UNIVERSITAT DE BARCELONA

Impact of RANK overexpression on mammary stem cell fate, alveolar cell differentiation and tumorigenesis

Alex Cordero Casanovas

UNIVERSITAT DE BARCELONA

FACULTAT DE MEDICINA

PROGRAMA DE BIOMEDICINA

Impact of RANK overexpression on mammary stem cell fate, alveolar cell differentiation and tumorigenesis

PhD candidate: **Alex Cordero Casanovas**

UNIVERSITY DE BARCELONA

FACULTY OF MEDICINE

CANCER EPIGENETICS AND BIOLOGY PROGRAMME (PEBC)

PROGRAME OF BIOMEDICINE

Impact of RANK overexpression on mammary stem cell fate, alveolar cell differentiation and tumorigenesis

Memory presented by Alex Cordero Casanovas to obtain the title of doctor by the University of Barcelona

Thesis director: Eva González Suárez

PhD Candidate: Alex Cordero Casanovas

Thesis tutor: Esteban Ballestar Tarín

ALEX CORDERO CASANOVAS, 2015.

AGRADECIMIENTOS

Los que me conocéis bien sabréis que no soy una persona dada a expresar los sentimientos abiertamente. Sin embargo, tras cinco duros años de duro trabajo, creo que merece la pena dedicar unas líneas a todas esas personas que directa o indirectamente han hecho posible el poder ver realizado mi "pequeño sueño" de ser doctor.

En primer lugar me gustaría expresar mi más sincero agradecimiento a la Dra. Eva González Suárez, la persona que confió en mí para poder realizar este proyecto. Gracias por guiarme en el complicado mundo de la ciencia, por tu dedicación, por exigirme para ser cada día mejor, y ayudarme a crecer tanto personal como profesionalmente.

Gracias a mis compañeros, a los de la "vieja" y los de la "nueva" escuela. Pasquale, Marta, Guille, Héctor, Jorge, Adrián, Eva, Adrià, Pili, Maria, Sergi, Toni, Gonzalo… Habéis sido los mejores compañeros de trabajo que habría podido soñar. Gracias por la ayuda, por compartir el día a día y estar ahí siempre, y por comportaros como verdaderos amigos. Os echaré muchísimo de menos, ya lo sabéis. Quisiera también hacer extensible este agradecimiento a la gente del PEBC, en especial a Laia, Carmen, Alexia, Catia, Paula, Octavio, Manu, Alex, Bárbara, Loren y Roser. Mención aparte merece Fer, el gurú del PEBC. El tener un problema y que la gente deje lo que está haciendo para ayudarte es una suerte que no siempre valoramos, pero no se puede pagar con nada. Es un orgullo para mí el haber podido trabajar junto con gente tan y tan válida, me siento más que afortunado por ello. Gracias también a mi gran profesor de Biología en el colegio, el señor Modest Mesa, por despertar mí curiosidad científica. A Josep María de Anta por darme esa primera oportunidad que toda persona necesita, y a Benja y Ester por su paciencia y amabilidad.

A mis amigos Carri, Kike, Charlie, Soto, Marcos, Santi…, los de toda la vida, por todos los buenos momentos que hemos pasado antes de la tesis, durante la misma y espero que por muchos años más. Gracias a Rodri, por convertirte en alguien tan importante en mi vida, a German por todos esos "buenos días" que te mantienen en contacto, y a aquellos que habéis dejado de ser compañeros de universidad para convertiros en amigos: Berni, Roser, Carla…

La familia. El sustento que toda persona necesita. Gracias a mi madre por cuidarme siempre sin condiciones, a mi padre por darme ese gen ganador que me permite luchar contra lo que sea, a mi avi Lluïs por darme los valores y mostrarme el tipo de

persona que quiero ser, y a toda la familia en general (Meri, Manu, Pol, Pepi, Marc, iaia Nuri, Gogó, Nery, Felipe) por todo el apoyo y cariño incondicional recibido.

Finalmente, gracias a ti, Camila. Mi pareja, mi compañera. Sin ti esto no habría ocurrido. Gracias por estar aquí, por ayudarme, comprenderme y quererme. Por esos viajes magníficos. Por la paciencia, la fuerza y el ejemplo. T'estimo molt, ara ens toca disfrutar a nosaltres!!!

Et dedico la tesi a tu, avi
sempre present…

INDEX

ABBREVIATIONS

-/-, +/+: homozygous
-/+: heterozygous
24h, 72h: 24 hours, 72 hours
-a647: Alexa 647
ANOVA: Analysis of variance
-APC: -Allophycocyanin
APRIL: A Proliferation-Inducing Ligand
BCMA: B Cell Maturation Antigen receptor
BrdU: 5-Bromo-2'-deoxyurdine
C/EBP: CCAAT/enhancer binding protein
CCND1: Cyclin D1
CD: Cluster of Differentiation
cDNA: Complementary DNA
CK: Cytokeratin
CSC: Cancer Stem Cell
Csnb: β-casein
CTRL: Control
-Cy7: Cyanine 7
DAB: 3,3'-Diaminobenzidine
DAPI: 4',6-diamidino-2-phenylindole
DM: Differentiation Medium
DMBA: 7,12-Dimethylbenz[α]anthracene
DMEM: Dulbecco's modified Eagle's medium
DNA: Deoxyribonucleic Acid
EDTA: Ethylenediaminetetraacetic Acid
EGF: Epidermal Growth Factor
ELDA: Extreme Limiting Dilution Analysis
Elf5: E74-Like Factor 5
ER: Estrogen Receptor
ERK: Extracellular signal-regulated kinases
FACS: Fluorescence-Activated Cell Sorting
FBS: Fetal Bovine Serum
-FITC: Fluorescein Isothiocyanate
FSC-H: Forward Scatter
G. 10,5/14,5/16.5: Gestation day 10,5/14,5/16.5
GFR: Growth Factor Reduced
GM: Growth Medium
GSEA: Gene Set Enrichment Analysis
H&E: Hematoxylin & Eosin
HEPES: 4-(2-hydroxyethyl)-1-piperazineethanesulfonic acid
HER2: v-erb-b2 Avian Erythroblastic Leukemia Viral Oncogene Homolog 2
HP: Hyperplasia
HRP: Horseradish Peroxidase
ID2: Inhibitor Of DNA Binding 2
IKB: Nuclear factor of Kappa light polypeptide gene enhancer in B-cells Inhibitor

ITS: Insulin, Transferring, Selenium
Jak-2: Janus Kinase 2
K5, K8, K14: Keratin 5,8,14
KO: Knock-Out
LDA: Limiting Dilution Assay
LP: Luminal Progenitor
LPS: Lipopolysaccharide
Ma-CFC: Colony Forming Cells
MAPK: Mitogen-Activated Protein Kinase
MaSC: Mammary Stem Cell
MEC: Mammary Epithelial Cell
MICs: Metastasis Initiating Cells
MIN: Mamamary Intra-epithelial Neoplasia
MMTV-: Mouse Mammary Tumor Virus
MPA: Medroxyprogesterone
mRNA: Messenger Ribonucleic Acid
NF-kB: Nuclear Factor Kappa-Light-Chain-Enhancer Of Activated B Cells
NG: Normal Gland
NOD: Nonobese Diabetic
OPG: Osteoprotegerin
P38: Mitogen-activated protein kinases 38
PBS: Phosphate Buffered Saline
-PE: Phycoerythrin
PFA: Paraformaldehyde
Pg: Progesterone
PgR: Progesterone Receptor
PI3K: Phosphoinositide-3-Kinase
PP1A: Protein Phosphatase 1
PRL: Prolatin
PrlR: Prolactin Receptor
RANK: Receptor Activator of Nuclear Factor κ B
RANKL: Receptor Activator for Nuclear Factor κ B Ligand
R-Fc: RANK-Fc
RNA: Ribonucleic Acid
ROCK: Rho-Associated Coil Kinase
Sca-1: Stem Cell Antigen-1
SCID: Severe Combined Immunodeficiency
SEM: Standard Error Of The Mean
SH2: Src Homology 2-like domain
Sma-1: Smooth Muscle Actin-1
SOCS: Suppressor of cytokine signaling
Sox-9: SRY (sex determining region Y)-Box 9
Src: Proto-oncogene tyrosine-protein kinase
SSC-A: Side Scatter
STAT5: Signal Transducer and Activator of Transcription 5A
SV0: Simian Vacuolating Virus 40
TACI: Transmembrane Activator and CAML-Interactor

TCGA: The Cancer Genome Atlas
TGF-β: Transforming Growth Factor β
TNF: Tumor Necrosis Factor
TRANCE: TNF-Related Activation-Induced Cytokine
Tris: Tris(Hydroxymethyl)Aminomethane
WAP: Whey Acidic Protein
WNT-4: Wingless-Type MMTV Integration Site Family, Member 4
WT: Wild-Type

GENERAL RESUME

Breast cancer is the second most common cancer worldwide, the fifth most common cause of cancer death, and the leading cause of cancer death in women. Distinct biological features and clinical behaviors turn cancer into a very heterogeneous disease, and although significant advances in the fight against breast cancer have been achieved during the last decades, a more profound understanding of their biology is still needed.

This thesis project is focused in RANK/RANKL signaling pathway, as during the last decade it has emerged as a key pathway in mammary gland development and tumorigenesis. RANK deletion or overexpression under the MMTV promoter disrupts mammary gland differentiation during pregnancy and lactation (Fata et al. 2000; Gonzalez-Suarez et al. 2007). It has been demonstrated that RANKL is downstream of progesterone and mediates its proliferative effects in the mammary gland (Beleut et al. 2010). Moreover, pharmacological inhibition of RANKL signaling prevents mammary tumor formation in WT mice under a carcinogenic treatment that includes a mutagen (dimethylbenz(a)anthracene, DMBA) and an analogous of progesterone (medroxiprogesterone, MPA) (Gonzalez-Suarez et al. 2010).

First, we aimed to elucidate how RANK signaling is regulating mammary gland differentiation. We demonstrated that RANK regulates different populations in mammary epithelial hierarchy. Indeed, constitutive activation of RANK in the mammary gland not only expands mammary stem cells (MaSC) and intermediate progenitors, but also reduced alveolar progenitors and impairs its differentiation into alveolar milk-producing cells through downregulation of the PrlR/STAT5/Elf5 signaling pathway. In addition we demonstrated that NF-KB, a signaling pathway activated downstream of RANK, regulates the balance between MEC self-renewal and differentiation.

Reproductive story and age have been linked to mammary tumorigenesis, and we found that increased levels of RANK in the mammary gland promote spontaneous tumor formation in mice under multiple gestations. We have also addressed the impact of RANK overexpression in two mouse models of spontaneous and metastatic hormone receptor negative breast cancer: MMTV-NEU and MMTV-PYMT. We demonstrated that RANK signaling plays a complex role in mammary tumorigenesis, affecting tumor initiation and/or aggressiveness in those oncogene-driven mouse models.

As we discovered that RANK signaling regulates mammary stem cell fate, we investigated whether this signaling pathway plays a role in the regulation of the cancer stem cell population. We demonstrated that RANK overexpression expands the cancer stem cell pool in PYMT-driven tumors, whereas RANK signaling blockage with RANK-Fc not only reduced this cancer stem cell population, but also induced tumor cell differentiation, resulting in decreased tumor recurrence and metastasis. Genetic deletion of RANK in MMTV-PYMT mice confirmed that RANK is important in tumor formation and mediates the metastatic potential of mammary tumor cells.

Altogether, our results supported that blocking RANKL could be a novel therapeutic therapy to treat both human hormone receptor positive and negative breast tumor subtypes.

INTRODUCTION

1. MAMMARY GLAND BIOLOGY

1.1. Anatomy of the mammary gland

The mammary gland is a type of exocrine gland that distinguishes mammals from all other animals for its capacity to synthesize, secrete and deliver milk to the newborn for its optimal nourishment, protection and development (Medina 1996). It is formed by two primary components: the parenchyma, responsible for milk production, and the stroma, that provides a substrate in which the parenchyma develops and functions (Medina 1996).

The mammary gland is a complex organ that consists of a number of different cell types: epithelial cells that form the ductal network of the gland; adipocytes, which constitute the fat pad and embeds the ductal network; vascular endothelial cells that make up the blood vessels; stromal cells including fibroblasts; and a variety of immune cells (Watson and Khaled 2008). Two main types of epithelium comprise the mammary gland, luminal (inner) and basal (outer). The luminal epithelium forms the ducts, and secreting alveoli during gestation. The basal epithelium consists essentially of highly elongated myoepithelial cells that surrounds the luminal layer (Hassiotou and Geddes 2013). Mammary stem cells (MaSC) are also found within the basal compartment (Kordon and Smith 1998).

1.2. Mammary gland development

Unlike most other organs, development of the mammary gland occurs predominantly after birth, following a time course of distinct phases. The mammary gland is a unique organ as it is capable of undergoing sequential cycles of development and differentiation under the control of steroid hormones (Figure 1).

1.2.1. Hormonal control in pubertal mammary gland development

At birth, the mammary epithelium is rudimentary, consisting of a few small ducts originating from the nipple that grow isometrically until puberty. At the onset of puberty, when mice are between 3-4 weeks of age, the mammary gland goes through a period of rapid expansion and remodeling. Elongation of the ductal tree during pubertal mammary development is possible due to the existence of club-shaped highly proliferative structures

called by terminal end buds (TEBs), which penetrate the fat pad under regulation of the surrounding stroma (Ball 1998). This growth is influenced by growth hormone (GH), estrogen and insulin-like growth factor-1 (IGF1) (Howlin, McBryan, and Martin 2006). GH is secreted from the pituitary gland and is an important global regulator of mammary gland development. GH effects on the mammary gland are mediated through its downstream IGF1 effector (Ruan and Kleinberg 1999; Gallego et al. 2001). GH binding to its receptor (GHR) in stromal fibroblasts induces IGF1, which then signals to the mammary epithelium. Indeed, growth hormone receptor (GHR) *knockout* mice display a dramatic (90%) reduction in serum IGF1 levels and delayed mammary gland development with eventual outgrowth of only a sparse tree (Y. Zhou et al. 1997; Gallego et al. 2001). The ovarian hormone estrogen acts in concern with IGF1 to generate the burst of proliferation required for ductal morphogenesis (Macias and Hinck 2012). Estrogen induces the release of amphiregulin (AREG), an epithermal growth factor (EGF) family member that generates additional growth factors in mammary epithelial cells (e.g. fibroblast growth factor, FGF), contributing to the rapid growth occurring in pubertal mammary glands.

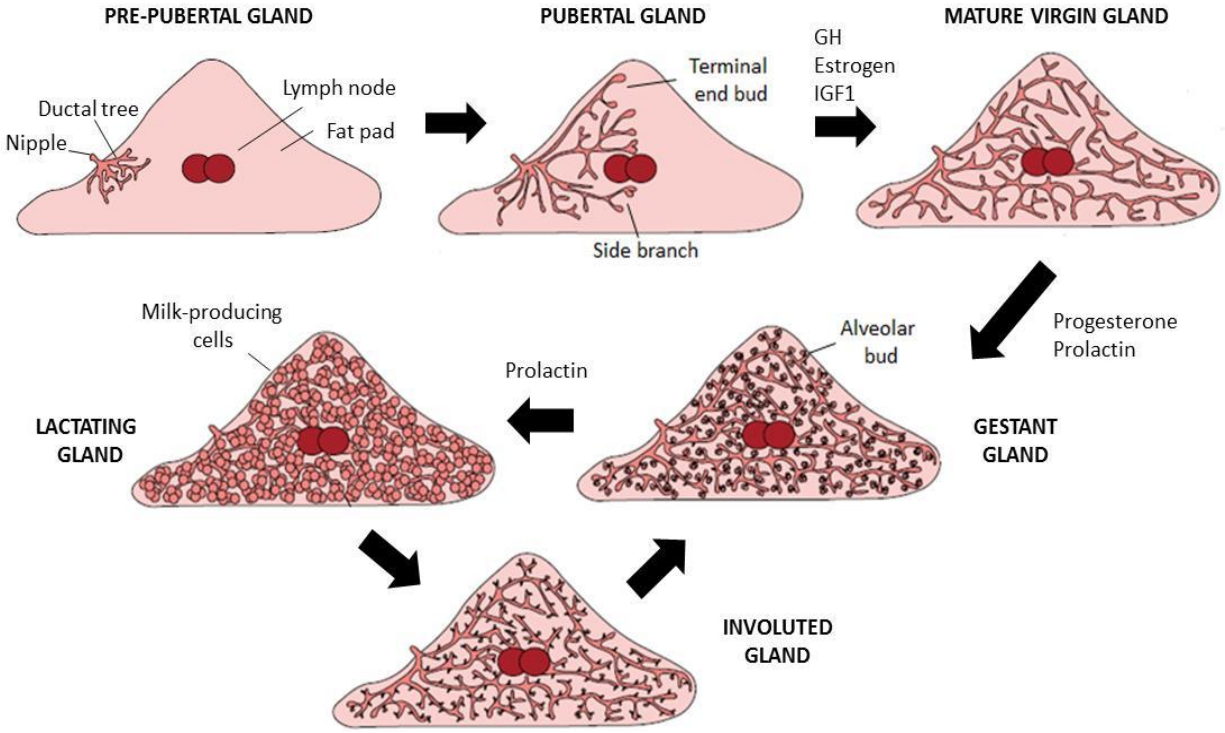

Figure 1: Schematic diagram of the mammary gland development**.** At birth the fat pad and a small rudimentary epithelial tree are present. During puberty the epithelium expands and the ductal network invades the whole fat pad. During pregnancy the epithelial ductal tree forms alveoli to produce milk for lactation. After weaning of the pups the milk-producing cells undergo apoptosis, a process termed involution and the gland returns to its virgin state. (Adapted from Watson CJ et.al. J. Reprod. Immunol. 2011).

1.2.2. Hormonal and transcriptional control in adult mammary gland development

When the mammary gland reaches its mature state, the majority of TEBs have reached the edge of the fat pad and have regressed. Virgin glands undergo cyclical development and regression of lateral and alveolar buds with each estrous cycle in response to ovarian hormones (Richert et al. 2000). Lateral buds that form branches have a layer of cap cells at the growing tip similar to TEBs. The alveolar buds subdivide to form rudimentary alveolar structures as postpubertal growth continues. These structures are composed of a single layer of epithelial cells enveloping a circular hollow center. However, progression of these alveolar buds into fully differentiated units capable of milk secretion only occurs during pregnancy-induced growth of the mammary gland.

1.2.2.1. Early pregnancy, a proliferative phase

The beginning of pregnancy is characterized by high proliferation of mammary epithelial cells (MECs), ductal side-branching and formation of alveolar buds under the stimuli of prolactin (PRL) and progesterone (PG) (Cathrin Brisken 2002; Neville, McFadden, and Forsyth 2002). These numerous changes in the mammary epithelium become crucial to prepare the mammary gland for lactation. The synergistic action of both hormones is supported by a positive feedback loop, as PRL secreted in the pituitary gland stimulates sustained secretion of ovarian PG, that in turn induces expression of prolactin receptor (PrlR) (Oakes, Hilton, and Ormandy 2006). Progesterone receptor (PR) and PrlR-null mice show severely impaired MEC proliferation and lobulo-alveoli formation, leading to lactation failure (Lydon et al. 1995; C. J. Ormandy et al. 1997).

Several cellular pathways are involved in mammary gland development during early pregnancy (Figure 2). WNT4 is a PG downstream target that stimulates epithelial ductal side-branching during early pregnancy (C. Brisken et al. 2000). RANKL is another PG downstream target essential to activate the RANKL/NF-kB/Cyclin D1 signaling pathway, which is crucial for the formation of alveolar structures during pregnancy and for PG-driven proliferation within alveoli (Conneely, Jericevic, and Lydon 2003; Yixue Cao and Karin 2003). RANKL also mediates the PG-induced Elf-5 expression, a member of the Ets transcription factors involved in mammary alveolar cell development during early pregnancy (Lee et al. 2013).

PRL is able to induce RANKL expression in mammary glands independently of PG (Fata et al. 2000; Christopher J. Ormandy et al. 2003). Alternatively, PRL can induce MECs proliferation independently of RANKL induction through insulin growth factor 2 (IGF2), a PRL-signaling target that lies upstream of Cyclin D1 transcription (Cathrin Brisken et al. 2002). PRL is also involved in the establishment of MEC polarity and cell-cell communication though Claudin-3 and Claudin-7, two members of the collagen family, and laminin (Christopher J. Ormandy et al. 2003; Oakes, Hilton, and Ormandy 2006).

1.2.2.2. Mid-pregnancy to lactation: the alveolar secretory differentiation phase

Proliferation levels in MECs decreases at mid-gestation whereas a subset of luminal cells differentiates in alveolar milk producing cells. Abrogation of proliferative PG signaling before lactation is required to enable terminal differentiation on the mammary gland (Piekorz et al. 2005; Ismail et al. 2002). Alveolar differentiated cells pour out the milk towards the ductal network, which ends at the nipple. Myoepithelial cells from the basal epithelium are contractile cells with properties of smooth muscle cells, and are responsible of the milk ejection from the alveoli during lactation as a response to pup suckling and oxytocin release from the pituitary gland (Moumen et al. 2011).

PRL is the major generator of lactational competence from mid-gestation onwards through activation of the downstream JAK2/STAT5 signaling pathway and transcription of Elf-5 (Hennighausen and Robinson 2005). STAT5 (signal traducer and activator of transcription 5) is the central transcriptional switch for a proper mammary gland cell differentiation and survival. STAT5 comprises two closely related isoforms, STAT5a and STAT5b, which are 96% identical at the protein level (Hennighausen and Robinson 2008). STAT5a is the main actor in normal mammary gland development representing 70% of total STAT5 levels (Yamaji et al. 2013). PRL binding to its receptor results in the tyrosine phosphorylation of Janus Kinase 2 (JAK2), which is permanently associated to PrlR (Campbell et al. 1994). Activated p-JAK2 proteins phosphorylate specific residues of PrlR, which are docking sites for STAT5 binding (Sutherland, Lindeman, and Visvader 2007). STAT5 is then phosphorylated at tyrosine residues, and subsequently p-STAT5 dissociates from the receptor, dimerizes in the cytoplasm and translocates into the nucleus for transcriptional regulation of its target genes, including milk proteins (Gouilleux et al. 1994; Wagner and Rui 2008). STAT5-null mice develop ducts but fail to form alveoli during pregnancy and lactation, and no milk expression is observed (X. Liu et al. 1997; Teglund et al. 1998; Miyoshi et al. 2001). Importantly, activated STAT5 under PRL stimuli induces β-

casein expression, and PG directly inhibits β-casein gene transcription in MECs *in vitro* by physical interaction with STAT5 (Buser et al. 2011), highlighting the importance of PG repression for a proper lactation in the mammary gland.

PRL signaling at mid-gestation induces the transcription of Elf5, which is expressed in luminal progenitor cells, increases during gestation and lactation, and specifies the alveolar cell fate (Harris et al. 2006; Oakes et al. 2008). Elf5 can bind to an ets-like domain in the proximal promoter of the whey acidic (WAP) milk protein and induce its expression (Thomas et al. 2000). Moreover, PrlR *knockout* mice form lobules capable of milk production after retroviral reexpression of Elf5, indicating that this transcription factor is a key regulator of the lobuloalveolar development (Harris et al. 2006). Interestingly, some studies show that Elf5 acts downstream of STAT5, as its transcription levels increase even when only one allele of either STAT5a or STAT5b is present in MECs (Yamaji et al. 2009; Lee and Ormandy 2012; Yamaji et al. 2013). In contrast, others have demonstrated that Elf5 binds to STAT5 promoter and transcriptionally activates STAT5, and Elf5-null mammary glands have reduced STAT5 expression and phosphorylation (Choi et al. 2009; Haricharan and Li 2014). These studies indicates the presence of a complex genetic regulatory network underlying the position of STAT5 and Elf5 in the mammary cell hierarchy (Lee and Ormandy 2012; Furth et al. 2011).

PrlR and JAK2-initiated STAT5 signaling in mammary glands at midgestation is modulated by several additional factors. Indeed, the protein tyrosine kinase Src is required for an increase in PrlR expression and activation of its downstream signaling cascade at midgestation (Okutani et al. 2001). Src-null mice exhibit a block in secretory activation due to impaired phosphorylation and activation of STAT5 and subsequently reduced β-casein expression, resulting in lactation failure and precocious mammary gland involution (Watkin et al. 2008). The epidermal growth factor ErbB4 (Her4), a member of the tyrosine kinase receptor ErbB family, is also necessary for mammary alveolar differentiation during pregnancy. Deletion of ErbB4 in the mammary epithelium leads to a failure to undergo complete functional differentiation (Long et al. 2003). Like the PrlR, stimulation of ErbB4 activates STAT5 to convey differentiation signals in alveolar luminal cells (Hennighausen and Robinson 2005). Moreover, the prosurvival protein AKT is an inducer of autocrine PRL secretion in the mammary epithelium, and it is essential for the activation of STAT5 and the development of a lactating mammary gland (C.-C. Chen et al. 2012). STAT5 is also found to transcriptionally activate AKT (Creamer et al. 2010), suggesting a positive feedback mechanism for maintaining STAT5 activation in the mammary gland during pregnancy and lactation.

In addition, the helix-loop-helix transcription factor ID2 show high levels during lactation and promotes differentiation in MECs cultures (Desprez, Sumida, and Coppé 2003), indicating that ID2 is essential for the differentiation of the mammary epithelium. The C/EBP family of proteins are important regulators of alveolar morphogenesis, and the isoform C/EBPβ plays an essential role attenuating PG expression resulting in MECs differentiation during pregnancy (Oakes, Hilton, and Ormandy 2006). Moreover, the NF1 family of transcription factors also play a role in functional alveolar differentiation as they regulate the transcription of milk protein genes such as those encoding WAP, α-lactalbumin and β-lactoglobulin (Murtagh, Martin, and Gronostajski 2003).

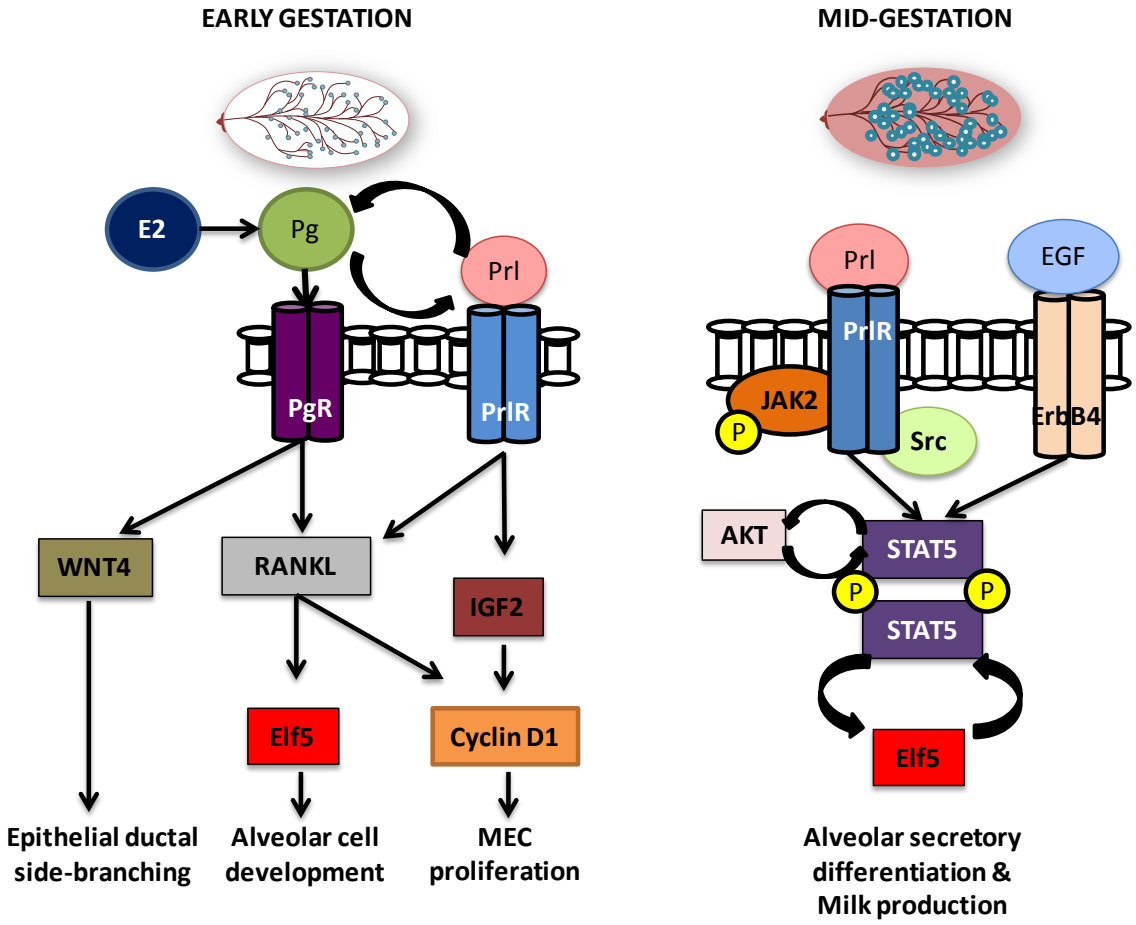

Figure 2: Schematic representation of the major signaling pathways that regulate mammary epithelial cell proliferation and alveolar secretory differentiation throughout gestation.

1.2.2.3. Involution: back to a virgin-like state

After lactation, the lack of demand causes milk accumulation in the mammary gland that initiates a process called involution. This process is characterized by high grade of apoptosis to remove milk-producing cells and a remodeling of the epithelial tree back to a simple ductal architecture (Lund et al. 1996). Two distinct phases of involution have been described. The first phase lasts around 48h, is reversible and involves apoptosis of alveolar cells. In a second irreversible phase, matrix metalloproteinases (MMPs) are responsible for reshaping the stroma, macrophages are recruited for clearing dead cells and adipocytes refill the mammary gland (Watson and Kreuzaler 2011).

Involution is characterized not only by a change in the STAT5 phosphorylation status that alters its activity state, resulting in the inactivation of both STAT5A and STAT5B isoforms, but also by activation of STAT3 (M. Li et al. 1997). Activation of STAT3 by the cytokine leukemia factor (LIF) during the first phase of involution results in alterations in PI3K-AKT signaling, restricting its prosurvival activity (Kritikou et al. 2003; Abell et al. 2005). This STAT3-induced AKT deactivation constitutes a mechanism by which STAT3 inhibits STAT5 at the onset of involution, since AKT can activate STAT5 (Haricharan and Li 2014; C.-C. Chen et al. 2012). Another mechanism by which STAT3 antagonizes prosurvival signaling is through upregulation of the insulin-like growth factor binding protein-5 (IGFBP5) (Chapman et al. 1999).

During the second phase of involution, LIF levels decline and STAT3 is activated by Oncostatin M (OSM), a member of the IL-6 cytokine family that has closest homology to LIF (Tiffen et al. 2008). OSM-induced STAT3 activation instigates the dephosphorylation of STAT5 even in the presence of PRL, indicating that OSM-OSM Receptor (OSMR) complex provides another signaling axis that activates STAT3 and inhibits STAT5 during involution (Tiffen et al. 2008; Haricharan and Li 2014).

1.2.2.4. Negative regulators of alveolar secretory differentiation

A balanced functioning of the PrlR-induced JAK2/STAT5 signaling pathway is essential for a proper regulation of the mammary gland cell differentiation during pregnancy. Hence, suppressor of cytokine signaling (SOCS) proteins and caveolin-1 have been described as part of the negative feedback loop, attenuating STAT5 phosphorylation and activation, keeping the signaling pathway under a strict regulatory control (Jasmin et al. 2006).

The SOCS protein family comprises eight members, which are induced by cytokines: SOCS 1-7 and cytokine-inducible SH2-containing protein (CIS). The most well-known members of the family are SOCS1, SOCS2, SOCS3 and CIS (Jasmin et al. 2006). The transcriptional regulation of SOCS proteins appears to be mediated, at least in part, by the STAT signaling pathway. Indeed, STAT-binding sequences were identified in the promoter region of SOCS genes (Naka et al. 1997). The protein CIS does not play a relevant role in mammary gland development, although its expression increases during lactation (Marine et al. 1999; Sutherland, Lindeman, and Visvader 2007).

SOCS1 binds to JAK2 and inhibits its kinase activity, targeting it for proteasomal degradation (Jasmin et al. 2006). SOCS1-null mice, which were rescued from neonatal death by deletion of the interferon gamma (IFNγ) gene, show an accelerated alveolar formation during pregnancy and precocious lactogenesis due to premature upregulation of p-STAT5 levels (Lindeman et al. 2001). In contrast to SOCS1, SOCS2 does not directly interact with JAK2, and its mechanism of action remains poorly understood (Sutherland, Lindeman, and Visvader 2007; Hennighausen and Robinson 2008). Although SOCS2 was found not to be essential for lactogenesis, the deletion of both alleles of SOCS2 can rescue the lactation defect observed in $PRLR^{+/-}$ heterozygous mice (Harris et al. 2006). Finally, SOCS3 is a critical repressor of STAT3-mediated mammary gland apoptosis during the involution phase, although its concrete role in lactation has not been elucidated (Sutherland et al. 2006).

The JAK2/STAT5 pathway can also be attenuated by membrane-bound proteins called caveolins. Caveolin-1 (Cav-1) expression is significantly downregulated during late gestation and lactation coinciding with PRL secretion (D. S. Park et al. 2001). Cav-1 depletion in the mammary gland results in a premature alveolar development during pregnancy due to hyperactivation of STAT5 (David S. Park et al. 2002). Importantly, Cav-1 prevents the access of JAK2 to the PrlR, thus negatively affecting STAT5 phosphorylation and a proper mammary gland differentiation during pregnancy (Hennighausen and Robinson 2008). Another negative regulator of alveolar differentiation is the transforming growth factor beta (TGF-β)/Smad signaling, which has been reported to downregulate prolactin-induced STAT5 activation and β-casein gene expression (Cocolakis et al. 2008; Wu et al. 2008).

1.3. Mammary epithelial hierarchy

1.3.1. Basal epithelium, a niche for Mammary Stem Cells

The continuous mammary gland development, differentiation and regression cycles during each estrous cycle highlight the plasticity of the mammary gland epithelium. The presence of stem cells in the mammary gland was demonstrated around 50 years ago, in groundbreaking experiments by DeOme and colleagues (Deome et al. 1959). They developed a technique that is still widely used today to test stem cell activity: the cleared fat pad transplantation (Figure 3). In this technique, the gland of 3 week-old recipient mouse (immunocompromised or not) is cleared by cutting out the endogenous epithelium, which at that point has not yet reached behind the lymph node. The remaining fat pad serves as environment for portions of normal mammary epithelium of donor mouse. If the piece transplanted contains stem cells they will be able to repopulate the gland, forming a ductal tree, end buds and even alveoli if the recipient mouse is mated. Subsequent studies demonstrated that successful engraftment could be obtained by injection of any segment of the mammary epithelial tree, indicating that repopulating cells, ie the MaSC, are widely distributed (Hoshino 1962; Daniel et al. 1968; Smith and Medina 1988). Furthermore the donor epithelial outgrowths can be serially transplanted in multiple generations (Daniel and Young 1971), resulting in the first *in vivo* experimental evidence providing the existence of mammary stem cells.

More recently, two landmark studies have changed the stem cell view and opened new possibilities. In two independent works carried out in 2006, John Stingl and Mark Shackleton identified new markers that can be used to isolate potential mammary stem cells by flow activated cell sorting (FACS) (Stingl et al. 2006; Shackleton et al. 2006). Identification of multipotent and self-renewing single cells that can reconstitute an entire mammary gland when injected *in vivo* defines them as MaSC. Thus, identification of MaSC-enriched populations relies on cell-surface markers and functional assays.

Heat stable antigen CD24 is a membrane glycoprotein heterogeneously expressed in the mammary epithelium. Three distinct populations in MECs stained with CD24 have been described: CD24high, CD24low and CD24negative (Sleeman et al. 2006). These populations represented luminal epithelial, basal myoepithelial and non-epithelial cells, respectively, as evidenced by cytoskeletal antigen staining analysis. Further mammary fat pad repopulation assays revealed that basal CD24low is enriched for mammary stem cells

(Sleeman et al. 2007). The characterization of additional cell-surface markers β-1 integrin (CD29) and α-6 integrin (CD49f) allow a better identification of mammary epithelial populations. Indeed, CD24low CD29high and CD24low CD49fhigh populations are considered enriched in MaSC as they show increased mammary repopulating ability *in vivo* (Stingl et al. 2006; Shackleton et al. 2006).

Different signaling pathways have been reported to control and preserve the mammary stem cell pool. The Notch and Hedgehog pathways, described as common regulators of stem cell fate in many tissues such as brain, skin and the hematopoietic system, regulate MaSC pool self-renewal and differentiation (S. Liu et al. 2006; Bouras et al. 2008). The increase in progesterone concentration during estrous cycle has also been reported to expand this MaSC pool (Joshi et al. 2010).

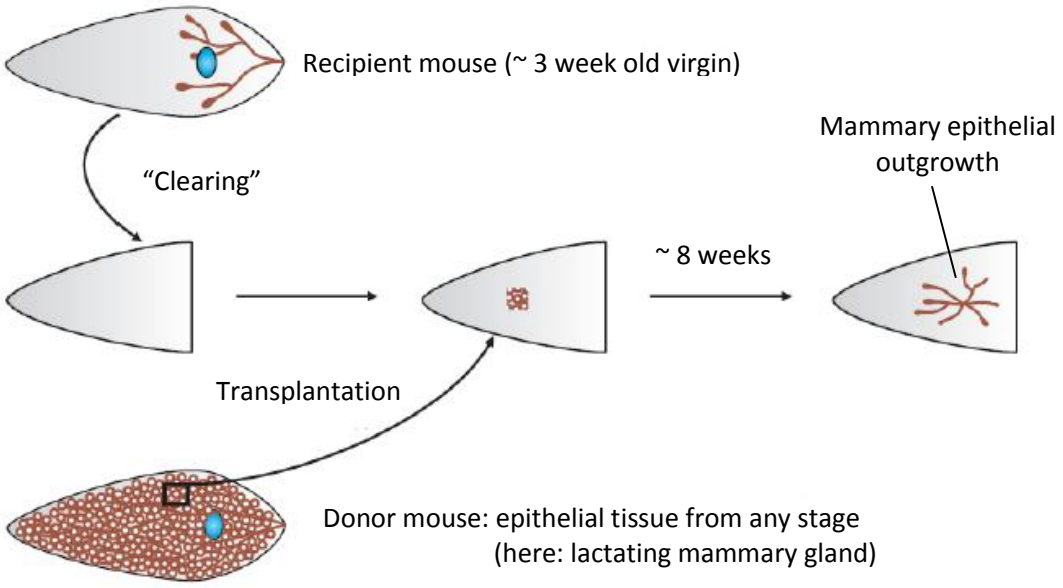

Figure 3: The cleared fat pad transplantation technique. Transplantation of donor epithelium into "cleared" recipient fat pads is a widely used stem cell assay to test *in vivo* outgrowth ability. (Adapted from DeOme K.B. et.al. Cancer Research, 1959).

1.3.2. Luminal epithelium is enriched in luminal progenitors

The luminal population contains a subset of hormone-sensing MECs that express both progesterone and estrogen receptors (Petersen, Høyer, and van Deurs 1987). PR expression is induced by estrogen via ER, and deletion of PR results in impaired lobuloalveolar development (Lydon et al. 1995). Luminal hormone-sensing MECs correspond to approximately 40% of total luminal cells and are considered mature luminal cells, as they showed low proliferative levels in an adult mammary gland (Clarke et al. 1997; Russo et al. 1999). Luminal proliferative cells are negative for PR and ER, suggesting a paracrine mechanism for PG-induced proliferation (Ismail et al. 2002; Shyamala et al. 2002). Indeed, transplantation of a mixture of wild type (WT) and PR-deficient MECs into a WT recipient mammary gland resulted in a rescued proliferation and morphogenesis of those PR-deficient MECs that were in close proximity to WT PR+ MECs, demonstrating the paracrine proliferation mechanism (C. Brisken et al. 1998).

Cells in the luminal compartment express higher levels of CD24 and lower CD29 and CD49f (CD24high CD29low CD49f low), compared to basal MECs. Moreover, it has been described the existence of luminal-restricted progenitor cells that generate colonies positive for luminal markers cytokeratin 8 and 18 (K8, K18) and negative for basal cytokeratin 5 and 14 (K5, K14) in low cell-density adherent cultures (Stingl et al. 2001). These MECs are called mammary colony forming cells (Ma-CFC), and show lower mammary repopulation ability when injected *in vivo*, compared to MaSC (Stingl et al. 2006). Moreover, the luminal progenitor ER- PR- population are also enriched in bipotent progenitor cells that produce colonies containing both luminal K8+ and basal K14+ cells *in vitro* (Z. Li et al. 2007; Chakrabarti et al. 2012; Stingl et al. 2001). These bipotent progenitor cells coincide with the previously called Ma-CFC, and this population also shows higher colony forming ability when compared to luminal ER+ PR+ cells (Sleeman et al. 2007).

The discovery of additional surface markers highlights a complex hierarchy within the luminal compartment. Expression of Sca-1 and Prominin-1 (CD133) in luminal CD24high MECs identify the hormone-sensing population ER, PR and PrlR positive (Sleeman et al. 2007). On the contrary β-3 integrin (CD61) and α-2 integrin (CD49b) are surface markers expressed in luminal progenitors, as CD24high CD61+ and CD24high CD49b+ showed higher colony forming ability compared to luminal CD24high MECs negative for these markers (Asselin-Labat et al. 2007; W. Li et al. 2009). In particular CD61+ identifies a

subset of luminal progenitor cells that differentiate into CD61- alveolar cells during pregnancy (Oakes et al. 2008).

Of the several genes implicated in alveolar morphogenesis regulation, Gata-3 and Elf5 have emerged as key regulators of luminal cell differentiation within the epithelial hierarchy. Gata-3 is essential for ductal and alveolar morphogenesis via regulation of the stem and CD61+ progenitor cell pools, and accumulation of CD24high CD29low CD61+ in Gata-3 deficient mice has been reported (Asselin-Labat et al. 2007). Elf5, a key transcriptor factor of alveolar commitment, is specifically expressed in the luminal progenitor CD61- population (Harris et al. 2006; Oakes et al. 2008). Unlike Gata-3, mammary glands of Elf5-deficient mice do not exhibit defects in ductal growth and morphogenesis. However, a pronounced defect in alveolar morphogenesis is evident during pregnancy in the absence of a single Elf5 allele (J. Zhou et al. 2005). Based on these discoveries, a model of mammary epithelial hierarchy has been described (Figure 4).

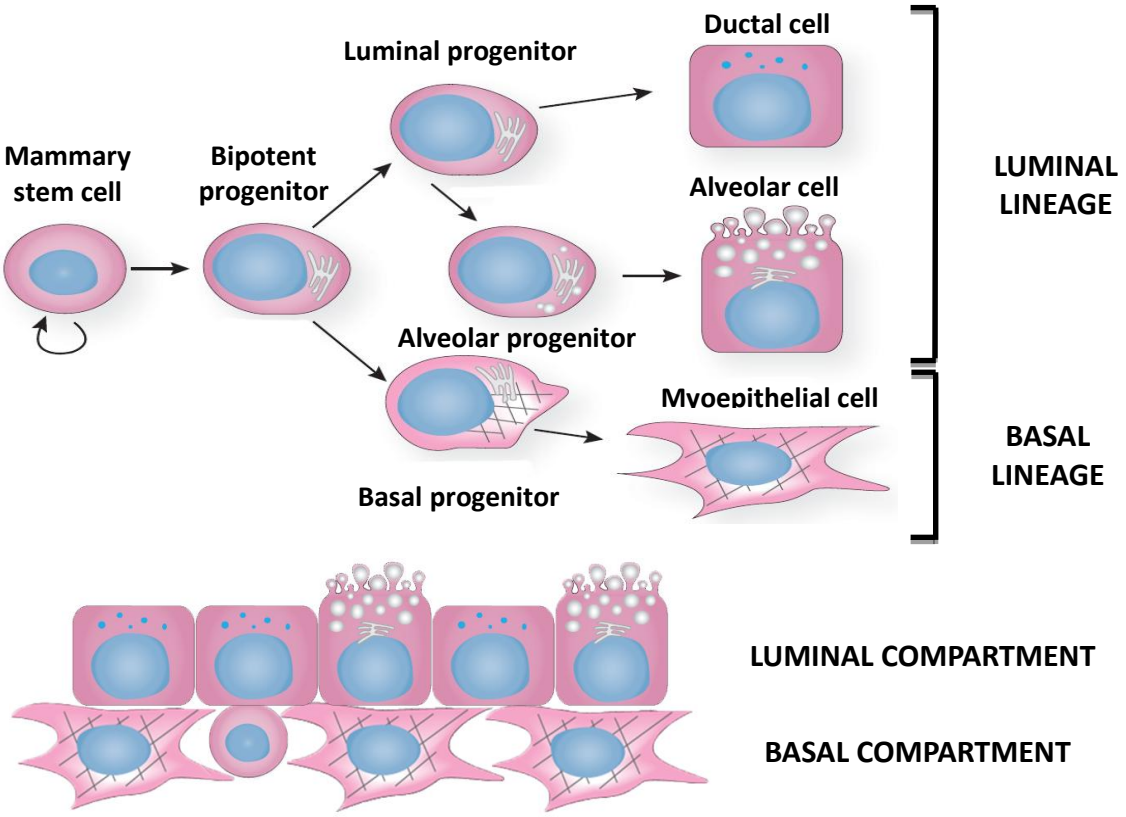

Figure 4: Mammary epithelium hierarchy. Existence of mammary stem cells (MaSC) in the basal compartment has been demonstrated. Differentiated ductal, alveolar (during gestation) and myoepithelial cells compose an adult mammary gland. Bipotent intermediate progenitors mediate the correct differentiation of the MaSC to give rise to a functional mammary gland. (Adapted from Hector Macias and Lindsay Hinck, Wiley Interdiscip Rev Dev Biol. 2012).

More recently, Van Keymeulen and colleagues in 2011 reported a new scenario in the mammary differentiation hierarchy model (Van Keymeulen et al. 2011). Genetic lineage-tracing experiments revealed that although the mammary gland initially develops from multipotent embryonic K14+ progenitors, giving rise to cells from both basal and luminal compartments; during puberty and adulthood the expansion and maintenance of each mammary epithelial lineage is ensured by the presence of two types of lineage-restricted stem cells (Van Keymeulen et al. 2011). Indeed, basal and luminal mammary epithelial cell populations are generated by different basal or luminal unipotent stem cells rather than being maintained by rare multipotent stem cells. The study argues that the experimental setting of the transplantation assays performed in previous studies forces the differentiation of the MaSC from the basal compartment into cells from both luminal and basal/myoepithelial lineages, while unperturbed mammary gland development relies on lineage-restricted unipotent stem cells.

2. BREAST CANCER

2.1. Incidence of breast cancer and molecular subtypes

Cancer is a term used for diseases characterized by uncontrolled cell growth. It causes tumors that can expand locally, invading nearby parts of the body, and may also spread to more distant parts and disseminate systemically. While normal cells are controlled by regulatory signals, cancer cells have the ability to proliferate uncontrolled, invade surrounding tissues and metastasize to distant organs.

Breast cancer is a type of cancer originating from breast tissue. Excluding non-melanoma skin cancers, breast cancer represents the most common cause of cancer in women and the second most common cause for female deaths worldwide (Weigelt, Peterse, and van't Veer 2005). The risk of breast cancer depends on both genetic and lifestyle factors. The latest are mainly related to events affecting hormonal status (for example parity and breast-feeding history or age of menarche and of menopause) and to environmental agents (ionizing radiation, fat-rich diet, alcohol consumption and so on) (Dumitrescu and Cotarla 2005).

Approximately in 5-10% of cases, breast cancers are due to strong inherited risk (Malone et al. 1998). Mutations in cancer predisposition genes BRCA1 and BRCA2 increase the relative risk of breast cancer by 10- to 20- fold, and account for approximately 80-90% of the familial breast cancer cases (S. Chen and Parmigiani 2007). They are tumor suppressor genes that when mutated, lead to the inability to regulate cell death and subsequently to uncontrolled cell growth, leading to cancer.

Classification of breast cancers follows different criteria: histopathology, histological grade, clinical stage, receptor status and molecular profile. Histologically, the most common breast cancers are developed from epithelial cells in the ducts (50-75%) and lobules (10-15%), known as invasive ductal carcinoma (IDC), and invasive lobular carcinoma (ILC), respectively. Less commonly, breast cancer can begin in the stromal tissues, including fatty and fibrous connective tissues of the breast (Dillon DA et al., 2010).

There are three receptors that have for long guided breast cancer classification: ER, PR and epidermal growth factor receptor 2 (ErbB2 or HER2). Based on receptor status, breast cancer subtypes can be defined as: endocrine receptor positive (ER+ or PR+), HER2 positive, triple negative (TNBC, ER-, PR-, HER2-) and triple positive (ER+, PR+ and HER2+).

Approximately 65% of breast cancers are the so-called luminal tumors, which express ER and PR and have usually a relatively good prognosis. Luminal B cancers differ from luminal A by having a poorer clinical outcome, being less responsive to the ER antagonist tamoxifen and having a stronger proliferative outcome and high rate of recurrence (Sørlie et al. 2001; Cheang et al. 2009; Prat and Perou 2011). Around 20-30% of breast tumors does not express hormone receptors but showed over-expression or amplification of HER2 receptor, and are called HER2+ tumors (Slamon et al. 1987). These clinically aggressive tumors are prone to frequent metastasis and recurrence and can be treated with trastuzumab, a monoclonal antibody that targets Her2 receptor (McKeage and Perry 2002). The triple positive tumor subtype can be considered the subset which most closely resembles the HER2-/hormone receptor positive tumors, with substantial differences in biology and clinical outcome (Vici et al. 2015). Approximately 10% of ER+ PR+ tumors are also HER2+, and preclinical evidences confirm that crosstalk between HER2 and ER signaling pathways contribute to resistance to endocrine therapy (Shou et al. 2004; Osborne and Schiff 2011). Simultaneous inhibition of both HER2 (trastuzumab) and ER (tamoxifen) pathways is believed more effective that ER inhibition alone (Vici et al. 2015). Finally the remaining 10-15% corresponds to TNBC. These tumors have the worse prognosis as they lack ER, PR and HER2 expression, and have increased likelihood of distant recurrence and of death, compared with other types of cancer (Dent et al. 2007). As no targeted therapies exist, TNBC are treated with systemic chemotherapy (Sorlie et al. 2003).

The scientific community is making a huge effort to find a cure for cancer and to eradicate it as a major cause of death (Ferlay et al. 2013). Despite significant progress in the treatment of breast cancer, the intrinsic heterogeneity of cancers and multiple mechanisms involved in tumor biology (Perou et al. 2000) hinders the finding for a definitive solution. For this reason, cancer research has been intensified with the aim to improve the understanding of tumor molecular biology and the development of more effective cancer treatments.

2.2. Mouse models of metastatic breast cancer

The vast majority of complications associated with breast cancer, including death, are due to metastasis developing in regional lymph nodes and in distant organs such as bone, lung, liver and brain (Fisher et al. 1983; Weigelt, Peterse, and van't Veer 2005). Thus, specific molecular changes occurring in both tumor cells and tumor microenvironment contribute to tumor cells detachment form the primary tumor mass, invasion into the tumor stroma,

entry into the bloodstream through nearby blood vessels or indirectly via the lymphatic system (intravasation), survival, extravasation and colonization of the target organ, and finally metastatic outgrowth (Chambers, Groom, and MacDonald 2002).

While studies in tissue cultures allow analyses of distinct molecular pathways that are triggered in a single cell, research in mouse models integrates the complexity of an organ and its different cell types with the hormonal and physiological dynamic status of the animal. Therefore, studies with mouse models have been developed because of their evolutional similarity to humans, short life span and easy handling. The possibility to activate (e.g. MYC, HER2/NEU) or delete (e.g. BRCA-1, P53) specific genes using genetically engineered mouse (GEM) models represent a valuable tool in shedding light on molecular alterations found in human breast cancers (D. Craig Allred and Medina 2008)

Mouse Mammary Tumor Virus (MMTV) is an oncoRNAvirus of the *Retroviridae* family. The MMTV-long terminal repeat (LTR) is one of the most common promoters used in directing transgene expression to the mammary gland, as it is hormonally stimulated by progesterone, glucocorticoids and dyhidrotestosterone, hormones that act during mammary gland development (Otten, Sanders, and McKnight 1988; Muñoz and Bolander 1989). Thus, MMTV-LRT is active throughout mammary development and its transcriptional activity increases with lactation under the influence of steroid hormones (Taneja et al. 2009).

MMTV-driven mouse models have been informative models for human breast cancer despite morphological, hormonal and lifestyle differences between both mice and humans (Taneja et al. 2009). Moreover, similarities in gene expression profile between human primary breast cancers and oncogene-induced mammary tumors in mouse models have been identified (Desai et al. 2002). While there are many advantages to using the mouse as a surrogate, there are also potential caveats, including that not a single mouse model recapitulates all the expression features of a given human breast tumor subtype, probably due to unknown specie-specific pathway differences (Herschkowitz et al. 2007). At present, the challenge is to test whether genes identified in gene expression profile analyses in human breast tumor samples could modulate mammary tumorigenesis in transgenic mouse models, like in the well-characterized MMTV-PYMT and MMTV-Neu. Comparative genomic analysis and cytokeratin expression profile revealed that tumors from these mouse models are highly similar to human luminal tumors (Herschkowitz et al. 2007).

MMTV-PyMT mouse model express the middle T protein of polyomavirus (SV40 virus), which activates several pathways such as RAS/MAPK and PI3K-AKT, essential for the regulation of cell proliferation, apoptosis, adhesion and migration (Fluck and Schaffhausen 2009). This results in widespread transformation of the mammary gland, with aggressive multifocal tumor formation at only 3-5 weeks of age, and high incidence of metastatic lesions in lymph nodes and lungs (Guy, Cardiff, and Muller 1992). A unique feature of MMTV-PyMT tumor-prone model is that primary tumors usually develop as single focus in epithelial ducts, resulting in multiple tumoral foci formation per mammary gland (E. Y. Lin et al. 2001). Tumor formation and progression in these mice particularly resembles the different stages of progression in human mammary tumorigenesis: hyperplasia, adenoma/MIN (mammary intraepithelial neoplasia), early carcinoma and late carcinoma (Elaine Y. Lin et al. 2003). Tumor cells of MMTV-PyMT adenocarcinomas loss hormone receptor expression (ER, PR) and β-1 integrin, and express high levels of Her2/neu and Cyclin D1 (Maglione et al. 2001; Elaine Y. Lin et al. 2003).

MMTV-Neu mouse model constitutively express the neu gene under the MMTV-promoter. Neu, the rat orthologue of human Her2 (ErbB2), belongs to the epithelial growth factor receptor (EGFR) family of receptor tyrosine kinases (RTKs), and is used as a clinically useful prognostic marker. Her2 overexpression has been observed in invasive human ductal carcinoma, and less frequently in benign breast disorders, such as hyperplasias and dysplasias (D. C. Allred et al. 1992; Mansour, Ravdin, and Dressler 1994). Continuous tyrosine kinase activity in MMTV-neu mice leads to uncontrolled cell proliferation resulting in mammary tumor formation at 8-11 months of age, with frequent lung metastasis in pure-strain FvB background (Bargmann, Hung, and Weinberg 1986; Muller et al. 1988; Guy, Cardiff, and Muller 1996). Indeed, Neu overexpression amplifies proliferative and apoptotic signaling pathways including RAS/MAPK, Pi3K-AKT or JNK (Olayioye et al. 2000; Yarden and Sliwkowski 2001). In addition, neu overexpression in mixed background (FvB x C57BL/6) glands results in mammary tumor formation with higher latencies (up to 18 months) compared to fully inbred FvB background mice (Rowse, Ritland, and Gendler 1998).

2.3. Cancer stem cells

The concept of cancer stem cells (CSC) was proposed more than three decades ago to explain heterogeneity of tumors and cancer cells. CSCs constitute a subpopulation of cells within tumors endowed with self-renewal and differentiation capacity that can generate the diverse non-stem cells that comprise a tumor (Reya et al. 2001). These cells have been

termed cancer stem cells to reflect their “stem like” properties and ability to continually sustain tumorigenesis, but they are not necessarily derived from normal mammary stem cells (McDermott and Wicha 2010; Owens and Naylor 2013). There is currently much interest in the role of breast CSCs in cancer disease and whether they provide a key to unlocking new insights into the mechanisms driving breast cancer progression, drug resistance and reoccurrence (Owens and Naylor 2013).

Importantly, a number of cell surface markers have been proved useful for the isolation of subsets enriched for CSCs in mammary gland tumors, although none of these surface markers are exclusively expressed by CSCs (Asselin-Labat et al. 2011; Lo et al. 2012). Thus, identification of CSC relies on their ability to form mammospheres in anchorage-independent growth assays (Dontu and Wicha 2005; Pece et al. 2010), and to initiate novel tumors when injected *in vivo* in the mammary gland of an immunocompromised mice (O’Brien, Kreso, and Jamieson 2010). More recently, new technological advances (lineage tracing) enable the study of CSCs in their primary setting, without the need for transplantation, in certain tissues such as the skin, brain, intestine and breast (Driessens et al. 2012; C.-C. Chen et al. 2012; Schepers et al. 2012; Zomer et al. 2013).

Importantly, CSCs are involved in the metastatic progression of breast cancer (Balic et al. 2006). This is particularly significant given that the vast majority of cancer deaths are due to secondary lesions that have disseminated from the original primary tumor. Moreover, most CSCs are believed to be resistant to conventional therapies such as chemotherapy and radiotherapy and are therefore preferentially preserved when cancer cells are targeted by these approaches (Eyler and Rich 2008; Morrison et al. 2010). Selective pressure in a genetically unstable environment can result in the acquisition of epigenetic or genetic changes that support CSC survival. Factors that influence this tumor environment include hypoxia or chemotherapy, which have been linked to CSC development (Owens and Naylor 2013).

It is important to note that CSC, that uniquely sustains malignant growth within the tumor, is not necessarily related to the tumor cell of origin, a normal cell that acquires the first cancer-promoting mutation (Visvader 2011). The intertumoral heterogeneity could be understood as that different tumor subtypes arise from distinct cells within the tissue that serve as the cell of origin. In addition, tumor maintenance depends on the continued expression of certain oncogenes, as process known as “oncogene addition” (Weinstein 2002). Transformation of distinct breast epithelial cells *in vitro* has indicated that the oncogene-target cell can critically influence the final phenotype of the tumor (Ince et al.

2007). Identification of the cell of origin may permit a systematic analysis of the genetic lesions responsible for tumor initiation and progression, serving as a valuable tool for the identification of early disease biomarkers. Indeed, lineage tracing experiments are the current “gold standard” for delineating the target cell of transformation in mouse models (Visvader 2011).

3. RANK/RANKL SIGNALING

3.1. Members of the pathway

RANK/RANKL signaling pathway is composed by three members: RANK, RANKL and OPG

RANK (Receptor Activator of Nuclear Factor k-B), also called tumor necrosis factor (TNF) receptor superfamily member 11A (TNFRSF11A) is a type I transmembrane protein. RANK assembles into functional trimers and is ubiquitously expressed in skeletal muscle, thymus, liver, colon, small intestine, adrenal gland, osteoclast, mammary gland epithelial cells, prostate and pancreas (Anderson et al. 1997; Fata et al. 2000; Theill, Boyle, and Penninger 2002; Boyle, Simonet, and Lacey 2003).

RANKL (Receptor Activator of Nuclear Factor k-B ligand), also called TNF ligand superfamily member 11A (TNFSF11A) is a type II homotrimeric transmembrane protein. RANKL is the only known ligand for RANK receptor (Xing, Schwarz, and Boyce 2005), and it is expressed as a membrane-bound and a secreted protein, which is derived from the membrane form as a result of either proteolytic cleavage or alternative splicing (Ikeda et al. 2001). RANKL is highly expressed in lymph nodes, thymus and lung, and at low levels in a variety of other tissues including spleen, bone marrow and leukocytes (Anderson et al. 1997; Wong et al. 1997; Yasuda et al. 1998a; Theill, Boyle, and Penninger 2002; Boyle, Simonet, and Lacey 2003).

OPG (Osteoprotegerin), also called TNF receptor superfamily member 11B (TNFRSF11B), is a decoy receptor for RANKL, acting as a natural inhibitor for RANK/RANKL signaling pathway (Yasuda et al. 1998). OPG is highly expressed in a variety of tissues including lung, liver, spleen, thymus, ovary, lymph node and bone marrow (Wada et al. 2006).

3.2. RANK/RANKL in bone remodeling and metastases

Bone system in the adult skeleton is renewed continuously in response to a variety of stimuli in a process called bone remodeling, which ensures the conservation and renewal of the bone matrix. Once formed, bone undergoes a cyclical process of break down

(resorption) and build-up (synthesis) throughout the skeleton, with the key involvement of osteoclasts and osteoblasts cells, respectively.

The discovery of RANK/RANKL/OPG system as a key regulator of bone remodeling was first brought to light in 1997 in a paper by Simonet et.al (Simonet et al. 1997). RANKL, expressed and secreted from osteoblasts, binds to its receptor RANK, expressed on osteoclasts precursors that in turn will differentiate into multinucleated activated osteoclasts (bone resorbing cells). OPG is secreted from osteoblasts and can bind to RANKL and compete for binding to RANK, thus blocking osteoclast activation (Kong et al. 1999; Dougall et al. 1999). Importantly, genetic ablations in both RANK and RANKL *knockout* mice ($RANK^{-/-}$, $RANKL^{-/-}$) leads to defective tooth eruption and a severe osteopetrosis due to complete lack in osteoclasts (Kong et al. 1999). Moreover the ablation of OPG in mice results in osteoporosis (Mizuno et al. 1998; Bucay et al. 1998).

Bone-related diseases such as osteoporosis, rheumatoid arthritis or cancer metastases affect millions of people worldwide. Decreased estrogen expression and increased RANKL that occurs after menopause in women lead to enhanced osteoclastogenesis and a process of osteoporosis over the time (Boyle, Simonet, and Lacey 2003). Furthermore the most common human cancers (lung, breast and prostate) often invade bone tissue causing skeletal complications due to metastases (Mundy 2002). Therefore bone environment and its high vascularity provides a particularly fertile ground for the establishment and growth of the circulating metastatic cells. In the case of breast cancer cells when present in the bone microenvironment, they overproduce the parathyroid hormone-related protein (PTHrP), which can promote osteoclastogenesis through upregulation of RANKL expression in osteoblasts (Southby et al. 1990). Consequently, active growth factors such as TGF-b and IGF-1 are released from bone matrix and cause proliferation of breast cancer cells, which in turn produce more PTHrP that perpetuate tumor activity. This “vicious cycle” promotes tumor cell growth, survival, angiogenesis, invasion and metastasis (Paget 1989; Mundy 2002).

Antiresorptive agents are important pharmacological options for the treatment of osteoporosis. In particular Denosumab, a human recombinant monoclonal antibody against RANKL, was developed and approved for the clinical use by the Food and Drug Administration and the European Commission in 2011 (http://www.cancer.gov/about-cancer/treatment/drugs/fda-denosumab). The antibody blocks RANK-RANKL binding and therefore inhibits osteoclast differentiation, activity and survival, resulting in decreased bone resorption (Moen and Keam 2011; Reginster 2011). Several clinical trials have also

demonstrated that denosumab is an effective inhibitor of bone metastasis (Body et al. 2010; Fizazi et al. 2012). This antibody is currently used as a highly and cost-effective therapy to reduce risk of osteoporosis in postmenopausal women and for skeleton-related complications in patients with bone metastases from breast and prostate solid tumors.

3.3. RANK/RANKL in the immune system

RANK and RANKL are important mediators of the interactions between bone system and the immune system. RANKL, expressed in activated T lymphocytes, can support osteoclastogenesis leading to certain autoimmune diseases such as rheumatoid arthritis, where local RANKL overstimulation couples inflammation to bone loss and finally results in bone destruction (Kong et al. 1999; Takayanagi 2007).

RANK signaling is also involved in the development and activation of the immune system. RANK- and RANKL-null mice completely lack lymph nodes, revealing a pivotal role of RANK signaling pathway during lymph node organogenesis. Most likely, loss of RANK or RANKL affects the lymph node inducer cells, resulting in their failure to form clusters in rudimentary mesenteric lymph nodes (Kong et al. 1999; Kim et al. 2000).

Moreover, RANK is highly expressed in the membrane of dendritic cells (DC), which are antigen-presenting cells specialized to capture antigens and initiate T cell immunity. Thus, RANKL expressed in T lymphocytes binds to its receptor in mature DC, resulting in the induction of anti-apoptotic and survival signals in mature DC, as well as the production of proinflamatory cytokines and cytokines that stimulate and induce T lymphocytes differentiation. Therefore, RANKL is likely to act as a positive feedback during productive T cell – DC interactions, leading to a faster immune response to future antigen exposures (Josien et al. 1999; Bachmann et al. 1999).

RANK and RANKL also play an essential role in the immunological tolerance. RANKL is expressed in intrathymic inducer cells, which are closely related with medullary thymic epithelial cells (mTECs). RANK expressed in mTECs binds to RANKL and induces the expression of the autoimmune regulator transcription factor (AIRE). AIRE regulates the expression of the self-tissue restricted antigens (TRAs) in the membrane of mTECs, thus regulating central tolerance and preventing T lymphocyte autoimmunity (Rossi et al. 2007; Akiyama et al. 2008). AIRE mutations lead to a multi-organ autoimmune disease in humans and autoimmunity in AIRE gene targeted mice (Leibbrandt and Penninger 2008).

Moreover, RANK signaling is also implicated in the establishment and maintenance of the peripheral autoimmunity. In particular, RANKL expression in keratinocytes of the skin is strongly upregulated following UV irradiation (Leibbrandt and Penninger 2008). Consequently, RANKL increase activates epidermal Langerhans cells (LC, dendritic cells of the skin), which express RANK. RANKL-activated LCs trigger an expansion of regulatory T cells (Tregs), which maintain immunological self-tolerance and suppress excessive immune responses to self-antigens, such as in autoimmune diseases or allergies (Sakaguchi 2005; Loser et al. 2006).

3.4. RANK/RANKL in the mammary gland

In addition to the crucial function in bone remodeling and the immune system, RANK signaling pathway plays also an important role in the morphogenesis of the mammary gland. The first evidence for that was described by Jimmie Fata and coworkers (Fata et al. 2000). They demonstrated that RANK- and RANKL-null mice show a strong defect in MEC proliferation, survival and development during gestation, resulting in a complete defect in alveoli differentiation and milk production. However, both RANK- and RANKL-null mice show normal glands at birth that develop without defects during puberty until adult nulliparous state (Fata et al. 2000), highlighting the importance of RANK signaling in mammary alveolar differentiation process.

RANK and RANKL expression is relatively low in virgin mammary glands. Expression profile analysis revealed that both RANK and RANKL distribution in the mammary gland is spatially and temporally regulated during gestation (Fata et al. 2000; Gonzalez-Suarez et al. 2007). RANKL is expressed in a subset of luminal cells responsive to progesterone (Mulac-Jericevic et al. 2003), and its expression increases greatly during early gestation, coinciding with the epithelial proliferative phase. RANKL expression gradually decreased during late gestation and lactation phase (Gonzalez-Suarez et al. 2007). Moreover, RANK protein expression significantly increased during gestation, reaching a peak at mid-gestation (days 14,5-15,5), and then decreases until lactation.

Importantly, RANK and RANKL overexpression also leads to defects in the differentiation of the mammary gland during pregnancy. Indeed, RANK overexpressing mice under the MMTV promoter (MMTV-RANK mice) show hyper-proliferative mammary glands during early pregnancy, and a complete blockade in the differentiation of lobulo-alveolar structures at mid-gestation (Gonzalez-Suarez et al. 2007). As a result, they are unable to produce milk and feed their pups. On the other hand, RANKL overexpressing mice (MMTV-

RANKL) show precocious ductal side-branching and alveologenesis in the pubescent mammary gland, with a persistent hyperproliferative phenotype in adult virgin and pregnant mammary glands (Fernandez-Valdivia et al. 2009). Together, these data indicates how a tight temporal and spatial regulation of RANK/RANKL signaling pathway is essential for a proper mammary gland development and differentiation during pregnancy.

3.4.1. Progesterone-RANKL signaling in mammary development and stem cell fate

RANKL plays a key role in mammary gland development, being the main mediator of progesterone signaling in the mammary epithelium (Fata et al. 2000; Mulac-Jericevic et al. 2003; Gonzalez-Suarez et al. 2007; Beleut et al. 2010). As mentioned above, RANKL expression increases during early to mid-pregnancy, when PG stimulates proliferation of MECs. It has been demonstrated that MECs proliferation levels in gestant RANKL-null mammary glands are restored after implantation of RANKL pellets *in vivo* (Fata et al. 2000). In addition, induced expression of RANKL in the mammary epithelium of PR-null mice rescues the lack of ductal side-branching and alveologenesis observed in those mice (Mukherjee et al. 2010).

It has been demonstrated that PG induces RANKL expression specifically in hormone-sensing ER+ PR+ cells. These cells are located in the luminal epithelium near responder ER-PR- cells (Mulac-Jericevic et al. 2003; Fernandez-Valdivia et al. 2009). Importantly, two different mechanisms underlie the PG-induced mammary gland proliferation: direct and indirect (Beleut et al. 2010). In the direct mechanism, PG binding to its receptor results in a fast CyclinD1 mediated cell proliferation, occurring 24h after the hormone stimuli. Indirect mechanism involves RANKL signaling and occurs 72h after the hormone stimuli. Thus, PG induces RANKL expression in PR+ cells. RANKL, by paracrine signaling binds to RANK in ER -PR- cells, inducing CyclinD1 expression and proliferation of these cells (figure 5). RANKL is also required for PG-induced proliferation in human mammary gland epithelium (Tanos et al. 2013).

MaSCs enriched population do not express ER and PR (Cathrin Brisken and Duss 2007; Joshi et al. 2010). This population is located in the mammary basal compartment and shows an 11-fold increase at mid-pregnancy compared to virgin glands, indicating that MaSC enriched population is highly responsive to hormones. Moreover, MaSC population significantly decreases in mice after ovaries removal (ovarectomization) (Asselin-Labat et al. 2010; Joshi et al. 2010).

RANK is expressed in luminal ER- PR- sensing cells, and more abundantly in cells from the basal compartment (Asselin-Labat et al. 2010; Joshi et al. 2010). Importantly (MMTV)-Cre rank $^{flox/\Delta}$ mice, with specific deletion of RANK in MECs, do not show an expansion in the basal CD24+CD49fhi population after medroxiprogesterone (MPA) treatment, a PG synthetic derivate, indicating that RANK/RANKL system mediates proliferation in the basal compartment (Schramek et al. 2010). RANK signaling inhibition with RANK-Fc, a competitive inhibitor of RANKL, results in significantly impaired clonogenic ability in MaSC enriched subpopulation (Asselin-Labat et al. 2010). Thus, RANKL derived from luminal ER+ PR+ cells is likely to induce an increase in the MaCS pool by paracrine signaling through RANK.

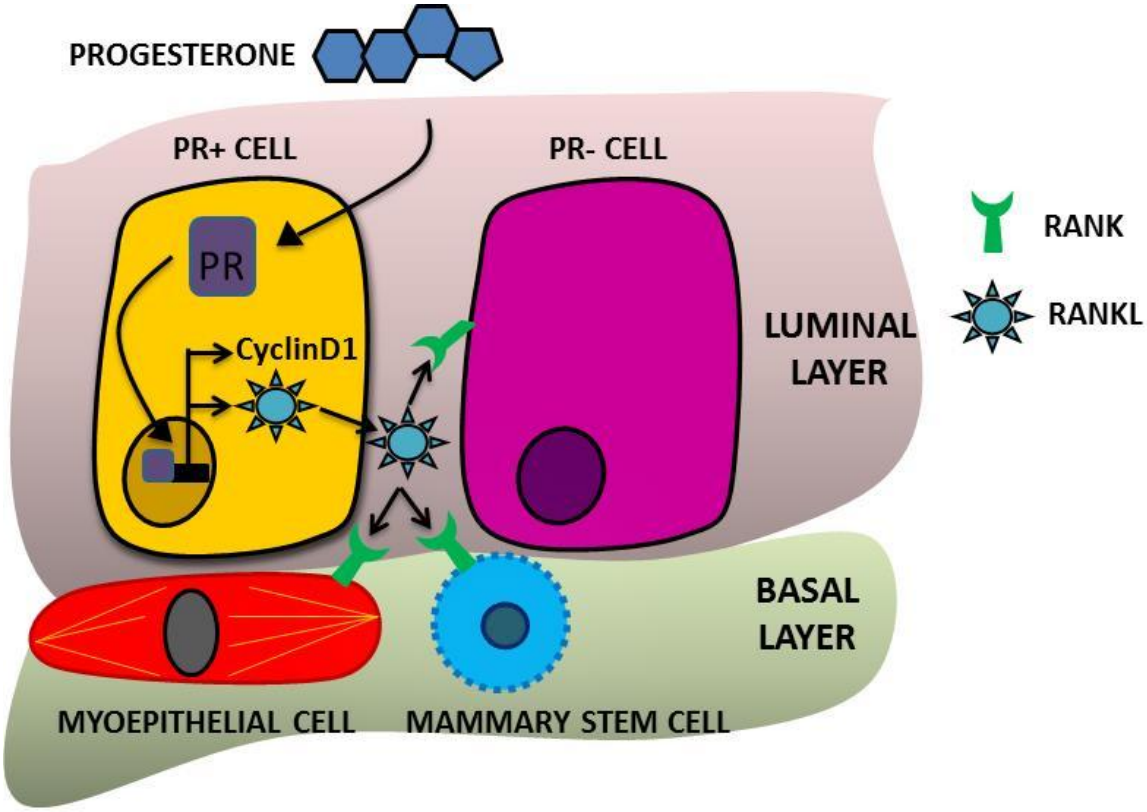

Figure 4: Schematic model of PR-RANKL signaling. Paracrine signaling of RANKL under progesterone stimuli. Progesterone binds to PR in the cytoplasm of luminal hormone-sensing cell. PR translocates to the nucleus and activates the expression of its target genes such as CyclinD1 and RANKL. CyclinD1 induces the proliferation of luminal hormone-sensing cells. RANKL binds to it receptor RANK located in luminal PR- cells or cells from the basal layer (myoepithelial cells and mammary stem cells), and activates CyclinD1-mediated proliferation by paracrine signaling.

3.4.2. RANK/RANKL in mouse mammary tumorigenesis

Progesterone is not only essential for a proper mammary gland development, but also promotes mammary tumor formation. Ablation of PR in mice results in a significantly reduced incidence of mammary tumors in response to carcinogen, compared to that observed in WT (Lydon et al. 1999; Soyal et al. 2002). In addition, organ cultures of PR-null glands show a failure to develop mammary pre-neoplastic lesions after *in vitro* exposure to chemical carcinogens (Chatterton et al. 2002). These observations highlight a specific role of PR as a crucial regulator of the intracellular signaling pathways responsible of the promotion of mammary tumorigenesis.

Fata el al demonstrated that RANK/RANKL signaling pathway promotes both survival and proliferation of mammary epithelia during pregnancy (Fata et al. 2000). Mid- to late pregnant (G.16,5) MMTV-RANK primary MECs cultured *in vitro* in 3D cultures show increased proliferation but also loss of milk secretion when treated with exogenous RANKL (Gonzalez-Suarez et al. 2007). In addition, an impaired apicobasal cell polarization and lumen formation have also been described in those MMTV-RANK MECs as a result of a defective apoptosis of cells from the luminal compartment (Gonzalez-Suarez et al. 2010), pointing to additional deffects in differentiation and polarization.

Importantly, mammary glands from aged MMTV-RANK mice (C57Bl/6 background) under multiple pregnancies show spontaneous tumor development and a higher incidence of pre-neoplasias compared to WT mice (Gonzalez-Suarez et al. 2010). To characterize the role of RANK/RANKL pathway in hormone-induced mammary tumor formation, WT and MMTV-RANK young virgin mice were treated with combined MPA and the carcinogen 7,12-dimethylbenz[α]anthracene (DMBA) (Aldaz et al. 1996). MPA treatment can trigger an enormous induction of RANKL expression not only in ER+ PR+ luminal cells from nulliparous WT, but also in the epithelial component of pre-neoplastic lesions and MINs (Gonzalez-Suarez et al. 2010; Schramek et al. 2010). MMTV-RANK mice under MPA-DMBA treatment showed a markedly enhanced susceptibility and decreased latency to mammary tumor formation compared to WT mice (figure 6A). Mammary pre-neoplastic lesions were clearly more abundant in MMTV-RANK mammary tissues that in WT. Moreover, multiple carcinomas were frequently present in MMTV-RANK mammary glands in contrast with focal lesions in WT glands (Gonzalez-Suarez et al. 2010).

Importantly, inhibition of RANKL signaling after treatment with RANK-Fc not only decreases tumor incidence and increases tumor latency in MMTV-RANK mice under MPA-

DMBA treatment, but also prevents tumor formation in WT mice (figure 6B). Moreover, RANKL inhibition with RANK-Fc in mammary glands from tumor-bearing WT and MMTV-RANK mice significantly reduces the proliferative index of normal mammary epithelium and pre-neoplastic hyperplasias, and increases apoptosis in MINs and adenocarcinomas (Gonzalez-Suarez et al. 2010). Similarly, deletion of RANK in the mammary gland results in increased mammary tumor latency and a markedly enhanced mice survival after MPA-DMBA treatment (Schramek et al. 2010).

The impact of RANK pathway in MEC survival in response to DNA damage was further investigated by Schramek et.al. (Schramek et al. 2010). Indeed, MECs were treated with DNA-damaging agents doxorubicin or γ-irradiation, which induce the upregulation of several pro-apoptotic molecules. Interestingly, treatment with MPA or RANKL *in vivo* resulted in marked protection from cell death in those treated MECs. Conversely, loss of RANK expression on MECs abrogated the protective effects of MPA on γ-irradiation induced cell death.

In addition, the role of RANK pathway in mammary tumor formation has been investigated in MMTV-neu, a model that spontaneously develop mammary tumors without an exogenous hormone requirement (Guy, Cardiff, and Muller 1992). RANK expression increases during MMTV-neu tumor progression, suggesting that RANK signaling may also play a role in this model (Gonzalez-Suarez et al. 2010). RANKL is mostly detected in the surrounding stroma and its expression in MMTV-neu tumor cells is undetectable in accordance the loss of PR. Importantly, RANK-Fc treatment in MMTV-neu mice before tumor formation does not significantly affect tumor latency, but significantly reduces the total number of pre-neoplastic lesions and tumors, as well as the incidence and number of lung metastasis per mouse (Gonzalez-Suarez et al. 2010). Conversely, RANKL treatment significantly increases the incidence and multiplicity of lung metastasis in MMTV-neu mice (Tan et al. 2011).

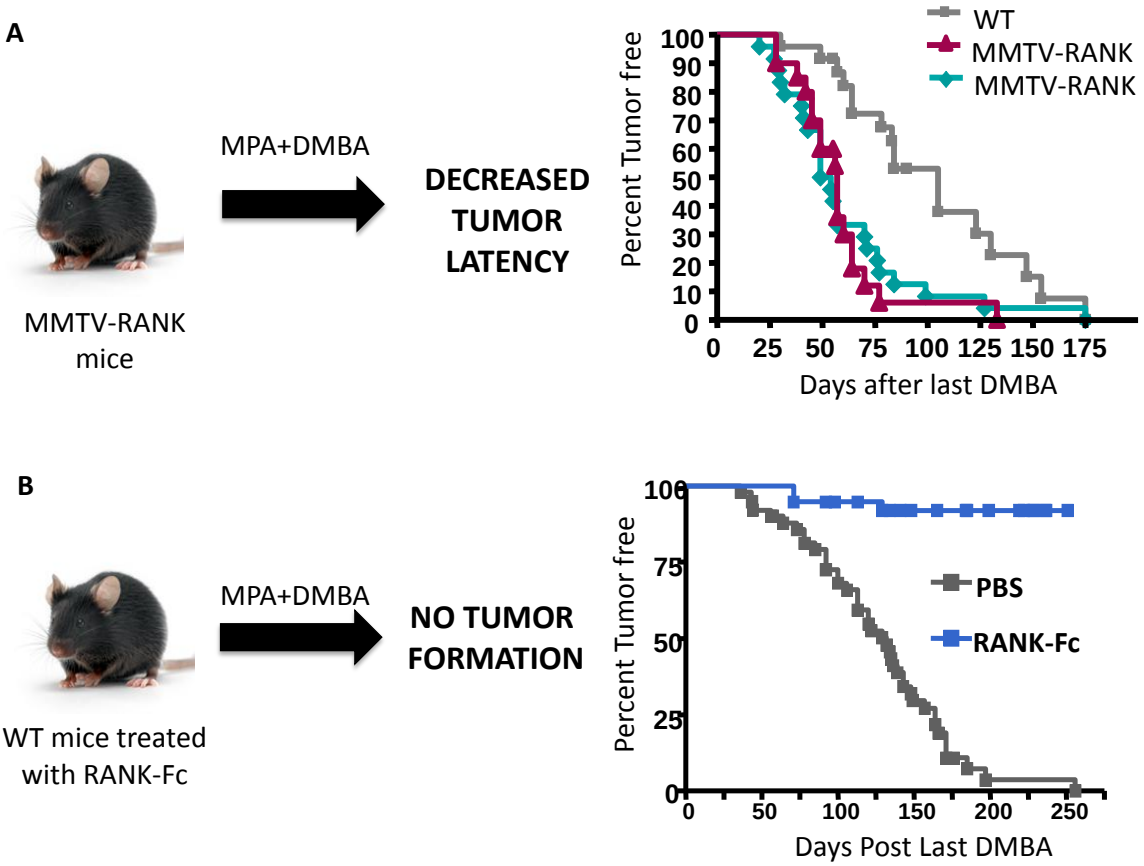

Figure 5: RANKL is the main mediator of the pro-tumorigenic effects of progesterone in the mammary gland. Schematic representation of Kaplan-Meyer curves of tumor latency. A. Tumor latency after MPA-DMBA treatment in WT mice and 2 different MMTV-RANK strains. B. Tumor latency after MPA-DMBA treatment in WT mice treated with RANK-Fc or PBS. (Adapted from Gonzalez-Suarez et.al. Nature 2010)

3.4.3. RANK/RANKL downstream signaling pathways

It has been recently shown that RANK overexpression in MCF10A human mammary gland epithelial cell line leads to constitutive activation of several pathways including NF-kB, PI3K-Akt and MAPK (Palafox et al. 2012). These signaling pathways downstream of RANK play a role in mammary gland development (Figure 6) (Gonzalez-Suarez et al. 2007; M. Liu et al. 2010; C.-C. Chen et al. 2012; Madrid et al. 2001; Whyte et al. 2009).

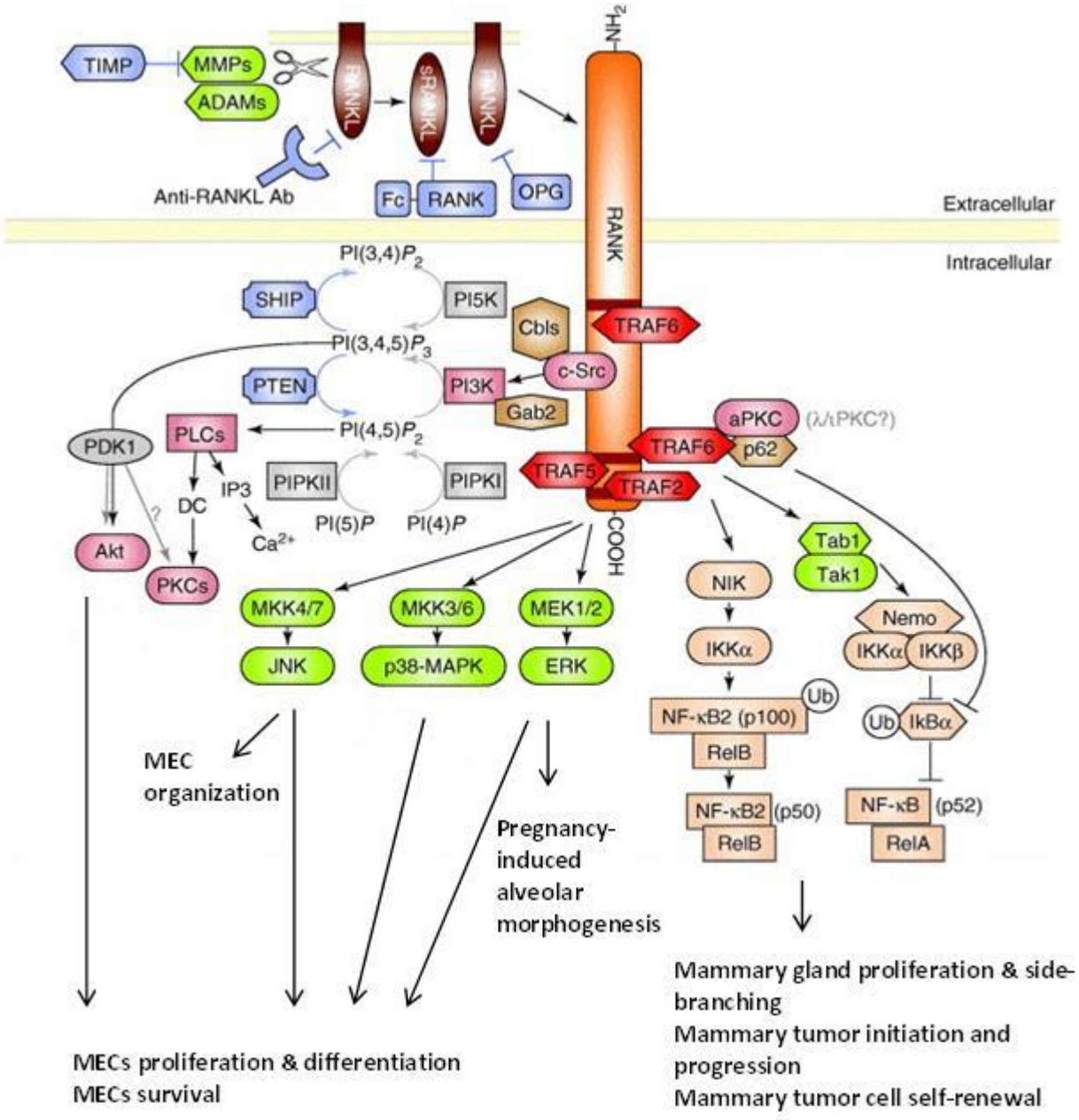

Figure 6: Signaling pathways activated downstream RANKL/RANK in osteoclasts and its major effects in mammary gland biology (Adapted from Wada et.al. TRENDS in Mol. Med. 2006).

3.4.3.1. NF-kB signaling pathway

NF-kB (Nuclear factor kappa-light-chain-enhancer of activated B cells) is a protein complex that plays a crucial role in various biological processes, including immune response, inflammation, cell growth and survival, and development (Hayden and Ghosh 2008; Vallabhapurapu and Karin 2009). Five NF-kB members exist in mammals including RelA (also named p65), RelB, c-Rel, NF-kB1 p50 and NF-kB2 p52 (Gilmore 2006). Distinct NF-kB complexes are formed from combinations of homo- and heterodimers of these family members that are retained in the cytoplasm by a family of NF-kB inhibitors, IKBs (IKB-α, β, ε) (Bonizzi and Karin 2004). NF-kB1 and NF-kB2 are produced as precursor proteins p105 and p100, respectively, and share structural homology with IkBs in their C-terminal portion (Sun and Ley 2008). Proteasome-mediated processing of p105 and p100 not only produces the mature NF-kB1 and NF-kB2 proteins (p50 and p52) but also results in disruption of the IkB-like function of these precursor proteins (Sun and Ley 2008).

Two main NF-κB-activating pathways exist in cells, canonical and alternative or non-canonical. The most common mechanism of regulation of NF-kB activity is through the canonical pathway, where IKK complex (IKKα-β) is activated by stimuli such as TNF-α or lipopolysaccharides (LPS). Activated p-IKK phosphorylates IKBα inhibitor protein resulting in its ubiquitination and degradation, and subsequent release of the p65-p50 heterodimer for activation and nuclear translocation (Karin 1999). The activation of the pathway promotes inflammation, cell survival and proliferation (Gerondakis et al. 2014). On the other hand, in the non-canonical NF-kB pathway specific members of the TNF cytokine family, such as CD40 or BAFF promote IKK-α phosphorylation by NIK. P-IKK-α in turn phosphorylates the p100 precursor of p52 to generate p52/RelB heterodimers. These heterodimers have affinity for a subset of NF-kB response elements and generate a distinctive gene expression pattern in the nucleus, which favors chemokine production and lymphoid stroma survival (Perkins 2007; Gerondakis et al. 2014).

Importantly, NF-kB pathway plays an essential role in mammary gland proliferation and side-branching during the post-natal development. Deletion of IKK-α in IKK-$\alpha^{AA/AA}$ ‘‘knockin’’ mice results in a severe lactation defect due to impaired MEC proliferation, similar than RANK-null mammary glands (Y. Cao et al. 2001). Moreover, activation of NF-kB signaling pathway impairs mammary alveolar secretory differentiation by a negative crosstalk between NF-kB and the PrlR/Jak2/Stat5, which occurs at the level of Stat5 tyrosine phosphorylation (Geymayer and Doppler 2000).

NF-kB signaling pathway is involved in the initiation and progression of breast cancer. Indeed, despite the high heterogeneity found between the different human breast tumor subtypes, an aberrant NF-kB becomes a common molecular feature among them (Sovak et al. 1999). Moreover, MPA-DMBA induced mammary adenocarcinomas in RANK-null mice had impaired activation of the NF-kB pathway (Schramek et al. 2010). In addition, NF-Kb pathway contributes to self-renewal of mammary tumor cells. Blockage of NF-kB activity leads to a decrease in tumor formation ability and reduces mammosphere growth in anchorage-independent conditions *in vitro* in MMTV-neu mice (Yixue Cao, Luo, and Karin 2007).

3.4.3.2. PI3K-AKT signaling pathway

PI3K-AKT signaling pathway regulates multiple biological processes such as apoptosis, metabolism, cell proliferation and cell growth (Carnero et al. 2008). When PI3K is activated by receptor tyrosine kinases, it phosphorylates PIP2 (phosphatidylinositol biphosphate) to generate PIP3 (phosphatidylinositol triphosphate), and activate the downstream AKT. AKT is expressed during mammary gland development, and its expression decreases at the onset of involution (Schwertfeger, Richert, and Anderson 2001).

Interestingly, AKT modulates PrlR/JAK2/STAT5 pathway activity through upregulation of Id2, a positive regulator of the pathway, and downregulation of Caveolin-1 and SOCS2 (C.-C. Chen et al. 2010). Constitutive activation of AKT in the mammary epithelium (MMTV-AKT) promotes precocious lipid droplets accumulation during pregnancy and delays post-weaning mammary involution by inhibiting apoptosis (Schwertfeger, Richert, and Anderson 2001; C.-C. Chen et al. 2010). In addition, PI3K-AKT pathway is also a key intracellular signaling system that drives tumor cell growth and survival. Hyperactivation of this pathway is implicated in the tumorigenesis in ER+ breast cancer and resistance to endocrine therapy (Ciruelos Gil 2014)

3.4.3.3. MAPK signaling pathway

The mitogen activated protein kinases (MAPK) signaling pathway acts as a molecular mediator of the intracellular signal transduction. Extracellular regulated kinase (ERK), the p38 pathway and JNK MAPK intracellular signaling cascades are active in proliferating

MECs, and implicated in breast cancer disease. Considering ERK signaling, the small GTPase Ras activates a set of MAPKs that finally activate ERK (Krishna and Narang 2008). In its active form, ERK phosphorylates a wide range of protein substrates that regulate MEC proliferation, differentiation and survival (Pearson et al. 2001). It has been shown that activation of ERK signaling pathway is required for pubertal ductal morphogenesis and pregnancy-induced alveolar morphogenesis (Whyte et al. 2009). In addition, ERK signaling plays a relevant role in breast cancer, enhancing tumor cell proliferation and invasiveness, preventing apoptosis and inducing resistance to tamoxifen (Whyte et al. 2009; McCubrey et al. 2007).

The p38 signaling pathway, which is activated by MAPK in response to stress signals or inflammatory cytokines, plays important roles in cell differentiation and apoptosis (Raingeaud et al. 1995; Hui et al. 2007). In addition, several studies reveal that activation of p38 signaling not only contributes to breast cancer cell progression, invasion and metastasis, but also in the resistance to tamoxifen in HER2+ breast tumors (Han et al. 2002; Galliher and Schiemann 2007; Gutierrez et al. 2005).

The c-Jun NH_2-terminal kinases (JNK), also known as stress-activated MAP kinases (SAPK), represent a third subgroup of MAPK that is activated by cytokines and exposure to environmental stress (Davis 2000). JNK phosphorylates c-Jun leading to activation of AP-1, which promotes cell proliferation (Jochum, Passegué, and Wagner 2001). In addition, JNK action has been reported to contribute to the normal MEC organization during acinus development. Indeed, inhibition of JNK action during acinus formation blocks the establishment of cell polarization, the formation of tight junctions and the lumen clearance (Murtagh, Martin, and Gronostajski 2003). JNK also contributes to mammary tumor cell proliferation, evidenced by the tumor cell cycle arrest in human breast cancer cell lines under inhibition of JNK signaling (Mingo-Sion et al. 2004).

OBJECTIVES

OBJECTIVES

The main objectives of this PhD thesis are as follows:

- Characterize the role of RANK signaling in mammary stem cell fate.
- Characterize the role of RANK in mammary alveolar cell differentiation during pregnancy.
- Investigate the cooperation of RANK signaling pathway with oncogenes using spontaneous tumor prone mouse models MMTV-PYMT and MMTV-neu.
- Analyze the role of RANK regulating the mammary Cancer Stem Cell (CSC) pool.

RESULTS

I hereby certify that the PhD student **ÀLEX CORDERO CASANOVAS** will present his thesis as a compendium of five publications. His contribution to each work is as follows:

ARTICLE 1: Pellegrini P*, **Cordero A***, Gallego MI, Dougall WC, Muñoz P, Pujana MA and Gonzalez-Suarez E.

* contributed equally

TITLE: "Constitutive activation of RANK in the mammary gland disrupts mammary cell fate leading to tumorigenesis".

JOURNAL: Stem Cells. 2013 Sep;31(9):1954-65. (Impact factor: 7,133)

Authors Pasquale Pellegrini and Alex Cordero Casanovas equally contributed to this study. Alex Cordero characterized the amplification of the mammary epithelium in MMTV-RANK model by whole mount analysis and cytokeratin quantification; Pasquale Pellegrini characterized the abnormalities in the cytokeratin distribution within the mammary epithelium. Afterwards both authors characterized mammary progenitor enriched populations by flow cytometry, and the functional activity of mammary progenitors using colony forming assays *in-vitro* and mammary repopulation assays *in-vivo*. Alex Cordero focused on the characterization of the MMTV-RANK driven tumorigenesis analyzing tumor histological heterogeneity and distribution of epithelial surface markers by flow citometry. Pasquale Pellegrini evaluated the impact of RANK signaling in physiological conditions by characterizing the correlation between RANK expression and accumulation of mammary progenitors in aged WT mammary glands and in WT tumors.

ARTICLE 2: Cordero A*, Pellegrini P*, Sanz-Moreno A, Trinidad EM, Serra-Musach J, Deshpande C, Dougall WC, Pujana MA and Gonzalez-Suarez E.

* contributed equally

TITLE: "RANKL impairs lactogenic differentiation through inhibition of the prolactin/Stat5 pathway".

JOURNAL: Under revision in Stem Cells, 2015. (Impact factor (2014): 6,523)

Authors Alex Cordero Casanovas and Pasquale Pellegrini equally contributed to this study. Pasquale Pellegrini focused on the treatment and evaluation of the RANKL pharmacological inhibition with RANK-Fc in WT mammary glands at different gestational timepoints. Pasquale Pellegrini also analyzed Elf5 expression by immunohistochemistry in those WT-treated glands. Alex Cordero focused on the study of both the PrlR/STAT5/Elf5 and NF-kB signaling pathways in virgin and gestant WT and MMTV-RANK mammary glands, as well as in WT RANK-Fc-treated glands, by qRT-PCR, western blot and immunohistochemistry. Alex Cordero also performed 3D cultures analysis of mammary epithelial cells from WT and MMTV-RANK at midgestation.

ARTICLE 3: Cordero A, Sanz-Moreno A, Yoldi G, and Gonzalez-Suarez E.

TITLE: "RANK overexpression delays mammary tumor formation in oncogene-driven NEU and PYMT mouse models but in turn contributes to tumor aggressiveness through Cancer Stem Cell enrichment"

JOURNAL: Manuscript in preparation

In this article Alex Cordero was responsible for generating all the results included in the current draft and participated in the writing of the manuscript.

ARTICLE 4: Pellegrini P*, Yoldi G*, Trinidad EM*, **Cordero A**, Gomez-Miragaya J, Serra-Musach J, Dougall WC, Muñoz P, Pujana MA, Planelles L and González-Suarez E.

* contributed equally

TITLE: "Therapeutic inhibition of RANK signaling reduces breast cancer recurrence by inducing tumor cell differentiation"

JOURNAL: Manuscript submitted

In this paper Alex Cordero contributed to the firsts steps of MMTV-PyMT;$RANK^{-/-}$ mouse model generation and performed MECs 3D cultures experiments and tumor initiating cell Limiting Dilution Assays (LDA) for MMTV-PyMT;$RANK^{-/-}$ mice in collaboration with Pasquale Pellegrini and Guillermo Yoldi. Alex Cordero also performed population analyses by Flow citometry (FACS) and analysis of the results in Diva software.

ARTICLE 5: García-Castro A, Zonca M, Florindo-Pinheiro D, Carvalho-Pinto CE, **Cordero A**, Gutiérrez del Fernando B, García-Grande A, Mañes S, Hahne M, González-Suárez E and Planelles L.

TITLE: "APRIL promotes breast tumor growth and metastasis and is associated with aggressive basal breast cancer"

JOURNAL: Carcinogenesis. 2015 May;36(5):574-84. (Impact factor 5,334)

In this paper Alex Cordero selected Luminal, Triple Negative Breast Cancer and HER2+ human breast tumors from a wide collection of human tumor samples from the University Hospital of Bellvitge (Barcelona). Alex Cordero designed primer sequences for hAPRIL, hTACI and hBCMA, performed qRT-PCR analysis for human APRIL, TACI and BCMA on tumor samples and analyzed the results.

In witness whereof, I hereby sign this in Hospitalet de Llobregat,

Barcelona, September 1st, 2015

Eva González Suárez, Ph.D

Metastasis and Transformation Group, Leader

Cancer Epigenetics and Biology Programme (PEBC)

Bellvitge Biomedical Research Institute (IDIBELL)

Avda. Gran Via 199-203

08908 L'Hospitalet de llobregat, Barcelona, Spain

(p) +34 932607500 ext. 3171

(f) +34 932607219

(e) egsuarez@idibell.cat

ARTICLE 1

"Constitutive activation of RANK in the mammary gland disrupts mammary cell fate leading to tumorigenesis"

STEM CELLS®

TISSUE-SPECIFIC STEM CELLS

Constitutive Activation of RANK Disrupts Mammary Cell Fate Leading to Tumorigenesis

PELLEGRINI PASQUALE,[a] CORDERO ALEX,[a] GALLEGO MARTA INES,[b] DOUGALL C. WILLIAM,[c] MUÑOZ PURIFICACIÓN,[a] PUJANA MIGUEL ANGEL,[d] GONZALEZ–SUAREZ EVA[a]

[a]Cancer Epigenetics and Biology Program, Bellvitge Biomedical Research Institute, IDIBELL, Barcelona, Spain; [b]Laboratory of Mammary Pathology, UFIEC, Instituto de Salud Carlos III, Majadahonda, Madrid, Spain; [c]Therapeutic Innovation Unit, Amgen, Inc., Seattle, Washington, USA; [d]Translational Research Laboratory, Breast Cancer Unit, Catalan Institute of Oncology, Bellvitge Biomedical Research Institute, IDIBELL, Barcelona, Spain

Key words: RANK • CD61 • Mammary stem cell fate • Bipotent progenitors • Breast adenocarcinomas

ABSTRACT

Receptor Activator of NF-kappa B (RANK) pathway controls mammary gland development in mice but its role in mammary stem cell fate remains undefined. We show that constitutive RANK signaling expands luminal and basal mammary compartments including mammary stem and luminal progenitor cell pools and interferes with the generation of CD61+ and Sca1+ luminal cells and *Elf5* expression. Impaired mammary cell commitment upon RANK overexpression leads to the accumulation of progenitors including K14+K8+ bipotent cells and the formation of heterogeneous tumors containing hyperplastic basal, luminal, and progenitor cells. *RANK* expression increases in wild-type mammary epithelia with age and parity, and spontaneous preneoplastic lesions express RANK and accumulate K14+K8+ cells. In human breast tumors, high *RANK* expression levels are also associated with altered mammary differentiation. These results suggest that increased RANK signaling interferes with mammary cell commitment, contributing to breast carcinogenesis. STEM CELLS *2013;31:1954-1965*

Disclosure of potential conflicts of interest is found at the end of this article.

INTRODUCTION

The mouse mammary epithelium consists of a branched ductal system that develops mainly during puberty and a lobuloalveolar compartment containing secretory epithelial cells that undergo functional differentiation and become milk-producing during pregnancy. Mammary epithelial cells can be organized in two main compartments, luminal and basal. Expression of hormone receptors (estrogen and progesterone receptors, ER and PR, respectively) is confined to the mature luminal cells that are characterized as being CD24high (hi) CD49flow (lo) Sca1+, whereas CD24hi CD49flo Sca1− cells are largely ER− progenitors [1] and contain the CD61+ luminal progenitors that establish the alveolar lineage during pregnancy [2,3]. The basal compartment, identified by the expression of CD24lo CD49fhi Sca1− CD61+, is mainly composed of contractile myoepithelial cells that surround ducts and alveoli and contains the population of mammary stem cells (MaSCs) identified by their ability to reconstitute an entire functional mammary gland [4–6]. Several cytokeratins are lineage markers within the mouse mammary epithelium: K5 and K14 mark basal/myoepithelial cells and are strongly expressed in MaSC, whereas K8/K18 expression marks luminal cells [7]. A hierarchical organization of mammary epithelia, in which MaSC give rise to differentiated cell types via a series of multipotent and lineage-restricted intermediates has been proposed [8].

MaSC and intermediate progenitors have been postulated as the cells of origin of tumors, as their long lifespan might allow them to accumulate enough genetic lesions to generate a tumor [9]. The observed expansion of MaSC and other progenitor populations with each round of pregnancy and estrous cycles [10,11] provides a potential mechanistic explanation for age and parity as risk factors for the development of mammary tumors [12].

RANK and its ligand, RANKL, are key regulators of mammary gland development [13,14]. The RANK signaling pathway mediates the major proliferative response of mouse mammary epithelium to progesterone during morphogenesis [10,11,15].

Disrupted mammary gland development during pregnancy and impaired lactation is observed as a consequence of RANK loss or overexpression [13,14]. Defective

Author contributions. P.P.: collection and/or assembly of data, data analysis and interpretation, final approval of manuscript; A.C.: collection and/or assembly of data; data analysis and interpretation; final approval of manuscript; M.I.G. and W.C.D: provision of study material, revisions of manuscript, final approval of manuscript; P.M.: revisions of manuscript, final approval of manuscript; P.A.M.: data analysis and interpretation, revisions of manuscript, final approval of manuscript; E.G.-S.: conception and design, financial support, collection and/or assembly of data, data analysis and interpretation, manuscript writing, and final approval of manuscript. PP and AC contributed equally to this work.

Correspondence: González-Suárez Eva, Ph.D., Cancer Epigenetics and Biology Program, Bellvitge Biomedical Research Institute, IDIBELL, Gran Via 199, L'Hospitalet de Llobregat, Barcelona 08908, Spain. Telephone: +34–932607253; Fax: +34–932607219; e-mail: egsuarez@idibell.cat Received January 23, 2013; accepted for publication May 8, 2013; first published online in STEM CELLS *EXPRESS* June 14, 2013. 1066-5099/2013/$30.00/0 doi: 10.1002/stem.1454

alveologenesis in RANK-null mice could be attributed to decreased proliferation and survival of mammary epithelial cells [13], whereas mouse mammary tumor virus (MMTV)-RANK mice show high mammary epithelial cell proliferation during pregnancy [14], pointing to a defect in differentiation. We have recently shown that activation of RANK signaling promotes mammary tumorigenesis in mice [16] and that RANK overexpression in human mammary cell lines induces stemness and promotes tumorigenesis and metastasis [17].

Here, we investigated the role of RANK signaling in MaSC fate and found that activation of RANK signaling expands basal and luminal compartments disrupting mammary lineage commitment, and results in the accumulation of intermediate progenitor cells, eventually leading to hyperplasia and tumorigenesis.

Materials and Methods

Mice

All research involving animals was performed at the IDIBELL animal facility and complied with protocols approved by the IDIBELL Committee on Animal Care. For cell proliferation analysis, 5-bromo-2′-deoxyuridine (BrdU, 30 mg/kg of mouse) was injected intraperitoneally 2 hours before killing.

Mammary Cell Isolation

Single cells were isolated from tumors and the mammary glands of virgin young (12–15 weeks), old (31–81 weeks), or pregnant mice, as described previously [18]. Briefly, fresh tissues were mechanically cutted with McIlwain tissue chopper and enzymatically digested with appropriate medium (Dulbecco's modified Eagle's medium [DMEM] F-12, 0.3% Collagenase A, 2.5U/mL dispase, 20 mM HEPES, and antibiotics) 40 minutes at 37°C. Samples were washed with Leibowitz L15 medium+10% fetal bovine serum (FBS) between each step. Erythrocytes were eliminated by treating samples with hypotonic lysis buffer and fibroblasts were excluded by incubation with DMEM F-12 + 10% FBS 1 hour at 37°C in a tissue culture flask (the majority of fibroblasts attach to the tissue culture plastic while most of epithelial organoids do not). Single epithelial cells were isolated by treating with trypsin (PAA Laboratories, Velizy-Villacoublay, France, http://www.paa.com) 2 minutes at 37°C and a mix of dispase (Gibco life technologies, Invitrogen Saint Aubin, France, http://www.invitrogen.com) DNAse (Invitrogen Saint Aubin, France, http://www.invitrogen.com) 5 minutes 37°C. Cell aggregates were removed by filtering cell suspension with 40 μm filter and counted.

Flow Cytometry

Single cells were labeled with antibodies against CD24-PE or CD24-FITC (M1/69 BD Pharmingen, San Diego, CA, http://www.bdbiosciences.com), CD29-FITC (HMβ1-1, BD Pharmingen), CD49f-APC (GoH3 R&D systems, Minneapolis, MN US, www.rndsystems.com), CD61-FITC or CD61-PE (2C9.G2 BD Pharmingen), Sca-1-PE or Sca1-APC (Ly-6A/E, BD Pharmingen), and CD49b-alexa 647 (HMα2 Biolegend, San Diego, CA, http://www.biolegend.com). Lymphocytes and endothelial cells were excluded in flow cytometry using CD45-PECy7 (30-F11 Biolegend) and CD31-PECy7 (390 Biolegend) antibodies, respectively. A population of 10,000 live cells was captured in all fluorescence-activated cell sorting (FACS) experiments. FACS analysis was performed using FACS Canto (Becton Dickinson, San Jose, CA) and Diva software package. Cell sorting was performed using FACS Aria cell sorter (BD Becton Dickinson, San Jose, CA).

Colony Forming Assays and Immunofluorescence

For colony-forming assays, sorted cells were plated as described previously [6] in growth medium that contains B27, 5% FBS, EGF (10 ng/mL), Hydrocortisone 0.5 μg/mL, Insulin 5 μg/mL, Cholera toxin 100 ng/mL, and penicillin/streptomycin and RANKL (1 μg/mL; Amgen Inc, Thousand Oaks, CA, USA, http://www.amgen.com) as indicated. ROCK inhibitor (10 μM Y-27632, Sigma Aldrich, Saint-Quentin Fallavier, http://www.sigmaaldrich.com/france) was added to basal cell cultures. After 15 days of culture, colonies were fixed with paraformaldehyde (PFA) 2% for keratins staining. K5 and K8 immunostaining on three-dimensional cultures was performed following standard procedures [19].

Cleared Fat Pad Transplantation

Primary mammary epithelial cells were freshly isolated from mouse mammary glands, sorted based on CD24 CD49f/Sca1 values and resuspended in Leibowitz L15 medium (Invitrogen) with 10% FBS and antibiotics, diluted 1:1 with Matrigel Matrix (BD Biosciences, San Diego, CA, http://www.bdbiosciences.com) for a final volume of 20–30 μL and CD24lo/CD49fhi cells were injected at limiting dilution in cleared mammary fat pads of 3–4 weeks old FVB mice. After 8 weeks, the transplanted fat pads were whole-mounted and carmine-stained. Outgrowths filling at least 25% of fat pat were scored. The proportion of stem/progenitor cells was determined using the Extreme Limiting Dilution Analysis (http://bioinf.wehi.edu.au/software/elda/).

Tissue Section Histology and Immunostaining

Mammary glands and tumors were fixed in 4% PFA or formalin and embedded in paraffin. For histological analysis, 3 μm sections were cut and stained with hematoxylin and eosin. Immunostaining was performed on 3 μm mammary gland/tumor sections. Antigen heat retrieval with citrate was used for all antibodies except for RANK (protease XXIV) and BrdU (protease XXIV and HCl 2 M) and primary antibodies were incubated overnight at 4°C. Antibodies used include RANK (AF692; R&D Systems), PR (A0098 Dako, Trappes, France, http://www.dako.fr), K5 (AF-138, Covance, Princeton, NJ, http://www.covance.com.), K14 (AF-64 Covance), K8 (TROMA, dshl, Developmental Studies Hybridoma Bank, Iowa City, Iowa), and SMA (1A4; A2547, Sigma), BrdU (G3G4, Kaufman laboratory; University of Illinois). The antigen–antibody complexes were detected with streptavidin horseradish peroxidase (Vector Laboratories, Burlingame, CA, USA, vector@vectorlabs.com) for RANK, K8 immunostainings. K5, K14, PR, and SMA were detected with EnVision technology (Dako, Trappes, France, http://www.dako.fr); BrdU was detected with labeled polymer-horse-radish peroxidase (DAKO). Peroxidase was finally revealed with 3,3-Diaminobenzidine DAB (DAKO). For immunofluorescence, opportune fluorochrome-conjugated secondary antibodies were added after primary incubation and then mounted with VECTASHIELD Mounting Media.

RNA Preparation and real time reverse transcription PCR

Total RNA of cells, mammary glands and tumors was prepared with Tripure Isolation Reagent (Roche, Basel, Switzerland, http://www.roche.ch/en/standorte/basel-hq.htm) in accordance with the manufacturer's instructions. After tissue dissociation, 20 ng/mL of messenger RNA (mRNA) or similar cell numbers were pretreated with DNase I (Ambion Invitrogen Saint Aubin, France, http://www.invitrogen.com). Single-stranded complementary DNA was produced by reverse transcription using 1 μg of RNA DNA-free in a 20-μL reaction (Applied Biosystems, Foster City, CA, http://www.appliedbiosystems.com). Quantitative polymerase chain reaction (PCR) was performed using the TaqMan probe-based system (Applied Biosystems) on the ABI 7900HT as per the manufacturer's instructions (Applied Biosystems; rank Mm00437135_m1, rankl Mm00441908_m1, wap Mm00839913_m1, k8

Mm00835759_m1, K14 Mm00516876_m1, elf5 Mm00468732_m1, slug Mm00441531_ m1, sox9 Mm00448840_m1).

Gene Set Enrichment Analysis (GSEA) Analyses

The GSEA tool was run using default values for all parameters. Preprocessed and normalized The Cancer Genome Atlas (TCGA) data were downloaded from the corresponding repository (version July 3, 2012; http://tcga-data.nci.nih.gov/tcga/tcgaHome2.jsp). Samples were clustered based on the expression of the 50 genes/probes from PAM50 and assigned to the intrinsic subtypes basal-like, HER2-enriched, luminal A, luminal B, or normal-like, based on a comparison with the PAM50 centroids [20]. The PAM50 confidence scores were >0.90 for all the basal-like and luminal A tumors except for two cases in each subtype. The GSEA leading edges were analyzed for enrichment in pathways annotated by the Kyoto Encyclopedia of Genes and Genomes (KEGG) using the Database for Annotation, Visualization and Integrated Discovery (DAVID) [21]. Only pathways over-represented at a false discovery rate <5% between the leading edge and the rest of the corresponding gene set were considered.

Statistical Analyses

Statistical analysis of the differences between two mouse cohorts or conditions was performed with a two-tailed Student's *t*-test. We used Microsoft Excell or GraphPad Prism software for calculations and expressed the results as the means ± SD. To calculate the significance of differences affecting several variables a multivariate analysis of variance (MANOVA) test has been carried out. The null hypothesis is that all the tumors are identical in all variables.

RESULTS

RANK Overexpression Results in Morphologically Aberrant Ducts that Contain Dual Positive K5/K8 Cells

As we have shown that RANK induces stemness in human mammary epithelial cell lines [17], we hypothesize that increased levels of RANK may alter the balance in mammary differentiated/progenitor cell populations. To evaluate this hypothesis, we used our previously generated MMTV-RANK mouse model [14] backcrossed to the FVB background, most commonly used in mammary studies (Supporting Information Fig. S1A). RANK overexpression in mammary epithelia led to constitutive activation of RANK pathway [14], resulting in mammary epithelial cell hyper-proliferation (Supporting Information Fig. S1D, S1E), impaired secretory alveologenesis and absence of *Wap* milk protein expression during pregnancy (Supporting Information Fig. S1B, S1C). These phenotypes led to a lactation failure that could not be rescued by multiple pregnancies in correlation with previous results [14]. Increased epithelial growth, enhanced ductal side-branching, and appearance of precocious small alveoli were observed in virgin MMTV-RANK glands (Fig. 1A; S1B) together with increased expression of basal, *K14*, and luminal, *K8*, mRNA markers as compared with wild type (WT) (Fig. 1B). Double immunofluorescence (IF) analyses of K5 and K8 (Fig. 1C) revealed frequent alterations within the basal and luminal compartments in young virgin MMTV-RANK glands. First, MMTV-RANK ducts often contained disorganized myoepithelium, occasionally with K5 cells that accumulate in several layers, areas lacking K5 expression in the outer layer or K5 cells localized within the luminal area, surrounded by K8+ cells. Second, accumulation of multiple layers of K8+ cells was noted in most young MMTV-RANK glands resulting in minimal luminal space or filled ducts (Fig. 1C, 1D). By contrast, in WT ducts, basal/myoepithelial K5 cells were well aligned and normally organized and a single layer of K8+ cells was detected. K14 and K5 showed similar staining patterns in the mammary glands of young WT and MMTV-RANK virgin glands; thus, K14 and K8 IF revealed similar phenotypes than K5 and K8 IF (data not shown). Additionally, both K5/K8 and K14/K8 double positive cells, which have been proposed as bipotent progenitors blocked in differentiation [22,23], were more common in MMTV-RANK ducts than in WT ducts (Fig. 1C, 1E). These observations demonstrate that enhanced activation of RANK signaling disrupts basal/luminal epithelial morphology resulting in aberrant ducts containing a hyperplastic luminal layer, a disorganized basal layer and expansion of dual positive K5/K8 (or K14/K8) cells, described as bipotent mammary progenitors.

RANK Overexpression Interferes with MaSC Fate in the Basal and Luminal Compartment

Given the disrupted mammary epithelia observed in MMTV-RANK glands, we next investigated whether RANK overexpression leads to alterations in mammary cell populations in virgin mice. Quantitative expression analysis (real time reverse transcriptase PCR [RT-qPCR]) of *Rank* in fluorescence-activated cell sorting (FACS)-sorted WT and MMTV-RANK mammary populations demonstrated that MMTV promoter directs *Rank* expression to basal (B: CD24lo CD49fhi) and luminal (L: CD24hi CD49flo) cells, both Sca1+ (LM: luminal mature) and Sca1− (LP: luminal progenitor enriched) fractions (Supporting Information Fig. S2A). FACS analyses of freshly isolated epithelial cells revealed a two fold increase in basal and 1.6-fold increase in luminal populations in MMTV-RANK as compared to WT mammary glands (Fig. 2A, 2B), in agreement with the abundant epithelia and increased expression of *K14* and *K8* markers observed (Fig. 1A, 1B). These findings further indicate that *Rank* overexpression under the MMTV promoter, induces an expansion of the mammary basal and luminal compartments. We next analyzed Sca1, CD61, and CD49b lineage markers expression to discriminate mammary subpopulations [1,2,24,25]. The distribution of Sca1+ and Sca1− cells was altered in MMTV-RANK luminal cells (Fig. 2A, 2B): in five of seven MMTV-RANK mice analyzed, there was a significant lower Sca1+ cell population within the luminal fraction compared with WT controls (Supporting Information Fig. S2B). Consistent with the known association between Sca1 and hormone receptor expression [1], the frequency of PR+ cells (detected by IHC analyses) was reduced in three of seven virgin MMTV-RANK mammary glands analyzed, compared to control glands (Fig. 2C). Thus, RANK overexpression results in a significant expansion of basal (CD24lo CD49fhi Sca1−) and luminal progenitor enriched (CD24hi CD49flo Sca1− PR−) compartments (Supporting Information Fig. S2C). The CD61+ luminal cells are contained in this latter fraction and are considered to be precursors of mature secretory alveolar cells [2]. A dramatic decline in the proportion of CD61+ cells was observed in the luminal fraction of MMTV-RANK compared with WT glands (Fig. 2A, 2B). The reduction in CD61 expression in MMTV-RANK luminal cells was corroborated by IF analysis of MMTV-RANK and WT virgin mammary glands (Fig. 2D). Moreover, MMTV-RANK glands contained more CD49bhi cells than WT glands (Fig. 2A, 2B). These findings demonstrate that RANK activation/overexpression disrupts the distribution of mammary populations in virgin glands.

To characterize the impaired alveolar differentiation that takes place in MMTV-RANK glands we analyzed the expression of lineage markers during pregnancy. The gestation

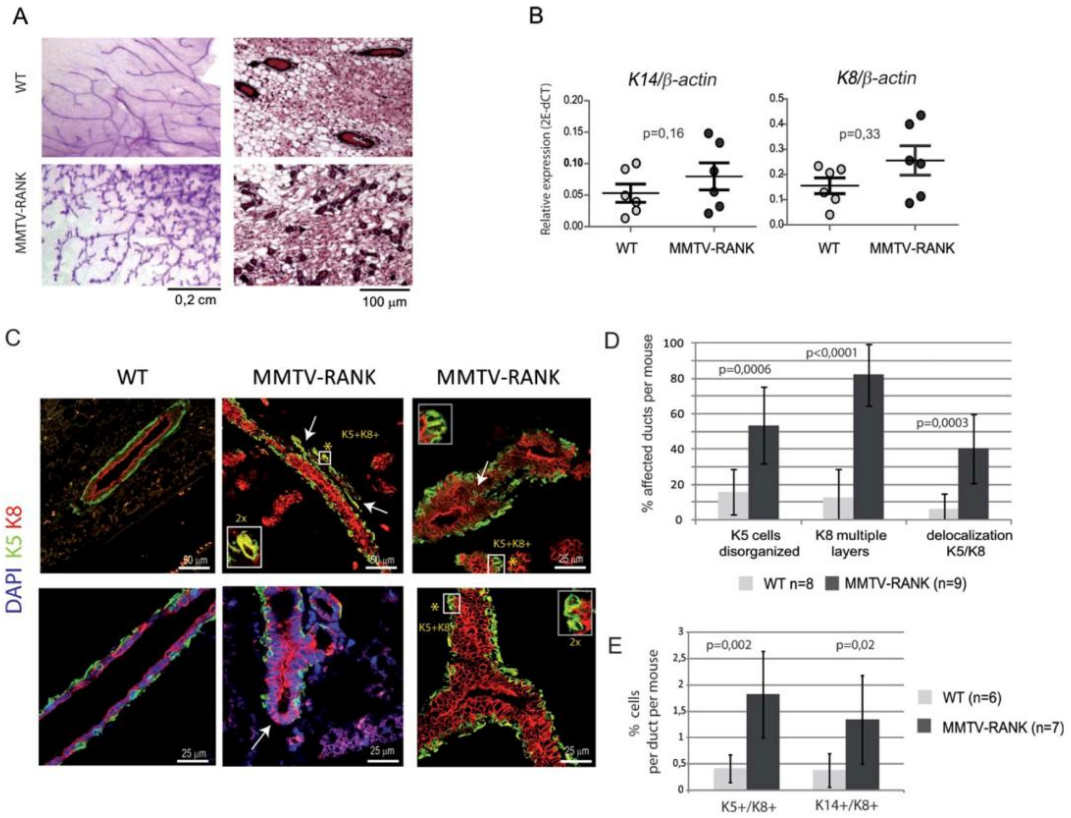

Figure 1. RANK overexpression disrupts epithelial morphology. See also Supporting Information Figure S1. **(A)**: Representative images of whole mounts and hematoxylin and eosin of virgin wild type (WT) and MMTV-RANK mammary glands. **(B)**: *K14* and *K8* messenger RNA expression relative to *β-actin* in the mammary glands of virgin WT and MMTV-RANK mice. Each dot represents one mouse. Mean, SEM, and *t*-test *p* values are shown. **(C)**: Representative images of K5 and K8 staining in mammary epithelia of virgin WT and MMTV-RANK mice (12–15 weeks old). Asterisks indicate double positive K5/K8 cells that are magnified in the insets. Arrows indicate other abnormalities including multilayer of K5+ cells, K5+ cell in the luminal area, or absence of K5 in the basal layer. **(D)**: Percentage of ducts per virgin mouse showing the indicated lesions. Between 5 and 7 ducts were analyzed per mouse. Mean, SD, and *t*-test *p* values are shown. Delocalization includes extra layer of K5+ cells, K5+ cells in the luminal area, and absence of K5 in the basal area as shown in C. **(E)**: Percentage of K5+/K8+ and K14+/K8+ cells versus total number of cells per duct in 12–15 weeks old virgin WT and MMTV-RANK mice. For each mouse, seven ducts were analyzed. Mean, SD, and *t*-test *p* values are shown. Abbreviations: DAPI, 4′6 Diamino-2-Phenylindole Dihydrochloride; MMTV-RANK, mouse mammary tumor virus-receptor activator of NF-kappa B; WT, wild type.

G14.5 WT glands contained fewer CD61+ cells in the luminal fraction than G10.5 or virgin WT glands, consistent with the differentiation of CD61+ luminal cells into alveolar mature secreting cells (Supporting Information Fig. S2D). In MMTV-RANK glands, the proportion of CD61+ in the luminal compartment was low at all time points (virgin, G10.5 and G14.5), despite the accumulation of luminal cells observed during pregnancy (Supporting Information Fig. S2D). Similarly, low levels of CD61+ luminal cells were observed in aged MMTV-RANK females, either virgin or multiparous (Supporting Information Fig. S2E). This dramatic reduction in the CD61+ alveolar progenitor population in MMTV-RANK glands would explain the lack of alveologenesis observed during pregnancy in these mice even after multiple pregnancies. The percentage of CD49bhi cells within the luminal population at G10.5 and G14.5 is significantly higher in MMTV-RANK than in WT glands suggesting that CD49bhi luminal cells accumulate in MMTV-RANK glands during pregnancy (Supporting Information Fig. S2D). Altogether these results demonstrate that RANK overexpression disrupts MaSC fate leading to unbalanced mammary epithelial cell populations in virgin and pregnant glands.

Activation of RANK Pathway Promotes MaSC and Luminal Progenitor Cell Activity

Given that RANK overexpression results in an expansion of the basal compartment, we investigated the impact on the MaSC contained in this population. Mammary transplantation assays into the cleared fat pad of FVB mice were used to test the repopulating ability of FACS-isolated basal cells (CD24lo CD49fhi) from virgin WT and MMTV-RANK mice. A 2.5-fold increase in the frequency of mammary repopulating units was found in assays using MMTV-RANK basal cells compared with WT cells (estimate 1/171 vs. 1/428, respectively, $p = 0.05$) (Fig. 3A), indicating that MMTV-RANK glands contain more MaSC than WT glands. Next, we tested the ability of basal WT and MMTV-RANK cells to form colonies in the presence or

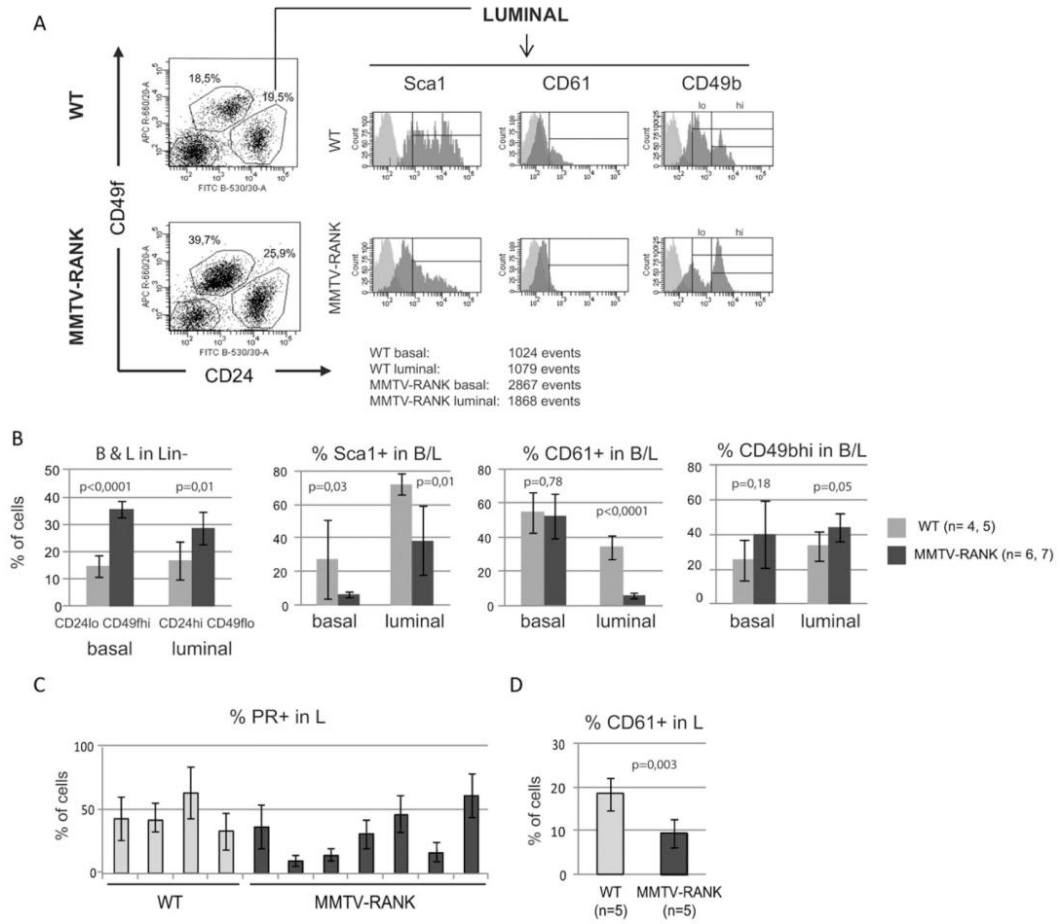

Figure 2. Constitutive expression of RANK alters mammary populations. See also Supporting Information Figure S2. **(A)**: Representative fluorescence-activated cell sorting dot plot and histograms showing mammary populations of virgin wild type (WT) and MMTV-RANK mice. Dot plot shows the expression of CD24 CD49f in the lineage negative Lin− (CD45− CD31−) population. Histograms show the expression of Sca1+, CD61+, and CD49bhi in luminal cells. Overlay with the corresponding negative control is shown. Numbers correspond to the percentages of the basal and luminal population in the Lin− population and the number of events quantified. **(B)**: Quantification of the percentage of CD24lo CD49fhi (basal, B) and CD24hi CD49flo (luminal, L) in the Lin− population, and the frequency of Sca1+, CD61+, and CD49b+ within the basal and luminal population of virgin WT and MMTV-RANK mice. A population of 10,000 live cells was captured, 62% and 78% of these cells are Lin− cells in WT and MMTV-RANK mammary glands, respectively. Mean, SD, and *t*-test *p* values are shown. **(C)**: Percentage of PR+ cells within the luminal compartment measured by immunohistochemistry in WT and MMTV-RANK virgin glands. Each bar represents one mouse. Six ducts per mouse were quantified. Mean and SD values are shown. **(D)**: Percentage of CD61+ cells within the luminal compartment determined by immunofluorescence in WT and MMTV-RANK virgin glands. Five ducts per mouse were quantified. Mean values, SD, and *t*-test *p* values are shown. Abbreviations: MMTV-RANK, mouse mammary tumor virus-receptor activator of NF-kappa B; PR, progesterone receptor; WT, wild type.

absence of RANKL. WT and MMTV-RANK basal cells form dense colonies with different morphologies (Fig. 3C). These colonies contained K5+ and K8+ as well as K5+/K8+ cells after 15 days of culture (Fig. 3C). As freshly isolated basal cells do not express *K8* (tested by RT-qPCR, data not shown), K8+ and K5+/K8+ cells must be derived from K5+ cells (Fig. 3C). K14 staining was similar to K5 in these colonies (data not shown). Frequency of colony formation was higher in MMTV-RANK basal cells as compared to WT and even higher upon exogenous RANKL stimulation (Fig. 3B). These results demonstrate that activation of RANK signaling results in an expansion of the MaSC/basal progenitor pool. To investigate the putative mechanism responsible for this expansion, we analyzed *Slug* and *Sox9* expression in FACS-sorted basal cells, as coexpression of these genes has been shown to induce MaSCs in the mouse mammary gland [26]. RT-qPCR analyses revealed higher expression of *Slug* and *Sox9* mRNA in some MMTV-RANK basal cells pools as compared to WT (Fig. 3D).

Elf5 mRNA expression has been shown to be enriched in the luminal progenitor fraction relative to basal and luminal mature cells [27]. In FACS-sorted luminal cells, a dramatic reduction in *Elf5* mRNA expression is found in MMTV-RANK as compared to WT cells indicating that the luminal compartment is disrupted in MMTV-RANK glands (Fig. 3D). To investigate the functional consequences of these alterations, we analyzed the colony-forming ability of WT and

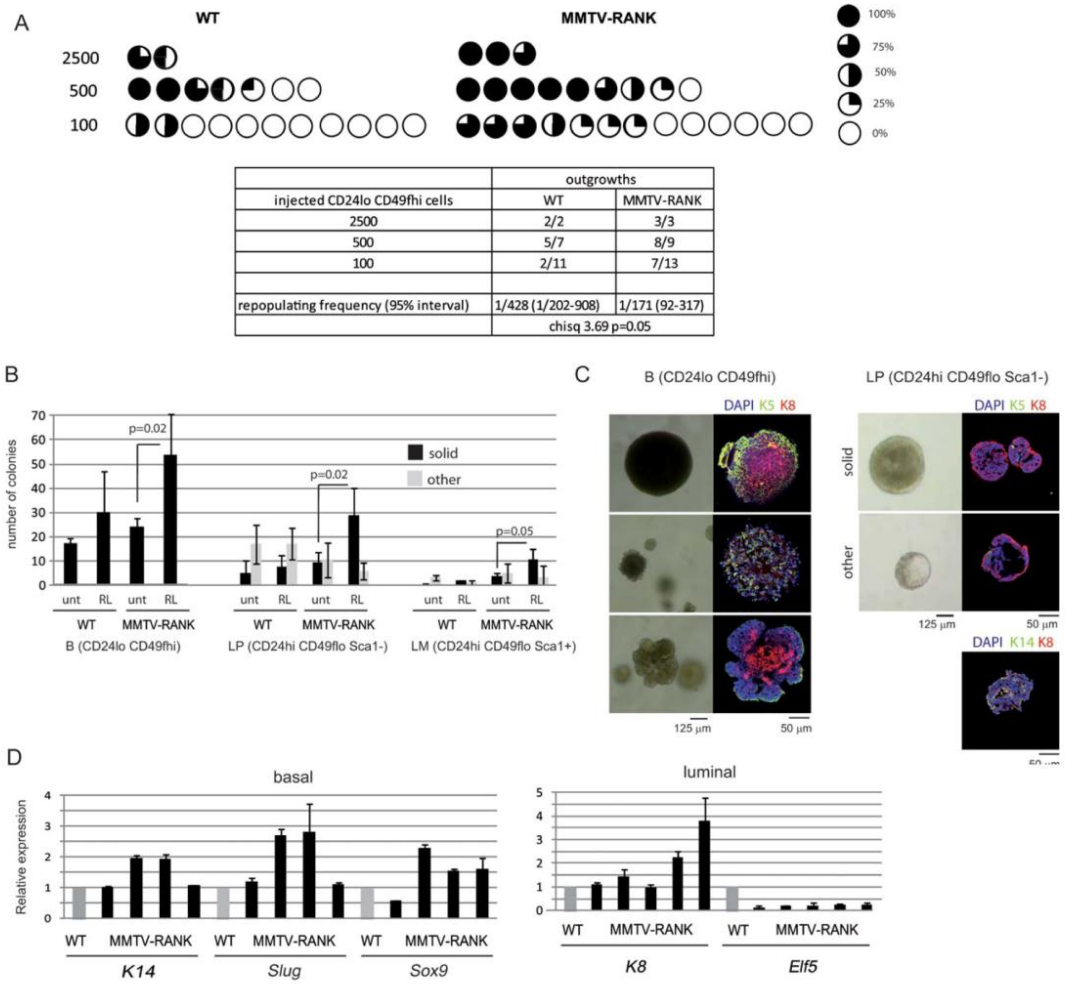

	outgrowths	
injected CD24lo CD49fhi cells	WT	MMTV-RANK
2500	2/2	3/3
500	5/7	8/9
100	2/11	7/13
repopulating frequency (95% interval)	1/428 (1/202-908)	1/171 (92-317)
	chisq 3.69 p=0.05	

Figure 3. RANK overexpression results in an expansion of the MaSC and luminal progenitor cell pool. **(A)**: Reconstitution efficiencies of wild type (WT) and MMTV-RANK basal CD24lo CD49fhi MECs. Each circle represents one transplanted fat pad and the percentage of reconstitution as indicated. Table indicates the ELDA quantification to calculate the frequency of MaSC. **(B)**: Number of colonies formed in matrigel by WT and MMTV-RANK indicated cell populations (basal [B], luminal progenitor [LP], and luminal mature [LM]) cultured with or without RANKL (RL or untreated). Luminal colonies were classified according to morphology as shown in C (solid/other). Each bar represents mean values for 4–6 independent experiments. In each experiment, a pool of 3–5 WT or MMTV-RANK mice was used. SD and *t*-test *p* values are included. **(C)**: Representative images showing morphology, and K5 or K14 (green), K8 (red) and DAPI (blue) staining found in colonies formed by basal **(B)** and LP cells. **(D)**: Expression of the indicated genes in MMTV-RANK fluorescence-activated cell sorting-sorted basal (CD24lo CD49fhi) and luminal (CD24hi CD49flo) cells relative to WT. Each dark bar represents values of cells isolated from an independent pool of 3–5 MMTV-RANK mice normalized to the expression found in WT pools (3–4 mice). For each sample measurements were done in duplicate and SD are shown. Abbreviations: DAPI, 4′6 Diamino-2-Phenylindole Dihydrochloride; LP; luminal progenitor; MMTV-RANK, mouse mammary tumor virus-receptor activator of NF-kappa B; RL, RANK ligand; WT, wild type.

MMTV-RANK luminal cells. Within the luminal population, Sca1−, CD49bhi, and CD61+ cells have all been shown to have enhanced clonogenic capacity in vitro as compared to Sca1+, CD49b−, and CD61− cells, respectively, and have therefore been identified as luminal progenitors [1,2,24]. Our data confirm that luminal Sca1− cells form more colonies than luminal Sca1+ cells in all comparisons (Fig. 3B). Upon RANKL stimulation, colony forming ability of MMTV-RANK Sca1− and Sca1+ luminal cells was significantly higher than the corresponding WT populations (Fig. 3B), and colonies showed a higher cellular density [6], (more solid colonies upon RANKL stimulation) (Fig. 3B, 3C). Colonies derived from WT and MMTV-RANK cells contained mostly K8+ and rarely K5+ cells, consistent with a luminal origin. Notably, many K8+ cells were also positive for K14, but not for K5 (Fig. 3C). Together, these results show that despite the decline in CD61+ luminal cells and disruption of the luminal compartment, MMTV-RANK luminal cells retain their clonogenic ability which is further enhanced by RANKL. These findings demonstrate that activation of RANK signaling disrupts MaSC fate in the basal and luminal compartments.

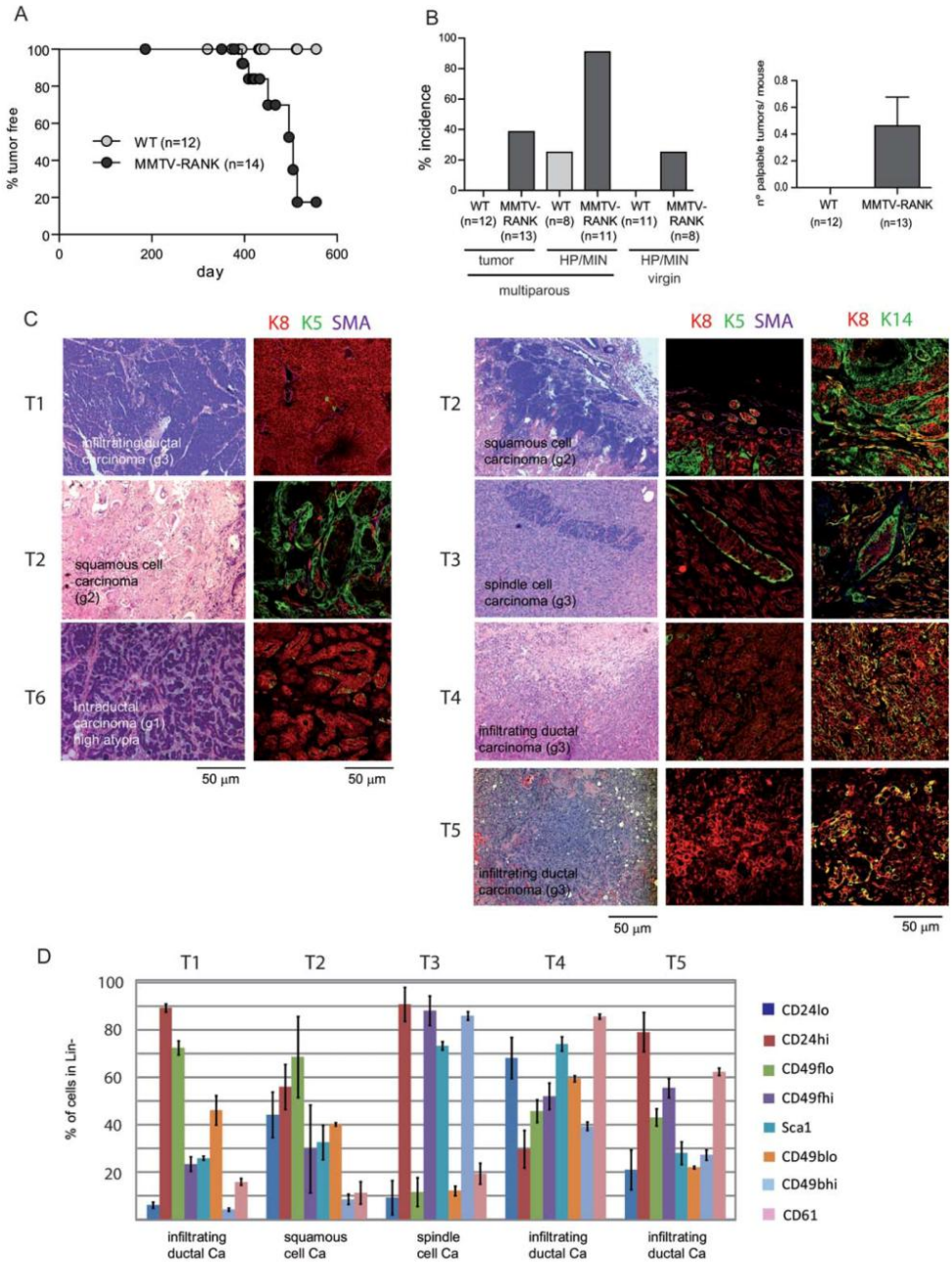

Figure 4. MMTV-RANK mice spontaneously develop preneoplastic lesions and tumors that are histologically heterogeneous and composed by distinct mammary populations. See also Supporting Information Figures S3, S4, and S5. (**A**): Kaplan Meier graph showing the percentage of palpable lesions in multiparous (at least three pregnancies) wild type (WT) and MMTV-RANK mice. (**B**): Left graph shows percentage of aged multiparous (MP) or virgin WT and MMTV-RANK mice showing preneoplastic lesions or tumors upon histological examination. Right graph shows the mean number of tumors per mouse. Mice free of lesions younger than 1 year or with less than three pregnancies for MP were not considered. (**C**): Representative histology (hematoxylin and eosin) and K5 or K14 (green), K8 (red), and SMA (magenta) immunostaining in MMTV-RANK spontaneous tumor lesions. All tumors are heterogeneous; staining for a representative area is shown. (**D**): Frequency of CD24hi/lo, CD49fhi/lo, Sca1+, CD61+, and CD49bhi/lo cells in Lin-population found in MMTV-RANK spontaneous tumors (T1–T5) analyzed by fluorescence-activated cell sorting. Positive/negative and high (hi)/low (lo) populations were set according to populations in the normal mammary gland. Measurements were performed in triplicate and mean and SD values are shown. Tumors are significantly different even when only CD24hi, CD49fhi, and Sca1+ are considered (MANOVA; Wilks Lambda: $p = 2.844e\text{-}13$). Abbreviations: MMTV-RANK, mouse mammary tumor virus-receptor activator of NF-kappa B; SMA, smooth muscle actin; WT, wild type; MANOVA, Multivariate Analysis of Variance.

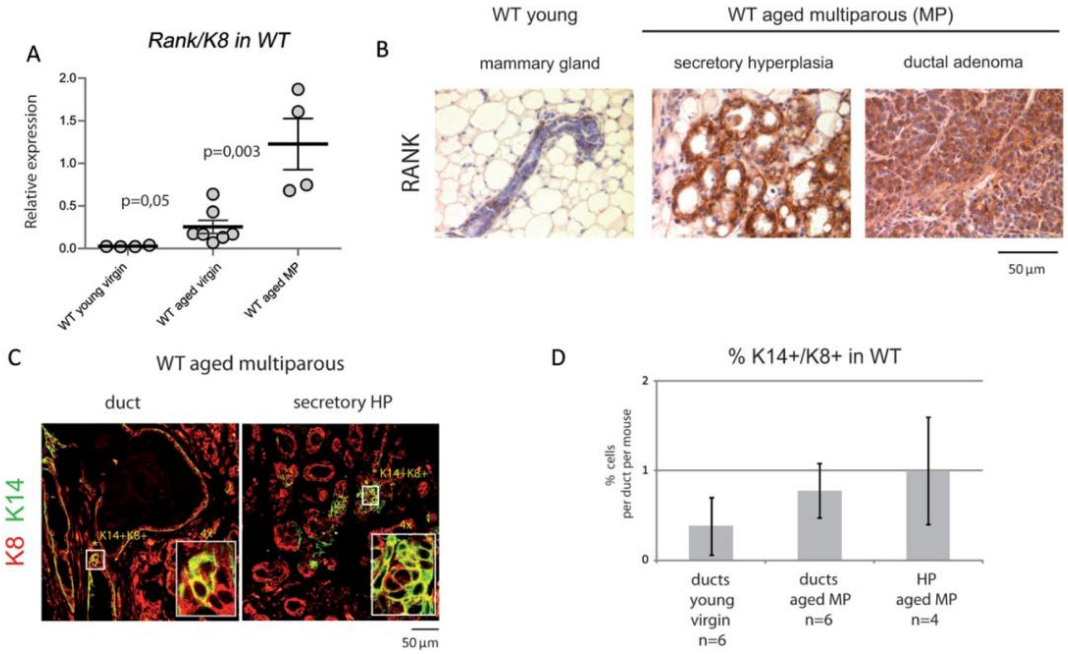

Figure 5. Physiological and pathophysiological upregulation of RANK in wild type (WT) mammary glands. See also Supporting Information Figure S6. (**A**): *RANK* expression relative to *K8* in mammary glands of young virgin, old virgin, and old multiparous (MP) WT mice. Each dot represents one mouse. Mean, SEM, and *t*-test *p* values are shown. For each sample measurements were performed in triplicate and mean was used. (**B**): Representative images of RANK expression as detected by IHC in normal ducts, secretory hyperplasia, and a low-grade adenoma of aged multiparous WT mouse (adenoma was found in a 90-week-old WT) and ducts from a young mouse. (**C**): Representative images of K8 (red) and K14 (green) staining in mammary epithelia from aged multiparous WT glands. K14+/K8+ are magnified in the insets. (**D**): Percentage of K14+/K8+ cells versus total number of cells per duct or hyperplastic structure (HP) of aged multiparous WT mice. Quantification in ducts from young virgin females is included for comparison. Five to seven ducts/structures were analyzed per mouse. Data represent the mean and SD. Abbreviations: HP, hyperplastic; MP, multiparous; WT, wild type; IHC, immunohistochemistry.

Spontaneous Preneoplastic Lesions and Heterogeneous Mammary Tumors in MMTV-RANK Mice

Our results show that RANK signaling disrupts mammary differentiation in virgin and parous glands, leading to the accumulation of MaSC, luminal and intermediate progenitors. K14+K8+ cells were found in the ducts from aged multiparous MMTV-RANK glands at frequency of 3.1%, a 2.3-fold increase when compared with the ducts of virgin young mice (Supporting Information Fig. S3B). We hypothesize that under continuous RANK stimulation, progenitors blocked in differentiation accumulate, acquire mutations, and might initiate tumorigenesis. After multiple pregnancies, 38% of elderly MMTV-RANK/FVB mice spontaneously developed high-grade invasive tumors with evidence of pulmonary metastasis (data not shown) and some mice showed multiple tumors (Fig. 4A–4C). Upon histological examination, preneoplastic lesions, including extensive hyperplasias and mammary intraepithelial neoplasias, were observed in most (90%) multiparous MMTV-RANK mammary glands and also in 25% of virgin aged MMTV-RANK mice (Fig. 4B; Supporting Information Fig. S3A). Age-matched multiparous WT mice exhibited only focal hyperplasias (25%) but no evidence of invasive tumors (Fig. 4A, 4B).

Invasive tumors (T1–T5) from MMTV-RANK mice showed a complex histological intra- and inter-tumor heterogeneity with different expression patterns of keratin and SMA staining despite all being RANK+ PR− (Fig. 4C; Supporting Information Figs. S3D, S4, S5). Consistent with the expansion of earlier progenitors observed in MMTV-RANK mice, each MMTV-RANK tumor was morphologically distinct, even in the case of tumors found in the same mouse (T2 and T3). MMTV-RANK tumors contained luminal (K8+) and/or basal (K5+, K14+, or SMA+) cells and importantly, cells coexpressing K14/K8, which were more frequent in the poorly differentiated tumors (T4 and T5). In contrast, K5+/K8+ cells were scarce in all tumors (Fig. 4C; Supporting Information Fig. S3D, S4, S5). FACS analyses revealed further heterogeneity between tumors (Fig. 4D; Supporting Information Fig. S3C, S3D). Higher expression levels of CD24 were found in tumors with high K8 expression, suggesting a luminal origin (T1 and T3), as opposed to K5+ tumors (T2). Expression of Sca1, CD61, and CD49b varied greatly between tumors and even within the same tumor (i.e., T5 contains two cell populations with different expression of CD49b and Sca1, which may be indicative of a polyclonal origin) (Fig. 4D; Supporting Information Fig. S3C, S3D). These results suggest that RANK overexpression disrupts mammary cell fate leading to extensively heterogeneous tumors that may originate from different populations of basal or luminal cells or alternatively from multipotent progenitors.

RANK Expression Increases with Age and Multiparity in WT Mice

Reproductive history and age have been linked to mammary tumorigenesis [12], and we found that increased levels of RANK expression promote spontaneous mammary tumors in

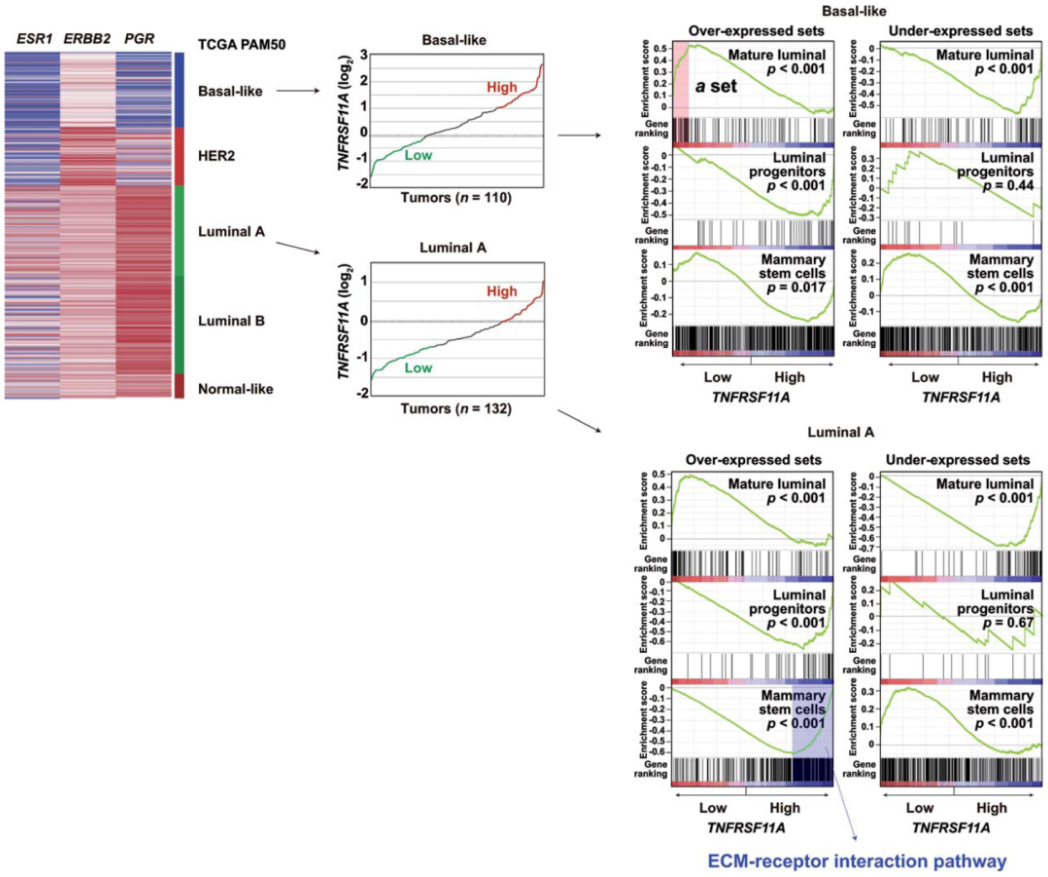

Figure 6. Association between *RANK* gene (also known as *TNFRSF11A*) expression differences among human breast tumors and the signatures that characterize mammary epithelial differentiation hierarchy. Left panel, TCGA tumors were classified into the intrinsic subtypes using the PAM50 predictor. The expression profiles of the genes encoding for ER, HER2, and PR (*ESR1*, *ERBB2*, and *PGR*, respectively) are shown. Middle panel, graphs showing the normalized expression values of *RANK* across basal-like and luminal A tumors; the first (low expression) and third (high expression) tertiles are highlighted. Right panels, GSEA graphical outputs for the association analysis between *RANK* tumor expression differences and the mammary epithelial differentiation signatures in basal-like and luminal A tumors. The signatures were previously identified as conserved in mice and human models, and specifically corresponding MaSC, luminal progenitors and luminal mature cells [29]. Each signature was analyzed using the gene subsets corresponding to over- or underexpression (Supporting Information Table 1). The GSEA enrichment scores and nominal *p* values are shown. The ECM-receptor interaction pathway was found significantly over-represented in the leading edge (false discovery rate <5% relative to rest of the given set) that defines the association between high *RANK* expression and the MaSC signature (overexpressed genes) in luminal A tumors. The rest of GSEA associations did not show significant over-representation of pathways beyond what was originally described for the signatures. Abbrevations: ER, estrogen receptor, IHC, immunohistochemistry, ECM, extra-cellular matrix.

mice. *Rank* mRNA expression, normalized to the epithelial content, was significantly higher in mammary glands from aged than young virgin WT (FVB) and was even higher in multiparous than in virgin glands (Fig. 5A). RANK protein is strongly expressed in spontaneous mammary secretory hyperplasias and ductal adenomas found occasionally in aged multiparous females compared with young virgin mammary tissues (Fig. 5B). Glands from aged multiparous WT mice showed a moderate increase in the frequency of basal and luminal cells as compared to younger WT and enhanced side branching, resembling the RANK-overexpressing glands (Supporting Information Fig. S6A, S6B). *Sox9* and *Elf5* expression levels increase with age and parities (Supporting Information Fig. S6C). While K14+K8+ cells were very rare in normal ducts of young virgin WT mice (Fig. 1C, 1E), their frequency increases in the ducts of elderly multiparous females and increases further in hyperplastic lesions (Fig. 5C, 5D). Our findings show that RANK expression increases with age and parity in the WT mammary gland, emulating some of the phenotypes observed in the MMTV-RANK glands.

RANK Expression Levels in Human Breast Adenocarcinomas Are Associated with Altered Mammary Differentiation

Previous work suggested a role for activated RANK signaling in human breast carcinogenesis; RANK expression was found in a subgroup of luminal and basal human mammary adenocarcinomas and was associated with tumor aggressiveness [17]. Based on these observations and the results presented

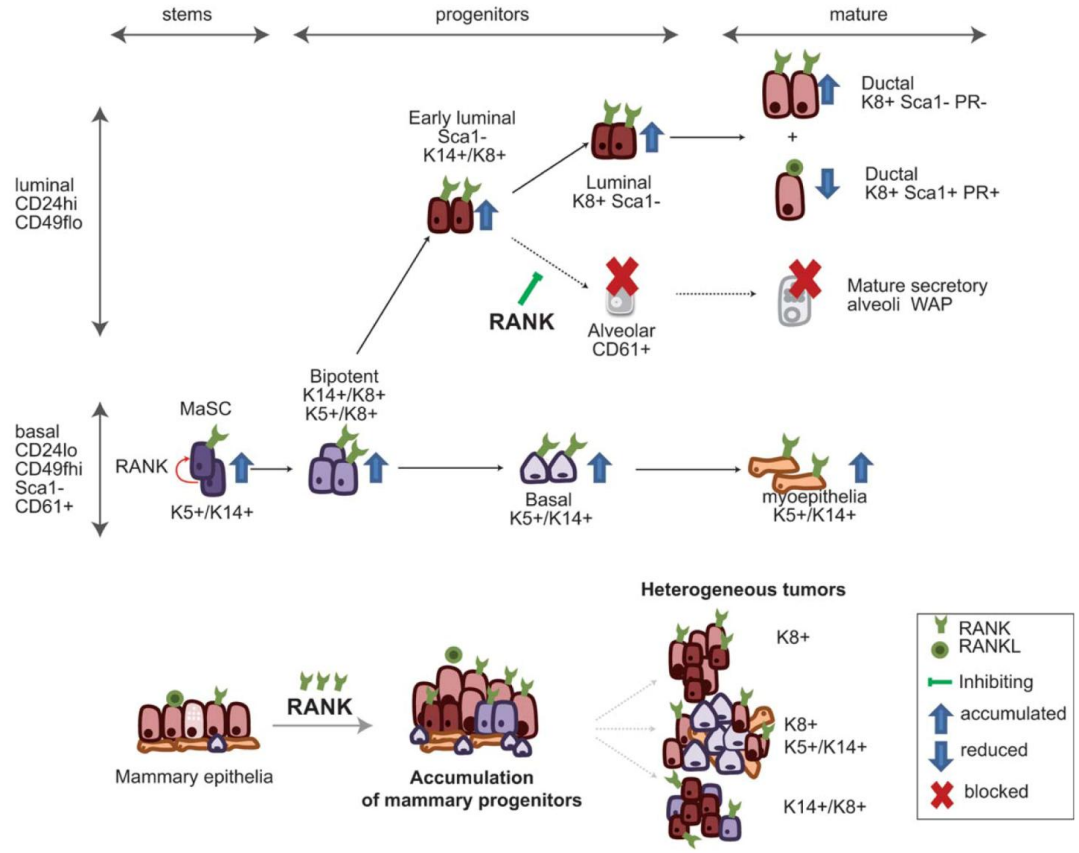

Figure 7. Schematic model showing RANK role in the regulation of mammary cell fate and breast cancer. Top: constitutive activation of RANK in virgin glands expands the luminal and basal compartment (including mammary stem cell) and disrupts luminal differentiation interfering with the generation of CD61+ luminal cells and Elf5 expression. Bottom: impaired cell commitment results in the accumulation of earlier progenitors, including bipotent K14+K8+ cells that during aging accumulate mutations and can initiate tumorigenesis. MMTV-RANK intertumor heterogeneity and the abundance of K14+/K8+ cells within the tumors suggest that each tumor may originate from progenitors that later differentiate into distinct phenotypes. Abbreviations: MaSC, mammary stem cell; RANK, receptor activator of NF-kappa B; RANKL, RANK ligand.

here, RANK expression in these tumors may be associated with alteration of cell differentiation programs. To assess this, hypothesis data from TCGA [28] were analyzed for the expression levels of the genes that characterize mammary differentiation hierarchy in mice and humans, including MaSC, luminal progenitors, and luminal mature cells [29]. The primary human tumors represented in TCGA dataset were first classified into the intrinsic subtypes using the PAM50 predictor. Subsequently, the basal-like and luminal A tumors were categorized into tertiles according to the expression levels of *RANK* (Fig. 6). No differences in the expression of the genes encoding for ER and PR were identified between the *RANK*-based basal-like or luminal A subgroups. Next, the ranks of expression differences between high and low *RANK*-expressing tumors were analyzed using the Gene Set Enrichment Analysis (GSEA) tool. The results revealed an association between high *RANK* expression in human breast tumors and altered mammary differentiation for both basal-like and luminal A tumors: while the gene sets that characterize MaSC and luminal progenitors were positively correlated with high *RANK* expression, an opposite pattern was observed for the gene sets that characterize the luminal mature cells (Fig. 6; Supporting Information Table 1). Regarding the link with altered signaling pathways, over-representation analysis in the GSEA leading edges only found the extracellular matrix (ECM)-receptor interaction pathway as significantly associated with high *RANK* expression and the MaSC signature (overexpressed genes) in luminal A tumors (Fig. 6). Specific interactions between cells and the ECM are mediated by transmembrane molecules, mainly integrins or other cell-surface-associated components and lead to a direct or indirect control of multiple cellular activities. The rest of leading edges did not show differences relative to what was described previously for the specific expression signatures [29]. Together, these results indicate that, akin to the observations made from mice studies, activated RANK signaling associates with a cell dedifferentiation profile in different subtypes of human breast cancer.

Discussion

The fact that RANK overexpression and RANK loss impaired mammary gland development [13,14] suggests that RANK

signaling controls mammary epithelial cell fate (schematized in Fig. 7). Our data reveal profound effects of the activated RANK/RANKL pathway on the mouse mammary epithelial hierarchy, affecting mammary cell fate and subsequently enhancing tumor initiation and progression. It was postulated that RANK signaling was the paracrine mediator of the expansion in the MaSC-enriched compartment driven by progesterone in mice [10,11]. As no specific markers allow the isolation of MaSC from the bulk of basal cells, the identification of MaSC relies on their ability to repopulate the mammary fat pad and their clonogenic potential. The increased repopulation frequency of basal MMTV-RANK cells and their enhanced ability to form colonies, supports that activation of RANK signaling expands the MaSC population. Increased expression of *Sox9* and *Slug*, genes that have recently been shown to mediate MaSC function [26] is observed in basal MMTV-RANK cells. These results corroborate in vivo our findings in human mammary epithelial cell lines, where we recently demonstrated that RANK overexpression induces stemness [17].

Constitutive activation of RANK in the mouse mammary gland expands not only the basal and MaSC population, but also the luminal compartment, and has dramatic effects on the distribution of luminal subpopulations. RANK overexpression resulted in an expansion of the luminal populations CD24hi CD49flo Sca1− and CD24hi CD49flo CD49b+ but interfered with the generation of the luminal CD24hi CD49flo CD61+ that establish the alveolar lineage during pregnancy [2,3]. MMTV-RANK luminal cells retained their clonogenic ability which has further enhanced by RANKL, despite the decrease in CD61+ luminal cells, suggesting that the colony-forming ability is likely compensated by other luminal progenitors. The significant decrease in *Elf5* expression in luminal cells from virgin MMTV-RANK mice fits with the notion that Elf5 is required for luminal cell differentiation [3]. Notably, it has been recently shown that Elf5 loss, akin RANK overexpression, induces MaSC activity and epithelial to mesenchymal transition (EMT) [17,22,30]. Our findings now indicate that the decline in the CD61+ alveolar progenitors contributes to the failure of alveologenesis and lactation in MMTV-RANK mice.

The hyperplastic epithelia, increased side branching and aberrant ducts observed in virgin MMTV-RANK glands is similar to that induced by progesterone treatment [31], suggesting that RANK expression is emulating aspects of acute progesterone stimuli. We hypothesize that RANK could contribute to the increased risk of breast cancer development associated with reproductive history and aging by accumulation of undifferentiated cells or progenitors. Several findings are consistent with this hypothesis: RANK expression increases in the WT mammary gland with age and parity; mammary ducts and hyperplastic lesions of aged multiparous WT females strongly express RANK and contain K14+/K8+ cells at higher frequencies than ducts from young females; RANK overexpression results in an expansion of K14+/K8+ cells in the virgin gland; spontaneous tumors found in aged multiparous MMTV-RANK mice contain K14+/K8+ cells, suggesting that these cells may contribute to tumorigenesis. In the aged human mammary gland similar changes, a reduction in myoepithelial cells and an increase in luminal cells expressing basal markers, resulting from an age-dependent expansion of defective multipotent progenitors, were reported [32] and RANKL was shown to induce the expression of basal cell markers and prevent milk production in human mammary acini [33]. Accumulation of K14+/K8+ cells, identified as intermediate progenitors blocked in differentiation and mislocalization of K14+ cells in the luminal compartment have been reported in the ducts of mice deficient for Elf5 during pregnancy and in spontaneous tumors [22,23]. We show that K14+K8+ cells are found in colonies derived from both basal and luminal cells, in contrast to K5+K8+ cells that are only found in basal colonies. K5+K8+ cells, in contrast to K14+K8+ cells were scarce in MMTV-RANK spontaneous. These results support that K5 and K14 mark different populations of cells [34], and situates K14+/K8+ cells at the edge basal/luminal differentiation.

Different breast tumor subtypes may originate from different classes of stem/progenitor cells [35]. In fact, it has been directly demonstrated that the cell of origin of a tumor is one of the key determinants of the tumor's histological features [36]. Inter- and intratumor heterogeneity observed in spontaneous MMTV-RANK tumors suggest that each tumor may originate from a different population of luminal and basal cells or from multipotent progenitors that later differentiate into distinct phenotypes. This tumor heterogeneity in MMTV-RANK mice contrasts with other MMTV-driven models such as MMTV-*neu* or MMTV-PyMT, which are highly clonal and homogenous [37–39]. Thus, RANK-induced changes in luminal, basal, and progenitor cells can cooperate with additional stochastic changes that occur in these cells to promote tumor initiation and progression.

We had previously shown that RANK is expressed in 50% of basal and 20% of luminal human breast adenocarcinomas and that RANK overexpression in human mammary cell lines induces stemness [17]. This GSEA analyses supports the hypothesis that *RANK* expression in luminal A and basal human breast adenocarcinomas is associated with a poorly differentiated phenotype and may therefore result in a poorer prognosis. At least signaling cascades mediated by protein kinases are induced by RANK signaling during osteoclastogenesis and activation —inhibitor of NF-κB kinase (IKK), c-Jun N-terminal kinase (JNK), p38, extracellular signal-regulated kinase (ERK), and Src pathways [40]. Future studies will reveal which of the downstream targets of RANK signal transduction in mammary epithelia mediate RANK-driven alterations in MaSC fate. In conclusion, this study, as represented in Figure 7, demonstrates that activated RANK signaling targets the basal and luminal compartments for expansion, impairing mammary cell fate and eventually leading to hyperplasia and tumorigenesis.

Conclusion

This study provides the first evidence that RANK is a master regulator of MaSC fate. Constitutive RANK expression interferes with basal and luminal cells commitment, resulting in the accumulation of MaSC, luminal and bipotent progenitors. Our data support the hypothesis that RANK driven expansion of mammary progenitors underlies RANK induced tumorigenesis and make an argument for a physiological upregulation of RANK in the mammary epithelia during aging and parity providing a mechanistic rationale for the increased risk of breast cancer with age.

Acknowledgments

We thank G. Boigues, S. Vila, and the IDIBELL animal facility for their assistance with mouse colonies; J. Climent and M.T. Soler for pathological assessment of mouse tumors; UB-SCT services for technical assistance; and O. Casanovas and L.

Planelles for useful discussions. This work was supported by grants from MICINN (SAF2008-01975; SAF2011–22893), AECC (Catalunya), FMM, Concern Foundation, and a Ramon y Cajal contract to G-S, E and by a grant from the ISCIII FIS (09/02483; to P.A.M.). PP is recipient of a FPI grant from the MICINN. P.P. and A.C. contributed equally to this work.

Disclosure of Potential Conflicts of Interest

The author W.C.D. is an employee and shareholder of Amgen Inc. All other authors indicate no potential conflicts of interest.

References

1 Sleeman KE, Kendrick H, Robertson D et al. Dissociation of estrogen receptor expression and in vivo stem cell activity in the mammary gland. J Cell Biol 2007;176:19–26.
2 Asselin-Labat ML, Sutherland KD, Barker H et al. Gata-3 is an essential regulator of mammary-gland morphogenesis and luminal-cell differentiation. Nat Cell Biol 2007;9:201–209.
3 Oakes SR, Naylor MJ, Asselin-Labat ML et al. The Ets transcription factor Elf5 specifies mammary alveolar cell fate. Genes Dev 2008;22:581–586.
4 Shackleton M, Vaillant F, Simpson KJ et al. Generation of a functional mammary gland from a single stem cell. Nature 2006;439:84–88.
5 Sleeman KE, Kendrick H, Ashworth A et al. CD24 staining of mouse mammary gland cells defines luminal epithelial, myoepithelial/basal and non-epithelial cells. Breast Cancer Res 2006;8:R7.
6 Stingl J, Eirew P, Ricketson I et al. Purification and unique properties of mammary epithelial stem cells. Nature 2006;439:993–997.
7 Mikaelian I, Hovick M, Silva KA et al. Expression of terminal differentiation proteins defines stages of mouse mammary gland development. Vet Pathol 2006;43:36–49.
8 Van Keymeulen A, Rocha AS, Ousset M et al. Distinct stem cells contribute to mammary gland development and maintenance. Nature 2011;479:189–193.
9 Smalley M, Ashworth A. Stem cells and breast cancer: A field in transit. Nat Rev Cancer 2003;3:832–844.
10 Asselin-Labat ML, Vaillant F, Sheridan JM et al. Control of mammary stem cell function by steroid hormone signalling. Nature 2010;465:798–802.
11 Joshi PA, Jackson HW, Beristain AG et al. Progesterone induces adult mammary stem cell expansion. Nature 2010;465:803–807.
12 Bernstein L. Epidemiology of endocrine-related risk factors for breast cancer. J Mammary Gland Biol Neoplasia 2002;7:3–15.
13 Fata JE, Kong YY, Li J et al. The osteoclast differentiation factor osteoprotegerin-ligand is essential for mammary gland development. Cell 2000;103:41–50.
14 Gonzalez-Suarez E, Branstetter D, Armstrong A et al. RANK overexpression in transgenic mice with mouse mammary tumor virus promoter-controlled RANK increases proliferation and impairs alveolar differentiation in the mammary epithelia and disrupts lumen formation in cultured epithelial acini. Mol Cell Biol 2007;27:1442–1454.
15 Beleut M, Rajaram RD, Caikovski M et al. Two distinct mechanisms underlie progesterone-induced proliferation in the mammary gland. Proc Natl Acad Sci U S A 2010;107:2989–2994.
16 Gonzalez-Suarez E, Jacob AP, Jones J et al. RANK ligand mediates progestin-induced mammary epithelial proliferation and carcinogenesis. Nature 2010;468:103–107.
17 Palafox M, Ferrer I, Pellegrini P et al. RANK induces epithelial-mesenchymal transition and stemness in human mammary epithelial cells and promotes tumorigenesis and metastasis. Cancer Res 2012;72:2879–2888.
18 Smalley MJ. Isolation, culture and analysis of mouse mammary epithelial cells. Methods Mol Biol 2010;633:139–170.
19 Debnath J, Brugge JS. Modelling glandular epithelial cancers in three-dimensional cultures. Nat Rev Cancer 2005;5:675–688.
20 Parker JS, Mullins M, Cheang MC et al. Supervised risk predictor of breast cancer based on intrinsic subtypes. J Clin Oncol 2009;27:1160–1167.
21 Huang da W, Sherman BT, Lempicki RA. Systematic and integrative analysis of large gene lists using DAVID bioinformatics resources. Nat Protoc 2009;4:44–57.
22 Chakrabarti R, Wei Y, Romano RA et al. Elf5 regulates mammary gland stem/progenitor cell fate by influencing notch signaling. Stem Cells 2012;30:1496–1508.
23 Li Z, Tognon CE, Godinho FJ et al. ETV6-NTRK3 fusion oncogene initiates breast cancer from committed mammary progenitors via activation of AP1 complex. Cancer Cell 2007;12:542–558.
24 Li W, Ferguson BJ, Khaled WT et al. PML depletion disrupts normal mammary gland development and skews the composition of the mammary luminal cell progenitor pool. Proc Natl Acad Sci U S A 2009;106:4725–4730.
25 Shehata M, Teschendorff A, Sharp G et al. Phenotypic and functional characterization of the luminal cell hierarchy of the mammary gland. Breast Cancer Res 2012;14:R134.
26 Guo W, Keckesova Z, Donaher JL et al. Slug and Sox9 cooperatively determine the mammary stem cell state. Cell 2012;148:1015–1028.
27 Kendrick H, Regan JL, Magnay FA et al. Transcriptome analysis of mammary epithelial subpopulations identifies novel determinants of lineage commitment and cell fate. Bmc Genom 2008;9:591.
28 Cancer Genome Atlas Network. Comprehensive molecular portraits of human breast tumours. Nature 2012;490:61–70.
29 Lim E, Wu D, Pal B et al. Transcriptome analyses of mouse and human mammary cell subpopulations reveal multiple conserved genes and pathways. Breast Cancer Res 2010;12:R21.
30 Chakrabarti R, Hwang J, Andres Blanco M et al. Elf5 inhibits the epithelial-mesenchymal transition in mammary gland development and breast cancer metastasis by transcriptionally repressing Snail2. Nat Cell Biol 2012;14:1212–1222.
31 Atwood CS, Hovey RC, Glover JP et al. Progesterone induces side-branching of the ductal epithelium in the mammary glands of peripubertal mice. J Endocrinol 2000;167:39–52.
32 Garbe JC, Pepin F, Pelissier FA et al. Accumulation of multipotent progenitors with a basal differentiation bias during aging of human mammary epithelia. Cancer Res 2012;72:3687–3701.
33 Thomas E, Lee-Pullen T, Rigby P et al. Receptor activator of NF-kappaB ligand promotes proliferation of a putative mammary stem cell unique to the lactating epithelium. Stem Cells 2012;30:1255–1264.
34 Sun P, Yuan Y, Li A et al. Cytokeratin expression during mouse embryonic and early postnatal mammary gland development. Histochem Cell Biol 2010;133:213–221.
35 Melchor L, Benitez J. An integrative hypothesis about the origin and development of sporadic and familial breast cancer subtypes. Carcinogenesis 2008;29:1475–1482.
36 Molyneux G, Geyer FC, Magnay FA et al. BRCA1 basal-like breast cancers originate from luminal epithelial progenitors and not from basal stem cells. Cell Stem Cell 2010;7:403–417.
37 Guy CT, Webster MA, Schaller M et al. Expression of the neu protooncogene in the mammary epithelium of transgenic mice induces metastatic disease. Proc Natl Acad Sci U S A 1992;89:10578–10582.
38 Lin EY, Jones JG, Li P et al. Progression to malignancy in the polyoma middle T oncoprotein mouse breast cancer model provides a reliable model for human diseases. Am J Pathol 2003;163:2113–2126.
39 Vaillant F, Asselin-Labat ML, Shackleton M et al. The mammary progenitor marker CD61/beta3 integrin identifies cancer stem cells in mouse models of mammary tumorigenesis. Cancer Res 2008;68:7711–7717.
40 Boyle WJ, Simonet WS, Lacey DL. Osteoclast differentiation and activation. Nature 2003;423:337–342.

See www.StemCells.com for supporting information available online.

FIGURES

Figure 1

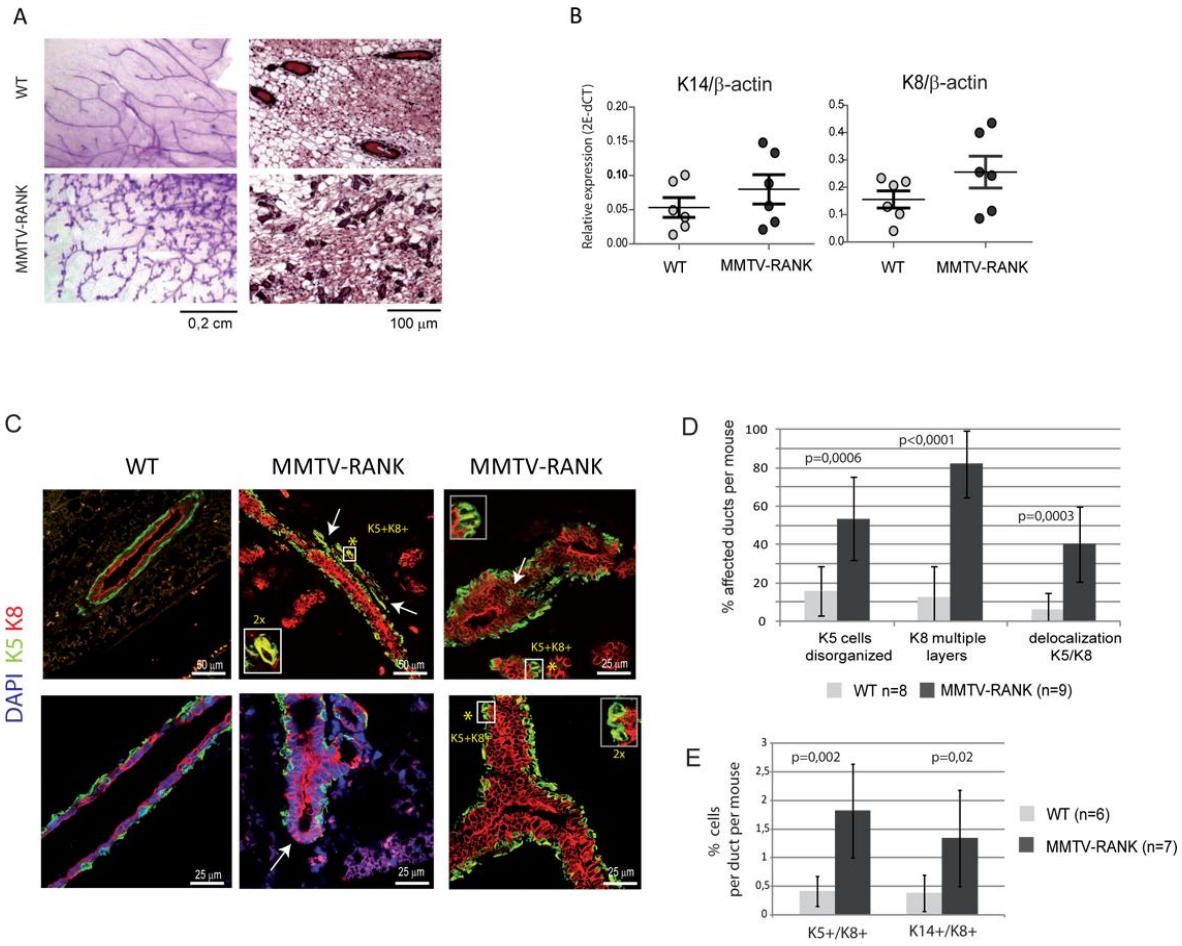

Figure 1: RANK overexpression disrupts epithelial morphology. See also Supporting Information Figure S1.

(A): Representative images of whole mounts and hematoxylin and eosin of virgin wild type (WT) and MMTV-RANK mammary glands.

(B): K14 and K8 messenger RNA expression relative to β-actin in the mammary glands of virgin WT and MMTV-RANK mice. Each dot represents one mouse. Mean, SEM, and t-test p values are shown.

(C): Representative images of K5 and K8 staining in mammary epithelia of virgin WT and MMTV-RANK mice (12– 15 weeks old). Asterisks indicate double positive K5/K8 cells that are magnified in the insets. Arrows indicate other abnormalities including multilayer of K51 cells, K51 cell in the luminal area, or absence of K5 in the basal layer.

(D): Percentage of ducts per virgin mouse showing the indicated lesions. Between 5 and 7 ducts were analyzed per mouse. Mean, SD, and t-test p values are shown. Delocalization includes extra layer of K5+ cells, K5+ cells in the luminal area, and absence of K5 in the basal area as shown in C.

(E): Percentage of K5+/K8+ and K14+/K8+ cells versus total number of cells per duct in 12–15 weeks old virgin WT and MMTV-RANK mice. For each mouse, seven ducts were analyzed. Mean, SD, and t-test p values are shown. Abbreviations: DAPI, 406 Diamino-2-Phenylindole Dihydrochloride; MMTV-RANK, mouse mammary tumor virus-receptor activator of NF-kappa B; WT, wild type.

Figure 2

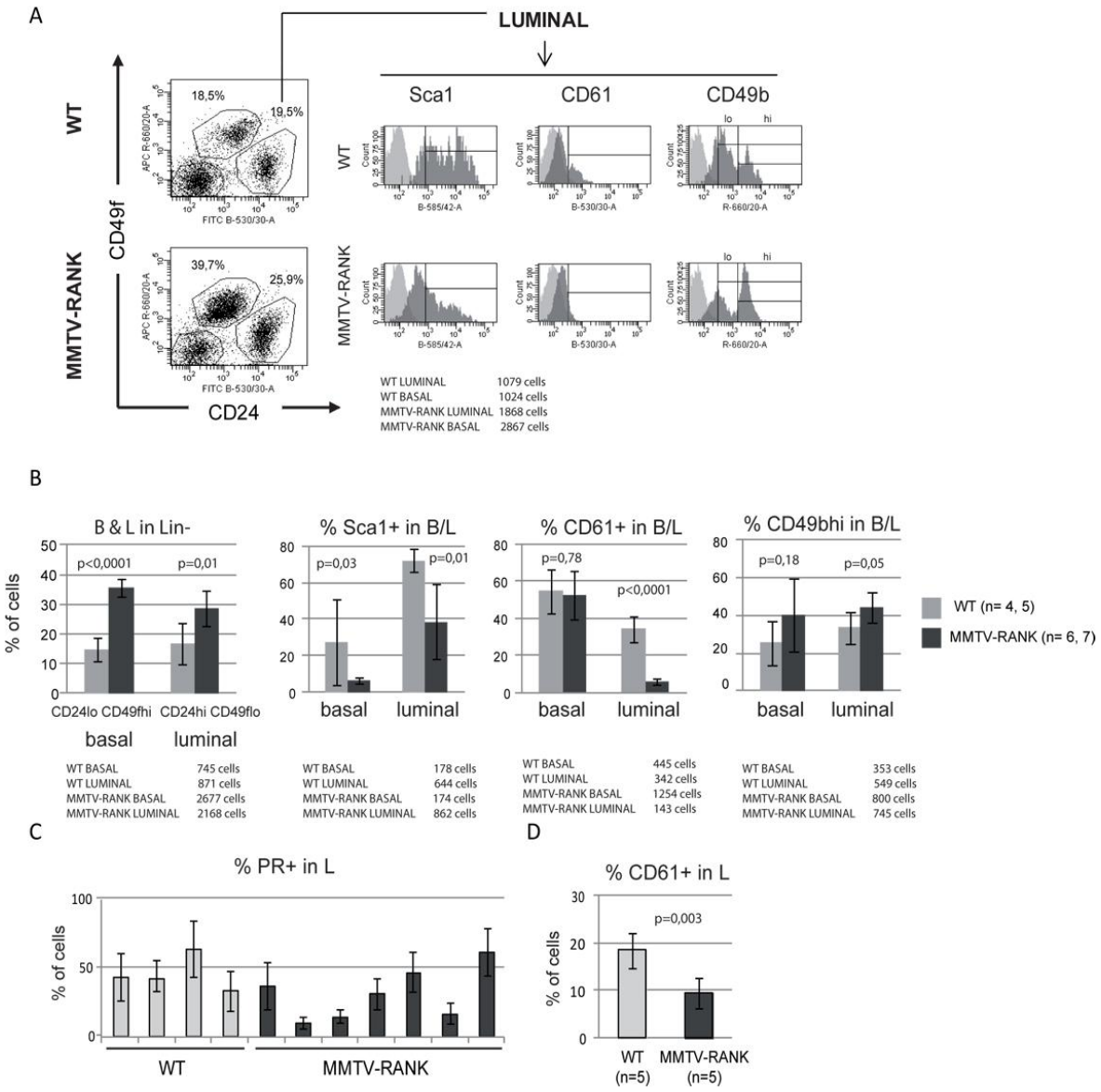

Figure 2. Constitutive expression of RANK alters mammary populations. See also Supporting Information Figure S2.

(A): Representative fluorescence-activated cell sorting dot plot and histograms showing mammary populations of virgin wild type (WT) and MMTV-RANK mice. Dot plot shows the expression of CD24 CD49f in the lineage negative Lin- (CD45- CD31-) population. Histograms show the expression of Sca1+, CD61+, and CD49bhi in luminal cells. Overlay with the corresponding negative control is shown. Numbers correspond to the percentages of the basal and luminal population in the Lin- population and the number of events quantified.

(B): Quantification of the percentage of CD24lo CD49fhi (basal, B) and CD24hi CD49flo (luminal, L) in the Lin- population, and the frequency of Sca1+, CD61+, and CD49b+ within the basal and luminal population of virgin WT and MMTV-RANK mice. A population of 10,000 live cells was captured, 62% and 78% of these cells are Lin- cells in WT and MMTV-RANK mammary glands, respectively. Mean, SD, and t-test p values are shown.

(C): Percentage of PR+ cells within the luminal compartment measured by immunohistochemistry in WT and MMTV-RANK virgin glands. Each bar represents one mouse. Six ducts per mouse were quantified. Mean and SD values are shown.

(D): Percentage of CD61+ cells within the luminal compartment determined by immunofluorescence in WT and MMTV-RANK virgin glands. Five ducts per mouse were quantified. Mean values, SD, and t-test p values are shown. Abbreviations: MMTV-RANK, mouse mammary tumor virus-receptor activator of NF-kappa B; PR, progesterone receptor; WT, wild type.

Figure 3

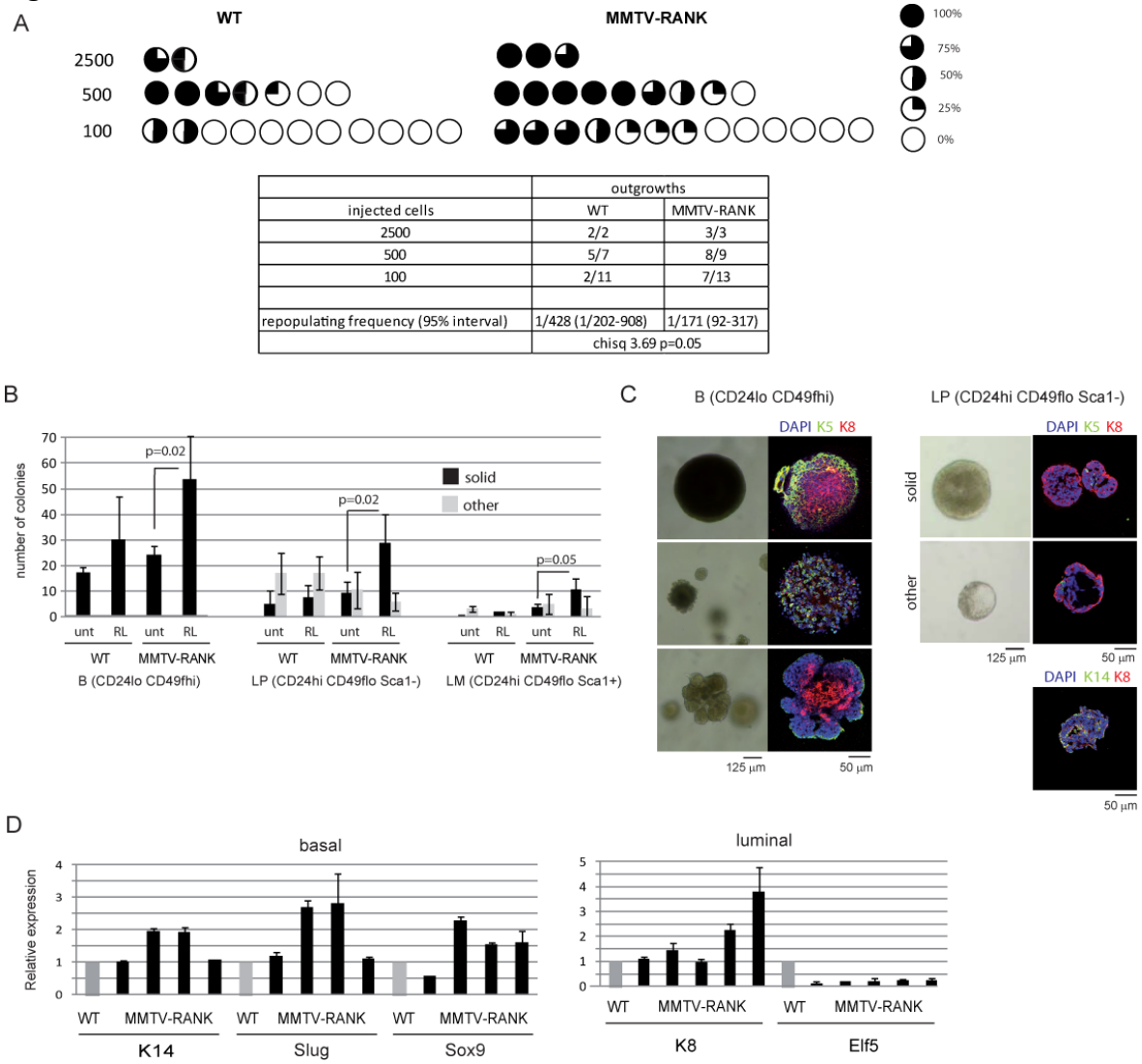

	outgrowths	
injected cells	WT	MMTV-RANK
2500	2/2	3/3
500	5/7	8/9
100	2/11	7/13
repopulating frequency (95% interval)	1/428 (1/202-908)	1/171 (92-317)
	chisq 3.69 p=0.05	

Figure 3. RANK overexpression results in an expansion of the MaSC and luminal progenitor cell pool.

(A): Reconstitution efficiencies of wild type (WT) and MMTV-RANK basal CD24lo CD49fhi MECs. Each circle represents one transplanted fat pad and the percentage of reconstitution as indicated. Table indicates the ELDA quantification to calculate the frequency of MaSC.

(B): Number of colonies formed in matrigel by WT and MMTV-RANK indicated cell populations (basal [B], luminal progenitor [LP], and luminal mature [LM]) cultured with or without RANKL (RL or untreated). Luminal colonies were classified according to morphology as shown in C (solid/other). Each bar represents mean values for 4–6 independent experiments. In each experiment, a pool of 3–5 WT or MMTV-RANK mice was used. SD and t-test p values are included.

(C): Representative images showing morphology, and K5 or K14 (green), K8 (red) and DAPI (blue) staining found in colonies formed by basal (B) and LP cells.

(D): Expression of the indicated genes in MMTV-RANK fluorescence-activated cell sorting-sorted basal (CD24lo CD49fhi) and luminal (CD24hi CD49flo) cells relative to WT. Each dark bar represents values of cells isolated from an independent pool of 3–5 MMTV-RANK mice normalized to the expression found in WT pools (3–4 mice). For each sample measurements were done in duplicate and SD are shown. Abbreviations: DAPI, 406 Diamino-2-Phenylindole Dihydrochloride; LP; luminal progenitor; MMTV-RANK, mouse mammary tumor virus-receptor activator of NF-kappa B; RL, RANK ligand; WT, wild type.

Figure 4

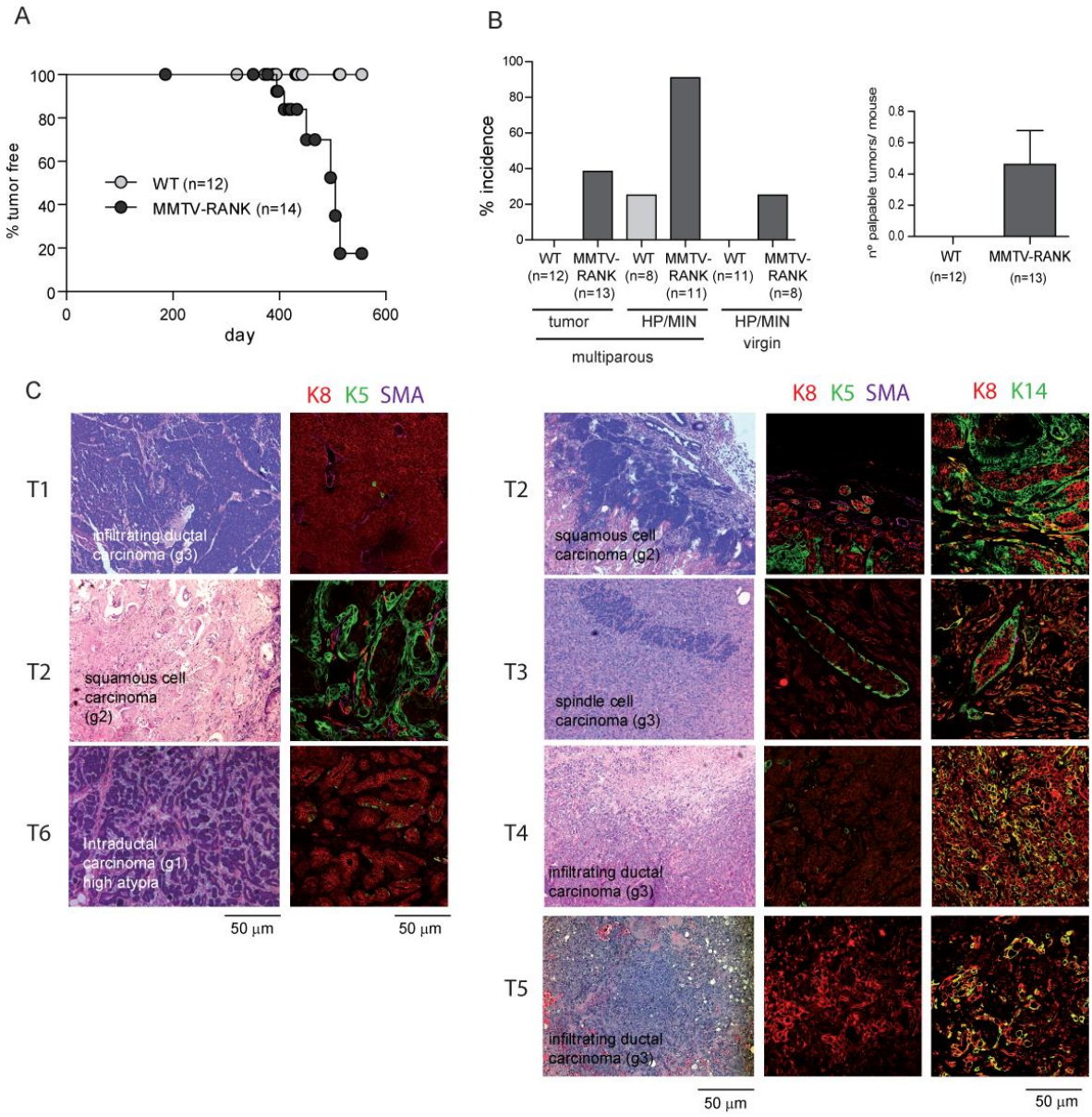
A
% tumor free
day
WT (n=12)
MMTV-RANK (n=14)
B
% incidence
WT (n=12)
MMTV-RANK (n=13)
WT (n=8)
MMTV-RANK (n=11)
WT (n=11)
MMTV-RANK (n=8)
tumor
HP/MIN
HP/MIN
multiparous
virgin
n° palpable tumors/ mouse
WT (n=12)
MMTV-RANK (n=13)
C
K8 K5 SMA
K8 K14
T1
infiltrating ductal carcinoma (g3)
T2
squamous cell carcinoma (g2)
T6
intraductal carcinoma (g1) high atypia
T3
spindle cell carcinoma (g3)
T4
infiltrating ductal carcinoma (g3)
T5
infiltrating ductal carcinoma (g3)
50 μm
D
T1
T2
T3
T4
T5
% of cells in Lin-
CD24lo
CD24hi
CD49flo
CD49fhi
Sca1
CD49blo
CD49bhi
CD61
infiltrating ductal Ca
squamous cell Ca
spindle cell Ca
infiltrating ductal Ca
infiltrating ductal Ca

Figure 4. MMTV-RANK mice spontaneously develop preneoplastic lesions and tumors that are histologically heterogeneous and composed by distinct mammary populations. See also Supporting Information Figures S3, S4, and S5.
(A): Kaplan Meier graph showing the percentage of palpable lesions in multiparous (at least three pregnancies) wild type (WT) and MMTV-RANK mice.
(B): Left graph shows percentage of aged multiparous (MP) or virgin WT and MMTV-RANK mice showing preneoplastic lesions or tumors upon histological examination. Right graph shows the mean number of tumors per mouse. Mice free of lesions younger than 1 year or with less than three pregnancies for MP were not considered.
(C): Representative histology (hematoxylin and eosin) and K5 or K14 (green), K8 (red), and SMA (magenta) immunostaining in MMTV-RANK spontaneous tumor lesions. All tumors are heterogeneous; staining for a representative area is shown.
(D): Frequency of CD24hi/lo, CD49fhi/lo, Sca1+, CD61+, and CD49bhi/lo cells in Lin-population found in MMTV-RANK spontaneous tumors (T1–T5) analyzed by fluorescence activated cell sorting. Positive/negative and high (hi)/low (lo) populations were set according to populations in the normal mammary gland. Measurements were performed in triplicate and mean and SD values are shown. Tumors are significantly different even when only CD24hi, CD49fhi, and Sca1+ are considered (MANOVA; Wilks Lambda: p=2.844e-13). Abbreviations: MMTV-RANK, mouse mammary tumor virus-receptor activator of NF-kappa B; SMA, smooth muscle actin; WT, wild type; MANOVA, Multivariate Analysis of Variance.

Figure 5

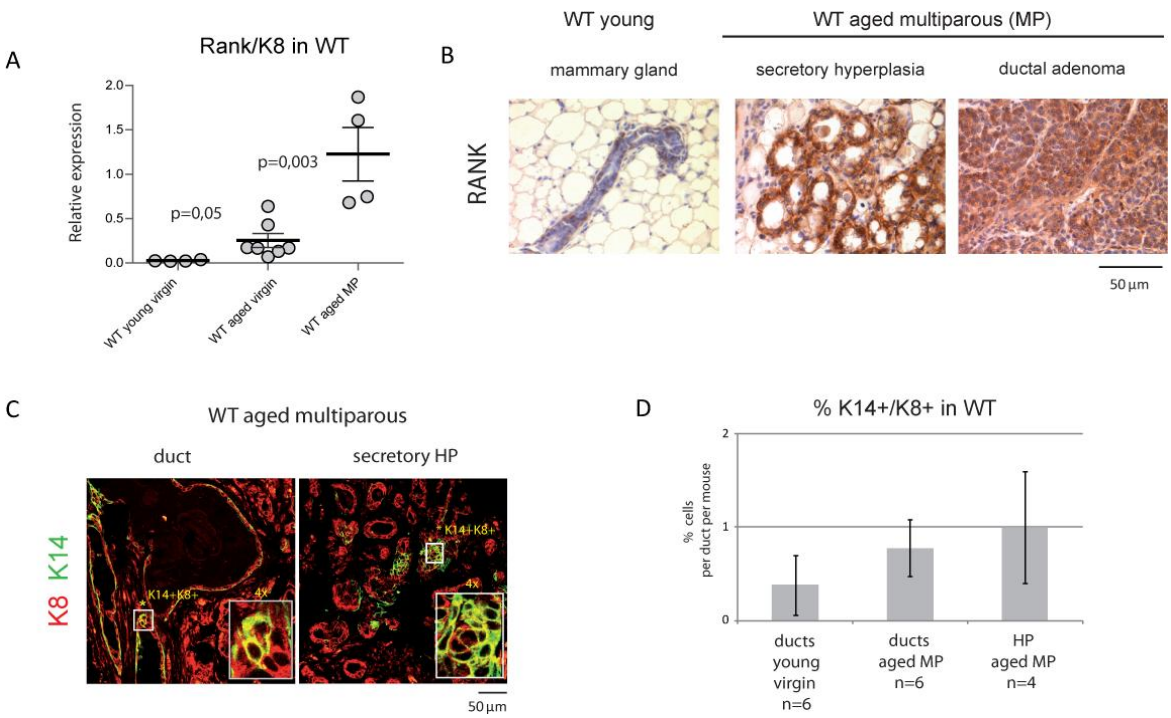

Figure 5. Physiological and pathophysiological upregulation of RANK in wild type (WT) mammary glands. See also Supporting Information Figure S6.

(A): RANK expression relative to K8 in mammary glands of young virgin, old virgin, and old multiparous (MP) WT mice. Each dot represents one mouse. Mean, SEM, and t-test p values are shown. For each sample measurements were performed in triplicate and mean was used.

(B): Representative images of RANK expression as detected by IHC in normal ducts, secretory hyperplasia, and a low-grade adenoma of aged multiparous WT mouse (adenoma was found in a 90-week-old WT) and ducts from a young mouse.

(C): Representative images of K8 (red) and K14 (green) staining in mammary epithelia from aged multiparous WT glands. K14+/K8+ are magnified in the insets.

(D): Percentage of K14+/K8+ cells versus total number of cells per duct or hyperplastic structure (HP) of aged multiparous WT mice. Quantification in ducts from young virgin females is included for comparison. Five to seven ducts/structures were analyzed per mouse. Data represent the mean and SD. Abbreviations: HP, hyperplastic; MP, multiparous; WT, wild type; IHC, immunohistochemistry.

Figure 6

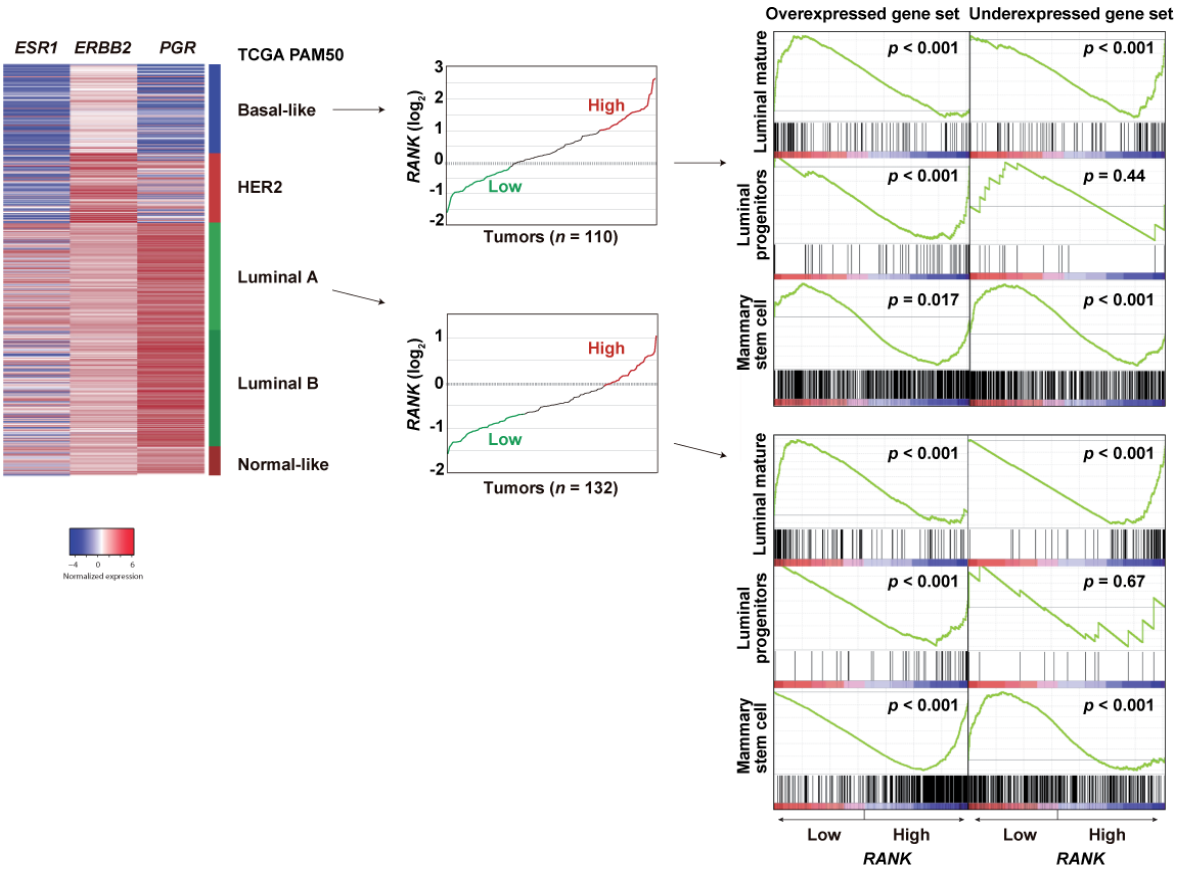

Figure 6. Association between RANK gene (also known as TNFRSF11A) expression differences among human breast tumors and the signatures that characterize mammary epithelial differentiation hierarchy. Left panel, TCGA tumors were classified into the intrinsic subtypes using the PAM50 predictor. The expression profiles of the genes encoding for ER, HER2, and PR (ESR+, ERBB2, and PGR, respectively) are shown. Middle panel, graphs showing the normalized expression values of RANK across basal-like and luminal A tumors; the first (low expression) and third (high expression) tertiles are highlighted. Right panels, GSEA graphical outputs for the association analysis between RANK tumor expression differences and the mammary epithelial differentiation signatures in basal-like and luminal A tumors. The signatures were previously identified as conserved in mice and human models, and specifically corresponding MaSC, luminal progenitors and luminal mature cells [29]. Each signature was analyzed using the gene subsets corresponding to over- or underexpression (Supporting Information Table 1). The GSEA enrichment scores and nominal p values are shown. The ECM-receptor interaction pathway was found significantly over-represented in the leading edge (false discovery rate <5% relative to rest of the given set) that defines the association between high RANK expression and the MaSC signature (overexpressed genes) in luminal A tumors. The rest of GSEA associations did not show significant over-representation of pathways beyond what was originally described for the signatures. Abbrevations: ER, estrogen receptor, IHC, immunohistochemistry, ECM, extra-cellular matrix.

Figure 7

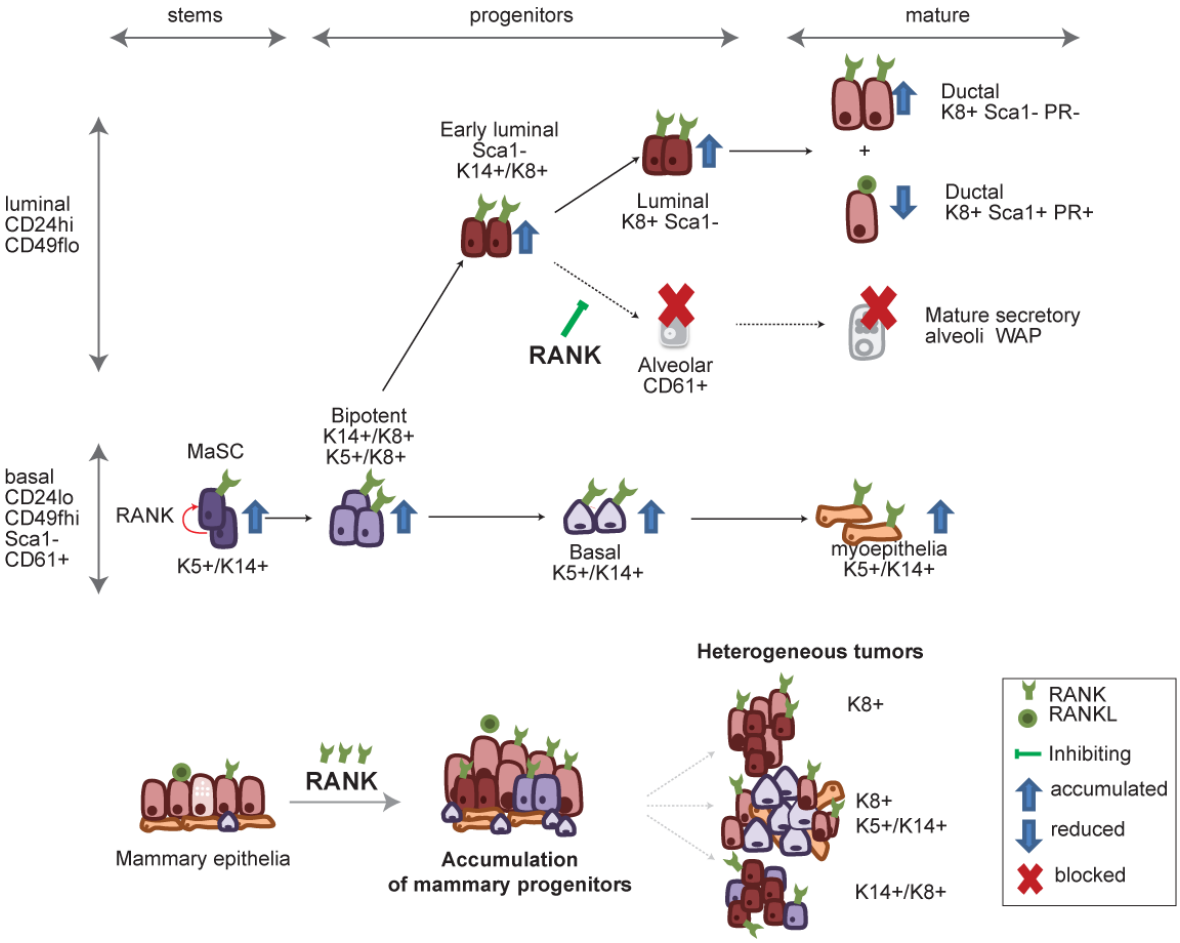

Figure 7. Schematic model showing RANK role in the regulation of mammary cell fate and breast cancer. Top: constitutive activation of RANK in virgin glands expands the luminal and basal compartment (including mammary stem cell) and disrupts luminal differentiation interfering with the generation of CD61+ luminal cells and Elf5 expression. Bottom: impaired cell commitment results in the accumulation of earlier progenitors, including bipotent K14+K8+ cells that during aging accumulate mutations and can initiate tumorigenesis. MMTV-RANK intertumor heterogeneity and the abundance of K14+/K8+ cells within the tumors suggest that each tumor may originate from progenitors that later differentiate into distinct phenotypes. Abbreviations: MaSC, mammary stem cell; RANK, receptor activator of NF-kappa B; RANKL, RANK ligand.

SUPPLEMENTAL INFORMATION

Supplemental Figure 1

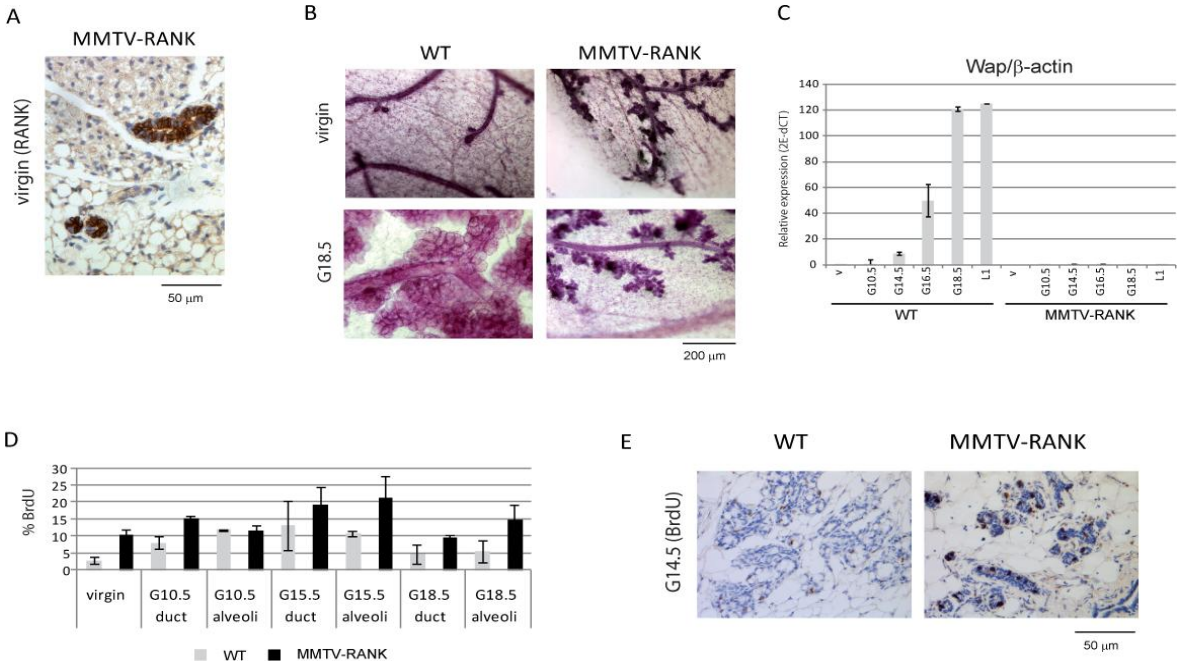

Supplemental Figure 1. RANK overexpression under the MMTV promoter impairs alveolar differentiation and promotes proliferation.

A. Representative image showing RANK expression in a normal duct of MMTV-RANK mice as measured by IHC.

B. Representative images of mammary whole mounts of virgin and late gestation (G18.5) WT and MMTV RANK mice.

C. mRNA expression levels of milk protein, Wap relative to β-actin in WT and MMTV-RANK glands at the indicated time points during gestation. Each bar represents mean values for two or three mice and SD are shown. Measurements for each sample were performed in triplicate and mean was used.

D. Frequency of BrdU positive cells in mammary glands of WT and MMTV-RANK mice at the indicated points. Each bar represents mean values and SD for two mice.

E. Representative images of BrdU immunostaining at G14.5 in WT and MMTV-RANK mammary glands.

Supplemental Figure 2

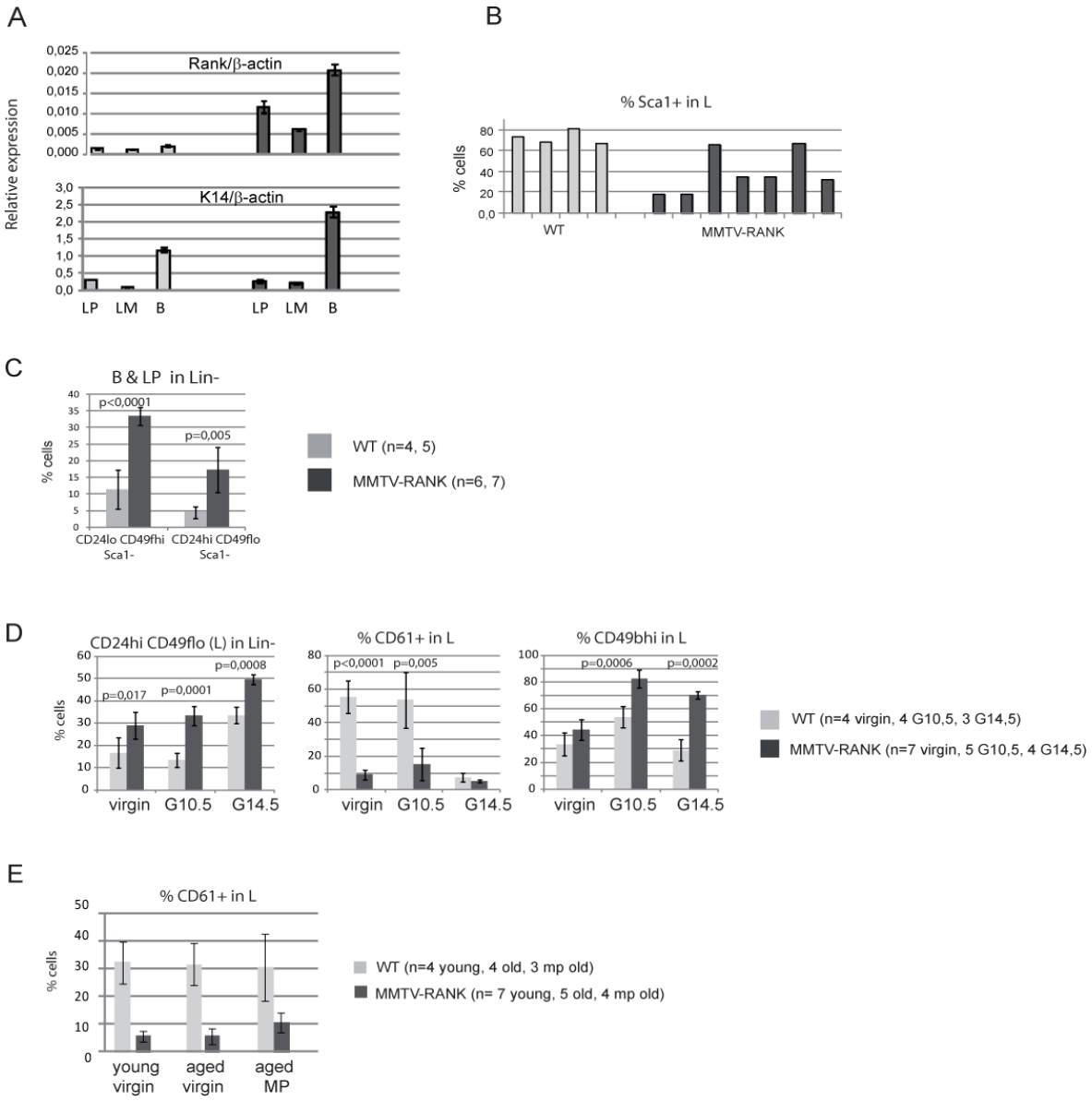

Supplemental Figure 2. RANK overexpression disrupts mammary populations in WT and MMTV-RANK mammary glands.

A. Expression of Rank and K14 mRNA relative to β-actin in FACS sorted populations of virgin WT and MMTV-RANK mammary glands. Basal (B): CD24lo CD49fhi Sca-1-, Luminal Progenitor (LP): CD24hi CD49flo Sca-1-, luminal mature (LM): CD24hi CD49fhi Sca-1+. Mammary cell pools from 2 WT and 3 MMTV-RANK mice were analyzed. Quantification was performed in duplicate, mean and SD values are shown.

B. Frequency of Sca-1+ cells within the luminal population of virgin WT and MMTV-RANK glands. Each bar represents one mouse.

C. Quantification of the percentage of CD24lo CD49fhi Sca-1- (B:basal) and CD24hi CD49flo Sca-1- (LP: luminal progenitor) in the Lin- population of virgin WT and MMTV-RANK mammary glands.

D. Quantification of the percentage of CD24+ CD49flo (luminal) in the Lin- population, and of CD61+ and CD49b+ referred to luminal cells of WT and MMTV-RANK virgin and pregnant mammary glands at the indicated points in gestation.

E. Quantification of the percentage of CD61+ cells in luminal cells of young virgin (12-15 weeks), aged virgin or multiparous (32-82 weeks) WT and MMTV-RANK mice.

Supplemental Figure 3

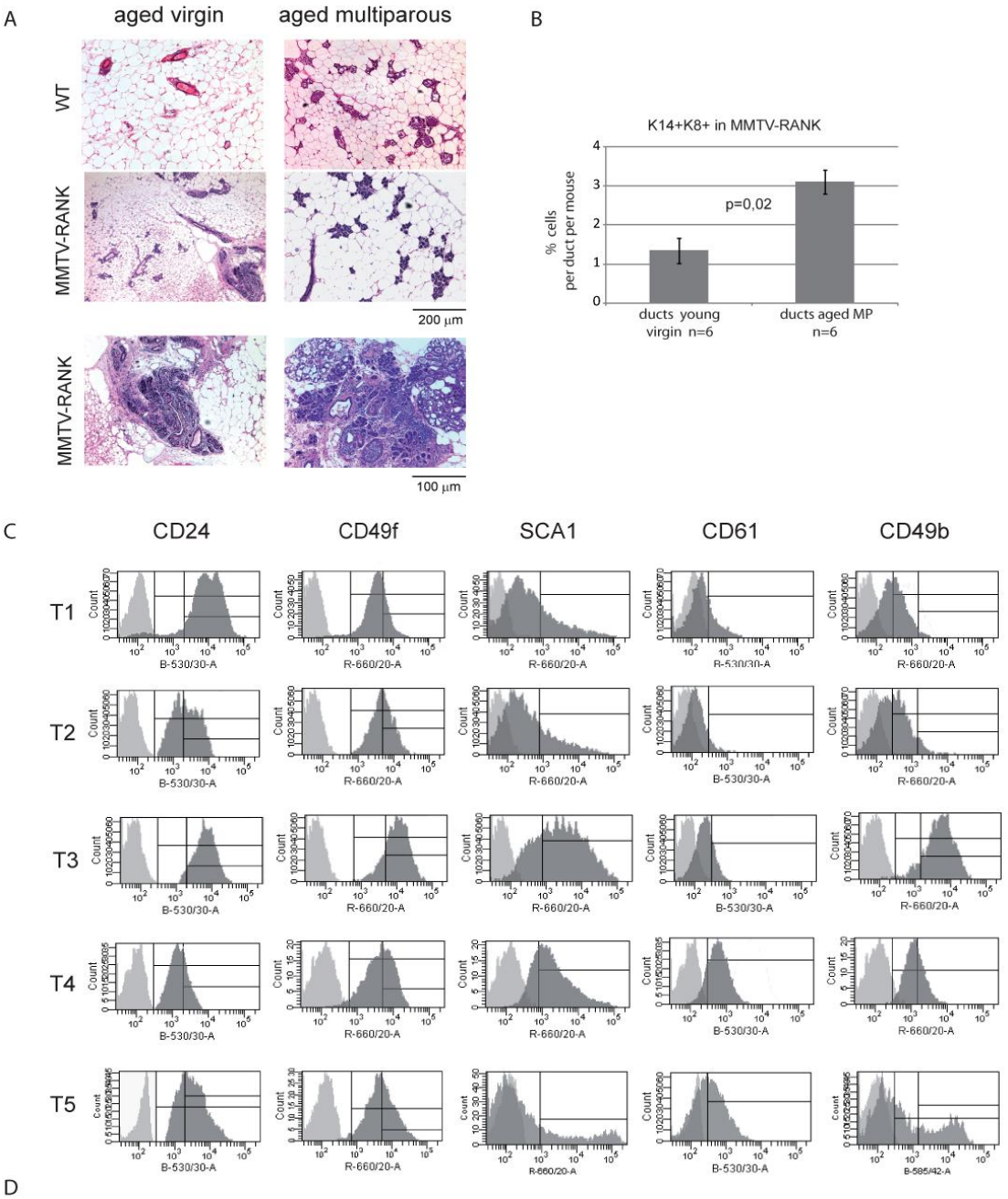

D

		RANK	PR	K8	K14	K5	SMA	K14+/K8+	K5+/K8+	CD24	CD49f	Sca1	CD61	CD49b
T1	infiltrating ductal carcinoma	+	-	+	-	-	-	-	-	hi	lo	-/lo	-/lo	-/lo
T2	squamous cell carcinoma (squamous area)	+	-	-	+	+	+	-	-					
T2	squamous cell carcinoma (infiltrating area)	+	-	+	+	+	+	+	-	lo	+	-/lo	-/lo	-/lo
T3	spindle cell carcinoma	+	-	+	+	-	-	+	-	hi	hi	+	-/lo	hi
T4	infiltrating ductal carcinoma poorly differentiated	+	-	+	+	-	-	++	-	lo	+	+	+	+
T5	infiltrating ductal carcinoma poorly differentiated	+	-	+	-	-	-	+	-	+	+	(-) (+)	+	(-/lo) (hi)
T6	intraductal carcinoma (high atypia)	+	+	+	+	+	+	-	-	n.a	n.a	n.a	n.a	n.a

Supplemental Figure 3. RANK overexpression results in preneoplasic lesions and tumors that are heterogeneous and contain K14+K8+ cells.
A. Representative images of H&E sections of aged virgin and multiparous mammary glands of WT and MMTV-RANK mice.

B. Percentage of K14+/K8+ cells versus total number of cells per duct of aged multiparous (MP) MMTV-RANK mice. Quantification in ducts from young females is included for comparison. 5-7 ducts/structures were analyzed per mouse. Mean, SD and t-test p values are shown.
C. FACS histograms showing CD24, CD49f, Sca-1, CD61 and CD49b staining within the Lin-, in four spontaneous MMTV-RANK tumors. For some markers axis for high/low populations are shown. Overlay with corresponding negative controls is shown.
D. Summary table of the tumor phenotypes. Most frequent profiles of the tumor cells are shown. n.a. not analyzed. Two populations were found in T5 with different CD49b and Sca-1 values as indicated. K14 refers to cells K14+ K8-. K5 refers to cells K5+ K8- and K8 to cells K8+K14-K5-.

Supplemental Figure 4

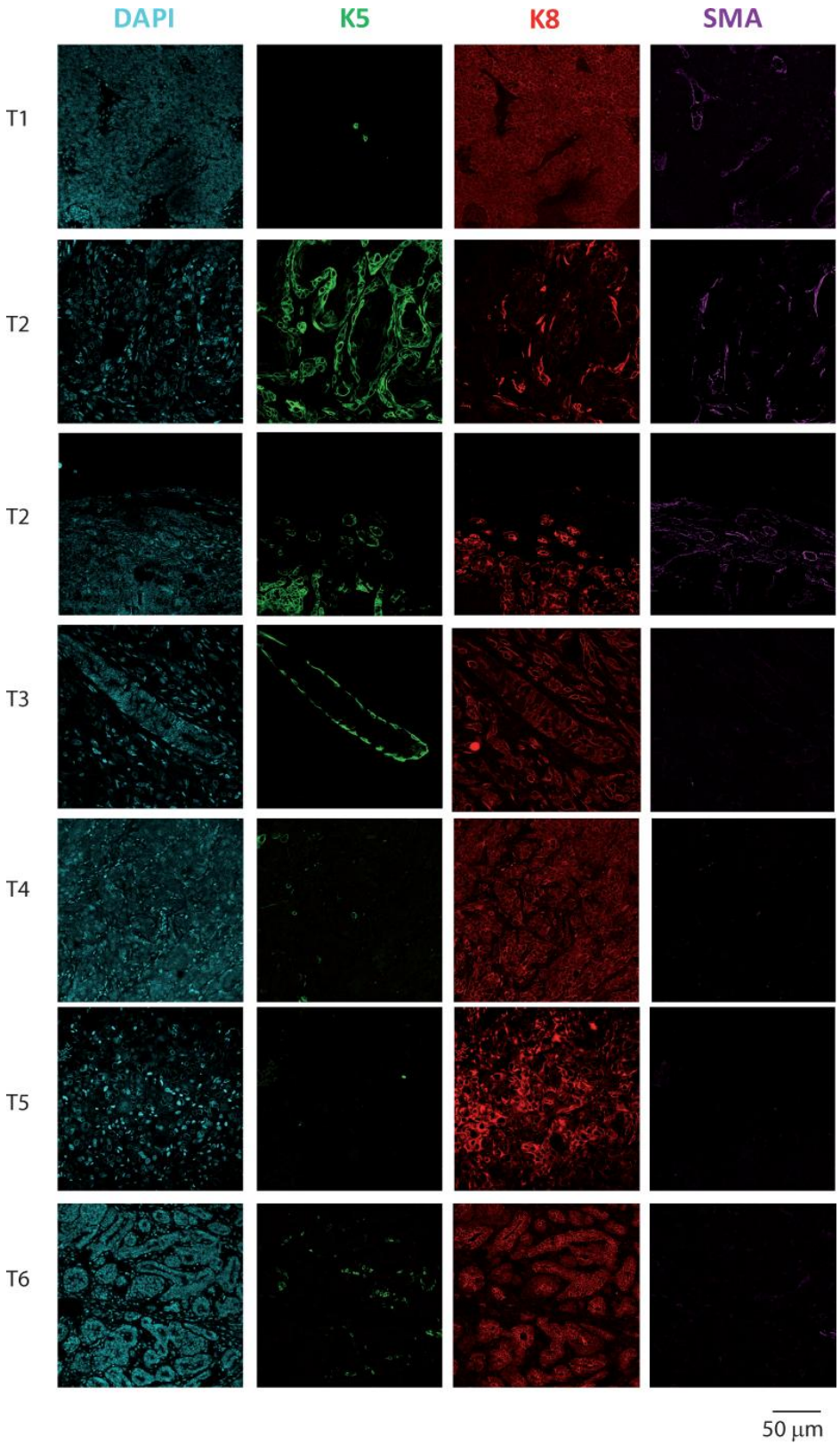

Supplemental Figure 4. Keratin profiles of MMTV-RANK spontaneous tumors reveal heterogeneity.
Representative images of DAPI, K5, K14, K8 and SMA immunostaining in spontaneous MMTV-RANK tumors.

Supplemental Figure 5

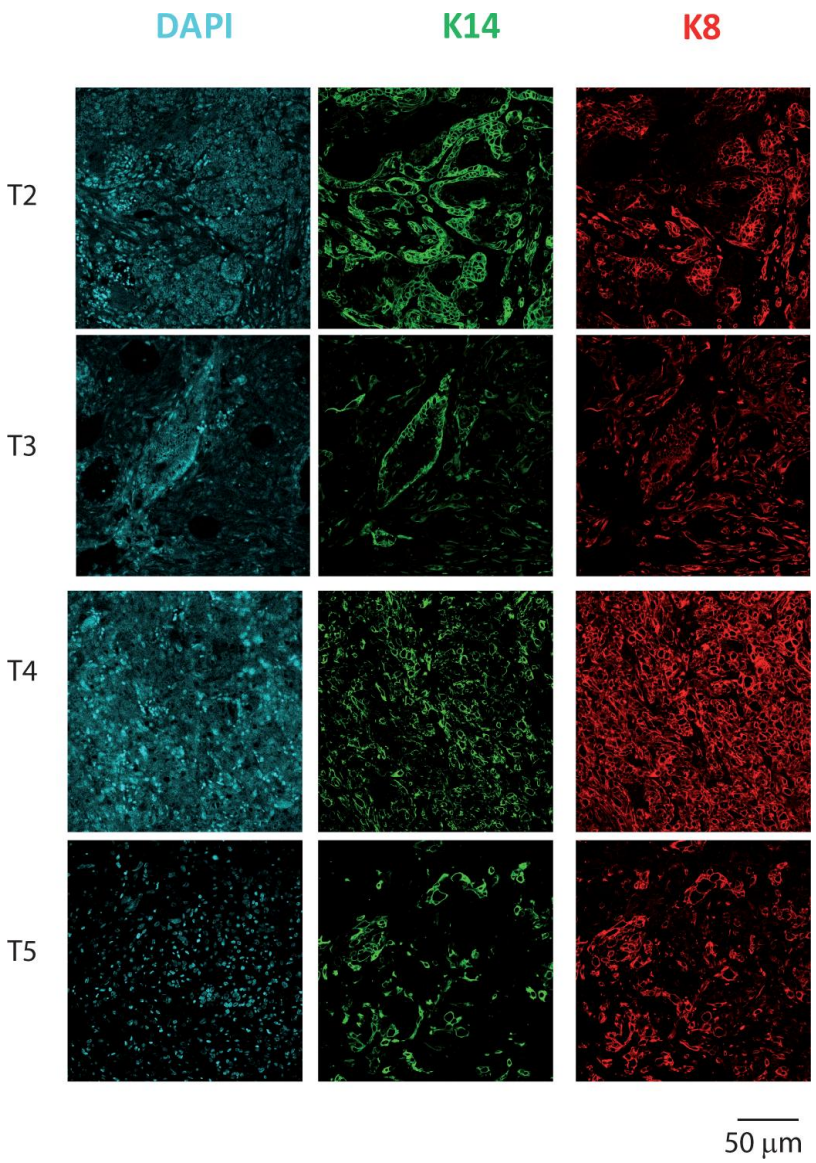

Supplemental Figure 5. Keratin profiles of MMTV-RANK spontaneous tumors reveal heterogeneity.
Representative images of DAPI, K5, K14, K8 and SMA immunostaining in spontaneous MMTV-RANK tumors.

Supplemental Figure 6

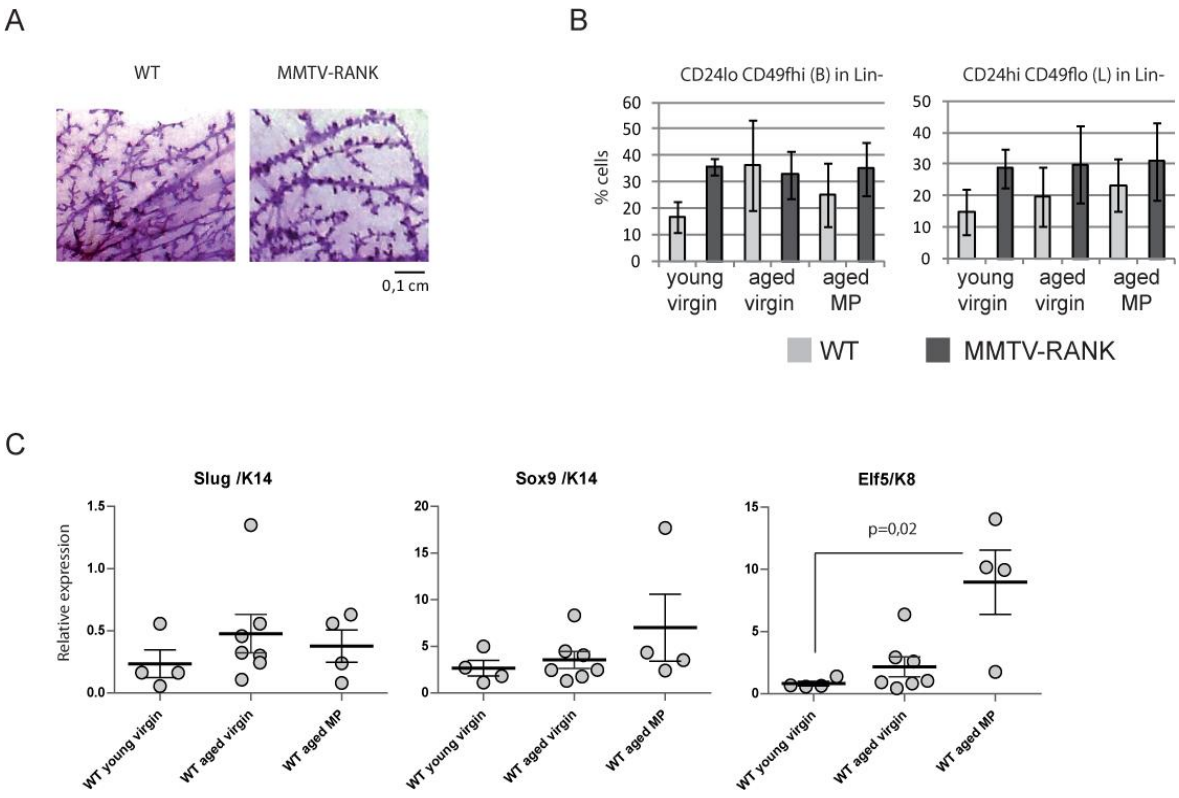

Supplemental Figure 6. Mammary glands of aged multiparous WT mice resemble those of MMTV-RANK mice.

A. Representative images of whole mounts of multiparous mammary glands of old WT and MMTV-RANK mice.

B. Quantification of the percentage of CD24lo CD49fhi (basal) and CD24hi CD49flo (luminal) in the Lin- population, of young virgin (12-15 weeks), aged virgin or multiparous (MP; 32-82 weeks) WT and MMTV-RANK mice.

C. Sox9 and Slug expression relative to K14, and Elf-5 expression relative to K8 in mammary glands of young virgin, old virgin and old multiparous (MP) WT mice. Each dot represents one mouse. Mean, SEM and significant t-test p values are shown. For each sample measurements were performed in triplicate and mean was used.

ANNEX 1

"NF-kB signaling in mammary stem cell fate"

ABSTRACT

RANK signaling pathway plays a key role regulating mammary gland development. RANK overexpression in virgin glands induces proliferation and impairs mammary stem cell fate, resulting in accumulation of mammary stem cells and intermediate progenitors. In this annex we introduce some preliminary results about the contribution of RANK downstream NF-kB signaling pathway to the mammary stem cell fate. Our results indicate a complex regulation of NF-kB signaling pathway in RANK overexpressing virgin and midgestant mammary glands. Colony forming assays from basal and luminal progenitors allowed us to follow the differentiation process for the basal and luminal compartment. Basal cells give rise to colonies that contained keratin 5, keratin 8 and cells co-expressing both keratins, demonstrating that they derive from MaSC or bipotent progenitors. In contrast, colonies derived from luminal Sca1- cells exclusively express keratin 8, evidencing their unipotent origin.

NF-kB inhibition significantly increases the number of colonies from both basal and luminal compartment but reduces their size. In the presence of NF-kB inhibitors reduced K8 expression in basal colonies and enhanced K5 expression in luminal colonies is observed. A nuclear phosphorylated IkBα is detected in basal but not in luminal colonies cultured in the presence of NF-kB inhibitors, suggesting an association between nuclear p-IKBα and stemness. No differences between WT and MMTV-RANK derived colonies are observed. These results support a role for NF-kB signaling in the differentiation of the basal lineage into luminal lineage and maintenance of luminal lineage within the mammary epithelium in both WT and MMTV-RANK acini.

Moreover, accumulation of mammary stem cells and luminal progenitors observed in MMTV-RANK mice is not mediated by enhanced activation of NF-kB signaling pathway.

INTRODUCTION

RANK/RANKL signaling pathway plays a key role in mammary gland development. We have recently shown that RANK overexpression in mammary glands increases proliferation of the mammary epithelium and disrupts mammary stem cell fate, resulting in accumulation of mammary stem cells (MaSC) and intermediate progenitors (Pellegrini et al. 2013). Moreover, activation of RANK signaling at midgestation impairs mammary alveolar differentiation and lactogenesis through inhibition of PrlR/STAT5/Elf5 signaling pathway (Cordero et.al, under revision).

Previous results demonstrate that RANK overexpression in MCF10A human mammary epithelial cells leads to constitutive activation of several pathways including NF-kB (Palafox et al. 2012), a protein complex that plays a crucial role in biological processes such as cell proliferation, immune response or cancer (Demicco et al. 2005; Liu et al. 2010; Kendellen et al. 2014). Five NF-kB members exist in mammals including RelA (p65), RelB, c-Rel, p50 and p52-p100, which form different complexes of homo- and heterodimers that are retained inactive in the cytoplasm by a family of NF-kB inhibitors, IKBs (IKB-α, β, ε) (Bonizzi y Karin 2004; Gilmore 2006). Importantly, two main NF-κB-activating pathways exist in cells: canonical and non-canonical. The most common mechanism of regulation of NF-kB activity is through the canonical pathway, where IKK complex (IKKα-β) is activated by diverse stimuli such as TNF-α or lipopolysaccharide (LPS). Activated p-IKK phosphorylates IKBα inhibitor protein resulting in its ubiquitination and degradation, and subsequent release of the p65-p50 heterodimer for activation and nuclear translocation (Karin 1999). The activation of the pathway promotes inflammation, cell survival and proliferation (Gerondakis et al. 2014). Alternatively, NF-kB signaling can also be activated through the non-canonical pathway, where specific members of the TNF cytokine family, such as CD40 or BAFF promote IKK-α phosphorylation by NIK. Activated p-IKK-α phosphorylates the p100 precursor of p52 to generate p52/RelB heterodimers that have affinity for a subset of NF-kB response elements and generate a distinctive gene expression pattern in the nucleus which favors chemokine production and lymphoid stroma survival (Perkins 2007; Gerondakis et al. 2014).

Multiple evidences suggest that NF-kB activity is important for mammary gland development. Indeed, virgin mice lacking the gene encoding for IkBα and therefore showing constitutive activation of NF-kB display an increased epithelial cell proliferation and lateral ductal branching (Brantley et al. 2001), a similar phenotype to that observed in MMTV-RANK mammary glands (Pellegrini et al. 2013). It has been previously demonstrated an activation of the canonical NF-kB pathway, with increased p65 nuclear

translocation, in MMTV-RANK MECs under RANKL stimulation *in vitro*, compared to WT (Gonzalez-Suarez et al. 2007). Moreover, activation of IKK-α in response to RANK engagement is required for CyclinD1 induction and proliferation of lobuloalveolar epithelial cells, evidenced by the defective MECs proliferation, as well as the retarded growth of the lobuloalveolar tree during pregnancy in IKK-$\alpha^{AA/AA}$ ''knockin'' mice (Y. Cao et al. 2001; Yixue Cao, Luo, y Karin 2007).

We therefore aimed to investigate whether RANK overexpression leads to enhanced activation of NF-kB signaling and its putative contribution to the accumulation of mammary stem cells and progenitors observed in virgin MMTV-RANK mammary glands (Pellegrini et al. 2013).

RESULTS AND DISCUSSION

1. Complex regulation of NF-kB signaling in MMTV-RANK mice

First, we analyzed the expression and activation of NF-kB in the mammary glands of WT and MMTV-RANK mice.

Analysis by immnunohistochemistry (IHC) in virgin WT and MMTV-RANK mammary glands showed slightly increased p65 staining in MMTV-RANK compared to WT ductal cells, where little p65 expression was found (Fig 1). Small alveoli, abundant in MMTV-RANK virgin glands (Pellegrini et al. 2013), showed higher levels of p65 expression than ductal cells (Fig 1A), although the staining looks mostly cytoplasmatic. Upon activation of the pathway p65 is phosphorylated and translocates to the nuclei. Thus, the expression levels and cellular localization of different NF-kB proteins was analyzed by western blot (Fig 2A). Cytoplasmatic, nuclear and chromatin protein extracts were obtained from virgin WT and MMTV-RANK MECs. Preliminary results revealed variable levels of p65, p-IkBα and p52/p100 in the cytoplasm of WT and MMTV-RANK virgin glands. No clear differences in p65 expression in the nuclear or chromatin fraction were observed. Nuclear p-IkBα was detected in 2 out of 3 MMTV-RANK virgin glands analyzed. IkBα cytoplasmic fraction was comparable between genotypes; in the chromatin fraction two IkBα bands with different molecular weights were observed but they were present in both WT and MMTV-RANK mammary cells. The higher band could correspond to a sumoylation modification that has been previously described (Desterro, Rodriguez, y Hay 1998; Carbia-Nagashima et al. 2007). Protein post-transcriptional modifications with the ubiquitin-like protein SUMO causes IkBα resistance to proteasome-mediated degradation (Demicco et al. 2005), although the function and physiological context for this modification remains to be addressed. Interestingly, MMTV-RANK mice showed lower p50 levels in the chromatin, and increased nuclear p-IKKα compared to WT (Fig 2A). The lack of differences in p65 suggested that this increase in p50 in WT MECs corresponds to p50 homodimers, which have been previously described to promote anti-inflammatory responses though transcription of interleukin-10 (IL-10) (S. Cao et al. 2006), suggesting a NF-kB-induced inflammatory response in RANK overexpressing mice. In addition, nuclear p-IKKα has been associated with tumor progression in human colorectal and prostate cancer (Margalef et al. 2012; Ammirante et al. 2013). The specific function of nuclear p-IKKα in mammary epithelial cells remains unexplored. Given the reduced progestin-driven mammary tumor onset in mice with deletion of IKKα in the mammary epithelium (Schramek et al. 2010),

this increase in nuclear p-IKKα levels could be related with pro-tumorigenic signals in MMTV-RANK mammary glands that would be later activated under hormonal stimuli. Together, these results suggested that alterations in NF-kB signaling pathway could have relevance in the RANK-overexpressing MECs phenotype and mammary tumor formation previously described (Pellegrini et al. 2013).

Previous data showed that mice overexpressing IkBα (MMTV-IkBα^{SR}) display no defects in virgin mammary gland but a transient delay in mammary ductal branching development at early pregnancy (Demicco et al. 2005). However, this delay is recovered at mid-late gestation due to nuclear CyclinD1 induction and activation of RelB/p52 non-canonical NF-kB, indicating that NF-kB is essential for mammary gland differentiation although different NF-kB complexes may be active at different points in development (Demicco et al. 2005; Pratt et al. 2009). A negative crosstalk between NF-kB and the PrlR/Jak2/Stat5 signaling pathway, which occurs at the level of Stat5 tyrosine phosphorylation, has been reported during pregnancy (Geymayer y Doppler 2000). We therefore analyzed the expression of NF-kB pathway in midgestant (G.14,5) WT and MMTV-RANK MECs. Preliminary results showed increased p-p65 and p65 cytoplasmic levels in MMTV-RANK MECs, but no expression of p-IkBα or differences in total IkBα were found between WT and MMTV-RANK MECs, indicating that canonical NF-kB pathway is not constitutively active in MMTV-RANK pregnant mice. Thus, our results suggested a complex regulation of NF-kB pathway at midgestation in RANK overexpressing glands, although further experiments are required to analyze other members of NF-kB pathway and their contribution to the MMTV-RANK phenotype.

Next, we aimed to discriminate the population within WT and MMTV-RANK virgin mammary glands showing NF-kB expression or activation. Using cell surface markers, we isolated virgin WT and MMTV-RANK CD45- CD31- lineage negative (Lin -) CD24hi CD49flo Sca1- (luminal Sca1- or luminal progenitors) and Lin - CD24hi CD49flo Sca1+ (luminal Sca1+ or luminal differentiated) populations. The Lin - CD24lo CD49fhi basal population was subdivided in CD24^{lo} CD49f^{hi} (MaSC enriched) and CD24^{lo} CD49f^{lo} (myoepithelia) as previously shown (Zhang et al. 2013) (Fig 3A). In agreement with previous data (Beg et al. 1995), WT unsorted cells stimulated with LPS (1,6 μg/mL) showed activation of canonical NF-kB pathway (Fig. 3B), evidenced by p65 nuclear translocation, demonstrating that NF-kB pathway could be activated *in vitro* in our 3D cultures.

Our results confirmed population purity, as luminal cells were cytokeratin 8 positive (K8+) and negative for cytokeratin 5 (K5-), whereas basal cells were K8-, K5+ (Fig 3C, left panel).

P65 expression was found exclusively in the cytoplasm of all four WT and MMTV-RANK cell populations indicating that the pathway is not active (Fig 3C, right panel). Importantly, we showed that p65 expression was more abundant in luminal Sca1- cells compared to luminal Sca1+, MaSC and myoepithelial cells in both WT and MMTV-RANK mice (Fig 3D, E). No differences in the frequency of p65+ cells, neither in the intensity of the staining were found between WT and MMTV-RANK populations (Fig 3D, E). Despite of the increase in p65 positive cells found in MMTV-RANK luminal Sca1+ population, very few cells were quantified, consistent with the disrupted luminal Sca1+ population described in MMTV-RANK mice (Pellegrini et al. 2013). In the basal compartment, the frequency of cells showing p65 cytoplasmic staining was higher in MaSC enriched population as compared to myoepithelial cells, but again no differences were detected between WT and MMTV-RANK cells (Fig 3D). Taken together these results indicate that p65 is expressed in luminal progenitor cells and, to a lesser extent, in MaSCs from both WT and MMTV-RANK. However, NF-kB canonical pathway is not active as no nuclear p65 staining was detected. In contrast to our data, Pratt et.al found p65 activation in 100% of CD24hi CD49flo sorted luminal cells, and absence of p65 expression in the basal CD24lo CD49fhi cells (Pratt et al. 2009). Differences with our results may be related to the sensitivity of the technique, estrous cycle, activation during cell isolation or mouse strain, and will be clarified in the future.

2. NF-kB inhibition interferes with differentiation and maintenance of the luminal lineage

Next, in order to functionally address the role of NF-kB pathway in mammary cell fate, we took advantage of *in vitro* 3D colony forming assays. It has been previously described that luminal progenitors and stem cells have higher colony forming ability (Shackleton et al. 2006; Stingl et al. 2006; Asselin-Labat et al. 2007). Thus, FACs-isolated basal and luminal Sca1- MECs from virgin WT and MMTV-RANK mice were seeded on 3D cultures, and the expression levels for p65, IkBα and p-IkBα were analyzed by IF after 24h and 4 days of culture in the presence of RANKL. Keratin staining (basal K5 and K14, luminal K8) was also analyzed to follow the cell differentiation process. After 24h of culture, K5+ expression was detected exclusively in basal cells, while K14+ expression was detected in both basal and luminal populations as previously reported (Shackleton et al. 2006) (Fig 4), suggesting that K14 could label bipotent progenitors that differentiate into basal or luminal lineages. Luminal MECs were K8+ K5- K14+, whereas basal MECs were K5+ K14+ and a faint K8+

staining was also found, suggesting that basal cells initiated the differentiation process into luminal cells. Moreover, a faint p65 staining was found mostly in the cytoplasm and no differences were detected in p65 or IkBα between basal and luminal single cells, nor between WT and MMTV-RANK cells (Fig 4). A small increase in cytoplasmic p-IkBα levels was observed in basal WT and MMTV-RANK MECs, compared to luminal MECs, suggesting a modest increase in NF-kB signaling in this population.

After 4 days in culture, MECs had already developed colonies. Basal colonies contained K5+ and K14+ cells as well as K8+ cells, evidencing the MaSC differentiation process into luminal cells (Fig 5). In contrast, luminal colonies contained K8+ and K14+ cells but no K5+ cells in both WT and MMTV-RANK cultures. P65 and IkBα staining was detected in MMTV-RANK luminal colonies at higher levels than WT luminal colonies, whereas basal WT and MMTV-RANK colonies expressed barely detectable p65 levels (Fig 5A), in correlation with previous results (Figs 3C, 3D). P-IkBα staining was not detected in any condition, whereas total IkBα was found in basal WT and MMTV-RANK colonies at similar levels. We could not detect p65 nuclear translocation in any condition. In contrast, nuclear p65 was observed in WT basal and luminal colonies under LPS treatment (Fig 5B).

As NF-kB activation is a transient and cyclical event (Gilmore 2006), we cannot rule out the possibility that we missed p65 nuclear translocation in our non-synchronized cultures or that the expression levels of nuclear p65 were below the limit of detection.

Next, we functionally assayed the impact of NF-kB pathway inhibition in our colony forming assays. Again, basal and luminal Sca1- populations were cultured *in vitro* in 3D cultures in the presence of RANKL and NF-kB inhibitors. We selected SN50, a synthetic peptide that blocks the nuclear translocation of p50/p65 complexes (Torgerson et al. 1998). In addition, we used the BAY family of NF-kB inhibitors. In particular, BAY65 inhibits IKK-β subunit, preventing IkBα phosphorylation and subsequent canonical NF-kB activation (Ziegelbauer et al. 2005; Suzuki et al. 2011), whereas BAY11 inhibits IkBα phosphorylation (Pierce et al. 1997; Keller et al. 2006). NF-kB inhibitors were added 24h after plating virgin WT and MMTV-RANK virgin MECs in 3D cultures. SN50 was used at two different concentrations (18μM and 72μM), as it has been reported that SN50 acts as a dominant negative and therefore its inhibitory effect increases with concentration (Lin et al. 1995). Efficiency of SN50 inhibition was corroborated by the decrease of p65 nuclear staining in LPS-treated MMTV-neu tumor cells pre-incubated with the inhibitor (Fig 6A). After 6 days in culture, SN50 inhibition at high concentrations (72μM) and BAY 11 (0,2μM) significantly increased the number of basal and luminal colonies in both WT and MMTV-

RANK as compared to the corresponding untreated controls (Fig 6B). Inhibition with SN50 at lower concentrations (18μM), BAY65 (5μM) and BAY11 (0,5μM) also generally increased the number of colonies to a lesser extent. Higher concentrations of BAY inhibitors completely abolished colony formation, which may be attributed to toxicity or alternatively that a fine regulation of NF-kB activation defines the phenotype; a minimal activation of NF-kB pathway is required to allow colony formation. Importantly, colony size was smaller in the presence of NF-kB inhibitors in basal and especially in luminal cultures, compared to untreated controls (Fig 6C). These results suggest that NF-kB inhibition alters mammary epithelial cell colony formation in both basal and luminal clusters in WT and MMTV-RANK. The increased number of smaller colonies suggests that inhibition of NF-kB increases the number of progenitor/MaSC but may interfere with proliferation and/or differentiation. Further experiments using genetic strategies will further enlighten the role of NF-kB regulating the balance between MECs self-renewal and differentiation.

In order to address whether inhibition of NF-kB interferes with the mammary differentiation process, we analyzed the levels of NF-kB (p65, p-IkBα and IkBα) and keratins (K5, K14 and K8) by IF in both basal and luminal progenitor Sca1- MECs from WT and MMTV-RANK treated with NF-kB inhibitors. After 6 days in culture, basal WT and MMTV-RANK MECs formed K5+/K14+ colonies with some luminal K8+ cells (Fig. 7), as previously observed (Fig. 4A). We found p65+ staining and low IkBα and p-IkBα expression exclusively in the cytoplasm in those colonies. Importantly, a decrease in K8+ cells was observed in both WT and MMTV-RANK basal colonies with inhibited NF-kB pathway (Fig. 7). These results suggested that inhibition of NF-kB pathway alters the differentiation of MaSCs (K5+) from the basal compartment into K8+ cells in both WT and MMTV-RANK under RANKL treatment *in vitro*. No differences in cytoplasmic p65 or IkBα expression were observed in WT and MMTV-RANK basal NF-kB inhibited colonies, whereas increased p-IkBα nuclear expression were observed (Fig. 7). Although the function of this nuclear p-IkBα in MECs remains unknown, recent data from Mulero et.al showed that nuclear p-IkBα has higher molecular weight than “normal” protein, evidencing post-transcriptional modifications with SUMO proteins (Mulero et al. 2013). Importantly, this nuclear phosphorylated/sumoylated form of IkBα (PS-IkBα) has implications in skin homeostasis, as decreased PS-IkBα protein levels have been associated with an induction of the keratinocyte differentiation process (Mulero et al. 2013). Thus, nuclear PS-IkBα may have a relevant role inducing stemness in NF-kB-inhibited mammary epithelial cells.

Consistent with previous observations (Fig 5A), luminal WT and MMTV-RANK MECs formed K8+ K14+ K5- colonies. These colonies showed higher cytoplasmic p65 expression levels compared to basal colonies, and extremely low p-IkBα (Fig 8). Luminal colonies treated with SN50 and, to a lesser extent, BAY65 and BAY11 inhibitors contained basal K5+ cells in contrast to corresponding untreated controls in both WT and MMTV-RANK. These results suggest that inhibition of NF-kB signaling alters mammary cell fate inducing luminal cell transdifferentiation into basal lineage. A reduction in cytoplasmic p65 expression but no changes in IkBα or p-IkBα were observed in WT and MMTV-RANK luminal colonies under NF-kB inhibition (Fig 8). In contrast to observations in basal cells, nuclear p-IkBα was not detected in colonies derived from luminal cells treated with any of the inhibitors. Further experiments and additional markers to differentiate luminal progenitors from luminal differentiated cells are required to clarify whether NF-kB also participates in the differentiation of luminal progenitor cells into mature luminal cells.

In conclusion, our results indicate that NF-kB is an essential regulator of the mammary cell fate, regulating the balance between self-renewal, differentiation and luminal cell fate. No differences between WT and MMTV-RANK acinar cultures were observed, suggesting that accumulation of MaSCs and luminal progenitors observed in MMTV-RANK mice is not mediated by enhanced activation of NF-kB pathway. Complementary strategies using additional specific inhibitors or genetic approaches are required to corroborate that NF-kB promotes differentiation of basal cells into the luminal lineage. As discussed above there are many potential intermediates between RANK signaling transduction in mammary epithelia that could be responsible of the subsequent changes observed in mammary stem cell fate.

Importantly, our results revealed a key role for NF-kB signaling in mammary cell fate, regulating the balance between self-renewal and differentiation. Inhibition of NF-kB not only interferes with differentiation of basal cells into luminal cells, but also induces transdifferentiation of luminal cells into basal cells. The nuclear phosphorylated form of IkBα could be involved in retaining the MaSC/basal phenotype preventing differentiation into the luminal lineage. In summary, activation of NF-kB pathway is essential for differentiation and maintenance of the mammary epithelial luminal lineage.

MATERIALS AND METHODS

Mice

All research involving animals was done in IDIBELL animal facility and complied with protocols approved by the IDIBELL Committee on Animal Care, local animal welfare laws, guidelines and policies. MMTV-RANK mice in FVB background were obtained through collaboration with Dr Bill Dougall (Oncology Research-AMGEN).

Mammary cell isolation and flow cytometry

Single cells were isolated from mammary glands as previously described (Smalley MJ et al, 2010, Zhang W et al, 2013). Briefly, fresh tissues were mechanically dissected with McIlwain tissue chopper and enzymatically digested with appropriate medium (DMEM F-12, 0.3% Collagenase A (Roche), 2.5U/mL dispase (GIBCO), 20 mM HEPES, and Penicilin/Streptomiciyn) 45 minutes at 37°C. Samples were washed with Leibowitz L15 medium 10% fetal bovine serum (FBS) between each step. Erythrocytes were eliminated by treating samples with hypotonic lysis buffer (Lonza Iberica), and fibroblasts were excluded by incubation with DMEM F-12 10% FBS 1 hour at 37ºC (the majority of fibroblasts attach to tissue culture plastic while most of epithelial organoids do not). Single epithelial cells were isolated by treating with trypsin 2 minutes at 37°C. Cell aggregates were removed treating with 2.5U/mL dispase (GIBCO), 20U/ml DNase (Invitrogene) 5 minutes at 37ºC. Cell suspension was finally filtered with 40 μm filter and counted. Single cells were then labeled with antibodies against CD24-FITC (5 μg/mL, M1/69 BD Pharmingen, San Diego, CA, http://www.bdbiosciences.com), CD49f-a647 (2,5 μg/mL, GoH3, BD Pharmingen), and Sca-1-PE (0,5 μg/mL, Ly-6A/E, BD Pharmingen), Lymphocytes and endothelial cells were excluded in flow cytometry using CD45-PECy7 (0,125 μg/mL, 30-F11 Biolegend) and CD31-PECy7 (0,5 μg/mL, 390 Biolegend) antibodies, respectively. Cell sorting was performed using MoFlo (Beckman Coulter) at 25psi and using a 100 mm tip.

Colony forming assays

For Colony forming assays in 3D cultures, 5.000 primary MECs isolated from virgin WT and MMTV-RANK females were plated in corresponding growth media. Basal CD24hi CD49fhi cells were plated in Basal medium (DMEM F12, FBS 1%, B27 1X, EGF 10 ng/mL, insulin 5 μg/mL, cholera toxin 100 ng/mL and Penicilin/Streptomiciyn). ROCK inhibitor (10 μM Y-27632, Sigma-Aldrich) was added to basal cultures. Luminal CD24hi CD49flo Sca1- cells

were plated in Luminal medium containing (DMEM F12, FBS 10%, EGF 10 ng/mL, insulin 5 µg/mL, cholera toxin 100 ng/mL and Penicilin/Streptomiciyn). Rankl-LZ (1 µg/ml; Amgen Inc) was added to both basal and luminal cultures.

Immunofluorescence

For 2D immunofluorescence, 5000 unsorted or FACS-isolated basal and luminal cells were resuspended in 10µl of corresponding growth media and left dry in a slide to get them fixed. Briefly, cells were then fixed in 2% paraformaldehyde (20 min), permeabilized with PBS containing 0,5% Triton X-100 (30 min), and washed twice with PBS 0.05% Tween-20. Antigens were blocked with 5%BSA 0.5% Tween-20 in PBS 1h, and primary antibodies against p65 (D14E12, Cell Signaling), K8 (TROMA, dshl, Developmental Studies Hybridoma Bank, Iowa City, Iowa), K5 (AF-138, Covance, Princeton, NJ) were incubated overnight at 4ºC. Opportune fluorochrome conjugated secondary antibodies (Invitrogen) were added after primary incubation, diluted 1:500 in PBS and incubated for 40 min. Cell nuclei were stained with DAPI (Sigma), and cells were mounted with Prolong ® Gold Antifade (Life Technologies).

3D acinar structures were stained as previously described (Debnath J, 2003). Briefly, acini were fixed in 2% paraformaldehyde (20 min), permeabilized with PBS containing 2% Triton X-100 (30 min), and washed with PBS-Glycine 100 mM (three washes of 15 min each). Antigens were blocked with IF buffer (PBS, 7.7 mM NaN_3, 0.1% bovine serum albumin, 0.2% Triton x-100, 0.05% Tween-20) + 10% goat serum for 1 h and then with IF buffer + goat serum + 20 µg/mL F(ab') fragment (Jackson ImmunoResearch) for 30 min. Primary antibodies for p65 (D14E12, Cell Signaling), p-IkB (S32/36, Cell Signaling), IkB (C-21, Santa Cruz), K8 (TROMA, dshl, Developmental Studies Hybridoma Bank, Iowa City, Iowa), K5 (AF-138, Covance, Princeton, NJ) and K14 (AF-64, Covance), were incubated overnight in a humid chamber. Opportune fluorochrome conjugated secondary antibodies (Invitrogen) were added after primary incubation, diluted 1:500 in IF buffer + 10% goat serum and incubated for 40 min. Acini were then washed with IF buffer and cell nuclei were stained with DAPI (Sigma), and then mounted with Prolong ® Gold Antifade (Life Technologies). Confocal analysis was carried out using Leica confocal microscope. Images were captured using LasAF software (Leica).

Tissue section histology and Immunostaining

For histological analysis, 4% PFA fixed, paraffin embedded mammary glands were cut in 3 µm sections. Antigen heat retrieval with citrate was performed before incubation with a primary antibody against p65 (D14E12, Cell Signaling). The antibody was incubated overnight at 4°C, detected with streptavidin horseradish peroxidase (Vector) and revealed with DAB substrate (DAKO).

Activation and Inhibition assays.

For NF-kB activation assays, cultured cells were incubated with LPS (1.6 µg/mL) for 30 minutes before IF staining.

For inhibition assays, FACS-isolated luminal and basal MECs from virgin WT and MMTV-RANK mice were plated in 3D cultures in the corresponding basal/luminal medium. 24h later, 5 µM BAY65 (NF-κB inhibitor; Calbiochem), 0,2 µM or 0,5 µM BAY11 (NF-κB inhibitor; Calbiochem) and 18 µM or 72 µM SN50 (NF-κB inhibitor; Enzo) were added to the medium during 24h or 6 days. 2h after addition of the inhibitor, RANKL was added to the medium. The treatment was refreshed daily for BAY inhibitors or every 48h for SN50 to avoid the degradation of inhibitors. Later, medium was removed and IF was performed, or protein extracts were collected.

Cell Fractionation and Western blot

For cytoplasm/nuclear/chromatin separations, WT and MMTV-RANK MECs were lysed in 10mM HEPES, 1.5mM MgCl2, 10mM KCl, 0.05%NP40 at pH 7.9, 10 min on ice and centrifuged at 13.000 rpm. Supernatants were recovered as cytoplasmic fraction and the pellets lysed in 5mM HEPES, 1.5mM MgCl2, 0.2 mM EDTA, 0.5mM DTT and 26% glycerol and sonicated 5 min three times to recover the soluble nuclear fractions. Pellet included the chromatin fraction. Western blotting with cell lysates was performed with standard protocols. Briefly, blots were blocked for 1 h at room temperature with 5% milk in 10 mM Tris-HCl pH 7.5, 150 mM NaCl containing 0.1% Tween 20 (TBST) and incubated overnight at 4ºC with primary antibodies reactive to p-P65 (#3033, Cell Signaling), p65 (D14E12, Cell Signaling), p-IkBα (S32/36, Cell Signaling), IkBα (C-21, Santa Cruz), p-IKK-α (sc-23470-R, Santa Cruz), p50 (sc-7178, Santa Cruz), p52-p100 (05-361, Upstate), Tubulin (T9026, Sigma-Aldrich) and β-actin (AC-74, Sigma.Aldrich). After washing, blots were incubated with horseradish peroxidase-conjugated secondary antibodies (1:2000, Promega) for 1 h at 20–25 °C, and revealed with enhanced chemiluminescence.

Statistical analysis

Statistical analyses were performed using GraphPad Prism software. Analysis of the differences between two mouse cohorts or conditions was performed with a two-tailed Student's t-test. Variability was calculated using standard error of measurement (SEM).

REFERENCES

Ammirante, Massimo, Ali I. Kuraishy, Shabnam Shalapour, Amy Strasner, Claudia Ramirez-Sanchez, Weizhou Zhang, Ahmed Shabaik, and Michael Karin. 2013. «An IKKα–E2F1–BMI1 cascade activated by infiltrating B cells controls prostate regeneration and tumor recurrence». *Genes & Development* 27 (13): 1435-40. doi:10.1101/gad.220202.113.

Asselin-Labat, Marie-Liesse, Kate D. Sutherland, Holly Barker, Richard Thomas, Mark Shackleton, Natasha C. Forrest, Lynne Hartley, et al. 2007. «Gata-3 Is an Essential Regulator of Mammary-Gland Morphogenesis and Luminal-Cell Differentiation». *Nature Cell Biology* 9 (2): 201-9. doi:10.1038/ncb1530.

Beg, A. A., W. C. Sha, R. T. Bronson, and D. Baltimore. 1995. «Constitutive NF-Kappa B Activation, Enhanced Granulopoiesis, and Neonatal Lethality in I Kappa B Alpha-Deficient Mice.» *Genes & Development* 9 (22): 2736-46. doi:10.1101/gad.9.22.2736.

Bonizzi, Giuseppina, and Michael Karin. 2004. «The Two NF-kappaB Activation Pathways and Their Role in Innate and Adaptive Immunity». *Trends in Immunology* 25 (6): 280-88. doi:10.1016/j.it.2004.03.008.

Brantley, Dana M., Chih-Li Chen, Rebecca S. Muraoka, Paul B. Bushdid, Jonathan L. Bradberry, Frances Kittrell, Daniel Medina, Lynn M. Matrisian, Lawrence D. Kerr, and Fiona E. Yull. 2001. «Nuclear Factor-κB (NF-κB) Regulates Proliferation and Branching in Mouse Mammary Epithelium». *Molecular Biology of the Cell* 12 (5): 1445-55.

Cao, Shanjin, Xia Zhang, Justin P. Edwards and David M. Mosser. 2006. «NF-κB1 (p50) Homodimers Differentially Regulate Pro- and Anti-inflammatory Cytokines in Macrophages». *The Journal of biological chemistry* 281 (36): 26041-50. doi:10.1074/jbc.M602222200.

Cao, Y., G. Bonizzi, T. N. Seagroves, F. R. Greten, R. Johnson, E. V. Schmidt and M. Karin. 2001. «IKKalpha Provides an Essential Link between RANK Signaling and Cyclin D1 Expression during Mammary Gland Development». *Cell* 107 (6): 763-75.

Cao, Yixue, Jun-Li Luo, and Michael Karin. 2007. «IkappaB Kinase Alpha Kinase Activity Is Required for Self-Renewal of ErbB2/Her2-Transformed Mammary Tumor-Initiating Cells». *Proceedings of the National Academy of Sciences of the United States of America* 104 (40): 15852-57. doi:10.1073/pnas.0706728104.

Carbia-Nagashima, Alberto, Juan Gerez, Carolina Perez-Castro, Marcelo Paez-Pereda, Susana Silberstein, Günter K. Stalla, Florian Holsboer, and Eduardo Arzt. 2007. «RSUME, a Small RWD-Containing Protein, Enhances SUMO Conjugation and Stabilizes HIF-1α during Hypoxia». *Cell* 131 (2): 309-23. doi:10.1016/j.cell.2007.07.044.

Demicco, Elizabeth G., Kathryn T. Kavanagh, Raphaëlle Romieu-Mourez, Xiaobo Wang, Sangmin R. Shin, Esther Landesman-Bollag, David C. Seldin and Gail E. Sonenshein. 2005. «RelB/p52 NF-kappaB Complexes Rescue an Early Delay in Mammary Gland Development in Transgenic Mice with Targeted Superrepressor IkappaB-Alpha Expression and Promote Carcinogenesis of the

Mammary Gland». *Molecular and Cellular Biology* 25 (22): 10136-47. doi:10.1128/MCB.25.22.10136-10147.2005.

Desterro, J. M., M. S. Rodriguez and R. T. Hay. 1998. «SUMO-1 Modification of IkappaBalpha Inhibits NF-kappaB Activation». *Molecular Cell* 2 (2): 233-39.

Gerondakis, Steve, Thomas S. Fulford, Nicole L. Messina and Raelene J. Grumont. 2014. «NF-κB Control of T Cell Development». *Nature Immunology* 15 (1): 15-25. doi:10.1038/ni.2785.

Geymayer, Sibylle and Wolfgang Doppler. 2000. «Activation of NF-κB p50/p65 Is Regulated in the Developing Mammary Gland and Inhibits STAT5-Mediated B-Casein Gene Expression». *The FASEB Journal* 14 (9): 1159-70.

Gilmore, T. D. 2006. «Introduction to NF-kappaB: Players, Pathways, Perspectives». *Oncogene* 25 (51): 6680-84. doi:10.1038/sj.onc.1209954.

Gonzalez-Suarez, Eva, Daniel Branstetter, Allison Armstrong, Huyen Dinh, Hal Blumberg and William C. Dougall. 2007. «RANK Overexpression in Transgenic Mice with Mouse Mammary Tumor Virus Promoter-Controlled RANK Increases Proliferation and Impairs Alveolar Differentiation in the Mammary Epithelia and Disrupts Lumen Formation in Cultured Epithelial Acini». *Molecular and Cellular Biology* 27 (4): 1442-54. doi:10.1128/MCB.01298-06.

Karin, M. 1999. «The Beginning of the End: IkappaB Kinase (IKK) and NF-kappaB Activation». *The Journal of Biological Chemistry* 274 (39): 27339-42.

Keller, Shannon A., Denise Hernandez-Hopkins, Jelena Vider, Vladimir Ponomarev, Elizabeth Hyjek, Elaine J. Schattner and Ethel Cesarman. 2006. «NF-kappaB Is Essential for the Progression of KSHV- and EBV-Infected Lymphomas in Vivo». *Blood* 107 (8): 3295-3302. doi:10.1182/blood-2005-07-2730.

Kendellen, M. F., J. W. Bradford, C. L. Lawrence, K. S. Clark and A. S. Baldwin. 2014. «Canonical and Non-Canonical NF-κB Signaling Promotes Breast Cancer Tumor-Initiating Cells». *Oncogene* 33 (10): 1297-1305. doi:10.1038/onc.2013.64.

Lin, Y. Z., S. Y. Yao, R. A. Veach, T. R. Torgerson and J. Hawiger. 1995. «Inhibition of Nuclear Translocation of Transcription Factor NF-Kappa B by a Synthetic Peptide Containing a Cell Membrane-Permeable Motif and Nuclear Localization Sequence». *The Journal of Biological Chemistry* 270 (24): 14255-58.

Liu, Manran, Toshiyuki Sakamaki, Mathew C. Casimiro, Nicole E. Willmarth, Andrew A. Quong, Xiaoming Ju, John Ojeifo, et al. 2010. «The Canonical NF-kappaB Pathway Governs Mammary Tumorigenesis in Transgenic Mice and Tumor Stem Cell Expansion». *Cancer Research* 70 (24): 10464-73. doi:10.1158/0008-5472.CAN-10-0732.

Mulero, María Carmen, Dolors Ferres-Marco, Abul Islam, Pol Margalef, Matteo Pecoraro, Agustí Toll, Nils Drechsel, et al. 2013. «Chromatin-Bound IκBα Regulates a Subset of Polycomb Target Genes in Differentiation and Cancer». *Cancer cell* 24 (2): 151-66. doi:10.1016/j.ccr.2013.06.003.

Palafox Marta, Irene Ferrer, Pasquale Pellegrini, Sergi Vila, Sara Hernandez-Ortega, Ander Urruticoechea, Fina Climent, et al. 2012. «RANK Induces Epithelial-Mesenchymal Transition and Stemness in Human Mammary Epithelial Cells and Promotes Tumorigenesis and Metastasis». *Cancer Research* 72 (11): 2879-88. doi:10.1158/0008-5472.CAN-12-0044.

Pellegrini, Pasquale, Alex Cordero, Marta I Gallego, William C. Dougall, Purificación Muñoz, Miguel Ángel Pujana and Eva González Suárez. 2013. «Constitutive activation of RANK disrupts mammary cell fate leading to tumorigenesis.» *Stem cells* 31 (9): 1954-65.

Perkins, Neil D. 2007. «Integrating Cell-Signalling Pathways with NF-κB and IKK Function». *Nature Reviews Molecular Cell Biology* 8 (1): 49-62. doi:10.1038/nrm2083.

Pierce, J. W., R. Schoenleber, G. Jesmok, J. Best, S. A. Moore, T. Collins and M. E. Gerritsen. 1997. «Novel Inhibitors of Cytokine-Induced IkappaBalpha Phosphorylation and Endothelial Cell Adhesion Molecule Expression Show Anti-Inflammatory Effects in Vivo». *The Journal of Biological Chemistry* 272 (34): 21096-103.

Pol Margalef, Vanesa Fernandez-Majada, Alberto Villanueva, Ricard Garcia-Carbonell, Mar Iglesias, Laura Lopez, Maria Martinez-Iniesta, Jordi Villa-Freixa, Mari Carmen Mulero, Montserrat Andreu, Ferran Torres, Marty W. Mayo, Anna Bigas and Lluís Espinosa. 2012. A truncated Form of IKKa is responsible for specific nuclear IKK activity in colorectal cancer. *Cell Rep* 2, 840-854, doi:S2211-1247(12)00268-910.1016/j.celrep.2012.08.028 (2012).

Pratt, M. a. C., E. Tibbo, S. J. Robertson, D. Jansson, K. Hurst, C. Perez-Iratxeta, R. Lau and M. Y. Niu. 2009. «The Canonical NF-kappaB Pathway Is Required for Formation of Luminal Mammary Neoplasias and Is Activated in the Mammary Progenitor Population». *Oncogene* 28 (30): 2710-22. doi:10.1038/onc.2009.131.

Schramek, Daniel, Andreas Leibbrandt, Verena Sigl, Lukas Kenner, John A. Pospisilik, Heather J. Lee, Reiko Hanada, et al. 2010. «Osteoclast differentiation factor RANKL controls development of progestin-driven mammary cancer». *Nature* 468 (7320): 98-102. doi:10.1038/nature09387.

Shackleton, Mark, François Vaillant, Kaylene J. Simpson, John Stingl, Gordon K. Smyth, Marie-Liesse Asselin-Labat, Li Wu, Geoffrey J. Lindeman and Jane E. Visvader. 2006. «Generation of a Functional Mammary Gland from a Single Stem Cell». *Nature* 439 (7072): 84-88. doi:10.1038/nature04372.

Stingl, John, Peter Eirew, Ian Ricketson, Mark Shackleton, François Vaillant, David Choi, Haiyan I. Li, y Connie J. Eaves. 2006. «Purification and Unique Properties of Mammary Epithelial Stem Cells». *Nature* 439 (7079): 993-97. doi:10.1038/nature04496.

Suzuki, Jun-Ichi, Masahito Ogawa, Susumu Muto, Akiko Itai, Mitsuaki Isobe, Yasunobu Hirata and Ryozo Nagai. 2011. «Novel IκB kinase inhibitors for treatment of nuclear factor-κB-related diseases». *Expert Opinion on Investigational Drugs* 20 (3): 395-405. doi:10.1517/13543784.2011.559162.

Torgerson, Troy R., Ann D. Colosia, John P. Donahue, Yao-Zhong Lin and Jacek Hawiger. 1998. «Regulation of NF-κB, AP-1, NFAT, and STAT1 Nuclear Import in T Lymphocytes by Noninvasive Delivery of Peptide Carrying the Nuclear Localization Sequence of NF-κB p50». *The Journal of Immunology* 161 (11): 6084-92.

Zhang, Weizhou, Wei Tan, Xuefeng Wu, Maxim Poustovoitov, Amy Strasner, Wei Li, Nicholas Borcherding, Majid Ghassemian and Michael Karin. 2013. «A NIK-IKKα Module Expands ErbB2-Induced Tumor-Initiating Cells by Stimulating Nuclear Export of p27/Kip1». *Cancer Cell* 23 (5): 647-59. doi:10.1016/j.ccr.2013.03.012.

Ziegelbauer, Karl, Florian Gantner, Nicholas W Lukacs, Aaron Berlin, Kinji Fuchikami, Toshiro Niki, Katsuya Sakai, et al. 2005. «A selective novel low-molecular-weight inhibitor of IκB kinase-β (IKK-β) prevents pulmonary inflammation and shows broad anti-inflammatory activity». *British Journal of Pharmacology* 145 (2): 178-92. doi:10.1038/sj.bjp.0706176.

FIGURES

Figure 1

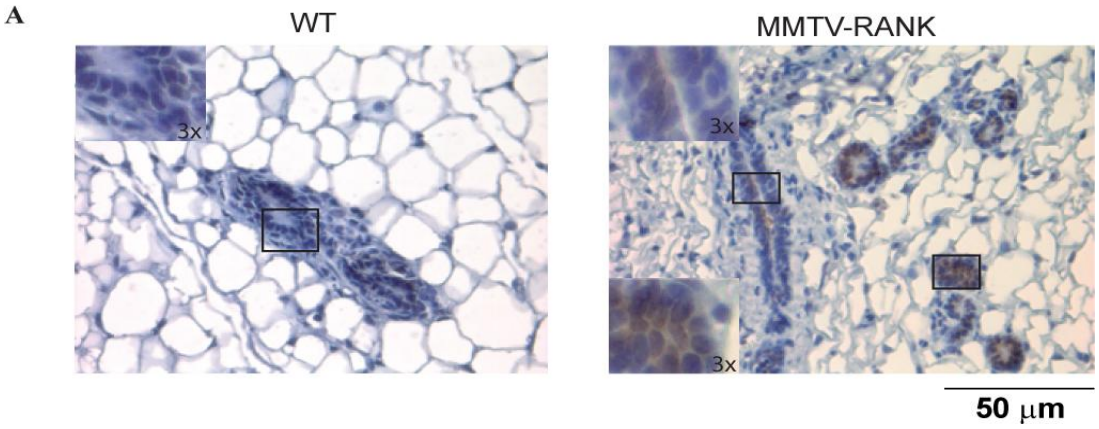

Figure 1. Higher levels of p65 cytoplasmic staining in MMTV-RANK mammary glands. Representative images of p65 protein expression detected by IHC in virgin WT and MMTV-RANK mammary glands. P65 positive cells in the cytoplasm are magnified in the insets.

Figure 2

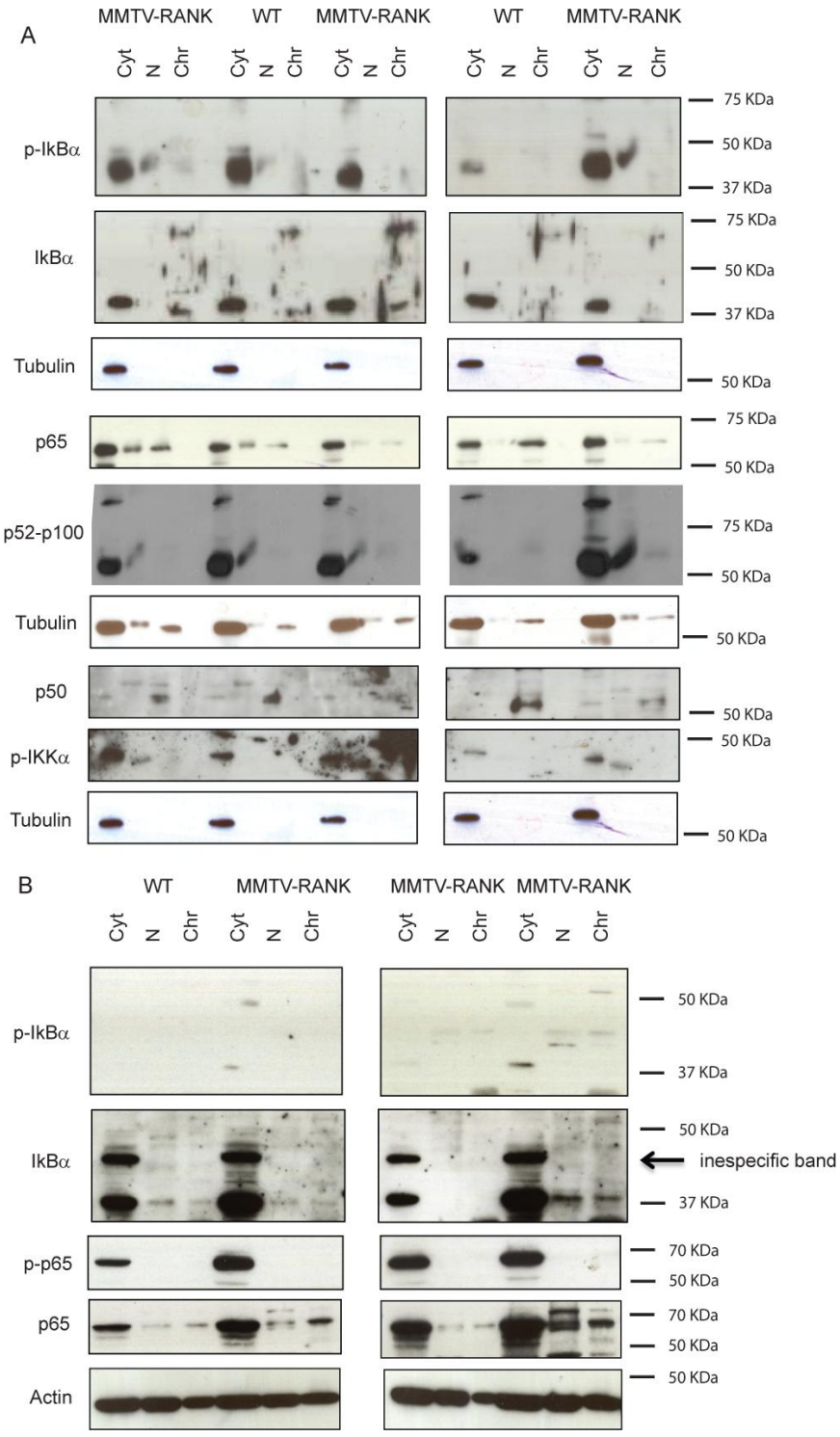

Figure 2. Complex regulation of NF-kB signaling in RANK overexpressing mammary glands.
A,B. Western blot analyses of the indicated genes in cytoplasmic, nuclear and chromatin protein extracts from virgin (A) and midgestant (B) WT and MMTV-RANK MECs. Tubulin and b-actin are shown as loading controls. Cytoplasmic, Cyt; Nuclear, N; Chromatin, Chr.

Figure 3

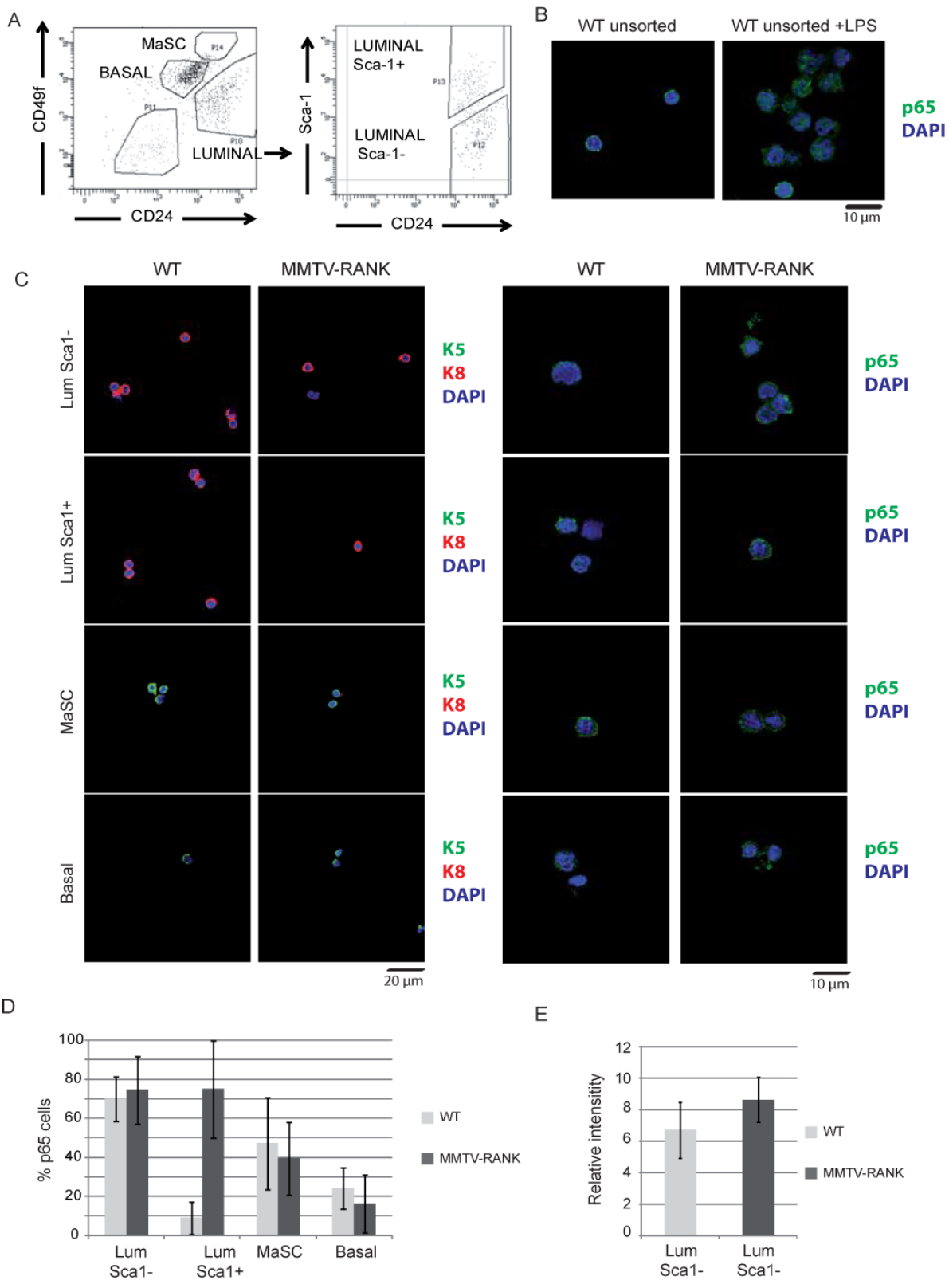
A
MaSC
BASAL
LUMINAL
CD49f
CD24
LUMINAL Sca-1+
LUMINAL Sca-1-
Sca-1
CD24
B
WT unsorted
WT unsorted +LPS
p65
DAPI
10 µm
C
WT
MMTV-RANK
WT
MMTV-RANK
Lum Sca1-
Lum Sca1+
MaSC
Basal
K5
K8
DAPI
p65
DAPI
20 µm
10 µm
D
% p65 cells
100
80
60
40
20
0
Lum Sca1-
Lum Sca1+
MaSC
Basal
WT
MMTV-RANK
E
Relative intensity
12
10
8
6
4
2
0
Lum Sca1-
Lum Sca1-
WT
MMTV-RANK

Figure 3. Enhanced p65 cytoplasmic staining in luminal progenitors and MaSC enriched populations in WT and MMTV-RANK.

A. Dot blots representing the mammary population identified by flow cytometry based on expression of CD24, CD49f and Sca1 surface markers.
B. Representative images showing p65 (green) and DAPI (blue) staining found in WT unsorted mammary epithelial cells. Cells were stimulated with LPS (1.6 µg/mL) during 30 minutes to induce p65 nuclear translocation.
C. Representative images showing K5 (green), K8 (red) and DAPI (blue) (left panel) or p65 (green) and DAPI (blue) (right panel) staining found in the indicated FACS-sorted populations in WT and MMTV-RANK.
D. Percentage of p65 positive cells in the indicated FACS-sorted populations in WT and MMTV-RANK. Mean and SD are shown.
E. P65 relative intensity in the indicated FACS-sorted populations in WT and MMTV-RANK. Mean and SD are shown.

Figure 4

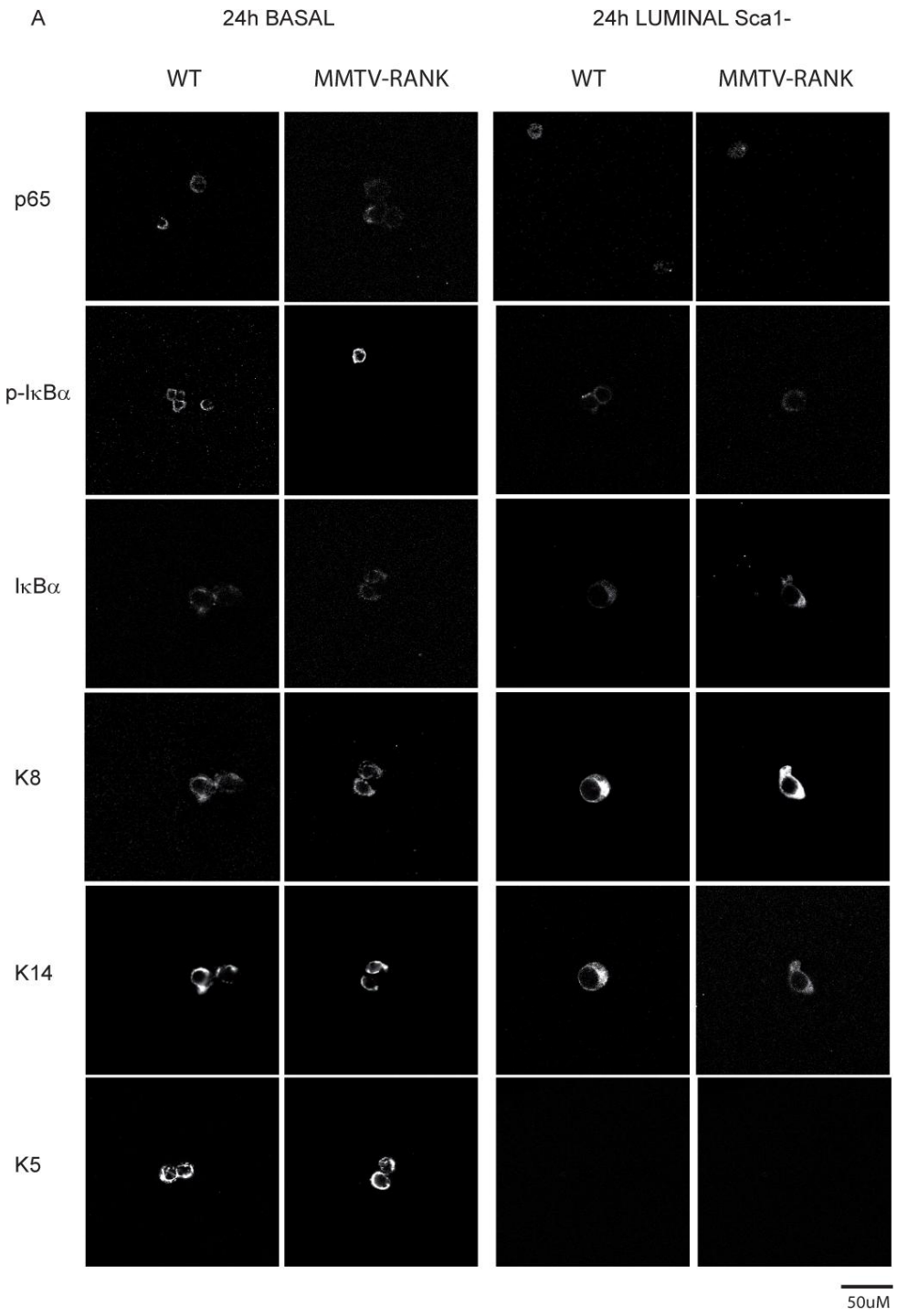

Figure 4. NF-kB canonical pathway in WT and MMTV-RANK basal and luminal progenitor populations after 24h in culture with RANKL.

Representative images showing p65, p-IkBα, IkBα, K8, K5 and K14 staining in WT and MMTV-RANK basal and luminal Sca1- FACS-sorted mammary epithelial cells after 24h in culture under RANKL stimuli.

Figure 5

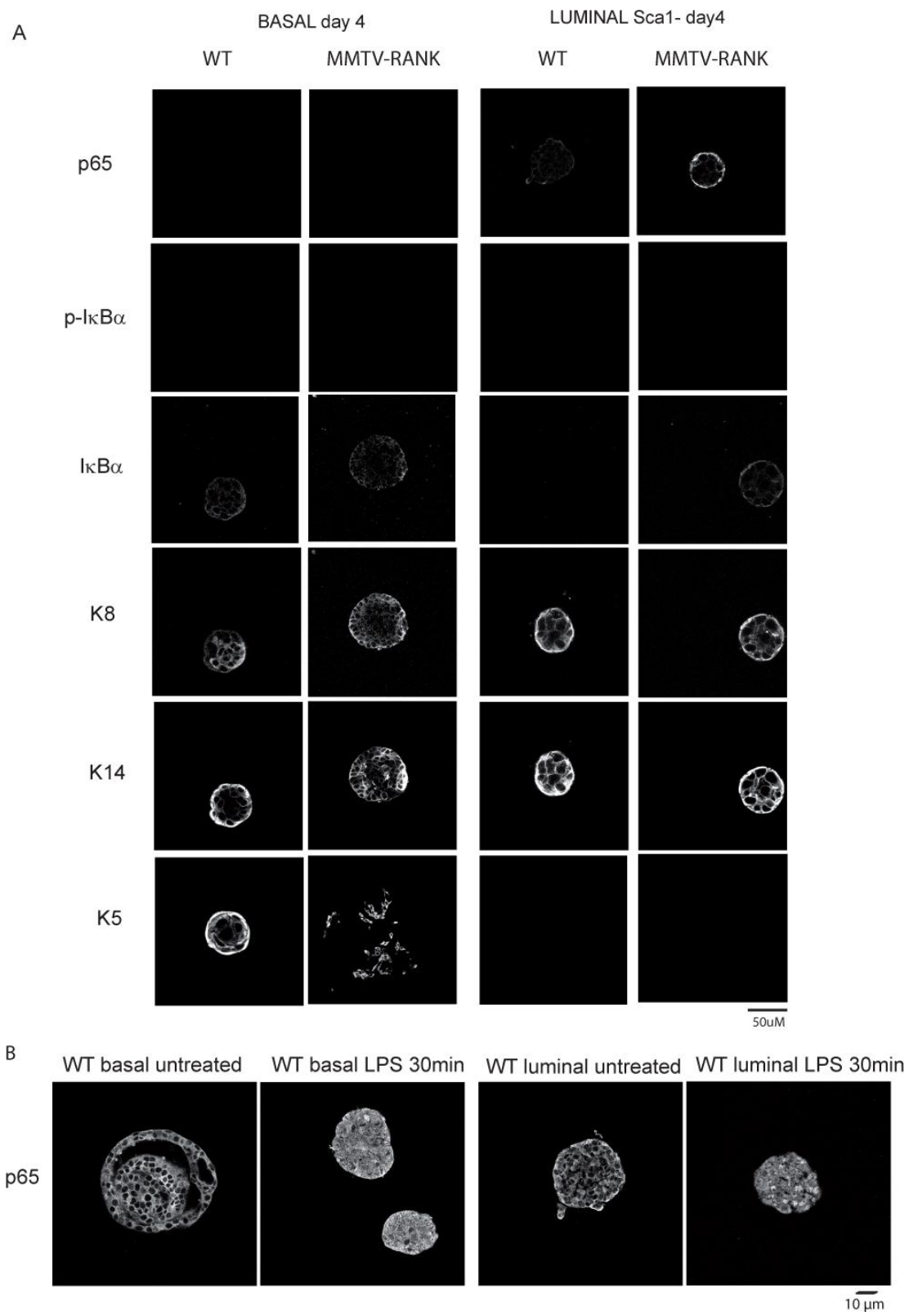
A
BASAL day 4
LUMINAL Sca1- day4
WT
MMTV-RANK
WT
MMTV-RANK
p65
p-IκBα
IκBα
K8
K14
K5
50uM
B
WT basal untreated
WT basal LPS 30min
WT luminal untreated
WT luminal LPS 30min
p65
10 µm

Figure 5. NF-kB canonical pathway in WT and MMTV-RANK basal and luminal colonies after 4 days in culture with RANKL.

A. Representative images showing p65, p-IkBα, IkBα, K8, K5 and K14 staining in WT and MMTV-RANK basal and luminal Sca1- colonies after 4 days in culture under RANKL stimuli.
B. Representative images showing p65 nuclear staining in WT basal and luminal Sca1- colonies under LPS (1.6 μg/mL) treatment during 30 minutes.

Figure 6

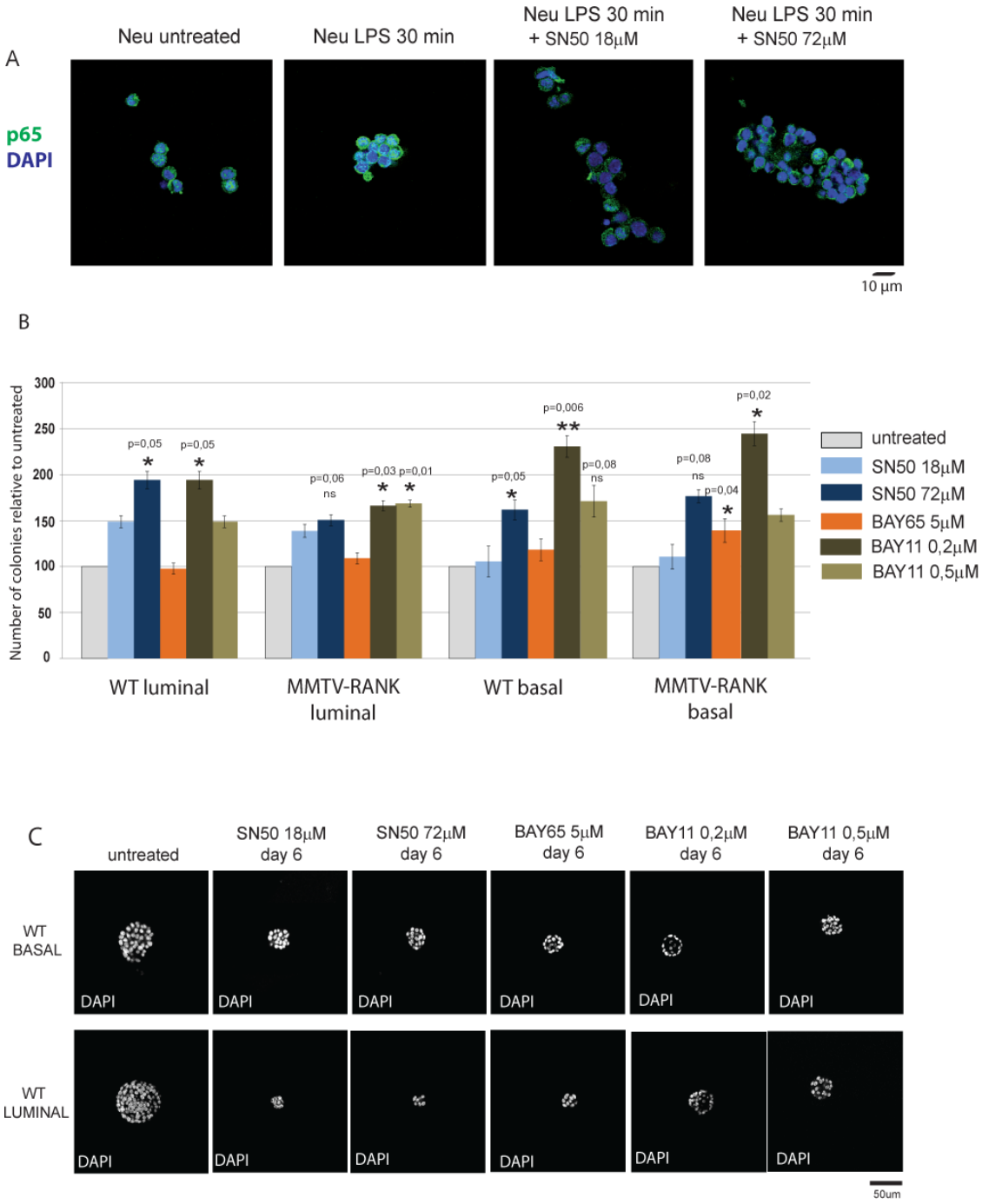

Figure 6. NF-kB inhibition enhanced colony formation ability but decreased colony size in basal and luminal WT and MMTV-RANK MECs.

A. Representative images showing p65 staining upon SN50 inhibition in LPS-treated MMTV-neu tumor cells preincubated with SN50 18μM and 72μM. P65 (green) and DAPI (blue) staining is shown. Cells were treated with LPS (1.6 μg/mL) during 30 minutes to induce p65 nuclear translocation.

B. Total number of colonies formed by WT and MMTV-RANK basal and luminal progenitor cells treated with SN50 (18μM and 72μM), BAY65 (5μM) or BAY11 (0,2μM and 0,5μM). Colony quantification relative to untreated colonies is represented. Results for one representative experiment out of 3 are shown. Experiment was performed in triplicates and mean, SEM and t-test p value are shown.
C. Representative images showing colony size from WT basal and luminal untreated or SN50 (18μM and 72μM), BAY65 (5μM) or BAY11 (0,2μM and 0,5μM) inhibited cultures. Nuclear DAPI (grey) staining is shown. Results for one representative experiment out of 3 are shown.

Figure 7

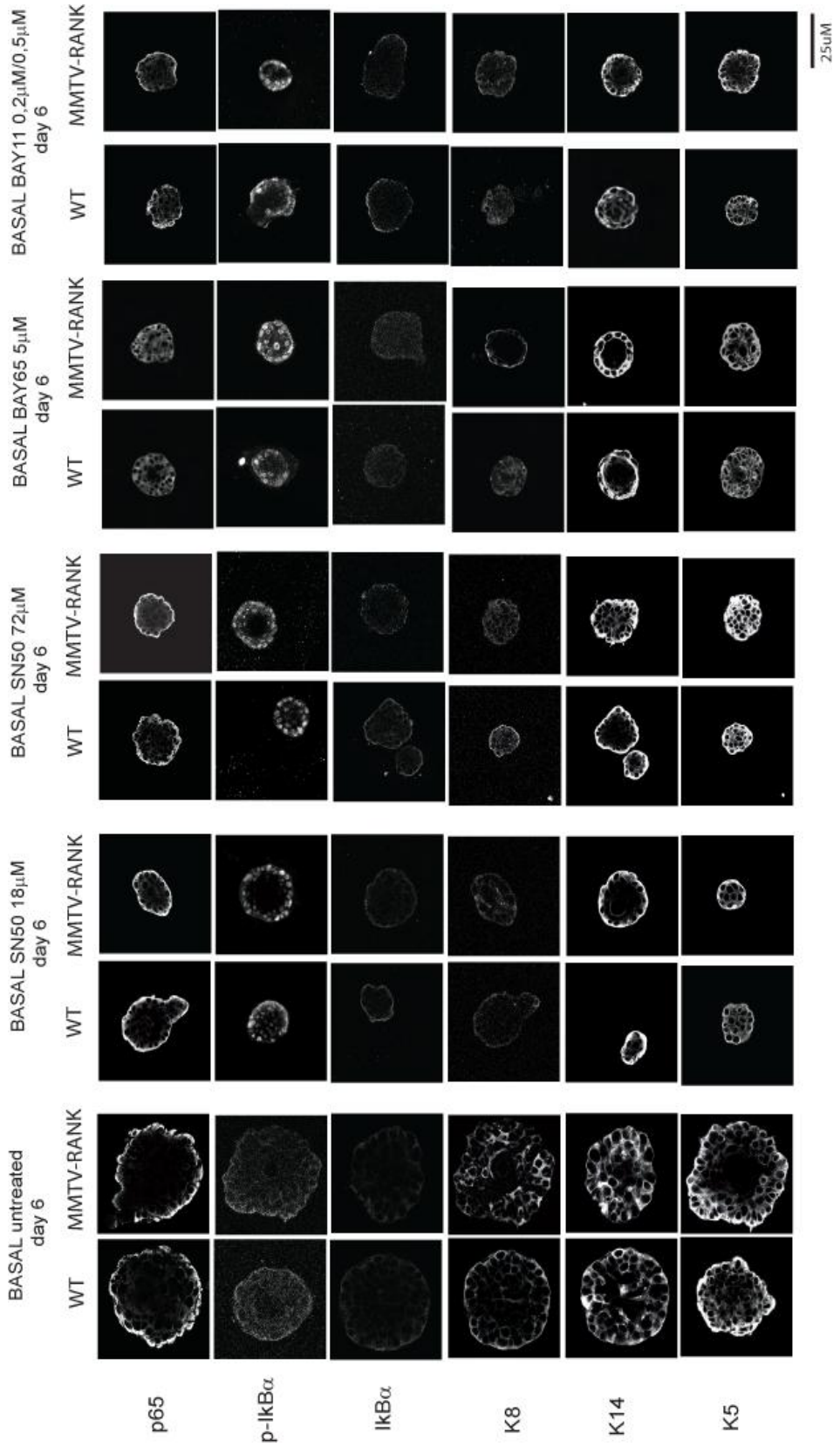
BASAL untreated day 6
BASAL SN50 18µM day 6
BASAL SN50 72µM day 6
BASAL BAY65 5µM day 6
BASAL BAY11 0,2µM/0,5µM day 6
WT
MMTV-RANK
p65
p-IkBα
IkBα
K8
K14
K5
25uM

Figure 7. Nuclear p-IkBα translocation and reduced K8+ luminal expression is observed in WT and MMTV-RANK basal colonies upon NF-kB-inhibition.
Representative images showing p65, p-IkBα, IkBα, K8, K5 and K14 staining (grey) in WT and MMTV-RANK basal colonies inhibited with SN50 (18μM and 72μM), BAY65 (5μM) or BAY11 (0,2μM and 0,5μM) during 6 days. Results for one representative experiment out of 3 are shown.

Figure 8

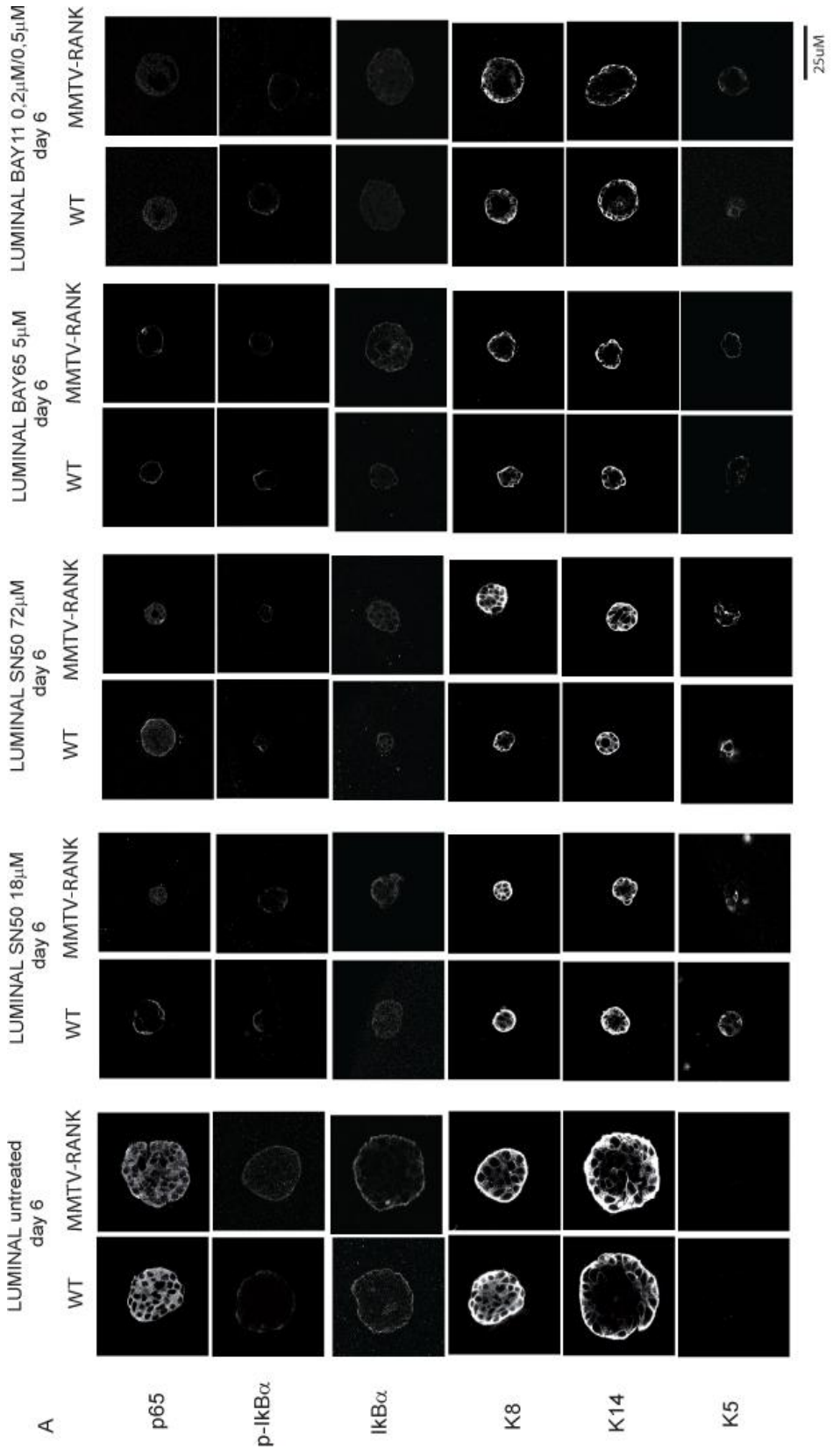
A
p65
p-IkBα
IkBα
K8
K14
K5
LUMINAL untreated day 6
WT
MMTV-RANK
LUMINAL SN50 18μM day 6
LUMINAL SN50 72μM day 6
LUMINAL BAY65 5μM day 6
LUMINAL BAY11 0,2μM/0,5μM day 6
25uM

Figure 8. Acquisition of K5 expression and reduction in p65 levels is observed in WT and MMTV-RANK luminal colonies upon NF-kB inhibition.
Representative images showing p65, p-IkBα, IkBα, K8, K5 and K14 staining (grey) in WT and MMTV-RANK luminal colonies inhibited with SN50 (18μM and 72μM), BAY65 (5μM) or BAY11 (0,2μM and 0,5μM) during 6 days. Results for one representative experiment out of 3 are shown.

ARTICLE 2

"Rankl impairs lactogenic differentiation through inhibition of the prolactin/Stat5 pathway"

Rankl impairs lactogenic differentiation through inhibition of the prolactin/Stat5 pathway

Cordero A[1*], Pellegrini P[1*], Sanz-Moreno A[1], Trinidad EM[1], Serra-Musach J[2], Deshpande C[3], Dougall WC[4], Pujana MA[2] and González Suarez E[1, #].

1. Cancer Epigenetics and Biology Program, Bellvitge Biomedical Research Institute, IDIBELL, Barcelona, Spain.

2. Breast Cancer and Systems Biology Unit, ICO, IDIBELL, Barcelona, Spain.

3. Department of Molecular Sciences and Computational Biology, Amgen Inc., Thousand Oaks (CA), USA

4. Therapeutic Innovation Unit, Amgen, Inc., Seattle (WA), USA

*These authors contributed equally to this work

#Corresponding author: Eva González-Suárez.

Cancer Epigenetics and Biology Program, Bellvitge Institute for Biomedical Research, IDIBELL.

Av. Gran Via de L'Hospitalet, 199. 08908 L'Hospitalet de Llobregat. Barcelona. Spain

egsuarez@idibell.cat www.pebc.cat Phone: +34 932607139 Fax: +34 932607219

CONFLICT OF INTEREST: C Deshpande & WC Dougall are employees and shareholders of Amgen Inc. All other authors declare no conflict of interest.

RUNNING TITLE: Rankl inhibits prolactin-driven Stat5 activation

KEY WORDS: Rank, Rankl, p-Stat5, mammary alveoli, prolactin, progesterone

ABSTRACT

Prolactin and progesterone both orchestrate the proliferation and differentiation of the mammary gland during gestation. Differentiation of milk secreting alveoli depends on the presence of Prolactin receptor (PrlR), the downstream Jak2-Stat5 pathway and the transcription factor Elf5. A strict regulation of Rank signaling is essential for the differentiation of the mammary gland and in particular for alveolar commitment. Impaired alveologenesis and lactation failure are observed in both, knockout and Rank overexpressing mice; however, the underlying molecular mechanism responsible for these phenotypes remains largely unknown. Using genome-wide expression analyses we show here that Rankl exposure leads to impaired secretory differentiation of alveolar cells not only in MMTV-RANK, but also in WT mammary acini. Conversely, pharmacological blockage of Rank signaling at midgestation in WT mice leads to precocious and exacerbated lactogenesis. Mechanistically, Rankl negatively regulates Stat5 phosphorylation and Elf5 expression at the onset of lactogenesis. Overall, we demonstrate that enhanced Rank signaling impairs secretory differentiation during pregnancy by inhibition of the prolactin/p-Stat5 pathway.

INTRODUCTION

The mammary gland undergoes profound tissue remodeling in response to progesterone and prolactin during pregnancy. In early gestation epithelial cells undergo extensive proliferation and form alveoli (alveologenesis), while in late pregnancy alveolar cells synthesize and secrete milk proteins (lactogenesis) (Cathrin Brisken 2002; Neville, McFadden, and Forsyth 2002). Progesterone is required for proliferation and ductal side-branching of the mammary epithelium in the cycling adult animal and for epithelial expansion and alveolar morphogenesis during pregnancy (C. Brisken et al. 1998; Mulac-Jericevic et al. 2003), whereas prolactin controls alveologenesis and lactogenesis. In fact, progesterone- and prolactin-receptor-deficient mice lack lobulo-alveoli (Lydon et al. 1995; Ormandy et al. 1997). The prolactin receptor (PrlR)/Jak2/p-Stat5 axis is responsible for mediating the biological responses initiated by prolactin (Oakes et al. 2008; Yamaji et al. 2009). Upon phosphorylation, activated Stat5 translocates to the nucleus and induces expression of its target genes including milk proteins (Gouilleux et al. 1994). The transcription factor Elf5, is expressed in luminal progenitor cells and specifies alveolar cell fate (Oakes et al. 2008). Lactation failure is observed in mice deficient in prolactin, its receptor (PrlR), Jak2, both isoforms of Stat5 (Stat5a, Stat5b) and Elf5 supporting a key role of this axis in lactogenesis (Ormandy et al. 1997; Horseman et al. 1997; Teglund et al. 1998; Wagner et al. 2004; Zhou et al. 2005).

The receptor activator of NF-kB (Rank) signaling pathway mediates the major proliferative response of mouse mammary epithelium to progesterone (Asselin-Labat et al. 2010; Beleut et al. 2010; Joshi et al. 2010). Mammary glands from Rank and Rankl knockout mice show impaired side-branching and alveolar development during pregnancy due to decreased proliferation and survival of mammary epithelial cells (MECs) (Fata et al. 2000). Conversely, forced expression of Rankl enhanced ductal side-branching and alveolar bud formation during puberty and epithelial cell proliferation in adult virgin animals (Fernandez-Valdivia et al. 2009). In contrast, Rank overexpression in the mammary epithelia impairs alveolar differentiation and lactation while it enhances proliferation in virgin and pregnant mammary epithelia (Gonzalez-Suarez et al. 2007; Pellegrini et al. 2013). Together these results point to an intriguing positive and negative dual regulation of alveolar differentiation by Rank signaling.

Studies of the regulation of Rankl by prolactin have also revealed contrasting data. It was initially shown that prolactin induced Rankl expression (Fata et al. 2000; Srivastava et al. 2003), but recent results using promoter ChIP analyses indicate that Rankl, at least in adult virgin MECs, is primarily a target of progesterone and not prolactin (Cathrin Brisken 2002, 200; Obr et al. 2013).

The molecular mechanism underlying the ambivalent role of Rankl signaling in alveologenesis and lactation remains unknown. Here, by using complementary strategies to activate or pharmacologically inhibit the pathway during pregnancy we demonstrate that Rank signaling prevents lactogenesis through inhibition of the Prolactin/p-Stat5 pathway.

RESULTS

Activation of Rank signaling at midgestation interferes with secretory alveologenesis

In order to investigate the mechanism underlying the defective alveologenesis in MMTV-RANK mice (Gonzalez-Suarez et al. 2007; Pellegrini et al. 2013), global gene expression profiles from primary acinar cultures of mammary epithelial cells from gestation day 16.5 (G16.5) WT and MMTV-RANK females at 8, 24 and 72 hours (h) were obtained. Cultures were established in the presence of prolactin, which induces differentiation into milk secreting acini (Barcellos-Hoff et al. 1989), and with or without Rankl (RL) to precisely determine the role of Rank signaling at midgestation (Fig. 1a). The number of differentially expressed genes increased from 8 h to 72 h in each comparison: WT/WT + RL; MMTV-RANK/MMTV-RANK + RL; WT/MMTV-RANK (Fig. 1b, Supplemental Table 1). Several genes were shared by all comparisons, including the WT/WT + RL (Fig. 1c). In all settings significantly associated biological processes of the up-regulated gene sets include those related to cell cycle/proliferation and programmed cell death, whereas the down regulated gene sets consist of processes related to lipid metabolism, cytokine production and inflammatory response (Fig. 1d). We focused on the WT/WT + RL signature given its physiological significance (Supplemental Table 1). Notably, exposure to RL in WT acini also correlated with a decreasing expression trend of differentiation-related genes, such as *Wap*, while proliferation-related genes, such as *Ccnd1,* show a higher expression with RL relative to non-treated WT acini (Fig. 2a). Other genes significantly down-regulated in WT acini exposed to Rankl include: prolactin receptor (*Prlr), Lao1*, milk protein genes (prolactin induced protein –*Pip*-, caseins- *Csna*, *Csnb, Csnd, Csng, Csnk- or lactalbumin, Lalba)* and milk lipid genes (*Fasn, Aldoc or Glut1)* (Supplemental Table 1). Ordering all genes according to their expression trend in this setting identified as significantly over-expressed pathways those known to be involved in cell proliferation, and also NF-kB and Wnt signaling among others (Fig. 2b, top panel). Conversely, under-expressed pathways were those linked to oxidative phosphorylation, and Ppar signaling (Fig. 2b, top panel). Consistent with these observations, the Rank signaling pathway gene set was also found significantly over-expressed with exposure to Rankl (Fig. 2b, bottom panel). Next, to assess if the observed gene expression changes are biologically relevant *in vivo*, data from mouse mammary gland development was analyzed (Anderson et al. 2007). Unsupervised analysis revealed that overexpressed genes with acini exposure to Rankl tend to be downregulated in normal late pregnancy (Fig. 2c, top panel), while under-expressed genes are mostly upregulated in normal late pregnancy and lactation (Fig. 2c, bottom panel). That is, exposure to Rankl caused gene

expression changes that are consistent with increased proliferation in early pregnancy but impaired lactogenesis *in vivo*. An enrichment analysis of predicted transcription binding sites at the promoters of the genes that were found to be over-expressed in Rankl-treated cultures identified NF-kB as a potential initial driver followed by E2Fs, commonly associated with proliferative signatures (Nevins 1992) and Stat5/6, well known regulators of mammary gland differentiation (Haricharan and Li 2014) (Fig. 2d). Together, these results support a negative role for Rank signaling in prolactin signaling and lactogenesis not only in MMTV-RANK, but also in WT acini.

RANKL treatment inhibits Stat5 phosphorylation in WT mammary acini

The microarray results suggested a negative regulation of milk production and lactogenesis by Rankl. Thus, we next evaluated key genes which are modulated during alveolar differentiation in acini from additional G14.5 WT and MMTV-RANK mice cultured in the presence of prolactin for 24 h +/- Rankl (Fig. 3a). Consistent with the lactation failure observed in MMTV-RANK mice and the enhanced proliferation, a decrease in *Wap*, *Csnb* and *PrlR* expression and an increase in *Ccnd1* were found in MMTV-RANK acini when compared to WT with or without Rankl (Fig. 3a). Some of the differences in gene expression did not reach significance probably due to heterogeneity between individuals as not even significant differences were found in *Rank* expression between WT and MMTV-RANK mice (Fig. 3a). No changes were observed in *Elf5* or *Stat5* mRNA expression between WT and MMTV-RANK in the absence of Rankl; however, after exposure to Rankl MMTV-RANK acini showed a significant decrease in Elf5 expression (Fig. 3a).

Next, we specifically addressed the impact of Rankl treatment in each WT and MMTV-RANK culture. A decrease in Rank expression was observed upon Rankl stimulation in WT and MMTV-RANK cultures confirming previous results (Gonzalez-Suarez et al. 2007). In accordance with the attenuated lactogenic signature already described addition of Rankl led to a decrease in milk protein gene expression (*Wap* and *Csnb)* in both WT and MMTV-RANK acini (Fig. 3b). The mRNA levels for *Prlr*, *Elf5* and *Stat5* in MMTV-RANK acini and *Prlr* and *Stat5* in WT, decreased significantly in the presence of Rankl (Fig. 3b), confirming array results and supporting that Rankl negatively regulates secretory differentiation and lactogenesis.

Given their critical role in the prolactin signaling pathway (Oakes et al. 2008; Gouilleux et al. 1994), activation of Stat5 and expression of Elf5 in acinar cultures was evaluated by western blot. Prolactin stimulation for 24 h (compared to growth media, GM) induced Stat5 phosphorylation and Elf5 expression in WT and MMTV-RANK acini (Fig. 3c). In contrast, Rankl activation impaired Stat5 phosphorylation and Elf5 expression in MMTV-RANK acini and, importantly, reduced p-Stat5 also in WT acini (Fig. 3c). In order

to understand whether Stat5 phosphorylation is directly regulated by Rankl, shorter time points were analyzed. A p-Stat5 increase was observed only 10 minutes after prolactin exposure in WT acini, and this induction was sustained after 30 and 60 minutes (Fig. 3d). Strikingly, Rankl also interfered with Stat5 phosphorylation in WT acini at these early time points supporting a non-transcriptional mechanism. A minimal induction of Stat5 phosphorylation was found in MMTV-RANK acini at 10 minutes but it is lost after 30 and 60 minutes of prolactin addition, independently of the presence of Rankl (Fig. 3d).

Rankl is known to activate Nf-kB consistent with the gene expression changes observed after 8-24 h (Fig. 2d). Enhanced IkB and p65 phosphorylation was observed 24 h after addition of prolactin while significantly higher levels of p-Ikb were found when Rankl was added to prolactin in WT acini (Fig. 3c). P-IkB and p-p65 levels were higher in MMTV-RANK than in the corresponding WT acini. A negative crosstalk between NF-kB and the PrlR/Jak2/Stat5 activation pathway, which occurs at the level of Stat5 tyrosine phosphorylation, has been reported (Geymayer and Doppler 2000). Thus, this exacerbated activation of the NF-kB pathway may contribute to reduce p-Stat5 in WT acini leading to impaired lactogenesis. However, p-IkB levels in WT acini at shorter time points did not increase in the presence of prolactin + Rankl (Fig. 3d), thus, additional mechanisms might contribute to the decreased Stat5 phosphorylation induced by Rankl. Overall, our results demonstrate that Rankl stimulation directly inhibits prolactin-induced Stat5 phosphorylation in MECs.

Defective Stat5 phosphorylation at midgestation underlies lactation failure in MMTV-RANK mice

Next, we sought to corroborate the significance of our findings *in vivo*. A reduction in *Csnb*, *Elf5* and *Prlr* mRNA expression, but not *Stat5*, was observed in MMTV-RANK mice as compared to WT when the same gestation time points were compared (Fig. 4a). Lower levels of milk, Elf5 and p-Stat5 protein expression were found in MMTV-RANK compared to WT glands at midgestation as revealed by IHC at G16.5 (Fig. 4b) and western blot at G14.5 (Fig. 4c) in correlation with the lack of secretory differentiation. These observations suggest that over-activation of Rank signaling at mid-gestation disrupts alveolar cell fate through negative regulation of p-Stat5/Elf5.

Interestingly, virgin MMTV-RANK mammary glands show slightly enhanced levels of p-Stat5, p-IkB and p-p65 than WT (Fig. 4c) which could explain the precocious alveolar formation observed in these glands. However, no clear differences in p-IkB and p-p65 were found between WT and MMTV-RANK G14.5 glands (Fig. 4c), suggesting that additional mechanisms contribute to the impaired Stat5 activation and lactogenesis in

MMTV-RANK such as the reduction in CD61 luminal cells and Elf5 expression we previously reported (Pellegrini et al. 2013). Our findings demonstrate that constitutive activation of the Rank pathway interferes with p-Stat5/Elf5 signaling at midgestation preventing lactogenesis.

Pharmacologic inhibition of Rankl at midgestation induces premature alveologenesis through activation of p-Stat5/Elf5 signaling

The reduced milk protein gene expression and increased proliferation observed upon Rankl stimulation in WT acini suggests that activation of Rank signaling plays a negative role in secretory alveologenesis. To interrogate the role of Rank pathway in the alveolar switch under physiological conditions *in vivo*, we inhibited Rank signaling at specific time points of gestation in WT females using the pharmacologic Rankl inhibitor, Rank-Fc (Gonzalez-Suarez et al. 2010). Rank -Fc was injected at G9.5 and G13.5 and mammary glands were harvested and analyzed 24 h later (Fig. 5a). *Rankl* mRNA levels were lower at G14.5 than at G10.5 as previously reported (Gonzalez-Suarez et al. 2007), but were not altered by Rank-Fc (Fig. 5e). Histological analysis showed that inhibition of Rankl induced precocious and enhanced secretory alveolar differentiation at G10.5 and G14.5, respectively, as compared to mock-injected animals (Fig. 5b). Reduced colony-forming ability and proliferation were observed in mammary cells from Rank-Fc-injected animals as compared to controls, suggesting that inhibition of Rankl induced differentiation (Fig. 5c-d). Blockage of Rankl led to premature (G10.5) or enhanced (G14.5) expression of *Wap* consistent with the morphological changes observed (Fig. 5e). Increased mRNA levels of *Elf5* (G10.5 and G14.5) and *Stat5* (G14.5) were observed 24 h after Rank-Fc-treatment (Fig. 5e). Although not significant, the increase in *Csnb* (G10.5) and *Prlr* and the decrease in *Pr* mRNA expression levels also supported that RANK-Fc treatment fostered secretory differentiation of alveolar cells. Western blot and immunohistochemistry analysis (Fig. 5f-g) confirmed increased milk and Elf5 protein expression and Stat5 phosphorylation in the mammary glands from Rank-Fc-injected mice than in control glands (Fig. 5f); however, no changes in IkB or p65 phosphorylation were observed 24h after Rank-Fc treatment (Fig. 5f).

Together, these results indicate that inhibition of Rank signaling at midgestation is required for the activation of p-Stat5 and induction of Elf5 that initiates alveolar secretory differentiation and milk production (Fig. 6).

DISCUSSION

Our study demonstrates that enhanced RANK/Rankl signaling affects lactogenic differentiation in mammary epithelial cells by inhibiting the prolactin-induced activation of STAT5 and expression of Elf5, required for lactation. Moreover we have found that the inhibition of Rankl at midpregnancy, resulted in increased Elf5 expression and activation of the STAT5 pathway leading to a premature secretory differentiation. In contrast to these data, an earlier study (H. J. Lee et al. 2013, 201) revealed that in virgin mice, RANKL is a mediator of progesterone-induced Elf5 expression favoring the differentiation of luminal cells and promoting alveologenesis. In fact, premature alveologenesis is observed in virgin MMTV-RANK glands. Collectively, these results provide a rationale for a dual role of Rank signaling during alveolar differentiation. Whilst the progesterone-Rankl-Rank axis is essential during early steps of alveolar development, later in pregnancy, it rather serves to inhibit prolactin-controlled events associated with lactogenic differentiation.

Indeed progesterone, similar to our data with Rankl, plays both a positive and negative role in mammary alveolar differentiation. Progesterone is required in early pregnancy for mammary epithelial cell expansion and proliferation, side-branching and alveolar morphogenesis. However, during mid-late pregnancy, progesterone suppresses lactogenesis mediated in part by the crosstalk between PR and Stat5 (Buser et al. 2007) consistent with our observations with Rankl herein. In fact, progesterone can suppress PrlR expression in late pregnancy mammary glands (Nishikawa et al. 1994). Our data demonstrate that Rankl inhibition of p-Stat5 contribute to the progesterone-mediated repression of milk protein gene expression during pregnancy (Neville, McFadden, and Forsyth 2002).

NF-kB plays an essential role in mammary gland proliferation and side-branching during pregnancy (Cao et al. 2001) but a negative crosstalk between NF-kB and the PrlR/Jak2/Stat5 activation pathway, which occurs at the level of Stat5 tyrosine phosphorylation, has also been reported (Geymayer and Doppler 2000). Rank is a well-known activator of NF-kB signaling, suggesting that an exacerbated activation of the NF-kB pathway, may contribute to reduce p-Stat5 in WT acini leading to impaired lactogenesis. Enhanced NF-kB activation was observed in MMTV-RANK and WT acini cultured in the presence of Rankl for 24h. However, whereas Rankl interferes with Stat5 phosphorylation as early as after 10, 30 or 60 minutes, no increased activation of NF-kB was detected in Rankl treated WT acini in these early time points. These results suggest that additional mechanisms contribute to the decreased Stat5 phosphorylation induced by Rankl.

Stat5 is phosphorylated by a variety of cytokine receptors depending on the cell type. In the mammary gland prolactin receptor recruits Jak2 which phosphorylates Stat5 (Oakes et al. 2008; Yamaji et al. 2009). It has also been shown that ErbB4 interacts with Stat5 leading to Stat5 phosphorylation in a Jak2 independent manner (Jones et al. 1999; Kabotyanski and Rosen 2003; Long et al. 2003). Other tyrosine kinases, such as c-Src can directly phosphorylate the activation site of Stat5 (Jones et al. 1999; Kabotyanski and Rosen 2003; Long et al. 2003). Further studies will be needed to address the putative role of these pathways in the Rankl- driven attenuation of Stat5 phosphorylation and activation.

Together, our results shed further light on the role of Rank signaling in mammary alveolar differentiation and provide a rationale for the apparently paradoxical phenotypes of impaired alveolar differentiation and lactation failure in Rank KO and MMTV-RANK mice (Fata et al. 2000; Gonzalez-Suarez et al. 2007). Rankl mediates positive and negative signals downstream of progesterone at discrete stages of alveologenesis and lactogenesis. Rank signaling, although essential during early pregnancy, must be shut down at midgestation to allow activation of Stat5, Elf5 induction and lactogenesis.

MATERIALS AND METHODS

Mice

All research involving animals was done in IDIBELL animal facility and complied with protocols approved by the IDIBELL Committee on Animal Care, local animal welfare laws, guidelines and policies. MMTV-RANK mice in FVB background were obtained through collaboration with Dr Bill Dougall (Oncology Research-AMGEN). For cell proliferation analysis, 5-bromo-2'-deoxyuridine (BrdU, 30 mg/kg of mouse) was injected intraperitoneally 2 h before sacrifice. RANK-Fc (10 mg/kg of mouse) was injected subcutaneously in G9.5 and G13.5 females 24 h before sacrifice.

Mammary gland cell isolation

Single cells were isolated from mammary glands as previously described (Smalley 2010). Briefly, fresh tissues were mechanically dissected with McIlwain tissue chopper and enzymatically digested with appropriate medium (DMEM F-12, 0.3% Collagenase A, 2.5U/mL dispase, 20 mM HEPES, and Penicilin/Streptomiciyn) 45 minutes at 37°C. Samples were washed with Leibowitz L15 medium 10% fetal bovine serum (FBS) between each step. Erythrocytes were eliminated by treating samples with hypotonic lysis buffer, and fibroblasts were excluded by incubation with DMEM F-12 10% FBS 1 hour at 37ºC (the majority of fibroblasts attach to tissue culture plastic while most of epithelial organoids do not). Single epithelial cells were isolated by treating with trypsin 2 minutes at 37°C. Cell aggregates were removed treating with 2.5 U/mL dispase (GIBCO), 20U/ml DNase (Invitrogene) 5 minutes at 37ºC. Cell suspension was finally filtered with 40 μm filter and counted.

3D cultures

For differentiation assays in 3D cultures, 600,000 primary MECs isolated from pregnant (G14.5 or G16.5) WT and MMTV-RANK females were plated in 6 well plates on top of growth factor reduced GFR-matrigel in growth medium (GM: DMEM F12, FBS 5%, EGF 10 ng/mL, hydrocortisone 0.5 μg/mL, insulin 5 μg/mL, cholera toxin 100 ng/mL and penicilin/streptomiciyn) for 24 h and then changed to MECs differentiation medium (DMEM F-12, prolactin 3 μg/mL, hydrocortisone 1 μg/mL, ITS (Insulin, transferring, selenium), cholera toxin 100 ng/mL, penicilin/streptomiciyn as previously described (de la Cruz et al. 2004) and Rankl-LZ (1 μg/ml; Amgen Inc) for the indicated time points (10, 30, 60 minutes, 8, 24 and 72h). Medium was replenished every two/three days. For cell isolation matrigel was dissolved with cold PBS-EDTA (5mM). Matrigel-free cell suspensions were then pelleted for RNA or protein isolation (G. Y. Lee et al. 2007).

Colony forming assays

For colony-forming assays 5000 cells were plated in GFR-matrigel cultures as previously described (Stingl et al. 2006) in growth medium that contains B27, 5% FBS, EGF (10 ng/mL), hydrocortisone 0,5 µg/mL, insulin 5 µg/mL, cholera toxin 100 ng/mL, Penicilin/Streptomiciyn and Rankl (1 µg/ml; Amgen Inc) as indicated and were quantified after 2 weeks.

Tissue section histology and Immunostaining

For histological analysis, 3 µm sections from 4% PFA fixed, paraffin embedded mammary glands were cut and stained with hematoxylin and eosin (H&E). Antigen heat retrieval with citrate or Tris-EDTA for Elf5 and p-Stat5 antibodies, was performed before incubation with antibodies against Elf5 (N-20, sc-9645, Santa Cruz), BrdU (G3G4, University of Illinois), p-Stat5 (9359S, Cell Signaling), or anti-milk serum (generously provided by Dr Nancy Hynes). All antibodies were incubated overnight at 4°C. The antigen-antibody complexes were detected with streptavidin horseradish peroxidase (Vector Laboratories) for Elf5, p-Stat5 and anti-milk immunostainings. Peroxidase was revealed with DAB (DAKO).

Western blot

Western blotting was performed with standard protocols. Primary antibodies reactive to mouse p-Stat5 (C11C5, Cell Signaling), Stat5 (C-17, Santa Cruz), Elf5 (N-20, Santa Cruz), p-p65 (S536, Cell Signaling), p65 (D14E12, Cell Signaling), p-IkB (S32/36, Cell Signaling), IkB (C-21, Santa Cruz), and β-actin (AC-74, Sigma) were used. Samples run in the same gel are shown in the same box. A divided box indicates that lanes of the gel have been removed.

Gene Expression Analysis Microarray Labeling and Hybridizations

RNA isolated with the RNAeasy Kit (Qiagen) was collected from WT and MMTV-RANK (C57Bl6) MECs grown in 3D cultures in differentiation media with or without Rankl. Each RL-treated sample was hybridized against its corresponding untreated sample in a fluor-reversed (Cy3/Cy5) pair of arrays. 200 ng of total RNA from each sample was amplified and labeled using Agilent Low RNA Input Linear Amplification labeling kit (Agilent Technologies, Palo Alto, CA). Labeled cRNA was generated by the incorporation of Cy3-CTP or Cy5-CTP (Perkin Elmer, Waltham, MA) during *in vitro* transcription and purified using the RNeasy mini kit (Qiagen, Valencia, CA) This cRNA was then hybridized to the 44K Whole Mouse Genome Oligo microarrays (G4122A Agilent Technologies, Palo Alto, CA) using the Agilent Gene Expression Hybridization kit

and washed using Agilent Gene Expression Wash Buffers following the provided protocols. Microarrays were scanned using the Agilent DNA Microarray Scanner, and data were extracted from images using the Agilent Feature Extraction (version 9.1) software.

Gene expression data analysis

The feature extracted files were imported into Rosetta Resolver 6.0 (Rosetta Biosoftware, Seattle, WA) for data analysis. The data from three replicate mice were combined using the Experiment Definition wizard in Resolver, and combined ratios were generated for each group using the default Agilent Ratio builder algorithm. A Resolver calculated P value of $\leq$ 0.0001 was applied to determine statistically significant differentially expressed genes between each group.

Venn diagrams to represent gene overlaps were generated using Venny interactive online software *http://bioinfogp.cnb.csic.es/tools/venny/index.html*. Genes up- and downregulated more than two-fold were selected. GO enrichment analysis was performed with the over-representation analysis tool from the ConsensusPathDB software developed in the Max Planck Institute for Molecular Genetics (Germany). Functional annotation was carried out choosing level 2-4 gene ontology categories of "biological processes" with the default P value cutoff ($p<0.01$). The expression trend (slope and Pearson's correlation coefficient (PCC) values) with exposure to RL were computed for each microarray probe across the 8 to 72 h time points and for each paired sample (e.g. each mice acini WT versus WT + RL). The PCCs were used in the pre-ranked Gene Set Expression Analysis (GSEA) tool with default parameters. The predicted transcription factor binding sites were analyzed using the Transfac GSEA sets and significantly associated sites were those with FDR < 5%. The Rank signaling pathway annotation was downloaded from WikiPathways. Preprocessed and normalized data from mouse normal mammary gland development was downloaded from the Gene Expression Omnibus (GEO) reference GSE8191 (Anderson et al. 2007). Unsupervised data clustering was performed using all microarray probes corresponding to the genes with the highest over-expression and under-expression lineal slope values (≥ 0.20 and ≤ 0.20, respectively) with exposure to RL in WT acini.

RNA preparation and Quantitative RT–PCR

Total RNA of mammary glands and cell cultures was prepared with Tripure Isolation Reagent (Roche) in accordance with the manufacturer's instructions. Tissue was dissociated using glass beads, (Sigma) and the PreCellys machine (2 cycles 30s 5500 rpm, pause 30 s). 20 ng/ml of mRNA were pretreated with DNase I (Ambion). Single-stranded cDNA was produced by reverse transcription using 1 µg of RNA DNA-free in a

20-µL reaction (Applied Biosystems). Quantitative PCR was performed using the TaqMan probe-based system: AB assays on demand (mouse *RANK, Rankl, Wap, Csnb, Ccnd1, Elf5, Stat5, PR* and *PrlR*) on the ABI 7900HT in accordance with the manufacturer's instructions (Applied Biosystems).

Statistical analysis

Statistical analyses were performed using GraphPad Prism. Analysis of the differences between two mouse cohorts or conditions was performed with a two-tailed unpaired Student's t-test. A t test against reference was used to test significance of fold changes. Statistical significant differences are indicated as (*p< 0.05; **p<0.01; ***p<0.001; ****p<0.0001).

ACKNOWLEDGEMENTS

This work was supported by grants to E González Suárez by MICINN (SAF2011-22893), AECC (Catalunya), FMM, Concern Foundation and a Ramon y Cajal contract. PP is recipient of a FPI grant from the MICINN. We thank A Bigas, L Espinosa, MA Glukhova, A Pietersen, M Bentires-Alj and N Hynes for sharing protocols and reagents.

CONFLICT OF INTEREST

C. Deshpande & W.C. Dougall are employees and shareholders of Amgen Inc. All other authors declare no conflict of interest.

AUTHOR CONTRIBUTIONS

AC, PP, ASM, EMT: Collection and/or assembly of data, data analysis and interpretation; final approval of manuscript. JSM, CD: data analyses, final approval of manuscript. WCD: Reagents, data analysis and interpretation; final approval of manuscript. MAP: data analysis and interpretation; final approval of manuscript, EGS: Conception and design, financial support, collection and/or assembly of data, data analysis and interpretation, manuscript writing and final approval of manuscript.

REFERENCES

Anderson, Steven M., Michael C. Rudolph, James L. McManaman, and Margaret C. Neville. 2007. “Key Stages in Mammary Gland Development. Secretory Activation in the Mammary Gland: It’s Not Just about Milk Protein Synthesis!” *Breast Cancer Research: BCR* 9 (1): 204. doi:10.1186/bcr1653.

Asselin-Labat, Marie-Liesse, François Vaillant, Julie M. Sheridan, Bhupinder Pal, Di Wu, Evan R. Simpson, Hisataka Yasuda, et al. 2010. “Control of Mammary Stem Cell Function by Steroid Hormone Signalling.” *Nature* 465 (7299): 798–802. doi:10.1038/nature09027.

Barcellos-Hoff, M. H., J. Aggeler, T. G. Ram, and M. J. Bissell. 1989. “Functional Differentiation and Alveolar Morphogenesis of Primary Mammary Cultures on Reconstituted Basement Membrane.” *Development (Cambridge, England)* 105 (2): 223–35.

Beleut, Manfred, Renuga Devi Rajaram, Marian Caikovski, Ayyakkannu Ayyanan, Davide Germano, Yongwon Choi, Pascal Schneider, and Cathrin Brisken. 2010. “Two Distinct Mechanisms Underlie Progesterone-Induced Proliferation in the Mammary Gland.” *Proceedings of the National Academy of Sciences of the United States of America* 107 (7): 2989–94. doi:10.1073/pnas.0915148107.

Brisken, Cathrin. 2002. “Hormonal Control of Alveolar Development and Its Implications for Breast Carcinogenesis.” *Journal of Mammary Gland Biology and Neoplasia* 7 (1): 39–48.

Brisken, C., S. Park, T. Vass, J. P. Lydon, B. W. O’Malley, and R. A. Weinberg. 1998. “A Paracrine Role for the Epithelial Progesterone Receptor in Mammary Gland Development.” *Proceedings of the National Academy of Sciences of the United States of America* 95 (9): 5076–81.

Buser, Adam C., Elizabeth K. Gass-Handel, Shannon L. Wyszomierski, Wolfgang Doppler, Susan A. Leonhardt, Jerome Schaack, Jeffrey M. Rosen, Harriet Watkin, Steven M. Anderson, and Dean P. Edwards. 2007. “Progesterone Receptor Repression of Prolactin/signal Transducer and Activator of Transcription 5-Mediated Transcription of the Beta-Casein Gene in Mammary Epithelial Cells.” *Molecular Endocrinology (Baltimore, Md.)* 21 (1): 106–25. doi:10.1210/me.2006-0297.

Cao, Y., G. Bonizzi, T. N. Seagroves, F. R. Greten, R. Johnson, E. V. Schmidt, and M. Karin. 2001. “IKKalpha Provides an Essential Link between RANK Signaling and Cyclin D1 Expression during Mammary Gland Development.” *Cell* 107 (6): 763–75.

de la Cruz, Laura, Kristin Steffgen, Andrea Martin, Carli McGee, and Helen Hathaway. 2004. “Apoptosis and Involution in the Mammary Gland Are Altered in Mice Lacking a Novel Receptor, beta1,4-Galactosyltransferase I.” *Developmental Biology* 272 (2): 286–309. doi:10.1016/j.ydbio.2004.03.041.

Fata, J. E., Y. Y. Kong, J. Li, T. Sasaki, J. Irie-Sasaki, R. A. Moorehead, R. Elliott, et al. 2000. “The Osteoclast Differentiation Factor Osteoprotegerin-Ligand Is Essential for Mammary Gland Development.” *Cell* 103 (1): 41–50.

Fernandez-Valdivia, Rodrigo, Atish Mukherjee, Yan Ying, Jie Li, Marilene Paquet, Francesco J. DeMayo, and John P. Lydon. 2009. “The RANKL Signaling Axis Is Sufficient to Elicit Ductal Side-Branching and Alveologenesis in the Mammary Gland of the Virgin Mouse.” *Developmental Biology* 328 (1): 127–39. doi:10.1016/j.ydbio.2009.01.019.

Geymayer, Sibylle, and Wolfgang Doppler. 2000. “Activation of NF-κB p50/p65 Is Regulated in the Developing Mammary Gland and Inhibits STAT5-Mediated β-Casein Gene Expression.” *The FASEB Journal* 14 (9): 1159–70.

Gonzalez-Suarez, Eva, Daniel Branstetter, Allison Armstrong, Huyen Dinh, Hal Blumberg, and William C. Dougall. 2007. “RANK Overexpression in Transgenic Mice with Mouse Mammary Tumor Virus Promoter-Controlled RANK Increases Proliferation and Impairs Alveolar Differentiation in the Mammary Epithelia and Disrupts Lumen Formation in Cultured Epithelial Acini.” *Molecular and Cellular Biology* 27 (4): 1442–54. doi:10.1128/MCB.01298-06.

Gonzalez-Suarez, Eva, Allison P. Jacob, Jon Jones, Robert Miller, Martine P. Roudier-Meyer, Ryan Erwert, Jan Pinkas, Dan Branstetter, and William C. Dougall. 2010. “RANK Ligand Mediates Progestin-Induced Mammary Epithelial Proliferation and Carcinogenesis.” *Nature* 468 (7320): 103–7. doi:10.1038/nature09495.

Gouilleux, F., H. Wakao, M. Mundt, and B. Groner. 1994. “Prolactin Induces Phosphorylation of Tyr694 of Stat5 (MGF), a Prerequisite for DNA Binding and Induction of Transcription.” *The EMBO Journal* 13 (18): 4361–69.

Haricharan, S., and Y. Li. 2014. “STAT Signaling in Mammary Gland Differentiation, Cell Survival and Tumorigenesis.” *Molecular and Cellular Endocrinology* 382 (1): 560–69. doi:10.1016/j.mce.2013.03.014.

Horseman, N. D., W. Zhao, E. Montecino-Rodriguez, M. Tanaka, K. Nakashima, S. J. Engle, F. Smith, E. Markoff, and K. Dorshkind. 1997. “Defective Mammopoiesis, but Normal Hematopoiesis, in Mice with a Targeted Disruption of the Prolactin Gene.” *The EMBO Journal* 16 (23): 6926–35. doi:10.1093/emboj/16.23.6926.

Jones, Frank E., Thomas Welte, Xin-Yuan Fu, and David F. Stern. 1999. “Erbb4 Signaling in the Mammary Gland Is Required for Lobuloalveolar Development and Stat5 Activation during Lactation.” *The Journal of Cell Biology* 147 (1): 77–88.

Joshi, Purna A., Hartland W. Jackson, Alexander G. Beristain, Marco A. Di Grappa, Patricia A. Mote, Christine L. Clarke, John Stingl, Paul D. Waterhouse, and Rama Khokha. 2010. “Progesterone Induces Adult Mammary Stem Cell Expansion.” *Nature* 465 (7299): 803–7. doi:10.1038/nature09091.

Kabotyanski, Elena B., and Jeffrey M. Rosen. 2003. “Signal Transduction Pathways Regulated by Prolactin and Src Result in Different Conformations of Activated Stat5b.” *The Journal of Biological Chemistry* 278 (19): 17218–27. doi:10.1074/jbc.M301578200.

Lee, Genee Y., Paraic A. Kenny, Eva H. Lee, and Mina J. Bissell. 2007. “Three-Dimensional Culture Models of Normal and Malignant Breast Epithelial Cells.” *Nature Methods* 4 (4): 359–65. doi:10.1038/nmeth1015.

Lee, Heather J., David Gallego-Ortega, Anita Ledger, Daniel Schramek, Purna Joshi, Maria M. Szwarc, Christina Cho, et al. 2013. “Progesterone Drives Mammary Secretory Differentiation via RankL-Mediated Induction of Elf5 in Luminal Progenitor Cells.” *Development* 140 (7): 1397–1401. doi:10.1242/dev.088948.

Long, Weiwen, Kay-Uwe Wagner, K. C. Kent Lloyd, Nadine Binart, Jonathan M. Shillingford, Lothar Hennighausen, and Frank E. Jones. 2003. “Impaired Differentiation and Lactational Failure of Erbb4-Deficient Mammary Glands Identify ERBB4 as an Obligate Mediator of STAT5.” *Development (Cambridge, England)* 130 (21): 5257–68. doi:10.1242/dev.00715.

Lydon, J. P., F. J. DeMayo, C. R. Funk, S. K. Mani, A. R. Hughes, C. A. Montgomery, G. Shyamala, O. M. Conneely, and B. W. O’Malley. 1995. “Mice Lacking Progesterone Receptor Exhibit Pleiotropic Reproductive Abnormalities.” *Genes & Development* 9 (18): 2266–78.

Mulac-Jericevic, Biserka, John P. Lydon, Francesco J. DeMayo, and Orla M. Conneely. 2003. “Defective Mammary Gland Morphogenesis in Mice Lacking the Progesterone Receptor B Isoform.” *Proceedings of the National Academy of Sciences of the United States of America* 100 (17): 9744–49. doi:10.1073/pnas.1732707100.

Neville, Margaret C., Thomas B. McFadden, and Isabel Forsyth. 2002. “Hormonal Regulation of Mammary Differentiation and Milk Secretion.” *Journal of Mammary Gland Biology and Neoplasia* 7 (1): 49–66.

Nevins, J. R. 1992. “E2F: A Link between the Rb Tumor Suppressor Protein and Viral Oncoproteins.” *Science (New York, N.Y.)* 258 (5081): 424–29.

Nishikawa, S., R. C. Moore, N. Nonomura, and T. Oka. 1994. “Progesterone and EGF Inhibit Mouse Mammary Gland Prolactin Receptor and Beta-Casein Gene Expression.” *The American Journal of Physiology* 267 (5 Pt 1): C1467–72.

Oakes, Samantha R., Matthew J. Naylor, Marie-Liesse Asselin-Labat, Katrina D. Blazek, Margaret Gardiner-Garden, Heidi N. Hilton, Michael Kazlauskas, et al. 2008. “The Ets Transcription Factor Elf5 Specifies Mammary Alveolar Cell Fate.” *Genes & Development* 22 (5): 581–86. doi:10.1101/gad.1614608.

Obr, Alison E., Sandra L. Grimm, Kathleen A. Bishop, J. Wesley Pike, John P. Lydon, and Dean P. Edwards. 2013. “Progesterone Receptor and Stat5 Signaling Cross Talk Through RANKL in Mammary Epithelial Cells.” *Molecular Endocrinology* 27 (11): 1808–24. doi:10.1210/me.2013-1077.

Ormandy, C. J., A. Camus, J. Barra, D. Damotte, B. Lucas, H. Buteau, M. Edery, et al. 1997. “Null Mutation of the Prolactin Receptor Gene Produces Multiple Reproductive Defects in the Mouse.” *Genes & Development* 11 (2): 167–78.

Pellegrini, Pasquale, Alex Cordero, Marta I Gallego, William C. Dougall, Purificación Muñoz, Miguel Ángel Pujana, and Eva González Suárez. 2013. “Constitutive Activation of RANK Disrupts Mammary Cell Fate Leading to Tumorigenesis.” *Stem Cells* 31 (9): 1954–65.

Smalley, Matthew J. 2010. “Isolation, Culture and Analysis of Mouse Mammary Epithelial Cells.” *Methods in Molecular Biology (Clifton, N.J.)* 633: 139–70. doi:10.1007/978-1-59745-019-5_11.

Srivastava, Sunil, Manabu Matsuda, Zhaoyuan Hou, Jason P. Bailey, Riko Kitazawa, Matthew P. Herbst, and Nelson D. Horseman. 2003. “Receptor Activator of NF-kappaB Ligand Induction via Jak2 and Stat5a in Mammary Epithelial Cells.” *The Journal of Biological Chemistry* 278 (46): 46171–78. doi:10.1074/jbc.M308545200.

Stingl, John, Peter Eirew, Ian Ricketson, Mark Shackleton, François Vaillant, David Choi, Haiyan I. Li, and Connie J. Eaves. 2006. “Purification and Unique Properties of Mammary Epithelial Stem Cells.” *Nature* 439 (7079): 993–97. doi:10.1038/nature04496.

Teglund, S., C. McKay, E. Schuetz, J. M. van Deursen, D. Stravopodis, D. Wang, M. Brown, S. Bodner, G. Grosveld, and J. N. Ihle. 1998. “Stat5a and Stat5b Proteins Have Essential and Nonessential, or Redundant, Roles in Cytokine Responses.” *Cell* 93 (5): 841–50.

Wagner, Kay-Uwe, Andrea Krempler, Aleata A. Triplett, Yongyue Qi, Nicholas M. George, Jianqiong Zhu, and Hallgeir Rui. 2004. “Impaired Alveologenesis and Maintenance of Secretory Mammary Epithelial Cells in Jak2 Conditional Knockout Mice.” *Molecular and Cellular Biology* 24 (12): 5510–20. doi:10.1128/MCB.24.12.5510-5520.2004.

Yamaji, Daisuke, Risu Na, Yonatan Feuermann, Susanne Pechhold, Weiping Chen, Gertraud W. Robinson, and Lothar Hennighausen. 2009. “Development of Mammary Luminal Progenitor Cells Is Controlled by the Transcription Factor STAT5A.” *Genes & Development* 23 (20): 2382–87. doi:10.1101/gad.1840109.

Zhou, Jiong, Renee Chehab, Josephine Tkalcevic, Matthew J. Naylor, Jessica Harris, Trevor J. Wilson, Sue Tsao, et al. 2005. “Elf5 Is Essential for Early Embryogenesis and Mammary Gland Development during Pregnancy and Lactation.” *The EMBO Journal* 24 (3): 635–44. doi:10.1038/sj.emboj.7600538.

FIGURES

Figure 1

a

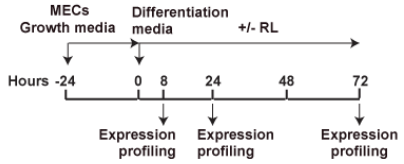

b

Differentially expressed

Hours	WT WT +RL	MMTV-Rank MMTV-Rank +RL	WT MMTV-Rank
8	0/0	73/11	93/91
24	20/54	152/177	83/177
72	171/341	607/341	379/572

c

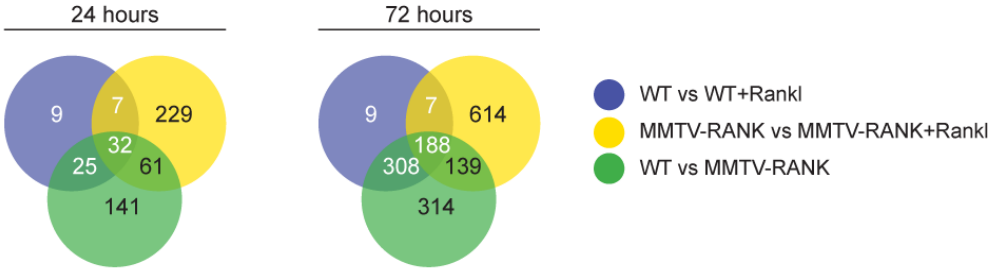

d

GO TERMS FROM GENES UPREGULATED IN ALL GROUPS (FC>2)

Gene ontology term	Category, level	Set size	Candidates contained	p-value	q-value
GO:0007049 cell cycle	BP 3	1175	40 (3.4%)	2.26e-31	2.76e-29
GO:0006996 organelle organization	BP 3	2205	30 (1.4%)	9.4e-12	2.87e-10
GO:0000226 microtubule cytoskeleton organization	BP 4	286	12 (4.2%)	3.07e-10	1.02e-08
GO:0006259 DNA metabolic process	BP 4	825	17 (2.1%)	2.64e-09	7.34e-08
GO:0033554 cellular response to stress	BP 3	1032	16 (1.6%)	4.37e-07	7.62e-06
GO:0036211 protein modification process	BP 4	2149	20 (0.9%)	3.46e-05	0.000304
GO:0022614 membrane to membrane docking	BP 4	5	2 (40.0%)	0.000124	0.000798
GO:0012501 programmed cell death	BP 4	1320	13 (1.0%)	0.000627	0.00326

GO TERMS FROM GENES DOWNREGULATED IN ALL GROUPS (FC>2)

Gene ontology term	Category, level	Set size	Candidates contained	p-value	q-value
GO:0070887 cellular response to chemical stimulus	BP 3	1268	15 (1.2%)	2.37e-05	0.001
GO:0006629 lipid metabolic process	BP 3	959	12 (1.3%)	0.000103	0.0026
GO:0071706 tumor necrosis factor superfamily cytokine production	BP 4	78	4 (5.1%)	0.000162	0.00521
GO:0001816 cytokine production	BP 3	412	7 (1.7%)	0.000556	0.00784
GO:0006810 transport	BP 2	2901	21 (0.7%)	0.000578	0.00763
GO:0009611 response to wounding	BP 3	693	9 (1.3%)	0.000619	0.00786
GO:0006954 inflammatory response	BP 4	427	7 (1.7%)	0.000651	0.0159
GO:0006631 fatty acid metabolic process	BP 4	273	5 (1.9%)	0.00257	0.0298

Figure 1. Gene expression analyses reveals overlapping genes and biological processes between MMTV-RANK and Rankl treatment in WT acini**.**

A. Scheme of microarray assay. Mammary epithelial cells from 3 WT and 3 MMTV-RANK G16,5 females were seeded in 3D cultures with growth media. After 24 h differentiation media (containing prolactin) with or without Rankl (RL) was added. RNA was collected 8, 24 and 72h later.

B. Differentially expressed genes (fold change higher than two-fold; red: up-regulated, blue: down-regulated) at the indicated time points for each signature.
C. Venn diagrams showing overlap between groups of genes up- and downregulated more than two-fold after 24 or 72 h of acinar Rankl (RL) treatment.
D. GO (Gene Ontology) enrichment analysis of genes up- or downregulated more than two-fold in all groups after 72 h of Rankl treatment. The most statistically significant and non-redundant GO terms for biological processes are represented.

Figure 2

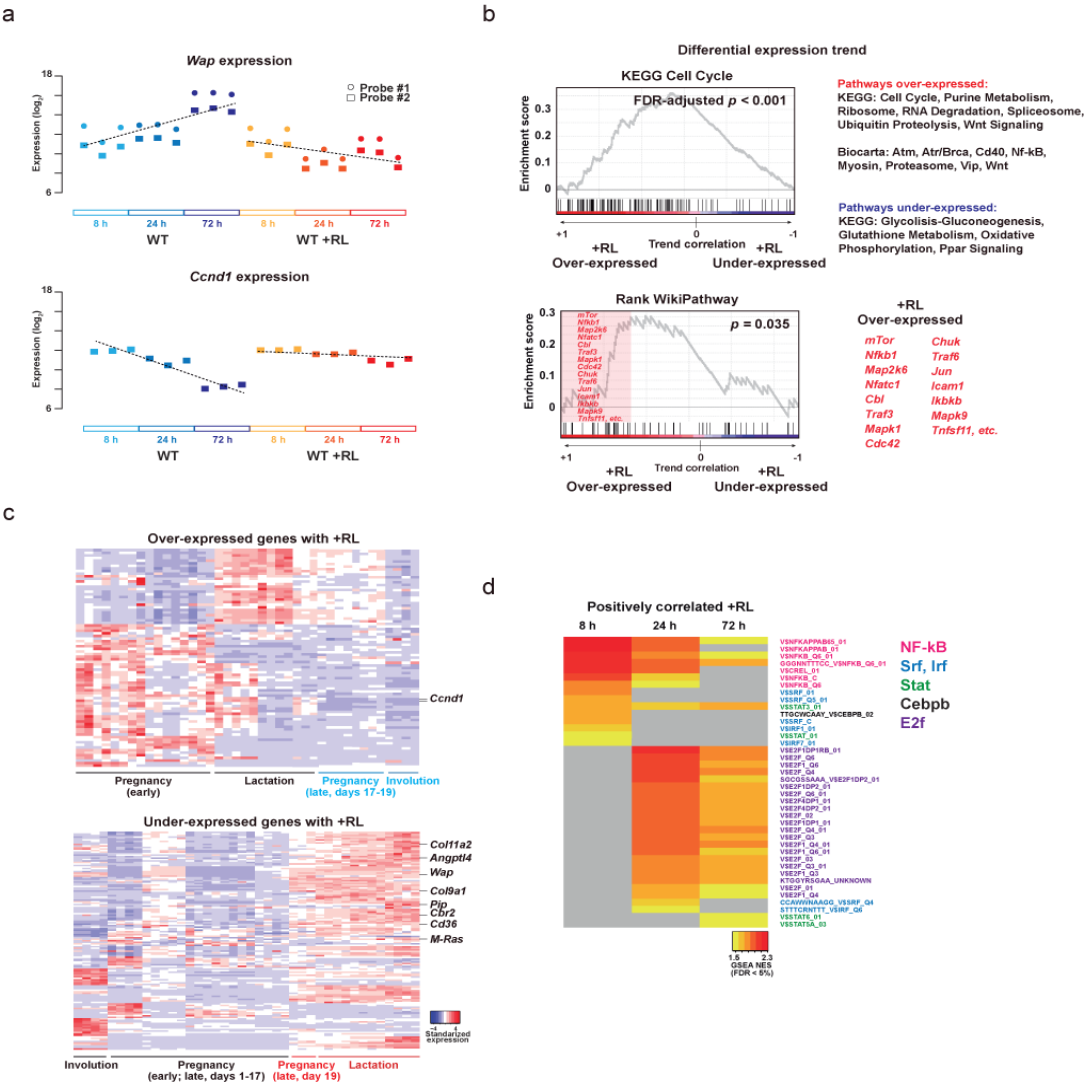

Figure 2. WT Acini gene expression changes with exposure to Rankl are consistent with increased proliferation and impaired alveolar differentiation**.**

A. Expression profiles of *Wap* and *Ccnd1* in WT acini exposed to RL. The results for two and one existing microarray probes of *Wap* and *Ccnd1*, respectively, are shown.

B. Top panel, GSEA graphical output for the association between over-expression of the KEGG Cell Cycle pathway and acini exposure to Rankl. Other significantly associated pathways are shown at the bottom, for KEGG and Biocarta annotations: red (top), over-expressed pathways; blue (bottom), under-expressed pathways, with WT acini exposure to RL. Bottom panel, GSEA graphical output for the association between over-expression of the Rank WikiPathway and acini exposure to Rankl. The top genes contributing to the over-expression association are listed.

C. Unsupervised heatmap clusters using the genes with the highest overexpression (top panel) and underexpression (bottom panel) slope values with acini exposure to Rankl. The developmental stages of the corresponding normal mice mammary gland samples are shown at the bottom of each cluster.

D. Profiles of predicted transcription factor binding sites significantly over-represented at 8, 24 and/or 72 h in acini exposed to Rankl. Coloured heatmap labels correspond to significant associations (false discovery rate (FDR) < 5%) and the scale is proportional to the enrichment score in the GSEA.

Figure 3

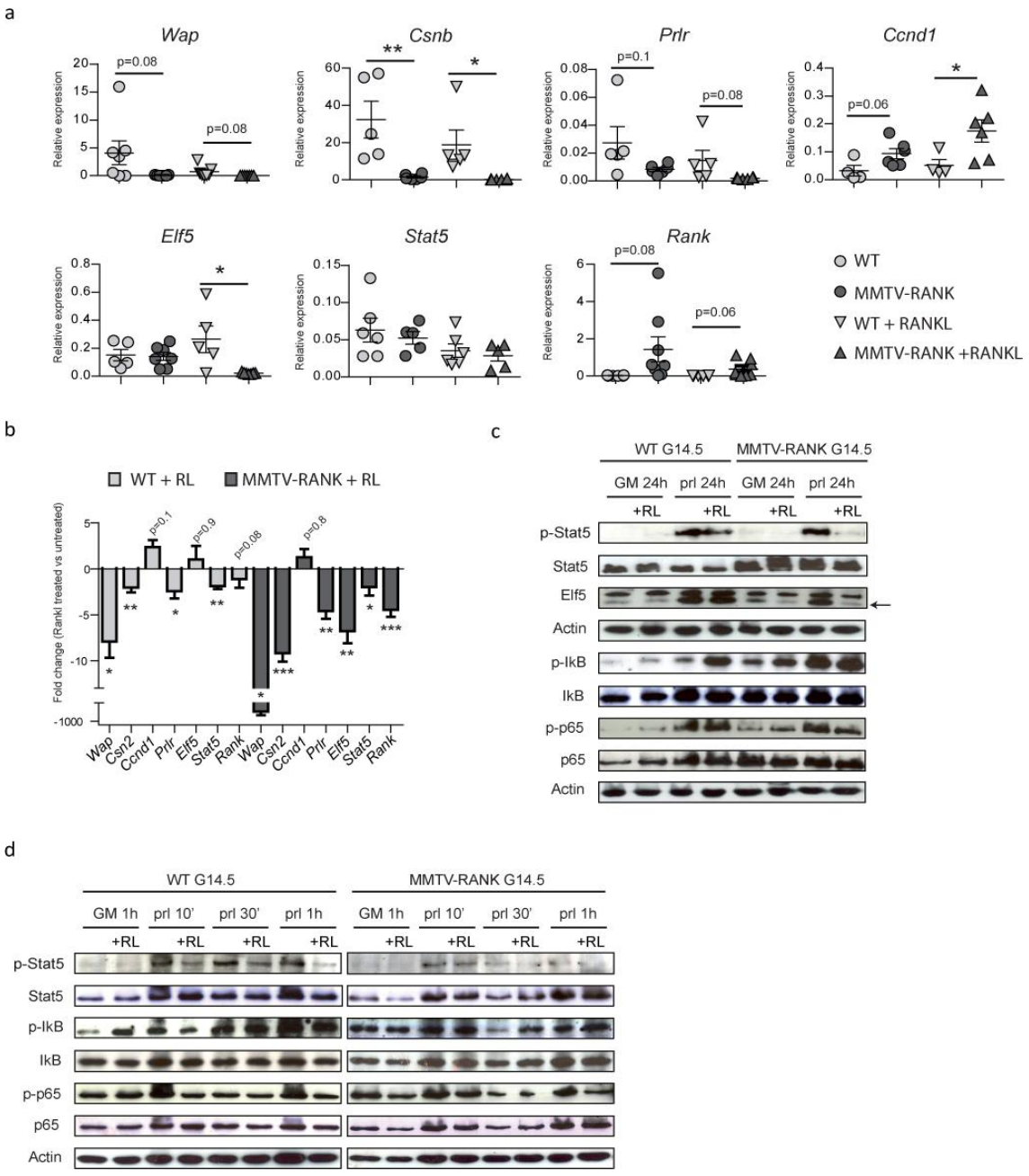

Figure 3: RANK signaling prevents alveolar secretory differentiation by negative regulation of p-Stat5 at midgestation.

A. mRNA expression levels of the indicated genes relative to *beta-actin* in WT and MMTV-RANK acini after 24 h of culture in differentiation media (prolactin, prl), with or without Rankl as determined by RT-PCR. Each dot represents mammary acini derived from one mouse at G14.5. Measurements were done in triplicate and means were used in the calculations. Significant differences are indicated by *.

B. Fold changes in the mRNA expression levels of the indicated genes in Rankl-treated relative to untreated mammary acinar cultures from WT and MMTV-RANK mice. Fold changes between paired treated and untreated samples were calculated, mean and SEM values are shown and t-test against reference was calculated for each gene. Cells derived from 4-8 different G14.5 mice were analyzed. Statistically significant differences are indicated.

C,D. Western blot analyses of the indicated proteins in WT and MMTV-RANK (G14.5) acinar cultures growing in GM and stimulated with prolactin (prl) with or without Rankl (RL) for 10, 30, 60 min or 24 h. Arrow in 3b indicates the Elf5 band. Results for one representative experiment out of 3 are shown. Spaces between sets of lanes indicate samples run on separate gels.

Figure 4

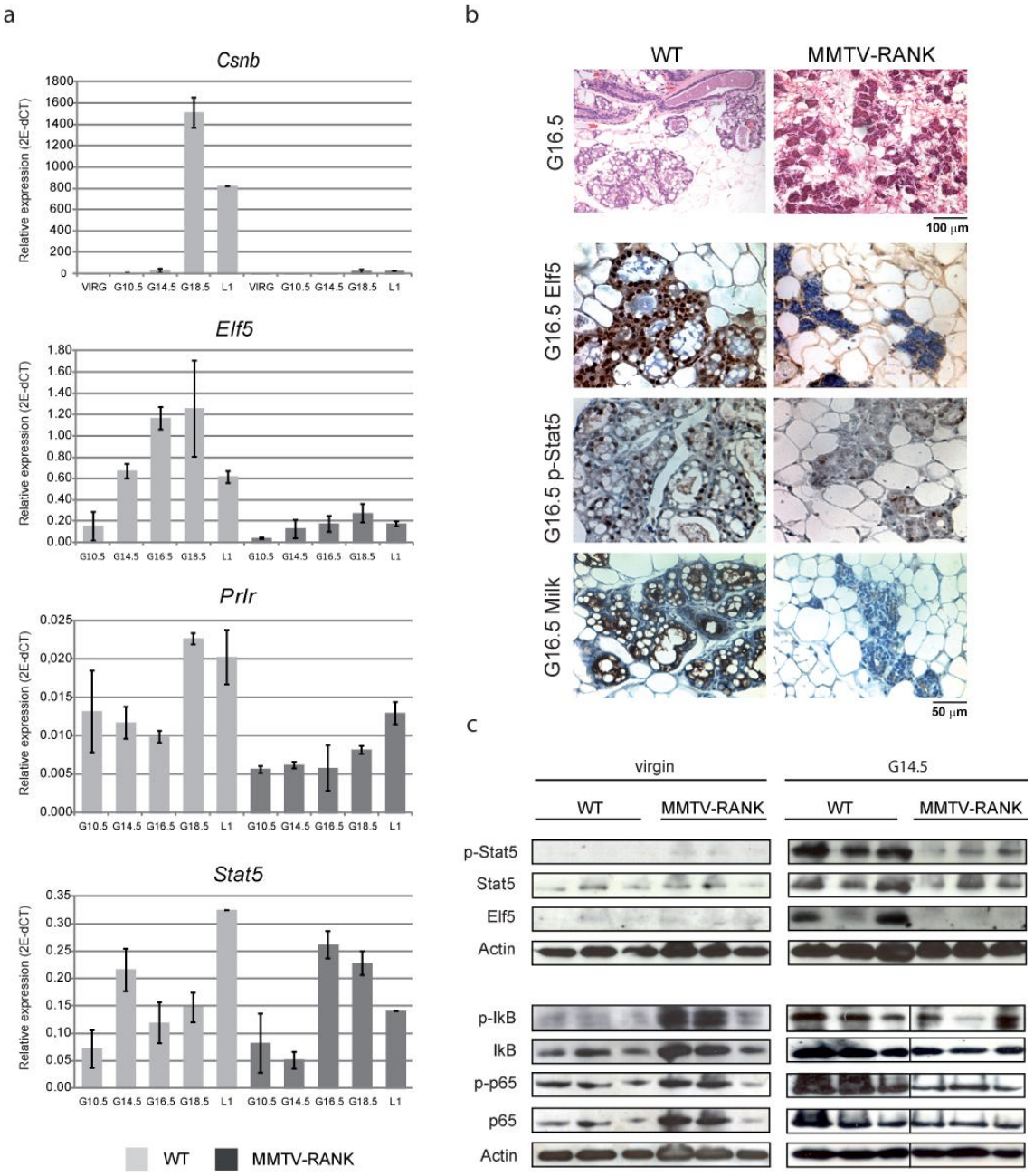

Figure 4: RANK overexpression during pregnancy interferes with p-Stat5 activation and Elf5 expression.

A. mRNA expression levels of indicated genes relative to *beta-actin* in WT and MMTV-RANK glands at the indicated time points during gestation. Each bar represents mean values for 2-3 mice and SD are indicated. For each sample measurements were done in triplicate and mean values were used in the calculations.

B. Representative H&E, Elf5, p-Stat5 and milk immunostainings at G16.5 of WT and MMTV-RANK mammary glands.

C. Western blot analyses of the indicated proteins in virgin and G14.5 mammary glands of WT and MMTV-RANK mice. Actin is shown as loading control. Spaces between sets of lanes indicate samples run on separate gels; thin black lines between lanes indicate splicing together of lanes run on the same gel.

Figure 5

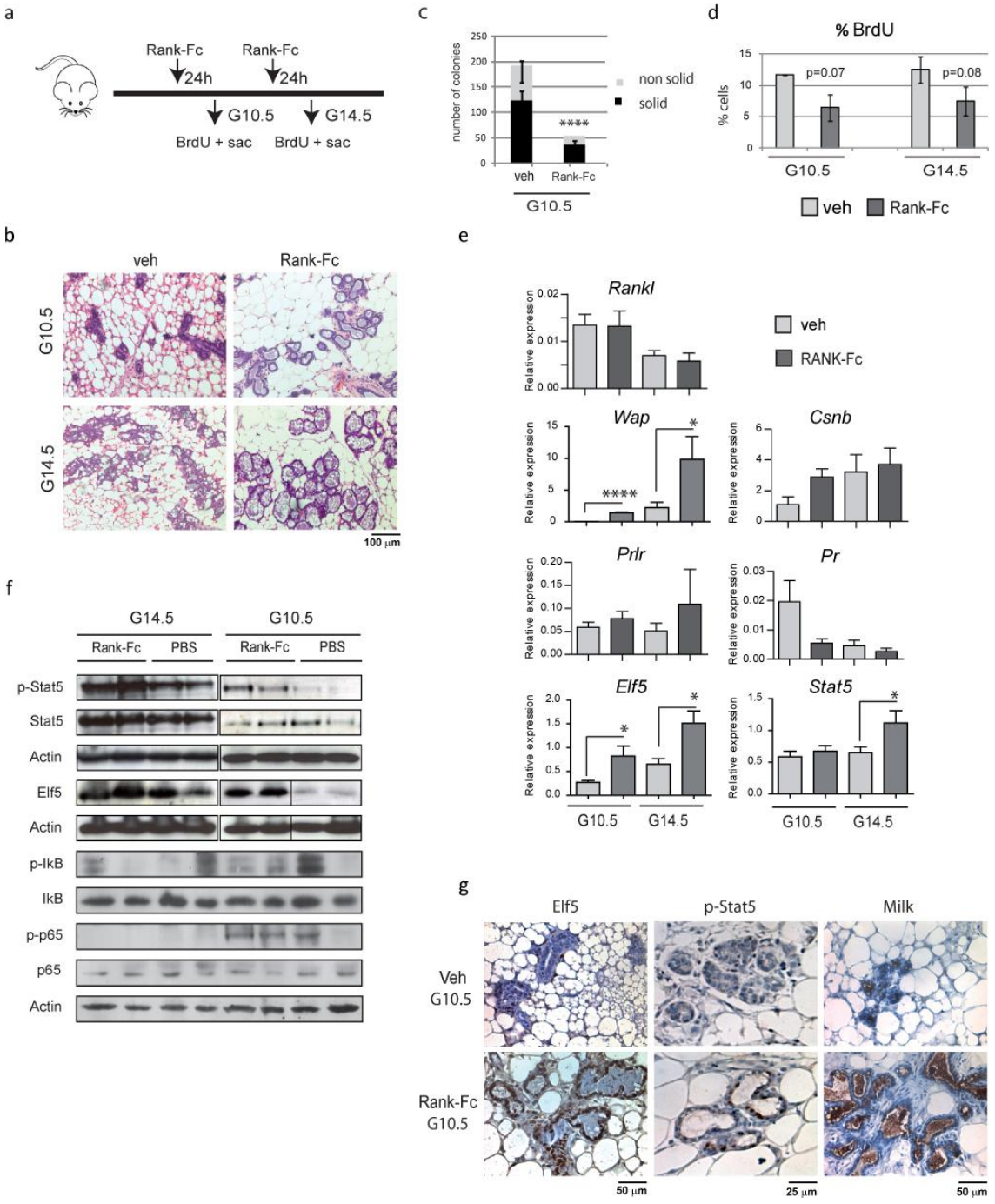

Figure 5: Pharmacological inhibition of Rankl during pregnancy induces precocious and exacerbated lactogenesis.

A. Schematic representation of Rank-Fc experiment. Pregnant WT females were injected with Rank-Fc (10 mg/kg) at midgestation and mammary glands were analyzed after 24 h.

B. Representative images of H&E at G10.5; G14.5 of WT mice 24 h after treatment with Rank - Fc or mock (veh).

C. Number of colonies (solid and non-solid) in matrigel formed by G10.5 MECs 24 h after Rank-Fc or mock treatment. The colony forming assay was done in triplicates and mean, SD values and *t* test probabilities for total number of colonies are shown. For solid colonies $p = 0.0003$, for non-solid $p = 0.02$. Results are representative of two independent experiments.

D. Percentage of proliferative cells measured by BrdU incorporation in Rank-Fc treated mice and controls. Each bar represents mean values for 3 mice and SD and p values are shown.
E. mRNA expression of indicated genes relative to *beta-actin* in G10.5; G14.5 mammary glands, 24 h after Rank-Fc or mock treatment. Each bar represents mean values for three mice; SEM and significant t test probabilities for significant differences are shown. Measurements for each sample were done in triplicates and mean values were used in the calculations.
F. Western blot analyses of the indicated proteins in WT G10.5, G14.5 mammary glands, 24 h after treatment with mock or Rank -Fc. Actin is shown as loading control.
Spaces between sets of lanes indicate samples run on separate gels; thin black lines between lanes indicate splicing together of lanes run on the same gel.
G. Representative images of Elf5, p-Stat5 and milk immunostainings at G10.5 in Rank -Fc treated WT mice and controls (veh).

Figure 6

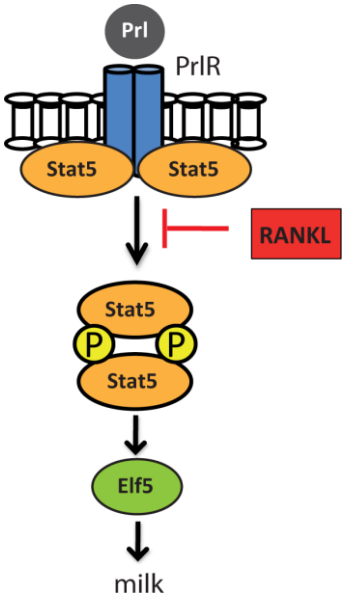

Figure 6: Rank signaling impairs lactogenesis through inhibition of prolactin/Stat5 pathway. Schematic representation of the negative role of Rankl in the PrlR/Stat5/Elf5 axis.

ANNEX 2

"Contribution of RANK downstream signaling pathways to the impaired STAT5 activation induced by RANKL at midgestation"

ABSTRACT

RANK signaling impairs mammary secretory differentiation during pregnancy through inhibition of the prolactin/STAT5/Elf5 pathway. In this annex we introduce some preliminary results investigating the mechanism by which RANKL stimulation interferes with prolactin induced-Stat5 phosphorylation. Our data suggest that NF-kB, PI3K-Akt, p38 and ERK pathways are not directly responsible of the impaired p-STAT5/Elf5 signaling induced by RANKL. Moreover, regulators of STAT5 phosphorylation such as STAT3, SOCS family and ErbB4 are not involved in RANKL-induced p-STAT5 impairment.

Overall, further investigations are required to elucidate the molecular mechanism that contributes to the impaired STAT5/Elf5 activation induced by RANKL at midgestation.

RESULTS AND DISCUSSION

RANK and its ligand, RANKL, are key regulators of mammary gland development (Fata et al. 2000; Gonzalez-Suarez et al. 2007). We have shown that RANKL inhibits mammary alveolar differentiation and lactogenesis at midgestation through inhibition of STAT5/Elf5 signaling (Cordero et.al, under revision). However, the molecular mechanism by which RANKL interferes with STAT5/Elf5 activation remains unknown.

We have previously shown that RANK overexpression in MCF10A human MECs leads to constitutive activation of several downstream pathways that play a role in mammary gland development, including NF-kB, PI3K-Akt, p38 and ERK (Palafox et al. 2012). NF-kB promotes mammary gland proliferation and side-branching during pregnancy (Cao et al. 2001), but a negative crosstalk between NF-kB and the PrlR/STAT5 activation in the mammary gland has been reported (Geymayer and Doppler 2000). PI3K-Akt signaling pathway regulates multiple biological processes including cell proliferation, and modulates PrlR/STAT5 activity through upregulation of Id2, a positive regulator of the pathway, and downregulation of negative modulators Caveolin-1 and Socs2 (Chen et al. 2010). The mitogen activated protein kinases (MAPK) ERK and p38 pathways are active in MECs and regulate cell proliferation, differentiation and survival (Pearson et al. 2001; Hui et al. 2007).

Our previous results showed activation of NF-kB pathway, evidenced by enhanced p-p65 and p-IkB levels, in WT and MMTV-RANK acini 24h after addition of prolactin (Cordero et. al, under revision). Higher levels of p-IkB were observed in WT acini under prolactin (DM) + RANKL treatment, compared to prolactin-treated acini. Moreover, p-IkB and p-p65 levels were higher in MMTV-RANK than in corresponding WT acini, suggesting that NF-kB activation could interfere with STAT5 phosphorylation observed at 24h, in agreement with previous observations (Geymayer and Doppler 2000). However, p-IkB levels did not increase in WT and MMTV-RANK acini treated with DM + RANKL at shorter time points, indicating that NF-kB is not responsible of the decreased STAT5 phosphorylation observed as early as after 10 minutes of prolactin + RANKL exposure (Cordero et. al, under revision), suggesting that additional mechanisms contribute to p-STAT5 inhibition.

Hence we tried to address the contribution of PI3K-Akt, p38 and ERK pathways to the PrlR/STAT5/Elf5 impairment induced by RANKL (Cordero et. al, under revision). Again, isolated MECs from WT and MMTV-RANK mice at midgestation (G.14,5) were seeded in 3D cultures in matrigel matrix, and treated with DM +/- RANKL stimuli. The protein levels for activated ERK, PI3K-Akt and p38 pathways were analyzed by WB. Our results showed a

severe reduction in p-ERK levels in WT MECs treated with DM during 24h, which was attenuated in the presence of RANKL, compared to corresponding controls in growth medium (GM, without prolactin) (Fig 1A). Moreover, p-ERK levels were higher in MMTV-RANK acini under prolactin +/- RANKL treatment, compared to corresponding WT acini. These results suggest that p-ERK signaling needs to be downregulated at midgestation to allow mammary alveolar differentiation, and the increased levels in MMTV-RANK acini and WT acini under DM + RANKL treatment could interfere with p-STAT5 activation. However, no differences in p-ERK were detected at shorter time points (10 min - 60 min), suggesting that additional mechanisms interfere with the impaired STAT5 phosphorylation observed in prolactin/RANKL treated cultures.

No clear differences in p-AKT or p-p38 levels were observed in both WT and MMTV-RANK MECs at any time point, irrespectively of RANKL (Fig. 1A,B). The slightly increased p-Akt levels observed in GM-treated MMTV-RANK MECs was probably related to the higher protein loading (actin) observed. Thus, ERK, PI3K-Akt and p38 signaling pathways are not involved in the inhibition of STAT5 phosphorylation driven by RANKL in differentiation media.

Next, we tried to functionally address the contribution of NF-kB, PI3K-Akt, p38 and ERK to the impaired mammary epithelial cell differentiation induced by RANKL using inhibitors. First, isolated MECs from midgestant (G.14,5) WT mice were cultured *in vitro* in GM and DM +/- RANKL, and the efficiency of NF-kB (Bay65), PI3K-Akt (LY294002), p38 (SB203580) and ERK (UO126) inhibitors was tested at protein level (Fig 2A). Reduced activation of the corresponding pathways was observed in the presence of the inhibitors (Fig 2A). In addition, the efficiency of NF-kB inhibitor peptide SN50 was tested *in vitro* (Fig 2B). Indeed, G.14,5 WT and MMTV-RANK acini were treated with GM or DM +/- RANKL and/or SN50 inhibitor. Lipopolysaccharide (LPS) was added to GM-treated cultures as a positive regulator of NF-kB signaling activation (Beg et al. 1995). As expected, increased nuclear p65 levels were observed in WT and MMTV-RANK acini treated with LPS during 30 minutes. However, SN50 inhibitor was not able to reduce p65 nuclear staining in WT and MMTV-RANK-treated acini. According to previous data (Gonzalez-Suarez et al. 2007), MMTV-RANK MECs under prolactin + RANKL treatment showed increased p65 nuclear translocation compared to WT. Moreover, SN50 not only was not able to reduce p65 nuclear translocation but it promoted this nuclear p65 signaling. These results reflect the complexity of NF-kB signaling regulation and feedback mechanisms. Further experiments and dose curve response need to be performed to demonstrate the efficiency of SN50 inhibitor in WT and MMTV-RANK midgestant acini *in vitro.*

WT and MMTV-RANK G.16,5 acini were treated *in vitro* with DM +/- RANKL +/- inhibitors for NF-kB (Bay65, Bay11, SN50), ERK (UO126), PI3K-AKT (LY294002) or p38 (SB203580). After 24h, the milk protein WAP mRNA expression levels were analyzed by RT-PCR as an indicator of lactogenic differentiation (Fig 2C). As previously shown, a clear increase in WAP levels were observed in WT MECs under prolactin treatment, which were significantly reduced in the presence of RANKL (Cordero et. al, under revision). Our results showed that WAP expression levels were not rescued in WT MECs treated with DM + RANKL + any of the inhibitors, suggesting that RANK downstream signaling pathways are not directly responsible of the impaired p-STAT5/Elf5 signaling and subsequent alveolar differentiation failure induced by RANKL. Moreover, WAP expression levels decreased in the presence of these inhibitors, except for the NF-kB peptide inhibitor SN50 (Fig 2C), suggesting that NF-kB, PI3K-Akt, p38 and ERK signaling pathways play a positive role in mammary alveologenesis. Consistent with previous observations, MMTV-RANK MECs showed impaired WAP levels under prolactin treatment that further decreased in the presence of RANKL (Cordero et. al, under revision). Again, WAP levels were not rescued in the presence of DM + RANKL + any of the inhibitors. Moreover, our results showed unexpected increased WAP levels in MMTV-RANK MECs treated with prolactin + BAY65 and SN50 inhibitors, compared to prolactin-treated MECs. These results suggest a complex role for RANK downstream signaling pathways in the regulation of the alveolar cell differentiation process. Moreover, the specific inhibition of NF-kB, PI3K-Akt, p38 and ERK does not rescue the impaired mammary epithelial differentiation induced by RANKL. Thus, additional mechanisms may contribute to the decreased STAT5 phosphorylation under RANK signaling overactivation.

Next, we addressed the contribution of the negative regulators of PrlR/JAK2/STAT5 signaling. Suppressor of cytokine signaling (SOCS) proteins and Caveolin-1 have been described as part of the negative feedback loop, attenuating STAT5 phosphorylation and activation, keeping the signaling pathway under a strict regulatory control (Jasmin et al. 2006). The SOCS protein family comprises eight members, although the most well-known are SOCS1, SOCS2 and SOCS3. In particular, SOCS1 binds to JAK2 and inhibits its kinase activity, targeting it for proteasomal degradation (Jasmin et al. 2006). SOCS2 mechanism of action remains poorly understood, although the deletion of both alleles of SOCS2 can rescue the lactation defect observed in $PRLR^{+/-}$ heterozygous mice (Harris et al. 2006). SOCS3 is a critical repressor of STAT3-mediated mammary gland apoptosis during involution, although its concrete role in lactation has not been elucidated (Sutherland et al. 2006). Caveolin-1 is a membrane-bound protein that prevents the PrlR-JAK2 binding, thus negatively regulating STAT5 phosphorylation and a proper mammary gland

differentiation during pregnancy (Hennighausen and Robinson 2008). Our results indicated that the mRNA expression levels of SOCS1, SOCS2, SOCS3 and caveolin-1 decreased in G.14,5 WT MECs treated with GM + RANKL for 24h, compared to GM (Fig 3). Moreover, we found an increase in SOCS1, SOCS3 and caveolin-1 in MECs under prolactin treatment, compared to GM. SOCS1, 2, 3 expression levels were not increased after prolactin + RANKL treatment. A modest increase in caveolin-1 levels were observed under DM + RANKL treatment and will be investigated in the future.

We have also interrogated the levels of ErbB4, a tyrosine kinase receptor that mediates STAT5 phosphorylation at late-stages of pregnancy and lactation (Jones et al. 1999). A clear increase in ErbB4 mRNA levels was observed during gestation in WT and MMTV-RANK glands compared to virgin glands (Fig. 4). Moreover, a slight increase in ErbB4 levels was observed in prolactin-treated WT MECs during 24h, which was further enhanced in the presence of RANKL, compared to corresponding GM-treated controls (Fig 4B). These results suggest that impaired lactogenic differentiation observed upon RANK signaling activation is not due to a reduction in ErbB4 expression.

Moreover, we asked the role of STAT3, which antagonizes with STAT5 lactogenic and survival activities, determining the end of lactation and apoptosis induction of mammary secretory cells (Bertucci et al. 2010; Humphreys et al. 2002). Moreover, STAT5 directly protects cells from the STAT3-mediated death signals (Clarkson et al. 2006). Thus, we analyzed if an increase in p-STAT3 levels could explain the lower p-STAT5 protein expression levels observed in midgestant MMTV-RANK mammary glands (Cordero et.al. under revision). Our preliminary results showed no differences in p-STAT3 expression levels in WT and MMTV-RANK mammary glands at midgestation (G.14,5-16,5) (Fig 5A). More experiments need to be performed to analyze if STAT3 is competing with STAT5 phosphorylation throughout gestation.

In conclusion, our results indicate that all the transcriptional changes observed in midgestant WT MECs under prolactin and RANKL treatment (and consequently in MMTV-RANK mice at midgestation) seem to be the consequence and not the cause of the impaired mammary alveolar differentiation phenotype, and cannot explain the RANKL short-term inhibitory effects in p-STAT5 levels previously reported (Cordero et.al, under revision). Further experiments are needed to elucidate other possible candidates that could contribute to this inhibitory effects such as c-Src, a tyrosine kinase that can directly phosphorylate the activation site of STAT5 (Okutani et al. 2001). Moreover, c-Src binds to activated RANK via its Src homology 2 (SH2) domain in the osteoclast cytoskeleton (Izawa et al. 2012).

MATHERIALS AND METHODS

Mice

All research involving animals was done in IDIBELL animal facility and complied with protocols approved by the IDIBELL Committee on Animal Care, local animal welfare laws, guidelines and policies. MMTV-RANK mice in FVB background were obtained through collaboration with Dr. Bill Dougall (Oncology Research-AMGEN).

3D cultures

For differentiation assays in 3D cultures, 600.000 primary mammary epithelial cells isolated from pregnant (G.14,5 or G.16,5) WT and MMTV-RANK females were plated in growth media that contains DMEM-F12, 5% FBS, EGF 10 ng/ml (E9644, Sigma-Aldrich), hydrocortinose 0,5 μg/ml (H-0888, Sigma-Aldrich), insulin 5 μg/ml (I-1882, Sigma-Aldrich), cholera toxin 100 ng/ml (C-8052, Sigma-Aldrich) and penicillin-strepromycin (15070-063, Invitrogen). After 24h the medium was changed to differentiation media containing DMEM-F12, prolactin 3 μg/ml (L6520, Sigma-Aldrich), hydrocortinose 1 μg/ml (H-0888, Sigma-Aldrich), ITS (insulin, transferrin, selenium; I3146, Sigma-Aldrich), cholera toxin 100 ng/ml (C-8052, Sigma-Aldrich) and penicillin-strepromycin (15070-063, Invitrogen) with/without Rankl-LZ (1 μg/ml; Amgen Inc). After 24h in culture MECs were isolated dissolving matrigel with cold PBS-EDTA (5 mM) for 30 minutes.

Inhibition assays

For inhibition assays, isolated MECs from WT and MMTV-RANK mice at midgestation (G.14,5 or G.16,5) were plated in 3D cultures in GM for 24h. WT and MMTV-RANK acini were then treated during 24h with 5 μM BAY65 (NF-κB inhibitor; Calbiochem), 10 μM BAY11 (NF-κB inhibitor; Calbiochem), 72 μM SN50 (NF-κB inhibitor; Enzo), 10μM SB203580 (p38 inhibitor: Calbiochem), 10 μM UO126 (ERK inhibitor; Calbiochem) or 10μM LY294002 (Pi3K-Akt inhibitor; Selleckchem). Inhibitors were added 2h before stimulation with prolactin (DM) +/- RANKL. After 24h in culture, the medium was removed and protein or RNA extracts were collected.

Inhibition assays for p65 quantification were performed in G.14,5 WT and MMTV-RANK MECs in 3D cultures. Again, MECs were plated in GM. After 24h, 72 μM SN50 (NF-κB inhibitor; Enzo) was added to the medium during 6 days. 2h after inhibitor addition, prolactin (DM) +/- RANKL were added to the medium. The treatment was refreshed every

48h to avoid degradation of the inhibitor. 6 days later the medium was removed and IF was performed.

RNA extraction and RT-PCR

Total RNA of acinar cultures was prepared with Tripure Isolation Reagent (11667165001 Roche). 20 ng/ml of mRNA were pretreated with DNase I (Ambion). cDNA was produced by reverse transcription using 1 µg of RNA in a 35-µL (Applied Biosystems). 20 ng/well of RNA/cDNA were used and analyses were performed in triplicate. Quantitative PCR was performed using LightCycler® 480 SYBR green. Primer sequences are indicated below.

mWAP Fwd → 5' TGCCTCATCAGCCTAGTTCTTG 3'
mWAP Rev → 5' CTGGAGCATTCTATCTTCATTGGG 3'
mErbB4 Fwd → 5' AATGCTGATGGTGGCAAGA 3'
mErbB4 Rev → 5' CATCACTTTGATGTGTGAATTTCC 3'
mSOCS1 Fwd → 5' GTGGTTGTGGAGGGTGAGAT 3'
mSOCS1 Rev → 5' CCTGAGAGGTGGGATGAGG 3'
mSOCS2 Fwd → 5' CGCGAGCTCAGTCAAACAG 3'
mSOCS2 Rev → 5' AGTTCCTTCTGGAGCCTCTTTT 3'
mSOCS3 Fwd → 5' ATTTCGCTTCGGGACTAGC 3'
mSOCS3 Rev → 5' AACTTGCTGTGGGTGACCAT 3'
mCav-1 Fwd → 5' CCAGGGAAACCTCCTCAGA 3'
mCav-1 Rev → 5' CCGGATGGGAACAGTGTAGA 3'
HK PP1A Fwd → 5' CAAATGCTGGACCAAACACAAACG 3'
HK PP1A Rev → 5' GTTCATGCCTTCTTTCACCTTCCC 3'

Western blot

Western blotting was performed with standard protocols. Briefly, cells were lysed with RIPA buffer (50 mM Tris-HCl at pH 7.6, 150mM NaCl, 1% NP-40, 0,5% Sodium deoxycholate, 0,1% SDS, 5mM EDTA). Proteases and phosphatases inhibitors (Roche) were added freshly to the lysis buffer. Blots were blocked for 1 h at room temperature with 5% milk in 10 mM Tris-HCl pH 7.5, 150 mM NaCl containing 0.1% Tween 20 (TBST) and incubated overnight at 4ºC with Primary antibodies reactive to mouse p-P65 (3033, , Cell Signaling), p-IkBα (S32/36, Cell Signaling), p-ERK (E7028, Sigma-Aldrich), p-AKT (4051, Cell Signaling), p-p38 (9211, Cell Signaling), p-STAT3 (9131, Cell Signaling) Tubulin (T9026, Sigma-Aldrich) and β-actin (AC-74, Sigma) were used. After washing, blots were incubated

with horseradish peroxidase-conjugated secondary antibodies (1:2000, Promega) for 1 h at 20–25 °C, and revealed with enhanced chemiluminescence.

Immunofluorescence

Acinar structures were stained as previously described (Debnath J, 2003). Briefly, acini were fixed in 2% paraformaldehyde (20 min), permeabilized with PBS containing 2% Triton X-100 (30 min), and washed with PBS-Glycine 100 mM (three washes of 15 min each). Antigens were blocked with IF buffer (PBS, 7.7 mM NaN_3, 0.1% bovine serum albumin, 0.2% Triton x-100, 0.05% Tween-20) + 10% goat serum for 1 h and then with IF buffer + goat serum + 20 µg/mL F(ab') fragment (Jackson ImmunoResearch) for 30 min. Primary antibodies against p65 (D14E12, Cell Signaling) and K8 (TROMA, dshl, Developmental Studies Hybridoma Bank, Iowa City, Iowa) were incubated overnight in a humid chamber. Opportune fluorochrome conjugated secondary antibodies (Invitrogen) were added after primary incubation, diluted 1:500 in IF buffer + 10% goat serum and incubated for 40 min. Acini were then washed with IF buffer and cell nuclei were stained with DAPI (Sigma), and then mounted with Prolong ® Gold Antifade (Life Technologies). Confocal analysis was carried out using Leica confocal microscope. Images were captured using LasAF software (Leica).

REFERENCES

Beg, A. A., W. C. Sha, R. T. Bronson, and D. Baltimore. 1995. “Constitutive NF-Kappa B Activation, Enhanced Granulopoiesis, and Neonatal Lethality in I Kappa B Alpha-Deficient Mice.” *Genes & Development* 9 (22): 2736–46. doi:10.1101/gad.9.22.2736.

Bertucci, Paola Y., Ana Quaglino, Andrea G. Pozzi, Edith C. Kordon, and Adali Pecci. 2010. “Glucocorticoid-Induced Impairment of Mammary Gland Involution Is Associated with STAT5 and STAT3 Signaling Modulation.” *Endocrinology* 151 (12): 5730–40. doi:10.1210/en.2010-0517.

Cao, Y., G. Bonizzi, T. N. Seagroves, F. R. Greten, R. Johnson, E. V. Schmidt, and M. Karin. 2001. “IKKalpha Provides an Essential Link between RANK Signaling and Cyclin D1 Expression during Mammary Gland Development.” *Cell* 107 (6): 763–75.

Chen, Chien-Chung, Robert B. Boxer, Douglas B. Stairs, Carla P. Portocarrero, Rachel H. Horton, James V. Alvarez, Morris J. Birnbaum, and Lewis A. Chodosh. 2010. “Akt Is Required for Stat5 Activation and Mammary Differentiation.” *Breast Cancer Research: BCR* 12 (5): R72. doi:10.1186/bcr2640.

Clarkson, Richard W. E., Marion P. Boland, Ekaterini A. Kritikou, Jennifer M. Lee, Tom C. Freeman, Paul G. Tiffen, and Christine J. Watson. 2006. “The Genes Induced by Signal Transducer and Activators of Transcription (STAT)3 and STAT5 in Mammary Epithelial Cells Define the Roles of These STATs in Mammary Development.” *Molecular Endocrinology (Baltimore, Md.)* 20 (3): 675–85. doi:10.1210/me.2005-0392.

Fata, J. E., Y. Y. Kong, J. Li, T. Sasaki, J. Irie-Sasaki, R. A. Moorehead, R. Elliott, et al. 2000. “The Osteoclast Differentiation Factor Osteoprotegerin-Ligand Is Essential for Mammary Gland Development.” *Cell* 103 (1): 41–50.

Geymayer, Sibylle, and Wolfgang Doppler. 2000. “Activation of NF-κB p50/p65 Is Regulated in the Developing Mammary Gland and Inhibits STAT5-Mediated β-Casein Gene Expression.” *The FASEB Journal* 14 (9): 1159–70.

Gonzalez-Suarez, Eva, Daniel Branstetter, Allison Armstrong, Huyen Dinh, Hal Blumberg, and William C. Dougall. 2007. “RANK Overexpression in Transgenic Mice with Mouse Mammary Tumor Virus Promoter-Controlled RANK Increases Proliferation and Impairs Alveolar Differentiation in the Mammary Epithelia and Disrupts Lumen Formation in Cultured Epithelial Acini.” *Molecular and Cellular Biology* 27 (4): 1442–54. doi:10.1128/MCB.01298-06.

Harris, Jessica, Prudence M. Stanford, Kate Sutherland, Samantha R. Oakes, Matthew J. Naylor, Fiona G. Robertson, Katrina D. Blazek, et al. 2006. “Socs2 and Elf5 Mediate Prolactin-Induced Mammary Gland Development.” *Molecular Endocrinology* 20 (5): 1177–87. doi:10.1210/me.2005-0473.

Hennighausen, Lothar, and Gertraud W. Robinson. 2008. “Interpretation of Cytokine Signaling through the Transcription Factors STAT5A and STAT5B.” *Genes & Development* 22 (6): 711–21. doi:10.1101/gad.1643908.

Hui, Lijian, Latifa Bakiri, Ewa Stepniak, and Erwin F. Wagner. 2007. “p38alpha: A Suppressor of Cell Proliferation and Tumorigenesis.” *Cell Cycle (Georgetown, Tex.)* 6 (20): 2429–33.

Humphreys, Robin C., Brian Bierie, Ling Zhao, Regina Raz, David Levy, and Lothar Hennighausen. 2002. “Deletion of Stat3 Blocks Mammary Gland Involution and Extends Functional Competence of the Secretory Epithelium in the Absence of Lactogenic Stimuli.” *Endocrinology* 143 (9): 3641–50. doi:10.1210/en.2002-220224.

Izawa, Takashi, Wei Zou, Jean C. Chappel, Jason W. Ashley, Xu Feng, and Steven L. Teitelbaum. 2012. “C-Src Links a RANK/αvβ3 Integrin Complex to the Osteoclast Cytoskeleton.” *Molecular and Cellular Biology* 32 (14): 2943–53. doi:10.1128/MCB.00077-12.

Jasmin, Jean-François, Isabelle Mercier, Federica Sotgia, and Michael P. Lisanti. 2006. “SOCS Proteins and Caveolin-1 as Negative Regulators of Endocrine Signaling.” *Trends in Endocrinology and Metabolism: TEM* 17 (4): 150–58. doi:10.1016/j.tem.2006.03.007.

Jones, F. E., T. Welte, X. Y. Fu, and D. F. Stern. 1999. “ErbB4 Signaling in the Mammary Gland Is Required for Lobuloalveolar Development and Stat5 Activation during Lactation.” *The Journal of Cell Biology* 147 (1): 77–88.

Okutani, Y., A. Kitanaka, T. Tanaka, H. Kamano, H. Ohnishi, Y. Kubota, T. Ishida, and J. Takahara. 2001. “Src Directly Tyrosine-Phosphorylates STAT5 on Its Activation Site and Is Involved in Erythropoietin-Induced Signaling Pathway.” *Oncogene* 20 (45): 6643–50. doi:10.1038/sj.onc.1204807.

Palafox, Marta, Irene Ferrer, Pasquale Pellegrini, Sergi Vila, Sara Hernandez-Ortega, Ander Urruticoechea, Fina Climent, et al. 2012. “RANK Induces Epithelial-Mesenchymal Transition and Stemness in Human Mammary Epithelial Cells and Promotes Tumorigenesis and Metastasis.” *Cancer Research* 72 (11): 2879–88. doi:10.1158/0008-5472.CAN-12-0044.

Pearson, Gray, Fred Robinson, Tara Beers Gibson, Bing-e Xu, Mahesh Karandikar, Kevin Berman, and Melanie H. Cobb. 2001. “Mitogen-Activated Protein (MAP) Kinase Pathways: Regulation and Physiological Functions.” *Endocrine Reviews* 22 (2): 153–83. doi:10.1210/edrv.22.2.0428.

Sutherland, Kate D, François Vaillant, Warren S Alexander, Tim M Wintermantel, Natasha C Forrest, Sheridan L Holroyd, Edward J McManus, et al. 2006. “C-Myc as a Mediator of Accelerated Apoptosis and Involution in Mammary Glands Lacking Socs3.” *The EMBO Journal* 25 (24): 5805–15. doi:10.1038/sj.emboj.7601455.

FIGURES

Figure 1

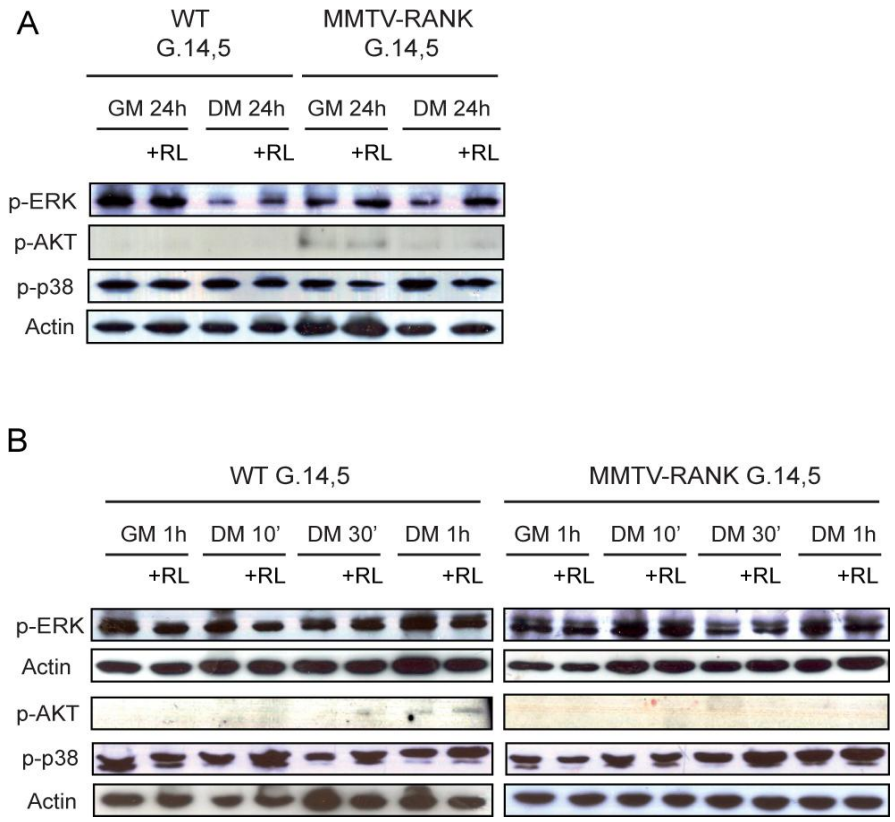

Figure 1. ERK, PI3K-Akt and p38 signaling pathways are not responsible of p-STAT5 inhibition induced by RANKL at short time points.
A,B. Western blot analyses of the indicated genes in WT and MMTV-RANK (G14.5) acinar cultures growing in GM and stimulated with prolactin (DM) with or without RANKL (RL) for 10, 30, 60 min or 24h. Actin is shown as loading control. Results for one representative experiment out of 2-3 are shown.

Figure 2

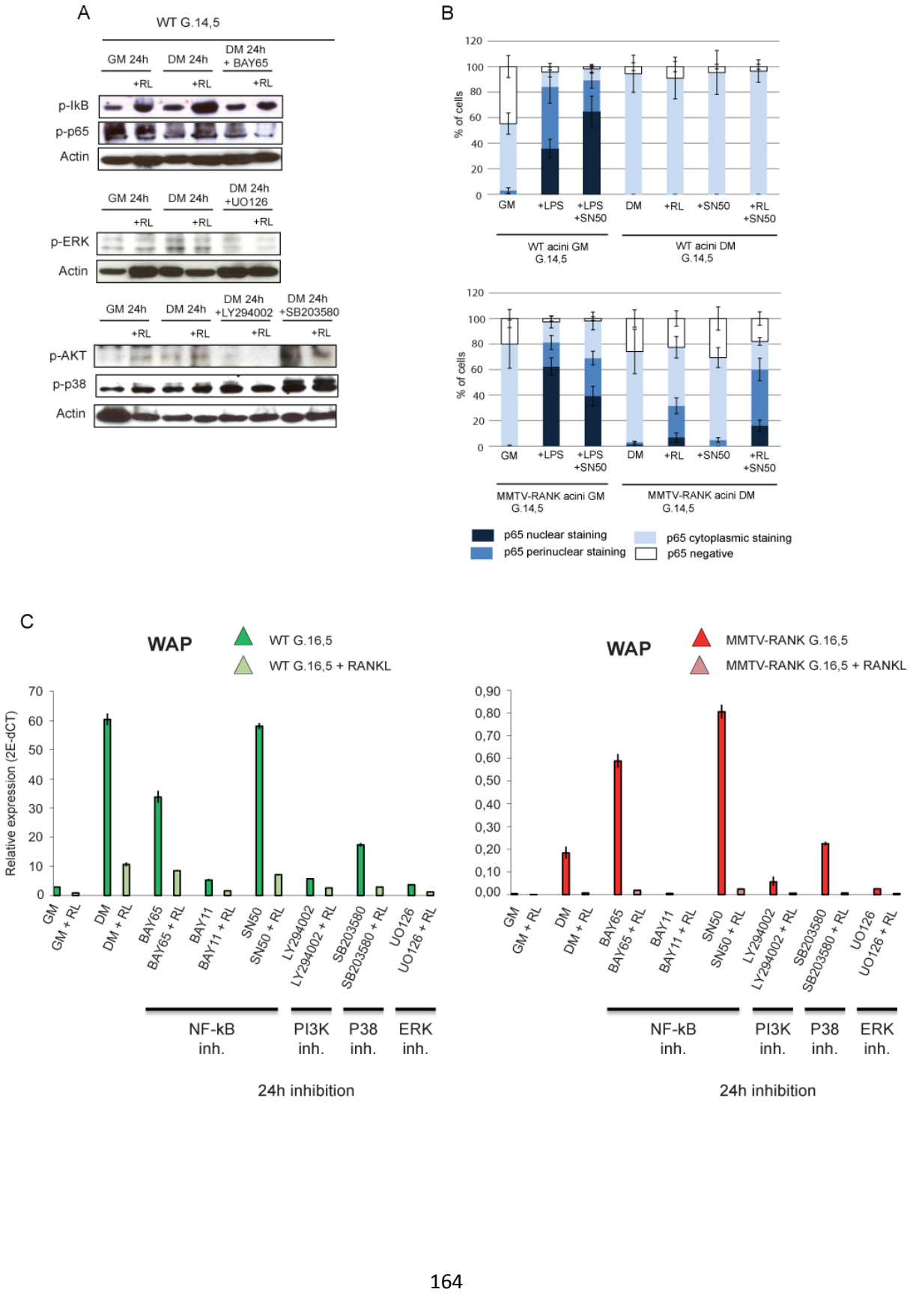
A
WT G.14,5
GM 24h
DM 24h
DM 24h + BAY65
+RL
p-IkB
p-p65
Actin
DM 24h +UO126
p-ERK
DM 24h +LY294002
DM 24h +SB203580
p-AKT
p-p38
B
% of cells
GM
+LPS
+LPS +SN50
DM
+RL
+SN50
+RL +SN50
WT acini GM G.14,5
WT acini DM G.14,5
MMTV-RANK acini GM G.14,5
MMTV-RANK acini DM G.14,5
p65 nuclear staining
p65 perinuclear staining
p65 cytoplasmic staining
p65 negative
C
WAP
WT G.16,5
WT G.16,5 + RANKL
Relative expression (2E-dCT)
GM
GM + RL
DM
DM + RL
BAY65
BAY65 + RL
BAY11
BAY11 + RL
SN50
SN50 + RL
LY294002
LY294002 + RL
SB203580
SB203580 + RL
UO126
UO126 + RL
NF-kB inh.
PI3K inh.
P38 inh.
ERK inh.
24h inhibition
MMTV-RANK G.16,5
MMTV-RANK G.16,5 + RANKL

Figure 2. RANK downstream NF-kB, ERK, PI3K-Akt and p38 pathways play a positive role on lactogenesis.

A. Western blot analyses of the indicated genes in WT (G14.5) acinar cultures growing in GM or DM +/- RANKL +/- specific inhibitors for NF-kB (5μM BAY65), ERK (10 μM UO126), PI3K-AKT (10μM LY294002) or p38 (10μM SB203580) pathways for 24h. Results for 1 or 2 experiments are shown.
B. Percentage of cells with positive (nuclear, perinuclear, cytoplasmic) or negative p65 staining in G.14,5 WT acini after 6 days in culture in GM +/- SN50 (72 μM) or DM +/- RANKL +/- SN50 (72 μM). GM treated cultures were stimulated with LPS (1.6 μg/mL) for 30 minutes to induce p65 nuclear translocation. Quantification, mean and SEM for 1 experiment is shown.
C. WAP mRNA expression levels, relative to PP1A, of acini isolated from WT and MMTV-RANK at G.16,5, and incubated in GM or DM +/- RANKL in the presence of the indicated specific inhibitors for 24 hours. Measurements for each sample were performed in triplicate and mean and SEM are shown. Note different scale used in WT and MMTV-RANK acinar cultures, as WT cultures express 100-fold higher levels of WAP than MMTV-RANK cultures.

Figure 3

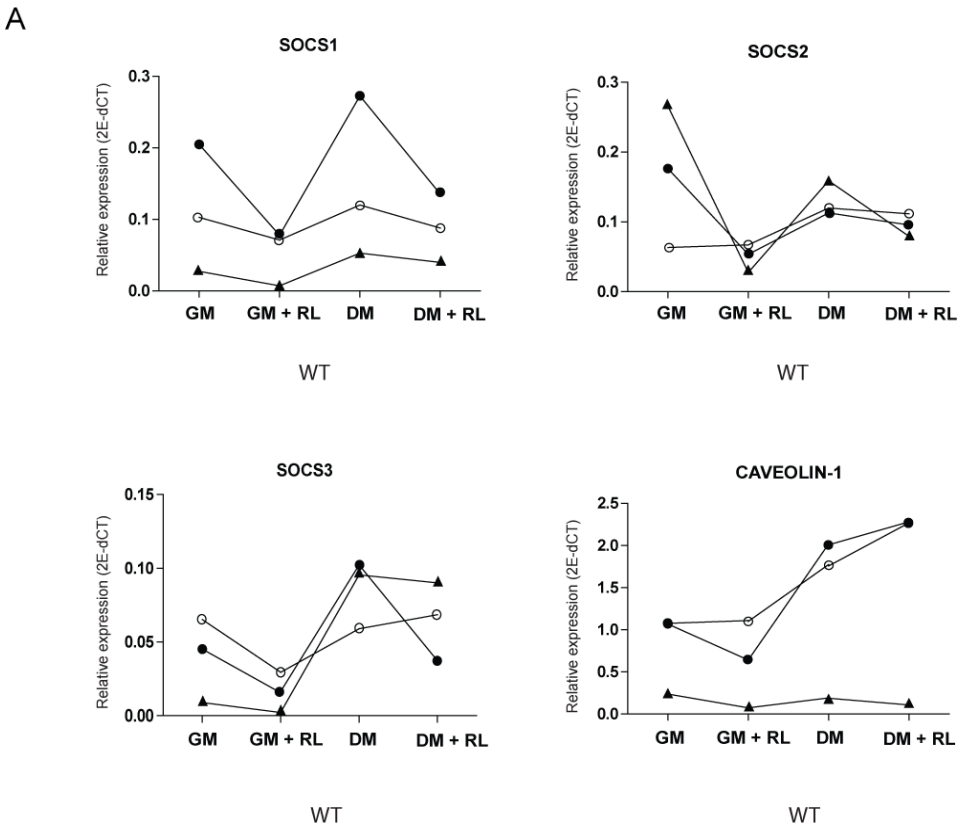

Figure 3. Expression levels of SOCS protein family members and caveolin-1 in WT acini treated with RANKL.

mRNA expression levels of the indicated genes relative to PP1A in WT acini cultured in GM or DM +/- RANKL. Each dot represents mammary acini derived from one mouse at G.14,5. Lines connecting dots represent different treatments in the same sample. Measurements were done in triplicate and means were used in the calculations.

Figure 4

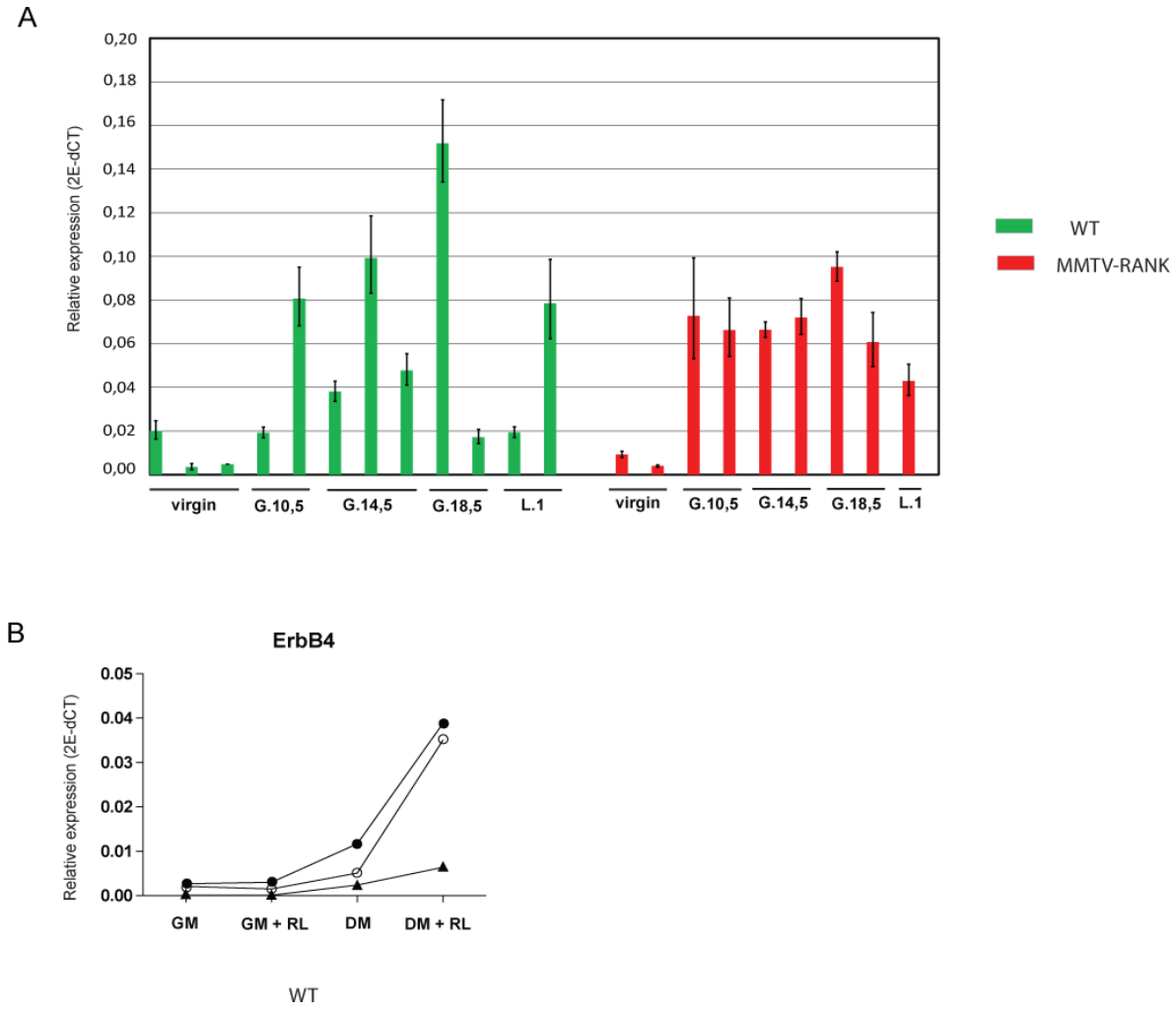

Figure 4. ErbB4 expression levels in WT and MMTV-RANK mammary epithelial cells.

A. ErbB4 mRNA expression levels relative to PP1A in WT and MMTV-RANK glands at the indicated time points during gestation. For each sample measurements were done in triplicate and mean and SD values were used in the calculations.

B. ErbB4 mRNA expression levels relative to PP1A in WT acini after 24h of culture in GM and DM +/- RANKL. Each dot represents mammary acini derived from one mouse at G.14,5. Lines connecting dots represent different treatments in the same sample. Measurements were done in triplicate and means were used in the calculations.

Figure 5

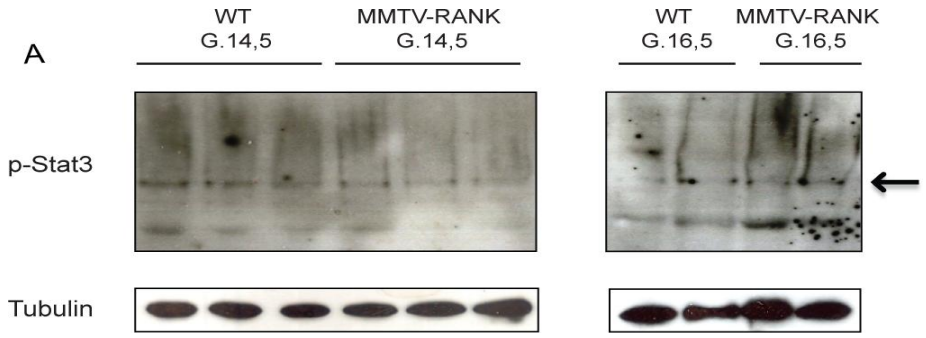

Figure 5. STAT3 activation in WT and MMTV-RANK mammary glands.
Western blot analysis of p-STAT3 levels in mammary glands from WT and MMTV-RANK at midgestation (G14,5-16,5). Arrow indicates p-STAT3 protein band. Tubulin is shown as loading control.

ARTICLE 3

"RANK overexpression delays mammary tumor formation in oncogene-driven NEU and PYMT mouse models but in turn contributes to tumor aggressiveness through Cancer Stem Cell enrichment"

RANK overexpression delays mammary tumor formation in oncogene-driven NEU and PYMT mouse models but in turn contributes to tumor aggressiveness through Cancer Stem Cell enrichment

Cordero A[1], Sanz-Moreno A[1], Yoldi G[1] and González-Suárez E[1,#]

[1] Cancer Epigenetics and Biology Program, Bellvitge Biomedical Research Institute, IDIBELL. Barcelona, Spain

[#] Corresponding author: Eva González-Suárez

Cancer Epigenetics and Biology Program, Bellvitge Biomedical Research Institute, IDIBELL. Barcelona, Spain

Av. Gran Via de l'Hospitalet, 199. 08908 L'Hospitalet de Llobregat. Barcelona. Spain

egsuarez@idibell.cat Phone: +34 932607139 Fax: +34 932607119

www.pebc.cat

KEY WORDS: RANK, MMTV-PYMT, MMTV-NEU, Cancer stem cell (CSC), tumor cell of origin, metastasis.

ABSTRACT

RANK signaling regulates mammary epithelial differentiation and mediates mammary tumorigenesis induced by progesterone and carcinogens. RANK overexpression leads to spontaneous mammary tumor formation with long latency in multiparous old mice, suggesting that RANK cooperates with oncogenic mutations to induce tumorigenesis. Thus, we directly addressed the impact of RANK overexpression in the oncogene-driven MMTV-NEU and MMTV-PYMT mouse models. Unexpectedly, we found a significant longer latency to tumor formation and reduced tumor incidence in transgenic mice overexpressing both RANK and NEU or RANK and PYMT as compared to the single mutants. RANK overexpression enhanced both basal and luminal mammary populations, and disrupted luminal subpopulations distribution, which could reduce the tumor cell of origin and delay tumorigenesis. However, both luminal and basal populations from NEU and PYMT overexpressing mice were able to form tumors and RANK overexpression in MMTV-NEU$^{+/-}$ mice prevented tumor initiation irrespectively of the population of origin. These results suggest that RANK overexpression attenuates tumorigenesis by alternative mechanisms.

Once tumors develop, RANK overxpression did not alter the MMTV-neu tumor phenotype but in the MMTV-PYMT background it increased tumor aggressiveness, with increased tumor growth and enhanced metastasis formation ability. MMTV-PYMT$^{+/-}$; RANK$^{+/tg}$ palpable lesions were enriched in K14+/K8+ coexpressing cells. Moreover, functional assays revealed an enrichment in the cancer stem cell (CSC) pool within MMTV-PYMT$^{+/-}$; RANK$^{+/tg}$ tumors.

Collectively, our results indicate that RANK signaling plays a complex role in tumorigenesis, affecting tumor initiation and/or aggressiveness in NEU- and PYMT-driven mammary tumors.

INTRODUCTION

RANK and its ligand, RANKL, are key regulators of mammary gland development, controlling proliferation and differentiation of the mammary epithelia during pregnancy (Fata et al. 2000; Gonzalez-Suarez et al. 2007). RANKL is expressed in progesterone receptor positive (PR+) mammary epithelial cells (MECs), and mediates the proliferative effects of progesterone in mouse (Fata et al. 2000; Beleut et al. 2010) and human mammary epithelium (Tanos et al. 2013). RANK deletion or overexpression results in disrupted mammary gland development during pregnancy and impaired lactation (Fata et al. 2000; Gonzalez-Suarez et al. 2007).

We have recently demonstrated that constitutive activation of RANK in the mammary gland, under the mouse mammary tumor virus (MMTV) promoter, disrupts mammary stem cell fate resulting in the accumulation of MaSC and intermediate progenitors (Pellegrini et al. 2013). Thus, RANK overexpression not only expands both basal $CD24^{lo}$ $CD29^{hi}$ $CD49f^{hi}$ and luminal $CD24^{hi}$ $CD29^{lo}$ $CD49f^{lo}$ mammary populations, but also decreases the expression of Sca-1 and CD61, described as markers of luminal differentiated cells and alveolar progenitors, respectively, and increases CD49b expression, a marker of luminal progenitor cells, within the luminal population (Sleeman et al. 2007; Asselin-Labat et al. 2007; W. Li et al. 2009; Shehata et al. 2012). Functional assays indicate that MMTV-RANK mice have more MaSC contained in the basal population, as they are more able to reconstitute an entire mammary gland when injected in limiting dilution assay (LDA) *in vivo* into a cleared fad pad FvB mammary gland, compared to wild type (WT) mice. Luminal progenitor cells are also expanded within luminal population in MMTV-RANK, as they are more able to form colonies *in vitro* in matrigel 3D cultures under RANKL stimuli, compared to WTcontrols.

MMTV-RANK mice spontaneously develop mammary adenocarcinomas after multiple gestations with a long latency. Consistent with the expansion of mammary progenitors observed in MMTV-RANK mice, each MMTV-RANK tumor is morphologically distinct and heterogeneous in terms of keratin staining, containing basal cells K5/K14+, luminal cells K8+, and abundant cells coexpressing K14+/K8+.

Moreover, MMTV-RANK mice show a shorter tumor latency compared to WT after a carcinogenic protocol that includes DMBA (dimethylbenz(a)anthracene) and MPA (medroxiprogesterone) (Gonzalez-Suarez et al. 2010; Schramek et al. 2010). Conversely, pharmacological inhibition of RANK with RANK-Fc, which binds to RANKL and blocks the

pathway, completely prevents MPA/DMBA-induced mammary tumor formation in WT mice.

MMTV-neu mice constitutively express the neu gene, the rat orthologue of human Her2 (ErbB2), resulting in mammary tumor and lung metastasis formation at 8-11 months of age (Muller et al. 1988a). Her2 is amplified in 30% of human breast cancers and it is a marker of poor prognosis (Slamon et al. 1987; Fantozzi and Christofori 2006). We have previously shown that preventive treatment with RANK-Fc before tumors arise leads to a significantly decreased number of tumoral foci per mouse and lung metastasis in MMTV-neu mice (Gonzalez-Suarez et al. 2010).

MMTV-PyMT mice express the middle T protein of the polyomavirus, which activates several pathways that regulate cell cycle and survival, resulting in aggressive multifocal adenocarcinoma formation at only 3-5 weeks of age, and high incidence of lung metastasis (Guy, Cardiff, and Muller 1992). Moreover, this model particularly resembles the different stages of progression in human mammary tumorigenesis, from hyperplasias to adenoma and advanced carcinomas, as well as loss of the expression of sex hormone receptors (ER, PR) and gain of Her2 and Cyclin D1 expression (Maglione et al. 2001; Herschkowitz et al. 2007).

RANK protein is expressed focally in MMTV-NEU normal mammary glands similarly to WT. Furthermore, a focal expression of RANK is observed in MMTV-PYMT residual non transformed mammary epithelium (Pellegrini P et.al, under revision), as this model show extensive hyperplasias before 4 weeks of age (Guy, Cardiff, and Muller 1992).

Mammary hyperplasias and invasive adenocarcinomas of both MMTV-NEU and MMTV-PYMT mice express high levels of RANK (Pellegrini P et.al, under revision). However, very low or undetectable levels of RANKL are detected in preneoplastic lesions and adenocarcinomas in MMTV-NEU and MMTV-PYMT mouse models (Gonzalez-Suarez et al. 2010; Schramek et al. 2010) (Pellegrini P et.al, under revision), in accordance with the loss of estrogen and progesterone receptors (ER, PR) during tumor progression of MMTV-NEU and MMTV-PYMT models (Lin et al. 2003), and the described RANKL expression in PR+ cells (Fernandez-Valdivia et al. 2009).

Recent publications highlight the importance of Cancer Stem Cells (CSC) in tumorigenesis (Reya et al. 2001; Yu et al. 2012). CSCs are a subpopulation of cells within tumors endowed with self-renewal and multilineage differentiation capacity which can cause relapse and metastasis (Sampieri and Fodde 2012; Merlos-Suárez et al. 2011; Overdevest

et al. 2011). These cells have been termed cancer stem cells to reflect their “stem like” properties and ability to continually sustain tumorigenesis, although they are not necessarily derived from stem cells (Owens and Naylor 2013; McDermott and Wicha 2010). CSCs are particularly difficult to isolate as there are no specific surface markers described for all tumors (Asselin-Labat et al. 2011; Lo et al. 2012, 49), although they can be functionally assayed by their enhanced ability to form non-adherent mammospheres, and to initiate novel tumors and metastasis when injected in vivo in limiting dilution assays (LDA) (Schramek et al. 2010; Pece et al. 2010; O’Brien, Kreso, and Jamieson 2010). Cancer stem cells are not necessarily related with the tumor cell of origin, the cell that acquires the first cancer-promoting mutation (Visvader 2011). Understanding the tumor cells of origin and how they contribute to breast cancer tumor phenotypes is one of the key challenges to the development of personalized medicine for breast cancer.

Given the long tumor latency previously observed in MMTV-RANK mice, we hypothesize that RANK cooperates with other oncogenic mutations to induce tumorigenesis. Unexpectedly our results indicate that RANK overexpression delays tumor initiation in oncogene-driven NEU and PYMT mouse models but promotes tumor aggressiveness through cancer stem cell enrichment.

RESULTS

RANK overexpression in an oncogenic MMTV-NEU and MMTV-PYMT background significantly delays mammary tumor onset

In order to investigate whether RANK overexpression cooperates with MMTV-NEU (Andrechek et al. 2000) and MMTV-PYMT (Guy, Cardiff, and Muller 2015) oncogene-driven mouse models, double transgenic mice were generated by crossing MMTV-RANK$^{+/tg}$ with MMTV-NEU$^{+/+}$ or MMTV-PYMT$^{+/-}$ mice, and their impact on tumor formation was analyzed.

Unexpectedly, MMTV-NEU$^{+/-}$; RANK$^{+/tg}$ mice showed a reduced tumor incidence (58% mice with tumors), compared to MMTV-NEU$^{+/-}$, where 100% mice developed tumors (Fig. 1A). Moreover, overexpression of RANK and NEU in the mammary gland resulted in a significantly delayed tumor latency (414 ± 115 days), compared to MMTV-NEU$^{+/-}$ mice (261 ± 87 days) (Fig. 1B). Once tumors developed, no clear changes in tumor growth or in their capacity to metastasize to lung were observed between both genotypes (Fig 1 C,D).

In the MMTV-PYMT$^{+/-}$; RANK$^{+/tg}$ mouse model all mice developed mammary tumors (Fig. 1A), and MMTV-PYMT$^{+/-}$; RANK$^{+/tg}$ mice presented significantly longer tumor latency (67 ± 16 days), compared to single transgenic MMTV-PYMT $^{+/-}$ mice (41 ± 7 days) (Fig.1B). However, MMTV-PYMT$^{+/-}$; RANK$^{+/tg}$ tumors grew significantly faster than MMTV-PYMT$^{+/-}$ (Fig. 1C), and displayed 100% lung metastasis incidence, with 30-90 metastatic foci per lung; by contrast, 70% MMTV-PYMT$^{+/-}$ mice presented lung metastasis, and several mice showed less than 10 metastatic foci per lung (Fig. 1D).

Thus, RANK overexpression non intuitively attenuates mammary tumorigenesis in MMTV-NEU and MMTV-PYMT mouse models.

RANK overexpression does not modify the tumor cell phenotype in MMTV-NEU background

Based on previous data showing that constitutive activation of RANK signaling in the mammary gland promotes heterogeneous mammary tumor formation (Pellegrini et al. 2013) we asked whether RANK overexpression altered the MMTV-NEU tumor phenotype.

Histological analysis revealed that both MMTV-NEU$^{+/-}$ and MMTV-NEU$^{+/-}$; RANK$^{+/tg}$ mice developed late stage carcinomas (data not shown). It has been shown that MMTV-NEU$^{+/-}$

tumors were positive for RANK (Gonzalez-Suarez et al. 2010)(Schramek et al. 2010)(Pellegrini P et.al, under revision). Quantitative expression analysis (RT-qPCR) demonstrated that mRNA RANK levels were significantly higher in MMTV-NEU$^{+/-}$; RANK$^{+/tg}$ mammary glands and tumors compared with MMTV-NEU$^{+/-}$ (Fig. 2A). Both genotypes formed luminal-like tumors that expressed high mRNA levels of luminal K8, and low levels of basal K14 (Fig. 2B). Moreover, all MMTV-NEU$^{+/-}$ and MMTV-NEU$^{+/-}$; RANK$^{+/tg}$ tumors were homogeneous in terms of keratin staining, with a generalized expression of luminal K8 in almost all tumoral cells and an extremely low expression of basal markers K5 and K14 (Fig. 2C). Additionally, freshly isolated tumor cells were analyzed by FACS (Supplemental Fig S1A), revealing that both genotypes developed CD24hi CD49flo tumors with high expression of CD61+ and low levels of Sca-1 and CD49b (Fig. 2D). These results indicated that RANK overexpression did not modify tumor cell phenotype in MMTV-NEU background, in accordance with no differences in tumor growth or metastasis ability found in this background.

RANK overexpression in MMTV-PYMT background increases CSC pool resulting in aggressive tumor formation and enhanced metastatic ability

In contrast to the MMTV-neu, RANK overexpression in MMTV-PYMT background resulted in a faster tumor growth and enhanced metastasis formation ability. We aimed to address what was the mechanism underlying this more aggressive phenotype in MMTV-PYMT$^{+/-}$; RANK$^{+/tg}$ tumors.

Previous data revealed that MMTV-PYMT adenocarcinomas express high levels of RANK compared with non-tumorigenic mammary epithelia (Pellegrini P et.al, under revision). Expression analysis demonstrated that double transgenic mice for RANK$^{+/tg}$ and PYMT$^{+/-}$ showed even higher levels of RANK, a 100-fold increase in mRNA RANK levels, compared to MMTV-PYMT$^{+/-}$ tumors (Fig 3A).

Tumor progression in MMTV-PYMT mice is characterized by loss of Progesterone Receptor (PR), alterations of the Smooth muscle Actin-1 (SMA-1) positive basal layer, and increased cytological atypia (Lin et al. 2003). Palpable lesions of MMTV-PYMT$^{+/-}$ and MMTV-PYMT$^{+/-}$; RANK$^{+/tg}$ were morphologically analyzed. Our results indicated that MMTV-PYMT$^{+/-}$ palpable lesions mostly contained late carcinoma poorly differentiated areas, while MMTV-PYMT$^{+/-}$; RANK$^{+/tg}$ palpable lesions contained extensive regions of MINs and early carcinomas (Supplemental Fig S2A). Analysis of keratin expression in tumors derived from both genotypes showed that they all express high levels of K8, but there was a significantly higher expression of K14 in RANK$^{+/tg}$ and PYMT$^{+/-}$ overexpressing mice (Fig

3B). Immunofluorescence analysis revealed that both MMTV-PYMT$^{+/-}$; RANK$^{+/tg}$ carcinomas and MINs contained a greater number of K14+ cells compared to MMTV-PYMT$^{+/-}$ (Fig. 3C, Supplemental Fig S2B). Furthermore, double transgenic mice displayed an increase in K8+/K14+ coexpressing cells within preneoplastic lesions and adenocarcinomas (Fig. 3C right panel, Supplemental Fig S2B), as previously observed in MMTV-RANK tumors (Pellegrini et al. 2013). In contrast, K5+ cells were scarce in MMTV-PYMT$^{+/-}$ and MMTV-PYMT$^{+/-}$; RANK$^{+/tg}$ late carcinomas (Fig. 3D). No differences in K5 expression, which was restricted to the basal membrane, were found in MMTV-PYMT$^{+/-}$ and MMTV-PYMT$^{+/-}$; RANK$^{+/tg}$ preneoplastic lesions (Supplemental Fig S2C). Taken together, these results indicate that RANK overexpression affects tumor cell characteristics in MMTV-PYMT tumor-prone model, leading to accumulation of bipotent K14+/K8+ cells.

Moreover, FACS analysis revealed a significant increase in CD61+ and CD49b+ cells within the CD45- CD31- (Lin -) CD24+ epithelial cells in MMTV-PYMT$^{+/-}$; RANK$^{+/tg}$ tumors, compared to MMTV-PYMT$^{+/-}$ (Fig. 3E). As CD61+ and CD49b+ cells are described to identify luminal progenitors in untransformed mammary glands (Shehata et al. 2012; Oakes et al. 2008), their increase in MMTV-PYMT$^{+/-}$; RANK$^{+/tg}$ tumors could suggest an enhanced stemness in these tumors, compared to MMTV-PYMT$^{+/-}$. These results prompted us to functionally test whether RANK overexpression leads to an increase in the cancer stem cell (CSC) population within tumors. Thus, MMTV-PYMT$^{+/-}$ and MMTV-PYMT$^{+/-}$; RANK$^{+/tg}$ tumor cells were isolated and cultured in suspension as tumorspheres, as it has been described that CSCs grow under anchorage-independent conditions (Dontu and Wicha 2005). The ability of MMTV-PYMT$^{+/-}$;RANK$^{+/tg}$ tumor cells to form secondary tumorspheres was significantly higher in number and size compared to MMTV-PYMT$^{+/-}$ (Fig. 3F), confirming an enrichment in CSC in mice overexpressing both RANK$^{+/tg}$ and PYMT$^{+/-}$.

Next, the ability of MMTV-PYMT$^{+/-}$ and MMTV-PYMT$^{+/-}$; RANK$^{+/tg}$ tumor cells to initiate novel tumors in the mammary gland of a WT host was evaluated by *in vivo* Limiting Dilution Assay (LDA). Our preliminary results revealed that the frequency of cancer stem cells is 1 in 918 in MMTV-PYMT$^{+/-}$; RANK$^{+/tg}$ tumor cells, significantly higher than in MMTV-PYMT$^{+/-}$, where this frequency is reduced to 1 in 2462 (p= 0,0155) (Supplemental Fig S2D). This may indicate that RANK overexpression plays an important role in tumor aggressiveness and relapse in MMTV-PYMT$^{+/-}$ background.

It has been extensively reported the relevance of RANK signaling in metastasis (Palafox et al. 2012). Thus, we directly test the metastatic ability of MMTV-PYMT$^{+/-}$ and MMTV-PYMT$^{+/-}$; RANK$^{+/tg}$ tumor cells by injecting them into the tail vein of *Foxn1*^{nu} recipient mice in LDA. MMTV-PYMT$^{+/-}$; RANK$^{+/tg}$ tumor cells showed a significant higher virtual frequency

of metastatic cells (1 in 1064 cells), compared to MMTV-PYMT$^{+/-}$ (1 in 6264 cells) (Fig 3G). Moreover the number of metastatic foci per lung was tendentially higher in *Foxn1*^{nu} mice injected with MMTV-PYMT$^{+/-}$; RANK$^{+/tg}$ tumor cells, compared to MMTV-PYMT$^{+/-}$ (Fig 3H).

Taken together, these results indicate that RANK overexpression in the MMTV-PYMT$^{+/-}$ mouse model promotes accumulation of K14+/K8+ coexpressing cells, increase CD49b+ and CD61+ population and an expansion of the CSC pool, resulting in aggressive tumor formation with higher metastatic-initiation potential, compared to MMTV-PYMT$^{+/-}$ mice.

RANK overexpression impairs NEU-induced tumor initiation from both luminal and basal mammary compartments

Next, we aimed to elucidate the mechanism underlying the delayed tumor latency observed in mice that constitutively express RANK and NEU in the mammary gland. One possible explanation is that RANK overexpression may reduce a specific population containing the tumor cell of origin, the cell that acquires the first cancer-promoting mutation, thus delaying the tumor initiation in those mice.

We have previously shown that RANK overexpression decreases the luminal Sca-1/CD61 positive population (Pellegrini et al. 2013), so we next analyzed if this phenotype was maintained in double transgenic mice for RANK and NEU. Histological analysis revealed that 25 week-old MMTV-NEU$^{+/-}$; RANK$^{+/tg}$ virgin glands had a hyperplastic mammary epithelium, with more precocious small alveoli, compared to MMTV-NEU$^{+/-}$ (Fig. 4A). Analysis by FACS (schematized in Supplemental Fig S1B) revealed that MECs from MMTV-NEU$^{+/-}$; RANK$^{+/tg}$ mice had the same alterations in mammary populations previously described for MMTV-RANK$^{+/tg}$ (Pellegrini et al. 2013), with increased basal (CD24lo CD49fhi) and luminal (CD24hi CD49flo) populations, and decreased Sca-1 and CD61 within the luminal population, compared to MMTV-NEU$^{+/-}$ (Fig 4B). Moreover, MMTV-NEU$^{+/-}$; RANK$^{+/tg}$ glands contained more CD49b+ cells than MMTV-NEU$^{+/-}$ glands. These findings confirmed that RANK overexpression in the MMTV-NEU$^{+/-}$ mouse model disrupts the distribution of mammary populations in virgin glands similarly than in MMTV-RANK$^{+/tg}$ mice. Moreover, MMTV-NEU$^{+/-}$; RANK$^{+/tg}$ mice resembled the phenotype observed in MMTV-RANK$^{+/tg}$ mice during gestation, with an impaired secretory differentiation of the mammary gland and lactation failure (Supplemental Fig S3)

Next, histological analyses in older virgin mice (30-55 week old) were performed. Our results indicated that MMTV-NEU$^{+/-}$; RANK$^{+/tg}$ mammary glands had higher incidence and number of hyperplasic lesions compared to MMTV-NEU$^{+/-}$ mice but no mammary

intraepithelial neoplasias (MINs) were detected (Fig 4C, D). In contrast, 30% of MMTV-NEU$^{+/-}$ mammary glands showed MINs (Fig 4C). This result suggests that constitutive activation of RANK in the mammary gland resulted in accumulation of hyperplastic lesions that do not progress into preneoplasic lesions and advanced carcinomas, leading to a significant delay in tumor formation in MMTV-NEU$^{+/-}$; RANK$^{+/tg}$ mice.

The identity of the tumor cell of origin for NEU and PYMT overexpressing mouse models remains controversial (Vaillant et al. 2008; Lo et al. 2012). We hypothesize that luminal Sca-1+ and/or CD61+ are the cell of origin in MMTV-NEU tumors, and therefore their decrease in MMTV-NEU$^{+/-}$; RANK$^{+/tg}$ mice could delay tumor formation. To investigate this hypothesis, basal (Lin- CD24lo CD49fhi), and luminal (Lin- CD24hi CD49flo) MECs isolated from non-transformed MMTV-NEU$^{+/-}$ and MMTV-NEU$^{+/-}$; RANK$^{+/tg}$ mammary glands (23-25 week old mice), were orthotopically implanted into the #2 mammary fad pad of immunocompromised SCID-BEIGE females (50.000 cells/MG). Importantly, our results showed that all mice injected with basal and luminal MECs from MMTV-NEU$^{+/-}$ animals developed palpable lesions with similar latency (Fig. 4E). Tumors derived from MMTV-NEU$^{+/-}$ basal and luminal MECs injections were analyzed, confirming that they all gave rise to highly homogeneous CD24+CD49f^{lo} CD61^{hi} CD49b^{lo} Sca1- tumors (Fig. 4F).

Strikingly, none of the mice injected with MMTV-NEU$^{+/-}$; RANK$^{+/tg}$ MECs developed tumors 6 months after the injection, suggesting that RANK overexpression alters the tumor formation capacity in the MMTV-NEU$^{+/-}$ mouse model irrespectively of the population implanted.

Altogether, these data indicates that both luminal and basal mammary populations can give rise to tumors that resemble the phenotype of primary tumors, suggesting that NEU oncogene target cells from both compartments and indistinctly leads to K8+ luminal tumor formation, and that RANK overexpression impairs NEU-induced tumor initiation irrespectively of the population of origin.

PYMT overexpression leads to luminal tumor formation regardless of the cell of origin and RANK expression levels

Next, we focused on MMTV-PYMT$^{+/-}$; RANK$^{+/tg}$ mice. Histological analysis of adult MMTV-PYMT$^{+/-}$ normal non-tumorigenic mammary glands could not be performed, as this model showed preneoplastic lesions at 4 weeks of age (Fig 5A), consistent with previous data (Guy, Cardiff, and Muller 1992). Thus, to elucidate the functional role for RANK signaling in PYMT-driven tumor initiation, we performed analysis of 2,2 - 2,6 week old pre-pubertal

glands, where only non-transformed mammary epithelium was observed (Fig 5B). Analysis by FACS showed an increase in CD24lo CD49fhi basal population, as well as enhanced CD49b+ population in MMTV-PYMT$^{+/-}$; RANK$^{+/tg}$ glands, compared to MMTV-PYMT$^{+/-}$ (Fig. 5C). Moreover, a significant decrease in CD61 expression within the luminal population was observed in MMTV-PYMT$^{+/-}$; RANK$^{+/tg}$ mice. Sca-1 was not detected neither in MMTV-PYMT$^{+/-}$ nor in MMTV-PYMT$^{+/-}$ mice, in accordance with the low expression of Sca-1 in pre-pubertal glands previously described (Bai and Rohrschneider 2010).

Next, the residual non-transformed mammary epithelium from 9-10 week-old MMTV-PYMT$^{+/-}$ and MMTV-PYMT$^{+/-}$; RANK$^{+/tg}$ mice was analyzed. In accordance with their multifocal origin (Lin et al. 2003), both genotypes had multiple stages of tumor progression, but preliminary results showed that double transgenic mice for RANK$^{+/tg}$ and PYMT showed less MINs compared to MMTV-PYMT$^{+/-}$ control mammary glands (Fig. 5D), as previously observed in MMTV-NEU$^{+/-}$ background.

In order to investigate the identity of the tumor cell of origin, MECs from 2,2 - 2,6 week old MMTV-PYMT$^{+/-}$ and MMTV-PYMT$^{+/-}$; RANK$^{+/tg}$ mice were isolated, before clonal populations were observed. Basal (Lin- CD24lo CD49fhi) and luminal CD61+ and CD61- (Lin- CD24hi CD49flo CD61+/-) cells were orthotopically implanted into the #2 mammary fad pad of immunocompromised SCID-BEIGE females (2.000 cells/MG). Again, MMTV-PYMT$^{+/-}$ basal and luminal CD61+/- populations gave rise to tumors with similar latency (Fig 5E). Contrary to what was observed in MMTV-NEU$^{+/-}$; RANK$^{+/tg}$, MMTV-PYMT$^{+/-}$; RANK$^{+/tg}$ MECs developed palpable lesions, although with lower frequency than single mutants MMTV-PyMT$^{+/-}$. No clear differences in tumor latency were observed between both genotypes (Fig. 5E, right panel). FACS analysis revealed that these tumors resemble the phenotype observed in primary tumors, with increased CD49b and CD61 levels in MMTV-PYMT$^{+/-}$; RANK$^{+/tg}$ irrespectively of the population of origin, mimicking the phenotype of primary tumors in this genotype (Fig 5F).

These results showed that both NEU and PYMT oncogenes overexpression lead to luminal tumor formation, regardless of the origin of the cell that acts as a target of transformation. In contrast to previous observations in MMTV-NEU$^{+/-}$;RANK$^{+/tg}$ mice, RANK overexpression in MECs from either basal and luminal CD61+/- populations did not prevent tumor initiation driven by PYMT, althouth it decreased the frequency, thus ruling out the hypothesis that the disrupted luminal populations in RANK overexpressing mice could be directly responsible of the delayed tumor initiation in those mice.

DISCUSSION

Our data reveals a complex role of RANK signaling in mammary tumorigenesis. MMTV-NEU$^{+/-}$ and MMTV-PYMT$^{+/-}$ oncogene-driven mouse models, when combined with MMTV-RANK$^{+/tg}$ mice, provide unexpected insights into the role of RANK in tumorigenesis.

Previous results support a positive role for RANK signaling in mammary tumor initiation. RANK overexpression leads to spontaneous mammary tumor formation with long latency in multiparous old mice (Pellegrini et al. 2013). Moreover, both MMTV-NEU$^{+/+}$ mice upon RANK-Fc preventive treatment (Gonzalez-Suarez et al. 2010) and MMTV-PYMT$^{+/-}$ mice with genetic deletion of RANK (MMTV-PYMT$^{+/-}$; RANK$^{-/-}$) (Pellegrini P et.al, under revision) show increased tumor latency and decreased tumor and metastasis incidence. Unexpectedly, our results show that double transgenic mice for RANK and NEU or PYMT have a significant delay in tumor onset. In addition, MMTV-NEU$^{+/-}$; RANK$^{+/tg}$ mice show a decrease in tumor incidence, compared to MMTV-NEU$^{+/-}$. These results indicate that high levels of RANK interfere with tumor initiation in both RANK and NEU or PYMT overexpressing mouse models.

Constitutive activation of RANK and NEU or PYMT in virgin mammary glands led to a similar phenotype to that observed in virgin MMTV-RANK mice (Pellegrini et al. 2013), with enhanced basal and luminal populations, and dramatic effects on the distribution of luminal subpopulations, leading to disrupted secretory differentiation and impaired lactation. These alterations could reduce the tumor cell of origin that acts as a target of transformation in Neu and PyMT driven tumors and explain their delayed latency to tumor formation. Many efforts are currently focused on finding the tumor cell of origin of different cancer subtypes (Visvader 2011), although its identity in NEU and PYMT overexpressing mouse models remains controversial (Vaillant et al. 2008; Lo et al. 2012; Lo and Chen 2013). We demonstrate that both luminal and basal populations in MMTV-NEU$^{+/-}$ and MMTV-PYMT$^{+/-}$ mammary glands are able to form tumors with similar latency and frequency, in accordance with previous data reported by Zhang et al. (Zhang et al. 2013). These results support an oncogene-dominant model where NEU and PYMT oncogenes target cells from both basal and luminal mammary populations and lead to formation of tumors that resemble MMTV-NEU$^{+/-}$ and MMTV-PYMT$^{+/-}$ primary tumors phenotype, ruling out our initial hypothesis.

Our results paradoxically show that MMTV-PYMT$^{+/-}$; RANK$^{+/tg}$ basal and luminal MECs are able to form tumors, whereas RANK overexpression prevents tumor formation in MMTV-NEU$^{+/-}$ MECs, irrespectively of the population of origin. One intriguing explanation for

these contradictory results could be that RANK overexpression in MMTV-NEU$^{+/-}$ leads to alterations in any of the downstream signaling pathways responsible for MECs proliferation and/or survival, such as NF-kB, MAPK or PI3K-AKT (Palafox et al. 2012). Thus, these alterations could interfere with RANK and NEU-induced tumor initiation in both basal and luminal populations. By contrast, the aggressive and multifocal PYMT-induced tumor formation would provide sufficient tumorigenic stimuli to initiate tumors, irrespectively of RANK overexpression (Fluck and Schaffhausen 2009). Further experiments will clarify the putative contribution of alterations in downstream signaling pathways to the observed phenotypes. Lineage tracing experiments (Kretzschmar and Watt 2012) should be performed to elucidate not only the progeny of the cell that originates tumors in physiological conditions (without transplantation), but also the specific contribution of RANK signaling in NEU and PYMT oncogene-driven mouse models.

The accumulation of hyperplasic lesions that do not progress into preneoplasic lesions and advanced carcinomas in MMTV-NEU$^{+/-}$; RANK$^{+/tg}$ mammary glands, and the decrease in early MINs observed in non-transformed adult MMTV-PYMT$^{+/-}$; RANK$^{+/tg}$ mammary glands are in line with the delayed tumor latency in RANK and NEU or PYMT overexpressing mice, and suggest that the blockage occurs in the transition from hyperplasias to MINs and adenocarcinomas. Importantly, these results suggest that RANK could be acting as a potent oncogene, as it has been shown that certain oncogenes can induce premature cell senescence or apoptosis (Serrano et al. 1997; Xu et al. 2014; Wajapeyee et al. 2008; Fearnhead et al. 1998). These biological processes constitute two major cell intrinsic mechanisms against tumor initiation and progression, and can be activated by multiple stimuli (Lowe, Cepero, and Evan 2004). Thus, the oncogene-induced senescence or apoptosis are tumor-suppressing defense mechanisms that occur in multiple human tumor types and tumor mouse models, and serve as the initial barrier to cancer development *in vivo* (Koumenis and Giaccia 1997; Courtois-Cox, Jones, and Cichowski 2008). To test this hypothesis, ongoing experiments aim to analyze senescence (e.g. β-galactosidase activity, P16 or P21 expression) and apoptosis (cleaved caspase-3 or TUNEL) in normal mammary glands, hyperplasias and preneoplasic lesions, in order to explain the delay in tumor formation observed in double transgenic mice for RANK and NEU or PYMT.

Our results show that MMTV-NEU$^{+/-}$ and MMTV-NEU$^{+/-}$; RANK$^{+/tg}$ mice form luminal K8+ tumors with low expression for basal markers K5 and K14. In contrast, we showed an accumulation of K14+/K8+ cells, but not K5+K8+ cells, in MMTV-PYMT$^{+/-}$; RANK$^{+/tg}$ preneoplastic lesions and adenocarcinomas as previously observed in MMTV-RANK$^{+/tg}$ mice (Pellegrini et al. 2013). Consistent with previous data, K14 and K5 are organized in

different gene clusters within tumors, and K14 is expressed not only in basal K5+ tumor cells, but also in luminal K8+, supporting that K14 and K5 mark different population of cells within mammary tumors (Z. Li et al. 2007; Herschkowitz et al. 2007). Expression of K5+ is restricted to basal populations in non-tumorigenic mammary glands, whereas K14 has been detected in both basal and luminal populations (Shackleton et al. 2006; Pellegrini et al. 2013). Cells coexpressing K14+/K8+ have been identified as intermediate progenitors blocked in differentiation in normal mammary glands, in contrast to K5+/K8+ that are only found in cells from the basal population (Chakrabarti et al. 2012).

In addition to K14+/K8+ cells, MMTV-PYMT$^{+/-}$; RANK$^{+/tg}$ tumors show an increase in CD61+ and CD49b+ cells, previously described to identify luminal progenitors in untransformed mammary glands (Shehata et al. 2012; Oakes et al. 2008). In accordance with the increased stemness induced by RANK activation in mouse and human mammary epithelium (Pellegrini et al. 2013; Palafox et al. 2012), these results suggest an enrichment in the CSC population in MMTV-PYMT$^{+/-}$; RANK$^{+/tg}$ tumors. CSC, important for their ability to self-renew, resistance to therapies and capacity to metastasize (Sampieri and Fodde 2012; Merlos-Suárez et al. 2011; Overdevest et al. 2011), become a promising target for the development of more reliable cancer therapies in the future. We show an enhanced tumor growth and metastasis ability in MMTV-PYMT$^{+/-}$; RANK$^{+/tg}$ tumors, compared to MMTV-PYMT$^{+/-}$. Moreover, tumorsphere and limiting dilution assays to test tumor and metastasis initiating ability demonstrate an enrichment in CSC population in MMTV-PYMT$^{+/-}$; RANK$^{+/tg}$ tumors. Conversely, we have recently shown a significant reduction in tumorsphere formation (*in vitro*) and tumor initiating (*in vivo*) ability in MMTV-PYMT$^{+/-}$; RANK$^{-/-}$ tumors and MMTV-PYMT$^{+/-}$ tumor cells after neoadjuvant RANK-Fc treatment (Pellegrini P et.al, under revision), supporting RANK as a key regulator of the CSC population in PYMT-driven tumors.

In accordance with their multifocal origin (Lin et al. 2003), PYMT overexpressing mice show multiple tumoral foci per mammary gland, and different stages of tumor progression. Interestingly we show that MMTV-PYMT$^{+/-}$; RANK$^{+/tg}$ palpable lesions contain less areas of late carcinoma and more MINs than MMTV-PYMT$^{+/-}$. Conversely, extensive early and/or late carcinomas areas were previously observed in MMTV-PYMT$^{+/-}$; RANK$^{-/-}$ palpable lesions (Pellegrini P et.al, under revision), leading to the contra-intuitive hypothesis that RANK attenuates tumor progression. As it has been reported that dissemination of metastatic cells is an early event in MMTV-PYMT$^{+/-}$ tumor progression (Hüsemann et al. 2008), our results suggest that this increase in preneoplasic regions could also be responsible of the faster tumor growth and increased metastasis observed in

MMTV-PYMT$^{+/-}$; RANK$^{+/tg}$ mice. Further *in vivo* functional characterization of preneoplasic lesions and advanced carcinomas will help to elucidate their specific contribution to tumor growth and metastasis formation in MMTV-PYMT$^{+/-}$ and MMTV-PYMT$^{+/-}$; RANK$^{+/tg}$ mice.

In conclusion, this study demonstrates that high levels of RANK interfere with tumor initiation in both RANK and NEU or PYMT tumor-prone mouse models, but in turn RANK signaling expands CSC population and increases tumor aggressiveness in PYMT-driven tumors, and consequently it could represent a useful therapeutic target for breast cancer treatment.

MATERIALS AND METHODS

Animals

All research involving animals was performed at the IDIBELL animal facility in compliance with protocols approved by the IDIBELL Committee on Animal Care and following nation and European Union regulations. MMTV-neu mice (N202 Mul; FvB background) and MMTV-PyMT (FVB/N-Tg(MMTV-PyVT)634Mul) were obtained from Jackson laboratory and have been described previously (Guy, Cardiff, and Muller 2015). MMTV-PYMT$^{+/-}$; RANK$^{+/+}$ and MMTV-NEU$^{+/-}$; RANK$^{+/tg}$ mice were obtained by crossing MMTV-PyMT$^{-/+}$ (FvB) strain and MMTV-NEU$^{+/+}$ (FvB) with MMTV-RANK$^{+/tg}$ (FvB) mice. Animals bearing tumors bigger than 1cm diameter were considered as endpoint criteria for sacrifice.

Mammary and tumor cell isolation

Single cells were isolated from mammary glands and tumors as previously described (Smalley MJ et al, 2010). Briefly, fresh tissues were mechanically dissected with McIlwain tissue chopper and enzymatically digested with appropriate medium (DMEM F-12, 0.3% Collagenase A, 2.5U/mL dispase, 20 mM HEPES, and Penicilin/Streptomiciyn) 45 minutes at 37°C. Samples were washed with Leibowitz L15 medium 10% fetal bovine serum (FBS) between each step. Erythrocytes were eliminated by treating samples with hypotonic lysis buffer (Lonza Iberica), and fibroblasts were excluded by incubation with DMEM F-12 10% FBS 1 hour at 37ºC (the majority of fibroblasts attach to tissue culture plastic while most of epithelial organoids do not). Single epithelial cells were isolated by treating with trypsin 2 minutes at 37°C. Cell aggregates were removed treating with 2.5U/mL dispase (GIBCO), 20U/ml DNase (Invitrogene) 5 minutes at 37ºC. Cell suspension was finally filtered with 40 μm filter and counted.

Flow Cytometry

Single cells were labeled with antibodies against CD24-PE or CD24-FITC (5 μg/mL, M1/69 BD Pharmingen, San Diego, CA, http://www.bdbiosciences.com), CD29-FITC (1,25 μg/mL, HMb1-1, BD Pharmingen), CD49f-a647 (2,5 μg/mL, GoH3, BD Pharmingen), CD61-PE or CD61-FITC (2,5 μg/mL, 2C9.G2, BD Pharmingen), Sca-1-APC or Sca-1-PE (0,5 μg/mL, Ly-6A/E, BD Pharmingen), and CD49b-a647 (1,25 μg/mL, HMa2 Biolegend, San Diego, CA, http://www.biolegend.com). Lymphocytes and endothelial cells were excluded in flow cytometry using CD45-PECy7 (0,125 μg/mL, 30-F11 Biolegend) and CD31-PECy7 (0,5

μg/mL, 390 Biolegend) antibodies, respectively. FACS analysis was performed using FACS Canto (Becton Dickinson, San Jose, CA) and Diva software package. Cell sorting was performed using MoFlo (Beckman Coulter) at 25psi and using a 100 mm tip.

Gene expression analysis

Total RNA of frozen tumor pieces was prepared with Tripure Isolation Reagent (11667165001 Roche) in accordance with the manufacturer's instructions. Frozen tumors tissues were fractionated using glass beads (G1152-100G, Sigma-Aldrich) and PreCellys® tissue homogenizer (Berting Technologies). cDNA was produced by reverse transcription using 1 μg of RNA following kit instructions (N8080234, Applied Biosystems). Quantitative PCR was performed using LightCycler® 480 SYBR green MasterMix (04707516001, Roche). Primer sequences are indicated in supplemental methods.

Tissue histology and immunostaining

Tissue samples were fixed in formalin and embedded in paraffin. 3 μm sections were cut for histological analysis and stained with hematoxylin and eosin. For characterization of MMTV-PYMT$^{+/-}$; RANK$^{+/tg}$ and MMTV-PyMT$^{-/+}$ tumors stage, hematoxilin-eosin stained tumor sections were classified as previously described (Lin EY et al., 2003). Histological areas were quantified with ImageJ and normalized to the whole section excluding non-epithelial areas.

Lung metastasis were detected and counted based on nuclear morphology and similarity with primary tumors. 15-16 cuts per lung were quantified in primary MMTV-PYMT$^{+/-}$; RANK$^{+/+}$ and MMTV-PyMT $^{-/+}$ tumors.

Immunostaining was performed on 3 μm tumor sections. Antigen heat retrieval with citrate was used for K8 (TROMA, dshl, Developmental Studies Hybridoma Bank, Iowa City, Iowa), K5 (AF-138, Covance, Princeton, NJ) and K14 (AF-64, Covance). Opportune fluorochrome conjugated secondary antibodies were added after primary incubation. Cell nuclei were stained with DAPI (Sigma), and then mounted with Prolong ® Gold Antifade (Life Technologies). Confocal analysis was carried out using Leica confocal microscope. Images were captured using LasAF software (Leica).

Tumor and metastasis limiting dilution assays

For tumor limiting dilution assays, mammary tumor cells were isolated as described, diluted 1:1 in matrigel matrix (254234, BD Biosciences) and injected in a final volume of 40

μL in the inguinal mammary fat pad. Cells isolated from three primary tumors of two MMTV-PYMT$^{+/-}$; RANK$^{+/tg}$ and two MMTV-PyMT$^{-/+}$ mice were pooled and injected in limiting dilution (1.000.000, 10.000, 1.000, 100 and 10 cells) in mammary fad pad of 8 week old WT mice (Fvb background).

For metastasis limiting dilution assay, mammary tumor cells were isolated as described Cells isolated from three primary tumors of two MMTV-PYMT$^{+/-}$; RANK$^{+/tg}$ and two MMTV-PyMT$^{-/+}$ mice were pooled, resuspended in 200 μL of cold PBS and injected intravenously (tail vein) in limiting dilution (100.000, 10.000, 1.000, 100 and 10 cells) in 5-week old *Foxn1*^{nu}mice (4 mice per dilution). Mice were sacrificed 8 week after cell injection and lungs were recovered for histological analysis.

Tumorsphere culture

MMTV-PYMT$^{+/-}$; RANK$^{+/+}$ and MMTV-PyMT$^{-/+}$ tumors were digested and filtered to obtain single cells, as previously described. Single cells were resuspended in serum-free DMEM F12 mammosphere medium containing 20 ng/mL EFG, 1x B27 and 4 μg/mL heparin (H3149, Sigma-Aldrich) as previously described (11). Briefly, primary tumorspheres were derived by plating 20.000 cells/ mL in 2mL of medium in triplicate into cell-suspension culture plates. After two weeks, tumorspheres were isolated by 5 min treatment with PBS-EDTA 5 mM + 5 min of trypsin at 37C° and plated for secondary tumorsphere at a concentration of 10.000 cells/mL in triplicate. Individual spheres were counted under a microscope and t-tests with SEM were calculated.

Statistical analysis

Statistical analyses were performed using GraphPad Prism software. Analysis of the differences between two mouse cohorts or conditions was performed with a two-tailed Student's t-test. Two-way analysis of variance (ANOVA) was used to analyze tumor growth curves. Estimation of tumor initiating cells in limiting dilutions was calculated using the extreme limiting dilution assay (ELDA) (Hu and Smyth 2009).

ACKNOWLEDGEMENTS

This work was supported by grants to E. González-Suárez by MICINN (SAF2008-01975; SAF2011-22893), FMM, Concern Foundation, Fundació La Marató de TV3 and a Ramon y Cajal program. We thank WC Dougall for providing reagents and MMTV-RANK$^{+/tg}$ mice. We also thank G. Boigues and the IDIBELL animal facility for their assistance with mouse colonies, A. Villanueva for technical support with metastasis assays and E. Castaño for her assistance with FACS analyses.

AUTHOR CONTRIBUTIONS

Alex Cordero: Collection and/or assembly, data analysis and interpretation, writing and final approval of manuscript. Guillermo Yoldi and Adrián Sanz: Collection and/or assembly of data, data analysis and interpretation, final approval of manuscript. Eva Gonzalez-Suarez: Conception and design, financial support, collection and/or assembly of data, data analysis and interpretation, writing and final approval of manuscript.

CONFLICT OF INTEREST

Authors declare no conflict of interest

REFERENCES

Andrechek, E. R., W. R. Hardy, P. M. Siegel, M. A. Rudnicki, R. D. Cardiff, and W. J. Muller. 2000. "Amplification of the neu/erbB-2 Oncogene in a Mouse Model of Mammary Tumorigenesis." *Proceedings of the National Academy of Sciences of the United States of America* 97 (7): 3444–49. doi:10.1073/pnas.050408497.

Asselin-Labat, Marie-Liesse, Kate D. Sutherland, Holly Barker, Richard Thomas, Mark Shackleton, Natasha C. Forrest, Lynne Hartley, et al. 2007. "Gata-3 Is an Essential Regulator of Mammary-Gland Morphogenesis and Luminal-Cell Differentiation." *Nature Cell Biology* 9 (2): 201–9. doi:10.1038/ncb1530.

Asselin-Labat, Marie-Liesse, Kate D. Sutherland, François Vaillant, David E. Gyorki, Di Wu, Sheridan Holroyd, Kelsey Breslin, et al. 2011. "Gata-3 Negatively Regulates the Tumor-Initiating Capacity of Mammary Luminal Progenitor Cells and Targets the Putative Tumor Suppressor Caspase-14." *Molecular and Cellular Biology* 31 (22): 4609–22. doi:10.1128/MCB.05766-11.

Bai, Lixia, and Larry R. Rohrschneider. 2010. "S-SHIP Promoter Expression Marks Activated Stem Cells in Developing Mouse Mammary Tissue." *Genes & Development* 24 (17): 1882–92. doi:10.1101/gad.1932810.

Beleut, Manfred, Renuga Devi Rajaram, Marian Caikovski, Ayyakkannu Ayyanan, Davide Germano, Yongwon Choi, Pascal Schneider, and Cathrin Brisken. 2010. "Two Distinct Mechanisms Underlie Progesterone-Induced Proliferation in the Mammary Gland." *Proceedings of the National Academy of Sciences of the United States of America* 107 (7): 2989–94. doi:10.1073/pnas.0915148107.

Chakrabarti, Rumela, Yong Wei, Rose-Anne Romano, Christina DeCoste, Yibin Kang, and Satrajit Sinha. 2012. "Elf5 Regulates Mammary Gland Stem/progenitor Cell Fate by Influencing Notch Signaling." *Stem Cells (Dayton, Ohio)* 30 (7): 1496–1508. doi:10.1002/stem.1112.

Courtois-Cox, S., S. L. Jones, and K. Cichowski. 2008. "Many Roads Lead to Oncogene-Induced Senescence." *Oncogene* 27 (20): 2801–9. doi:10.1038/sj.onc.1210950.

Dontu, Gabriela, and Max S. Wicha. 2005. "Survival of Mammary Stem Cells in Suspension Culture: Implications for Stem Cell Biology and Neoplasia." *Journal of Mammary Gland Biology and Neoplasia* 10 (1): 75–86. doi:10.1007/s10911-005-2542-5.

Fantozzi, Anna, and Gerhard Christofori. 2006. "Mouse Models of Breast Cancer Metastasis." *Breast Cancer Research: BCR* 8 (4): 212. doi:10.1186/bcr1530.

Fata, J. E., Y. Y. Kong, J. Li, T. Sasaki, J. Irie-Sasaki, R. A. Moorehead, R. Elliott, et al. 2000. "The Osteoclast Differentiation Factor Osteoprotegerin-Ligand Is Essential for Mammary Gland Development." *Cell* 103 (1): 41–50.

Fearnhead, Howard O., Joe Rodriguez, Eve-Ellen Govek, Wenjun Guo, Ryuji Kobayashi, Greg Hannon, and Yuri A. Lazebnik. 1998. "Oncogene-Dependent Apoptosis Is Mediated by Caspase-9."

Proceedings of the National Academy of Sciences 95 (23): 13664–69. doi:10.1073/pnas.95.23.13664.

Fernandez-Valdivia, Rodrigo, Atish Mukherjee, Yan Ying, Jie Li, Marilene Paquet, Francesco J. DeMayo, and John P. Lydon. 2009. "The RANKL Signaling Axis Is Sufficient to Elicit Ductal Side-Branching and Alveologenesis in the Mammary Gland of the Virgin Mouse." *Developmental Biology* 328 (1): 127–39. doi:10.1016/j.ydbio.2009.01.019.

Fluck, Michele M., and Brian S. Schaffhausen. 2009. "Lessons in Signaling and Tumorigenesis from Polyomavirus Middle T Antigen." *Microbiology and Molecular Biology Reviews: MMBR* 73 (3): 542–63, Table of Contents. doi:10.1128/MMBR.00009-09.

Gonzalez-Suarez, Eva, Daniel Branstetter, Allison Armstrong, Huyen Dinh, Hal Blumberg, and William C. Dougall. 2007. "RANK Overexpression in Transgenic Mice with Mouse Mammary Tumor Virus Promoter-Controlled RANK Increases Proliferation and Impairs Alveolar Differentiation in the Mammary Epithelia and Disrupts Lumen Formation in Cultured Epithelial Acini." *Molecular and Cellular Biology* 27 (4): 1442–54. doi:10.1128/MCB.01298-06.

Gonzalez-Suarez, Eva, Allison P. Jacob, Jon Jones, Robert Miller, Martine P. Roudier-Meyer, Ryan Erwert, Jan Pinkas, Dan Branstetter, and William C. Dougall. 2010. "RANK Ligand Mediates Progestin-Induced Mammary Epithelial Proliferation and Carcinogenesis." *Nature* 468 (7320): 103–7. doi:10.1038/nature09495.

Guy, C. T., R. D. Cardiff, and W. J. Muller. 1992. "Induction of Mammary Tumors by Expression of Polyomavirus Middle T Oncogene: A Transgenic Mouse Model for Metastatic Disease." *Molecular and Cellular Biology* 12 (3): 954–61.

Guy, C T, R D Cardiff, and W J Muller. 2015. "Induction of Mammary Tumors by Expression of Polyomavirus Middle T Oncogene: A Transgenic Mouse Model for Metastatic Disease." Accessed January 8. http://www.ncbi.nlm.nih.gov/pmc/articles/PMC369527/.

Herschkowitz, Jason I., Karl Simin, Victor J. Weigman, Igor Mikaelian, Jerry Usary, Zhiyuan Hu, Karen E. Rasmussen, et al. 2007. "Identification of Conserved Gene Expression Features between Murine Mammary Carcinoma Models and Human Breast Tumors." *Genome Biology* 8 (5): R76. doi:10.1186/gb-2007-8-5-r76.

Hüsemann, Yves, Jochen B. Geigl, Falk Schubert, Piero Musiani, Manfred Meyer, Elke Burghart, Guido Forni, et al. 2008. "Systemic Spread Is an Early Step in Breast Cancer." *Cancer Cell* 13 (1): 58–68. doi:10.1016/j.ccr.2007.12.003.

Hu, Yifang, and Gordon K. Smyth. 2009. "ELDA: Extreme Limiting Dilution Analysis for Comparing Depleted and Enriched Populations in Stem Cell and Other Assays." *Journal of Immunological Methods* 347 (1-2): 70–78. doi:10.1016/j.jim.2009.06.008.

Koumenis, C., and A. Giaccia. 1997. "Transformed Cells Require Continuous Activity of RNA Polymerase II to Resist Oncogene-Induced Apoptosis." *Molecular and Cellular Biology* 17 (12): 7306–16.

Kretzschmar, Kai, and Fiona M. Watt. 2012. “Lineage Tracing.” *Cell* 148 (1): 33–45. doi:10.1016/j.cell.2012.01.002.

Lin, Elaine Y., Joan G. Jones, Ping Li, Liyin Zhu, Kathleen D. Whitney, William J. Muller, and Jeffrey W. Pollard. 2003. “Progression to Malignancy in the Polyoma Middle T Oncoprotein Mouse Breast Cancer Model Provides a Reliable Model for Human Diseases.” *The American Journal of Pathology* 163 (5): 2113–26. doi:10.1016/S0002-9440(10)63568-7.

Li, Wenjing, Brian J. Ferguson, Walid T. Khaled, Maxine Tevendale, John Stingl, Valeria Poli, Tina Rich, Paolo Salomoni, and Christine J. Watson. 2009. “PML Depletion Disrupts Normal Mammary Gland Development and Skews the Composition of the Mammary Luminal Cell Progenitor Pool.” *Proceedings of the National Academy of Sciences* 106 (12): 4725–30. doi:10.1073/pnas.0807640106.

Li, Zhe, Cristina E. Tognon, Frank J. Godinho, Laura Yasaitis, Hanno Hock, Jason I. Herschkowitz, Chris L. Lannon, et al. 2007. “ETV6-NTRK3 Fusion Oncogene Initiates Breast Cancer from Committed Mammary Progenitors via Activation of AP1 Complex.” *Cancer Cell* 12 (6): 542–58. doi:10.1016/j.ccr.2007.11.012.

Lo, P.-K., and H. Chen. 2013. “Cancer Stem Cells and Cells of Origin in MMTV-Her2/neu-Induced Mammary Tumorigenesis.” *Oncogene* 32 (10): 1339–40. doi:10.1038/onc.2012.456.

Lo, P.-K., D. Kanojia, X. Liu, U. P. Singh, F. G. Berger, Q. Wang, and H. Chen. 2012. “CD49f and CD61 Identify Her2/neu-Induced Mammary Tumor-Initiating Cells That Are Potentially Derived from Luminal Progenitors and Maintained by the Integrin-TGFβ Signaling.” *Oncogene* 31 (21): 2614–26. doi:10.1038/onc.2011.439.

Lowe, Scott W., Enrique Cepero, and Gerard Evan. 2004. “Intrinsic Tumour Suppression.” *Nature* 432 (7015): 307–15. doi:10.1038/nature03098.

Maglione, Jeannie E., Drew Moghanaki, Lawrence J. T. Young, Cathyryne K. Manner, Lesley G. Ellies, Sasha O. Joseph, Benjamin Nicholson, Robert D. Cardiff, and Carol L. MacLeod. 2001. “Transgenic Polyoma Middle-T Mice Model Premalignant Mammary Disease.” *Cancer Research* 61 (22): 8298–8305.

McDermott, Sean P., and Max S. Wicha. 2010. “Targeting Breast Cancer Stem Cells.” *Molecular Oncology* 4 (5): 404–19. doi:10.1016/j.molonc.2010.06.005.

Merlos-Suárez, Anna, Francisco M. Barriga, Peter Jung, Mar Iglesias, María Virtudes Céspedes, David Rossell, Marta Sevillano, et al. 2011. “The Intestinal Stem Cell Signature Identifies Colorectal Cancer Stem Cells and Predicts Disease Relapse.” *Cell Stem Cell* 8 (5): 511–24. doi:10.1016/j.stem.2011.02.020.

Muller, W. J., E. Sinn, P. K. Pattengale, R. Wallace, and P. Leder. 1988a. “Single-Step Induction of Mammary Adenocarcinoma in Transgenic Mice Bearing the Activated c-Neu Oncogene.” *Cell* 54 (1): 105–15.

Oakes, Samantha R., Matthew J. Naylor, Marie-Liesse Asselin-Labat, Katrina D. Blazek, Margaret Gardiner-Garden, Heidi N. Hilton, Michael Kazlauskas, et al. 2008. “The Ets Transcription Factor Elf5 Specifies Mammary Alveolar Cell Fate.” *Genes & Development* 22 (5): 581–86. doi:10.1101/gad.1614608.

O’Brien, Catherine Adell, Antonija Kreso, and Catriona H. M. Jamieson. 2010. “Cancer Stem Cells and Self-Renewal.” *Clinical Cancer Research* 16 (12): 3113–20. doi:10.1158/1078-0432.CCR-09-2824.

Overdevest, Jonathan B., Shibu Thomas, Glen Kristiansen, Donna E. Hansel, Steven C. Smith, and Dan Theodorescu. 2011. “CD24 Offers a Therapeutic Target for Control of Bladder Cancer Metastasis Based on a Requirement for Lung Colonization.” *Cancer Research* 71 (11): 3802–11. doi:10.1158/0008-5472.CAN-11-0519.

Owens, Thomas W., and Matthew J. Naylor. 2013. “Breast Cancer Stem Cells.” *Frontiers in Physiology* 4: 225. doi:10.3389/fphys.2013.00225.

Palafox, Marta, Irene Ferrer, Pasquale Pellegrini, Sergi Vila, Sara Hernandez-Ortega, Ander Urruticoechea, Fina Climent, et al. 2012. “RANK Induces Epithelial-Mesenchymal Transition and Stemness in Human Mammary Epithelial Cells and Promotes Tumorigenesis and Metastasis.” *Cancer Research* 72 (11): 2879–88. doi:10.1158/0008-5472.CAN-12-0044.

Pece, Salvatore, Daniela Tosoni, Stefano Confalonieri, Giovanni Mazzarol, Manuela Vecchi, Simona Ronzoni, Loris Bernard, Giuseppe Viale, Pier Giuseppe Pelicci, and Pier Paolo Di Fiore. 2010. “Biological and Molecular Heterogeneity of Breast Cancers Correlates with Their Cancer Stem Cell Content.” *Cell* 140 (1): 62–73. doi:10.1016/j.cell.2009.12.007.

Pellegrini, Pasquale, Alex Cordero, Marta I Gallego, William C. Dougall, Purificación Muñoz, Miguel Ángel Pujana, and Eva González Suárez. 2013. “Constitutive Activation of RANK Disrupts Mammary Cell Fate Leading to Tumorigenesis.” *Stem Cells* 31 (9): 1954–65.

Reya, T., S. J. Morrison, M. F. Clarke, and I. L. Weissman. 2001. “Stem Cells, Cancer, and Cancer Stem Cells.” *Nature* 414 (6859): 105–11. doi:10.1038/35102167.

Sampieri, Katia, and Riccardo Fodde. 2012. “Cancer Stem Cells and Metastasis.” *Seminars in Cancer Biology*, Novel Concepts in Cancer Metastasis, 22 (3): 187–93. doi:10.1016/j.semcancer.2012.03.002.

Schramek, Daniel, Andreas Leibbrandt, Verena Sigl, Lukas Kenner, John A. Pospisilik, Heather J. Lee, Reiko Hanada, et al. 2010. “Osteoclast Differentiation Factor RANKL Controls Development of Progestin-Driven Mammary Cancer.” *Nature* 468 (7320): 98–102. doi:10.1038/nature09387.

Serrano, M., A. W. Lin, M. E. McCurrach, D. Beach, and S. W. Lowe. 1997. “Oncogenic Ras Provokes Premature Cell Senescence Associated with Accumulation of p53 and p16INK4a.” *Cell* 88 (5): 593–602.

Shackleton, Mark, François Vaillant, Kaylene J. Simpson, John Stingl, Gordon K. Smyth, Marie-Liesse Asselin-Labat, Li Wu, Geoffrey J. Lindeman, and Jane E. Visvader. 2006. “Generation of a Functional Mammary Gland from a Single Stem Cell.” *Nature* 439 (7072): 84–88. doi:10.1038/nature04372.

Shehata, Mona, Andrew Teschendorff, Gemma Sharp, Nikola Novcic, I Alasdair Russell, Stefanie Avril, Michael Prater, et al. 2012. “Phenotypic and Functional Characterisation of the Luminal Cell Hierarchy of the Mammary Gland.” *Breast Cancer Research : BCR* 14 (5): R134. doi:10.1186/bcr3334.

Slamon, D. J., G. M. Clark, S. G. Wong, W. J. Levin, A. Ullrich, and W. L. McGuire. 1987. “Human Breast Cancer: Correlation of Relapse and Survival with Amplification of the HER-2/neu Oncogene.” *Science (New York, N.Y.)* 235 (4785): 177–82.

Sleeman, Katherine E., Howard Kendrick, David Robertson, Clare M. Isacke, Alan Ashworth, and Matthew J. Smalley. 2007. “Dissociation of Estrogen Receptor Expression and in Vivo Stem Cell Activity in the Mammary Gland.” *The Journal of Cell Biology* 176 (1): 19–26. doi:10.1083/jcb.200604065.

Tanos, Tamara, George Sflomos, Pablo C. Echeverria, Ayyakkannu Ayyanan, Maria Gutierrez, Jean-Francois Delaloye, Wassim Raffoul, et al. 2013. “Progesterone/RANKL Is a Major Regulatory Axis in the Human Breast.” *Science Translational Medicine* 5 (182): 182ra55. doi:10.1126/scitranslmed.3005654.

Vaillant, François, Marie-Liesse Asselin-Labat, Mark Shackleton, Natasha C. Forrest, Geoffrey J. Lindeman, and Jane E. Visvader. 2008. “The Mammary Progenitor Marker CD61/beta3 Integrin Identifies Cancer Stem Cells in Mouse Models of Mammary Tumorigenesis.” *Cancer Research* 68 (19): 7711–17. doi:10.1158/0008-5472.CAN-08-1949.

Visvader, Jane E. 2011. “Cells of Origin in Cancer.” *Nature* 469 (7330): 314–22. doi:10.1038/nature09781.

Wajapeyee, Narendra, Ryan W. Serra, Xiaochun Zhu, Meera Mahalingam, and Michael R. Green. 2008. “Oncogenic BRAF Induces Senescence and Apoptosis through Pathways Mediated by the Secreted Protein IGFBP7.” *Cell* 132 (3): 363–74. doi:10.1016/j.cell.2007.12.032.

Xu, Yingxi, Na Li, Rong Xiang, and Peiqing Sun. 2014. “Emerging Roles of the p38 MAPK and PI3K/AKT/mTOR Pathways in Oncogene-Induced Senescence.” *Trends in Biochemical Sciences* 39 (6): 268–76. doi:10.1016/j.tibs.2014.04.004.

Yu, Zuoren, Timothy G. Pestell, Michael P. Lisanti, and Richard G. Pestell. 2012. “Cancer Stem Cells.” *The International Journal of Biochemistry & Cell Biology* 44 (12): 2144–51. doi:10.1016/j.biocel.2012.08.022.

Zhang, Weizhou, Wei Tan, Xuefeng Wu, Maxim Poustovoitov, Amy Strasner, Wei Li, Nicholas Borcherding, Majid Ghassemian, and Michael Karin. 2013. “A NIK-IKKα Module Expands ErbB2-Induced Tumor-Initiating Cells by Stimulating Nuclear Export of p27/Kip1.” *Cancer Cell* 23 (5): 647–59. doi:10.1016/j.ccr.2013.03.012.

FIGURES

Figure 1

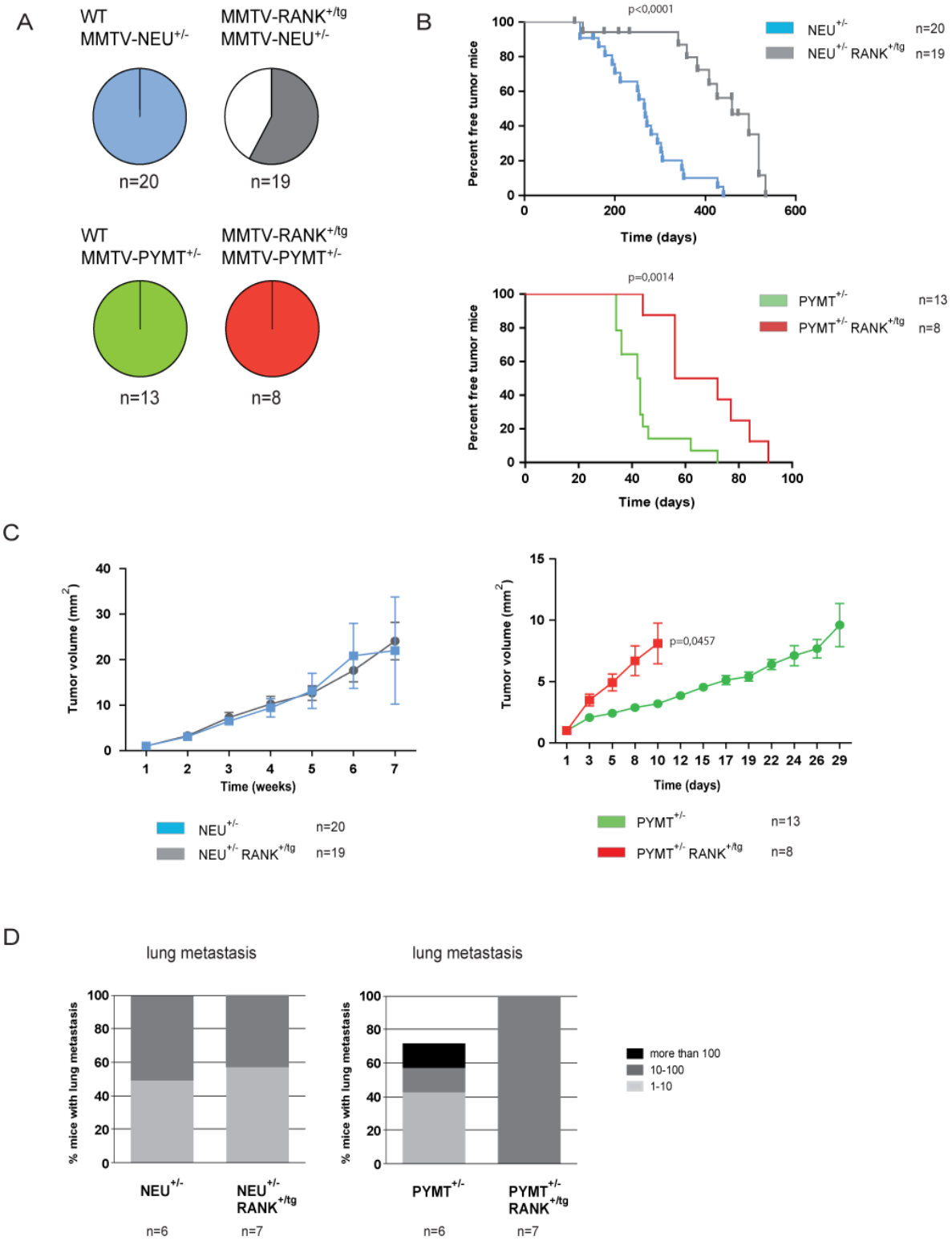

Figure 1. RANK overexpression in an oncogenic MMTV-NEU and MMTV-PYMT background significantly delays mammary tumor onset

A. Pie charts representing frequency of MMTV-NEU$^{+/-}$, MMTV-NEU$^{+/-}$; RANK$^{+/tg}$, MMTV-PYMT$^{+/-}$ and MMTV-PYMT$^{+/+}$; RANK$^{+/tg}$ mice with tumors.
B. Kinetics of palpable tumor onset with age in the indicated genotypes. 20 MMTV-NEU$^{+/-}$, 19 MMTV-NEU$^{+/-}$; RANK$^{+/tg}$ (upper graph), 13 MMTV-PYMT$^{+/-}$ and 8 MMTV-PYMT$^{+/+}$; RANK$^{+/tg}$ (lower graph) mice were analyzed. Statistical difference between groups was evaluated by Log-rank test.
C. Growth curves of MMTV-NEU$^{+/-}$, MMTV-NEU$^{+/-}$; RANK$^{+/tg}$, MMTV-PYMT$^{+/-}$ and MMTV-PYMT$^{+/-}$; RANK$^{+/tg}$ tumors relative to initial volume. Mean tumor volume +/- SEM for each mouse model is represented at each time point and values were normalized to their volume on the first day of detection. Statistical t-test is shown.
D. Percentage of MMTV-NEU$^{+/-}$, MMTV-NEU$^{+/-}$; RANK$^{+/tg}$, MMTV-PYMT$^{+/-}$ and MMTV-PYMT$^{+/+}$; RANK$^{+/tg}$ females with lung metastasis. Entire lungs were step-sectioned at 75 □m and individual metastases identified histologically. Total number of metastasis foci per mouse is indicated.

Figure 2

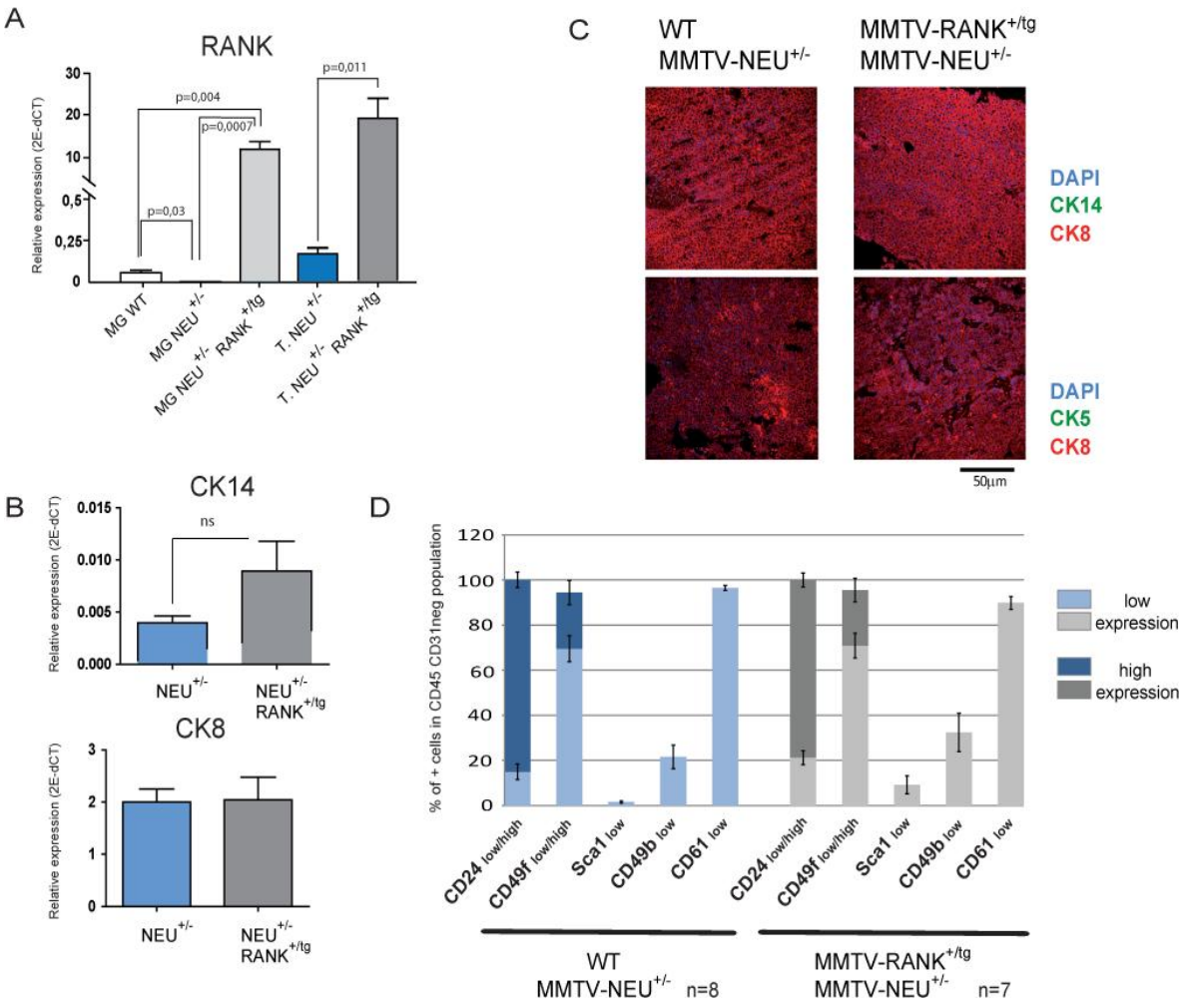

Figure 2. RANK overexpression does not modify tumor cell phenotype in MMTV-NEU background

A. mRNA expression of RANK relative to PP1A measured by RT-PCR in WT mammary gland and MMTV-NEU$^{+/-}$ and MMTV-NEU$^{+/-}$; RANK$^{+/tg}$ mammary glands and tumors. Mean, SEM and t-test p value for 4-5 independent mammary glands and tumors are shown. Quantifications were performed in triplicate and mean values were used in the calculations.

B. mRNA expression of indicated genes relative to PP1A measured by RT-PCR in MMTV-NEU$^{+/-}$ and MMTV-NEU$^{+/-}$; RANK$^{+/tg}$ tumors. Mean, SEM and t-test p value for 5 independent mammary glands and tumors are shown. Quantifications were performed in triplicate and mean values were used in the calculations.

C. Representative K8 (red) and K14/K5 (green) immunostaining in MMTV-NEU$^{+/-}$ and MMTV-NEU$^{+/-}$; RANK$^{+/tg}$ spontaneous tumor lesions.

D. Frequency of CD24$^{hi/lo}$, CD49f$^{hi/lo}$, Sca1+, CD49b+ and CD61+ cells in lineage negative CD45-CD31- population found in MMTV-NEU$^{+/-}$ and MMTV-NEU$^{+/-}$; RANK$^{+/tg}$ spontaneous tumors analyzed by FACS. Positive/negative and high (hi)/low (lo) populations were set according to populations in the normal mammary gland. Mean and SEM for 7-8 independent tumors for each genotype are shown.

Figure 3

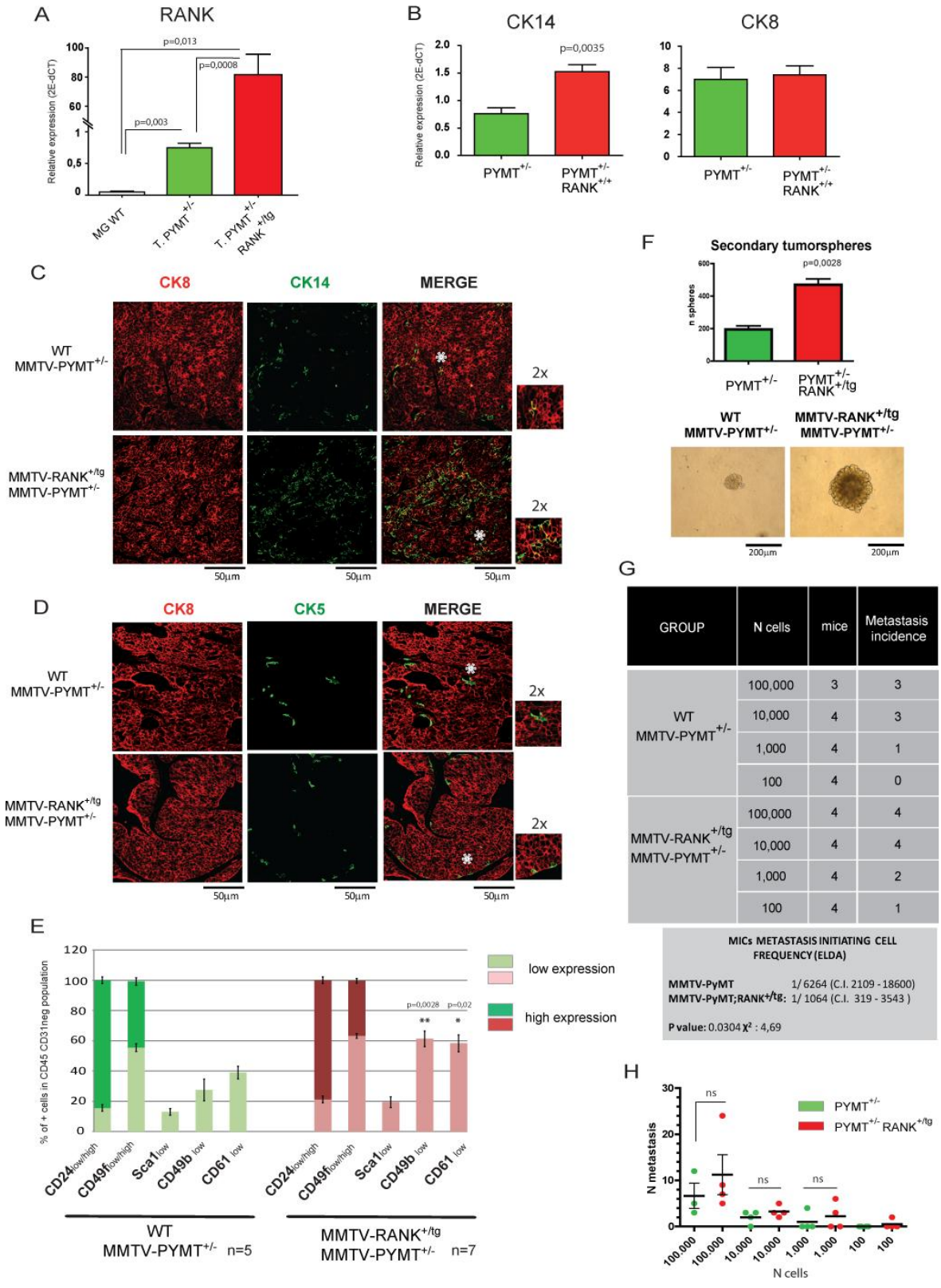

GROUP	N cells	mice	Metastasis incidence
WT MMTV-PYMT$^{+/-}$	100,000	3	3
	10,000	4	3
	1,000	4	1
	100	4	0
MMTV-RANK$^{+/tg}$ MMTV-PYMT$^{+/-}$	100,000	4	4
	10,000	4	4
	1,000	4	2
	100	4	1

MICs METASTASIS INITIATING CELL FREQUENCY (ELDA)

MMTV-PyMT 1/ 6264 (C.I. 2109 - 18600)
MMTV-PyMT;RANK$^{+/tg}$: 1/ 1064 (C.I. 319 - 3543)

P value: 0.0304 χ^2 : 4,69

Figure 3. RANK overexpression in MMTV-PYMT background increases the CSC pool resulting in aggressive tumor formation and enhanced metastatic ability

A. mRNA expression of RANK relative to PP1A measured by RT-PCR in WT mammary gland and MMTV-PYMT$^{+/-}$ and MMTV-PYMT$^{+/-}$; RANK$^{+/tg}$ tumors. Mean, SEM and t-test p value for 4 independent mammary glands and tumors are shown. Quantifications were performed in triplicate and mean values were used in the calculations.

B. mRNA expression of indicated genes relative to PP1A measured by RT-PCR in MMTV-PYMT$^{+/-}$ and MMTV-PYMT$^{+/-}$; RANK$^{+/tg}$ tumors. Mean, SEM and t-test p value for 4 independent mammary glands and tumors are shown. Quantifications were performed in triplicate and mean values were used in the calculations.

C. Representative K14 (green) and K8 (red) immunostaining in MMTV-PYMT$^{+/-}$ and MMTV-PYMT$^{+/-}$; RANK$^{+/tg}$ spontaneous adenocarcinomas. Asterisks indicate double positive K14+K8+ cells that are magnified (2x) in the insets.

D. Representative K5 (green) and K8 (red) immunostaining in MMTV-PYMT$^{+/-}$ and MMTV-PYMT$^{+/-}$; RANK$^{+/tg}$ spontaneous adenocarcinomas. Asterisks indicate K5+ cells that are magnified (2x) in the insets. Note that no K5+K8+ cells were found.

E. Frequency of CD24$^{hi/lo}$, CD49f$^{hi/lo}$, Sca1+, CD49b+ and CD61+ cells in lineage negative population found in MMTV-PYMT$^{+/-}$ and MMTV-PYMT$^{+/-}$; RANK$^{+/tg}$ spontaneous tumors analyzed by FACS. Positive/negative and high (hi)/low (lo) populations were set according to populations in the normal mammary gland. Mean, SEM and t-test p values for 5-7 independent tumors for each genotype are shown. Significance for each population in MMTV-PYMT$^{+/-}$; RANK$^{+/tg}$ tumors was calculated comparing to the corresponding MMTV-PYMT$^{+/-}$.

F. Number of secondary tumorspheres formed by MMTV-PYMT$^{+/-}$ and MMTV-PYMT$^{+/-}$; RANK$^{+/+}$ tumors. Each bar is representative of a pool of 3 independent tumors. 5.000 cells/ml from primary mammospheres were plated in triplicate in anchorage-independent conditions, and tumorspheres were quantified after 2 weeks. Mean, SEM and t-test p value are shown. Representative pictures of secondary tumorspheres derived from each genotype are also shown.

G. Table showing limiting dilution assay to test the metastasis-initiating ability of MMTV-PYMT$^{+/-}$ and MMTV-PYMT$^{+/-}$; RANK$^{+/+}$ tumor cells. Cells from two independent tumors per genotype were pooled for injections in limiting dilution in the tail vein of *Foxn1*^{nu} females. Presence of lung metastasis was scored 8 weeks after injection. Entire lungs were step-sectioned at 100 mm and individual metastases identified histologically. The metastasis-initiating cell frequencies (with confidence intervals) for each group were calculated by ELDA; p- and chi-square values are shown.

H. Quantification of the absolute number of lung metastasis in *Foxn1*^{nu} mice that received an intravenous injection of 100.000, 10.000, 1.000 or 100 MMTV-PYMT$^{+/-}$ and MMTV-PYMT$^{+/-}$; RANK$^{+/+}$ tumor cells. Each dot represents the lung of one mouse, and 3-4 lungs per condition were quantified. Mean values for each condition are shown.

Figure 4

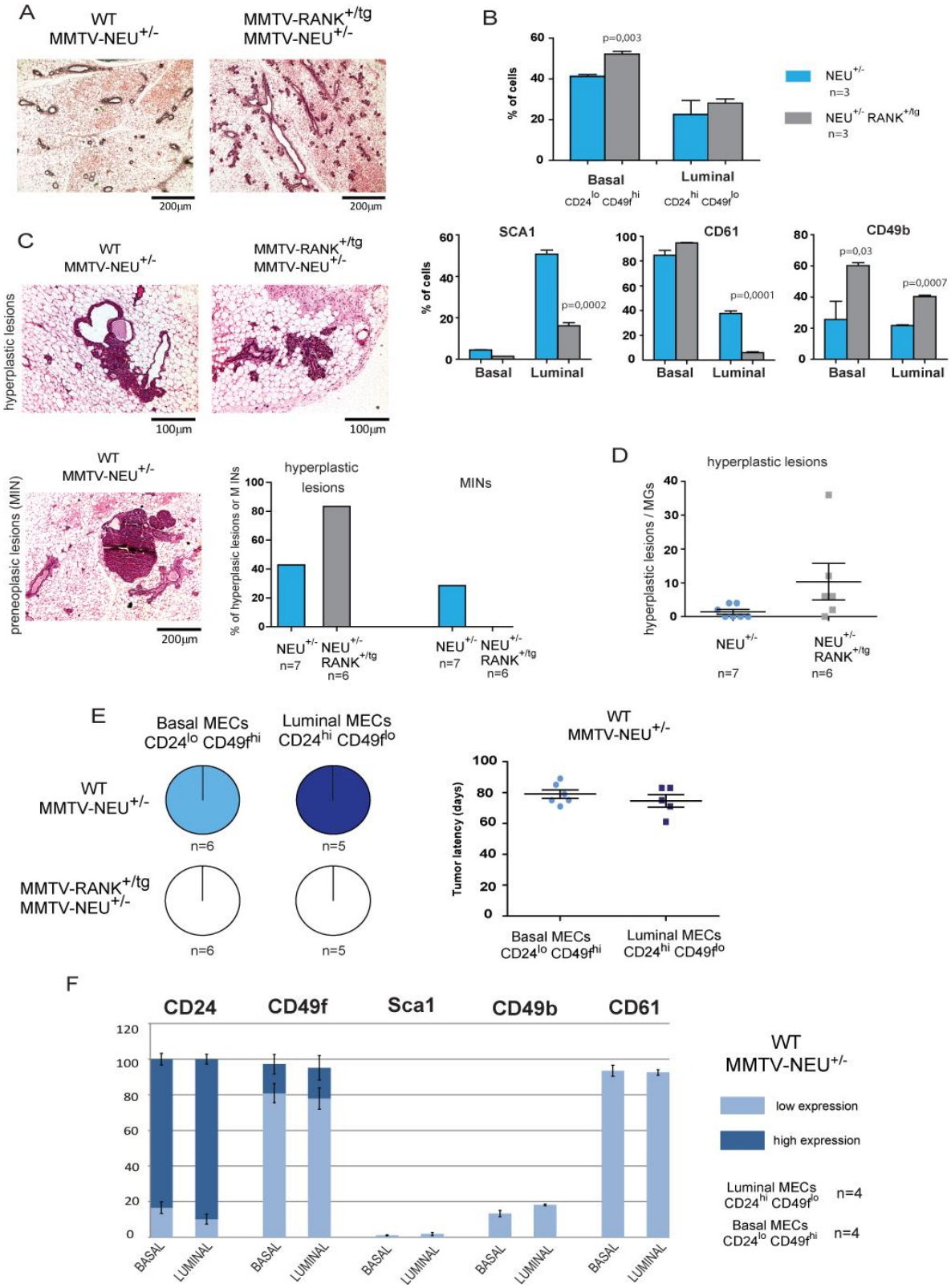
A
WT
MMTV-NEU+/-
MMTV-RANK+/tg
MMTV-NEU+/-
200µm
B
% of cells
p=0,003
NEU+/- n=3
NEU+/- RANK+/tg n=3
Basal
CD24lo CD49fhi
Luminal
CD24hi CD49flo
C
hyperplastic lesions
100µm
SCA1
p=0,0002
CD61
p=0,0001
CD49b
p=0,03
p=0,0007
Basal
Luminal
preneoplasic lesions (MIN)
% of hyperplasic lesions or MINs
hyperplastic lesions
MINs
NEU+/- n=7
NEU+/- RANK+/tg n=6
D
hyperplastic lesions / MGs
E
Basal MECs
CD24lo CD49fhi
Luminal MECs
CD24hi CD49flo
n=6
n=5
Tumor latency (days)
F
CD24
CD49f
Sca1
CD49b
CD61
BASAL
LUMINAL
low expression
high expression
Luminal MECs CD24hi CD49flo n=4
Basal MECs CD24lo CD49fhi n=4

Figure 4. RANK overexpression impairs NEU-induced tumor initiation from both luminal and basal mammary compartments

A. Representative images of H&E of MMTV-NEU$^{+/-}$ and MMTV-NEU$^{+/-}$; RANK$^{+/tg}$ mammary glands (20-25 weeks old mice), before palpable lesions were detected.
B. FACS quantification of the percentage of CD24lo CD49fhi (basal) and CD24hi CD49flo (luminal) in the CD45- CD31- Lineage negative (Lin -) population (top panel), and the frequency of Sca1+, CD61+ and CD49b+ within the basal and luminal populations of virgin MMTV-NEU$^{+/-}$ and MMTV-NEU$^{+/-}$; RANK$^{+/tg}$ mice (bottom panel). Mean, SEM and t-test p values for 3 mice per genotype are shown.
C. Representative images of H&E showing hyperplasic lesions (top panel), mammary intraepithelial neoplasia (MIN) (bottom panel)
D. Incidence of hyperplasic lesions and MINs detected in 30-55 week old MMTV-NEU$^{+/-}$ (n=7) and/or MMTV-NEU$^{+/-}$; RANK$^{+/tg}$ (n=6) mammary glands. Only mammary glands without palpable lesions were considered. Each dot represents one mammary gland.
E. Quantification of total number of hyperplasic lesions detected in 30-55 week old MMTV-NEU$^{+/-}$ (n=7) and/or MMTV-NEU$^{+/-}$; RANK$^{+/tg}$ (n=6). Each dot represents one mammary gland. Mean and SEM are shown.
F. Left panel: pie charts representing tumor incidence in mice injected with Lin- basal CD24lo CD49fhi or luminal CD24hi CD49flo MECs from virgin MMTV-NEU$^{+/-}$ and MMTV-NEU$^{+/-}$; RANK$^{+/tg}$ mice. Right panel: tumor latency for tumors derived from MMTV-NEU$^{+/-}$ basal and luminal MECs injection is also shown.
G. Frequency of CD24$^{hi/lo}$, CD49f$^{hi/lo}$, Sca1+, CD49b+ and CD61+ cells in the Lin- population found in tumors derived from MMTV-NEU$^{+/-}$ Basal/Luminal MECs injection. Positive/negative and high (hi)/low (lo) populations were set according to populations in the normal mammary gland (Sup Fig S1). Mean and SEM for 4 independent tumors per group are shown.

Figure 5

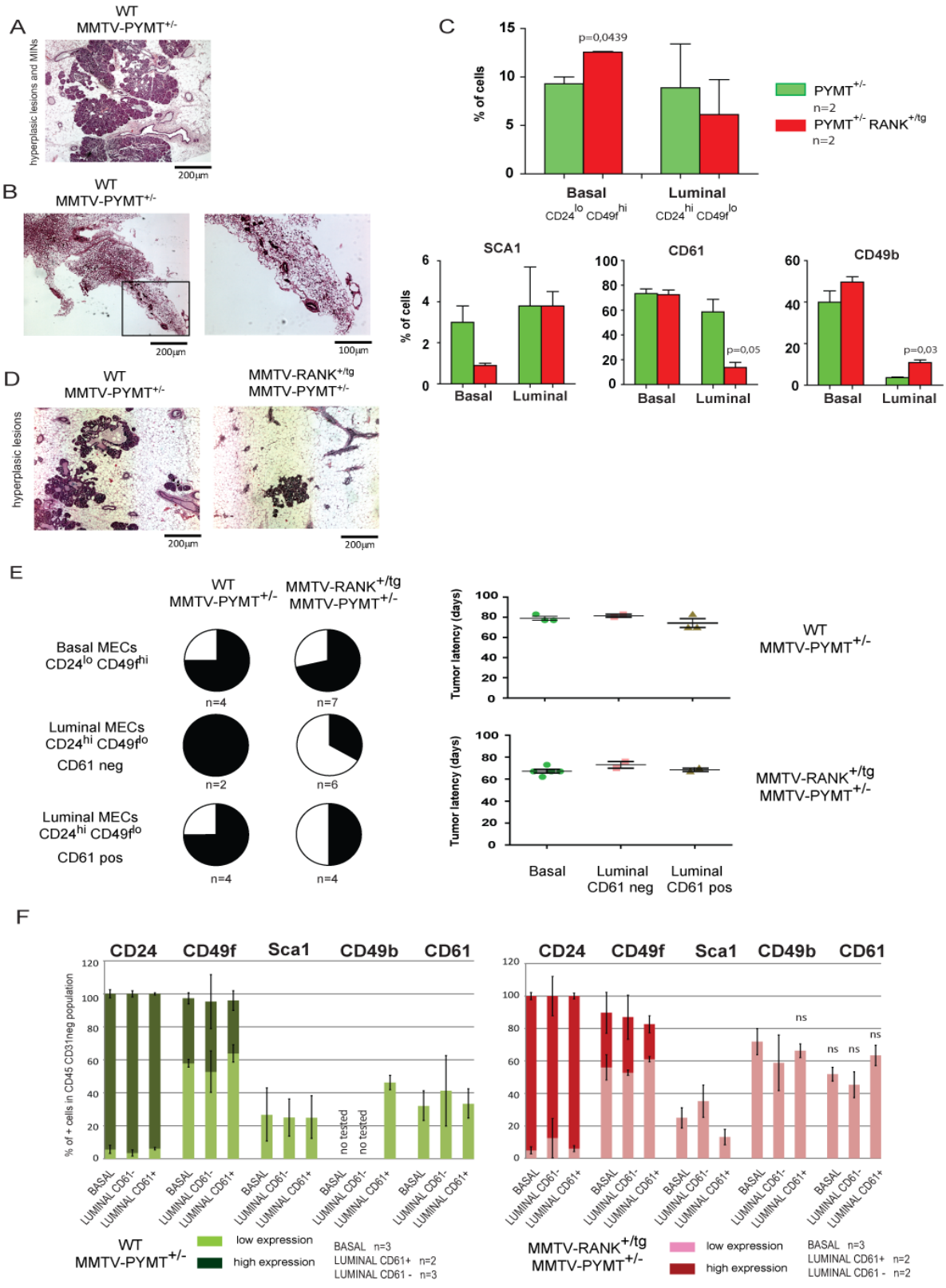
A
WT
MMTV-PYMT+/-
hyperplasic lesions and MINs
200µm
B
WT
MMTV-PYMT+/-
200µm
100µm
C
% of cells
p=0,0439
PYMT+/-
n=2
PYMT+/- RANK+/tg
n=2
Basal
CD24lo CD49fhi
Luminal
CD24hi CD49flo
SCA1
CD61
CD49b
p=0,05
p=0,03
D
WT
MMTV-PYMT+/-
MMTV-RANK+/tg
MMTV-PYMT+/-
hyperplasic lesions
200µm
E
WT
MMTV-PYMT+/-
MMTV-RANK+/tg
MMTV-PYMT+/-
Basal MECs
CD24lo CD49fhi
n=4
n=7
Luminal MECs
CD24hi CD49flo
CD61 neg
n=2
n=6
Luminal MECs
CD24hi CD49flo
CD61 pos
n=4
n=4
Tumor latency (days)
WT
MMTV-PYMT+/-
MMTV-RANK+/tg
MMTV-PYMT+/-
Basal
Luminal
CD61 neg
Luminal
CD61 pos
F
CD24
CD49f
Sca1
CD49b
CD61
% of + cells in CD45 CD31neg population
no tested
BASAL
LUMINAL CD61-
LUMINAL CD61+
WT
MMTV-PYMT+/-
low expression
high expression
BASAL n=3
LUMINAL CD61+ n=2
LUMINAL CD61 - n=3
ns
MMTV-RANK+/tg
MMTV-PYMT+/-

Figure 5. PYMT overexpression leads to luminal tumor formation regardless of the cell of origin.

A. Representative image of H&E of MMTV-PYMT$^{+/-}$ pre-pubertal mammary gland (4 week old mice) (n=1).
B. Representative image of H&E of MMTV-PYMT$^{+/-}$ (n=1) and MMTV-PYMT$^{+/-}$; RANK$^{+/tg}$ (n=1) pre-pubertal mammary glands (2,6 weeks old mice).
C. FACS quantification of the percentage of CD24lo CD49fhi (basal) and CD24hi CD49flo (luminal) in the Lin- population, and the frequency of Sca1+, CD61+ and CD49b+ within the basal and luminal populations of virgin MMTV-PYMT$^{+/-}$ and MMTV-PYMT$^{+/-}$; RANK$^{+/tg}$ mice of 2.2-2.6 weeks old glands. Note low frequency of mammary epithelial cells and Sca1+ population. Mean, SEM and t-test p values for 2 mice per genotype are shown.
D. Representative image of H&E showing early preneoplasic lesions detected in 9-10 week old MMTV-PYMT$^{+/-}$ (n=2) and MMTV-PYMT$^{+/-}$; RANK$^{+/tg}$ (n=2) residual mammary epithelia.
E. Left panel: pie charts representing tumor incidence in mice injected with basal CD24lo CD49fhi, luminal CD24hi CD49flo CD61- and luminal CD24hi CD49flo CD61+ MECs from virgin MMTV-PYMT$^{+/-}$ and MMTV-PYMT$^{+/-}$; RANK$^{+/tg}$ mice. Right panel: Tumor latency for these tumors is also shown.
F Frequency of CD24$^{hi/lo}$, CD49f$^{hi/lo}$, Sca1+, CD49b+ and CD61+ cells in the Lin- population found in tumors derived from MMTV-PYMT$^{+/-}$ and MMTV-PYMT$^{+/-}$; RANK$^{+/tg}$ Basal, Luminal CD61- and Luminal CD61+ MECs injection. Positive/negative and high (hi)/low (lo) populations were set according to populations in the normal mammary gland. Mean, SEM, t-test p value and number of tumors analyzed are shown. Significance for each marker in MMTV-PYMT$^{+/-}$; RANK$^{+/tg}$ tumors was calculated comparing to the corresponding MMTV-PYMT$^{+/-}$.

SUPPLEMENTAL INFORMATION

Supplemental Figure 1

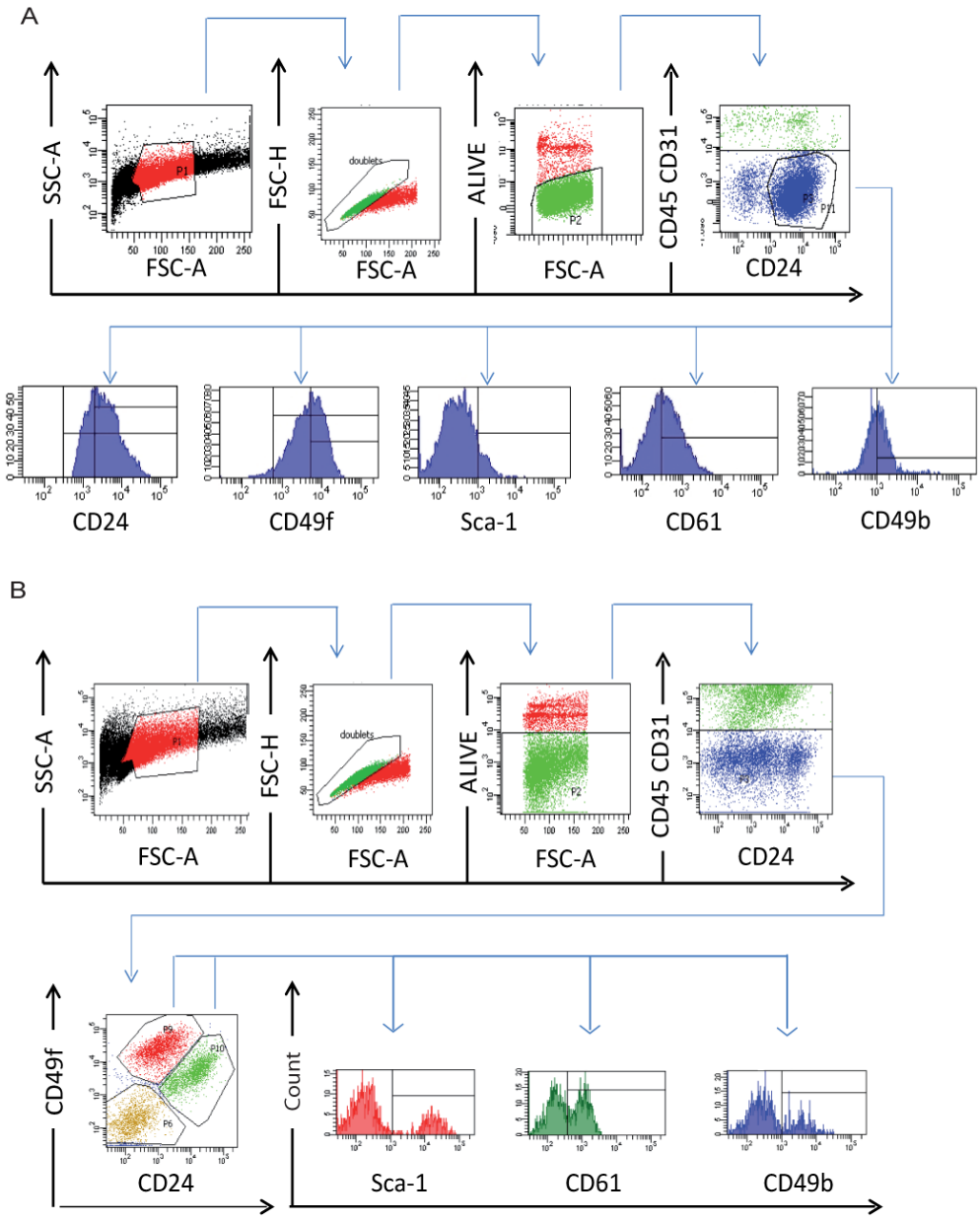

Figure S1. (Related to Figure 2,3,4,5). FACS gating scheme

A. Dot blots and histograms representing the hierarchy identified by flow cytometry analysis for MMTV-NEU$^{+/-}$, MMTV-NEU$^{+/-}$; RANK$^{+/tg}$, MMTV-PYMT$^{+/-}$ and MMTV-PYMT$^{+/+}$; RANK$^{+/tg}$ tumor cells. Positive/negative and high (hi)/ low (lo) populations were set according to populations in the normal mammary gland.

B. Dot blots and histograms representing the hierarchy identified by flow cytometry analysis for MMTV-NEU$^{+/-}$, MMTV-NEU$^{+/-}$; RANK$^{+/tg}$, MMTV-PYMT$^{+/-}$ and MMTV-PYMT$^{+/+}$; RANK$^{+/tg}$ mammary epithelial cells. Positive populations are defined based on single positive controls.

Supplemental Figure 2

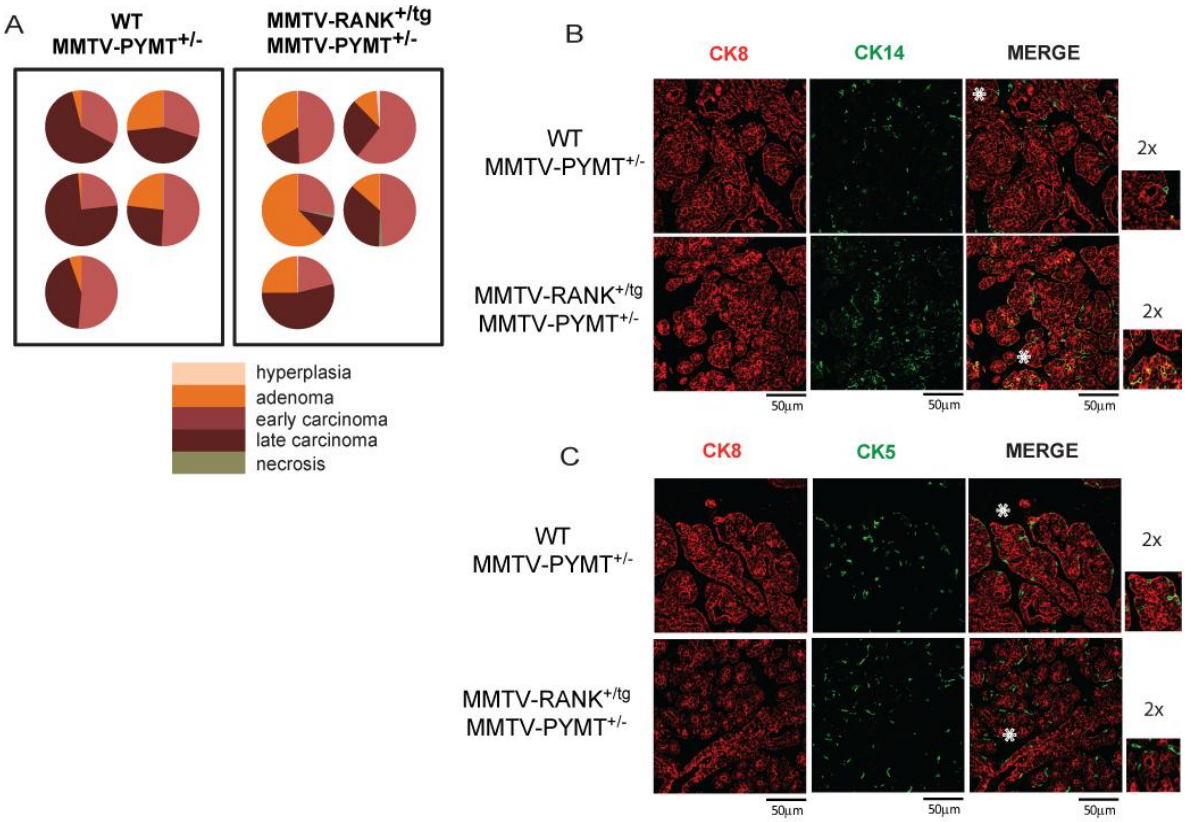

D

GROUP	N cells	CSCs: N fat pads	CSCs: Tumor incidence
WT MMTV-PYMT$^{+/-}$	10^6	8	8
	10.000	6	4
	1.000	6	2
	100	6	5
	10	6	3
MMTV-RANK$^{+/tg}$ MMTV-PYMT$^{+/-}$	10^6	8	8
	10.000	6	5
	1.000	6	6
	100	6	5
	10	6	3

CSCs CANCER STEM CELL FREQUENCY (ELDA)

MMTV-PyMT 1/ 2462 (C.I. 921 - 6583)
MMTV-PyMT;RANK$^{+/tg}$: 1/ 918 (C.I. 357 -2361)

P value: 0.0155 χ^2: 5,86

Figure S2. (Related to Figure 3). MMTV-PYMT$^{+/-}$; RANK$^{+/tg}$ tumors show more preneoplasic regions and an increase in K14+/K8+ cells in preneoplasic lesions and tumor initiating ability compared to MMTV-PYMT

A. Pie charts representing quantification of histological areas of MMTV-PYMT$^{+/-}$ and MMTV-PYMT$^{+/-}$; RANK$^{+/tg}$ tumors, as defined in Lin EY et.al. (2003). Tumor size at sacrifice was comparable for both genotypes.

B. Representative K14 (green) and K8 (red) immunostaining in MMTV-PYMT$^{+/-}$ and MMTV-PYMT$^{+/-}$; RANK$^{+/tg}$ preneoplasic lesions. Asterisks indicate double positive K14+/K8+ cells which are magnified (2x) in the insets.
C. Representative K5 (green) and K8 (red) immunostaining in MMTV-PYMT$^{+/-}$ and MMTV-PYMT$^{+/-}$; RANK$^{+/tg}$ spontaneous tumor lesions. Asterisks indicate K5+ cells that are magnified (2x) in the insets.
D. Table showing limiting dilution assay to test the tumor initiating ability of MMTV-PYMT$^{+/-}$ and MMTV-PYMT$^{+/-}$; RANK$^{+/tg}$ tumor cells. 2 independent MMTV-PYMT$^{+/-}$ and MMTV-PYMT$^{+/-}$; RANK$^{+/tg}$ tumors were pooled and indicated number of cells were injected into #4 (inguinal) WT (FvB) mammary gland. The TIC frequencies (with confidence intervals) for each group were calculated by ELDA; p- and chi-square values are shown.

Supplemental Figure 3

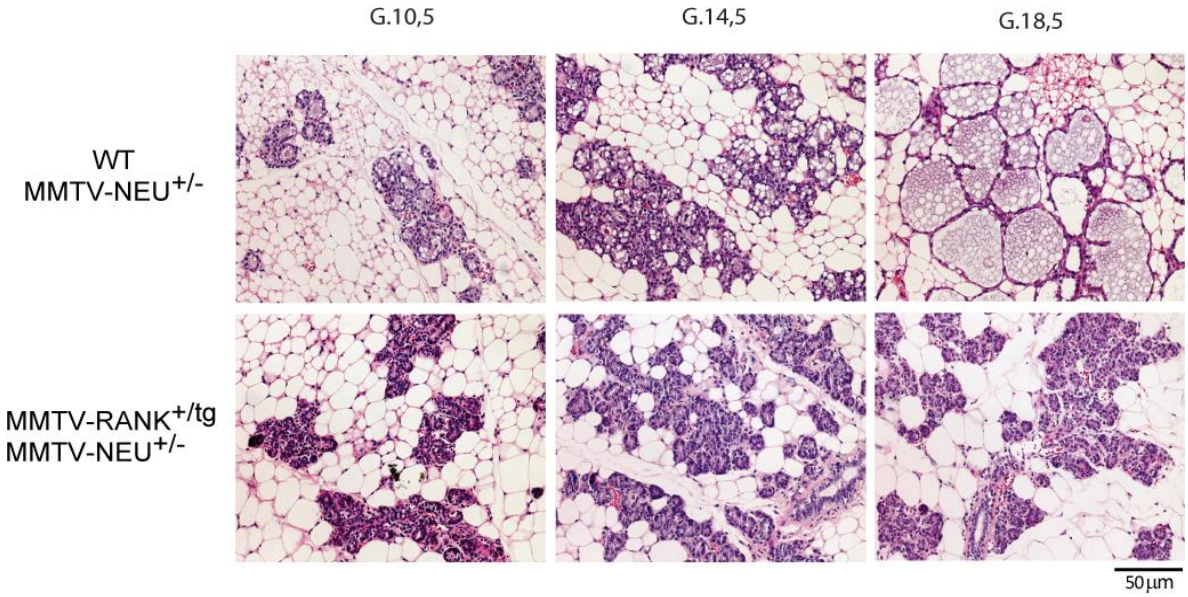

Figure S3. (Related to Figure 4). RANK overexpression in MMTV-NEU background impairs mammary alveolar secretory differentiation and lactation during pregnancy
Representative images of H&E of MMTV-NEU$^{+/-}$ and MMTV-NEU$^{+/-}$; RANK$^{+/tg}$ mammary glands at the indicated days during gestation.

SUPPLEMENTAL METHODS

Primers for genotyping

RANK Fwd	5’ CAGATGCGAACCAGGAAAG 3’
RANK Rev	5’ CAGATGCGAACCAGGAAAG 3’
NEU Fwd	5’ TTTCCTGCAGCAGCCTACGC 3’
NEU Rev	5’ CGGAACCCACATCAGGCC 3’
HK B965S Fwd	5’ CCTAGCTGTCACCAACCCTTT 3’
HK N1227AS Rev	5’ GACGAAGAGCATCACAAGGAG 3’

PYMT Fwd	5’ GGAAGCAAGTACTTCACAAGGG 3’
PYMT Rev	5’ GGAAAGTCACTAGGAGCAGGG 3’
HK PYMT Fwd	5’ TTTCCTGCAGCAGCCTACGC 3’
HK PYMT Rev	5’ CGGAACCCACATCAGGCC 3’

Primers for SYBR GREEN qRT-PCR

RANK Fwd	5’ CAGATGCGAACCAGGAAAG 3’
RANK Rev	5’ CAGATGCGAACCAGGAAAG 3’
CK14 Fwd	5’ TGAGAGCCTCAAGGAGGAGC 3’
CK14 Rev	5’ TCTCCACATTGACGTCTCCAC 3’
CK8 Fwd	5’ ATTGACAAGGTGCGCTTCCT 3’
CK8 Rev	5’ CTCCACTTGGTCTCCAGCATC 3’
HK PP1A Fwd	5’ CAAATGCTGGACCAAACACAAACG 3’
HK PP1A Rev	5’ GTTCATGCCTTCTTTCACCTTCCC 3’

ARTICLE 4

"Therapeutic inhibition of RANK signaling reduces breast cancer recurrence by inducing tumor cell differentiation"

Therapeutic Inhibition of RANK signaling reduces breast cancer recurrence by inducing tumor cell differentiation

Pellegrini P[1*], Yoldi G[1*], Trinidad EM[1*], Cordero A[1], Gomez-Miragaya J[1], Serra-Musach[2] J[2], Dougall WC[3], Muñoz P[1], Pujana MA[2], Planelles L[4] and González-Suarez E[1, #]

[1]Cancer Epigenetics and Biology Program, Bellvitge Biomedical Research Institute, IDIBELL, Barcelona, Spain.

[2]Breast Cancer and Systems Biology Unit, ICO, IDIBELL, Barcelona, Spain.

[3] Therapeutic Innovation Unit, Amgen Inc., Seattle, WA, USA

[4]Centro Nacional de Biotecnología/CSIC, UAM Cantoblanco, 28049 Madrid, Spain.

[*] contributed equally

[#]Corresponding author: Eva González-Suárez

Cancer Epigenetics and Biology Program, Bellvitge Institute for Biomedical Research, IDIBELL.

Av. Gran Via de L'Hospitalet, 199, 08908 L'Hospitalet de Llobregat, Barcelona, Spain

egsuarez@idibell.cat

Phone: +34 932607139 Fax: +34 932607219

www.pebc.cat

RUNNING TITLE: RANKL inhibition induces tumor cell differentiation

KEYWORDS: RANK, breast cancer, cancer stem cells, tumor differentiation therapy

ABSTRACT

RANK expression is associated with poor prognosis in breast cancer but its therapeutic potential remains unknown. RANK is mostly expressed in hormone receptor negative adenocarcinomas. In contrast to RANK, RANKL is rarely found on tumor cells, suggesting additional roles for RANK signaling beyond its action as a paracrine mediator of progesterone.

Here, using complementary genetic and pharmacological approaches we demonstrate that therapeutic inhibition of RANK signaling drastically reduces the cancer stem cell pool as revealed by a reduction in tumor and metastasis initiation ability and increased sensitivity to chemotherapy. Mechanistically, neoadjuvant RANKL inhibition induces the transcription factor *Tfap2b* and a luminal differentiation program, reducing the Sca1- population, enriched in tumor initiating ability. Our results suggest that RANKL inhibition could decrease recurrence and metastasis in breast cancer patients based on its ability to induce tumor cell differentiation.

INTRODUCTION

Multiple evidences support the existence of tumor initiating cells also called, cancer stem cells (CSCs) in breast cancer. CSC are able to self-renew but also to differentiate and recapitulate the molecular heterogeneity of initial tumor, being responsible of disease recurrence and metastasis, and resistance to conventional therapies such as radiation or chemotherapy (Li et al. 2008). The CSC hypothesis has attracted much attention due to the potential for discovery and development of CSC-related therapies aiming to eliminate the CSC population. Another way to control tumor progression is to induce differentiation of CSCs. Differentiation therapy could force CSCs to differentiate terminally and lose their self-renewal property. The first differentiation agent successfully used in the clinic was all-trans retinoic acid in the treatment of acute promyelocytic leukemia (Tallman et al. 1997). Retinoid signaling has also been shown to regulate breast CSC self-renewal and differentiation (Ginestier et al. 2009).

Altered regulation of developmental pathways has been proposed to play an important role in tumorigenesis and to contribute to the observed heterogeneity in breast cancer (Dontu et al. 2003). Several transcription factors such as: GATA3, FOXA1, ESR1, and more recently TFAP2, PDEF, have shown to promote luminal differentiation, by inducing expression of luminal genes and repressing basal genes, in mammary development and in breast cancer (Asselin-Labat et al. 2007; Bogachek et al. 2014; Buchwalter et al. 2013; Cyr et al. 2015; Ross-Innes et al. 2012). Characterization of the factors that regulate mammary gland differentiation is important for understanding the mechanisms of breast cancer initiation and progression and for developing targeted treatments for each tumor subtype.

RANKL is expressed in progesterone receptor-positive (PR+) mammary epithelial cells and acts as a paracrine mediator of the mitogenic effects of progesterone in mouse (Beleut et al. 2010; Fata et al. 2000) and human mammary epithelium (Tanos et al. 2013). Overexpression of RANK in mammary epithelial cells enhances proliferation, impairs alveolar differentiation and disrupts mammary epithelial cell fate, resulting in the accumulation of mammary stem cells (MaSC) and progenitors (Gonzalez-Suarez et al. 2007; Palafox et al. 2012; Pellegrini et al. 2013; Schramek et al. 2010). Moreover, we and others have shown that RANKL mediates the early steps of progesterone-driven mammary tumorigenesis in mice (Schramek et al. 2010; Gonzalez-Suarez et al. 2010; González-Suárez 2011). However, in human adenocarcinomas RANK is predominantly expressed in hormone receptor-negative (HR-) tumors, supporting progesterone-independent roles for RANK signaling in human breast cancer. In contrast to RANK, RANKL is rarely expressed on

tumor cells, but it is expressed in tumor-infiltrating lymphocytes (Palafox et al. 2012; González-Suárez 2011; Pfitzner et al. 2014). Hormone receptor-negative tumors are linked to a poor prognosis based on the high rates of recurrence and metastasis and the lack of targeted therapies. RANK expression in human adenocarcinomas is associated with reduced overall survival, accelerated bone metastasis formation and aggressive tumor phenotypes (Pfitzner et al. 2014; Santini et al. 2011), but the mechanism underlying these effects and the therapeutic potential of RANKL inhibition once tumors are established remains unexplored.

The MMTV-PyMT breast cancer mouse model shows a widespread transformation of the mammary gland with multifocal adenocarcinoma at an early age and a high incidence of lung metastasis (Guy, Cardiff, and Muller 1992; Maglione et al. 2001). Tumor cells of invasive PyMT adenocarcinomas do not express hormone receptors (HR) or RANKL, but do express high levels of RANK (Schramek et al. 2010; Gonzalez-Suarez et al. 2010), similar to what is seen in human breast tumors.

RANKL inhibitors are currently used for the treatment of bone related pathologies, osteoporosis and bone metastasis. Here we demonstrate that therapeutic inhibition of RANK signaling reduces recurrence and metastasis by inducing tumor cell differentiation.

RESULTS

RANK deletion increases tumor latency, decreases tumor incidence and impairs lung metastasis in MMTV-PyMT mice

MMTV-PyMT preneoplasic lesions and adenocarcinomas expressed high levels of RANK compared with non-tumorigenic mammary epithelia (Fig. 1A, B) suggesting a functional role for this pathway in PyMT-driven tumors. RANKL expression was found in non-tumorigenic ducts and hyperplasias (Fig. 1A) but was lost in MMTV-PyMT adenocarcinomas, consistent with the loss of PR positivity (Fig. 1A, Supplemental Fig. S-1) (Lin et al. 2003). RANKL expression was found in draining lymph nodes and tumor infiltrating leucocytes of MMTV-PyMT tumor-bearing mice (Fig. 1A, B). Analyses of FACS-sorted MMTV-PyMT tumor populations (Supplemental Fig. S2) revealed that *Rankl* mRNA was predominantly found in tumor-infiltrating CD4+ and CD8+ T lymphocytes (CD45+ CD11b- CD4+ and CD45+ CD11b- CD8+) (Fig. 1C). This profile was consistent with the expression pattern of RANK and RANKL in human breast adenocarcinomas (Palafox et al. 2012; Gonzalez-Suarez et al. 2010; Pfitzner et al. 2014), highlighting the relevance of the MMTV-PyMT tumor model to the study of human pathology.

Then, the impact of RANKL stimulation on RANK expressing tumor cells using 3D cultures derived from late stage carcinomas was addressed. These cultures have been extensively used as they mimic physiological conditions in normal and tumoral mammary gland (Barcellos-Hoff et al. 1989; Lee et al. 2007). RANKL stimulation resulted in increased acinar size in MMTV-PyMT tumor acini (Fig. 1D). No significant changes in proliferation (measured as the percentage of Ki67 positive cells) were found, but decreased apoptosis (percentage of cleaved caspase-3-positive cells) was observed in RANKL-treated tumor cultures which may be responsible of their larger size (Fig. 1E). MMTV-PyMT RANKL-treated acinar cultures showed an “invasive-like” phenotype, revealed by isolated cells surrounding the acini (Fig. 1D). To test the impact of these changes *in vivo*, 10^5 tumor cells from RANKL-treated and control MMTV-PyMT acini were injected into the mammary gland of *Foxn1*^{nu} mice. Remarkably, a significantly higher growth rate was detected in tumors arising from 2-week RANKL-treated acini compared with that of controls (Fig. 1F). Moreover, an increase in the number of lung metastatic foci was observed in mice injected with 10^5 tumor cells derived from RANKL-treated acini compared with those injected with control cells (Fig. 1G). These results demonstrate that activation of RANK signaling in could promote tumor growth and metastasis in MMTV-PyMT primary tumor cells.

Neoadjuvant inhibition of RANKL signaling decreases the frequency of tumor-initiating cells

Next, we induced RANK signaling *in vivo* in tumor bearing MMTV-PyMT mice using RANKL (Fig. 2A) at doses previously demonstrated to activate the pathway (Gonzalez-Suarez et al. 2007). After 2 weeks of RANKL treatment no significant changes in tumor growth, tumor cell proliferation (Ki67) or apoptosis (cleaved caspase 3) were observed (Fig. 2B-C). However, palpable lesions from control mice contained extensive areas of dilated ducts and hyperplasias full of secretory material, in contrast to those of RANKL treated MMTV-PyMT mice which showed a higher cell density (Fig. 2D-E). Secretions contained milk proteins as revealed by immunostaining with an anti-milk antibody (Fig 2E). These results indicate that short-term *in vivo* activation of RANK signaling is not sufficient to change the growth of established tumors, but may influence tumor cell differentiation and therefore the CSC population and tumor initiating ability.

Aiming to mimic the clinical procedure in breast cancer patients, the putative benefit of neoadjuvant and adjuvant treatment with RANKL inhibitors in tumor recurrence was interrogated. As shown in Fig. 3A, cells isolated from one single MMTV-PyMT carcinoma were orthotopically injected in syngeneic WT mice, which were randomized 1:1 for neoadjuvant RANK-Fc or mock treatment (passage 1) for 4 weeks, using doses and schedule treatments previously shown to inhibit RANK signaling (Gonzalez-Suarez et al. 2010). Using cells derived from a single tumor we avoid confounding effects due to primary tumor heterogeneity. Cells isolated from both treatment arms were injected into the fat pad of syngeneic WT recipients (passage 2) in limiting dilutions (mimicking occult disease) and again randomized 1:1 for additional RANK-Fc (adjuvant) or mock treatment to determine whether pharmacological inhibition of RANK signaling could alter the population of CSCs and their tumor-initiating ability. No significant differences in tumor growth or the frequency of apoptotic cells were observed after RANK-Fc treatments (Fig. 3B, C). However, tumor cells that were pre-treated with RANK-Fc showed a 10-fold decrease in tumor-initiating ability ($p=2.99E^{-5}$) (Fig. 3D). The estimated number of tumor-initiating cells in the control group was 1 in 206, whereas in the RANK-Fc pretreated pool (neoadjuvant) it was only 1 in 1,929. Two additional weeks of RANK-Fc treatment (pre& post-RANK-Fc) reduced the tumor-initiating cell frequency to 1 in 2,353 ($p=7.48E^{-6}$), whereas adjuvant RANK-Fc alone (post-RANK-Fc) decreased the virtual tumor-initiating cell frequency from 1 in 206 to 1 in 466 (Fig. 3D). Concomitantly, the ability to form secondary tumorspheres was significantly impaired in cells derived from the RANK-Fc-pretreated pool (Fig. 3E), consistent with a reduction in CSC population (Dontu and Wicha

2005). These results demonstrated that pretreatment with RANK-Fc reduced tumor-initiation ability, and suggested that neoadjuvant treatment with RANKL inhibitors may reduce the risk of relapse by depleting the population of CSCs.

Pharmacological inhibition of RANK signaling induces lactogenic differentiation of tumor cells

To investigate the molecular mechanism underlying the reduction in tumor initiation ability, global gene expression profiles from all RANK-Fc treatment arms were carried out. GSEA revealed as significantly associated gene sets to RANKL inhibition, protein export, exopeptidase activity, extracellular matrix, fatty acid metabolism or PPAR signaling (Fig 4A). We noticed that several of RANK-Fc regulated genes are normally expressed during alveologenesis and lactogenesis, this is, during differentiation of mammary epithelial cells into milk-secreting alveoli (Anderson et al. 2007): *Pip* (prolactin-induced protein), caseins (*Csn2, Csn1s1, Csn1s2a Csn1s2b*), *Wap* (whey acidic protein), *Glycam1* (glycosylation-dependent adhesion molecule), Lpl (*lipoprotein lipase*) (Supplemental Table 1 and Fig. 4B). In addition multiple members of the secretoglobin family were induced in the RANK-Fc treated tumors (*Scgb1b27, Scgb1b30, Scgb2b2, Scgb2b20, Scgb2b26, Scgb2b27*) (Supplemental Table 1). In fact, the genes significantly up-regulated with mammary lactation (Anderson et al. 2007) were found to be significantly over-expressed in the tumors treated with RANK-Fc (Fig. 4B, C).

Quantitative RT-PCR analyses confirmed mRNA up-regulation of *Csn2*, *Pip*, *Scgb1b27* and *Scgb2b27* in the RANK-Fc pre- and post-treated tumors (Fig. 4D). Immunostaining with anti-milk antibody confirmed that RANKL inhibition induced differentiation of late-adenocarcinoma cells into milk secreting cells (Fig. 4E). Conversely, RANKL treatment in MMTV-PyMT tumor acinar cultures induced a significant downregulation of *Csn2, Pip* and *Scgb2b27* (Fig. 4F), in correlation with the reduction of milk protein secretion found in palpable lesions from RANKL-treated MMTV-PyMT mice (Fig. 2E).

These results demonstrate that pharmacological inhibition of RANK signaling in PyMT tumor-bearing mice promoted tumor cells differentiation into an apocrine, milk-secreting phenotype that mimics mammary lactogenesis, which can contribute to the reduction in tumor initiating ability.

RANK deletion increases tumor latency, decreases tumor incidence and impairs lung metastasis in MMTV-PyMT mice

In order to further understand the relevance of RANK pathway in HR- mammary adenocarcinomas MMTV-PyMT$^{+/-}$;RANK$^{-/-}$ mice were obtained. Genetic deletion of RANK in the MMTV-PyMT background significantly delayed tumor onset (Fig. 5A) and reduced tumor incidence (Fig. 5B, C). In accordance with their multifocal origin (Lin et al. 2003), MMTV-PyMT$^{+/-}$;RANK$^{+/+}$ (PyMT;RANK$^{+/+}$) palpable lesions showed multiple stages of tumor progression: areas of early and/or late carcinomas surrounded by adenomas and hyperplastic epithelia. MMTV-PyMT;RANK$^{-/-}$ (PyMT;RANK$^{-/-}$) lesions also contained extensive areas of early and/or late carcinoma indicating that tumors can progress to the invasive stage in the absence of RANK. For most PyMT;RANK$^{-/-}$ lesions one predominant stages was found throughout the whole PyMT;RANK$^{-/-}$ palpable mass indicating that palpable lesions arise from a single tumor focus (Fig. 5D). In fact, a lower diversity index was found in the PyMT;RANK$^{-/-}$palpable lesions (Fig 5E) and the number of preneoplasic lesions quantified in mammary gland whole mounts was also significantly reduced in PyMT;RANK$^{-/-}$ compared with control mice (Fig. 5F). Lung metastases were found in 100% of PyMT;RANK$^{+/+}$ mice with early/late carcinomas, and several mice showed extensive areas of metastasis with 30-200 metastatic foci per lung; by contrast, almost all PyMT;RANK$^{-/-}$ were devoid of lung metastasis, even those bearing late carcinomas (Fig. 5G). Thus, RANK deletion severely impairs epithelial cell increases tumor latency, decreases tumor incidence and impairs lung metastasis in the MMTV-PyMT tumor-prone model.

RANK loss in tumor cells depletes the tumor and metastasis-initiating cell pools and increases apoptosis and sensitivity to docetaxel

To rule out the progesterone/RANKL-mediated effects acting in early tumorigenesis (Gonzalez-Suarez et al. 2010) and the influence of the RANK-null microenvironment (Dougall et al. 1999), PyMT;RANK$^{-/-}$ and PyMT;RANK$^{+/+}$ tumors cells, isolated from established carcinomas were orthotopically implanted in the mammary fat pads of syngeneic WT females. PyMT;RANK$^{-/-}$ tumor cells had a significantly longer latency to tumor formation when implanted in WT mice than did PyMT;RANK$^{+/+}$ tumor cells, indicating a tumor cell autonomous defect (Fig. 6A). Longer latency to tumor formation was also observed when PyMT;RANK$^{+/+}$ tumor cells were orthotopically implanted in RANK null hosts compared with WT, but no synergic effect was observed after implantation of PyMT;RANK$^{-/-}$ in RANK null hosts (Fig. 6A).

PyMT;RANK$^{-/-}$ tumors growing in WT hosts contained more apoptotic cells as revealed by cleaved caspase 3 quantification (Fig. 6B, 7C, right panel) and extensive non-viable areas relative to PyMT;RANK$^{+/+}$ tumors (Fig. 6C, left panel). This demonstrates that tumor cell survival is impaired in the absence of RANK which may contribute to the delayed tumor formation observed. Next, we examined whether the absence of RANK sensitized tumors to docetaxel, one of the most common chemotherapies used in breast cancer. PyMT;RANK$^{+/+}$ and PyMT;RANK$^{-/-}$ tumor cells were transplanted in the fat pad of WT mice and docetaxel treatment was started when tumors reached a diameter of 6 mm. As shown in Fig. 6D, PyMT/RANK$^{-/-}$ tumors were more sensitive to docetaxel than control tumors.

Next, we aimed to determine whether loss of RANK signaling exclusively on tumor cells also reduced the cancer stem cell pool as observed after pharmacological treatment with RANKL inhibitors. PyMT;RANK$^{-/-}$ tumor cells were significantly less able to give rise to tumorspheres after two passages than PyMT;RANK$^{+/+}$ tumor cells, independently of the initial host (Fig. 6E), highlighting an extenuation of a self-renewal capability that is tumor cell-autonomus (Dontu and Wicha 2005). Limiting dilution assays (LDA) in WT hosts using PyMT;RANK$^{-/-}$ tumor cells and corresponding controls isolated from late-stage adenocarcinomas revealed that the frequency of tumor-initiating cells (TICs) in PyMT;RANK$^{+/+}$ tumors was 1 in 285, whereas in PyMT;RANK$^{-/-}$ tumors it was reduced to 1 in 1,078 ($p=0.05$) (Fig. 6F). To clarify whether the impaired metastasis observed in the PyMT;RANK$^{-/-}$ mice (Fig. 6F) is a consequence of the attenuated tumorigenesis observed in these mice or an intrinsic tumor cell defect, PyMT;RANK$^{+/+}$ and PyMT;RANK$^{-/-}$ tumor cells were injected into the tail vein of *Foxn1*^{nu} recipients in LDA. PyMT;RANK$^{+/+}$ tumor cells efficiently colonized the lung: virtual frequency of metastatic cells was 1 in 2,952 cells (Fig. 7G). Strikingly, in the PyMT;RANK$^{-/-}$ pool a 10-fold (1 in 29,420) decrease in the frequency of metastasis-initiating cells (MICs) was observed (Fig. 6G). Moreover, mice injected with 10^5 PyMT;RANK$^{+/+}$ cells showed 18–133 metastatic foci, whereas in mice injected with the same number of PyMT/RANK$^{-/-}$ cells, only 0–9 metastatic foci were found (Fig. 6H), implying that RANK expression in tumor cells is a key mediator of metastasis.

Taken together, our results demonstrate that tumor cell autonomous mechanisms are sufficient to reduce the CSC population. RANK loss in advanced adenocarcinomas depleted the pool of tumor and metastasis-initiating cells, decreased survival and sensitized tumors to docetaxel, highlighting RANK as a new therapeutic target for breast cancer patients.

RANK loss or inhibition induces the expression of AP2 transcription factors drivers of the luminal differentiation in mammary epithelial cells.

To understand further the molecular mechanism underlying tumor cell differentiation and reduction in CSC observed after neoadjuvant RANKL inhibition we focused on genes specifically induced in tumors that received neoadjuvant RANK-Fc treatment as opposed to untreated or adjuvant treatments (Supplementary Table 1).

Neoadjuvant RANKL inhibition significantly induced the expression of activator protein 2 transcription factor: *Tfap2b* (Supplementary Table 1). The AP2 transcription factor family is a set of developmentally regulated, retinoic acid (RA) inducible genes; loss of expression of the AP2 genes is associated with poor survival and metastasis (Bar-Eli 1999; Gee et al. 1999). RANKL treatment for 24h significantly reduced the *Tfap2a, Tfap2b* and *Tfap2c* mRNA expression in tumor cultures of PyMT cells (Fig 7A). Moreover, overexpression of Tfap2a and Tfap2c in the mammary gland and RANK genetic loss lead to a strikingly similar phenotype (Fata et al. 2000; Jäger et al. 2003; Zhang et al. 2003, 200), therefore we analyze Tfap2 expression levels in the mammary glands of RANK null mice. A significant increase in the expression levels of *Tfap2a* and *Tfap2b* mRNA was observed in the RANK null mammary epithelia (Fig 7B). Together these results demonstrate than RANK signaling negatively regulates *Tfap2* expression.

Recent studies demonstrate that Tfap2 govern the luminal epithelial phenotype in mammary development and carcinogenesis (Bogachek et al. 2014; Cyr et al. 2015). Consistent with a tumor cell- luminal differentiation phenotype GSEA analyses of the genes that characterize mammary differentiation hierarchy in mice and humans (Lim et al. 2010), revealed that the mature luminal up-regulated set and the mammary stem cell down-regulated set, were over-expressed on the RANK-Fc treated tumors (Fig. 7C). Importantly, *Spdef*, which also promotes luminal differentiation and inhibits prostate carcinogenesis (Buchwalter et al. 2013; Cheng et al. 2014) was the top gene in these associations (Fig 7C). In addition, the genes up-regulated by TFAP2C in human breast cancer cells (Woodfield et al. 2010) were found to be significantly overexpressed in the tumors that received neoadjuvant RANK-Fc treatment (Fig 7D). mRNA expression analyses confirmed upregulation of *Tfap2b*, and the luminal genes Sp*def* and *Fbp1* (regulated by Tfap2) (Cyr et al. 2015) and downregulation of the basal genes *p63*, *krt14* in the pre-RANK-Fc treated tumors (Fig. 7E). Higher levels of *cdkn1a/p21*, also known to be regulated by Tfap2 (Scibetta et al. 2010), were observed in pre-RANK-Fc treated groups (Fig 7E). No significant changes in *krt8,* other luminal transcription factors such, *foxa1, gata3*, *esr1*,

elf5 and *Rspo1*, *axin2*, recently shown to amplify mammary progenitors in the healthy gland (Joshi et al. 2015), were observed between groups (Fig 7E). Concomitantly, higher levels of *Tfap2b, Tfap2c and p21* and lower levels of *krt14* were also found in PyMT RANK-/- tumor cells isolated from PyMT RANK-/- tumors transplanted into WT hosts as compared to control PyMT; RANK+/+ (Fig 7F). Together these results indicate that RANK signaling inhibition leads to the induction of a luminal differentiation program driven by Tfap2.

To investigate the clinical relevance of our findings we analyzed an expression dataset from lymph-node negative breast cancer patients that developed distant metastasis (Wang et al. 2005). Thus, the expression of *TFAP2B* was found to be significantly associated with good prognosis, as measured by the absence of distant metastasis: probe 215686_x_at Cox regression hazard ratio (HR) = 0.25, 95% confidence interval (CI) = 0.11 – 0.57, p=0.001 (Fig 7G). A similar estimation was revealed when considering only those tumors with a luminal phenotype (ER+): HR = 0.24, 95% CI = 0.09 – 0.63, p=0.004 (Fig 7G). Consistent with these observations, and with the proposed cancer-promoting role for enhanced RANK signaling, associations with relapse free were also observed for *TNFRSF11B* (also called OPG*),* the canonical negative regulator of the RANK pathway: 204933_s_at probe HR = 0.49, 95% confidence interval (CI) = 0.31 – 0.78, p=0.002; in luminal tumors (ER+): HR =0.33, 95% CI = 0.17 – 0.62, p=0.0006. Accordingly, *TFAP2B* and *TNFRSF11B* were found significantly co-expressed: Pearson's correlation coefficient = 0.14, p=0.018. Together these data indicate that defined AP2 transcription factors mediate the response to RANKL inhibition and, thus, metastasis impairment and good prognosis.

RANK signaling inhibition depletes the pool of Sca1- tumor initiating cells

Next, we aimed to identify the CSC population regulated by RANK in our models. Despite multiple efforts the identity of the surface markers that identify CSCs in MMTV-PyMT remains controversial (Malanchi et al. 2012; Vaillant et al. 2008). Thus, we analyzed epithelial surface markers previously shown to be enriched in MaSC, progenitors or tumor and metastasis initiation ability (Malanchi et al. 2012; Vaillant et al. 2008; Sleeman et al. 2007) in all RANK-Fc treated groups (Supplemental Fig. S2). The levels of CD49f, CD49b, CD61 and CD90 within the epithelial CD45- CD31- CD24+ cells were comparable for all treatment arms; in contrast, Sca1+/hi cells were more abundant in tumors pretreated with RANK-Fc, which show a lower tumor initiating ability (Fig. 8A, B). In the normal mammary gland Sca1 identifies a population of luminal mature cells, enriched in ER+/PR+ associated genes, in accordance with the observed increase in AP2 transcription factors and their role

inducing luminal differentiation. Despite the increase in Sca1+, we could not detect an increase in PR+ cells after RANK-Fc treatment as revealed by immunohistochemistry (Fig 8C). Similarly, no differences in the frequency of CD49f, CD49b, CD61 and CD90 were found between PyMT;RANK$^{-/-}$ orthotopic tumors and controls (Fig 8D) but an increase in the Sca1+/hi population was found in PyMT;RANK$^{-/-}$ orthotopic tumors as compared to the corresponding controls (Fig 8D).

As surface markers may vary in different tumor subtypes, models and stage of progression, functional assays were performed to evaluate whether Sca1 expression discriminates CSC population in the MMTV-PyMT tumors. Secondary tumorspheres of Sca1-/lo tumor cells were larger and five times as numerous as those of Sca1+/hi cells (Fig. 8E-F). Strikingly, LDA assays revealed the TIC frequency is significantly enhanced by 200-fold in Sca1-/lo compared with Sca1+/hi tumor cells (Fig. 8G), indicating that the Sca1-/lo population is enriched in CSCs. Altogether these results demonstrated that RANK loss or RANKL inhibition reduced the frequency of CSCs, which is enriched in a Sca1-/lo population.

DISCUSSION

Our results reveal a central role of RANK signaling enhancing recurrence and metastasis in aggressive breast tumors that can be therapeutically exploited. The MMTV-PyMT model is ideal for investigating the role of RANK signaling in HR- late-stage carcinomas, as the expression profile of RANK and RANKL resembles that found in human breast adenocarcinomas, with RANK being expressed in tumor cells and RANKL in infiltrating lymphocytes (Palafox et al. 2012; Gonzalez-Suarez et al. 2010; Pfitzner et al. 2014).

Constitutive deletion of RANK in MMTV-PyMT increases tumor latency and decreases tumor incidence, in agreement with the lower incidence of preneoplasic lesions and tumors found in MMTV-neu mice upon RANK-Fc preventive treatment (Gonzalez-Suarez et al. 2010), further supporting the role of RANK signaling in early stages of tumorigenesis [18]. It has been reported that dissemination of metastatic cells is an early event in MMTV-neu and MMTV-PyMT tumor progression (Hüsemann et al. 2008). However, the significant reduction in tumors and metastasis-initiating ability of RANK null carcinoma cells demonstrates that RANK is essential for their intrinsic metastatic potential, and not a consequence of the reduced incidence of preneoplastic lesions and tumors in PyMT; RANK-/- mice.

Our previous data demonstrated that overexpression of RANK under the MMTV promoter, disrupts mammary cell fate and differentiation resulting in accumulation of MaSC and luminal progenitors (Pellegrini et al. 2013). In human basal cell lines RANK overexpression increased the frequency of the CD44+CD24- cells, which are enriched in tumor initiating potential in HR- breast cancer (Palafox et al. 2012). Here we show that pharmacological inhibition using RANK-Fc induces tumor cell differentiation and reduces the pool of CSCs in late-stage tumors. These results demonstrate that RANK signaling regulates the balance between self-renewal and differentiation, not only during mammary gland development but also on breast adenocarcinomas. Breast tumors can be easily removed in surgery but mortality is due to tumor recurrence and metastasis driven by the surviving CSC. RANKL inhibitors, although unable to reduce tumor growth, can be used as differentiation therapy of CSC that can then be eliminated with conventional therapies. Moreover, RANK null tumor cells are more susceptible to taxanes than RANK expressing tumor cells, supporting the use of neoadjuvant RANKL inhibitors in the clinical setting to reduce the frequency of tumor relapse and metastasis and to increase sensitivity to chemotherapy. The impaired tumor and metastasis initiation ability observed in RANK null tumor cells as compared to controls, demonstrates that tumor cell intrinsic mechanisms mediate the

observed reduction in CSC. However, we cannot discard that the tumor cell extrinsic mechanisms induced by RANK signaling inhibition in the microenvironment can also contribute to reduce recurrence. In fact, longer latency to tumor formation was observed when RANK positive tumor cells were implanted in RANK null mice, although no synergic effect was observed when RANK was missing in both tumor cells and hosts.

We found that RANK-Fc treatment in MMTV-PyMT late-carcinomas induces tumor cell differentiation leading to the expression of genes involved in secretory differentiation and milk secretion. The best characterized members of the human Scgb family, mammoglobins, have been successfully used as tumor biomarkers; high levels of mammoglobin mRNA expression are associated with favorable clinicopathological features and low risk of relapse (Span et al. 2004), and are expressed under differentiation conditions (Dontu et al. 2003).

Mechanistically, we found that RANK signaling negatively regulates the AP2 transcription factors. The AP2 transcription factor family is a set of developmentally regulated, retinoic acid (RA) inducible genes, which regulate vertebrate embryogenesis, proliferation and tumorigenesis. Considerable amino acid identity exists between the TFAP2A, TFAP2B, and TFAP2C proteins, and indeed these transcription factors can all bind to essentially the same recognition site (Bosher et al. 1996). TFAP2A has been shown to function as a tumor suppressor in several solid tumors including breast cancer, which may be driven by its transcriptional regulation of p53 and p21 (Scibetta et al. 2010; McPherson, Loktev, and Weigel 2002). It has been suggested that AP2 factors can mediate retinoic acid responsiveness (McPherson, Woodfield, and Weigel 2007) and TFAP2A transcriptional activity has been shown to be essential for retinoic acid-induced neuronal differentiation of mesenchymal stem cells (Bi et al. 2014). Although little is known about TFAP2B in mammary epithelia our results suggest that, similarly to other members of the family, TFAP2B promotes differentiation in luminal tumors, and it is associated with good prognoses. Moreover, the positive correlation between the RANKL inhibitor, *OPG*, and *TFAP2B* expression in human breast tumors and their association with metastasis free phenotype support the clinical implication of our findings.

Overexpression of TFAP2A and TFAP2C mimics the mammary phenotype of RANK null mice: a simpler, sparser, ductal network and a dramatic reduction in the frequency of the alveolar buds and lactation failure, due to a significant increase in apoptosis and reduction of proliferation (Fata et al. 2000; Jäger et al. 2003; Zhang et al. 2003). Furthermore, recent findings have highlighted a critical role for TFAP2C and TFAP2A in maintaining the luminal phenotype through the induction of luminal-associated genes and repression of basal-

associated genes in mammary epithelia and breast cancer cell lines (Bogachek et al. 2014; Cyr et al. 2015). Sca-1/Ly6A is found in the luminal differentiated cell cluster, characterized by the expression of ER, PR, and according to our data it is likely to be regulated by Tfap2 or other transcription factors determinant of the luminal phenotype. Although RANKL inhibition induced *Tfap2, Pdef, Fbp1* and Sca1, it could not reinstitute ER/PR expression in PyMT adenocarcinomas.

In human breast cancer cells TFAP2 negatively regulates cancer stem cell markers (Bogachek et al. 2014). The decrease in Sca1- cells upon genetic deletion of RANK or RANK-Fc neoadjuvant treatment and their enhanced mammosphere-forming and tumor-initiating potential demonstrate that this population is enriched in CSCs in the PyMT tumors. Accordingly, RANK overexpression leads to an expansion of the CD24+ Sca1-, luminal progenitor population (Pellegrini et al. 2013) and Joshi et al recently reported a reduction in the Sca1- luminal progenitors in the mammary glands of RANK-deficient mice (Joshi et al. 2015). Previous results also support that repression of Sca1 enhances tumor initiation in MMTV-wnt models (Batts et al. 2011). CSC markers extensively used in breast cancer are associated with clinical and molecular characteristics in HR- breast cancer but not in luminal tumors (Ali et al. 2011). Although MMTV-PyMT adenocarcinomas lose the expression of HR during tumor progression they are luminal tumors. The relevance of Sca1/Ly6a as a CSC marker in human luminal adenocarcinomas deserves further investigation.

In summary, we have now demonstrated that inhibition of RANK signaling in breast adenocarcinomas would target and differentiate the CSC population, decreasing tumor- and metastasis-initiating ability, and enhancing sensitivity to chemotherapy. Therefore, RANKL inhibitors could have therapeutic benefits in breast cancer patients beyond its current use for controlling skeletal-related events, by reducing tumor relapse and metastasis.

MATERIALS AND METHODS

Animals

All research involving animals was performed at the IDIBELL animal facility in compliance with protocols approved by the IDIBELL Committee on Animal Care and following national and European Union regulations. MMTV-PyMT (FVB/N-Tg(MMTV-PyVT)634Mul) were obtained from the Jackson Laboratory and have been described previously (Guy, Cardiff, and Muller 1992). MMTV-PyMT$^{-/+}$;RANK$^{-/-}$ mice were obtained by crossing the MMTV-PyMT (FvB/N) strain with RANK$^{+/-}$ (C57BL/6) mice (Dougall et al. 1999). Littermates with the same genetic background were used as controls in all experiments. Mice were backcrossed for at least five generations with RANK$^{+/-}$ (C57BL/6) before transplantation into syngeneic C57BL/6 mice. RANKL-LZ and RANK-Fc reagents and RANK$^{+/-}$ (C57BL/6) mice were obtained from Dr. Bill Dougall (Amgen Inc.). *Foxn1^{nu}*, Scid/Beige and Nod/Scid mice were obtained from Charles River.

Whole-mounts analysis

Preneoplasic lesions were quantified in the mammary glands of mice between 90 and 150 days of age by fixation with Carnoy's solution (ethanol 95%, chloroform and glacial acetic acid at 6:3:1) 2 hours at RT. Then, they were washed 15 minutes with ethanol 70% and rinsed in distilled water. Overnight staining was performed at 4ºC with carmine alum at 0,002% and then dehydrated at RT.

Tumor cell isolation

Fresh tissues were mechanically dissected with a McIlwain tissue chopper and enzymatically digested with appropriate medium (DMEM F-12, 0.3% Collagenase A, 2.5 U/mL dispase, 20 mM HEPES and antibiotics) for 30 min at 37°C. Samples were washed with Leibowitz L15 medium containing 10% fetal bovine serum (FBS) between each step. Erythrocytes were eliminated by treating samples with hypotonic lysis buffer (Lonza Iberica). Single epithelial cells were isolated by treating with trypsin (PAA Laboratories) for 2 min at 37°C. Cell aggregates were removed by filtering the cell suspension with a 40-µm filter and counted as described (Smalley 2010).

Orthotopic transplants, metastasis and limiting dilution assays

For orthotopic transplants and tumor-limiting dilution assays tumor cells isolated from MMTV-PyMT (FVB), MMTV-PyMT;RANK$^{+/+}$ (C57BL/6) or MMTV-PyMT;RANK$^{-/-}$ (C57BL/6)

mice were mixed 1:1 with Matrigel matrix (BD Biosciences) and orthotopically implanted in the inguinal mammary gland of 6-10-week-old syngeneic females. Mice were monitored for tumor formation for a maximum of 38 weeks. In all assays, tumor-initiating potential was defined as the ability to form palpable, growing tumors of ≥2 mm diameter. For metastasis assays, the indicated number of tumor cells were resuspended in 200 µL of cold PBS and injected intravenously in 6-10-week-old *Foxn1*^{nu} females. Lungs were recovered 8-10 weeks later for histological analysis. For metastasis scoring entire lungs were step-sectioned at 100 µm and individual metastases identified histologically.

RANKL or RANK-Fc treatments in vivo

For short-term experiments, RANKL (25 µg/mouse, Amgen Inc.) was injected subcutaneously three times a week for 2 weeks in tumor-bearing MMTV-PyMT FVB (10-14 weeks old) females. Treatment started when tumors were approximately 3 mm of diameter. For neoadjuvant or adjuvant treatments, RANK-Fc (10 mg/kg; Amgen Inc.) was injected subcutaneously three times a week (for 4 weeks in passage 1 and for 2 weeks in passage 2), starting 24 h after orthotopic injection of MMTV-PyMT tumor cells into syngeneic WT FVB mice.

Docetaxel treatment

500,000 PyMT;RANK$^{+/+}$ and PyMT;RANK$^{-/-}$ tumor cells were orthotopically implanted in the inguinal glands of syngeneic WT mice. Docetaxel (Actavis, 20 mg/ml) was administered at 25 mg/kg intraperitoneally twice per week. Treatment started when tumors reached 6 mm of diameter and was interrupted when the residual tumors shrank below 2 mm.

Tumor acinar cultures and growth/metastasis assays from acinar cultures

For 3D acinar cultures, isolated MMTV-PyMT tumor cells were seeded on top of growth factor reduced matrigel (10,000 cells/well in 8-well chamber slides; 500,000 cells/well in 6-well paltes) in growth medium (DMEM-F12, 5% FBS, 10 ng/ml of EGF, 100 ng/ml cholerin toxin, 5 µg/ml insulin and 1x Penicillin/Streptomycin with or without RANKL (1 µg/mL). After 24 h cells were collected for RNA analyses or medium was changed to differentiation medium containing DMEM F-12, prolactin 3 µg/mL (Sigma-Aldrich), hydrocortisone 1 µg/mL, ITS (Sigma-Aldrich), cholera toxin 100 ng/mL and penicillin/streptomycin, as previously described (Hathaway and Shur 1996) with or without RANKL (1 µg/mL). Medium was replenished three times a week and maintained in culture for 15 days. Acinar diameters were quantified with ImageJ software (Wayne Rasband, NIH). Matrigel was dissolved by treatment with cold PBS-EDTA 5 mM for 25 min

on ice, washed with PBS, and tumor cells were obtained after digestion with trypsin for 5 min at 37°C.

Tissue histology and immunostaining

Tissue samples were fixed in formalin and embedded in paraffin. 3-µm sections were cut for histological analysis and stained with hematoxylin and eosin. Entire lungs were step-sectioned at 100 µm and individual metastases identified histologically. 15-16 cuts per lung were quantified unless macroscopic metastases were apparent at necropsy, in which case only 3 cuts were quantified. For immunostaining, 3-µm tissue sections were used. Antigen heat retrieval with citrate was used for PR (DAKO), SMA-1 (Sigma-Aldrich), mRANKL (R&D Systems), Ki67 (Thermo Scientific), cleaved caspase-3 (Cell Signaling) antibodies and rabbit anti-milk serum (kindly provided by Prof. Nancy E. Hynes). mRANK (R&D Systems) immunostaining was performed, pre-treating sections with Protease XXIV 5 U/mL (Sigma-Aldrich) for 15 min at room temperature. All antibodies were incubated overnight at 4°C, detected with biotinylated secondary antibodies and streptavidin horseradish peroxidase (Vector) and revealed with DAB substrate (DAKO).

Immunofluorescence

Immunofluorescence of Ki67 and cleaved caspase-3 in acinar cultures were performed as previously described (Debnath, Muthuswamy, and Brugge 2003). Briefly, acini were fixed in 2% paraformaldehyde (20 min), permeabilized with PBS containing 0.5% Triton X-100 (15 min), and washed with PBS-Glycine 100 mM (three washes of 15 min each). Antigens were blocked with IF buffer (PBS, 7.7 mM NaN_3, 0.1% bovine serum albumin, 0.2% Triton x-100, 0.05% Tween-20) + 10% goat serum for 1 h and then with IF buffer + goat serum + 20 µg/mL F(ab') fragment (Jackson ImmunoResearch) for 30 min. Primary antibodies were incubated overnight in a humid chamber. Antibody-antigen complexes were detected using Alexa-488-conjugated anti-rabbit (Invitrogen) diluted 1:500 in IF buffer + 10% goat serum and incubated for 40 min. Acini were then washed with IF buffer and the nuclei stained with DAPI. Confocal analysis was carried out using a Leica confocal microscope. Images were captured using LasAF software (Leica). The percentage of Ki67 or caspase-3+ cells was calculated with ImageJ software.

Flow cytometry

Single cells were resuspended and blocked with PBS 2% FBS and IgG blocking reagent for 10 min on ice. For leucocyte analyses cells were incubated with CD45-APC-Cy7 (0.125 µg/mL; 30-F11, Biolegend), CD4-PE-Cy7 (2 µg/mL; RM4-5, Biolegend), CD11b-APC (2.5

μg/mL; M1/70, Biolegend), CD8-PE or CD8-FITC (1 μg/mL; 53-6.7, Biolegend), Gr1-FITC (2 μg/mL; RB6-8C5, Biolegend), F4/80-PE (1.25 μg/mL, BM8, Biolegend) for 30 min on ice. To analyze epithelial markers, cells were incubated with the following antibodies: CD24-FITC (5 μg/mL; M1/69), CD61-FITC (2.5 μg/mL; 2C9.G2), Sca-1-APC (0.5 μg/mL; Ly-6A/E) all from BD Pharmingen, CD49b-Alexa 647 (1.25 μg/Ml; HMa2, Biolegend), CD90-PE (1 μg/Ml; HIS51, Bioscience) and CD49f-a647 (2.5 μg/mL; GoH3, R&D Systems). Lymphocytes and endothelial cells were excluded in flow cytometry using CD45-PECy7 (0.125 μg/mL; 30-F11) or CD45-APC Cy7 (0.125 μg/mL; 30-F11) and CD31-PECy7 (0.5 μg/mL; 390) all from Biolegend. FACS analysis was performed using FACS Canto, FACS Aria (Becton Dickinson) and Diva software. Cells were sorted using MoFlo (Beckman Coulter) at 25 psi and a 100-μm tip.

Tumorsphere culture

Cells isolated from primary tumors were resuspended in serum-free DMEM F12 mammosphere medium containing 20 ng/mL of EFG, 1x B27 and 4 μg/mL heparin (Sigma-Aldrich), as previously described (Dontu and Wicha 2005) with 2% of growth factor reduced matrigel. Primary tumorspheres were derived by plating 20,000 cells/mL in 2 mL of medium onto cell-suspension culture plates. After 14 days, tumorspheres were isolated by 5 min treatment with PBS-EDTA 1 mM + 5 min of trypsin at 37°C and plated for secondary tumorsphere formation at a concentration of 5,000 cells/mL in triplicate. Individual spheres from each replicate well were counted under a microscope.

RNA extraction and RT-PCR

Total RNA of tissue, sorted cells and acinar cultures were prepared with Tripure Isolation Reagent (Roche); Matrigel cultures were dissolved with cold PBS-EDTA (5 mM) on ice for 30 min. Matrigel-free cell suspensions were then pelleted at maximum speed and resuspended in TriPure Isolation Reagent for RNA isolation. Frozen tumor tissues were fractionated using glass beads (Sigma-Aldrich) and the PrecCellys® 24 tissue homogenizer (Berting Technologies). cDNA was produced by reverse transcription using 1 μg of RNA in a 35 μL reaction following the kit instructions (Applied Biosystems). 20 ng/well of RNA/cDNA were used for tissue/acinar cultures and 5,000 cells/well for sorted cells. Analyses were performed in triplicate. Quantitative PCR was performed using TaqMan or LightCycler® 480 SYBR green.Primer sequences and TaqMan probes are indicated below.

RNA labeling and hybridization to Agilent microarrays

RNA quality was assessed using a TapeStation (Agilent Technologies). RNA concentration and dye incorporation was measured using a UV-VIS spectrophotometer (Nanodrop 1000, Agilent Technologies, Wilmington, DE, USA). Hybridization to SurePrint G3 Mouse Gene Expression Microarray (ID G4852A, Agilent Technologies) was conducted following manufacturer's two-color protocol (Two-Color Microarray-Based Gene Expression Analysis v. 6.5, Agilent Technologies), and dye swaps (Cy3 and Cy5) were performed for RNA amplified from each sample. Microarray chips were then washed and immediately scanned using a DNA Microarray Scanner (Model G2505C, Agilent Technologies).

Microarray analysis

Microarray data were feature extracted using Feature Extraction Software (v. 10.7) available from Agilent, using the default variables. Outlier features on the arrays were flagged by the same software package. Data analysis was performed using *Bioconductor* package, under R environment. Data preprocessing and differential expression analysis was performed using *limma* and *RankProd* package, and latest gene annotations available was used. Raw feature intensities were background corrected using *normexp* background correction algorithm. Within-array normalization was done using spatial and intensity-dependent *loess. Aquantile* normalization was used to normalize between arrays. The expression of each gene is reported as the as the *base 2 logarithm* of ratio of the value obtained of each condition relative to control condition. A gene is considered differentially expressed if it displays a *pfp* (proportion of false positives) less than 0.05 by non-parametric test. The GSEA was run using default values for all parameters. Raw microarray data has been deposited in GEO, access number GSE66085. The mature luminal and stem cell gene sets were taken from the original publication (Lim et al. 2010). The differentially expressed genes between lactation and pregnancy were identified using the GEO GSE8191 dataset (Anderson et al. 2007) and the TFAP2C regulated genes in breast cancer cells using the GEO GSE8640 dataset (Woodfield et al. 2010). Cox proportional hazard regression analyses were applied to evaluate associations with prognosis (relapse or distant metastasis) at the level of microarray probes.

Statistical analysis

Statistical analyses were performed using GraphPad Prism. Differences between pairs of mouse cohorts or conditions were analyzed with a two-tailed Student's t-test or an F-test. Fold changes between expression values for RANKL or RANK-Fc treated tumors or tumor

cells and untreated controls were calculated, and one sample t test against a reference value of 1 was used. Two-way analysis of variance was used to compare tumor growth curves. The Mantel-Cox test was used for tumor-free survival studies. Tumor-initiating cells in limiting dilutions were estimated using the extreme limiting dilution assay (ELDA) (Hu and Smyth 2009).

Primers

NAME		**SEQUENCE 5'→3'**
mRANK	TaqMan	Mm00437135_m1
mRANKL	TaqMan	Mm00441908_m1
mACTINβ	TaqMan	4352341e-1003012
Rank	FWD	CAGATGCGAACCAGGAAAGT
	REV	TCTTCATTCCAGGTGTCCAAG
Rankl	FWD	TCCTGAGACTCCATGAAAACG
	REV	CCCACAATGTGTTGCAGTTC
Rpl38	FWD	AGGATGCCAAGTCTGTCAAGA
	REV	TCCTTGTCTGTGATAACCAGGG
Csn2	FWD	TCCACAACATTCCGTTTCTG
	REV	AGCATGATCCAAAGGTGAAAA
Pip	FWD	TCAGTGCTGTGACACTCTTCT
	REV	GTGTTTCAACTGTAACTTGCACA
Scgb1b27	FWD	TCTGATAGGACCTTGACCGAG
	REV	GGCAATTGGTTTCCGTGAGA
Scgb2b27	FWD	AGGGGACACTTCTTCTGCTG
	REV	TGGGGACTCTTTAATTTGGTGG
p21	FWD	CGCGGTGTCAGAGTCTAGG
	REV	GGACATCACCAGGATTGGAC
Hprt	FWD	TCAGTCAACGGGGGACATAAA
	REV	GGGGCTGTACTGCTTAACCAG
Rspo1	FWD	CTGAGCTGGACACACATCG
	REV	AACAGAGCTCACAGCCCTTG
Krt14	FWD	TGAGAGCCTCAAGGAGGAGC
	REV	TCTCCACATTGACGTCTCCAC
Krt15	FWD	GAGTGGGGAAGGAGTTGGAC
	REV	GCCACTGCCAACACCAAT
p63	FWD	GCATGGGAGCCAACATTCC
	REV	TGTCTCCAGCCATTGGCAT

Axin2	FWD	TGTGAGATCCACGGAAACA
	REV	GTGGCTGGTGCAAAGACATA
Tfap2a	FWD	CTTACCTCACGCCATCGAG
	REV	TTGCTGTTGGACTTGGACAG
Tfap2b	FWD	GACAGCCTCTCGTTGCAC
	REV	TGACTGACTGGTCCAATAGGTTC
Tfap2c	FWD	AGTATGAAGAGGATTGCGAGGA
	REV	CGCGGGACTGTAGAGATGTT
Krt8	FWD	ATTGACAAGGTGCGCTTCCT
	REV	CTCCACTTGGTCTCCAGCATC
Gata3	FWD	GCAGGCATTGCAAAGGTAGT
	REV	AGCACAGGCAGGGAGTGT
Foxa1	FWD	CACGCAGGAGGCCTACTCCT
	REV	TGTTGGCGTAGGACATGTTG
Esr1	FWD	GGAAGCTCCTGTTTGCTCCT
	REV	CGGAACCGACTTGACGTAG
Spdef	FWD	AGGTGCAATCGATGGTTGTG
	REV	AAAAGCCACTTCTGCACGTT
Fbp1	FWD	CGCTACCTGTGTTCTTGTGTCT
	REV	CACAAGGCAGTCAATGTTGG
Elf5	FWD	GGACTCCGTAACCCATAGCA
	REV	TACTGGTCGCAGCAGAATTG

Online supplemental material includes 2 Supplemental Figures and 1 Supplemental Excel Table summarizing genes regulated by RANK-Fc treatment obtained from microarray results.

ACKNOWLEDGEMENTS

We thank, L Alcaraz and D Amoros (Bioarray) for microarray analyses, NE Hynes for providing anti-milk serum, M. Glukhova's group for sharing protocols, G. Boigues and the IDIBELL animal facility for their assistance with mouse colonies, A. Villanueva for technical support with metastasis assays, and E. Castaño for her assistance with FACS analyses.

This work was supported by grants to E. González-Suárez by Ministerio de Ciencia e Innovación (SAF2008-01975; SAF2011-22893), Fundacion Mutua Madrileña, Concern Foundation, Fundació La Marató de TV3 and a Ramón y Cajal program and by grants to M.A. Pujana from the ISCIII (PI12/01528) and AGAUR (SGR 2014-364), and by grants to L. Planelles from the ISCIII (PI10/01556) and the Ramón y Cajal program. P. Pellegrini and J Gomez-Miragaya are recipients of an FPI grant from the Ministerio de Ciencia e Innovacion. The funders had no role in study design, data collection and analysis, decision to publish, or preparation of the manuscript.

AUTHOR CONTRIBUTIONS

P Pellegrini: Collection and assembly of data, data analysis and interpretation, writing and final approval of manuscript. G Yoldi, EM Trinidad, A Cordero, JG Miragaya, J Serra-Musach: Collection and assembly of data, data analysis and interpretation, final approval of manuscript. P Muñoz, MA Pujana, WC Dougall, L Planelles: data analysis and interpretation, and final approval of manuscript. E Gonzalez-Suarez: Conception and design, financial support, collection and assembly of data, data analysis and interpretation, writing and final approval of manuscript.

CONFLICT OF INTEREST

WC Dougall is employee and stock holder of Amgen Inc. All other declare that they have no conflict of interest.

REFERENCES

Ali, H. Raza, Sarah-Jane Dawson, Fiona M. Blows, Elena Provenzano, Paul D. Pharoah, and Carlos Caldas. 2011. "Cancer Stem Cell Markers in Breast Cancer: Pathological, Clinical and Prognostic Significance." *Breast Cancer Research: BCR* 13 (6): R118. doi:10.1186/bcr3061.

Anderson, Steven M., Michael C. Rudolph, James L. McManaman, and Margaret C. Neville. 2007. "Key Stages in Mammary Gland Development. Secretory Activation in the Mammary Gland: It's Not Just about Milk Protein Synthesis!" *Breast Cancer Research: BCR* 9 (1): 204. doi:10.1186/bcr1653.

Asselin-Labat, Marie-Liesse, Kate D. Sutherland, Holly Barker, Richard Thomas, Mark Shackleton, Natasha C. Forrest, Lynne Hartley, et al. 2007. "Gata-3 Is an Essential Regulator of Mammary-Gland Morphogenesis and Luminal-Cell Differentiation." *Nature Cell Biology* 9 (2): 201–9. doi:10.1038/ncb1530.

Barcellos-Hoff, M. H., J. Aggeler, T. G. Ram, and M. J. Bissell. 1989. "Functional Differentiation and Alveolar Morphogenesis of Primary Mammary Cultures on Reconstituted Basement Membrane." *Development (Cambridge, England)* 105 (2): 223–35.

Bar-Eli, M. 1999. "Role of AP-2 in Tumor Growth and Metastasis of Human Melanoma." *Cancer Metastasis Reviews* 18 (3): 377–85.

Batts, Torey D., Heather L. Machado, Yiqun Zhang, Chad J. Creighton, Yi Li, and Jeffrey M. Rosen. 2011. "Stem Cell Antigen-1 (sca-1) Regulates Mammary Tumor Development and Cell Migration." *PloS One* 6 (11): e27841. doi:10.1371/journal.pone.0027841.

Beleut, Manfred, Renuga Devi Rajaram, Marian Caikovski, Ayyakkannu Ayyanan, Davide Germano, Yongwon Choi, Pascal Schneider, and Cathrin Brisken. 2010. "Two Distinct Mechanisms Underlie Progesterone-Induced Proliferation in the Mammary Gland." *Proceedings of the National Academy of Sciences of the United States of America* 107 (7): 2989–94. doi:10.1073/pnas.0915148107.

Bi, Yang, Min Gong, Yun He, Xiaojian Zhang, Xiaoqin Zhou, Yun Zhang, Guoxin Nan, et al. 2014. "AP2α Transcriptional Activity Is Essential for Retinoid-Induced Neuronal Differentiation of Mesenchymal Stem Cells." *The International Journal of Biochemistry & Cell Biology* 46 (January): 148–60. doi:10.1016/j.biocel.2013.11.009.

Bogachek, Maria V., Yizhen Chen, Mikhail V. Kulak, George W. Woodfield, Anthony R. Cyr, Jung M. Park, Philip M. Spanheimer, Yingyue Li, Tiandao Li, and Ronald J. Weigel. 2014. "Sumoylation Pathway Is Required to Maintain the Basal Breast Cancer Subtype." *Cancer Cell* 25 (6): 748–61. doi:10.1016/j.ccr.2014.04.008.

Bosher, J. M., N. F. Totty, J. J. Hsuan, T. Williams, and H. C. Hurst. 1996. "A Family of AP-2 Proteins Regulates c-erbB-2 Expression in Mammary Carcinoma." *Oncogene* 13 (8): 1701–7.

Buchwalter, Gilles, Michele M. Hickey, Anne Cromer, Laura M. Selfors, Ruwanthi N. Gunawardane, Jason Frishman, Rinath Jeselsohn, et al. 2013. “PDEF Promotes Luminal Differentiation and Acts as a Survival Factor for ER-Positive Breast Cancer Cells.” *Cancer Cell* 23 (6): 753–67. doi:10.1016/j.ccr.2013.04.026.

Cheng, Xin-Hua, Markaisa Black, Vladimir Ustiyan, Tien Le, Logan Fulford, Anusha Sridharan, Mario Medvedovic, Vladimir V. Kalinichenko, Jeffrey A. Whitsett, and Tanya V. Kalin. 2014. “SPDEF Inhibits Prostate Carcinogenesis by Disrupting a Positive Feedback Loop in Regulation of the Foxm1 Oncogene.” *PLoS Genetics* 10 (9): e1004656. doi:10.1371/journal.pgen.1004656.

Cyr, A. R., M. V. Kulak, J. M. Park, M. V. Bogachek, P. M. Spanheimer, G. W. Woodfield, L. S. White-Baer, et al. 2015. “TFAP2C Governs the Luminal Epithelial Phenotype in Mammary Development and Carcinogenesis.” *Oncogene* 34 (4): 436–44. doi:10.1038/onc.2013.569.

Debnath, Jayanta, Senthil K. Muthuswamy, and Joan S. Brugge. 2003. “Morphogenesis and Oncogenesis of MCF-10A Mammary Epithelial Acini Grown in Three-Dimensional Basement Membrane Cultures.” *Methods*, Epithelial polarity and morphogenesis, 30 (3): 256–68. doi:10.1016/S1046-2023(03)00032-X.

Dontu, Gabriela, Wissam M. Abdallah, Jessica M. Foley, Kyle W. Jackson, Michael F. Clarke, Mari J. Kawamura, and Max S. Wicha. 2003. “In Vitro Propagation and Transcriptional Profiling of Human Mammary Stem/progenitor Cells.” *Genes & Development* 17 (10): 1253–70. doi:10.1101/gad.1061803.

Dontu, Gabriela, and Max S. Wicha. 2005. “Survival of Mammary Stem Cells in Suspension Culture: Implications for Stem Cell Biology and Neoplasia.” *Journal of Mammary Gland Biology and Neoplasia* 10 (1): 75–86. doi:10.1007/s10911-005-2542-5.

Dougall, W. C., M. Glaccum, K. Charrier, K. Rohrbach, K. Brasel, T. De Smedt, E. Daro, et al. 1999. “RANK Is Essential for Osteoclast and Lymph Node Development.” *Genes & Development* 13 (18): 2412–24.

Fata, J. E., Y. Y. Kong, J. Li, T. Sasaki, J. Irie-Sasaki, R. A. Moorehead, R. Elliott, et al. 2000. “The Osteoclast Differentiation Factor Osteoprotegerin-Ligand Is Essential for Mammary Gland Development.” *Cell* 103 (1): 41–50.

Gee, J. M., J. F. Robertson, I. O. Ellis, R. I. Nicholson, and H. C. Hurst. 1999. “Immunohistochemical Analysis Reveals a Tumour Suppressor-like Role for the Transcription Factor AP-2 in Invasive Breast Cancer.” *The Journal of Pathology* 189 (4): 514–20. doi:10.1002/(SICI)1096-9896(199912)189:4<514::AID-PATH463>3.0.CO;2-9.

Ginestier, Christophe, Julien Wicinski, Nathalie Cervera, Florence Monville, Pascal Finetti, François Bertucci, Max S. Wicha, Daniel Birnbaum, and Emmanuelle Charafe-Jauffret. 2009. “Retinoid Signaling Regulates Breast Cancer Stem Cell Differentiation.” *Cell Cycle (Georgetown, Tex.)* 8 (20): 3297–3302.

González-Suárez, Eva. 2011. “RANKL Inhibition: A Promising Novel Strategy for Breast Cancer Treatment.” *Clinical & Translational Oncology: Official Publication of the Federation of Spanish*

Oncology Societies and of the National Cancer Institute of Mexico 13 (4): 222–28. doi:10.1007/s12094-011-0646-5.

Gonzalez-Suarez, Eva, Daniel Branstetter, Allison Armstrong, Huyen Dinh, Hal Blumberg, and William C. Dougall. 2007. "RANK Overexpression in Transgenic Mice with Mouse Mammary Tumor Virus Promoter-Controlled RANK Increases Proliferation and Impairs Alveolar Differentiation in the Mammary Epithelia and Disrupts Lumen Formation in Cultured Epithelial Acini." *Molecular and Cellular Biology* 27 (4): 1442–54. doi:10.1128/MCB.01298-06.

Gonzalez-Suarez, Eva, Allison P. Jacob, Jon Jones, Robert Miller, Martine P. Roudier-Meyer, Ryan Erwert, Jan Pinkas, Dan Branstetter, and William C. Dougall. 2010. "RANK Ligand Mediates Progestin-Induced Mammary Epithelial Proliferation and Carcinogenesis." *Nature* 468 (7320): 103–7. doi:10.1038/nature09495.

Guy, C. T., R. D. Cardiff, and W. J. Muller. 1992. "Induction of Mammary Tumors by Expression of Polyomavirus Middle T Oncogene: A Transgenic Mouse Model for Metastatic Disease." *Molecular and Cellular Biology* 12 (3): 954–61.

Hathaway, H. J., and B. D. Shur. 1996. "Mammary Gland Morphogenesis Is Inhibited in Transgenic Mice That Overexpress Cell Surface beta1,4-Galactosyltransferase." *Development (Cambridge, England)* 122 (9): 2859–72.

Hüsemann, Yves, Jochen B. Geigl, Falk Schubert, Piero Musiani, Manfred Meyer, Elke Burghart, Guido Forni, et al. 2008. "Systemic Spread Is an Early Step in Breast Cancer." *Cancer Cell* 13 (1): 58–68. doi:10.1016/j.ccr.2007.12.003.

Hu, Yifang, and Gordon K. Smyth. 2009. "ELDA: Extreme Limiting Dilution Analysis for Comparing Depleted and Enriched Populations in Stem Cell and Other Assays." *Journal of Immunological Methods* 347 (1-2): 70–78. doi:10.1016/j.jim.2009.06.008.

Jäger, Richard, Uwe Werling, Stephan Rimpf, Andrea Jacob, and Hubert Schorle. 2003. "Transcription Factor AP-2gamma Stimulates Proliferation and Apoptosis and Impairs Differentiation in a Transgenic Model." *Molecular Cancer Research: MCR* 1 (12): 921–29.

Joshi, Purna A., Paul D. Waterhouse, Nagarajan Kannan, Swami Narala, Hui Fang, Marco A. Di Grappa, Hartland W. Jackson, Josef M. Penninger, Connie Eaves, and Rama Khokha. 2015. "RANK Signaling Amplifies WNT-Responsive Mammary Progenitors through R-SPONDIN1." *Stem Cell Reports* 5 (1): 31–44. doi:10.1016/j.stemcr.2015.05.012.

Lee, Genee Y., Paraic A. Kenny, Eva H. Lee, and Mina J. Bissell. 2007. "Three-Dimensional Culture Models of Normal and Malignant Breast Epithelial Cells." *Nature Methods* 4 (4): 359–65. doi:10.1038/nmeth1015.

Lim, Elgene, Di Wu, Bhupinder Pal, Toula Bouras, Marie-Liesse Asselin-Labat, François Vaillant, Hideo Yagita, Geoffrey J Lindeman, Gordon K Smyth, and Jane E Visvader. 2010. "Transcriptome Analyses of Mouse and Human Mammary Cell Subpopulations Reveal Multiple Conserved Genes and Pathways." *Breast Cancer Research: BCR* 12 (2): R21. doi:10.1186/bcr2560.

Lin, Elaine Y., Joan G. Jones, Ping Li, Liyin Zhu, Kathleen D. Whitney, William J. Muller, and Jeffrey W. Pollard. 2003. “Progression to Malignancy in the Polyoma Middle T Oncoprotein Mouse Breast Cancer Model Provides a Reliable Model for Human Diseases.” *The American Journal of Pathology* 163 (5): 2113–26. doi:10.1016/S0002-9440(10)63568-7.

Li, Xiaoxian, Michael T. Lewis, Jian Huang, Carolina Gutierrez, C. Kent Osborne, Meng-Fen Wu, Susan G. Hilsenbeck, et al. 2008. “Intrinsic Resistance of Tumorigenic Breast Cancer Cells to Chemotherapy.” *Journal of the National Cancer Institute* 100 (9): 672–79. doi:10.1093/jnci/djn123.

Maglione, Jeannie E., Drew Moghanaki, Lawrence J. T. Young, Cathyryne K. Manner, Lesley G. Ellies, Sasha O. Joseph, Benjamin Nicholson, Robert D. Cardiff, and Carol L. MacLeod. 2001. “Transgenic Polyoma Middle-T Mice Model Premalignant Mammary Disease.” *Cancer Research* 61 (22): 8298–8305.

Malanchi, Ilaria, Albert Santamaria-Martínez, Evelyn Susanto, Hong Peng, Hans-Anton Lehr, Jean-Francois Delaloye, and Joerg Huelsken. 2012. “Interactions between Cancer Stem Cells and Their Niche Govern Metastatic Colonization.” *Nature* 481 (7379): 85–89. doi:10.1038/nature10694.

McPherson, Lisa A., Alexander V. Loktev, and Ronald J. Weigel. 2002. “Tumor Suppressor Activity of AP2alpha Mediated through a Direct Interaction with p53.” *The Journal of Biological Chemistry* 277 (47): 45028–33. doi:10.1074/jbc.M208924200.

McPherson, Lisa A., George W. Woodfield, and Ronald J. Weigel. 2007. “AP2 Transcription Factors Regulate Expression of CRABPII in Hormone Responsive Breast Carcinoma.” *The Journal of Surgical Research* 138 (1): 71–78. doi:10.1016/j.jss.2006.07.002.

Palafox, Marta, Irene Ferrer, Pasquale Pellegrini, Sergi Vila, Sara Hernandez-Ortega, Ander Urruticoechea, Fina Climent, et al. 2012. “RANK Induces Epithelial-Mesenchymal Transition and Stemness in Human Mammary Epithelial Cells and Promotes Tumorigenesis and Metastasis.” *Cancer Research* 72 (11): 2879–88. doi:10.1158/0008-5472.CAN-12-0044.

Pellegrini, Pasquale, Alex Cordero, Marta I Gallego, William C. Dougall, Purificación Muñoz, Miguel Ángel Pujana, and Eva González Suárez. 2013. “Constitutive Activation of RANK Disrupts Mammary Cell Fate Leading to Tumorigenesis.” *Stem Cells* 31 (9): 1954–65.

Pfitzner, Berit Maria, Daniel Branstetter, Sibylle Loibl, Carsten Denkert, Bianca Lederer, Wolfgang Daniel Schmitt, Frank Dombrowski, et al. 2014. “RANK Expression as a Prognostic and Predictive Marker in Breast Cancer.” *Breast Cancer Research and Treatment* 145 (2): 307–15. doi:10.1007/s10549-014-2955-1.

Ross-Innes, Caryn S., Rory Stark, Andrew E. Teschendorff, Kelly A. Holmes, H. Raza Ali, Mark J. Dunning, Gordon D. Brown, et al. 2012. “Differential Oestrogen Receptor Binding Is Associated with Clinical Outcome in Breast Cancer.” *Nature* 481 (7381): 389–93. doi:10.1038/nature10730.

Santini, Daniele, Gaia Schiavon, Bruno Vincenzi, Laura Gaeta, Francesco Pantano, Antonio Russo, Cinzia Ortega, et al. 2011. “Receptor Activator of NF-kB (RANK) Expression in Primary Tumors Associates with Bone Metastasis Occurrence in Breast Cancer Patients.” *PloS One* 6 (4): e19234. doi:10.1371/journal.pone.0019234.

Schramek, Daniel, Andreas Leibbrandt, Verena Sigl, Lukas Kenner, John A. Pospisilik, Heather J. Lee, Reiko Hanada, et al. 2010. “Osteoclast Differentiation Factor RANKL Controls Development of Progestin-Driven Mammary Cancer.” *Nature* 468 (7320): 98–102. doi:10.1038/nature09387.

Scibetta, Angelo G., Ping-Pui Wong, KaYi V. Chan, Monica Canosa, and Helen C. Hurst. 2010. “Dual Association by TFAP2A during Activation of the p21cip/CDKN1A Promoter.” *Cell Cycle (Georgetown, Tex.)* 9 (22): 4525–32.

Sleeman, Katherine E., Howard Kendrick, David Robertson, Clare M. Isacke, Alan Ashworth, and Matthew J. Smalley. 2007. “Dissociation of Estrogen Receptor Expression and in Vivo Stem Cell Activity in the Mammary Gland.” *The Journal of Cell Biology* 176 (1): 19–26. doi:10.1083/jcb.200604065.

Smalley, Matthew J. 2010. “Isolation, Culture and Analysis of Mouse Mammary Epithelial Cells.” *Methods in Molecular Biology (Clifton, N.J.)* 633: 139–70. doi:10.1007/978-1-59745-019-5_11.

Span, Paul N., Esmé Waanders, Peggy Manders, Joop J. T. M. Heuvel, John A. Foekens, Mark A. Watson, Louk V. A. M. Beex, and Fred C. G. J. Sweep. 2004. “Mammaglobin Is Associated with Low-Grade, Steroid Receptor-Positive Breast Tumors from Postmenopausal Patients, and Has Independent Prognostic Value for Relapse-Free Survival Time.” *Journal of Clinical Oncology: Official Journal of the American Society of Clinical Oncology* 22 (4): 691–98. doi:10.1200/JCO.2004.01.072.

Tallman, M. S., J. W. Andersen, C. A. Schiffer, F. R. Appelbaum, J. H. Feusner, A. Ogden, L. Shepherd, et al. 1997. “All-Trans-Retinoic Acid in Acute Promyelocytic Leukemia.” *The New England Journal of Medicine* 337 (15): 1021–28. doi:10.1056/NEJM199710093371501.

Tanos, Tamara, George Sflomos, Pablo C. Echeverria, Ayyakkannu Ayyanan, Maria Gutierrez, Jean-Francois Delaloye, Wassim Raffoul, et al. 2013. “Progesterone/RANKL Is a Major Regulatory Axis in the Human Breast.” *Science Translational Medicine* 5 (182): 182ra55. doi:10.1126/scitranslmed.3005654.

Vaillant, François, Marie-Liesse Asselin-Labat, Mark Shackleton, Natasha C. Forrest, Geoffrey J. Lindeman, and Jane E. Visvader. 2008. “The Mammary Progenitor Marker CD61/beta3 Integrin Identifies Cancer Stem Cells in Mouse Models of Mammary Tumorigenesis.” *Cancer Research* 68 (19): 7711–17. doi:10.1158/0008-5472.CAN-08-1949.

Wang, Yixin, Jan G. M. Klijn, Yi Zhang, Anieta M. Sieuwerts, Maxime P. Look, Fei Yang, Dmitri Talantov, et al. 2005. “Gene-Expression Profiles to Predict Distant Metastasis of Lymph-Node-Negative Primary Breast Cancer.” *Lancet (London, England)* 365 (9460): 671–79. doi:10.1016/S0140-6736(05)17947-1.

Woodfield, George W., Yizhen Chen, Thomas B. Bair, Frederick E. Domann, and Ronald J. Weigel. 2010. “Identification of Primary Gene Targets of TFAP2C in Hormone Responsive Breast Carcinoma Cells.” *Genes, Chromosomes & Cancer* 49 (10): 948–62. doi:10.1002/gcc.20807.

Zhang, J., S. Brewer, J. Huang, and T. Williams. 2003. “Overexpression of Transcription Factor AP-2alpha Suppresses Mammary Gland Growth and Morphogenesis.” *Developmental Biology* 256 (1): 127–45.

FIGURES

Figure 1

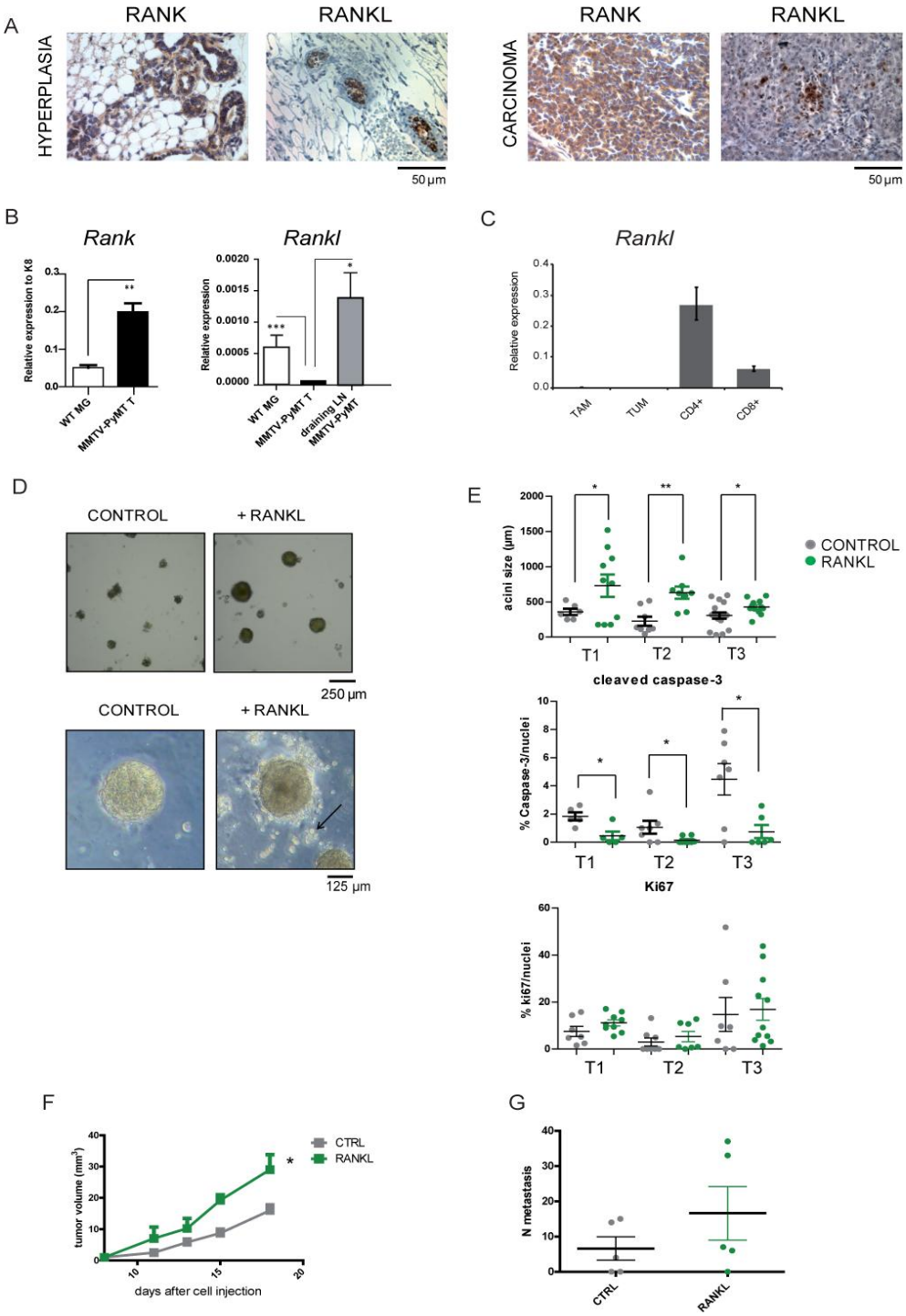

Figure 1. RANKL treatment decreases apoptosis in MMTV-PyMT-derived tumor cells *in vitro.*

A. Representative images of RANK and RANKL protein expression detected by IHC in MMTV-PyMT preneoplasic lesions (hyperplasia) and adenocarcinomas. Note that RANKL expression in carcinoma lesions is found not in the tumor cells but in tumor infiltrating lymphocytes. See also expression patterns in Supplemental Fig. 1.

B. mRNA expression of *Rank* and *Rankl* in 7 WT, 8 MMTV-PyMT tumors and three draining lymph nodes of MMTV-PyMT tumor-bearing mice. Expression relative to β-actin is shown. Mean, SEM and t-test probabilities are shown.

C. *Rankl* mRNA expression relative to *Rpl38* measured by RT-PCR in FACS-sorted tumor cells (CD45-), macrophages (CD45+ CD11b+ F4/80+ Gr1-), CD4+ lymphocytes (CD45+ CD11b- CD3+ CD4+) and CD8+ (CD45+ CD11b- CD3+ CD8+). Cells from four independent MMTV-PyMT tumors were sorted as shown in Supplemental Fig. S2.

D. Representative pictures of MMTV-PyMT tumor acini cultured in Matrigel with or without RANKL (1 μg/mL) for 15 days.

E. Diameter (μm), percentage of cleaved caspase 3+ and percentage of ki67+ nuclei of MMTV-PyMT tumor acini cultured in Matrigel, treated or not treated with RANKL for 15 days. Each dot represents one acinus, and results from three independent tumors (T1, T2 and T3) are shown. SEM and t-test statistics are shown.

F. Tumor growth curves derived from MMTV-PyMT tumor cells cultured for 15 days with or without RANKL after injection in the fat pads of Scid/Beige mice. Tumor volume is normalized to the first measurement. 100,000 cells per mammary gland were injected. Each mean and SEM is representative of six tumors and t-test statistics are shown.

G. Quantification of lung metastatic foci derived from tumor cells cultured for 15 days with or without RANKL after intravenous injection in Nod/Scid mice. 100,000 cells were injected and mice were sacrificed 9 weeks after tumor-cell injection. Each dot represents one mouse. Entire lungs were step-sectioned at 100 μm and individual metastases identified. The total number of metastatic foci per mouse is indicated.

Figure 2

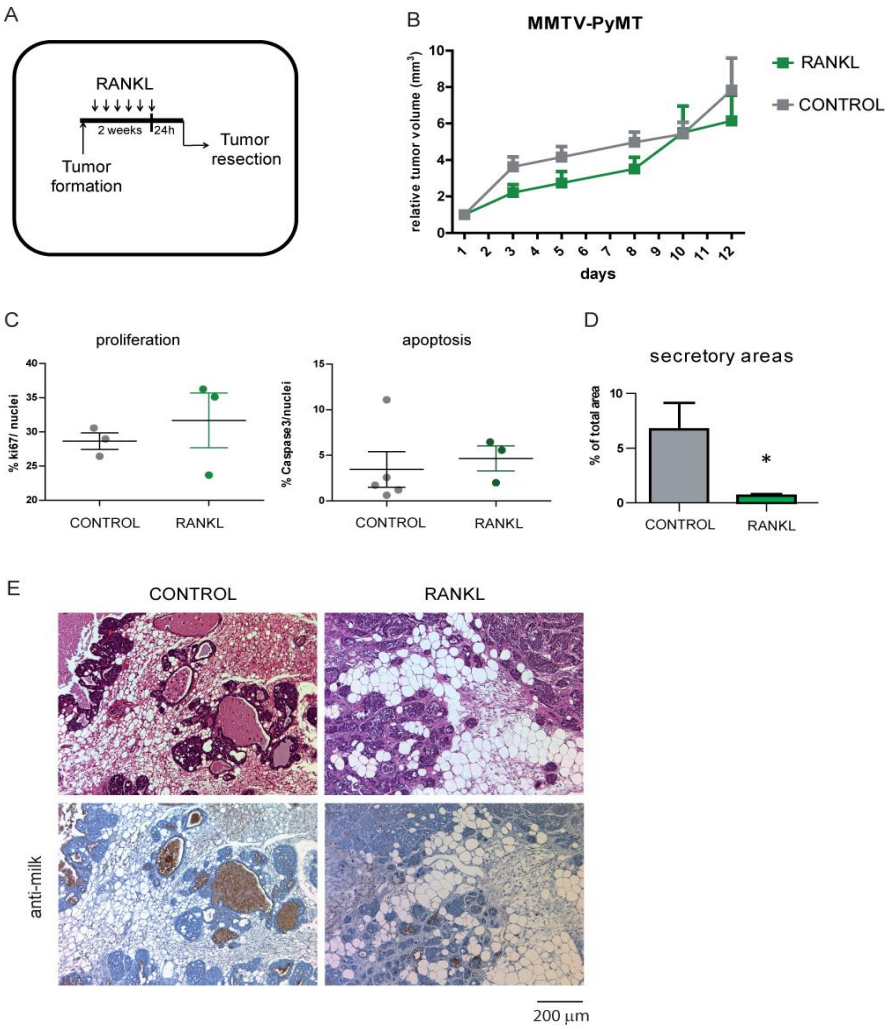

Figure 2. Short-term RANKL treatment *in vivo* does not change MMTV-PyMT tumor growth but modulates tumor cell differentiation.

A. Schematic overview of short-term RANKL (25 µg/mouse) or control (vehicle, PBS) treatment in MMTV-PyMT tumor-bearing females. Five mice per treatment arm were included. Treatment (3 times per week) started when tumors reached 3 mm of diameter. Mice received 6 doses, and tumors were excised and analyzed 24 h after the last dose.

B. Tumor volume of MMTV-PyMT mice undergoing RANKL treatment. Mean and SEM of five mice per treatment are shown. Tumor volume is normalized to the volume on the first day of treatment (day 1).

C. Percentage of tumor cell proliferation (Ki67) and apoptosis (cleaved caspase-3) after 2 weeks of RANKL or control of MMTV-PyMT tumor-bearing mice. Each dot represents one independent tumor from one mouse. Six sections per tumor were quantified. The mean and SEM for each group is shown.

D. Percentage of secretory areas relative to total tumor area identified in MMTV-PYMT primary tumors after 2 weeks of RANKL or control. 3-5 mice per treatment arm were considered.

E. Representative images of H&E showing secretory areas identified in MMTV-PYMT primary tumors and milk protein staining after 2 weeks of RANKL treatment.

Figure 3

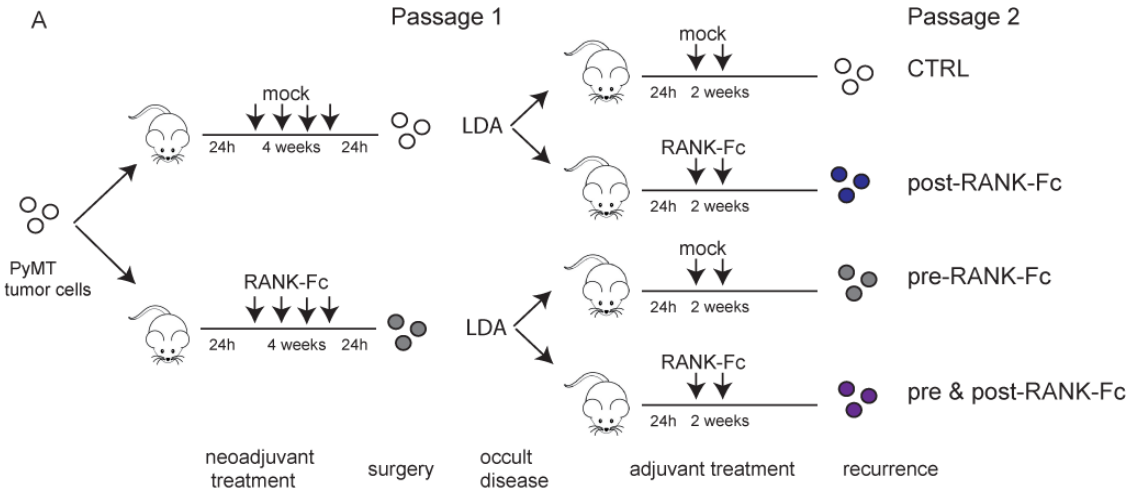

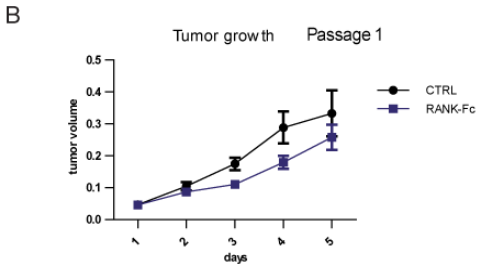

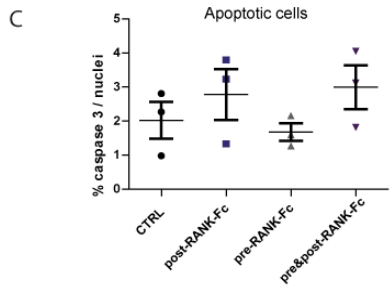

D

GROUP	N cells	N fat pad	N tumors	TIC frequency
CTRL	100,000	4	4	1/ 206 (C.I. 599 - 70.9)
	10,000	6	6	
	1,000	6	5	
	100	6	6	
post RANK-Fc	100,000	6	6	1/ 466 (C.I. 1,138-190.7)
	10,000	6	6	
	1,000	6	4	
	100	6	4	
pre RANK-Fc	100,000	6	6	1/ 1,929 (C.I. 5,431-685.1)
	10,000	6	5	
	1,000	6	5	
	100	6	2	
pre&post RANK-Fc	100,000	6	6	1/ 2,353 (C.I. 6,378 -868.3)
	10,000	6	5	
	1,000	6	3	
	100	6	3	

GROUP	P value	χ^2
CTRL vs post RANK-Fc	0.13	2.27
CTRL vs pre RANK-Fc	2.99 E-5	17.4
CTRL vs pre&post RANK-Fc	7.48 E-6	7.41
pre RANK-Fc vs pre&post RANK-Fc	0.701	0.147

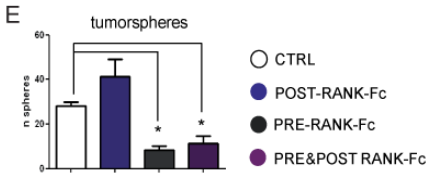

Figure 3. Neoadjuvant inhibition of RANK signaling depletes the pool of MMTV-PyMT tumor-initiating cells.

A. Schematic overview of RANK-Fc treatments in orthotopic MMTV-PyMT tumors. One million cells isolated from one MMTV-PyMT carcinoma were injected into the inguinal fat pads of syngeneic WT mice (FVB), which were randomized 1:1 for RANK-Fc (10 mg/kg, three times per week) or mock treatment starting 24 h later. After 4 weeks of treatment, tumors were surgically excised and cells isolated from at least three RANK-Fc-treated MMTV-PyMT tumors (passage 1,

neoadjuvant treatment) were pooled and injected into the fat pad of syngeneic WT (Passage 2) mice in limiting dilutions (mimicking occult disease); again, mice from both groups were randomized 1:1 for additional RANK-Fc (adjuvant) or mock treatment for 2 weeks. The same was done for the control arm in passage 1. The total number of tumors was scored after 26 weeks.

B. Tumor growth of passage 1 RANK-Fc treated MMTV-PyMT orthotopic tumors. Day 1 is the first day that palpable and growing tumors were detected.

C. Percentage of tumor cell apoptosis (cleaved caspase 3) in passage 2 RANK-Fc-treated and controls MMTV-PyMT orthotopic tumors.

D. Table showing limiting dilution assay to test the tumor-initiating ability of MMTV-PyMT tumor cells after RANK-Fc treatments. Tumor-initiating cell frequencies (with confidence intervals) for each group were calculated by ELDA; chi-square values and associated probabilities are shown.

E. Number of secondary tumorspheres (n spheres) formed by RANK-Fc-treated MMTV-PyMT orthotopic tumors from the indicated treatment groups (P2). Each bar represents data from four tumors. 20,000 cells/mL for primary and 5,000 cells/mL for secondary mammospheres were plated in triplicate and tumorspheres were quantified after 2 weeks. Mean, SEM and t-test statistics are shown.

Figure 4

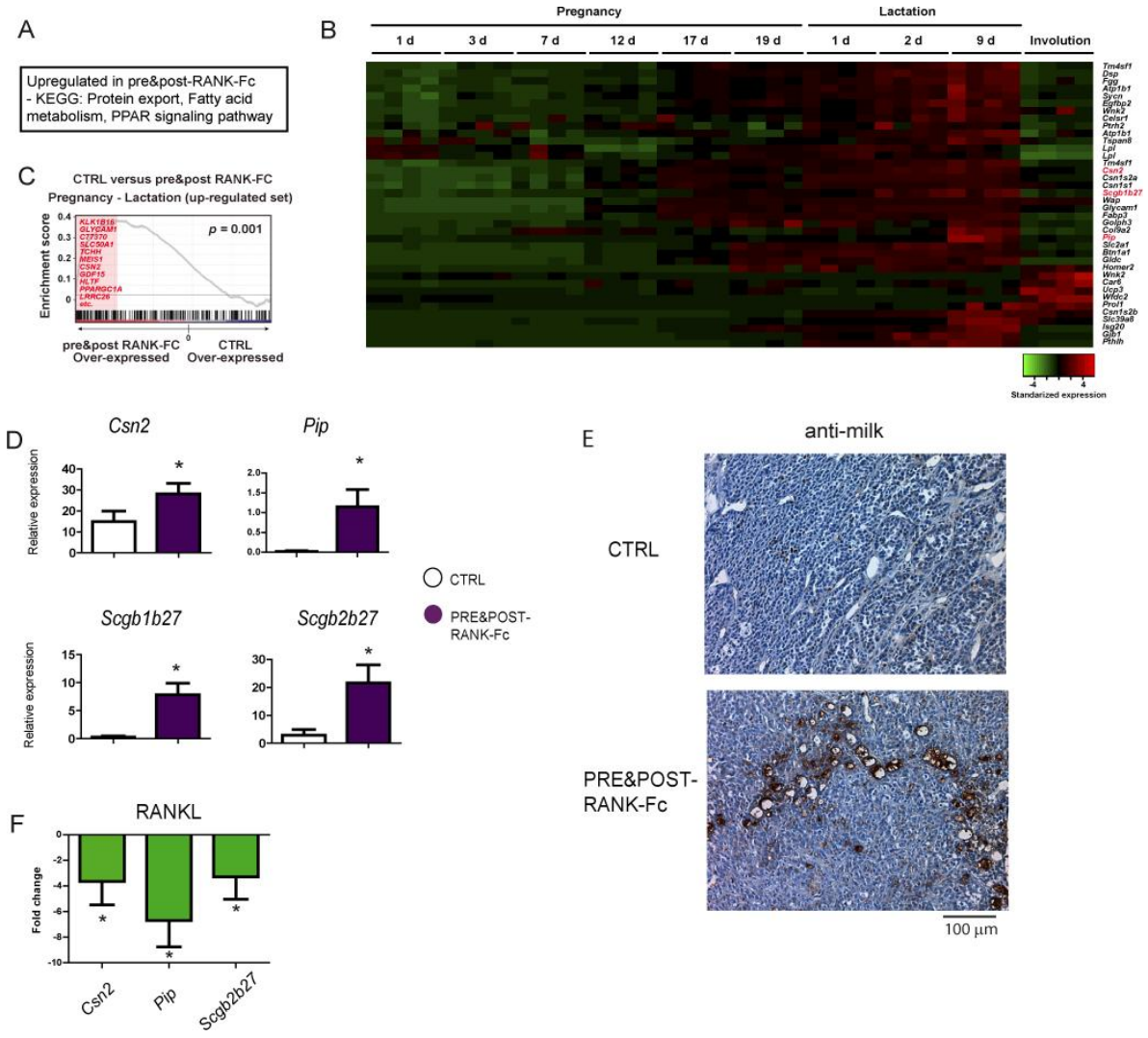

Figure 4. RANKL inhibition induces differentiation of tumor cells into milk secreting cells.

A. Top panel: Significantly associated genes sets and pathways for KEGG annotations are shown

B. Heatmap showing the expression profile in mammary gland development of differentially expressed genes between RANK-Fc treated tumor and controls. Note that genes are up-regulated during late pregnancy, lactation and involution. Genes further validated by RT-PCR are shown in red.

C. GSEA graphical output for the association between lactation over-expressed genes and RANK-Fc treatment. The top genes contributing to this association are listed.

D. mRNA expression levels of *Csn2, Pip, Scgb1b27, Scgb2b27* relative to *HPRT* in RANK-Fc treated or control MMTV-PyMT orthotopic tumors. Each bar is representative of three independent tumors. Mean, SEM and t-test statistics are shown.

E. Representative images of milk staining in control and pre&post-RANK-Fc treated tumors.

F. Fold change of mRNA expression levels of indicated genes in RANKL treated 3D acinar cultures of MMTV-PyMT tumor cells relative to untreated controls. Cultures from three independent tumors were analyzes. Mean, SEM, and t test p values are shown.

Figure 5

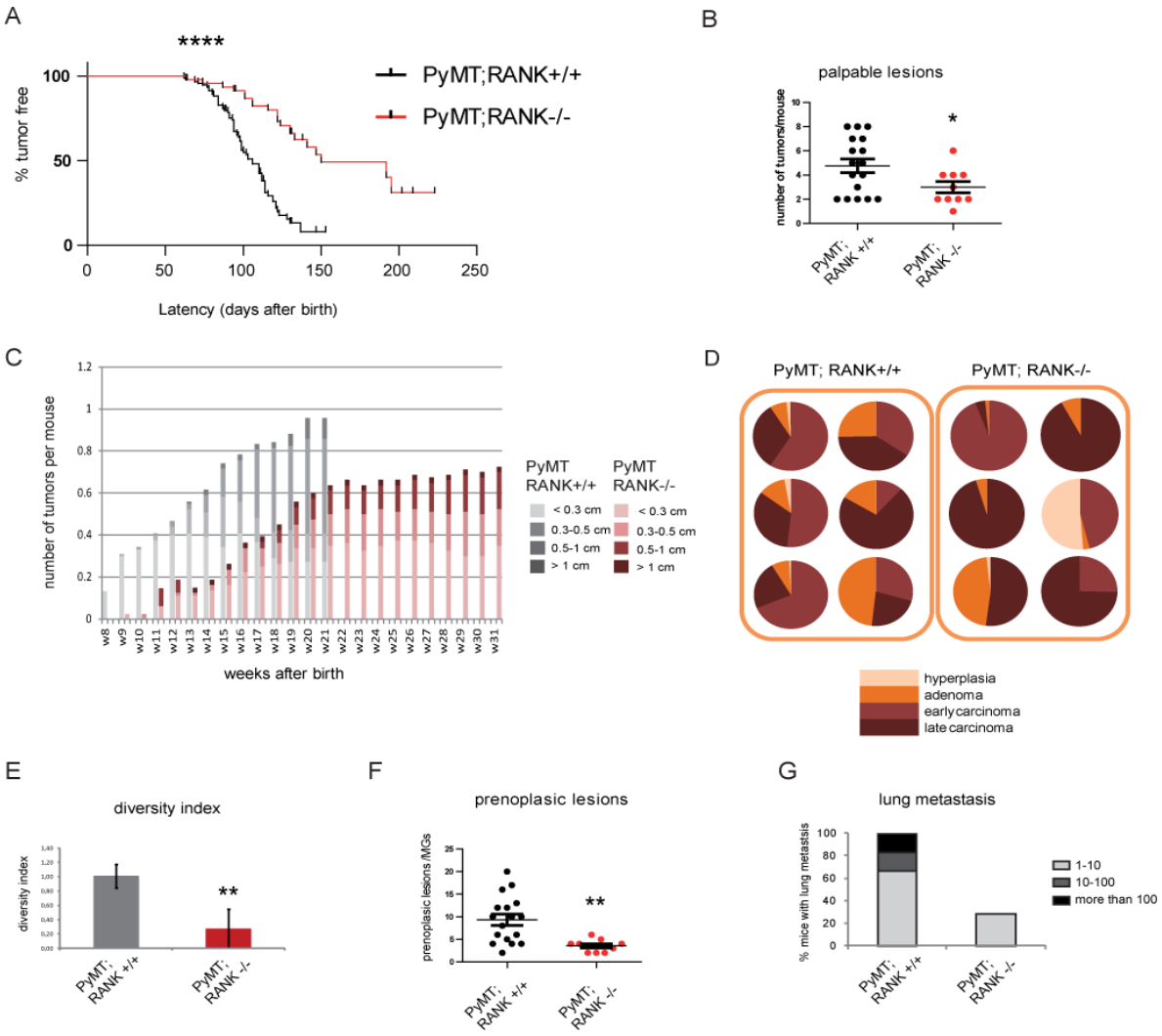

Figure 5. Constitutive deletion of RANK increases tumor latency, decreases tumor incidence, and prevents lung metastasis of MMTV-PyMT tumors.

A. Kinetics of palpable tumor onset with age in the indicated genotypes. 18 PyMT; $RANK^{+/+}$ and 10 PyMT;$RANK^{-/-}$ (F5) mice were analyzed. All palpable lesions were considered. The difference between the groups was evaluated by the log-rank test.

B. Number of palpable lesions bigger than 0.3 cm of diameter detected at necropsy in 17 PyMT; $RANK^{+/+}$ and 10 PyMT;$RANK^{-/-}$ (F5) mice.

C. Cumulative number of palpable lesions per mouse in 18 PyMT;$RANK^{+/+}$ and 10 PyMT;$RANK^{-/-}$ mice with age (in weeks). Tumors were classified by their diameter as indicated. All PyMT;$RANK^{+/+}$ and PyMT;$RANK^{-/-}$ mice died after week 21 and 31, respectively; for mice dying before total number of tumors detected at necropsy was considered.

D. Pie charts representing quantification of histological areas as defined in Supplemental Fig. S1 and [23] of PyMT;$RANK^{-/-}$ and PyMT;$RANK^{+/+}$ tumors. Tumor size at sacrifice was similar for the two genotypes (1 cm diameter).

E. Shannon-Wiener diversity test of palpable PyMT;RANK$^{-/-}$ and PyMT;RANK$^{+/+}$ lesions. Each bar represent the mean of 6 tumors and t-test statistics are shown.

F. Number of preneoplasic regions per mammary gland detected in mammary whole mounts of in PyMT;RANK$^{+/+}$ (n=9) and PyMT;RANK$^{-/-}$ (n=5) (F5) females 13-22 weeks old. Only mammary glands without tumors were considered. Each dot represents one mammary gland. Mean, SEM and t test p value are shown.

G. Percentage of PyMT;RANK$^{+/+}$ (n=6) and PyMT;RANK$^{-/-}$ (n=7) (F5) females with lung metastasis. Entire lungs were step-sectioned at 100 □m and individual metastases identified histologically. The total number of metastatic foci per mouse is indicated.

Figure 6

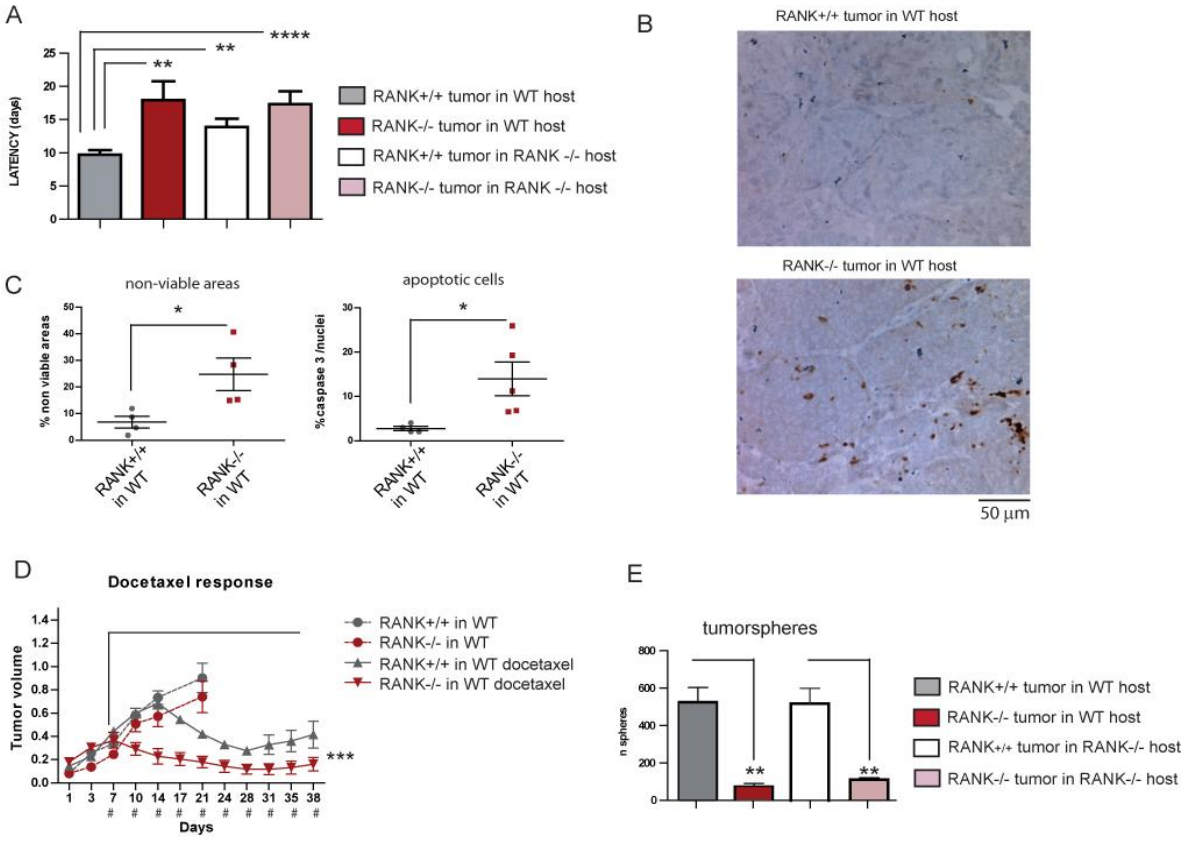

F

GROUP	N cells	N fat pad	N tumors
PyMT;RANK+/+	10,000	4	4
	1,000	4	3
	100	4	4
	10	4	0
PyMT;RANK-/-	10,000	4	4
	1,000	4	2
	100	4	1
	10	4	0

TUMOR-INITIATING CELL (TIC) FREQUENCY

PyMT;RANK +/+
1/ 285 (C.I. 913-89)

PyMT;RANK-/-
1/ 1,078 (C.I. 3,572-326)

P value : 0.05 χ^2: 3.58

G

GROUP	N cells	mice	Metastasis incidence
PyMT;RANK+/+	100,000	4	4
	10,000	4	4
	1,000	4	0
	100	4	1
PyMT;RANK-/-	100,000	4	3
	10,000	4	3
	1,000	4	1
	100	4	0

METASTASIS-INITIATING CELL (MIC) FREQUENCY

PyMT;RANK +/+
1 / 2,952 (C.I. 9,374-929)

PyMT;RANK-/-
1/ 29,420 (C.I. 93,261-9,281)

P value : 0.00262 χ^2: 9.06

H

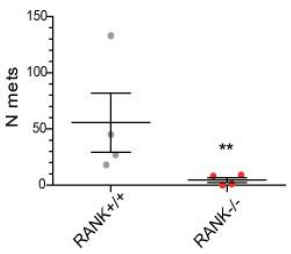

Figure 6. RANK-null tumors contain fewer tumor and metastasis-initiating cells, have enhanced apoptosis and are more sensitive to docetaxel.

A. Latency to tumor formation of PyMT;RANK$^{+/+}$ and PyMT;RANK$^{-/-}$ tumor cells orthotopically implanted in WT and RANK$^{-/-}$ syngeneic mice (C57Bl6). 10^6 cells were injected per mammary gland and 22 tumors from each group were quantified. Times in days from injection are shown.

B. Representative pictures of cleaved caspase 3 staining in transplants from PyMT;RANK$^{+/+}$ and PyMT;RANK$^{-/-}$ tumor cells in syngeneic WT hosts.

C. Quantification of the percentage of non-viable areas versus total tumor area (left panel) and caspase 3-positive nuclei (right panel) in transplants from PyMT;RANK$^{+/+}$ and PyMT;RANK$^{-/-}$ tumor cells in syngeneic WT hosts. Each dot represents an independent transplanted primary tumor and t –test statistic are shown.

D. Relative tumor volume of PyMT;RANK$^{+/+}$ and PyMT;RANK$^{-/-}$ tumors treated with docetaxel (25 mg/kg) twice per week. Volume was calculated as length*width/100. Treatment started when tumors reached a diameter of 6 mm. # indicate docetaxel doses. Probabilities of t test for docetaxel-treated PyMT;RANK$^{+/+}$ and PyMT;RANK$^{-/-}$ tumors is shown.

E. Number (n) of tertiary tumorspheres formed by PyMT;RANK$^{+/+}$ and PyMT;RANK$^{-/-}$ tumor cells. No differences in mammosphere frequency or size were observed in primary or secondary passages. Each bar represents four tumors. The mean, SEM and t-test statistics are shown.

F-G. Table showing limiting dilution assay to test the tumor-initiating ability (F) and metastasis-initiating ability (G) of PyMT;RANK$^{+/+}$ and PyMT;RANK$^{-/-}$ tumor cells. Cells from two tumors per genotype were pooled for injections in limiting dilutions in number 4 mammary glands of syngeneic WT females (F) or in the tail vein of *Foxn1*^{nu} females (G), respectively. Presence of lung metastasis was scored 8 weeks after injection. TICs and MICs frequencies (with confidence intervals) for each group were calculated by ELDA; p- and chi-square values are shown.

H. Quantification of the absolute number of lung metastasis in *Foxn1*^{nu} mice that received an intravenous injection of 10^5 PyMT;RANK$^{+/+}$ and PyMT;RANK$^{-/-}$ tumor cells. Each dot represents the lung of one mouse. The mean, SEM and probabilities of significant F-tests are shown.

Figure 7

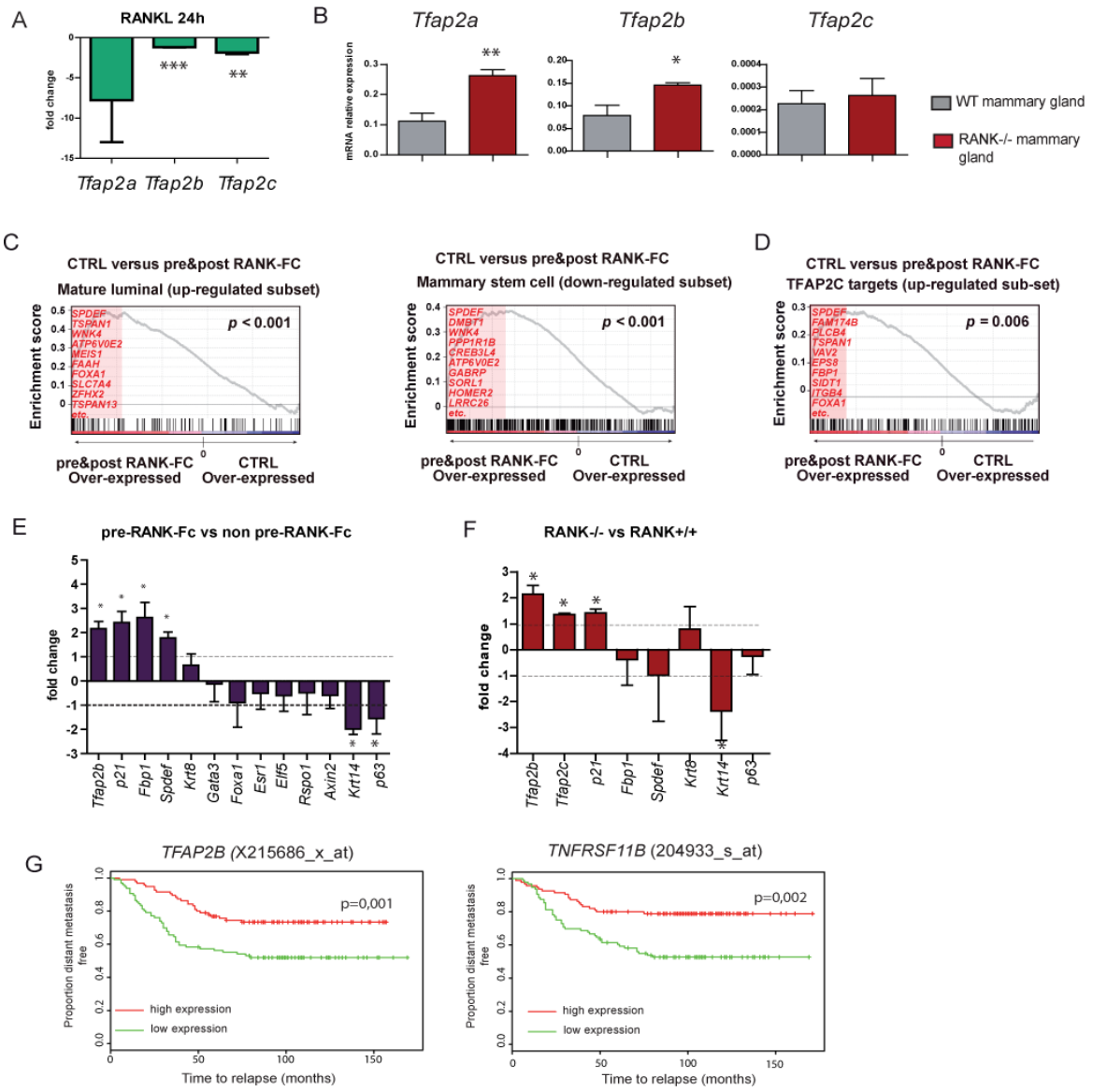

Figure 7. RANK loss or inhibition induces the expression of AP2 transcription factors.

A. Fold changes in mRNA expression of indicated genes in PyMT tumor cultures treated with RANKL for 24h relative to untreated cultures. Each bar is representative of three cultures derived from three independent tumors. Mean, SEM and t-test statistics are shown.

B. mRNA expression levels of indicated genes relative to *KRT8* in PyMT RANK+/+ and PyMT;RANK-/- mammary glands. Each bar is representative of three independent mammary glands. Mean, SEM and t-test statistics are shown.

C. GSEA graphical outputs for the association between mammary mature luminal (up-regulated genes in mature luminal) and stem (down-regulated genes in stem) cells gene sets and RANK-Fc treatment. The top genes contributing to the association are listed.

D. GSEA graphical outputs for the association between TFAP2C up-regulated genes sets in human breast cancer and RANK-Fc treatment. The top genes contributing to the association are listed.

E. Fold changes in mRNA expression of indicated genes in PyMT tumors that received neoadjuvant RANK-Fc treatment relative to expression in the other treatment arms. Each bar is representative of six independent tumors. Mean, SEM and t-test statistics are shown.

F. Fold changes in mRNA expression of indicated genes in PyMT;RANK-/- sorted tumor cells relative to expression in PyMT;RANK+/+ sorted tumor cells. Each bar is representative of three-four independent tumors. Mean, SEM and t-test statistics are shown.

G. Association between *TFAP2B* (left panel) and *TNFRSF11B (*right panel*)* tumor expression and distant metastasis in lymph-node negative breast cancer patients (Gene Expression Omnibus data GSE2034). Graphs show the proportion of distant metastasis-free patients over time (months) and stratified according to the first (low expression) or the third (high expression) tertiles.

Figure 8

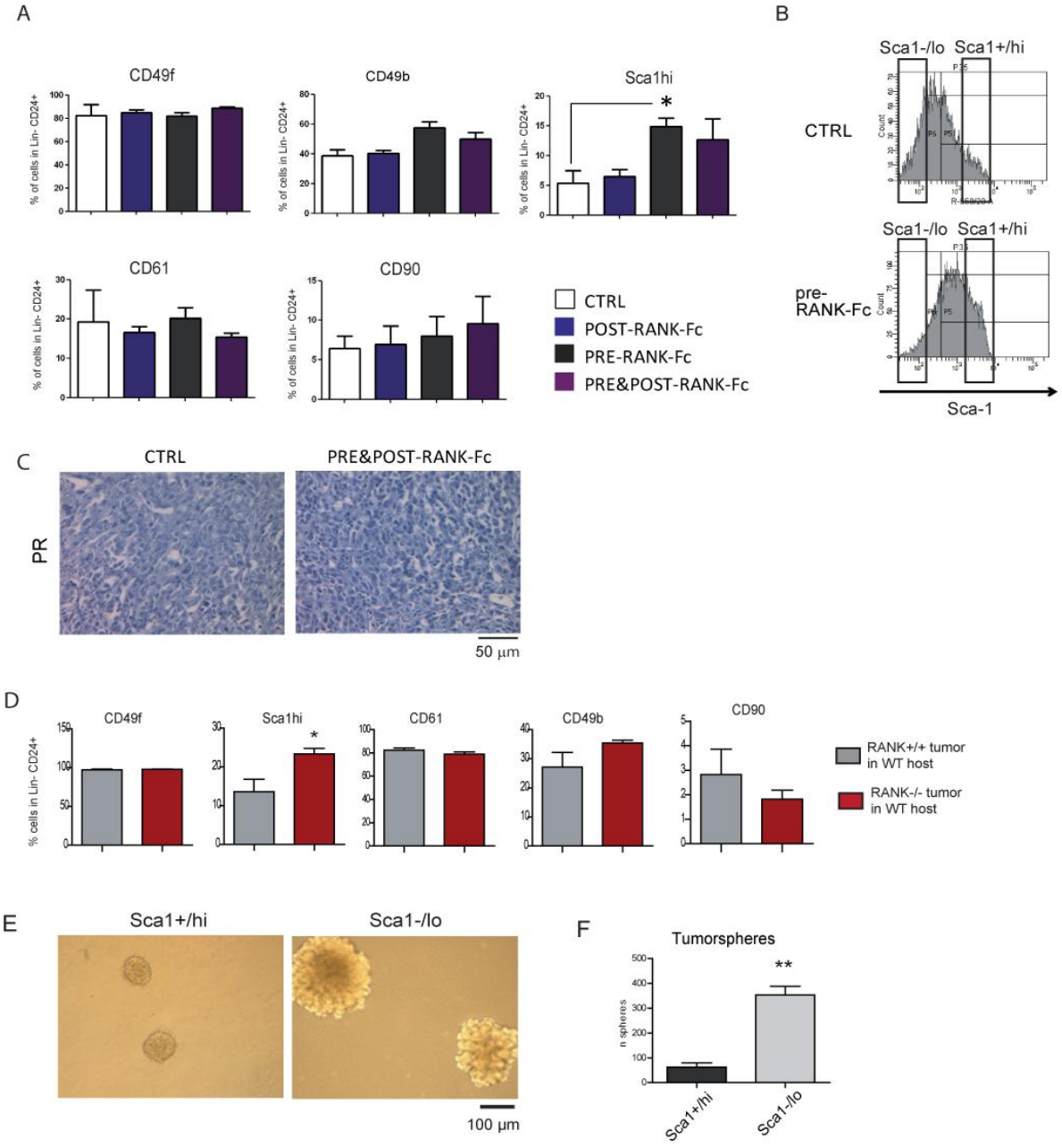

G

GROUP	N cells	N fat pad	N tumors
Sca1+/hi	100,000	4	3
	10,000	4	3
	1,000	4	2
	100	4	3
Sca1-/lo	100,000	4	4
	10,000	4	4
	1,000	4	4
	100	4	3

TICs: TUMOR INITIATING CELL FREQUENCY (ELDA)

Sca1+/hi : 1/ 15767.4 (C.I. 56295 - 4416.4)

Sca1-/lo : 1/ 72.6 (C.I. 246 - 21.7)

P value: 1.04E-11 $\chi^2 = 46.3$

Figure 8. RANK-Fc neoadjuvant treatment reduces the Sca1- tumor cell population.

A. Frequency of the indicated populations within tumor CD45- CD31- CD24+ cells determined by flow cytometry in RANK-Fc-treated or control MMTV-PyMT orthotopic tumors. Each bar represents data from four mice in two independent experiments. Mean, SEM and t-test statistics are shown.

B. Representative histograms of Sca1+/hi and Sca1-/lo populations in control and pre-RANK-Fc treated tumors.

C. Representative images of PR immunostaining in control and pre&post-RANK-Fc treated tumors.

D. Frequency of the indicated populations within tumor cells (CD45- CD31- CD24+), as analyzed by flow cytometry in PyMT;$RANK^{+/+}$ and PyMT;$RANK^{-/-}$ orthotopic transplants. Each bar represents the mean and SEM of 3-5 independent tumors. Probabilities of significant t tests are shown.

E. Representative images of tumorspheres derived from FACS-sorted Sca1+/hi and Sca1- tumor cells from MMTV-PyMT orthotopic tumors.

F. Number of secondary tumorspheres (n spheres) of FACS-sorted Sca1+/hi and Sca1-/lo tumor cells from MMTV-PyMT orthotopic tumors. Each bar is representative of two tumors quantified in triplicate. 20,000 cells/mL were plated in triplicate and tumorspheres were quantified after 2 weeks. Mean, SEM and probabilities of significant t tests are shown.

G. Table showing limiting dilution assay to test the tumor-initiating ability of Sca1+/hi and Sca1-/lo tumor cells in WT (FVB) females. Cells were FACs-sorted from control tumors and injected in limiting dilutions into number 4 mammary glands. Tumor initiating cell frequencies (with confidence intervals) for each group were calculated by ELDA; chi-square values and associated probabilities are shown.

SUPPLEMENTAL INFORMATION

Supplemental Figure 1

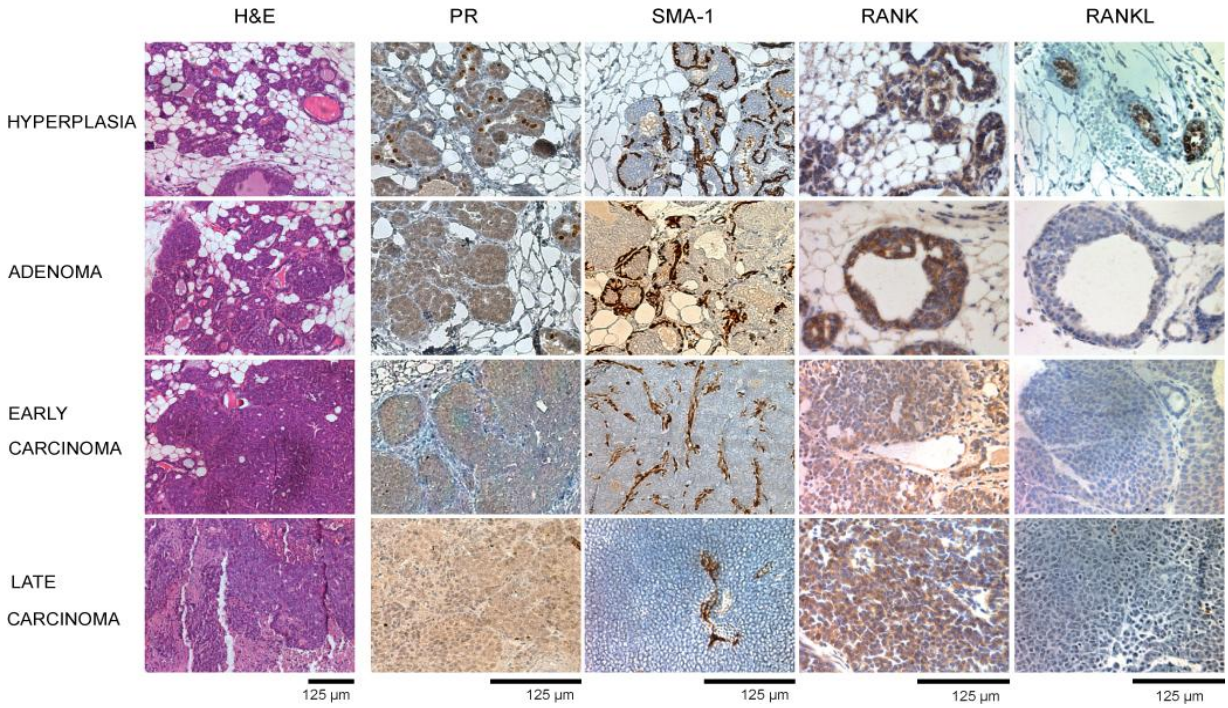

Figure S1. RANK and RANKL expression during MMTV-PyMT tumor progession
Representative pictures of hematoxylin eosin (H&E), PR (progesterone receptor), Sma-1, Rank and Rankl protein expression in MMTV-PyMT palpable lesions by immunostaining. Note the loss of PR (nuclear staining) and RANKL expression in adenoma and loss of a continuous layer of Sma-1 in the transition to carcinoma and late carcinoma.

Supplemental Figure 2

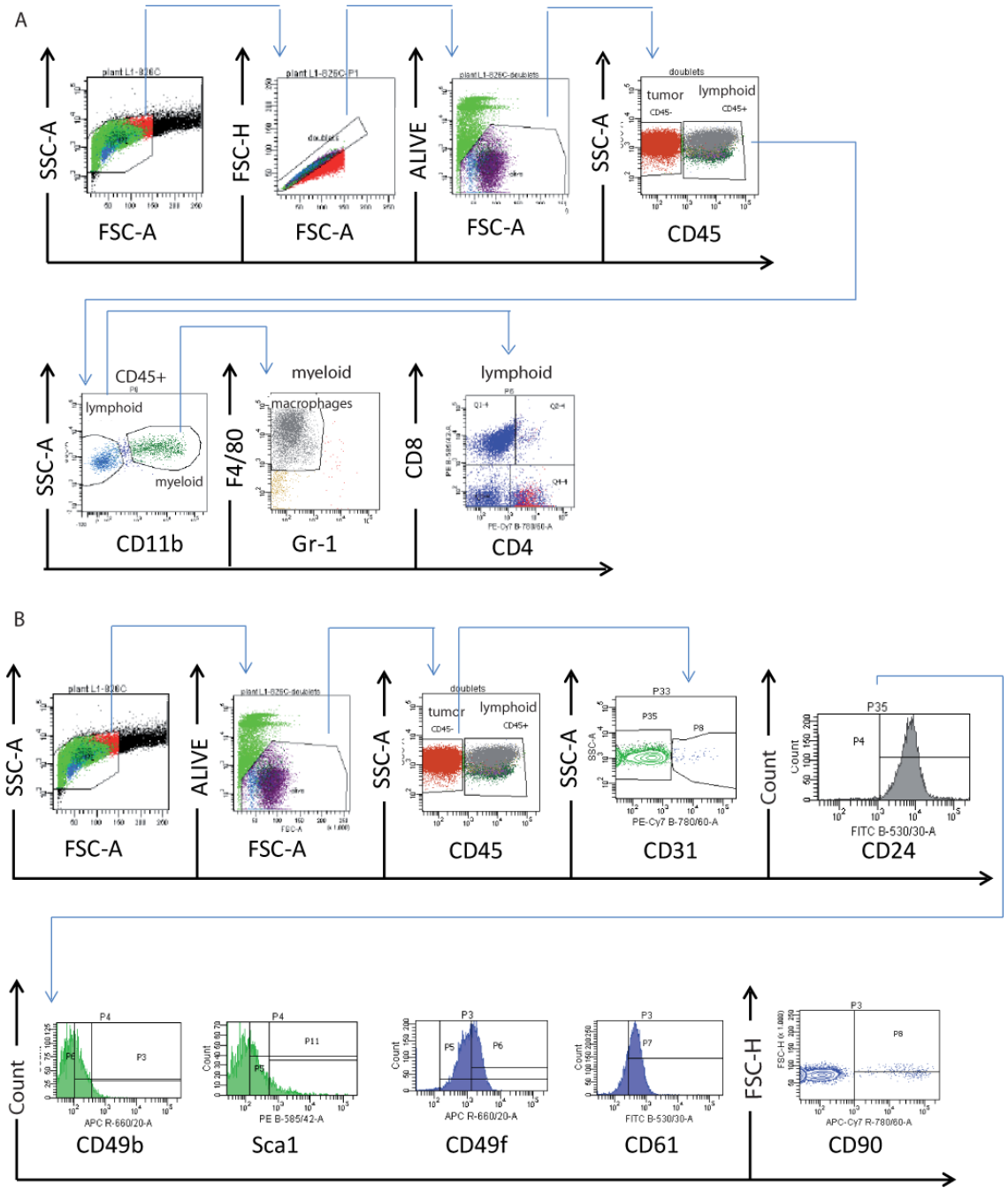

Figure S2. FACS gating scheme.
Dot-blots and histograms representing the hierarchy identified by flow cytometry analyses for the selection of tumor infiltrating leucocytes and epithelial cells in MMTV-PyMT tumors. Positive populations or mean values are defined based on isotope or FMO ("fluorescence minus one") controls.

ARTICLE 5

"APRIL promotes breast tumor growth and metastasis and is associated with aggressive basal breast cancer"

OXFORD

Carcinogenesis, 2015, Vol. 36, No. 5, 574–584

doi:10.1093/carcin/bgv020
Advance Access publication March 6, 2015
Original Manuscript

ORIGINAL MANUSCRIPT

APRIL promotes breast tumor growth and metastasis and is associated with aggressive basal breast cancer

Araceli García-Castro[1,†], Manuela Zonca[1,†], Douglas Florindo-Pinheiro[1], Carla E.Carvalho-Pinto[1,2], Alex Cordero[3], Burgo Gutiérrez del Fernando[1], Aránzazu García-Grande[4], Santos Mañes[1], Michael Hahne[5], Eva González-Suárez[3] and Lourdes Planelles[1,*]

[1]Immunology and Oncology Department, Centro Nacional de Biotecnología/CSIC, UAM Cantoblanco, Madrid, Spain, [2]Immunobiology Department, Universidade Federal Fluminense, Niterói, Rio de Janeiro, Brazil, [3]Cancer Epigenetics and Biology Program, Bellvitge Biomedical Research Institute, IDIBELL, Barcelona, Spain, [4]Flow Cytometry Core Facility, Hospital Universitario Puerta de Hierro Majadahonda, Madrid, Spain and [5]Institute de Génétique Moléculaire de Montpellier, Montpellier, France

*To whom correspondence should be addressed. Tel: +34 915854855; Fax: +34 913720493;Email: lplanelles@cnb.csic.es

†These authors contributed equally to this work.

Abstract

APRIL (a proliferation-inducing ligand) is a cytokine of the tumor necrosis factor family associated mainly with hematologic malignancies. APRIL is also overexpressed in breast carcinoma tissue lesions, although neither its role in breast tumorigenesis nor the underlying molecular mechanism is known. Here, we show that several breast cancer cell lines express APRIL and both its receptors, B cell maturation antigen (BCMA) and transmembrane activator and CAML-interactor (TACI), independently of luminal or basal tumor cell phenotype, and that the mitogen-activated protein kinases p38, ERK1/2, and JNK1/2 are activated in response to APRIL. The inflammatory stimulus poly I:C, a toll-like receptor (TLR) 3 ligand, enhanced APRIL secretion. Silencing experiments decreased cell proliferation, demonstrating that APRIL is a critical autocrine factor for breast tumor growth. Studies of 4T1 orthotopic breast tumors in APRIL transgenic mice showed that an APRIL-enriched environment increased tumor growth and promoted lung metastasis associated with enhanced tumor cell proliferation; BCMA and TACI expression suggests that both participate in these processes. We detected APRIL, BCMA and TACI in human luminal, triple-negative breast carcinomas and HER2 breast carcinomas, with increased levels in more aggressive basal tumors. APRIL was observed near Ki67$^+$ nuclei and was distributed heterogeneously in the cancer cells, in the leukocyte infiltrate, and in the myoepithelial layer adjacent to the tumor area; these results imply that APRIL provides proliferation signals to tumor cells through paracrine and autocrine signaling. Our study identifies participation of APRIL signaling in breast cancer promotion; we propose impairment of this pathway as a potential therapeutic strategy.

Introduction

Breast cancer is the most commonly diagnosed tumor type, and its incidence grows annually (1). The last decade has seen much progress in our understanding of the biology of breast cancer, a complex and heterogeneous disease (reviewed in ref. 2). Based on molecular and genetic profiles, breast carcinomas were recently classified in six major subsets that include luminal A, luminal B, human epidermal growth factor receptor 2 (HER2)-enriched, basal-like, normal breast and claudin-low carcinomas (3). Luminal carcinomas express luminal markers, estrogen receptor and/or progesterone receptor (PR), account for 60–80% of diagnosed cases, and generally have a good prognosis (4). HER2-enriched carcinomas are HER2 positive and make up 15–20% of cases, whereas basal-like carcinomas express basal/myoepithelial markers, are frequently negative for estrogen receptor, PR

Received: August 1, 2014; **Revised:** February 8, 2015; **Accepted:** February 15, 2015

Abbreviations

BCMA	B cell maturation antigen
TACI	transmembrane activator and CAML-interactor
TLR	toll-like receptor
HER2	human epidermal growth factor receptor 2
PR	progesterone receptor
HSPG	heparan sulfate proteoglycans
MAP	mitogen-activated protein
qPCR	quantitative real-time polymerase chain reaction
TNBC	triple-negative breast carcinomas.

and HER2 (triple negative), and represents 10–20% of all breast cancers. HER2-enriched and basal-like are usually more aggressive and have a poorer prognosis than the luminal subtype (5), although anti-HER2 treatment has substantially improved survival of HER2-enriched carcinoma patients in the last decade (6). Even so, 20–30% of all breast cancer patients develop metastatic disease that remains incurable, with a median survival between 2 and 4 years depending on subtype (7). Better understanding is thus needed for the molecular mechanisms and signaling pathways that govern the processes of breast carcinoma formation, maintenance and expansion and this knowledge must be translated into more effective therapeutic strategies.

Cytokines and other soluble factors are key molecules in breast cancer development and progression (8). They can be secreted by tumor cells and by cells in the tumor environment, and establish complex communication networks to promote tumor cell proliferation and survival, epithelial-to-mesenchymal transition, as well as tumor cell invasion and metastasis. They are also involved in tumor lymphocyte recruitment and modulate the type of immune response generated, which contributes to disease outcome (9). APRIL (a proliferation-inducing ligand) is a TNF family cytokine originally named for its ability to stimulate tumor cell proliferation *in vitro* (10). Cells of the immune system as well as epithelial and adipose-derived mesenchymal stem cells can secrete APRIL (11–13), which binds to two known receptors, the transmembrane activator and calcium-modulator and cyclophilin ligand interactor (TACI) and the B cell maturation antigen (BCMA) (14,15); APRIL also binds heparan sulfate proteoglycans (HSPG) on the cell surface, which are highly expressed in tumor cells (16).

The association between APRIL and cancer has been studied mainly for leukemia and lymphoma, due to the initial description of APRIL receptors in B cells (17) and to the observation that APRIL transgenic mice develop lymphoid tumors (18). In these hematological malignancies, APRIL overexpression correlates with disease progression and is a poor prognostic factor for patient survival (19,20); it protects tumor cells from spontaneous and drug-induced apoptosis, promotes cell cycle progression and enhances cell survival and/or proliferation (21,22). In human solid tumors, APRIL overexpression has been detected in many cancer types (23–34). APRIL induces growth arrest in hepatocellular carcinoma cells (28), and promotes tumor growth and/or metastasis in glioblastoma (30), pancreatic cell lines (31), and in *in vivo* colon carcinoma models (32). Data on APRIL relevance in breast cancer are very limited (23,33,34). APRIL is overexpressed in breast tissue lesions and is detected in cancer cells, but is associated mainly with the stroma and non-malignant structures (23,34). Its involvement in breast tumorigenesis and metastasis, its association with breast carcinoma subtypes, and the underlying molecular mechanisms are not known.

Here, we show that APRIL as well as BCMA and TACI are expressed in human luminal and basal-like breast carcinoma cell lines as well as in primary breast carcinomas. We found that APRIL signals through p38, ERK1/2 and JNK1/2 mitogen-activated protein (MAP) kinases, and show that Toll-like receptor (TLR)3 activation induces APRIL secretion in breast cancer cells. Loss-of-function experiments demonstrated that APRIL sustains cell proliferation in an autocrine manner. *In vivo* studies using 4T1 orthotopic tumors confirmed that ectopic APRIL promotes breast tumor growth and lung metastasis. Moreover, we found higher APRIL and TACI expression in human triple-negative breast carcinomas (TNBC) compared with luminal breast carcinomas, which suggests association of this APRIL signaling pathway with tumor aggressiveness.

Methods

Mouse, cell lines and human tumor samples

B6-Tg(Lck-hAPRIL) mice were previously described by Michael Hahne's laboratory (17) and backcrossed at least 10 times onto the BALB/c background to generate the BALB/c-Tg (Lck-hAPRIL) mice used in these experiments and termed APRIL-Tg for short. APRIL-Tg and wild type littermates were bred in-house under specific pathogen-free conditions. Animal experiments were supervised by the Centro Nacional de Biotecnología Ethics Committee, in compliance with national, institutional and EU guidelines. Human breast carcinoma cell lines MDA-MB231, MDA-MB468, MCF7, T47D (35) and the murine 4T1 cell line, derived from a spontaneous mammary tumor in BALB/c mice, were obtained from the American Type Culture Collection (ATCC, Manassas). ATCC ensures authenticity of these cell lines using short tandem repeat DNA profiling. Short tandem repeat authentication of cell lines was conducted by the Genomics Core Facility at the Instituto de Investigaciones Biomedicas 'Alberto Sols' and verified with the ATCC data base. A certificate of analysis was provided. Cells were kept in culture and used no longer than 3–4 months after authentication. Cells were cultured according to supplier's recommendations; for culture media, see Supplementary Table 1 is available at *Carcinogenesis* Online. For quantitative real-time polymerase chain reaction (qPCR) analysis, samples from breast cancer patients were collected from the University Hospital of Bellvitge (Barcelona, Spain), using protocols approved by the IDIBELL ethics committee and according to Declaration of Helsinki. Samples were collected immediately after surgery, frozen and stored at −80°C. For immunohistochemical studies, nine IDC tissue samples were obtained from the CNIO Tumor Biobank (Madrid, Spain), with anonymized patient data and consent (36). Molecular characteristics of human samples are provided in Supplementary Table 2 is available at *Carcinogenesis* Online (samples used for molecular analyses) and S3 (samples for IHC analyses). We used the hAPRIL ELISA kit (eBioscience) to quantify APRIL protein in 37 human serum samples from breast carcinoma patients with three carcinoma subtypes (luminal, $n = 20$; triple negative breast carcinoma, TNBC, $n = 12$; HER2-enriched, $n = 5$; obtained from Biobank HUB-ICO-IDIBELL, Barcelona, Spain).

RNA isolation and quantitative RT-PCR

Total RNA was isolated from each tumor cell line and from 4T1 tumors and lungs of 4T1-orthotransplanted WT and APRIL-Tg mice, using TRI Reagent (Sigma–Aldrich). RNA (1–2 µg) was used for reverse transcription with the High Capacity cDNA Reverse Transcription Kit (Life Technologies). qPCR assay was performed on an ABI 7900 Fast Real-time PCR System using TaqMan Fast Universal PCR master mix (Life Technologies). β-*Actin* and *Pum1* served as internal housekeeping genes depending on the experiment. RNA extraction and qPCR from human breast tumors were performed as described (37), and mRNA levels were normalized to the *PP1A* gene. Primer sequences (Sigma–Aldrich) are shown in Supplementary Table 4 (available at *Carcinogenesis* Online).

Immunofluorescence

Breast cell lines were plated on fibronectin-coated slides and incubated (3–6 h, 37°C), then fixed with 2% paraformaldehyde solution, permeabilized with 0.1% Triton X-100 (5 min, 20°C) and incubated with primary antibody anti-hAPRIL ED2 (overnight, 4°C; Alexis Biochemicals) that recognizes both full length and processed APRIL. Then cells were incubated

with a Cy2-conjugated secondary antibody followed by DAPI. Samples were mounted in Vectashield medium (Vector Laboratories) and images were recorded in a confocal microscope (Olympus Fluoview 10) with a ×20 objective lens, using FV10-ASW 1.6 software (Olympus). Brightness and/or contrast were adjusted with ImageJ software (National Institutes of Health).

Western blot

To evaluate APRIL expression, MCF7, T47D, MDA-MB231 and MDA-MB468 cells were lysed with lysis buffer (Roche), and proteins quantified and analyzed by Western blot following standard procedures (38). As positive control, we used HEK-293T cells transfected with APRIL (293T-APRIL). To study APRIL induction by TLR ligands, MDA-MB231 and MDA-MB468 cells were cultured with ultrapure LPS (2 µg/ml), flagellin (0.5 µg/ml) or poly I:C (20 µg/ml; all from InvivoGen) and supernatants were collected at 24 and 48 h. Blots were probed with Aprily5 anti-hAPRIL antibody (Alexis Biochemicals), which recognizes full-length and cleaved APRIL. To analyze APRIL and TLR3 signaling, cells were starved overnight, and then stimulated with hAPRIL (200 ng/ml; R&D Systems) or poly I:C (20 µg/ml) in a time course. We used anti-phospho-ERK1/2 (Thr202/Tyr204), -ERK1/2, -phospho-p38 (Thr180/Tyr182), -p38, -JNK1/2, -IκBα and phospho- IκBα antibodies (Cell Signaling Technology); anti-phospho-JNK1/2 (Thr183/Tyr185, Invitrogen, Life Technologies), and appropriate HRP-conjugated secondary antibodies (Dako).

Proliferation assays

We quantified cell proliferation at 48 h using a thymidine incorporation assay. Briefly, cells from each cell line were cultured (10^4 cells/well, 96 flat-well plates), alone or with 100 ng/ml hAPRIL (MegaAPRIL, Alexis Biochemicals). [^{3}H]thymidine (1 CµCi/well) was added to the culture for the last 8 h and thymidine incorporation was measured in a liquid scintillation counter (Wallac Trilux 1450 Microbeta, Perkin Elmer). Three independent assays were performed, with at least 15 wells per condition.

To determine proliferation after APRIL silencing, similar experiments were performed with cells previously transfected with APRIL-specific and control small interference RNA (ON-TARGETplus SMARTpool, Dharmacon) following supplier's protocols for adherent cells. APRIL-reduction efficiency was evaluated by Western blot.

4T1 tumor transplantation model

Basal 4T1 cells (10^5) were injected into the 4th mammary gland of 8- to 10-week-old female APRIL-Tg and control mice (8–15 mice/group). After detection, tumors were measured weekly with calipers and volume calculated (length × width^2/2). Mice were killed at different time points; tumors and lungs were excised, weighed and photographed, respectively, and optimal cutting temperature compound embedded for analysis.

Immunohistochemistry

Mouse 4T1 tumors

To detect hAPRIL and Ki67, a 8-µm-thick cryosections were fixed in neutral-buffered formalin (Sigma–Aldrich), then incubated overnight with mouse-on-mouse blocking reagent (Vector Laboratories). Sections were reblocked with 40% goat serum in TBS-Tween (blocking solution, 1 h) and incubated with anti-hAPRIL antibody Aprily2 (overnight, 4°C; Alexis Biochemicals), followed by alkaline phosphatase (AP)-anti-mouse antibody (Sigma–Aldrich). We subsequently incubated the sections with anti-Ki67 antibody (overnight, 4°C; Invitrogen), followed by horseradish peroxidase (HP)-anti-rabbit antibody (Dako). AP was developed with the Blue AP substrate kit (Vector Laboratories) and HP with 3-amino-9-ethylcarbazole (AEC, Sigma–Aldrich). All slides were counterstained in Mayer's hematoxylin (20–60 s; Sigma–Aldrich) and mounted with Faramount aqueous mounting medium (Sigma–Aldrich).

Human breast carcinoma samples

Slides of 5-µm-thick formalin-fixed paraffin-embedded breast tumor biopsies were prepared and sequentially deparaffinized. Antigen was heat-retrieved in 10 mM sodium citrate buffer (pre-heat steamer, 30 min). Endogenous peroxidase was blocked with TBS 3% H_2O_2; sections were incubated with primary anti-hAPRIL and -Ki67, and antigen–antibody complexes were detected as above for mouse sections.

Image analysis and statistics

Tumor sections were imaged with a Microdigital Camera (Olympus DP70) mounted on an axioplan microscope (Leica). We analyzed the percentage of Ki67 stained area with Image Pro V6.0 software (Media Cybernetics) and GraphPad Prism 5 (GraphPad Software) to assess statistical significance. For Ki67 quantification, at least 7 fields per mouse and 5 mice per group were analyzed. *P* values indicate comparisons between two groups using unpaired, two-tailed Student's *t* tests; ***$P < 0.0005$, **$P < 0.005$ and *$P < 0.05$.

Results

Breast carcinoma cell lines express APRIL and its receptors BCMA and TACI. APRIL production is induced after TLR3 activation

To study the relationship between breast cancer and APRIL, we first analyzed APRIL expression in four human breast carcinoma cell lines with different features. MCF7 and T47D cells have a luminal-like phenotype and are ERα$^+$PR$^+$HER2$^-$, and MDA-MB468 and MDA-MB231 cells are basal A and B phenotypes, respectively, and all are ERα$^-$PR$^-$HER2$^-$ (36). Basal TNBC are generally more aggressive and invasive than luminal carcinomas (5). Quantitative expression analysis (qPCR) of *April* mRNA showed *April* transcripts in all four cell lines, with a maximum 19-fold difference between MCF7 (lowest) and MDA-MB468 (highest) (Figure 1A).

Unique in its family, APRIL protein is processed at the Golgi apparatus and secreted through vesicular transport outside the cell (39). Both full-length APRIL (≈30 kDa) and processed APRIL (≈17 kDa) can be detected intracellularly while only the processed form is secreted outside the cells. Protein analysis confirmed mRNA results and showed that luminal and basal breast carcinoma cells expressed both APRIL forms (Figure 1B and Supplmentary Figure 7, available at *Carcinogenesis* Online), with higher levels in MDA-MB468 and T47D cells compared to MCF7 and MDA-MB231 cells. Multiple bands for full-length APRIL have been previously described and might be due to post-translational modifications (40). Confocal analysis for protein visualization and localization within cells showed APRIL in cytoplasm, with a punctate pattern typical of the Golgi apparatus (Figure 1C), where this cytokine is cleaved (39). These data demonstrate that breast carcinoma cells express APRIL independently of their luminal/basal phenotype.

We also analyzed APRIL receptors BCMA and TACI by qPCR and detected *Bcma* and *Taci* transcripts in the four cell lines, with higher levels in MDA-MB231 and MDA-MB468 compared to T47D and MCF cells (Figure 1D), suggesting a direct correlation between APRIL receptor expression and cell aggressiveness. Flow cytometry analysis confirmed BCMA and TACI expression in the cell lines (Supplementary Figure S1, available at *Carcinogenesis* Online).

Given that APRIL is expressed in breast carcinoma cells, we studied the factors that regulate its expression. As TLR ligands induce APRIL secretion in hematopoietic and intestinal epithelial cells (12,40), we tested poly I:C (TLR3 ligand), LPS (TLR4), and flagellin (TLR5). APRIL measurement in MDA-MB468 and MDA-MB231 supernatants at various times post-stimulation indicated that poly I:C, but not LPS or flagellin, clearly enhanced APRIL secretion (Figure 1E and Supplementary Figure 8, available at *Carcinogenesis* Online). Poly I:C is a mimic of viral double-stranded RNA; interest in TLR signaling in breast and other cancers has increased, given its pro- and antitumor activities (41,42). TLR3 activation induces apoptosis in some breast cancer cell lines (43,44), but also stimulates tumorigenesis (42), probably by activating molecules associated with tumor cell survival and apoptosis resistance. Indeed, we found that poly

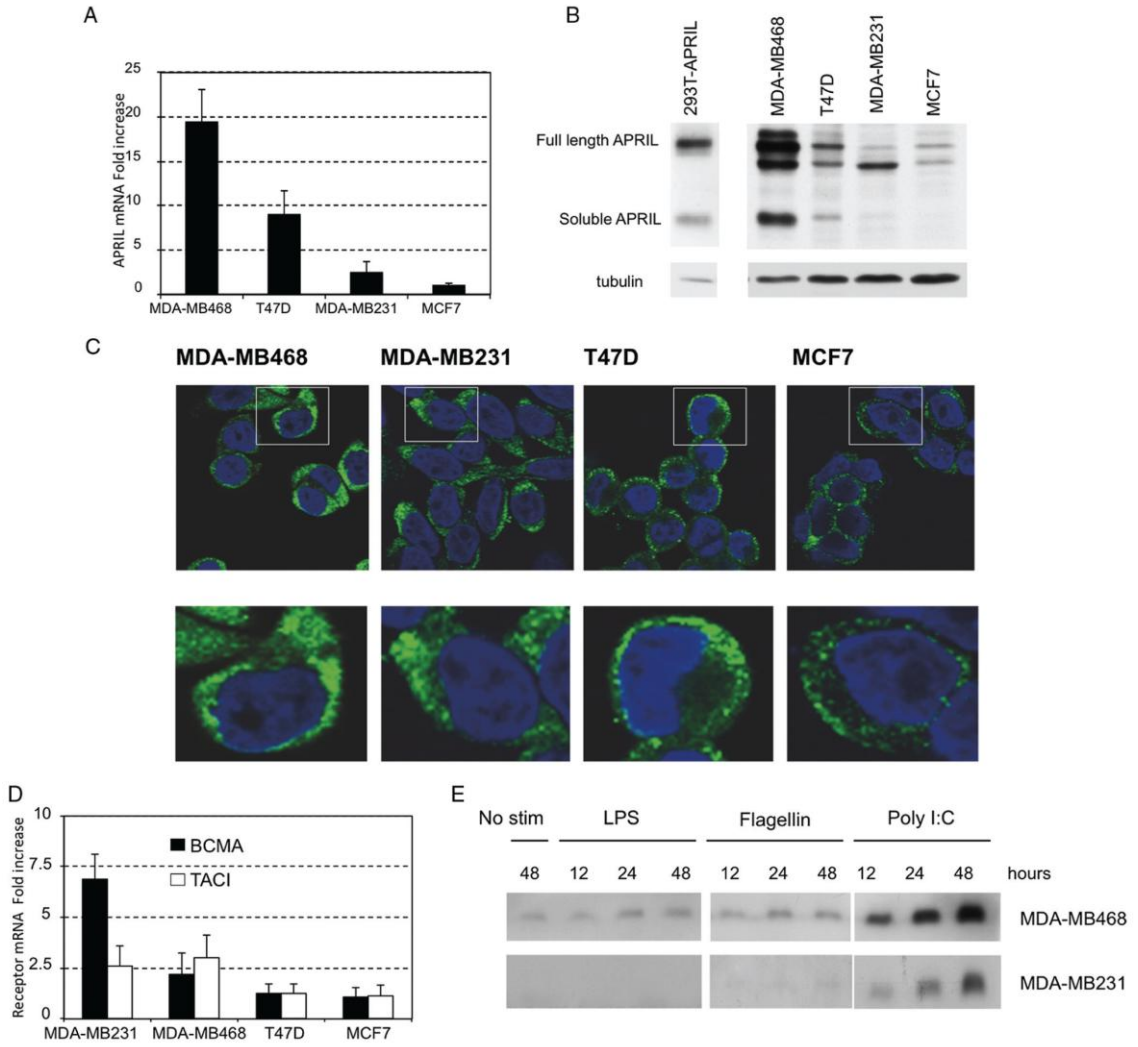

Figure 1. APRIL, BCMA and TACI are expressed in breast carcinoma cells. Toll-like receptor ligand 3 induces APRIL secretion. APRIL mRNA and protein expression levels were analyzed in four breast carcinoma cell lines (MDA-MB468, MDA-MB231, T47D, MCF7). (**A**) Relative APRIL mRNA expression in each cell line compared to MCF7 cells. Values are mean ± SD ($n = 3$ independent experiments). (**B**) Western blot analysis of cell lysates showing bands for full length and processed APRIL forms. (**C**) Confocal microscopy images show APRIL expression (green) in cytoplasm of cell lines labeled with anti-hAPRIL antibody and DAPI (blue). (**D**) Relative BCMA and TACI mRNA expression in each cell line compared to MCF7 cells. Values are mean ± SD ($n = 3$ independent experiments). (**E**) MDA-MB468 and MDA-MB231 cells were unstimulated or stimulated with LPS, flagellin or poly I:C. Western blot analysis shows soluble APRIL in culture supernatants at different times.

I:C activated the NFκB signaling pathway in MDA-MB231 cells (Supplementary Figures 2 and 9, available at *Carcinogenesis* Online). Effects of TLR3 activation on APRIL secretion and NFκB function might explain its tumorigenic activity.

APRIL activates MAP kinases ERK1/2 and JNK1/2 and sustains breast carcinoma cell proliferation

The finding that breast carcinoma cells express TACI and BCMA predicted that signaling through these receptors might promote tumor growth. We analyzed APRIL-mediated signaling via the MAP kinases ERK1/2, p38 and JNK1/2, which have been implicated in breast cancer tumorigenesis (45). Analysis of the phosphorylation kinetics in MDA-MB231 cells, which have the highest receptor levels in our cell panel, showed that APRIL rapidly induced JNK1/2 phosphorylation, followed by that of ERK1/2 (Figure 2A and Supplementary Figure 10, available at *Carcinogenesis* Online). Slight phosphorylation was also observed for p38, indicating that the three MAP kinases are activated after APRIL binding in MDA-MB231 cells.

To explore APRIL-mediated biological effects, we studied cell proliferation in response to exogenous APRIL in a [^{3}H]thymidine assay. APRIL enhanced proliferation in the four breast carcinoma cells with a greater effect on MDA-MB231 (149%) and MDA-MB468 (139%) compared to T47D (118%) and MCF7 cells (111%) (Figure 2B, % relative to untreated cells). We performed silencing experiments to test whether APRIL promotes tumor growth through autocrine signaling. APRIL was efficiently depleted by specific small interference RNA (ON-TARGETplus; Figure 2C for MDA-MB468 and Supplementary Figures 3 and 11, available at

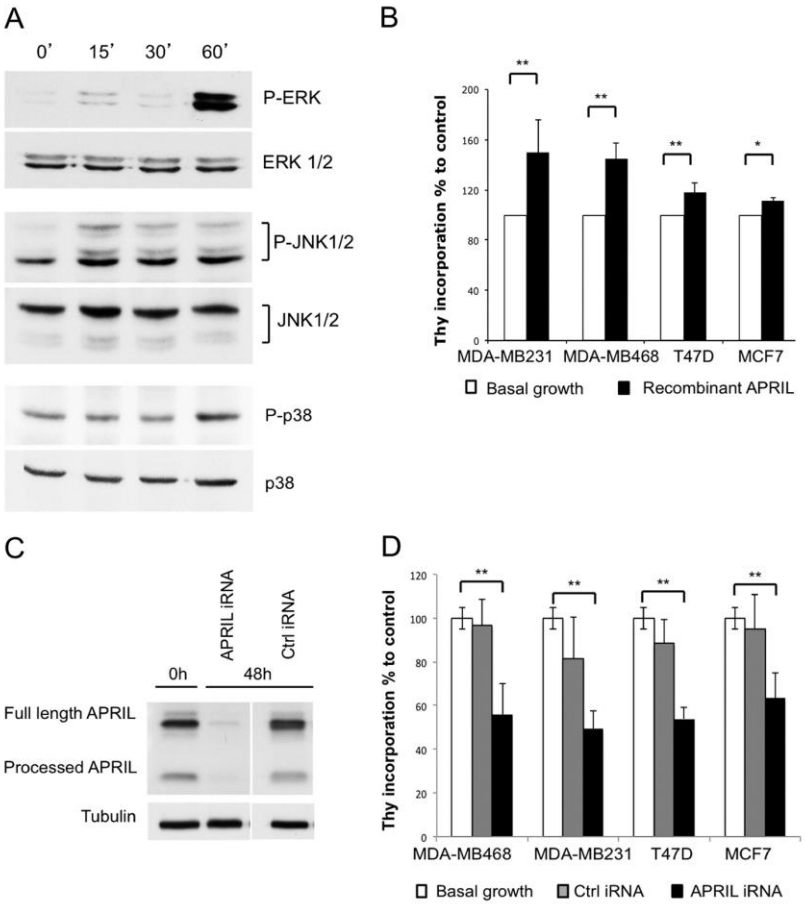

Figure 2. APRIL activates ERK1/2, JNK1/2 and p38 MAP kinases and enhances proliferation of breast carcinoma cells. (**A**) Western blot analysis of lysates from MDA-MB231 cells activated with APRIL (0, 15, 30 and 60 min). Phosphorylation pattern for ERK1/2, JNK1/2 and p38. (**B**) Proliferation rate ([^{3}H]thymidine incorporation) at 48 h of MDA-MB231, MDA-MB468, MCF7 and T47D cells cultured with recombinant APRIL referred to untreated cells (100%). (**C**) Western blot shows APRIL expression in MDA-MB468 after APRIL silencing at 48 h. (**D**) Proliferation rate ([^{3}H]thymidine incorporation) at 48 h of cell lines used in B, after transfection with Ctrl- or APRIL-iRNA and referred to untreated cells (100%). (**B**, **D**) Values are mean ± SD (n = 5 independent experiments); *$P \leq 0.05$, **$P \leq 0.005$.

Carcinogenesis Online). At 48 h, cell proliferation was significantly reduced in all four APRIL-depleted cell lines (Figure 2D). MCF7-APRIL-KO cell proliferation was reduced by 37% of control values, whereas that of MDA-MB231-APRIL-KO cells was reduced by 51% of control values. The greater MDA-MB231 response compared to MCF7 carcinoma cells coincides with increased APRIL receptor levels. These results show that autocrine APRIL stimulates proliferation of basal and luminal breast cancer cells, confirming APRIL signaling is functional in breast carcinoma, with greater activity in aggressive MDA-MB231 cells.

Ectopic APRIL promotes tumor growth and metastasis in 4T1 orthotopic tumors through BCMA and TACI

APRIL is a soluble cytokine detectable in the serum of healthy donors that is increased in chronic lymphocytic leukemia patients (19). We hypothesized that in breast carcinoma patients, circulating APRIL can reach the tumor via the bloodstream and provide support to malignant cells. To determine the paracrine effect of APRIL on breast tumor promotion *in vivo*, we evaluated tumor growth and metastasis in a mouse model that overexpresses human APRIL (APRIL-Tg) (17). In these mice, hAPRIL is expressed under the lck distal promoter and is found in the circulation (Supplementary Figure 4A, is available at *Carcinogenesis* Online). Mouse basal breast carcinoma 4T1 cells express preferentially TACI receptor and are APRIL-sensitive (Supplementary Figure 4B and C, available at *Carcinogenesis* Online). After 4T1 cells transplantation into the mammary fat pad, 4T1 tumors grew more rapidly and were larger in APRIL-Tg females than in the control littermates (Figure 3A). Significant differences in tumor volume were detected from day 25 (4T1Control, mean 71.3 ± 30 mm^3; 4T1APRIL, 153.8 ± 38.7 mm^3; day 25; $P < 0.005$) and in tumor weight from day 19 (4T1Control, 0.27 ± 0.03 g; 4T1APRIL, 0.39 ± 0.08 g; day 19; $P < 0.05$), until the end of the experiment.

Based on our *in vitro* results, we measured cell proliferation (Ki67) and human APRIL expression in tumor lesions by immunohistochemical analysis. 4T1 tumors from APRIL-Tg mice showed increased proliferation (measured as % Ki67-positive

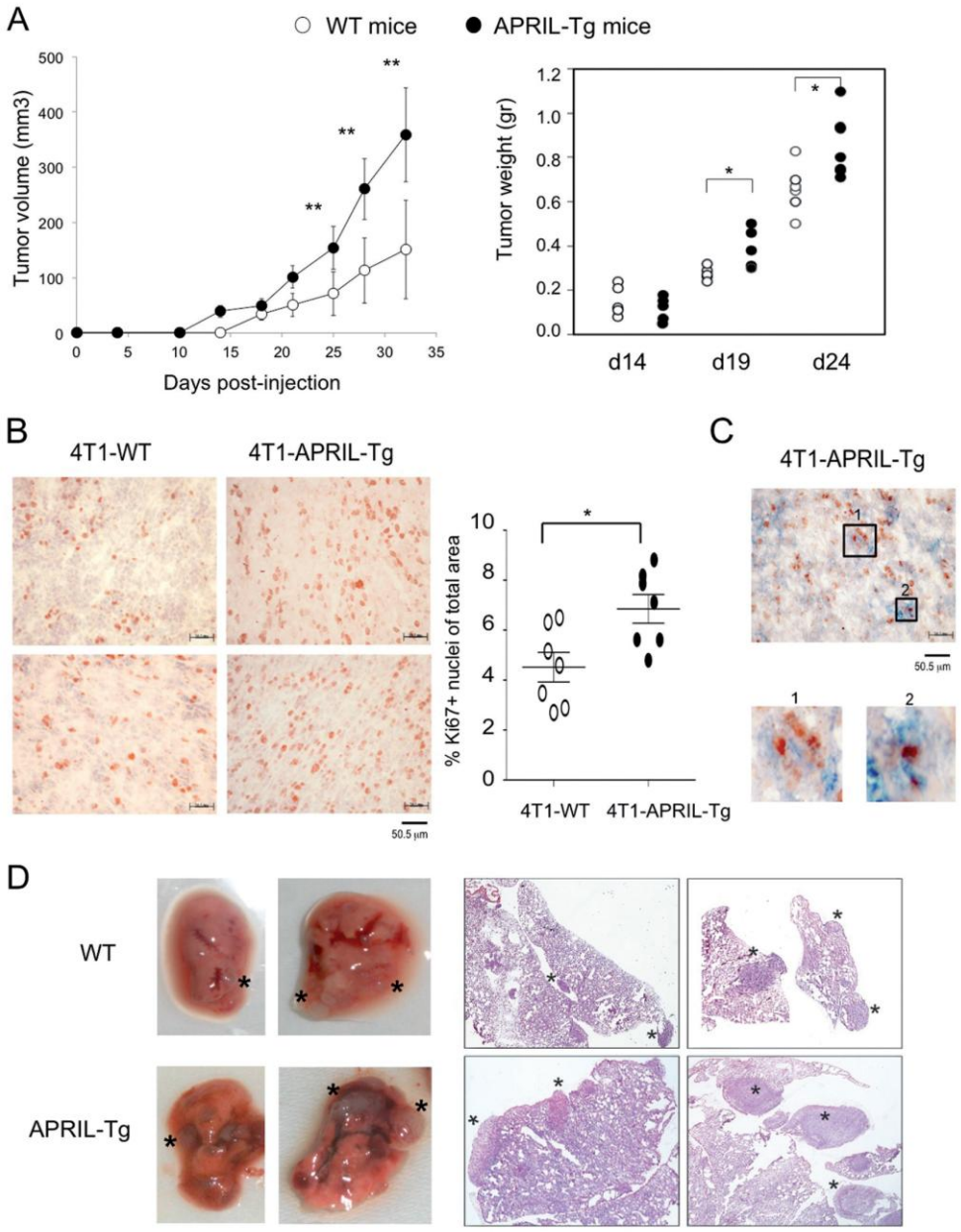

Figure 3. 4T1 tumor growth and lung metastasis are enhanced in an APRIL-enriched environment. 4T1 cells (10^5) were transplanted into the mammary fat pad of syngeneic WT and APRIL-Tg female mice. (**A**) Mean tumor volume ± SD measured twice weekly (left) and individual tumor weight at different times of killing (right) of 4T1 tumors from WT (white circles) and APRIL-Tg (black circles) mice; $n = 6$/group. (**B**) Expression analysis of Ki67 in 4T1 tumors. Representative images of Ki67 staining in 4T1 tumor sections from WT (4T1-WT) and APRIL-Tg (4T1-APRIL-Tg) mice at day 39. Quantification of Ki67-positive area relative to total area (right graph); each point represents the mean of 10 fields from a 4T1 tumor of a WT mouse (black circle) or APRIL-Tg mouse (black squares); $n = 7$/group, mean ± SD is shown. (**C**) Representative image of APRIL (blue) and Ki67 (brown) staining in a 4T1-APRIL-Tg tumor at day 39. Inset, magnification of double-positive APRIL$^+$Ki67$^+$ cells. $^*P \leq 0.05$; $^{**}P \leq 0.005$. (**D**) Representative images of lung macrometastases (day 39) in WT and APRIL-Tg mice. Asterisks mark some metastases. One representative experiment of three is shown.

nuclei/area) compared to controls (Figure 3B) and stained positively for hAPRIL (Figure 3C).

We examined the metastasic potential of 4T1 cells in the same type of assay, after cell transplantation into the mammary fat pad. At day 39, inspection of lungs and H&E analysis showed increased pulmonary colonization and larger metastases in APRIL-Tg mice than in wild type littermates (Figure 3D). To determine the role of APRIL receptors, we used qPCR to analyze

BCMA and TACI in transplanted 4T1 tumors and lung metastases, and normalized mRNA levels to *Pum1* gene. Results for both mouse genotypes showed a clear increase in *Bcma* and *Taci* transcripts in lung metastases compared to transplanted tumors (Figure 4), which suggests that both participate in the metastatic process. *Bcma* and *Taci* transcript levels were also significantly higher in lung metastases from APRIL-Tg compared to control mice (Figure 4), which was linked to increased endogenous *April* (Supplementary Figure 5, available at *Carcinogenesis* Online) and larger metastases in the transgenic mice. Transplanted 4T1 tumors showed no differences in *Bcma*, *Taci* and *mApril* mRNA between control and APRIL-Tg mice (Figure 4, Supplementary Figure 5, available at *Carcinogenesis* Online), suggesting that the pathway is active in both mouse groups and that enhanced tumor growth in APRIL-Tg mice is due to ectopic APRIL protein, that gives an additional ligand source to the tumors. These results provide evidence that APRIL contributes to breast carcinoma and enhances tumor growth and metastasis through BCMA and TACI receptors.

APRIL, BCMA and TACI are overexpressed in human basal-like breast carcinomas

To date, the APRIL pathway has not been analyzed in the distinct breast carcinoma subtypes. We measured APRIL, BCMA and TACI by qPCR in a panel of ductal breast carcinomas containing luminal, TNBC and HER2 samples, the three most frequent subtypes (for sample information, see Supplementary Table 2, available at *Carcinogenesis* Online). We found *April* transcripts in most samples (13 of 14), with significantly increased levels in TNBC (0.037 ± 0.021) compared with luminal carcinomas (0.017 ± 0.012) (Figure 5A). For the receptors, we observed greater incidence of *Bcma* and *Taci* transcripts in TNBC and HER2 than in luminal samples (Figure 5B). Similar to *April*, *Taci* receptor levels were significantly higher in TNBC than in luminal carcinomas, suggesting direct correlation between the APRIL/TACI pathway and breast carcinoma aggressiveness.

We analyzed APRIL protein expression by IHC in tissue sections from nine ductal breast carcinomas (sample data in Supplementary Table 3, available at *Carcinogenesis* Online). APRIL staining in luminal, TNBC and HER2 carcinomas (Figure 6A, Supplementary Figure 6A, available at *Carcinogenesis* Online) confirmed our previous results; staining was detected at several sites within tumor sections, including epithelial cells of the basal layer near tumor areas, normal ducts, transformed tumor cell cytoplasm and the leukocyte infiltrate (Figure 6A, insets). Measurement of APRIL protein in the serum of breast carcinoma patients (n = 37; luminal, TNBC and Her2 subtypes) showed a concentration similar to that of healthy donor control sera (Supplementary Figure 6B, available at *Carcinogenesis* Online).

As APRIL stimulated breast carcinoma growth in our experimental models, we analyzed the proliferative status of APRIL-positive carcinomas and tested for simultaneous expression of APRIL and Ki67. APRIL-positive areas were also enriched in Ki67$^+$ nuclei (Figure 6B), with cells double positive for both markers (Figure 6B, inset). These data suggest that APRIL expressed in the tumor lesions sustains proliferation of the malignant breast carcinoma cells; more extensive studies are under way to confirm this observation.

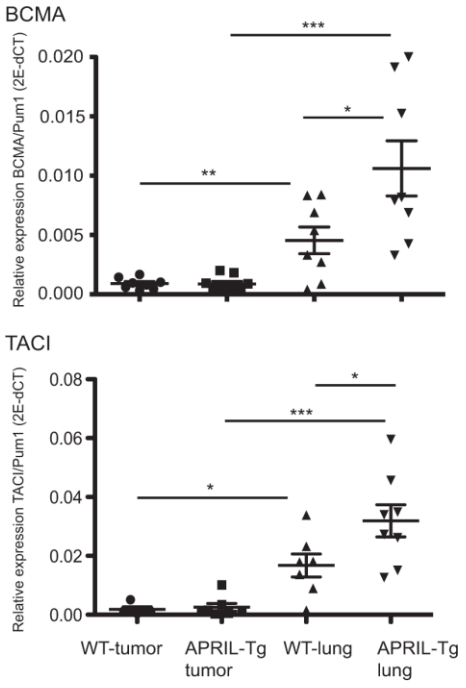

Figure 4. BCMA and TACI expression profile in 4T1 transplanted tumors and lung metastases. mRNA expression of *Bcma* (upper) and *Taci* (lower) in 4T1 tumors and lung metastases from 4T1-transplanted control (n = 8) and APRIL-Tg mice (n = 9), measured by qPCR and normalized to *Pum1*. *P ≤0.05, **P ≤0.005, ***P ≤0.0005.

Discussion

A sustained proliferative signal is one of the signatures of cancer cells. After cell transformation, several mechanisms promote proliferation and provide tumors with independence from normal regulation of cell control (2). We show that APRIL is expressed by malignant luminal and basal breast carcinoma cells, as well as by other cells in the tumor environment, to generate autocrine and paracrine signaling loops that enhance tumor cell proliferation and promote tumor growth and metastasis.

APRIL was initially described in the late 1990s based on its ability to induce proliferation of distinct types of cell lines (10). Initial data showed that APRIL is overexpressed in leukemia and lymphoma, and promotes tumorigenesis, but newer reports indicate a role for this cytokine beyond hematopoietic malignancies (23–34). There are currently three descriptive studies of APRIL in breast cancer (23,33,34). They found overexpressed APRIL protein (23,33) or RNA (34) in tissue lesions although none of them analyzed specific histological subtypes or the implication of APRIL pathway in breast cancer promotion.

BCMA and TACI are expressed mainly and abundantly in lymphoid cells, with few reports regarding solid tumors. Our group and others have nonetheless described BCMA and/or TACI expression in non-lymphoid cell linages such as adipose-related cells (13), renal carcinoma (25), squamous and basal cell carcinoma (26), hepatocarcinoma (28), glioma (29) and glioblastoma (30). Variation between studies is probably based on the distinct approaches, tools and sample types used to detect these receptors.

Here, we show that four breast carcinoma cell lines as well as primary breast carcinomas express APRIL, BCMA and TACI, and that their expression is not restricted to the basal/luminal phenotype. The mechanisms that induce the APRIL pathway during

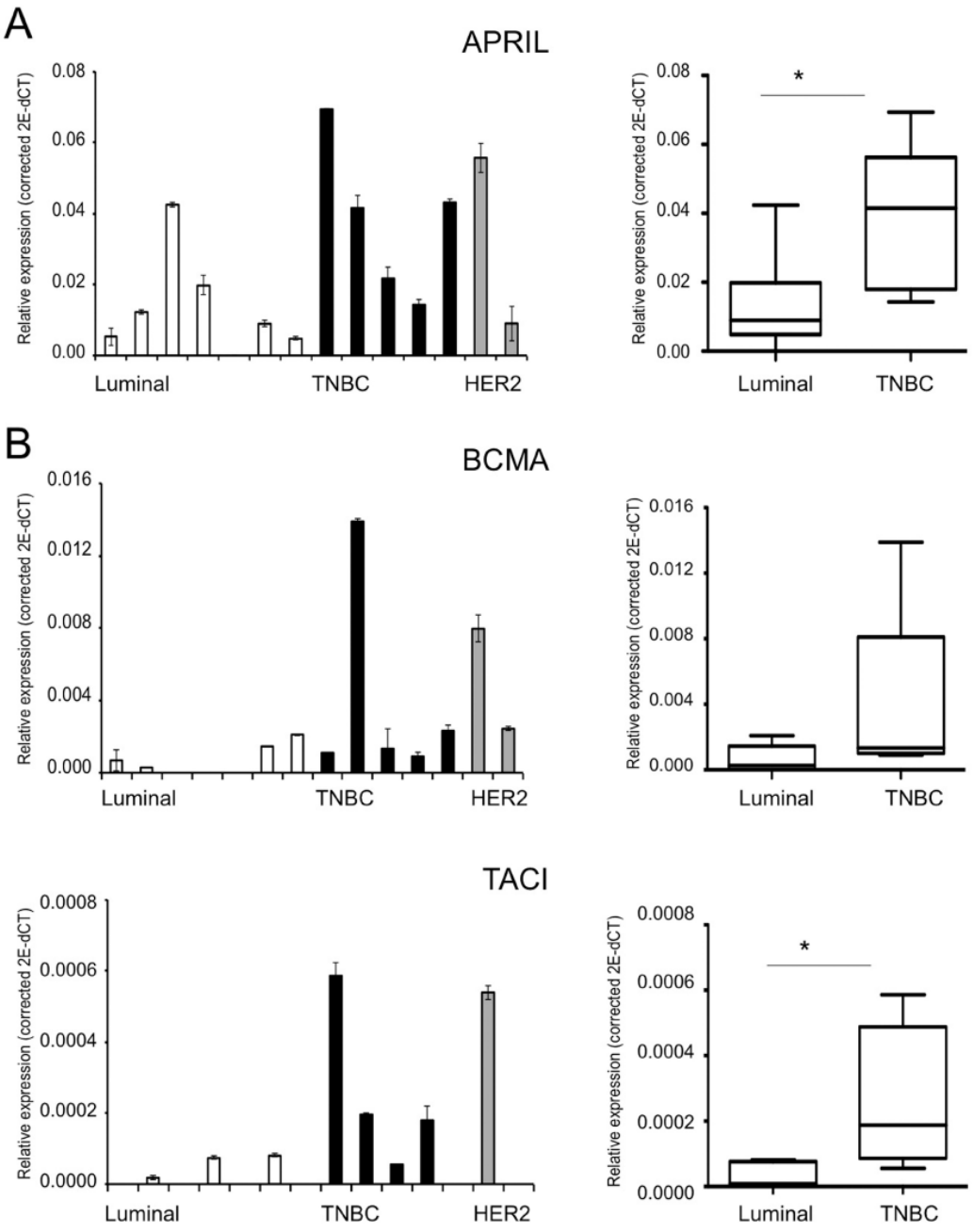

Figure 5. APRIL, BCMA and TACI expression is increased in TNBC breast carcinomas. mRNA expression of (**A**) APRIL and (**B**) BCMA and TACI in a panel of luminal ($n = 7$), TNBC ($n = 5$), and HER2 ($n = 2$) breast carcinoma samples, measured by qPCR relative to PP1A. Left graphs show mean ± SD from triplicate determinations; right graphs show mean ± SD of data grouped by sample subtype (luminal and TNBC samples). *$P \leq 0.05$.

breast malignant transformation remain undetermined. We found that TLR3 activation in cell lines promotes APRIL secretion and activates the NFκB transcription factor, which might also explain why some breast carcinoma cells such as MDA-MB231 are resistant to poly I:C-induced apoptosis (43,44). NFκB is associated with tumor cell survival and apoptosis resistance (46), is reported to be more active in basal than in luminal breast carcinomas (47), and is crucial in promoting transcription of the human *April* gene (48). Further studies are needed to determine the link between NFκB and other signaling pathways with APRIL in breast carcinoma and to establish whether TLR3 mediates APRIL production *in vivo*. There is evidence that endogenous

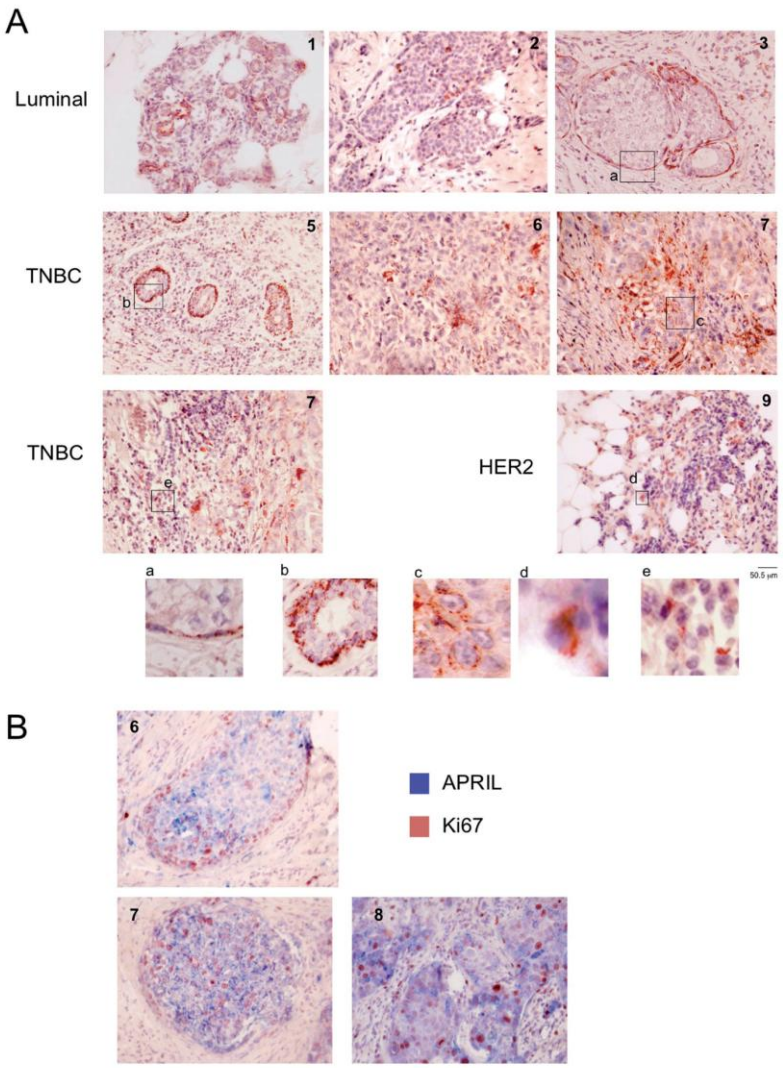

Figure 6. Luminal, TNBC and HER2 carcinomas express APRIL protein heterogeneously and near proliferating areas. (**A**) Immunohistochemistry study of APRIL expression in paraffin-embedded IDC. Representative images of APRIL staining (brown) are shown. Inset, magnifications of indicated areas showing APRIL at distinct sites, (a) basal epithelial layer, (b) 'normal' ducts, (c, d) tumor cell cytoplasm, and (e) inflammatory infiltrate. (**B**) Representative images of three IDC showing immunostaining of APRIL (blue) and Ki67 (brown). Numbers correspond to sample ID (see Supplementary Table 3, available at *Carcinogenesis* Online)

or damage-associated molecular pattern (DAMP) molecules released from damaged/necrotic tissues activate TLR and promote tumor development (49); this could also be the case for APRIL.

Coexpression of APRIL and its receptors enables autocrine proliferation of tumor cells, as we confirmed in APRIL silencing assays. Basal MDA-MB231 and MDA-MB468 cells were more responsive to APRIL than luminal-like MCF7 and T47D cells, based on their higher receptor expression pattern; this suggests that the APRIL pathway is more active in aggressive carcinoma cells. APRIL also binds HSPG on the tumor cell surface, which is critical for the proliferation-mediated effect (16). We thus cannot exclude that HSPG in the breast carcinoma cells might contribute to the differences observed by concentrating the ligand or by direct signaling. We show that after binding, APRIL induces phosphorylation of JNK1/2, ERK1/2 and p38 in MDA-MB231 cells. These three MAP kinases are overexpressed in breast cancer and their activation enhances cancer cell survival and proliferation (45). Switching on the APRIL pathway provides malignant cells a mechanism to sustain activation of their MAP kinase signaling and promote tumor progression. Breast carcinoma cells expressed BCMA and TACI receptors; it is possible that both of these as well as HSPG contribute to this effect. We reduced BCMA and TACI expression in MDA-MB231 cells using small interference RNA but we did not detect consistent differences in cell proliferation, attributable to the poor efficiency of receptor silencing. Current experiments using CRISPR technology (clustered, regularly interspaced, short palindromic repeats) to

silence receptor genes will provide new data about the specific function of BCMA and TACI signaling in breast cancer.

In solid tumors, it has been described that APRIL triggers different signaling pathways depending on the cellular and tissue context inducing pleiotropic functions. APRIL binding to BCMA activates a JNK2-FOXO3-GADD45 pathway in HCC cell lines and promotes cell growth arrest (28). In addition, APRIL binding to BCMA in transfected 293 cells (50) and to TACI in B cell lines (15) activates NFkB and JNK pathways that are related to cell survival and proliferation. In breast cancer, knock down studies for BCMA and TACI are needed to clarify their specific function.

In addition to its autocrine role as a tumor-promoting factor, APRIL paracrine signaling is described in cancers such as leukemia or glioblastoma (reviewed in ref. 11). Our results indicate that this is probably to be the case in breast carcinoma, as we and others found APRIL expression in tumor cells, in tumor-infiltrating leukocytes, and in 'normal' epithelial cells near the tumor area (33). APRIL is detected in serum (17) and could reach tumor lesions via the circulation. Our data using orthotopic 4T1 tumor transplants in APRIL-overexpressing mice indicate that high serum APRIL levels promote tumor growth and lung metastasis and suggest that both BCMA and TACI have an important role in the metastatic process, as receptor expression was higher in the lungs compared to 4T1 transplanted tumors. In pancreatic cancer patients, serum APRIL levels are proposed as diagnostic and prognostic references, alone or in combination with other conventional markers (27). Our results nonetheless indicate that breast carcinoma behaves differently, as we observe no differences in serum APRIL levels.

There are currently no data regarding APRIL, BCMA and TACI expression in different breast carcinoma subtypes. We detected expression of all three in luminal, TNBC and HER2 carcinomas, and higher levels of APRIL and TACI mRNA transcripts in TNBC than in luminal samples, indicating that overexpression of APRIL and TACI in human breast cancer cells increases their aggressiveness and may result in poorer clinical outcome. Two reports have evaluated APRIL association with tumor grade in breast carcinoma, with contrasting results (33,34). This disparity might reflect the different experimental approaches used (protein versus mRNA), but also sample heterogeneity, as no specific subtypes were analyzed nor were histopathological features provided (hormone receptor, HER2 or Ki67 expression). We found higher APRIL expression in grade 3 TNBC than in grade 3 luminal samples (not shown), which underlines the importance of subtype analysis. Moreover, we and others found APRIL expression in normal epithelial structures (33) and in the inflammatory infiltrate of breast carcinoma tissue lesions, what implies a role for this cytokine in mammary tissue beyond cancer pathology and also in the inflammatory response. It would be interesting to investigate the function of APRIL in mammary gland development, in which cell proliferation and apoptosis are key events.

In summary, we identify an APRIL signaling pathway that functions and participates in human mammary tumorigenesis. Breast carcinoma cells express APRIL, BCMA and TACI to sustain their proliferation. Studies with human breast carcinoma samples and with mice indicate that APRIL signaling is linked to tumor cell aggressiveness, growth and metastasis.

Supplementary Data

Supplementary Tables 1–5 and Supplementary Figures 1–11 can be found at http://carcin.oxfordjour- nals.org/

Funding

Instituto de Salud Carlos III ISCIII (PI07-1184, PI10-01556 to L.P.); Comunidad de Madrid/CAM (CCG08-CSIC/SAL-3726 to L.P., IMMUNOTHERCAN, S2010/BMD-2326 to S.M.); Ministerio de Ciencia e Innovación (SAF2011-24453 to S.M.).

Acknowledgments

We thank Biobank HUB-ICO-IDIBELL (Barcelona, Spain) for providing us with serum samples of breast carcinoma patients, A.C. and Y.R.C. for helpful comments and C.M. for editorial assistance. A.G.C. held a PhD fellowship from the Madrid regional government, M.Z. was a PhD fellow of the La Caixa Foundation International Fellowship Programme (La Caixa/CNB), C.E.C.P. was financed by the CNPq Science Exchange Program (Brasil) and L.P. was supported by the Spanish Ministry of Education and Science Ramón y Cajal program.

Conflict of Interest Statement: None declared.

References

1. Siegel, R. et al. (2013) Cancer statistics, 2013. CA. Cancer J. Clin., 63, 11–30.
2. Hanahan, D. et al. (2011) Hallmarks of cancer: the next generation. Cell, 144, 646–674.
3. Perou, C.M. et al. (2000) Molecular portraits of human breast tumours. Nature, 406, 747–752.
4. Eroles, P. et al. (2012) Molecular biology in breast cancer: intrinsic subtypes and signaling pathways. Cancer Treat. Rev., 38, 698–707.
5. Dent, R. et al. (2007) Triple-negative breast cancer: clinical features and patterns of recurrence. Clin. Cancer Res., 13(15 Pt 1), 4429–4434.
6. Slamon, D.J. et al. (2001) Use of chemotherapy plus a monoclonal antibody against HER2 for metastatic breast cancer that overexpresses HER2. N. Engl. J. Med., 344, 783–792.
7. Kennecke, H. et al. (2010) Metastatic behavior of breast cancer subtypes. J. Clin. Oncol., 28, 3271–3277.
8. Lippitz, B.E. (2013) Cytokine patterns in patients with cancer: a systematic review. Lancet. Oncol., 14, e218–e228.
9. Quail, D.F. et al. (2013) Microenvironmental regulation of tumor progression and metastasis. Nat. Med., 19, 1423–1437.
10. Hahne, M. et al. (1998) APRIL, a new ligand of the tumor necrosis factor family, stimulates tumor cell growth. J. Exp. Med., 188, 1185–1190.
11. Planelles, L. et al. (2008) The expanding role of APRIL in cancer and immunity. Curr. Mol. Med., 8, 829–844.
12. He, B. et al. (2007) Intestinal bacteria trigger T cell-independent immunoglobulin A(2) class switching by inducing epithelial-cell secretion of the cytokine APRIL. Immunity, 26, 812–826.
13. Alexaki, V.I. et al. (2009) Adipocytes as immune cells: differential expression of TWEAK, BAFF, and APRIL and their receptors (Fn14, BAFF-R, TACI, and BCMA) at different stages of normal and pathological adipose tissue development. J. Immunol., 183, 5948–5956.
14. Gras, M.P. et al. (1995) BCMAp: an integral membrane protein in the Golgi apparatus of human mature B lymphocytes. Int. Immunol., 7, 1093–1106.
15. Xia, X.Z. et al. (2000) TACI is a TRAF-interacting receptor for TALL-1, a tumor necrosis factor family member involved in B cell regulation. J. Exp. Med., 192, 137–143.
16. Hendriks, J. et al. (2005) Heparan sulfate proteoglycan binding promotes APRIL-induced tumor cell proliferation. Cell Death Differ., 12, 637–648.
17. Stein, J.V. et al. (2002) APRIL modulates B and T cell immunity. J. Clin. Invest., 109, 1587–1598.
18. Planelles, L. et al. (2004) APRIL promotes B-1 cell-associated neoplasm. Cancer Cell, 6, 399–408.
19. Planelles, L. et al. (2007) APRIL but not BLyS serum levels are increased in chronic lymphocytic leukemia: prognostic relevance of APRIL for survival. Haematologica, 92, 1284–1285.

20. Schwaller, J. et al. (2007) Neutrophil-derived APRIL concentrated in tumor lesions by proteoglycans correlates with human B-cell lymphoma aggressiveness. Blood, 109, 331–338.
21. Chiu, A. et al. (2007) Hodgkin lymphoma cells express TACI and BCMA receptors and generate survival and proliferation signals in response to BAFF and APRIL. Blood, 109, 729–739.
22. Quinn, J. et al. (2011) APRIL promotes cell-cycle progression in primary multiple myeloma cells: influence of D-type cyclin group and translocation status. Blood, 117, 890–901.
23. Mhawech-Fauceglia, P. et al. (2006) The source of APRIL up-regulation in human solid tumor lesions. J. Leukoc. Biol., 80, 697–704.
24. Mhawech-Fauceglia, P. et al. (2008) Role of the tumour necrosis family ligand APRIL in solid tumour development: Retrospective studies in bladder, ovarian and head and neck carcinomas. Eur. J. Cancer, 44, 2097–2100.
25. Pelekanou, V. et al. (2011) Detection of the TNFSF members BAFF, APRIL, TWEAK and their receptors in normal kidney and renal cell carcinomas. Anal. Cell. Pathol. (Amst)., 34, 49–60.
26. Alexaki, V.I. et al. (2012) B-cell maturation antigen (BCMA) activation exerts specific proinflammatory effects in normal human keratinocytes and is preferentially expressed in inflammatory skin pathologies. Endocrinology, 153, 739–749.
27. Wang, F. et al. (2011) Serum APRIL, a potential tumor marker in pancreatic cancer. Clin. Chem. Lab. Med., 49, 1715–1719.
28. Notas, G. et al. (2012) APRIL binding to BCMA activates a JNK2-FOXO3-GADD45 pathway and induces a G2/M cell growth arrest in liver cells. J. Immunol., 189, 4748–4758.
29. Pelekanou, V. et al. (2013) BAFF, APRIL, TWEAK, BCMA, TACI and Fn14 proteins are related to human glioma tumor grade: immunohistochemistry and public microarray data meta-analysis. PLoS One, 8, e83250.
30. Deshayes, F. et al. (2004) Abnormal production of the TNF-homologue APRIL increases the proliferation of human malignant glioblastoma cell lines via a specific receptor. Oncogene, 23, 3005–3012.
31. Wang, F. et al. (2008) Lentivirus-mediated short hairpin RNA targeting the APRIL gene suppresses the growth of pancreatic cancer cells *in vitro* and *in vivo*. Oncol. Rep., 20, 135–139.
32. Lascano, V. et al. (2012) The TNF family member APRIL promotes colorectal tumorigenesis. Cell Death Differ., 19, 1826–1835.
33. Pelekanou, V. et al. (2008) Expression of TNF-superfamily members BAFF and APRIL in breast cancer: immunohistochemical study in 52 invasive ductal breast carcinomas. BMC Cancer, 8, 76.
34. Moreaux, J. et al. (2009) APRIL is overexpressed in cancer: link with tumor progression. BMC Cancer, 9, 83.
35. Neve, R.M. et al. (2006) A collection of breast cancer cell lines for the study of functionally distinct cancer subtypes. Cancer Cell, 10, 515–527.
36. Tardáguila, M. et al. (2013) CX3CL1 promotes breast cancer via transactivation of the EGF pathway. Cancer Res., 73, 4461–4473.
37. Palafox, M. et al. (2012) RANK induces epithelial-mesenchymal transition and stemness in human mammary epithelial cells and promotes tumorigenesis and metastasis. Cancer Res., 72, 2879–2888.
38. Zonca, M. et al. (2012) APRIL and BAFF proteins increase proliferation of human adipose-derived stem cells through activation of Erk1/2 MAP kinase. Tissue Eng. Part A, 18, 852–859.
39. López-Fraga, M. et al. (2001) Biologically active APRIL is secreted following intracellular processing in the Golgi apparatus by furin convertase. EMBO Rep., 2, 945–951.
40. Hardenberg, G. et al. (2007) Specific TLR ligands regulate APRIL secretion by dendritic cells in a PKR-dependent manner. Eur. J. Immunol., 37, 2900–2911.
41. Conforti, R. et al. (2010) Opposing effects of toll-like receptor (TLR3) signaling in tumors can be therapeutically uncoupled to optimize the anticancer efficacy of TLR3 ligands. Cancer Res., 70, 490–500.
42. Yu, L. et al. (2013) Dual character of Toll-like receptor signaling: protumorigenic effects and anti-tumor functions. Biochim. Biophys. Acta, 1835, 144–154.
43. Salaun, B. et al. (2006) TLR3 can directly trigger apoptosis in human cancer cells. J. Immunol., 176, 4894–4901.
44. Inao, T. et al. (2012) Antitumor effects of cytoplasmic delivery of an innate adjuvant receptor ligand, poly(I:C), on human breast cancer. Breast Cancer Res. Treat., 134, 89–100.
45. Adeyinka, A. et al. (2002) Activated mitogen-activated protein kinase expression during human breast tumorigenesis and breast cancer progression. Clin. Cancer Res., 8, 1747–1753.
46. Cao, Y. et al. (2003) NF-kappaB in mammary gland development and breast cancer. J. Mammary Gland Biol. Neoplasia, 8, 215–223.
47. Shapochka, D.O. et al. (2012) Relationship between NF-κB, ER, PR, Her2/neu, Ki67, p53 expression in human breast cancer. Exp. Oncol., 34, 358–363.
48. Xu, J. et al. (2012) Transcription of promoter from the human APRIL gene regulated by Sp1 and NF-kB. Neoplasma, 59, 341–347.
49. Yu, L. et al. (2012) Exogenous or endogenous Toll-like receptor ligands: which is the MVP in tumorigenesis? Cell. Mol. Life Sci., 69, 935–949.
50. Hatzoglou, A. et al. (2000) TNF receptor family member BCMA (B cell maturation) associates with TNF receptor-associated factor (TRAF) 1, TRAF2, and TRAF3 and activates NF-kappa B, elk-1, c-Jun N-terminal kinase, and p38 mitogen-activated protein kinase. J. Immunol., 165, 1322–1330.

SUPPLEMENTAL INFORMATION

Supplemental Table 1

CELL CULTURE CONDITIONS FOR BREAST CARCINOMA CELL LINES

CELL LINE	CULTURE MEDIUM
MDA-MB231	DMEM high glucose, 10% FBS, 2mM L-Glutamine, 100U/ml Penicillin/Streptomycin
MDA-MB468	Leibovitz's L15, 10% FBS, 100U/ml Penicillin/Streptomycin (no CO2)
MCF7	MEM high glucose, 10% FBS, 2mM L-Glutamine, 1% Non-Essential Amino Acids, 1mM Sodium Pyruvate, 100U/ml Penicillin/Streptomycin
T47D	RPMI high glucose, FBS 10%, 2mM L-Glutamine, 1mM Sodium Pyruvate, 1.5gr/l Sodium Bicarbonate, 0.2 U/ml Bovine Insulin, 100U/ml Penicillin/Streptomycin
4T1	DMEM high glucose, 10% FBS, 2mM L-Glutamine, 100U/ml Penicillin/Streptomycin

DMEM and RPMI from Lonza
MEM, Leibovitz's, FBS, L-Glutamine Sodium Pyruvate, Sodium Bicarbonate and Penicillin/Streptomycin from Gibco
Bovine Insulin from Sigma-Aldrich

Supplemental Table 1: Cell culture Media.
Table shows media conditions used to culture breast carcinoma cell lines.

Supplemental Table 2

Human samples used for molecular analysis

ID	Histology	Grade	ER (%)	PR (%)	HER2	Ki67 (%)
1	IDC	3	POS 100	POS 95	NEG	15-20
2	IDC	3	100	60	NEG	30
3	IDC	2	100	80	NEG	35
4	IDC	3	90	30	NEG	40
5	IDC	2	85	NEG	NEG	65
6	IDC	1	95	100	NEG	<5
7	MC	3	NEG	30	NEG	80
8	IDC	3	NEG	NEG	NEG	70
9	IDC	3	NEG	NEG	NEG	90
10	IDC	3	NEG	NEG	NEG	70
11	MC		NEG	NEG	NEG	60
12	MC	3	NEG	NEG	NEG	20
13	IDC	2	NEG	NEG	POS	15
14	MC	3	NEG	NEG	POS	15

IDC: Invasive ductal carcinoma
MC: Metaplastic carcinoma
POS: POSITIVE
NEG: NEGATIVE

Supplemental Table 2. Human samples used for molecular analysis.
Table shows the molecular characteristics of fourteen ductal breast carcinomas used for RNA analysis. ER, estrogen receptor; PR, progesterone receptor; HER2, Human Epidermal Growth Factor Receptor 2.

Supplemental Table 3

Human samples used for IHC analysis

ID	Histology	Grade	ER	PR	HER2	Ki67
1	IDC	1	POS	NEG	NEG	+
2	IDC	2	POS	POS	NEG	++
3	IDC	2	NEG	POS	NEG	+
4	IDC	1	POS	POS	NEG	+++
5	IDC	2	NEG	NEG	NEG	+++
6	IDC	3	NEG	NEG	NEG	+++
7	IDC	3	NEG	NEG	NEG	+++
8	IDC	2	NEG	NEG	NEG	+++
9	IDC	3	POS	POS	+++	++

IDC: Invasive ductal carcinoma
POS: POSITIVE
NEG: NEGATIVE
HER2 and Ki67: + low expression, ++ medium expression, +++ high expression

Supplemental Table 3. Human samples used for IHC analysis. Table shows the molecular characteristics of nine invasive ductal breast carcinomas used for immunohistochemical analysis. ER, estrogen receptor; PR, progesterone receptor; HER2, Human Epidermal Growth Factor Receptor 2.

Supplemental Table 4

GENES	SEQUENCE 5'-3'
hAPRIL Fw	AAGGGTATCCCTGGCAGAGT
hAPRIL Rv	GCAGGACAGAGTG CTGCTT
hTACI Fw	TGCAAAACCATTTGCAACC
hTACI Rv	AGAACTTGCCTTGCTCCTTG
hBCMA Fw	TTTTCGTGCTAATGTTTTTGCTAA
hBCMA Rv	TTCATCACCAGTCCTGCTCTTTTC
hBeta-actin Fw	CCCAGCACAATGAAGATCAA
hBeta-actin Fw	CGATCCACACGGAGTACTTG
hPP1A Fw	ATGCTGGACCCAACACAAAT
hPP1A Rv	TCTTTCACTTTGCCAAACACC
mAPRIL Fw	GGTGGTATCTCGGGAAGGAC
mAPRIL Rv	CCCCTTGATGTAAATGAAAGACA
mBCMA Fw	TCCCTCATGGCGCAACAGTG
mBCMA Rv	ACCAAGGTCAGCCCCAAGAAGAT
mTACI Fw	GAGCTCGGGAGACCACAG
mTACI Rv	TGGTCGCTACTTAGCCTCAAT
PUM1 Fw	AGCAGCCTTAGCTATTCCTCCTCT
PUM1 Rv	ATCTTCCACTGCCGTTTGTGAGTC

Supplemental Table 4. Primer sequences.
Table shows primer sequences used for qPCR amplification.

Supplemental Figure 1

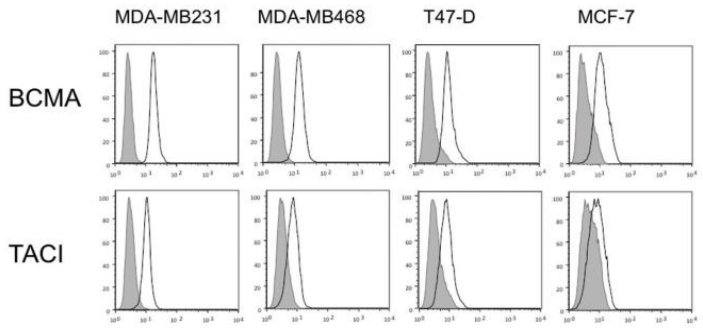

Supplemental Figure 1. BCMA and TACI receptors are expressed in breast carcinoma cells. Expression of APRIL receptors BCMA and TACI in carcinoma cell lines (MDA-MB231, MDA-MB468, T47D, MCF7). Cells were stained with anti-BCMA (polyclonal goat antibody, R&D) and –TACI (clone 1A1-K21-M22, BD Bioscience) antibodies; samples were acquired in a LSR II flow cytometer (BD Bioscience) and analyzed with FlowJo software. Histogram overlays show isotype control (shaded) and BCMA and TACI receptors (solid line).

Supplemental Figure 2

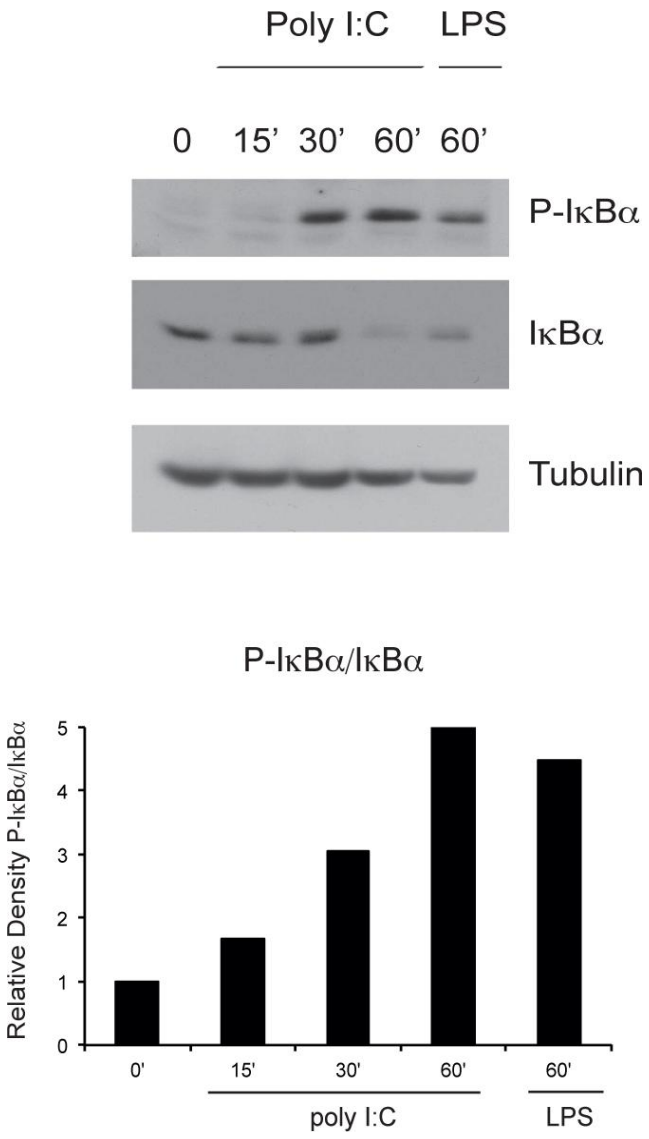

Supplemental Figure 2. Poly I:C induces NF-kB activation in MDAMB231 cells.
Western Blot shows IκBα phosphorylation and degradation in MDA-MB231 cells stimulated with poly I:C in a time course (LPS, positive control). Graph below shows the ratio P-IκBα/IκBα; relative band intensity was quantified by ImageJ software.

Supplemental Figure 3

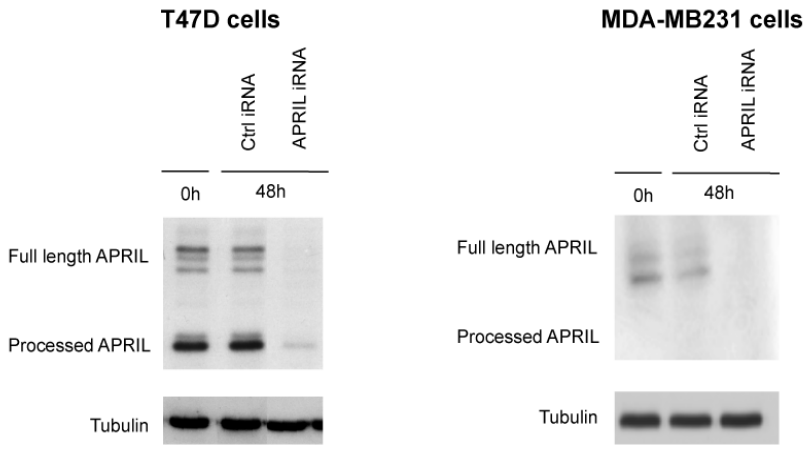

Supplemental Figure 3. APRIL expression after silencing experiments in breast carcinoma cell lines.
Western blot show APRIL expression at 48 hours in T47D and MDA-MB231 cells after transfection with Ctrl- and APRIL-iRNA. Time 0h represents untransfected cells.

Supplemental Figure 4

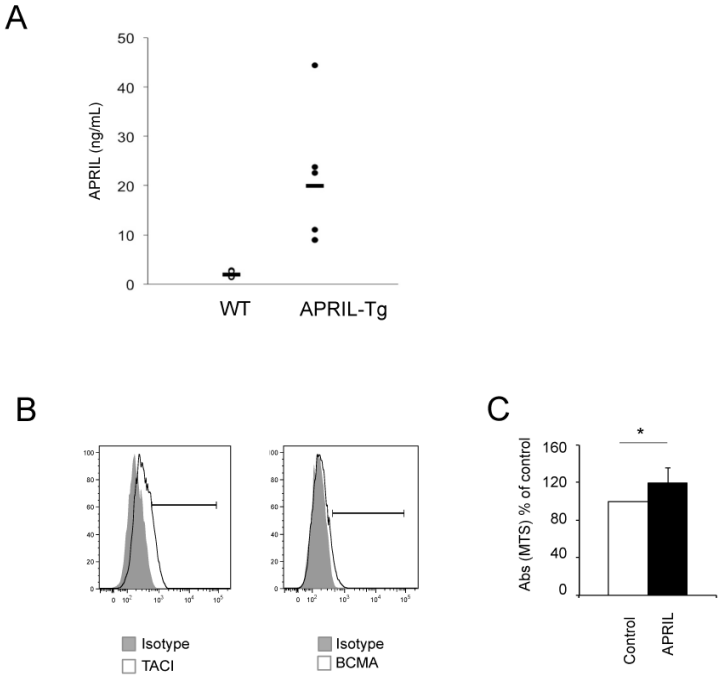

Supplemental Figure 4. 4T1 orthotopic tumors in APRIL-Tg mice.
(A) Graph shows quantification of hAPRIL protein in the blood of APRILTg and WT mice determined by ELISA using a commercial kit (Bender MedSystem). Mean is shown, *n* = 6/group.
(B) BCMA and TACI expression in 4T1 cells. 4T1 cells were stained with anti-mBCMA (clone 161616, R&D) and mTACI antibodies (clone 8F10, BD) and analyzed by flow cytometry. Histogram overlays show isotype control (shaded) and BCMA and TACI receptors (solid line).
(C) Graph shows 4T1 proliferation in response to APRIL assessed by MTS assay. Briefly, 4T1 cells (5 x 10^3 cells/well) were cultured alone or with 200 ng/ml mAPRIL (R&D Systems), 48h hours later CellTiter AQueous One Solution Cell Proliferation Assay (Promega) was added (20 µl/well) and absorbance was measured in an ELISA reader (OD 492 nm). The experiment was repeated twice (*n* = 8). *p ≤0.05

Supplemental Figure 5

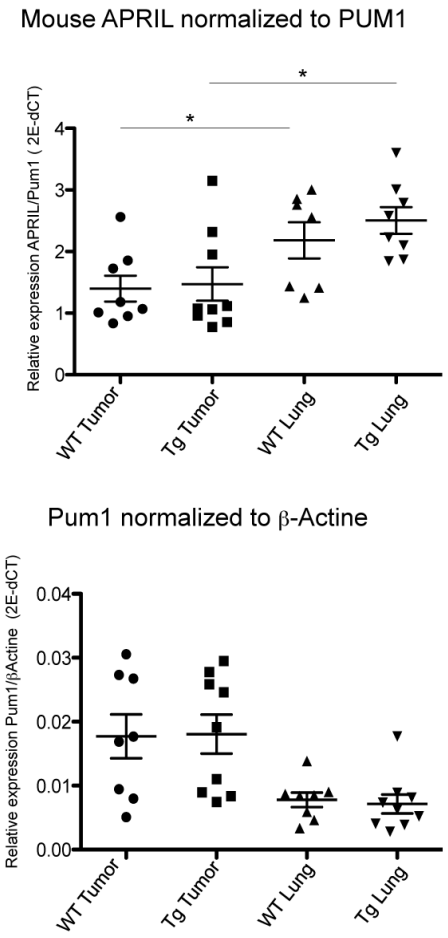

Supplemental Figure 5. Endogenous APRIL expression in 4T1 transplanted tumors and lung metastases.
Upper graph shows mRNA expression of mouse *April* in 4T1 tumors and lung metastases from 4T1- transplanted Control (*n* = 8) and APRIL-Tg mice (*n* = 9), measured by qPCR and normalized to *Pum1*. Lower graph shows mRNA expression of *Pum1* gene in the same samples normalized to β-actin. * p ≤0.05.

Supplemental Figure 6

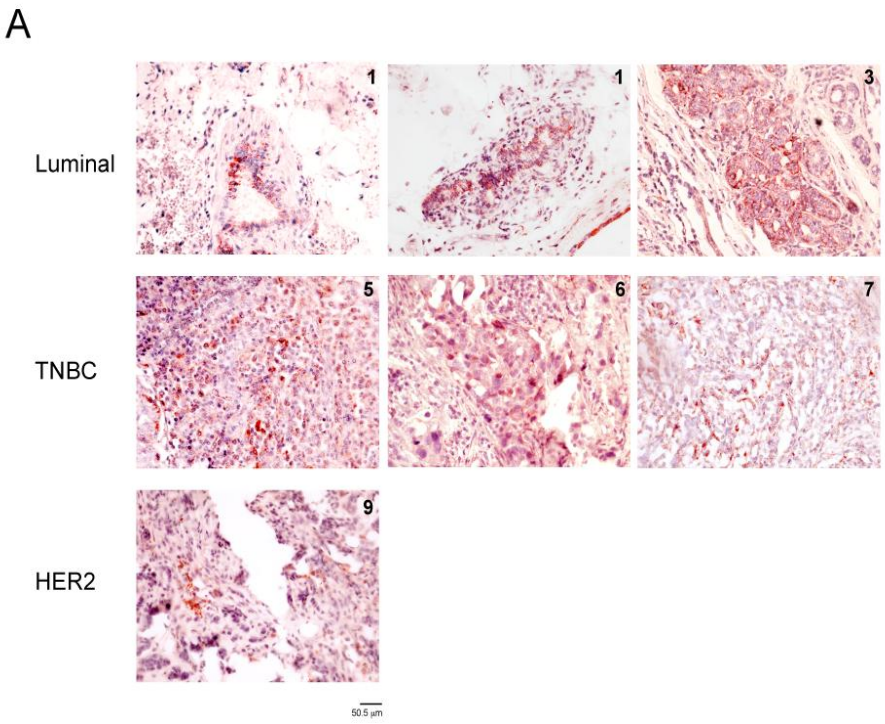

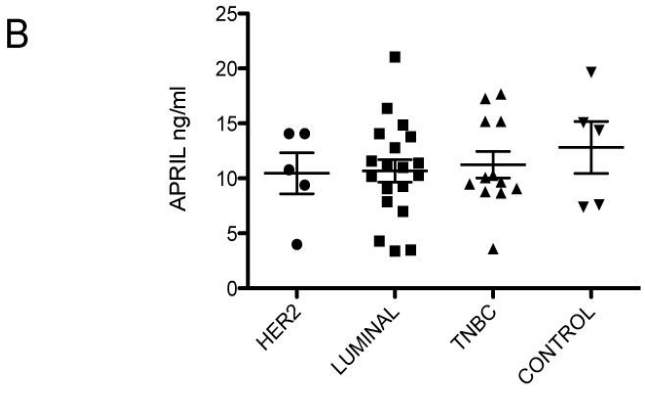

Supplemental Figure 6. APRIL expression in serum and tissue lesions of patients with Luminal, TNBC and HER2 breast cancer**.**
(A) Immunohistochemistry study of APRIL expression in paraffin-embedded luminal, TNBC and HER2 breast carcinoma lesions. Representative images of APRIL staining (brown) are shown. Numbers correspond to sample ID (Supplementary Table S2).
(B) APRIL concentration in the serum of breast carcinoma patients from luminal, TNBC and HER2 subtypes, measured by ELISA (eBioscience).

Supplemental Figure 7

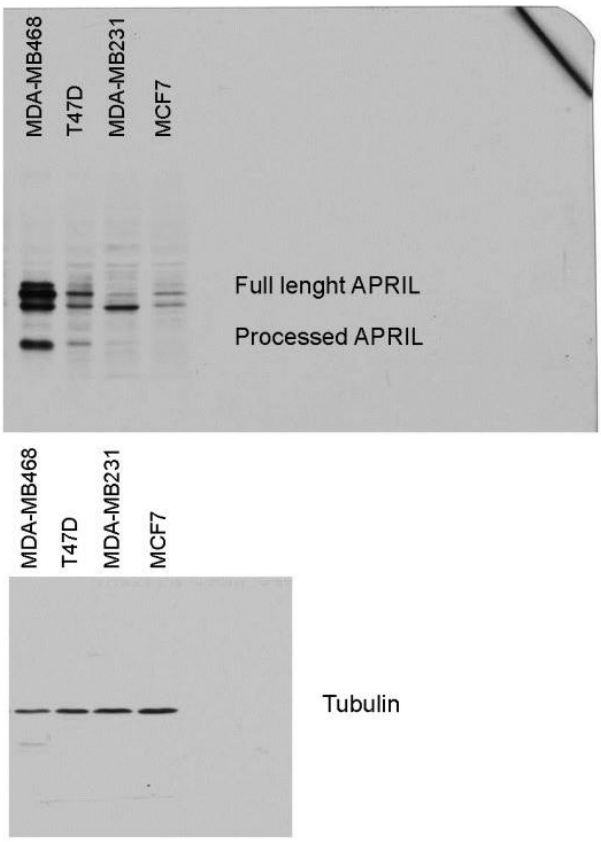

Supplemental Figure 7. APRIL expression in breast carcinoma cells.
Full-length blots show APRIL and tubulin expression in breast carcinoma cell lines.

Supplemental Figure 8

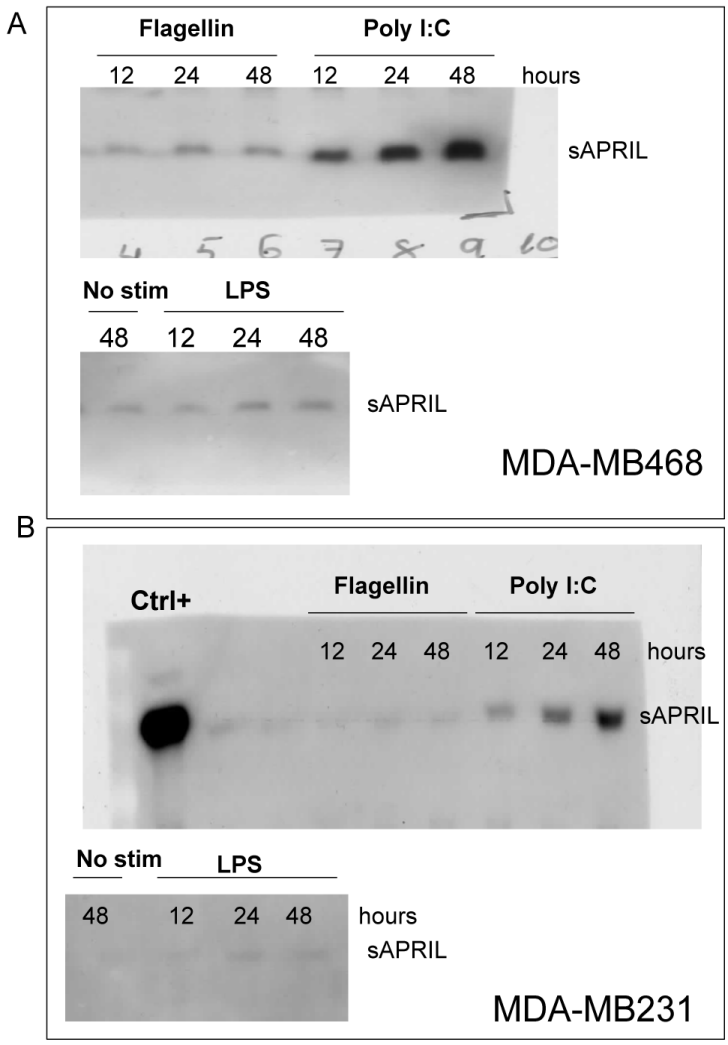

Supplemental Figure 8. Toll-like receptor ligand 3 induces APRIL secretion.
Full-length blots show soluble APRIL in the supernatants of MDA-MB468 (A) and MDA-MB231 (B) cells after TLR ligand stimulation.

Supplemental Figure 9

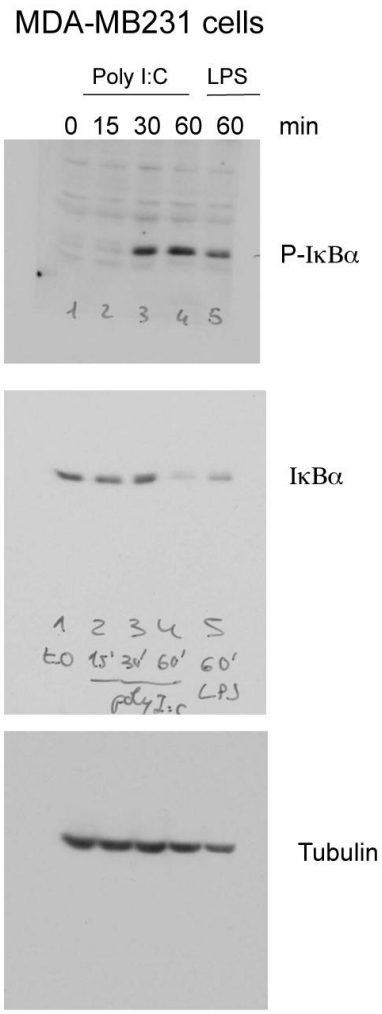

Supplementary Figure S9. Poly I:C induces NFκB activation in MDAMB231 cells.
Full-length blots show IκBα phosphorylation, IκBα degradation and tubulin expression in MDA-MB231 cells stimulated with poly I:C and LPS.

Supplemental Figure 10

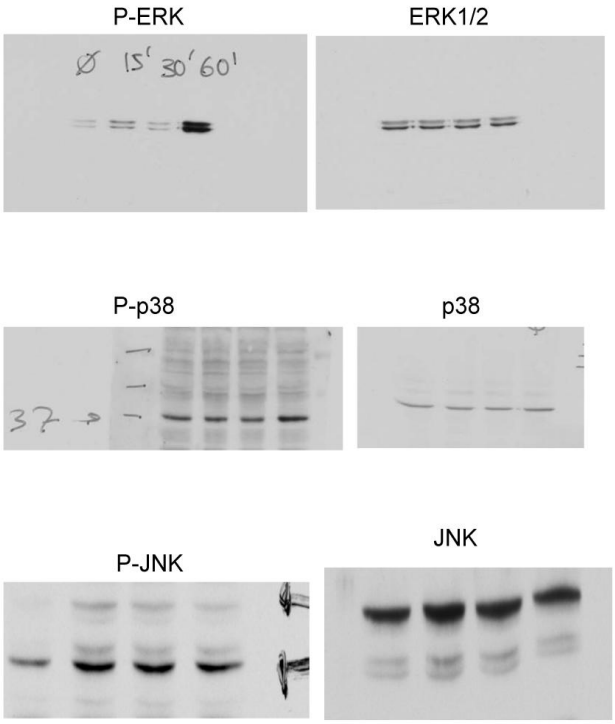

Supplemental Figure 10. APRIL activates ERK1/2, JNK1/2 and p38 MAP kinases in breast carcinoma cells**.**
Full-length blots show a time course for P-ERK, ERK, P-p38, p38, P-JNK and JNK in MDA-MB231 cells stimulated with APRIL.

Supplemental Figure 11

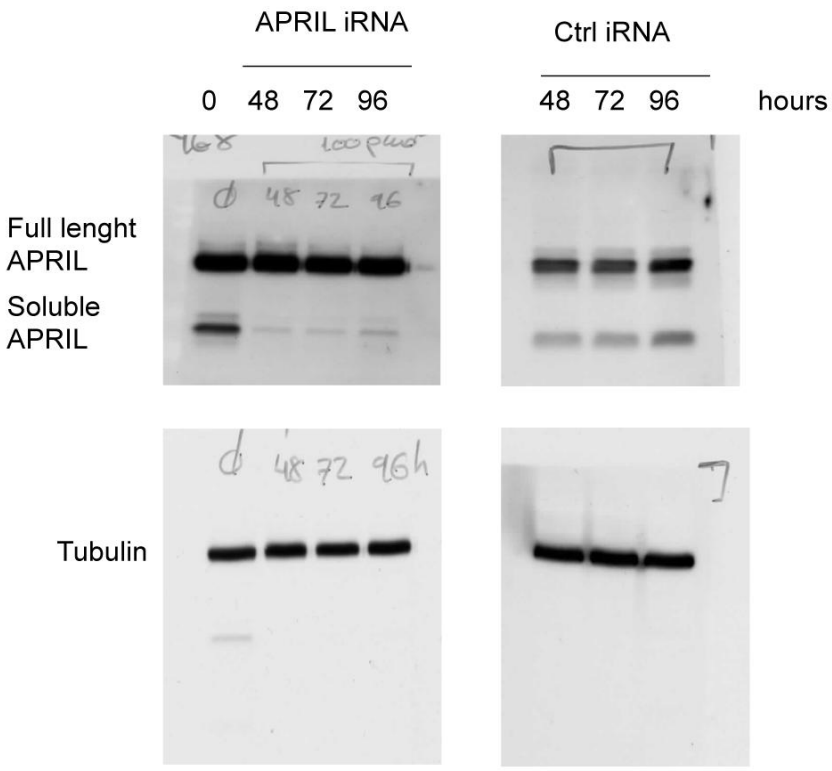

Supplemental Figure 11. APRIL expression after silencing experiments in breast carcinoma cell lines.
Full-length blots show APRIL and tubulin expression in MDA-MB231 cell transfected with control- or APRIL-interference RNA.

GENERAL DISCUSSION

GENERAL DISCUSSION

RANK/RANKL signaling pathway has emerged as a key pathway in the biology of the mammary gland. This thesis has been focused on the study of the impact of RANK overexpression in the development of the mammary gland and its differentiation during pregnancy, as well as in mammary tumor formation.

1. RANK/RANKL pathway in mammary gland development

1.1 RANK signaling pathway in mammary stem cell fate and alveolar commitment

The mammary gland is a unique organ, as it undergoes a variety of morphological changes throughout its development and differentiation during gestation mostly in response to hormonal stimulus (Hennighausen and Robinson 2001).

RANK/RANKL signaling pathway plays an essential role in the morphogenesis of the mammary gland. Indeed, RANK loss or overexpression in the mammary gland of genetically modified mouse models results in impaired lobulo-alveolar development of the gland during gestation and a subsequent lactation defect (Fata et al. 2000; Gonzalez-Suarez et al. 2007), suggesting that a tight regulation of RANK signaling is required for a proper mammary development.

Progesterone drives the epithelial cell expansion, ductal side-branching and alveolar morphogenesis of the mammary gland during early gestation (Brisken et al. 1998; Mulac-Jericevic et al. 2003). Previous published data reveals that RANKL signaling mediates the major proliferative response of mouse mammary epithelium to progesterone during mammary gland morphogenesis (Asselin-Labat et al. 2010; Joshi et al. 2010; Beleut et al. 2010). We have demonstrated that constitutive activation of RANK in the mammary gland results in an increased epithelial growth, enhanced ductal side-branching and precocious

small alveoli in virgin MMTV-RANK, a similar phenotype to that observed in WT virgin mammary glands under progesterone treatment *in vivo* (Atwood et al. 2000). The mimicking of acute progesterone stimuli driven by RANK overexpression supports that RANK mediates progesterone effects during mammary gland development.

RANK is expressed in basal and luminal mammary epithelial cells, and we found that MMTV-RANK mice overexpress RANK in both mammary populations. RANKL expression is restricted to a subset of luminal cells that are ER+PR+ (Beleut et al. 2010). Our results showed that RANK overexpression resulted in an expansion of both basal and luminal populations in virgin and pregnant mice. Importantly, previous studies suggested that RANKL signaling could mediate the expansion of the mammary stem cell population by paracrine signaling driven by progesterone in mice (Asselin-Labat et al. 2010; Joshi et al. 2010). This hypothesis was further supported by the decreased MaSC self-renewal ability *in vitro* in progesterone-treated mice with specific deletion of RANK in the mammary epithelium (Schramek et al. 2010). Consistent with these data, we showed that constitutive activation of RANK signaling in the mammary gland resulted in an expansion of mammary stem cells, as evidenced not only by the increased mammary repopulating ability *in vivo* in MMTV-RANK MECs, compared to WT, but also by the higher Sox9 and Slug expression, both genes that have been described to mediate MaSC function (Guo et al. 2012). These results are in correlation with previous findings in our laboratory, with increased frequency of breast cancer stem cells in RANK overexpressing human breast cell lines (Palafox et al. 2012).

In addition to RANK signaling, previous published data reveals that WNT signaling pathway contributes to the regulation of MaSC self-renewal and differentiation responses in the mouse mammary gland (Zeng and Nusse 2010; van Amerongen, Bowman, and Nusse 2012). Importantly, it has been recently shown that progesterone-triggered RANKL/RANK paracrine signaling stimulates the expression of R-spondin1 (Rspo1) protein in luminal ER-PR- cells (Joshi et al. 2015), which in turn cooperates with Wnt4 promoting basal MaSC-enriched and luminal progenitor cell expansion (Cai et al. 2014). Consistently, our global gene expression profiles from WT and MMTV-RANK primary acinar cultures at midgestation showed a clear up-regulation in Rspo1 expression not only in MMTV-RANK, but also in WT RANKL-treated acini, compared to WT. These results suggest that Rspo1-induced Wnt4 signaling mediated by the RANK pathway might contribute to the increased mammary repopulating ability in RANK overexpressing mice.

Further characterization of lineage-specific keratins supported an increase in K5+/K8+ and K14+/K8+ double positive cells, compared to WT glands. These cells have been proposed as bipotent progenitors blocked in differentiation (Li et al. 2007; Chakrabarti et al. 2012). In addition, we showed that K14+/K8+ cells were found *in vitro* in colonies derived from basal and luminal populations, consistent with previous data (Shackleton et al. 2006), whereas K5+/K8+ were only found in basal colonies. Previous studies demonstrate that mammary glands initially develops from multipotent embryonic K5+K14+ progenitors, which gave rise to both myoepithelial cells and luminal cells (Van Keymeulen et al. 2011). K5 expression is confined to the mammary basal compartment, whereas K14 is expressed in both basal and luminal compartments in pre-pubertal mammary glands, supporting that K5 and K14 mark different populations of cells within the mammary epithelium (Sun et al. 2010). Together, our results indicate that MMTV-RANK mice accumulate intermediate progenitors at different stages of differentiation within the mammary epithelium hierarchy.

Despite the increased proliferation of the mammary epithelium and the expansion of both RANK+ basal MaSC-enriched and luminal populations, our results indicated that MMTV-RANK mice showed an impaired alveolar differentiation and lactation failure during pregnancy as previously reported (Gonzalez-Suarez et al. 2007). These results suggest that the lack of alveologenesis in RANK overexpressing mice is not due to a reduced volume of luminal cells in favour to basal cells, and point out to a specific defect in the alveolar commitment.

Moreover, RANK overexpression has dramatic effects on the distribution of luminal subpopulations within the mammary epithelium. MMTV-RANK glands showed a decrease in Sca-1 and PR, both markers of luminal differentiation (Sleeman et al. 2007; Chou, Provot, and Werb 2010), as well as increased CD24+CD49b+ and CD24+Sca1- mammary populations within the luminal compartment. Previous published data have shown that these populations have higher colony forming ability *in vitro*, indicating that they are enriched in luminal progenitor cells (Sleeman et al. 2007; Shehata et al. 2012).

In contrast, a significant decrease in luminal CD61+ alveolar progenitors was shown in both virgin and early gestant MMTV-RANK mice. Despite this important drop in CD61 levels, luminal cells derived from MMTV-RANK mammary glands did not reduce their clonogenic ability *in vitro*, which was enhanced under RANKL treatment. These results demonstrated the existence of different luminal progenitors within the mammary gland. Elf5 is a transcription factor highly expressed in luminal CD61+ progenitor population that

specifies the alveolar-cell fate during pregnancy (Oakes et al. 2008). Our results showed that luminal cells derived from virgin MMTV-RANK glands have a decreased Elf5 expression, consistent with the decreased luminal CD61+ population, providing a rationale for the impaired alveolar differentiation observed in these mice. Similar to MMTV-RANK, previous data reveals that the amount of CD61+ cells is profoundly reduced in mammary glands from virgin and gestant STAT5 or Elf5 *knockout* mice, resulting in a deficient mammary alveologenesis and lactation failure (Zhou et al. 2005; Choi et al. 2009; Yamaji et al. 2009).

Mammary secretory differentiation at midgestation depends on the binding of prolactin to its receptor (PrlR), the activation of the downstream JAK2-STAT5 signaling pathway, and the transcription of Elf5 (Hennighausen and Robinson 2001; Srivastava et al. 2003; Harris et al. 2006). Importantly, our results showed a severe reduction in PrlR, p-STAT5 and Elf5 levels at midgestation in MMTV-RANK mammary glands, and therefore a subsequent complete alteration in the transcripts for milk proteins β-casein and WAP, compared to WT mice. These results suggest that constitutive activation of RANK signaling in the mammary gland at midgestation disrupts alveolar cell fate through negative regulation of the prolactin-induced STAT5/Elf5 signaling pathway.

Previous data indicate a negative regulation in PrlR and β-casein expression levels induced by progesterone in WT mice during gestation (Nishikawa et al. 1994). Our results demonstrated a disrupted mammary alveolar differentiation under physiological levels of RANK in midgestant WT acini treated with RANKL *in vitro,* evidenced by a significant decrease in WAP, β-casein, PrlR and p-STAT5 levels. Together, these data support that RANKL signaling repress functional alveologenesis and milk protein gene expression in WT mice during pregnancy, and therefore that contributes to the negative regulation of lactogenesis driven by progesterone.

The modest increase in Elf5 levels observed in RANKL-treated WT acini could be explained by recent published data by Lee et.al, where they demonstrate that progesterone induces Elf5 expression and precocious mammary gland differentiation in the virgin mammary gland by paracrine signaling through RANKL. In contrast, we showed that inhibition of RANKL signaling *in vivo* with Rank-Fc in WT mammary glands during gestation increased Elf5 and STAT5 levels, forcing the differentiation of luminal cells towards a premature lactating phenotype with significantly increased WAP expression levels. A significant reduction in the colony forming ability *in vitro* confirmed a more differentiated phenotype in RANKL-inhibited WT mice, compared to corresponding non-treated WT controls.

Collectively, these data support that progesterone-RANKL axis plays both positive and negative roles in the development of the mammary gland. During early gestation, progesterone-RANKL signaling is required to induce mammary gland proliferation and differentiation. At midgestation, progesterone-RANKL interferes with alveolar differentiation and lactation, mediated in part by a negative crosstalk between progesterone receptor and STAT5 as previously described (Buser et al. 2007). Moreover, we have also demonstrated that RANK overexpression signaling expands basal and luminal mammary compartments and disrupts mammary lineage commitment, preventing the formation of a functional milk-producing mammary gland by inhibiting the PrlR/STAT5/Elf5 signaling pathway.

1.2 Functional dissection of molecular pathways activated by RANK

Recent findings from our laboratory show that over-activation of RANK signaling pathway in MCF10A human breast epithelial cell line results in a constitutive activation of several pathways, including NF-kB, PI3K-Akt, p38 and ERK (Palafox et al. 2012). These signaling pathways downstream of RANKL/RANK play a positive role in the morphogenesis of the mammary gland and its differentiation during pregnancy (Madrid et al. 2001; Gonzalez-Suarez et al. 2007; Whyte et al. 2009; Liu et al. 2010; C.-C. Chen et al. 2012), suggesting that they can contribute to the disrupted mammary cell fate or the impaired alveolar secretory differentiation during pregnancy in RANK overexpressing glands.

1.2.1 NF-kB signaling pathway in epithelial cell fate of the virgin mammary gland

Multiple evidences indicate that NF-kB signaling pathway is important for mammary gland development (Yixue Cao and Karin 2003). Indeed, non-canonical NF-kB signaling pathway controls mammary epithelial cell proliferation in response to RANK signaling via Cyclin D1 (Y. Cao et al. 2001). Gonzalez-Suarez et.al demonstrated an activation of the canonical NF-kB pathway, with increased p65 nuclear translocation, in MMTV-RANK MECs under RANKL stimulation *in vitro*, compared to WT (Gonzalez-Suarez et al. 2007). These results led to

the hypothesis that enhanced activation of NF-kB could mediate the expansion in MaSC and luminal progenitors observed in MMTV-RANK mammary glands. However, in this thesis we could not detect clear differences neither in nuclear or cytoplasmic p65 levels, nor in p52-p100 expression between WT and MMTV-RANK virgin mammary glands. These results suggested that either NF-kB pathway was not constitutively active or we were not able to see its activation at the protein level in MMTV-RANK mammary epithelial cells in the absence of acute RANKL stimuli. In agreement, we did not observe activation of NF-kB signaling, revealed by P-IkB or P-p65, in FACs-isolated basal CD24lo CD49fhi or luminal CD24hi CD49flo population, contrary to previous published data (Pratt et al. 2009), neither in WT nor in MMTV-RANK cells. Activation of NF-kB signaling is a transient and cyclical event due to repeated degradation and re-synthesis of IkB inhibitory members (Gilmore 2006; Hoffmann, Natoli, and Ghosh 2006). Therefore, one possible explanation could be that we missed p65 nuclear translocation in WT and RANK overexpressing MECs. In fact, a clear phenotype was observed in the presence of several inhibitors of NF-kB signaling, suggesting that the pathway is indeed active.

It has been reported that NF-kB signaling pathway regulates cell fate decisions in the immune system and mammary tumors (Liu et al. 2010; X. Zhang et al. 2013). We demonstrated that NF-kB is an essential regulator of the mammary stem cell fate, controlling the balance between MaSC self-renewal and differentiation into the luminal lineage. According to published data, post-transcriptional IkBα modifications including phosphorylation and sumoylation result in alterations in skin homeostasis, as decreased PS-IkBα is associated with an induction of the keratinocyte differentiation process (Mulero et al. 2013; Perkins 2013). Therefore, we hypothesize that the increased PS-IkBα form observed in NF-kB-inhibited WT and MMTV-RANK basal cultures might play a relevant role inducing stemness in the mammary epithelium. In addition, inhibition of NF-kB signaling in the luminal compartment promoted luminal cell transdifferentiation into basal lineage, supporting that NF-kB signaling pathway is also essential for differentiation and maintenance of the luminal lineage in the mammary epithelium. Importantly, given the lack of differences between WT and MMTV-RANK basal and luminal colonies, we demonstrate that the alterations in mammary cell fate previously described in RANK overexpressing glands cannot be uniquely explained by enhanced activation of NF-kB signaling pathway.

1.2.2. NF-kB, MAPK and PI3K/Akt signaling pathways in mammary alveolar secretory differentiation

According to published data, increased RANK/RANKL signaling throughout gestation activates canonical NF-kB signaling and consequently mammary epithelial cell proliferation in WT and MMTV-RANK glands (Gonzalez-Suarez et al. 2007). However, NF-kB pathway disrupts STAT5 tyrosine phosphorylation and β-casein gene expression at midgestation (Geymayer and Doppler 2000). PI3K-Akt and MAPK signaling pathways play a relevant role during gestation modulating the PrlR/JAK2/STAT5 signaling and the mammary epithelial cell differentiation process (C.-C. Chen et al. 2010; Schwertfeger, Richert, and Anderson 2001; Nyga et al. 2005). We demonstrated that NF-kB, PI3K-Akt, p38 and ERK play a positive role in mammary gland alveologenesis, evidenced by decreased WAP mRNA expression levels in midgestant WT MECS treated *in vitro* with specific inhibitors for these signaling pathways. However, WAP levels were not rescued in the presence of prolactin + RANKL + inhibitors, suggesting that none of these pathways downstream of RANK are directly responsible of the impaired secretory alveologenesis induced by RANKL. In addition, despite the increased NF-kB and, to a lesser extent, ERK protein levels found in midgestant WT and MMTV-RANK MECs after 24h prolactin + RANKL treatments *in vitro*, we demonstrated that alterations in p-STAT5 levels in both WT and MMTV-RANK MECs under short-term treatments could not be explained by increased levels in any of these signaling pathways downstream of RANK. Together, these data suggest that additional mechanisms may contribute to the impaired STAT5 phosphorylation under RANK signaling overactivation.

The complexity of the JAK2/STAT5 signaling pathway regulation in the mammary gland is given by the numerous regulatory mechanisms that can attenuate STAT5 phosphorylation during pregnancy (W. Chen, Daines, and Khurana Hershey 2004). Preliminary results suggested that expression levels for the family of inducible suppressors of cytokine signaling (SOCS) proteins, which are induced by activated STAT5 forming a negative feedback loop that attenuates STAT5 phosphorylation (Alexander and Hilton 2004; Jasmin et al. 2006), were not increased in midgestant WT MECS under RANKL treatment. In addition expression levels of ErbB4, a tyrosine kinase receptor that phosphorylates STAT5 in a JAK2 independent manner (Jones et al. 1999; Long et al. 2003), were increased in WT MECs under prolactin + RANKL treatment, suggesting that lactogenic differentiation

impairment observed upon RANK signaling activation may not be due to reduction in ErbB4 levels.

Another possible mechanism regulating STAT5 lactogenic activity could be STAT3, which antagonizes with STAT5 and determines the end of lactation (Humphreys et al. 2002; Desrivières et al. 2006). Our preliminary results showed no differences in p-STAT3 levels between midgestant WT and MMTV-RANK mammary glands, although further experiments need to clarify whether STAT3 is competing with STAT5 activation throughout gestation.

Given that activation of JAK2/STAT5 signaling is a reversible process, its deactivation can also be achieved through counteracting enzymes, such as the phosphotyrosine phosphatases SHP1 and SHP2 (Valentino and Pierre 2006). Interaction of their homology 2 (SH2) domains with STAT5 phosphorylated tyrosine residues triggers their phosphatase activity disrupting STAT5 activation (Desrivières et al. 2006). Other phosphotyrosine phosphatases involved in the regulation of JAK2/STAT5 pathway include CD45, a transmembrane molecule active in hematopoietic cells (Irie-Sasaki et al. 2001), and PTP1B and TC-PTP phosphatases (Aoki and Matsuda 2002). In addition alterations in c-Src, a tyrosine kinase that binds to activated RANK via its SH2 domain and can directly tyrosine-phosphorylate the activation site of STAT5 (Okutani et al. 2001; Izawa et al. 2012), can also play a relevant role in the negative regulation of JAK2/STAT5 signaling pathway in RANK overexpressing mammary glands.

Future projects in our laboratory will aim to enquire the molecular mechanisms by which enhanced RANK/RANKL signaling in the mammary gland at midgestation interferes with JAK2/STAT5 activation and subsequent lactation defect.

2. RANK and RANKL in mammary tumorigenesis

2.1. RANK overexpression in spontaneous mammary tumor formation

Progesterone and their synthetic derivatives (progestins), commonly used in combined hormone replacement therapy in postmenopausal women, have been associated with an increased risk of breast cancer (Pike et al. 1997). During last years, RANK signaling

pathway has emerged as a key regulator in mammary gland tumorigenesis, being the main mediator of the protumorigenic effects of progesterone in the mammary gland (Gonzalez-Suarez et al. 2010; Schramek et al. 2010).

Aging and reproductive story are two recognized risk factors in human breast carcinogenesis (Bernstein 2002; Medina 2004). Our results showed that elderly MMTV-RANK virgin mice show extensive hyperplasias, consistent with previous observations (Gonzalez-Suarez et al. 2007), but do not form tumors. Previous data showed that MPA alone was not enough stimuli to give rise to tumors in virgin mice (Gonzalez-Suarez et al. 2010). These results indicate that physiological levels of progesterone were probably not sufficient to induce mammary tumor formation in virgin MMTV-RANK mice, suggesting that progesterone peaks accumulated through successive gestational periods could induce protumorigenic effects in multipregnant MMTV-RANK mammary glands.

The increased mammary epithelial cell proliferation induced by progesterone-RANKL axis, together with the expansion of both basal and luminal mammary gland populations in virgin MMTV-RANK mice, resulted in frequent alterations in the mammary epithelium, such as accumulation of multiple luminal layers or disorganization of both basal and luminal mammary epithelial cells. These morphological abnormalities in RANK overexpressing virgin glands could be considered as early preneoplastic lesions, in agreement with the spontaneous mammary tumor formation in MMTV-RANK mice after multiple gestations.

It has been previously shown that K14 and K5 are organized in different gene clusters within tumors (Z. Li et al. 2007). In addition, K14 is expressed not only in basal K5+ tumor cells, but also in luminal K8+, supporting that K14 and K5 mark different population of cells within mammary tumors (Li et al. 2007; Herschkowitz et al. 2007). Importantly, each mammary tumor derived from multiparous MMTV-RANK mice was very heterogeneous in terms of clinical and molecular features, and contained several K14+/K8+ cells, whereas in contrast K5+/K8+ cells were scarce in these tumors. This result is in line with the accumulation of K14+/K8+ bipotent progenitors in virgin MMTV-RANK mammary glands described above, and suggests a direct link between alterations in mammary stem cell fate and tumor initiation in RANK overexpressing mice. According to previous data, the different sporadic and familial breast tumor subtypes in humans may have their origin in different types of stem or progenitor cells (Melchor and Benítez 2008). Therefore, the high inter- and intratumor heterogeneity observed in spontaneous MMTV-RANK tumors suggests that each tumor may originate from stem or progenitors that differentiate into different tumor cell phenotypes. An alternative cell target of transformation in

multipregnant MMTV-RANK mice could be the parity-induced mammary epithelial cells (PI-MEC). These cells originated during pregnancy have stem cell properties and do not undergo apoptosis during post-lactational remodeling (K.-U. Wagner et al. 2002; Matulka, Triplett, and Wagner 2007). Moreover, PI-MECs have been proposed to be the tumorigenic target for some multiparous MMTV-driven oncogenic models such as MMTV-NEU mice (Henry et al. 2004), and therefore their accumulation along the successive MMTV-RANK pregnancies could lead to acquisition of mutations and consequently initiation of mammary tumors in MMTV-RANK mice.

The identity of the cell(s) that originates MMTV-RANK tumors remains unknown. Previous data indicated that these tumor cells of origin represent one of the key determinants of the tumor's histological features (Molyneux et al. 2010). The final resultant tumor phenotype depends on the reciprocal interaction between the plasticity of tumor cells along tumor progression, and the differentiating capabilities of the oncogenic event(s) (Abollo-Jimenez et al. 2011). Thus, characterization of highly heterogeneous advanced mammary tumors from RANK overexpressing mice does not allow us to determine whether these tumors derive from multipotent poorly differentiated stem/progenitor cells, basal and luminal accumulated mammary epithelial populations, or both hypotheses. These observations suggest that tracing different cell lineages (Kretzschmar and Watt 2012) during mammary gland development and tumor initiation would elucidate the cell(s) that acquire the genetic hit(s) resulting in tumor formation in RANK overexpressing mice.

Analyses in WT mammary glands revealed that the expression levels of RANK increases with age and parity. Moreover, we showed that mammary ducts, preneoplastic lesions and tumors from aged multiparous WT females strongly expressed RANK and exhibited an accumulation of K14+/K8+ cells. These results suggested that RANK-driven phenotypes are reproduced in elderly WT mammary glands and therefore it could have clinical relevance in humans. Indeed, similar changes have been reported in aged women breast, with an age-dependent expansion of multipotent progenitors and luminal cells expressing basal markers (K14) (Garbe et al. 2012). As women receiving combined estrogen plus progesterone replacement therapy, but not estrogen alone, have an increased risk of developing breast cancer (Chlebowski et al. 2013), the association between progesterone-RANKL signaling with aging and reproductive story highlight RANK as a candidate biomarker for breast cancer prediction risk.

2.2. Cooperation of RANK signaling with other oncogenes in spontaneous tumor-prone mouse models

Mammary gland tumors induced by MPA/DMBA *in vivo* are PR+, and RANKL is expressed in PR+ cells, acting as a mediator of progesterone; therefore RANK signaling is associated with ER+PR+ tumor subtype (Gonzalez-Suarez et al. 2010). However, it has been described that RANK is mostly expressed in hormone receptor negative human adenocarcinomas. These tumors lacking ER and PR expression are described to have a poor prognosis based on a reduced overall survival, aggressive tumor phenotypes, high rates of recurrence and metastasis, and the lack of targeted therapies (Santini et al. 2011; Pfitzner et al. 2014). We decided to investigate the cooperation of RANK overexpression in pregnancy-independent MMTV-NEU or MMTV-PYMT oncogene-driven models which develop ER-PR- tumors. The expression profile of RANK and RANKL in NEU and PYMT overexpressing mammary carcinomas resemble that found in human breast ER-PR- adenocarcinomas, and therefore these mouse models become ideal tools to investigate the role of RANK signaling in hormone receptor negative late-stage carcinomas.

Importantly, two simultaneous studies published in 2010 showed contradictory results on the effect of RANK signaling on mammary tumor formation capacity in NEU overexpressing mice. Schramek et al showed that specific deletion of RANK in mammary epithelia did not alter both incidence and latency to mammary tumor formation in MMTV-NeuT mice (Schramek et al. 2010). In contrast, Gonzalez-Suarez et.al showed that blockage of RANKL/RANK signaling with RANK-Fc in MMTV-NEU$^{+/+}$ mice before tumor onset significantly decreases the incidence of spontaneous preneoplastic lesions, tumors and lung metastasis (Gonzalez-Suarez et al. 2010). Now we demonstrated that genetic deletion of RANK in PYMT-overexpressing glands (MMTV-PYMT$^{+/-}$; RANK$^{-/-}$) resulted in a significant delay in tumor formation, as well as reduced tumor and metastasis incidence, supporting a positive role for RANK signaling in early stages of tumorigenesis and metastatic spread to the lungs. These discrepancies between Schramek results and ours could be explained because the (MMTV)-Cre rank$^{flox/\Delta}$ system might not be 100% efficient (K. U. Wagner et al. 1997; K. U. Wagner et al. 2001). Moreover, although the MMTV promoter is expressed in most mammary epithelial cells, it is not expressed in the stroma, which constitutes a critical regulator in mammary tumorigenesis (Wiseman and Werb 2002; Vargo-Gogola and Rosen 2007). By contrast, we genetically delete RANK in both the

mammary epithelium and the stroma, and RANK-Fc will block RANK signaling in both compartments.

It has been previously shown that tumor cells can disseminate systemically from earliest epithelial alterations in MMTV-NEU and MMTV-PYMT mice, being an early event in tumor progression in these transgenic mouse models (Hüsemann et al. 2008). Importantly, the significant reduction in tumor and metastasis-initiating ability in MMTV-PYMT$^{+/-}$; RANK$^{-/-}$ tumor cells compared to MMTV-PYMT$^{+/-}$; RANK$^{+/+}$, when injected in limiting dilution, demonstrates that RANK is essential for the intrinsic metastatic potential of tumor cells, independently of primary tumor incidence.

According to these data, one can speculate that RANK signaling overexpression would positively contribute to mammary tumorigenesis in MMTV-NEU and MMTV-PYMT mouse models. Unexpectedly, we found that RANK overexpression reduced tumor incidence in MMTV-NEU$^{+/+}$ mammary glands, and significantly increased tumor latency in both MMTV-NEU$^{+/+}$ and MMTV-PYMT$^{+/-}$ glands, indicating that high levels of RANK interfere with tumor initiation in these oncogene-driven mouse models.

Based on these unexpected results we analyzed mammary glands from both MMTV-NEU$^{+/+}$; RANK$^{+/tg}$ and MMTV-PYMT$^{+/-}$; RANK$^{+/tg}$ mice, and we confirmed the same alterations in mammary cell fate previously described in virgin MMTV-RANK glands (discussed above) (Pellegrini et al. 2013). Understanding the relation between normal epithelial cell types and mammary tumors is essential to gaining insight into cell types predisposed to tumorigenesis. Despite the efforts made, the cell that originates mammary tumors in MMTV-NEU and MMTV-PYMT mice remains controversial. Some studies support that given the high luminal progenitor signature in NEU and PYMT overexpressing tumors, luminal progenitor-enriched population contains the tumor cell of origin in those oncogene-driven mouse models (Lim et al. 2010; Visvader 2009; Shackleton et al. 2006). In contrast, other studies support that NEU and PYMT induced mammary tumors can arise from both basal and luminal mammary populations (Asselin-Labat et al. 2011; W. Zhang et al. 2013). In accordance with the latter, our results demonstrated that basal and luminal CD61+/- mammary populations from MMTV-NEU$^{+/+}$ and MMTV-PYMT$^{+/-}$ mice were able to initiate tumors when transplanted into mammary glands from immunocompromised mice with similar incidence and latency. These results supported a NEU and PYMT oncogene-dominant model. RANK overexpression prevented tumor initiation from luminal and basal MMTV-neu cells but not in MMTV-PyMT. Importantly, these studies have some limitations; perhaps the most important disadvantage of using cell transplantation assays is that single cells may not behave in the context of a graft as they do during normal tissue

homeostasis (Watt and Jensen 2009; Kretzschmar and Watt 2012). This is particularly relevant in the context of the mammary gland, because MECs are normally organized and connected by intercellular junctions but are disaggregated into single-cell suspensions for transplantation disrupting paracrine signaling. If we consider that MMTV-PYMT$^{+/-}$; RANK$^{+/tg}$ primary tumors showed a faster growth and enhanced metastatic ability compared to MMTV-PYMT$^{+/-}$, we hypothesize that transplantation of both basal and luminal MMTV-PYMT$^{+/-}$; RANK$^{+/tg}$ MECs could induce a cellular switch that would offset the differences in both tumor latency and aggressiveness when compared to between MMTV-PYMT$^{+/-}$ MECs. By contrast, as no differences in mammary tumor growth were observed between MMTV-NEU$^{+/+}$ and MMTV-NEU$^{+/+}$; RANK$^{+/tg}$ mice, the significantly higher tumor latency observed in MMTV-NEU$^{+/+}$; RANK$^{+/tg}$ primary tumors might explain the lack for tumor formation when injecting MMTV-NEU$^{+/+}$; RANK$^{+/tg}$ MECs, irrespectively of the population of origin. . Further lineage tracing experiments in physiological conditions (Kretzschmar and Watt 2012) are required to elucidate not only the tumor cell of origin, but also the specific contribution of RANK signaling in NEU and PYMT oncogene-driven mouse models.

RANK overexpression in MMTV-NEU mammary glands resulted in an accumulation of hyperplastic lesions that do not progress into preneoplastic lesions and advanced carcinomas. In addition, our results also indicated a decrease in early MINs in non-transformed adult MMTV-NEU$^{+/+}$; RANK$^{+/tg}$ mammary glands. These results indicated a blockage in the transition from hyperplastic epithelium or hyperplastic lesions to MINs and adenocarcinomas. One possible explanation for this blockage in RANK and NEU or PYMT overexpressing glands could be that RANK behaves as a potent oncogene, as it has been shown that certain oncogenes can induce premature cell senescence or apoptosis in a process called oncogene-induced senescence/apoptosis (OIS/OIA) (Serrano et al. 1997; Wajapeyee et al. 2008). This hypothesis is supported by recent data from Xu et al, where they demonstrate a role for the RANK-activated downstream MAPK p38 and PI3K/AKT/mTOR signaling pathways inducing DNA damage responses, chromatin remodeling or chronic inflammation, processes leading to oncogene-induced senescence (Xu et al. 2014; Freund et al. 2010). In addition, OIS/OIA processes can also be induced by oncogenes such as *ras*, *BRAF^{V600E}*, *E2F1, Cdc6*, and by inactivation of tumor-suppressor genes including *PTEN, p53, p16* or *p21* (Courtois-Cox, Jones, and Cichowski 2008), therefore supporting that OIS/OIA are not mediated by a simple and linear pathway, but by an intricate signaling network (Xu et al. 2014). In our laboratory we are currently carrying out experiments to identify whether high levels of senescence or apoptosis in normal glands, hyperplasias and preneoplastic lesions could explain the delayed latency to

tumor formation in MMTV-NEU$^{+/+}$; RANK$^{+/tg}$ and MMTV-PYMT$^{+/-}$; RANK$^{+/tg}$ mice, compared to single mutants.

2.2.1. Contribution of RANK signaling to tumor aggressiveness and cancer stem cell pool expansion

Molecular characterization of mammary tumors derived from MMTV-NEU$^{+/+}$ and MMTV-NEU$^{+/+}$; RANK$^{+/tg}$ glands revealed that both genotypes formed homogeneous luminal tumors highly enriched for CD61+ cells, consistent with previous observations in NEU overexpressing mice (Vaillant et al. 2008).

We have also demonstrated that MMTV-PYMT$^{+/-}$; RANK$^{+/tg}$ preneoplastic lesions and adenocarcinomas showed an accumulation of K14+/K8+ cells, as previously observed in MMTV-RANK$^{+/tg}$ tumors, whereas a scarce presence of K5+/K8+ cells was observed. In addition, the significant increased tummorsphere formation ability *in vitro* (Dontu and Wicha 2005) and metastasis initiation ability *in vivo* demonstrated an enrichment in cancer stem cell population in MMTV-PYMT$^{+/-}$; RANK$^{+/tg}$ tumors.

Cancer stem cells are a subpopulation of tumor cells that share some characteristics with adult stem cells, such as self-renewal, ability to differentiate and quiescence (Jordan, Guzman, and Noble 2006). CSCs remain mostly in the resting stage of the cell cycle, and therefore are resistant to chemotherapy that mostly targets proliferating cells (Y. Zhang et al. 2012). Contrary to MMTV-PYMT$^{+/-}$; RANK$^{+/tg}$, genetic loss of RANK in MMTV-PYMT$^{+/-}$ tumor cells resulted in a significant reduction in tumorsphere and metastasis initiating ability. In addition, these tumors showed enhanced sensitivity to docetaxel, one of the most common chemotherapy agents used to treat patients with hormone-receptor negative tumors (Yagata, Kajiura, and Yamauchi 2011). We have also analyzed the relevance of pharmacological inhibition of RANKL (RANK-Fc) in MMTV-PYMT$^{+/-}$ tumors, as it represents a more clinically relevant model than constitutive genetic deletion of RANK. *In vivo* and *in vitro* analyses demonstrated a significant decrease in CSCs in PYMT overexpressing tumors under RANK-Fc treatment. Moreover, these RANK-Fc-treated tumor cells were less able to initiate tumors when implanted in a new host as compared to untreated cells. Together, these results support the use of neoadjuvant treatment with

RANKL inhibitors to reduce the frequency of tumor relapse and metastasis, and to increase the sensitivity to docetaxel in the clinical setting.

In addition, these PYMT-overexpressing RANK-Fc-treated tumors showed an up-regulation of several genes that are normally expressed during mammary alveologenesis and lactation, such as prolactin-induced protein (Pip), caseins and also multiple members of the secretoglobin family including mammoglobins (Anderson et al. 2007). Mammoglobins has been successfully used as breast cancer biomarker since their expression is associated with favorable clinicopathological features and low risk of relapse (Watson and Fleming 1996; Span et al. 2004). Therefore, this lactogenic tumor cell differentiation can contribute to the reduction in tumor-initiating ability in RANK-Fc-treated MMTV-PYMT tumors.

Importantly in humans, an increased RANK mRNA expression has been observed in ER-PR- breast tumors, which are more aggressive than other subtypes of tumors and contain a higher frequency of human breast cancer stem cells enriched CD44+/CD24- population (Palafox et al. 2012; Park et al. 2010; Ricardo et al. 2011). In addition, RANK could expand the CSC population in human cell lines (Palafox et al. 2012) as it does in MMTV-PYMT$^{+/-}$ mouse model. In accordance with these data, our Gene Set Enrichment Analysis (GSEA) results demonstrated that high RANK expression in human breast tumors correlates with high expression of genes sets that characterize mammary stem cells and luminal progenitors, and low expression of genes representative for luminal differentiation.

Altogether, we demonstrated that RANK signaling plays a complex role in mammary tumorigenesis, as it affects not only the bulk of progesterone-induced proliferative cells, but also the cancer stem cells self-renewal and differentiation ability. Therefore, blocking RANKL could be a novel therapy to treat both human hormone receptor positive and negative breast tumor subtypes. These data are clinically relevant, as an inhibitor of RANKL (Denosumab) is currently being used in the clinics for the treatment of tumor derived bone metastasis. If the results presented and discussed in this thesis project are confirmed, patients will effectively benefit from this new therapeutic strategy against breast cancer.

CONCLUSIONS

CONCLUSIONS

1. RANK signaling is a positive regulator of mammary stem cells, bipotent K14+K8+ progenitors and luminal progenitor cells.
2. RANK overexpression disrupts cell fate in virgin mammary glands, decreases CD61- alveolar progenitors and Sca1+ luminal mature cells and increases CD49b luminal progenitors.
3. NF-kB signaling pathway regulates the differentiation of the basal lineage into luminal lineage and maintenance of luminal lineage within the mammary epithelium in both WT and MMTV-RANK acini.
4. Accumulation of mammary stem cells and luminal progenitors observed in MMTV-RANK mice is not mediated by enhanced activation of NF-kB signaling pathway.
5. RANKL impairs alveolar secretory differentiation by inhibiting PrlR/JAK2/STAT5 signaling and transcription of Elf5 at midgestation not only in MMTV-RANK but also in WT mice.
6. Pharmacological inhibition of RANK (Rank-Fc) in physiological conditions induces precocious (G.10,5) and exacerbated (G.14,5) mammary alveologenesis through induction of the PrlR/JAK2/STAT5 signaling pathway.
7. RANKL downstream signaling pathways NF-kB, PI3K-AKT and MAPK play a positive role in mammary alveologenesis and are not directly responsible of the alveolar impairment induced by RANKL.
8. RANK overexpression results in an aberrant organization of the mammary epithelium affecting both basal (K14+ and K5+) and luminal (K8+) lineages.
9. Multiple gestations in aged MMTV-RANK mice lead to spontaneous preneoplastic lesions and tumors that are highly heterogeneous and composed by distinct mammary populations.
10. RANK overexpression in an oncogenic NEU or PYMT background delays mammary tumor formation.
11. MMTV-PYMT$^{+/-}$; RANK$^{+/tg}$ well-established tumors are more aggressive, with enhanced growing ability, expanded K14+K8+ cells, and higher capacity to metastasize, compared to MMTV-PYMT+/- tumors.

12. Basal CD24lo CD49fhi and Luminal CD24hi CD49flo CD61+/- MECs are able to initiate tumors in MMTV-neu and MMTV-PYMT mice.
13. Deletion of RANK in MMTV-PYMT mouse model increases tumor latency, decreases tumor growth and incidence, blocks lung metastasis and increases the sensitivity of these tumors to docetaxel.
14. Neoadjuvant RANKL inhibition with RANK-Fc in MMTV-PYMT mice induces tumor cell differentiation and decreases the cancer stem cell pool resulting in a reduced tumor-initiating ability.

BIBLIOGRAPHY

BIBLIOGRAPHY

Abell, Kathrine, Antonio Bilancio, Richard W. E. Clarkson, Paul G. Tiffen, Anton I. Altaparmakov, Thomas G. Burdon, Tomoichiro Asano, Bart Vanhaesebroeck, and Christine J. Watson. 2005. "Stat3-Induced Apoptosis Requires a Molecular Switch in PI(3)K Subunit Composition." *Nature Cell Biology* 7 (4): 392–98. doi:10.1038/ncb1242.

Akiyama, Taishin, Yusuke Shimo, Hiromi Yanai, Junwen Qin, Daisuke Ohshima, Yuya Maruyama, Yukiko Asaumi, et al. 2008. "The Tumor Necrosis Factor Family Receptors RANK and CD40 Cooperatively Establish the Thymic Medullary Microenvironment and Self-Tolerance." *Immunity* 29 (3): 423–37. doi:10.1016/j.immuni.2008.06.015.

Aldaz, C. M., Q. Y. Liao, M. LaBate, and D. A. Johnston. 1996. "Medroxyprogesterone Acetate Accelerates the Development and Increases the Incidence of Mouse Mammary Tumors Induced by Dimethylbenzanthracene." *Carcinogenesis* 17 (9): 2069–72.

Alexander, Warren S., and Douglas J. Hilton. 2004. "The Role of Suppressors of Cytokine Signaling (SOCS) Proteins in Regulation of the Immune Response." *Annual Review of Immunology* 22: 503–29. doi:10.1146/annurev.immunol.22.091003.090312.

Allred, D. C., G. M. Clark, R. Molina, A. K. Tandon, S. J. Schnitt, K. W. Gilchrist, C. K. Osborne, D. C. Tormey, and W. L. McGuire. 1992. "Overexpression of HER-2/neu and Its Relationship with Other Prognostic Factors Change during the Progression of in Situ to Invasive Breast Cancer." *Human Pathology* 23 (9): 974–79.

Allred, D. Craig, and Daniel Medina. 2008. "The Relevance of Mouse Models to Understanding the Development and Progression of Human Breast Cancer." *Journal of Mammary Gland Biology and Neoplasia* 13 (3): 279–88. doi:10.1007/s10911-008-9093-5.

Anderson, D. M., E. Maraskovsky, W. L. Billingsley, W. C. Dougall, M. E. Tometsko, E. R. Roux, M. C. Teepe, R. F. DuBose, D. Cosman, and L. Galibert. 1997. "A Homologue of the TNF Receptor and Its Ligand Enhance T-Cell Growth and Dendritic-Cell Function." *Nature* 390 (6656): 175–79. doi:10.1038/36593.

Anderson, Steven M., Michael C. Rudolph, James L. McManaman, and Margaret C. Neville. 2007. "Key Stages in Mammary Gland Development. Secretory Activation in the Mammary Gland: It's Not Just about Milk Protein Synthesis!" *Breast Cancer Research: BCR* 9 (1): 204. doi:10.1186/bcr1653.

Aoki, Naohito, and Tsukasa Matsuda. 2002. "A Nuclear Protein Tyrosine Phosphatase TC-PTP Is a Potential Negative Regulator of the PRL-Mediated Signaling Pathway: Dephosphorylation and Deactivation of Signal Transducer and Activator of Transcription 5a and 5b by TC-PTP in Nucleus." *Molecular Endocrinology (Baltimore, Md.)* 16 (1): 58–69. doi:10.1210/mend.16.1.0761.

Asselin-Labat, Marie-Liesse, Kate D. Sutherland, Holly Barker, Richard Thomas, Mark Shackleton, Natasha C. Forrest, Lynne Hartley, et al. 2007. “Gata-3 Is an Essential Regulator of Mammary-Gland Morphogenesis and Luminal-Cell Differentiation.” *Nature Cell Biology* 9 (2): 201–9. doi:10.1038/ncb1530.

Asselin-Labat, Marie-Liesse, Kate D. Sutherland, François Vaillant, David E. Gyorki, Di Wu, Sheridan Holroyd, Kelsey Breslin, et al. 2011. “Gata-3 Negatively Regulates the Tumor-Initiating Capacity of Mammary Luminal Progenitor Cells and Targets the Putative Tumor Suppressor Caspase-14.” *Molecular and Cellular Biology* 31 (22): 4609–22. doi:10.1128/MCB.05766-11.

Asselin-Labat, Marie-Liesse, François Vaillant, Julie M. Sheridan, Bhupinder Pal, Di Wu, Evan R. Simpson, Hisataka Yasuda, et al. 2010. “Control of Mammary Stem Cell Function by Steroid Hormone Signalling.” *Nature* 465 (7299): 798–802. doi:10.1038/nature09027.

Atwood, C. S., R. C. Hovey, J. P. Glover, G. Chepko, E. Ginsburg, W. G. Robison, and B. K. Vonderhaar. 2000. “Progesterone Induces Side-Branching of the Ductal Epithelium in the Mammary Glands of Peripubertal Mice.” *The Journal of Endocrinology* 167 (1): 39–52.

Bachmann, M. F., B. R. Wong, R. Josien, R. M. Steinman, A. Oxenius, and Y. Choi. 1999. “TRANCE, a Tumor Necrosis Factor Family Member Critical for CD40 Ligand-Independent T Helper Cell Activation.” *The Journal of Experimental Medicine* 189 (7): 1025–31.

Balic, Marija, Henry Lin, Lillian Young, Debra Hawes, Armando Giuliano, George McNamara, Ram H. Datar, and Richard J. Cote. 2006. “Most Early Disseminated Cancer Cells Detected in Bone Marrow of Breast Cancer Patients Have a Putative Breast Cancer Stem Cell Phenotype.” *Clinical Cancer Research: An Official Journal of the American Association for Cancer Research* 12 (19): 5615–21. doi:10.1158/1078-0432.CCR-06-0169.

Ball, S. M. 1998. “The Development of the Terminal End Bud in the Prepubertal-Pubertal Mouse Mammary Gland.” *The Anatomical Record* 250 (4): 459–64.

Bargmann, C. I., M. C. Hung, and R. A. Weinberg. 1986. “Multiple Independent Activations of the Neu Oncogene by a Point Mutation Altering the Transmembrane Domain of p185.” *Cell* 45 (5): 649–57.

Beleut, Manfred, Renuga Devi Rajaram, Marian Caikovski, Ayyakkannu Ayyanan, Davide Germano, Yongwon Choi, Pascal Schneider, and Cathrin Brisken. 2010. “Two Distinct Mechanisms Underlie Progesterone-Induced Proliferation in the Mammary Gland.” *Proceedings of the National Academy of Sciences of the United States of America* 107 (7): 2989–94. doi:10.1073/pnas.0915148107.

Bernstein, Leslie. 2002. “Epidemiology of Endocrine-Related Risk Factors for Breast Cancer.” *Journal of Mammary Gland Biology and Neoplasia* 7 (1): 3–15.

Body, Jean-Jacques, Allan Lipton, Julie Gralow, Guenther G Steger, Guozhi Gao, Howard Yeh, and Karim Fizazi. 2010. “Effects of Denosumab in Patients with Bone Metastases with and without Previous Bisphosphonate Exposure.” *Journal of Bone and Mineral Research* 25 (3): 440–46. doi:10.1359/jbmr.090810.

Bonizzi, Giuseppina, and Michael Karin. 2004. “The Two NF-kappaB Activation Pathways and Their Role in Innate and Adaptive Immunity.” *Trends in Immunology* 25 (6): 280–88. doi:10.1016/j.it.2004.03.008.

Bouras, Toula, Bhupinder Pal, François Vaillant, Gwyndolen Harburg, Marie-Liesse Asselin-Labat, Samantha R. Oakes, Geoffrey J. Lindeman, and Jane E. Visvader. 2008. “Notch Signaling Regulates Mammary Stem Cell Function and Luminal Cell-Fate Commitment.” *Cell Stem Cell* 3 (4): 429–41. doi:10.1016/j.stem.2008.08.001.

Boyle, William J., W. Scott Simonet, and David L. Lacey. 2003. “Osteoclast Differentiation and Activation.” *Nature* 423 (6937): 337–42. doi:10.1038/nature01658.

Brisken, Cathrin. 2002. “Hormonal Control of Alveolar Development and Its Implications for Breast Carcinogenesis.” *Journal of Mammary Gland Biology and Neoplasia* 7 (1): 39–48.

Brisken, Cathrin, Ayyakkannu Ayyannan, Cuc Nguyen, Anna Heineman, Ferenc Reinhardt, Jian Tan, S. K. Dey, G. Paolo Dotto, Robert A. Weinberg, and Tian Jan. 2002. “IGF-2 Is a Mediator of Prolactin-Induced Morphogenesis in the Breast.” *Developmental Cell* 3 (6): 877–87.

Brisken, Cathrin, and Stephan Duss. 2007. “Stem Cells and the Stem Cell Niche in the Breast: An Integrated Hormonal and Developmental Perspective.” *Stem Cell Reviews* 3 (2): 147–56.

Brisken, C., A. Heineman, T. Chavarria, B. Elenbaas, J. Tan, S. K. Dey, J. A. McMahon, A. P. McMahon, and R. A. Weinberg. 2000. “Essential Function of Wnt-4 in Mammary Gland Development Downstream of Progesterone Signaling.” *Genes & Development* 14 (6): 650–54.

Brisken, C., S. Park, T. Vass, J. P. Lydon, B. W. O’Malley, and R. A. Weinberg. 1998. “A Paracrine Role for the Epithelial Progesterone Receptor in Mammary Gland Development.” *Proceedings of the National Academy of Sciences of the United States of America* 95 (9): 5076–81.

Bucay, Nathan, Ildiko Sarosi, Colin R. Dunstan, Sean Morony, John Tarpley, Casey Capparelli, Sheila Scully, et al. 1998. “Osteoprotegerin-Deficient Mice Develop Early Onset Osteoporosis and Arterial Calcification.” *Genes & Development* 12 (9): 1260–68.

Buser, Adam C., Elizabeth K. Gass-Handel, Shannon L. Wyszomierski, Wolfgang Doppler, Susan A. Leonhardt, Jerome Schaack, Jeffrey M. Rosen, Harriet Watkin, Steven M. Anderson, and Dean P. Edwards. 2007. “Progesterone Receptor Repression of Prolactin/signal Transducer and Activator of Transcription 5-Mediated Transcription of the Beta-Casein Gene in Mammary Epithelial Cells.” *Molecular Endocrinology (Baltimore, Md.)* 21 (1): 106–25. doi:10.1210/me.2006-0297.

Buser, Adam C., Alison E. Obr, Elena B. Kabotyanski, Sandra L. Grimm, Jeffrey M. Rosen, and Dean P. Edwards. 2011. “Progesterone Receptor Directly Inhibits β-Casein Gene Transcription in Mammary Epithelial Cells through Promoting Promoter and Enhancer Repressive Chromatin Modifications.” *Molecular Endocrinology (Baltimore, Md.)* 25 (6): 955–68. doi:10.1210/me.2011-0064.

Cai, Cheguo, Qing Cissy Yu, Weimin Jiang, Wei Liu, Wenqian Song, Hua Yu, Lei Zhang, Ying Yang, and Yi Arial Zeng. 2014. “R-spondin1 Is a Novel Hormone Mediator for Mammary Stem Cell Self-Renewal.” *Genes & Development* 28 (20): 2205–18. doi:10.1101/gad.245142.114.

Campbell, G. S., L. S. Argetsinger, J. N. Ihle, P. A. Kelly, J. A. Rillema, and C. Carter-Su. 1994. “Activation of JAK2 Tyrosine Kinase by Prolactin Receptors in Nb2 Cells and Mouse Mammary Gland Explants.” *Proceedings of the National Academy of Sciences of the United States of America* 91 (12): 5232–36.

Cao, Y., G. Bonizzi, T. N. Seagroves, F. R. Greten, R. Johnson, E. V. Schmidt, and M. Karin. 2001. “IKKalpha Provides an Essential Link between RANK Signaling and Cyclin D1 Expression during Mammary Gland Development.” *Cell* 107 (6): 763–75.

Cao, Yixue, and Michael Karin. 2003. “NF-kappaB in Mammary Gland Development and Breast Cancer.” *Journal of Mammary Gland Biology and Neoplasia* 8 (2): 215–23.

Cao, Yixue, Jun-Li Luo, and Michael Karin. 2007. “IkappaB Kinase Alpha Kinase Activity Is Required for Self-Renewal of ErbB2/Her2-Transformed Mammary Tumor-Initiating Cells.” *Proceedings of the National Academy of Sciences of the United States of America* 104 (40): 15852–57. doi:10.1073/pnas.0706728104.

Carnero, Amancio, Carmen Blanco-Aparicio, Oliver Renner, Wolfgang Link, and Juan F.M. Leal. 2008. “The PTEN/PI3K/AKT Signalling Pathway in Cancer, Therapeutic Implications.” *Current Cancer Drug Targets* 8 (3): 187–98. doi:10.2174/156800908784293659.

Chakrabarti, Rumela, Yong Wei, Rose-Anne Romano, Christina DeCoste, Yibin Kang, and Satrajit Sinha. 2012. “Elf5 Regulates Mammary Gland Stem/progenitor Cell Fate by Influencing Notch Signaling.” *Stem Cells (Dayton, Ohio)* 30 (7): 1496–1508. doi:10.1002/stem.1112.

Chambers, Ann F., Alan C. Groom, and Ian C. MacDonald. 2002. “Dissemination and Growth of Cancer Cells in Metastatic Sites.” *Nature Reviews. Cancer* 2 (8): 563–72. doi:10.1038/nrc865.

Chapman, Rachel S., Paula C. Lourenco, Elizabeth Tonner, David J. Flint, Stefan Selbert, Kiyoshi Takeda, Shizuo Akira, Alan R. Clarke, and Christine J. Watson. 1999. “Suppression of Epithelial Apoptosis and Delayed Mammary Gland Involution in Mice with a Conditional Knockout of Stat3.” *Genes & Development* 13 (19): 2604–16.

Chatterton, Robert T., John P. Lydon, Rajendra G. Mehta, Esnar T. Mateo, Ashley Pletz, and V. Craig Jordan. 2002. “Role of the Progesterone Receptor (PR) in Susceptibility of Mouse Mammary Gland

to 7,12-Dimethylbenz[a]anthracene-Induced Hormone-Independent Preneoplastic Lesions in Vitro." *Cancer Letters* 188 (1-2): 47–52.

Cheang, Maggie C. U., Stephen K. Chia, David Voduc, Dongxia Gao, Samuel Leung, Jacqueline Snider, Mark Watson, et al. 2009. "Ki67 Index, HER2 Status, and Prognosis of Patients with Luminal B Breast Cancer." *Journal of the National Cancer Institute* 101 (10): 736–50. doi:10.1093/jnci/djp082.

Chen, Chien-Chung, Robert B. Boxer, Douglas B. Stairs, Carla P. Portocarrero, Rachel H. Horton, James V. Alvarez, Morris J. Birnbaum, and Lewis A. Chodosh. 2010. "Akt Is Required for Stat5 Activation and Mammary Differentiation." *Breast Cancer Research: BCR* 12 (5): R72. doi:10.1186/bcr2640.

Chen, Chien-Chung, Douglas B. Stairs, Robert B. Boxer, George K. Belka, Nelson D. Horseman, James V. Alvarez, and Lewis A. Chodosh. 2012. "Autocrine Prolactin Induced by the Pten-Akt Pathway Is Required for Lactation Initiation and Provides a Direct Link between the Akt and Stat5 Pathways." *Genes & Development* 26 (19): 2154–68. doi:10.1101/gad.197343.112.

Chen, Jian, Yanjiao Li, Tzong-Shiue Yu, Renée M. McKay, Dennis K. Burns, Steven G. Kernie, and Luis F. Parada. 2012. "A Restricted Cell Population Propagates Glioblastoma Growth after Chemotherapy." *Nature* 488 (7412): 522–26. doi:10.1038/nature11287.

Chen, Weiguo, Michael O. Daines, and Gurjit K. Khurana Hershey. 2004. "Turning off Signal Transducer and Activator of Transcription (STAT): The Negative Regulation of STAT Signaling." *Journal of Allergy and Clinical Immunology* 114 (3): 476–89. doi:10.1016/j.jaci.2004.06.042.

Chen, Sining, and Giovanni Parmigiani. 2007. "Meta-Analysis of BRCA1 and BRCA2 Penetrance." *Journal of Clinical Oncology: Official Journal of the American Society of Clinical Oncology* 25 (11): 1329–33. doi:10.1200/JCO.2006.09.1066.

Chlebowski, Rowan T., JoAnn E. Manson, Garnet L. Anderson, Jane A. Cauley, Aaron K. Aragaki, Marcia L. Stefanick, Dorothy S. Lane, et al. 2013. "Estrogen Plus Progestin and Breast Cancer Incidence and Mortality in the Women's Health Initiative Observational Study." *JNCI Journal of the National Cancer Institute* 105 (8): 526–35. doi:10.1093/jnci/djt043.

Choi, Yeon Sook, Rumela Chakrabarti, Rosalba Escamilla-Hernandez, and Satrajit Sinha. 2009. "Elf5 Conditional Knockout Mice Reveal Its Role as a Master Regulator in Mammary Alveolar Development: Failure of Stat5 Activation and Functional Differentiation in the Absence of Elf5." *Developmental Biology* 329 (2): 227–41. doi:10.1016/j.ydbio.2009.02.032.

Chou, Jonathan, Sylvain Provot, and Zena Werb. 2010. "GATA3 in Development and Cancer Differentiation: Cells GATA Have It!" *Journal of Cellular Physiology* 222 (1): 42–49. doi:10.1002/jcp.21943.

Ciruelos Gil, Eva Maria. 2014. “Targeting the PI3K/AKT/mTOR Pathway in Estrogen Receptor-Positive Breast Cancer.” *Cancer Treatment Reviews* 40 (7): 862–71. doi:10.1016/j.ctrv.2014.03.004.

Clarke, Robert B., Anthony Howell, Christopher S. Potten, and Elizabeth Anderson. 1997. “Dissociation between Steroid Receptor Expression and Cell Proliferation in the Human Breast.” *Cancer Research* 57 (22): 4987–91.

Cocolakis, Eftihia, Meiou Dai, Loren Drevet, Joanne Ho, Eric Haines, Suhad Ali, and Jean-Jacques Lebrun. 2008. “Smad Signaling Antagonizes STAT5-Mediated Gene Transcription and Mammary Epithelial Cell Differentiation.” *The Journal of Biological Chemistry* 283 (3): 1293–1307. doi:10.1074/jbc.M707492200.

Conneely, Orla M., Biserka M. Jericevic, and John P. Lydon. 2003. “Progesterone Receptors in Mammary Gland Development and Tumorigenesis.” *Journal of Mammary Gland Biology and Neoplasia* 8 (2): 205–14.

Creamer, Bradley A., Kazuhito Sakamoto, Jeffrey W. Schmidt, Aleata A. Triplett, Richard Moriggl, and Kay-Uwe Wagner. 2010. “Stat5 Promotes Survival of Mammary Epithelial Cells through Transcriptional Activation of a Distinct Promoter in Akt1.” *Molecular and Cellular Biology* 30 (12): 2957–70. doi:10.1128/MCB.00851-09.

Courtois-Cox, S., S. L. Jones, and K. Cichowski. 2008. “Many Roads Lead to Oncogene-Induced Senescence.” *Oncogene* 27 (20): 2801–9. doi:10.1038/sj.onc.1210950.

Daniel, C. W., K. B. De Ome, J. T. Young, P. B. Blair, and L. J. Faulkin. 1968. “The in Vivo Life Span of Normal and Preneoplastic Mouse Mammary Glands: A Serial Transplantation Study.” *Proceedings of the National Academy of Sciences of the United States of America* 61 (1): 53–60.

Daniel, C. W., and L. J. Young. 1971. “Influence of Cell Division on an Aging Process. Life Span of Mouse Mammary Epithelium during Serial Propagation in Vivo.” *Experimental Cell Research* 65 (1): 27–32.

Davis, R. J. 2000. “Signal Transduction by the JNK Group of MAP Kinases.” *Cell* 103 (2): 239–52.

Dent, Rebecca, Maureen Trudeau, Kathleen I. Pritchard, Wedad M. Hanna, Harriet K. Kahn, Carol A. Sawka, Lavina A. Lickley, Ellen Rawlinson, Ping Sun, and Steven A. Narod. 2007. “Triple-Negative Breast Cancer: Clinical Features and Patterns of Recurrence.” *Clinical Cancer Research: An Official Journal of the American Association for Cancer Research* 13 (15 Pt 1): 4429–34. doi:10.1158/1078-0432.CCR-06-3045.

Deome, K. B., L. J. Faulkin, H. A. Bern, and P. B. Blair. 1959. “Development of Mammary Tumors from Hyperplastic Alveolar Nodules Transplanted into Gland-Free Mammary Fat Pads of Female C3H Mice.” *Cancer Research* 19 (5): 515–20.

Desai, Kartiki V., Nianqing Xiao, Weili Wang, Lisa Gangi, John Greene, John I. Powell, Robert Dickson, et al. 2002. “Initiating Oncogenic Event Determines Gene-Expression Patterns of Human Breast Cancer Models.” *Proceedings of the National Academy of Sciences of the United States of America* 99 (10): 6967–72. doi:10.1073/pnas.102172399.

Desprez, Pierre-Yves, Tomoki Sumida, and Jean-Philippe Coppé. 2003. “Helix-Loop-Helix Proteins in Mammary Gland Development and Breast Cancer.” *Journal of Mammary Gland Biology and Neoplasia* 8 (2): 225–39.

Desrivières, Sylvane, Christian Kunz, Itamar Barash, Vida Vafaizadeh, Corina Borghouts, and Bernd Groner. 2006. “The Biological Functions of the Versatile Transcription Factors STAT3 and STAT5 and New Strategies for Their Targeted Inhibition.” *Journal of Mammary Gland Biology and Neoplasia* 11 (1): 75–87. doi:10.1007/s10911-006-9014-4.

Dontu, Gabriela, and Max S. Wicha. 2005. “Survival of Mammary Stem Cells in Suspension Culture: Implications for Stem Cell Biology and Neoplasia.” *Journal of Mammary Gland Biology and Neoplasia* 10 (1): 75–86. doi:10.1007/s10911-005-2542-5.

Dougall, W. C., M. Glaccum, K. Charrier, K. Rohrbach, K. Brasel, T. De Smedt, E. Daro, et al. 1999. “RANK Is Essential for Osteoclast and Lymph Node Development.” *Genes & Development* 13 (18): 2412–24.

Driessens, Gregory, Benjamin Beck, Amélie Caauwe, Benjamin D. Simons, and Cédric Blanpain. 2012. “Defining the Mode of Tumour Growth by Clonal Analysis.” *Nature* 488 (7412): 527–30. doi:10.1038/nature11344.

Dumitrescu, R. G., and I. Cotarla. 2005. “Understanding Breast Cancer Risk -- Where Do We Stand in 2005?” *Journal of Cellular and Molecular Medicine* 9 (1): 208–21.

Eyler, Christine E., and Jeremy N. Rich. 2008. “Survival of the Fittest: Cancer Stem Cells in Therapeutic Resistance and Angiogenesis.” *Journal of Clinical Oncology: Official Journal of the American Society of Clinical Oncology* 26 (17): 2839–45. doi:10.1200/JCO.2007.15.1829.

Fata, J. E., Y. Y. Kong, J. Li, T. Sasaki, J. Irie-Sasaki, R. A. Moorehead, R. Elliott, et al. 2000. “The Osteoclast Differentiation Factor Osteoprotegerin-Ligand Is Essential for Mammary Gland Development.” *Cell* 103 (1): 41–50.

Ferlay, J., E. Steliarova-Foucher, J. Lortet-Tieulent, S. Rosso, J. W. W. Coebergh, H. Comber, D. Forman, and F. Bray. 2013. “Cancer Incidence and Mortality Patterns in Europe: Estimates for 40 Countries in 2012.” *European Journal of Cancer (Oxford, England: 1990)* 49 (6): 1374–1403. doi:10.1016/j.ejca.2012.12.027.

Fernandez-Valdivia, Rodrigo, Atish Mukherjee, Yan Ying, Jie Li, Marilene Paquet, Francesco J. DeMayo, and John P. Lydon. 2009. “The RANKL Signaling Axis Is Sufficient to Elicit Ductal Side-

Branching and Alveologenesis in the Mammary Gland of the Virgin Mouse." *Developmental Biology* 328 (1): 127–39. doi:10.1016/j.ydbio.2009.01.019.

Fernando Abollo-Jimenez, Elena Campos-Sanchez, Ana Sagrera, Maria Eugenia Muñoz, Ana Isabel Galan, Rafael Jimenez and Cesar Cobaleda (2011). The Dark Side of Cellular Plasticity: Stem Cells in Development and Cancer, Cancer Stem Cells Theories and Practice, Prof. Stanley Shostak (Ed.), ISBN: 978-953-307-225-8, InTech, DOI: 10.5772/13969. Available from: http://www.intechopen.com/books/cancer-stem-cells-theories-and-practice/the-dark-side-of-cellular-plasticity-stem-cells-in-development-and-cancer

Fisher, B., M. Bauer, D. L. Wickerham, C. K. Redmond, E. R. Fisher, A. B. Cruz, R. Foster, B. Gardner, H. Lerner, and R. Margolese. 1983. "Relation of Number of Positive Axillary Nodes to the Prognosis of Patients with Primary Breast Cancer. An NSABP Update." *Cancer* 52 (9): 1551–57.

Fizazi, K., L. Albiges, C. Massard, B. Escudier, and Y. Loriot. 2012. "Novel and Bone-Targeted Agents for CRPC." *Annals of Oncology* 23 (suppl 10): x264–67. doi:10.1093/annonc/mds353.

Fluck, Michele M., and Brian S. Schaffhausen. 2009. "Lessons in Signaling and Tumorigenesis from Polyomavirus Middle T Antigen." *Microbiology and Molecular Biology Reviews: MMBR* 73 (3): 542–63, Table of Contents. doi:10.1128/MMBR.00009-09.

Freund, Adam, Arturo V. Orjalo, Pierre-Yves Desprez, and Judith Campisi. 2010. "Inflammatory Networks during Cellular Senescence: Causes and Consequences." *Trends in Molecular Medicine* 16 (5): 238–46. doi:10.1016/j.molmed.2010.03.003.

Furth, Priscilla A., Rebecca E. Nakles, Sarah Millman, Edgar S. Diaz-Cruz, and M. Carla Cabrera. 2011. "Signal Transducer and Activator of Transcription 5 as a Key Signaling Pathway in Normal Mammary Gland Developmental Biology and Breast Cancer." *Breast Cancer Research: BCR* 13 (5): 220. doi:10.1186/bcr2921.

Gallego, M. I., N. Binart, G. W. Robinson, R. Okagaki, K. T. Coschigano, J. Perry, J. J. Kopchick, T. Oka, P. A. Kelly, and L. Hennighausen. 2001. "Prolactin, Growth Hormone, and Epidermal Growth Factor Activate Stat5 in Different Compartments of Mammary Tissue and Exert Different and Overlapping Developmental Effects." *Developmental Biology* 229 (1): 163–75. doi:10.1006/dbio.2000.9961.

Galliher, Amy J., and William P. Schiemann. 2007. "Src Phosphorylates Tyr284 in TGF-Beta Type II Receptor and Regulates TGF-Beta Stimulation of p38 MAPK during Breast Cancer Cell Proliferation and Invasion." *Cancer Research* 67 (8): 3752–58. doi:10.1158/0008-5472.CAN-06-3851.

Garbe, James C., Francois Pepin, Fanny A. Pelissier, Klara Sputova, Agla J. Fridriksdottir, Diana E. Guo, Rene Villadsen, et al. 2012. "Accumulation of Multipotent Progenitors with a Basal Differentiation Bias during Aging of Human Mammary Epithelia." *Cancer Research* 72 (14): 3687–3701. doi:10.1158/0008-5472.CAN-12-0157.

Gerondakis, Steve, Thomas S. Fulford, Nicole L. Messina, and Raelene J. Grumont. 2014. “NF-κB Control of T Cell Development.” *Nature Immunology* 15 (1): 15–25. doi:10.1038/ni.2785.

Geymayer, Sibylle, and Wolfgang Doppler. 2000. “Activation of NF-κB p50/p65 Is Regulated in the Developing Mammary Gland and Inhibits STAT5-Mediated β-Casein Gene Expression.” *The FASEB Journal* 14 (9): 1159–70.

Geymayer, Sibylle, and Wolfgang Doppler. 2000. “Activation of NF-κB p50/p65 Is Regulated in the Developing Mammary Gland and Inhibits STAT5-Mediated β-Casein Gene Expression.” *The FASEB Journal* 14 (9): 1159–70.

Gilmore, T. D. 2006. “Introduction to NF-kappaB: Players, Pathways, Perspectives.” *Oncogene* 25 (51): 6680–84. doi:10.1038/sj.onc.1209954.

Gonzalez-Suarez, Eva, Daniel Branstetter, Allison Armstrong, Huyen Dinh, Hal Blumberg, and William C. Dougall. 2007. “RANK Overexpression in Transgenic Mice with Mouse Mammary Tumor Virus Promoter-Controlled RANK Increases Proliferation and Impairs Alveolar Differentiation in the Mammary Epithelia and Disrupts Lumen Formation in Cultured Epithelial Acini.” *Molecular and Cellular Biology* 27 (4): 1442–54. doi:10.1128/MCB.01298-06.

Gonzalez-Suarez, Eva, Allison P. Jacob, Jon Jones, Robert Miller, Martine P. Roudier-Meyer, Ryan Erwert, Jan Pinkas, Dan Branstetter, and William C. Dougall. 2010. “RANK Ligand Mediates Progestin-Induced Mammary Epithelial Proliferation and Carcinogenesis.” *Nature* 468 (7320): 103–7. doi:10.1038/nature09495.

Gouilleux, F., H. Wakao, M. Mundt, and B. Groner. 1994. “Prolactin Induces Phosphorylation of Tyr694 of Stat5 (MGF), a Prerequisite for DNA Binding and Induction of Transcription.” *The EMBO Journal* 13 (18): 4361–69.

Guo, Wenjun, Zuzana Keckesova, Joana Liu Donaher, Tsukasa Shibue, Verena Tischler, Ferenc Reinhardt, Shalev Itzkovitz, et al. 2012. “Slug and Sox9 Cooperatively Determine the Mammary Stem Cell State.” *Cell* 148 (5): 1015–28. doi:10.1016/j.cell.2012.02.008.

Gutierrez, M. Carolina, Simone Detre, Stephen Johnston, Syed K. Mohsin, Jiang Shou, D. Craig Allred, Rachel Schiff, C. Kent Osborne, and Mitch Dowsett. 2005. “Molecular Changes in Tamoxifen-Resistant Breast Cancer: Relationship between Estrogen Receptor, HER-2, and p38 Mitogen-Activated Protein Kinase.” *Journal of Clinical Oncology: Official Journal of the American Society of Clinical Oncology* 23 (11): 2469–76. doi:10.1200/JCO.2005.01.172.

Guy, C. T., R. D. Cardiff, and W. J. Muller. 1992. “Induction of Mammary Tumors by Expression of Polyomavirus Middle T Oncogene: A Transgenic Mouse Model for Metastatic Disease.” *Molecular and Cellular Biology* 12 (3): 954–61.

Han, Qiwei, Jay Leng, Dafang Bian, Chitladda Mahanivong, Kevin A. Carpenter, Zhixing K. Pan, Jiahuai Han, and Shuang Huang. 2002. “Rac1-MKK3-p38-MAPKAPK2 Pathway Promotes Urokinase Plasminogen Activator mRNA Stability in Invasive Breast Cancer Cells.” *The Journal of Biological Chemistry* 277 (50): 48379–85. doi:10.1074/jbc.M209542200.

Haricharan, S., and Y. Li. 2014. “STAT Signaling in Mammary Gland Differentiation, Cell Survival and Tumorigenesis.” *Molecular and Cellular Endocrinology* 382 (1): 560–69. doi:10.1016/j.mce.2013.03.014.

Harris, Jessica, Prudence M. Stanford, Kate Sutherland, Samantha R. Oakes, Matthew J. Naylor, Fiona G. Robertson, Katrina D. Blazek, et al. 2006. “Socs2 and elf5 Mediate Prolactin-Induced Mammary Gland Development.” *Molecular Endocrinology (Baltimore, Md.)* 20 (5): 1177–87. doi:10.1210/me.2005-0473.

Hassiotou, Foteini, and Donna Geddes. 2013. “Anatomy of the Human Mammary Gland: Current Status of Knowledge.” *Clinical Anatomy* 26 (1): 29–48. doi:10.1002/ca.22165.

Hayden, Matthew S., and Sankar Ghosh. 2008. “Shared Principles in NF-kappaB Signaling.” *Cell* 132 (3): 344–62. doi:10.1016/j.cell.2008.01.020.

Hennighausen, L., and G. W. Robinson. 2001. “Signaling Pathways in Mammary Gland Development.” *Developmental Cell* 1 (4): 467–75.

Hennighausen, Lothar, and Gertraud W. Robinson. 2005. “Information Networks in the Mammary Gland.” *Nature Reviews. Molecular Cell Biology* 6 (9): 715–25. doi:10.1038/nrm1714.

Henry, MaLinda D., Aleata A. Triplett, Keon Bong Oh, Gilbert H. Smith, and Kay-Uwe Wagner. 2004. “Parity-Induced Mammary Epithelial Cells Facilitate Tumorigenesis in MMTV-Neu Transgenic Mice.” *Oncogene* 23 (41): 6980–85. doi:10.1038/sj.onc.1207827.

Herschkowitz, Jason I., Karl Simin, Victor J. Weigman, Igor Mikaelian, Jerry Usary, Zhiyuan Hu, Karen E. Rasmussen, et al. 2007. “Identification of Conserved Gene Expression Features between Murine Mammary Carcinoma Models and Human Breast Tumors.” *Genome Biology* 8 (5): R76. doi:10.1186/gb-2007-8-5-r76.

Hinohara, Kunihiko, Seiichiro Kobayashi, Hajime Kanauchi, Seiichiro Shimizu, Kotoe Nishioka, Ei-ichi Tsuji, Kei-ichiro Tada, et al. 2012. “ErbB Receptor Tyrosine kinase/NF-κB Signaling Controls Mammosphere Formation in Human Breast Cancer.” *Proceedings of the National Academy of Sciences of the United States of America* 109 (17): 6584–89. doi:10.1073/pnas.1113271109.

Hoffmann, A., G. Natoli, and G. Ghosh. 2006. “Transcriptional Regulation via the NF-kappaB Signaling Module.” *Oncogene* 25 (51): 6706–16. doi:10.1038/sj.onc.1209933.

Hoshino, K. 1962. “Morphogenesis and Growth Potentiality of Mammary Glands in Mice. I. Transplantability and Growth Potentiality of Mammary Tissue of Virgin Mice.” *Journal of the National Cancer Institute* 29 (November): 835–51.

Howlin, Jillian, Jean McBryan, and Finian Martin. 2006. “Pubertal Mammary Gland Development: Insights from Mouse Models.” *Journal of Mammary Gland Biology and Neoplasia* 11 (3-4): 283–97. doi:10.1007/s10911-006-9024-2.

Hui, Lijian, Latifa Bakiri, Ewa Stepniak, and Erwin F. Wagner. 2007. “p38alpha: A Suppressor of Cell Proliferation and Tumorigenesis.” *Cell Cycle (Georgetown, Tex.)* 6 (20): 2429–33.

Humphreys, Robin C., Brian Bierie, Ling Zhao, Regina Raz, David Levy, and Lothar Hennighausen. 2002. “Deletion of Stat3 Blocks Mammary Gland Involution and Extends Functional Competence of the Secretory Epithelium in the Absence of Lactogenic Stimuli.” *Endocrinology* 143 (9): 3641–50. doi:10.1210/en.2002-220224.

Hüsemann, Yves, Jochen B. Geigl, Falk Schubert, Piero Musiani, Manfred Meyer, Elke Burghart, Guido Forni, et al. 2008. “Systemic Spread Is an Early Step in Breast Cancer.” *Cancer Cell* 13 (1): 58–68. doi:10.1016/j.ccr.2007.12.003.

Ikeda, T., M. Kasai, M. Utsuyama, and K. Hirokawa. 2001. “Determination of Three Isoforms of the Receptor Activator of Nuclear Factor-kappaB Ligand and Their Differential Expression in Bone and Thymus.” *Endocrinology* 142 (4): 1419–26. doi:10.1210/endo.142.4.8070.

Ince, Tan A., Andrea L. Richardson, George W. Bell, Maki Saitoh, Samuel Godar, Antoine E. Karnoub, James D. Iglehart, and Robert A. Weinberg. 2007. “Transformation of Different Human Breast Epithelial Cell Types Leads to Distinct Tumor Phenotypes.” *Cancer Cell* 12 (2): 160–70. doi:10.1016/j.ccr.2007.06.013.

Ismail, Preeti M., Jie Li, Francesco J. DeMayo, Bert W. O’Malley, and John P. Lydon. 2002. “A Novel LacZ Reporter Mouse Reveals Complex Regulation of the Progesterone Receptor Promoter During Mammary Gland Development.” *Molecular Endocrinology* 16 (11): 2475–89. doi:10.1210/me.2002-0169.

Irie-Sasaki, Junko, Takehiko Sasaki, Wataru Matsumoto, Anne Opavsky, Mary Cheng, Grant Welstead, Emily Griffiths, et al. 2001. “CD45 Is a JAK Phosphatase and Negatively Regulates Cytokine Receptor Signalling.” *Nature* 409 (6818): 349–54. doi:10.1038/35053086.

Izawa, Takashi, Wei Zou, Jean C. Chappel, Jason W. Ashley, Xu Feng, and Steven L. Teitelbaum. 2012. “C-Src Links a RANK/αvβ3 Integrin Complex to the Osteoclast Cytoskeleton.” *Molecular and Cellular Biology* 32 (14): 2943–53. doi:10.1128/MCB.00077-12.

Jasmin, Jean-François, Isabelle Mercier, Federica Sotgia, and Michael P. Lisanti. 2006. “SOCS Proteins and Caveolin-1 as Negative Regulators of Endocrine Signaling.” *Trends in Endocrinology and Metabolism: TEM* 17 (4): 150–58. doi:10.1016/j.tem.2006.03.007.

Jochum, W., E. Passegué, and E. F. Wagner. 2001. “AP-1 in Mouse Development and Tumorigenesis.” *Oncogene* 20 (19): 2401–12. doi:10.1038/sj.onc.1204389.

Jones, Frank E., Thomas Welte, Xin-Yuan Fu, and David F. Stern. 1999. “Erbb4 Signaling in the Mammary Gland Is Required for Lobuloalveolar Development and Stat5 Activation during Lactation.” *The Journal of Cell Biology* 147 (1): 77–88.

Jordan, Craig T., Monica L. Guzman, and Mark Noble. 2006. “Cancer Stem Cells.” *New England Journal of Medicine* 355 (12): 1253–61. doi:10.1056/NEJMra061808.

Joshi, Purna A., Hartland W. Jackson, Alexander G. Beristain, Marco A. Di Grappa, Patricia A. Mote, Christine L. Clarke, John Stingl, Paul D. Waterhouse, and Rama Khokha. 2010. “Progesterone Induces Adult Mammary Stem Cell Expansion.” *Nature* 465 (7299): 803–7. doi:10.1038/nature09091.

Josien, R., B. R. Wong, H. L. Li, R. M. Steinman, and Y. Choi. 1999. “TRANCE, a TNF Family Member, Is Differentially Expressed on T Cell Subsets and Induces Cytokine Production in Dendritic Cells.” *Journal of Immunology (Baltimore, Md.: 1950)* 162 (5): 2562–68.

Karin, M. 1999. “The Beginning of the End: IkappaB Kinase (IKK) and NF-kappaB Activation.” *The Journal of Biological Chemistry* 274 (39): 27339–42.

Kim, Dongku, Reina E. Mebius, John D. MacMicking, Steffen Jung, Tom Cupedo, Yaneth Castellanos, Jaerang Rho, et al. 2000. “Regulation of Peripheral Lymph Node Genesis by the Tumor Necrosis Factor Family Member Trance.” *The Journal of Experimental Medicine* 192 (10): 1467–78.

Kong, Y. Y., H. Yoshida, I. Sarosi, H. L. Tan, E. Timms, C. Capparelli, S. Morony, et al. 1999. “OPGL Is a Key Regulator of Osteoclastogenesis, Lymphocyte Development and Lymph-Node Organogenesis.” *Nature* 397 (6717): 315–23. doi:10.1038/16852.

Kordon, E. C., and G. H. Smith. 1998. “An Entire Functional Mammary Gland May Comprise the Progeny from a Single Cell.” *Development* 125 (10): 1921–30.

Kretzschmar, Kai, and Fiona M. Watt. 2012. “Lineage Tracing.” *Cell* 148 (1): 33–45. doi:10.1016/j.cell.2012.01.002.

Krishna, M., and H. Narang. 2008. “The Complexity of Mitogen-Activated Protein Kinases (MAPKs) Made Simple.” *Cellular and Molecular Life Sciences: CMLS* 65 (22): 3525–44. doi:10.1007/s00018-008-8170-7.

Kritikou, Ekaterini A., Andrew Sharkey, Kathrine Abell, Paul J. Came, Elizabeth Anderson, Richard W. E. Clarkson, and Christine J. Watson. 2003. “A Dual, Non-Redundant, Role for LIF as a Regulator of Development and STAT3-Mediated Cell Death in Mammary Gland.” *Development (Cambridge, England)* 130 (15): 3459–68.

Lee, Heather J., David Gallego-Ortega, Anita Ledger, Daniel Schramek, Purna Joshi, Maria M. Szwarc, Christina Cho, et al. 2013. “Progesterone Drives Mammary Secretory Differentiation via RankL-Mediated Induction of Elf5 in Luminal Progenitor Cells.” *Development* 140 (7): 1397–1401. doi:10.1242/dev.088948.

Lee, Heather J., and Christopher J. Ormandy. 2012. “Elf5, Hormones and Cell Fate.” *Trends in Endocrinology and Metabolism: TEM* 23 (6): 292–98. doi:10.1016/j.tem.2012.02.006.

Leibbrandt, Andreas, and Josef M. Penninger. 2008. “RANK/RANKL: Regulators of Immune Responses and Bone Physiology.” *Annals of the New York Academy of Sciences* 1143 (November): 123–50. doi:10.1196/annals.1443.016.

Li, M., X. Liu, G. Robinson, U. Bar-Peled, K. U. Wagner, W. S. Young, L. Hennighausen, and P. A. Furth. 1997. “Mammary-Derived Signals Activate Programmed Cell Death during the First Stage of Mammary Gland Involution.” *Proceedings of the National Academy of Sciences of the United States of America* 94 (7): 3425–30.

Lim, Elgene, Di Wu, Bhupinder Pal, Toula Bouras, Marie-Liesse Asselin-Labat, François Vaillant, Hideo Yagita, Geoffrey J Lindeman, Gordon K Smyth, and Jane E Visvader. 2010. “Transcriptome Analyses of Mouse and Human Mammary Cell Subpopulations Reveal Multiple Conserved Genes and Pathways.” *Breast Cancer Research: BCR* 12 (2): R21. doi:10.1186/bcr2560.

Lindeman, G. J., S. Wittlin, H. Lada, M. J. Naylor, M. Santamaria, J. G. Zhang, R. Starr, et al. 2001. “SOCS1 Deficiency Results in Accelerated Mammary Gland Development and Rescues Lactation in Prolactin Receptor-Deficient Mice.” *Genes & Development* 15 (13): 1631–36. doi:10.1101/gad.880801.

Lin, Elaine Y., Joan G. Jones, Ping Li, Liyin Zhu, Kathleen D. Whitney, William J. Muller, and Jeffrey W. Pollard. 2003. “Progression to Malignancy in the Polyoma Middle T Oncoprotein Mouse Breast Cancer Model Provides a Reliable Model for Human Diseases.” *The American Journal of Pathology* 163 (5): 2113–26. doi:10.1016/S0002-9440(10)63568-7.

Lin, E. Y., A. V. Nguyen, R. G. Russell, and J. W. Pollard. 2001. “Colony-Stimulating Factor 1 Promotes Progression of Mammary Tumors to Malignancy.” *The Journal of Experimental Medicine* 193 (6): 727–40.

Liu, Manran, Toshiyuki Sakamaki, Mathew C. Casimiro, Nicole E. Willmarth, Andrew A. Quong, Xiaoming Ju, John Ojeifo, et al. 2010. “The Canonical NF-kappaB Pathway Governs Mammary

Tumorigenesis in Transgenic Mice and Tumor Stem Cell Expansion." *Cancer Research* 70 (24): 10464–73. doi:10.1158/0008-5472.CAN-10-0732.

Liu, Suling, Gabriela Dontu, Ilia D. Mantle, Shivani Patel, Nam-shik Ahn, Kyle W. Jackson, Prerna Suri, and Max S. Wicha. 2006. "Hedgehog Signaling and Bmi-1 Regulate Self-Renewal of Normal and Malignant Human Mammary Stem Cells." *Cancer Research* 66 (12): 6063–71. doi:10.1158/0008-5472.CAN-06-0054.

Liu, X., G. W. Robinson, K. U. Wagner, L. Garrett, A. Wynshaw-Boris, and L. Hennighausen. 1997. "Stat5a Is Mandatory for Adult Mammary Gland Development and Lactogenesis." *Genes & Development* 11 (2): 179–86.

Li, Wenjing, Brian J. Ferguson, Walid T. Khaled, Maxine Tevendale, John Stingl, Valeria Poli, Tina Rich, Paolo Salomoni, and Christine J. Watson. 2009. "PML Depletion Disrupts Normal Mammary Gland Development and Skews the Composition of the Mammary Luminal Cell Progenitor Pool." *Proceedings of the National Academy of Sciences* 106 (12): 4725–30. doi:10.1073/pnas.0807640106.

Li, Zhe, Cristina E. Tognon, Frank J. Godinho, Laura Yasaitis, Hanno Hock, Jason I. Herschkowitz, Chris L. Lannon, et al. 2007. "ETV6-NTRK3 Fusion Oncogene Initiates Breast Cancer from Committed Mammary Progenitors via Activation of AP1 Complex." *Cancer Cell* 12 (6): 542–58. doi:10.1016/j.ccr.2007.11.012.

Long, Weiwen, Kay-Uwe Wagner, K. C. Kent Lloyd, Nadine Binart, Jonathan M. Shillingford, Lothar Hennighausen, and Frank E. Jones. 2003. "Impaired Differentiation and Lactational Failure of Erbb4-Deficient Mammary Glands Identify ERBB4 as an Obligate Mediator of STAT5." *Development (Cambridge, England)* 130 (21): 5257–68. doi:10.1242/dev.00715.

Lo, P.-K., D. Kanojia, X. Liu, U. P. Singh, F. G. Berger, Q. Wang, and H. Chen. 2012. "CD49f and CD61 Identify Her2/neu-Induced Mammary Tumor-Initiating Cells That Are Potentially Derived from Luminal Progenitors and Maintained by the Integrin-TGFβ Signaling." *Oncogene* 31 (21): 2614–26. doi:10.1038/onc.2011.439.

Loser, Karin, Annette Mehling, Stefanie Loeser, Jenny Apelt, Annegret Kuhn, Stephan Grabbe, Thomas Schwarz, Josef M. Penninger, and Stefan Beissert. 2006. "Epidermal RANKL Controls Regulatory T-Cell Numbers via Activation of Dendritic Cells." *Nature Medicine* 12 (12): 1372–79. doi:10.1038/nm1518.

Lund, L. R., J. Rømer, N. Thomasset, H. Solberg, C. Pyke, M. J. Bissell, K. Danø, and Z. Werb. 1996. "Two Distinct Phases of Apoptosis in Mammary Gland Involution: Proteinase-Independent and -Dependent Pathways." *Development (Cambridge, England)* 122 (1): 181–93.

Lydon, J. P., F. J. DeMayo, C. R. Funk, S. K. Mani, A. R. Hughes, C. A. Montgomery, G. Shyamala, O. M. Conneely, and B. W. O'Malley. 1995. "Mice Lacking Progesterone Receptor Exhibit Pleiotropic Reproductive Abnormalities." *Genes & Development* 9 (18): 2266–78.

Lydon, J. P., G. Ge, F. S. Kittrell, D. Medina, and B. W. O'Malley. 1999. "Murine Mammary Gland Carcinogenesis Is Critically Dependent on Progesterone Receptor Function." *Cancer Research* 59 (17): 4276–84.

Macias, Hector, and Lindsay Hinck. 2012. "Mammary Gland Development." *Wiley Interdisciplinary Reviews. Developmental Biology* 1 (4): 533–57. doi:10.1002/wdev.35.

Madrid, L. V., M. W. Mayo, J. Y. Reuther, and A. S. Baldwin. 2001. "Akt Stimulates the Transactivation Potential of the RelA/p65 Subunit of NF-Kappa B through Utilization of the Ikappa B Kinase and Activation of the Mitogen-Activated Protein Kinase p38." *The Journal of Biological Chemistry* 276 (22): 18934–40. doi:10.1074/jbc.M101103200.

Maglione, Jeannie E., Drew Moghanaki, Lawrence J. T. Young, Cathyryne K. Manner, Lesley G. Ellies, Sasha O. Joseph, Benjamin Nicholson, Robert D. Cardiff, and Carol L. MacLeod. 2001. "Transgenic Polyoma Middle-T Mice Model Premalignant Mammary Disease." *Cancer Research* 61 (22): 8298–8305.

Malone, K. E., J. R. Daling, J. D. Thompson, C. A. O'Brien, L. V. Francisco, and E. A. Ostrander. 1998. "BRCA1 Mutations and Breast Cancer in the General Population: Analyses in Women before Age 35 Years and in Women before Age 45 Years with First-Degree Family History." *JAMA* 279 (12): 922–29.

Mansour, E. G., P. M. Ravdin, and L. Dressler. 1994. "Prognostic Factors in Early Breast Carcinoma." *Cancer* 74 (1 Suppl): 381–400.

Marine, J. C., C. McKay, D. Wang, D. J. Topham, E. Parganas, H. Nakajima, H. Pendeville, et al. 1999. "SOCS3 Is Essential in the Regulation of Fetal Liver Erythropoiesis." *Cell* 98 (5): 617–27.

Matulka, Laurice A., Aleata A. Triplett, and Kay-Uwe Wagner. 2007. "Parity-Induced Mammary Epithelial Cells Are Multipotent and Express Cell Surface Markers Associated with Stem Cells." *Developmental Biology* 303 (1): 29–44. doi:10.1016/j.ydbio.2006.12.017.

McCubrey, James A., Linda S. Steelman, William H. Chappell, Stephen L. Abrams, Ellis W. T. Wong, Fumin Chang, Brian Lehmann, et al. 2007. "Roles of the Raf/MEK/ERK Pathway in Cell Growth, Malignant Transformation and Drug Resistance." *Biochimica Et Biophysica Acta* 1773 (8): 1263–84. doi:10.1016/j.bbamcr.2006.10.001.

McDermott, Sean P., and Max S. Wicha. 2010. "Targeting Breast Cancer Stem Cells." *Molecular Oncology* 4 (5): 404–19. doi:10.1016/j.molonc.2010.06.005.

McKeage, Kate, and Caroline M. Perry. 2002. "Trastuzumab: A Review of Its Use in the Treatment of Metastatic Breast Cancer Overexpressing HER2." *Drugs* 62 (1): 209–43.

Medina, Daniel. 1996. “The Mammary Gland: A Unique Organ for the Study of Development and Tumorigenesis.” *Journal of Mammary Gland Biology and Neoplasia* 1 (1): 5–19. doi:10.1007/BF02096299.

Medina, Daniel. 2004. “Breast Cancer: The Protective Effect of Pregnancy.” *Clinical Cancer Research: An Official Journal of the American Association for Cancer Research* 10 (1 Pt 2): 380S – 4S.

Melchor, Lorenzo, and Javier Benítez. 2008. “An Integrative Hypothesis about the Origin and Development of Sporadic and Familial Breast Cancer Subtypes.” *Carcinogenesis* 29 (8): 1475–82. doi:10.1093/carcin/bgn157.

Mingo-Sion, Amy M., Peter M. Marietta, Erich Koller, Douglas M. Wolf, and Carla L. Van Den Berg. 2004. “Inhibition of JNK Reduces G2/M Transit Independent of p53, Leading to Endoreduplication, Decreased Proliferation, and Apoptosis in Breast Cancer Cells.” *Oncogene* 23 (2): 596–604. doi:10.1038/sj.onc.1207147.

Miyoshi, K., J. M. Shillingford, G. H. Smith, S. L. Grimm, K. U. Wagner, T. Oka, J. M. Rosen, G. W. Robinson, and L. Hennighausen. 2001. “Signal Transducer and Activator of Transcription (Stat) 5 Controls the Proliferation and Differentiation of Mammary Alveolar Epithelium.” *The Journal of Cell Biology* 155 (4): 531–42. doi:10.1083/jcb.200107065.

Mizuno, A., N. Amizuka, K. Irie, A. Murakami, N. Fujise, T. Kanno, Y. Sato, et al. 1998. “Severe Osteoporosis in Mice Lacking Osteoclastogenesis Inhibitory Factor/osteoprotegerin.” *Biochemical and Biophysical Research Communications* 247 (3): 610–15.

Moen, Marit D., and Susan J. Keam. 2011. “Denosumab: A Review of Its Use in the Treatment of Postmenopausal Osteoporosis.” *Drugs & Aging* 28 (1): 63–82. doi:10.2165/11203300-000000000-00000.

Morrison, Ryan, Stephen M. Schleicher, Yunguang Sun, Kenneth J. Niermann, Sungjune Kim, Daniel E. Spratt, Christine H. Chung, and Bo Lu. 2010. “Targeting the Mechanisms of Resistance to Chemotherapy and Radiotherapy with the Cancer Stem Cell Hypothesis.” *Journal of Oncology* 2011 (October): e941876. doi:10.1155/2011/941876.

Moumen, Mejdi, Aurélie Chiche, Stéphanie Cagnet, Valérie Petit, Karine Raymond, Marisa M. Faraldo, Marie-Ange Deugnier, and Marina A. Glukhova. 2011. “The Mammary Myoepithelial Cell.” *The International Journal of Developmental Biology* 55 (7-9): 763–71. doi:10.1387/ijdb.113385mm.

Mukherjee, Atish, Selma M. Soyal, Jie Li, Yan Ying, Bin He, Francesco J. DeMayo, and John P. Lydon. 2010. “Targeting RANKL to a Specific Subset of Murine Mammary Epithelial Cells Induces Ordered Branching Morphogenesis and Alveologenesis in the Absence of Progesterone Receptor Expression.” *FASEB Journal: Official Publication of the Federation of American Societies for Experimental Biology* 24 (11): 4408–19. doi:10.1096/fj.10-157982.

Mulac-Jericevic, Biserka, John P. Lydon, Francesco J. DeMayo, and Orla M. Conneely. 2003. “Defective Mammary Gland Morphogenesis in Mice Lacking the Progesterone Receptor B Isoform.” *Proceedings of the National Academy of Sciences of the United States of America* 100 (17): 9744–49. doi:10.1073/pnas.1732707100.

Mulero, María Carmen, Dolors Ferres-Marco, Abul Islam, Pol Margalef, Matteo Pecoraro, Agustí Toll, Nils Drechsel, et al. 2013. “Chromatin-Bound IκBα Regulates a Subset of Polycomb Target Genes in Differentiation and Cancer.” *Cancer Cell* 24 (2): 151–66. doi:10.1016/j.ccr.2013.06.003.

Muller, W. J., E. Sinn, P. K. Pattengale, R. Wallace, and P. Leder. 1988. “Single-Step Induction of Mammary Adenocarcinoma in Transgenic Mice Bearing the Activated c-Neu Oncogene.” *Cell* 54 (1): 105–15.

Mundy, Gregory R. 2002. “Metastasis to Bone: Causes, Consequences and Therapeutic Opportunities.” *Nature Reviews. Cancer* 2 (8): 584–93. doi:10.1038/nrc867.

Muñoz, B., and F. F. Bolander. 1989. “Prolactin Regulation of Mouse Mammary Tumor Virus (MMTV) Expression in Normal Mouse Mammary Epithelium.” *Molecular and Cellular Endocrinology* 62 (1): 23–29.

Murtagh, Janice, Finian Martin, and Richard M. Gronostajski. 2003. “The Nuclear Factor I (NFI) Gene Family in Mammary Gland Development and Function.” *Journal of Mammary Gland Biology and Neoplasia* 8 (2): 241–54.

Naka, T., M. Narazaki, M. Hirata, T. Matsumoto, S. Minamoto, A. Aono, N. Nishimoto, et al. 1997. “Structure and Function of a New STAT-Induced STAT Inhibitor.” *Nature* 387 (6636): 924–29. doi:10.1038/43219.

Neville, Margaret C., Thomas B. McFadden, and Isabel Forsyth. 2002. “Hormonal Regulation of Mammary Differentiation and Milk Secretion.” *Journal of Mammary Gland Biology and Neoplasia* 7 (1): 49–66.

Nishikawa, S., R. C. Moore, N. Nonomura, and T. Oka. 1994. “Progesterone and EGF Inhibit Mouse Mammary Gland Prolactin Receptor and Beta-Casein Gene Expression.” *The American Journal of Physiology* 267 (5 Pt 1): C1467–72.

Nyga, Rémy, Christian Pecquet, Noria Harir, Haihua Gu, Isabelle Dhennin-Duthille, Aline Régnier, Valérie Gouilleux-Gruart, Kaïss Lassoued, and Fabrice Gouilleux. 2005. “Activated STAT5 Proteins Induce Activation of the PI 3-kinase/Akt and Ras/MAPK Pathways via the Gab2 Scaffolding Adapter.” *The Biochemical Journal* 390 (Pt 1): 359–66. doi:10.1042/BJ20041523.

Oakes, Samantha R., Heidi N. Hilton, and Christopher J. Ormandy. 2006. “The Alveolar Switch: Coordinating the Proliferative Cues and Cell Fate Decisions That Drive the Formation of

Lobuloalveoli from Ductal Epithelium." *Breast Cancer Research: BCR* 8 (2): 207. doi:10.1186/bcr1411.

Oakes, Samantha R., Matthew J. Naylor, Marie-Liesse Asselin-Labat, Katrina D. Blazek, Margaret Gardiner-Garden, Heidi N. Hilton, Michael Kazlauskas, et al. 2008. "The Ets Transcription Factor Elf5 Specifies Mammary Alveolar Cell Fate." *Genes & Development* 22 (5): 581–86. doi:10.1101/gad.1614608.

O'Brien, Catherine Adell, Antonija Kreso, and Catriona H. M. Jamieson. 2010. "Cancer Stem Cells and Self-Renewal." *Clinical Cancer Research* 16 (12): 3113–20. doi:10.1158/1078-0432.CCR-09-2824.

Okutani, Y., A. Kitanaka, T. Tanaka, H. Kamano, H. Ohnishi, Y. Kubota, T. Ishida, and J. Takahara. 2001. "Src Directly Tyrosine-Phosphorylates STAT5 on Its Activation Site and Is Involved in Erythropoietin-Induced Signaling Pathway." *Oncogene* 20 (45): 6643–50. doi:10.1038/sj.onc.1204807.

Olayioye, M. A., R. M. Neve, H. A. Lane, and N. E. Hynes. 2000. "The ErbB Signaling Network: Receptor Heterodimerization in Development and Cancer." *The EMBO Journal* 19 (13): 3159–67. doi:10.1093/emboj/19.13.3159.

Ormandy, Christopher J., Matthew Naylor, Jessica Harris, Fiona Robertson, Nelson D. Horseman, Geoffrey J. Lindeman, Jane Visvader, and Paul A. Kelly. 2003. "Investigation of the Transcriptional Changes Underlying Functional Defects in the Mammary Glands of Prolactin Receptor Knockout Mice." *Recent Progress in Hormone Research* 58: 297–323.

Ormandy, C. J., A. Camus, J. Barra, D. Damotte, B. Lucas, H. Buteau, M. Edery, et al. 1997. "Null Mutation of the Prolactin Receptor Gene Produces Multiple Reproductive Defects in the Mouse." *Genes & Development* 11 (2): 167–78.

Osborne, C. Kent, and Rachel Schiff. 2011. "Mechanisms of Endocrine Resistance in Breast Cancer." *Annual Review of Medicine* 62 (1): 233–47. doi:10.1146/annurev-med-070909-182917.

Otten, A. D., M. M. Sanders, and G. S. McKnight. 1988. "The MMTV LTR Promoter Is Induced by Progesterone and Dihydrotestosterone but Not by Estrogen." *Molecular Endocrinology (Baltimore, Md.)* 2 (2): 143–47. doi:10.1210/mend-2-2-143.

Owens, Thomas W., and Matthew J. Naylor. 2013. "Breast Cancer Stem Cells." *Frontiers in Physiology* 4: 225. doi:10.3389/fphys.2013.00225.

Paget, S. 1989. "The Distribution of Secondary Growths in Cancer of the Breast. 1889." *Cancer Metastasis Reviews* 8 (2): 98–101.

Palafox, Marta, Irene Ferrer, Pasquale Pellegrini, Sergi Vila, Sara Hernandez-Ortega, Ander Urruticoechea, Fina Climent, et al. 2012. "RANK Induces Epithelial-Mesenchymal Transition and

Stemness in Human Mammary Epithelial Cells and Promotes Tumorigenesis and Metastasis." *Cancer Research* 72 (11): 2879–88. doi:10.1158/0008-5472.CAN-12-0044.

Park, David S., Hyangkyu Lee, Philippe G. Frank, Babak Razani, Andrew V. Nguyen, Albert F. Parlow, Robert G. Russell, James Hulit, Richard G. Pestell, and Michael P. Lisanti. 2002. "Caveolin-1-Deficient Mice Show Accelerated Mammary Gland Development During Pregnancy, Premature Lactation, and Hyperactivation of the Jak-2/STAT5a Signaling Cascade." *Molecular Biology of the Cell* 13 (10): 3416–30. doi:10.1091/mbc.02-05-0071.

Park, D. S., H. Lee, C. Riedel, J. Hulit, P. E. Scherer, R. G. Pestell, and M. P. Lisanti. 2001. "Prolactin Negatively Regulates Caveolin-1 Gene Expression in the Mammary Gland during Lactation, via a Ras-Dependent Mechanism." *The Journal of Biological Chemistry* 276 (51): 48389–97. doi:10.1074/jbc.M108210200.

Park, So Yeon, Hee Eun Lee, Hailun Li, Michail Shipitsin, Rebecca Gelman, and Kornelia Polyak. 2010. "Heterogeneity for Stem Cell-Related Markers according to Tumor Subtype and Histologic Stage in Breast Cancer." *Clinical Cancer Research: An Official Journal of the American Association for Cancer Research* 16 (3): 876–87. doi:10.1158/1078-0432.CCR-09-1532.

Pearson, Gray, Fred Robinson, Tara Beers Gibson, Bing-e Xu, Mahesh Karandikar, Kevin Berman, and Melanie H. Cobb. 2001. "Mitogen-Activated Protein (MAP) Kinase Pathways: Regulation and Physiological Functions." *Endocrine Reviews* 22 (2): 153–83. doi:10.1210/edrv.22.2.0428.

Pece, Salvatore, Daniela Tosoni, Stefano Confalonieri, Giovanni Mazzarol, Manuela Vecchi, Simona Ronzoni, Loris Bernard, Giuseppe Viale, Pier Giuseppe Pelicci, and Pier Paolo Di Fiore. 2010. "Biological and Molecular Heterogeneity of Breast Cancers Correlates with Their Cancer Stem Cell Content." *Cell* 140 (1): 62–73. doi:10.1016/j.cell.2009.12.007.

Pellegrini, Pasquale, Alex Cordero, Marta I Gallego, William C. Dougall, Purificación Muñoz, Miguel Ángel Pujana, and Eva González Suárez. 2013. "Constitutive Activation of RANK Disrupts Mammary Cell Fate Leading to Tumorigenesis." *Stem Cells* 31 (9): 1954–65.

Perkins, Neil D. 2007. "Integrating Cell-Signalling Pathways with NF-κB and IKK Function." *Nature Reviews Molecular Cell Biology* 8 (1): 49–62. doi:10.1038/nrm2083.

Perou, Charles M., Therese Sørlie, Michael B. Eisen, Matt van de Rijn, Stefanie S. Jeffrey, Christian A. Rees, Jonathan R. Pollack, et al. 2000. "Molecular Portraits of Human Breast Tumours." *Nature* 406 (6797): 747–52. doi:10.1038/35021093.

Petersen, O. W., P. E. Høyer, and B. van Deurs. 1987. "Frequency and Distribution of Estrogen Receptor-Positive Cells in Normal, Nonlactating Human Breast Tissue." *Cancer Research* 47 (21): 5748–51.

Pfitzner, Berit Maria, Daniel Branstetter, Sibylle Loibl, Carsten Denkert, Bianca Lederer, Wolfgang Daniel Schmitt, Frank Dombrowski, et al. 2014. “RANK Expression as a Prognostic and Predictive Marker in Breast Cancer.” *Breast Cancer Research and Treatment* 145 (2): 307–15. doi:10.1007/s10549-014-2955-1.

Piekorz, Roland P., Sébastien Gingras, Angelika Hoffmeyer, James N. Ihle, and Yacob Weinstein. 2005. “Regulation of Progesterone Levels during Pregnancy and Parturition by Signal Transducer and Activator of Transcription 5 and 20α-Hydroxysteroid Dehydrogenase.” *Molecular Endocrinology* 19 (2): 431–40. doi:10.1210/me.2004-0302.

Pike, M. C., R. K. Peters, W. Cozen, N. M. Probst-Hensch, J. C. Felix, P. C. Wan, and T. M. Mack. 1997. “Estrogen-Progestin Replacement Therapy and Endometrial Cancer.” *Journal of the National Cancer Institute* 89 (15): 1110–16.

Pratt, Aleix, and Charles M. Perou. 2011. “Deconstructing the Molecular Portraits of Breast Cancer.” *Molecular Oncology* 5 (1): 5–23. doi:10.1016/j.molonc.2010.11.003.

Pratt, M. a. C., E. Tibbo, S. J. Robertson, D. Jansson, K. Hurst, C. Perez-Iratxeta, R. Lau, and M. Y. Niu. 2009. “The Canonical NF-kappaB Pathway Is Required for Formation of Luminal Mammary Neoplasias and Is Activated in the Mammary Progenitor Population.” *Oncogene* 28 (30): 2710–22. doi:10.1038/onc.2009.131.

Raingeaud, J., S. Gupta, J. S. Rogers, M. Dickens, J. Han, R. J. Ulevitch, and R. J. Davis. 1995. “Pro-Inflammatory Cytokines and Environmental Stress Cause p38 Mitogen-Activated Protein Kinase Activation by Dual Phosphorylation on Tyrosine and Threonine.” *The Journal of Biological Chemistry* 270 (13): 7420–26.

Reginster, Jean-Yves. 2011. “Antifracture Efficacy of Currently Available Therapies for Postmenopausal Osteoporosis.” *Drugs* 71 (1): 65–78. doi:10.2165/11587570-000000000-00000.

Reya, T., S. J. Morrison, M. F. Clarke, and I. L. Weissman. 2001. “Stem Cells, Cancer, and Cancer Stem Cells.” *Nature* 414 (6859): 105–11. doi:10.1038/35102167.

Ricardo, Sara, André Filipe Vieira, Renê Gerhard, Dina Leitão, Regina Pinto, Jorge F. Cameselle-Teijeiro, Fernanda Milanezi, Fernando Schmitt, and Joana Paredes. 2011. “Breast Cancer Stem Cell Markers CD44, CD24 and ALDH1: Expression Distribution within Intrinsic Molecular Subtype.” *Journal of Clinical Pathology* 64 (11): 937–46. doi:10.1136/jcp.2011.090456.

Richert, M. M., K. L. Schwertfeger, J. W. Ryder, and S. M. Anderson. 2000. “An Atlas of Mouse Mammary Gland Development.” *Journal of Mammary Gland Biology and Neoplasia* 5 (2): 227–41.

Rossi, Simona W., Mi-Yeon Kim, Andreas Leibbrandt, Sonia M. Parnell, William E. Jenkinson, Stephanie H. Glanville, Fiona M. McConnell, et al. 2007. “RANK Signals from CD4(+)3(-) Inducer

Cells Regulate Development of Aire-Expressing Epithelial Cells in the Thymic Medulla." *The Journal of Experimental Medicine* 204 (6): 1267–72. doi:10.1084/jem.20062497.

Rowse, G. J., S. R. Ritland, and S. J. Gendler. 1998. "Genetic Modulation of Neu Proto-Oncogene-Induced Mammary Tumorigenesis." *Cancer Research* 58 (12): 2675–79.

Ruan, W., and D. L. Kleinberg. 1999. "Insulin-like Growth Factor I Is Essential for Terminal End Bud Formation and Ductal Morphogenesis during Mammary Development." *Endocrinology* 140 (11): 5075–81. doi:10.1210/endo.140.11.7095.

Russo, J., X. Ao, C. Grill, and I. H. Russo. 1999. "Pattern of Distribution of Cells Positive for Estrogen Receptor Alpha and Progesterone Receptor in Relation to Proliferating Cells in the Mammary Gland." *Breast Cancer Research and Treatment* 53 (3): 217–27.

Sakaguchi, Shimon. 2005. "Naturally Arising Foxp3-Expressing CD25+CD4+ Regulatory T Cells in Immunological Tolerance to Self and Non-Self." *Nature Immunology* 6 (4): 345–52. doi:10.1038/ni1178.

Santini, Daniele, Gaia Schiavon, Bruno Vincenzi, Laura Gaeta, Francesco Pantano, Antonio Russo, Cinzia Ortega, et al. 2011. "Receptor Activator of NF-kB (RANK) Expression in Primary Tumors Associates with Bone Metastasis Occurrence in Breast Cancer Patients." *PloS One* 6 (4): e19234. doi:10.1371/journal.pone.0019234.

Schepers, Arnout G., Hugo J. Snippert, Daniel E. Stange, Maaike van den Born, Johan H. van Es, Marc van de Wetering, and Hans Clevers. 2012. "Lineage Tracing Reveals Lgr5+ Stem Cell Activity in Mouse Intestinal Adenomas." *Science (New York, N.Y.)* 337 (6095): 730–35. doi:10.1126/science.1224676.

Schramek, Daniel, Andreas Leibbrandt, Verena Sigl, Lukas Kenner, John A. Pospisilik, Heather J. Lee, Reiko Hanada, et al. 2010. "Osteoclast Differentiation Factor RANKL Controls Development of Progestin-Driven Mammary Cancer." *Nature* 468 (7320): 98–102. doi:10.1038/nature09387.

Schwertfeger, Kathryn L., Monica M. Richert, and Steven M. Anderson. 2001. "Mammary Gland Involution Is Delayed by Activated Akt in Transgenic Mice." *Molecular Endocrinology* 15 (6): 867–81. doi:10.1210/mend.15.6.0663.

Serrano, M., A. W. Lin, M. E. McCurrach, D. Beach, and S. W. Lowe. 1997. "Oncogenic Ras Provokes Premature Cell Senescence Associated with Accumulation of p53 and p16INK4a." *Cell* 88 (5): 593–602.

Shackleton, Mark, François Vaillant, Kaylene J. Simpson, John Stingl, Gordon K. Smyth, Marie-Liesse Asselin-Labat, Li Wu, Geoffrey J. Lindeman, and Jane E. Visvader. 2006. "Generation of a Functional Mammary Gland from a Single Stem Cell." *Nature* 439 (7072): 84–88. doi:10.1038/nature04372.

Shehata, Mona, Andrew Teschendorff, Gemma Sharp, Nikola Novcic, I Alasdair Russell, Stefanie Avril, Michael Prater, et al. 2012. “Phenotypic and Functional Characterisation of the Luminal Cell Hierarchy of the Mammary Gland.” *Breast Cancer Research: BCR* 14 (5): R134. doi:10.1186/bcr3334.

Shou, Jiang, Suleiman Massarweh, C. Kent Osborne, Alan E. Wakeling, Simale Ali, Heidi Weiss, and Rachel Schiff. 2004. “Mechanisms of Tamoxifen Resistance: Increased Estrogen Receptor-HER2/neu Cross-Talk in ER/HER2–Positive Breast Cancer.” *Journal of the National Cancer Institute* 96 (12): 926–35. doi:10.1093/jnci/djh166.

Shyamala, G., Y.-C. Chou, S. G. Louie, R. C. Guzman, G. H. Smith, and S. Nandi. 2002. “Cellular Expression of Estrogen and Progesterone Receptors in Mammary Glands: Regulation by Hormones, Development and Aging.” *The Journal of Steroid Biochemistry and Molecular Biology* 80 (2): 137–48.

Simonet, W. S., D. L. Lacey, C. R. Dunstan, M. Kelley, M. S. Chang, R. Lüthy, H. Q. Nguyen, et al. 1997. “Osteoprotegerin: A Novel Secreted Protein Involved in the Regulation of Bone Density.” *Cell* 89 (2): 309–19.

Slamon, D. J., G. M. Clark, S. G. Wong, W. J. Levin, A. Ullrich, and W. L. McGuire. 1987. “Human Breast Cancer: Correlation of Relapse and Survival with Amplification of the HER-2/neu Oncogene.” *Science (New York, N.Y.)* 235 (4785): 177–82.

Sleeman, Katherine E., Howard Kendrick, Alan Ashworth, Clare M. Isacke, and Matthew J. Smalley. 2006. “CD24 Staining of Mouse Mammary Gland Cells Defines Luminal Epithelial, Myoepithelial/basal and Non-Epithelial Cells.” *Breast Cancer Research: BCR* 8 (1): R7. doi:10.1186/bcr1371.

Sleeman, Katherine E., Howard Kendrick, David Robertson, Clare M. Isacke, Alan Ashworth, and Matthew J. Smalley. 2007. “Dissociation of Estrogen Receptor Expression and in Vivo Stem Cell Activity in the Mammary Gland.” *The Journal of Cell Biology* 176 (1): 19–26. doi:10.1083/jcb.200604065.

Smith, G. H., and D. Medina. 1988. “A Morphologically Distinct Candidate for an Epithelial Stem Cell in Mouse Mammary Gland.” *Journal of Cell Science* 90 (Pt 1) (May): 173–83.

Sorlie, Therese, Robert Tibshirani, Joel Parker, Trevor Hastie, J. S. Marron, Andrew Nobel, Shibing Deng, et al. 2003. “Repeated Observation of Breast Tumor Subtypes in Independent Gene Expression Data Sets.” *Proceedings of the National Academy of Sciences of the United States of America* 100 (14): 8418–23. doi:10.1073/pnas.0932692100.

Sørlie, T., C. M. Perou, R. Tibshirani, T. Aas, S. Geisler, H. Johnsen, T. Hastie, et al. 2001. “Gene Expression Patterns of Breast Carcinomas Distinguish Tumor Subclasses with Clinical Implications.” *Proceedings of the National Academy of Sciences of the United States of America* 98 (19): 10869–74. doi:10.1073/pnas.191367098.

Southby, J., M. W. Kissin, J. A. Danks, J. A. Hayman, J. M. Moseley, M. A. Henderson, R. C. Bennett, and T. J. Martin. 1990. “Immunohistochemical Localization of Parathyroid Hormone-Related Protein in Human Breast Cancer.” *Cancer Research* 50 (23): 7710–16.

Sovak, M. A., M. Arsura, G. Zanieski, K. T. Kavanagh, and G. E. Sonenshein. 1999. “The Inhibitory Effects of Transforming Growth Factor beta1 on Breast Cancer Cell Proliferation Are Mediated through Regulation of Aberrant Nuclear Factor-kappaB/Rel Expression.” *Cell Growth & Differentiation: The Molecular Biology Journal of the American Association for Cancer Research* 10 (8): 537–44.

Soyal, Selma, Preeti M. Ismail, Jie Li, Biserka Mulac-Jericevic, Orla M. Conneely, and John P. Lydon. 2002. “Progesterone’s Role in Mammary Gland Development and Tumorigenesis as Disclosed by Experimental Mouse Genetics.” *Breast Cancer Research: BCR* 4 (5): 191–96.

Span, Paul N., Esmé Waanders, Peggy Manders, Joop J. T. M. Heuvel, John A. Foekens, Mark A. Watson, Louk V. A. M. Beex, and Fred C. G. J. Sweep. 2004. “Mammaglobin Is Associated with Low-Grade, Steroid Receptor-Positive Breast Tumors from Postmenopausal Patients, and Has Independent Prognostic Value for Relapse-Free Survival Time.” *Journal of Clinical Oncology: Official Journal of the American Society of Clinical Oncology* 22 (4): 691–98. doi:10.1200/JCO.2004.01.072.

Srivastava, Sunil, Manabu Matsuda, Zhaoyuan Hou, Jason P. Bailey, Riko Kitazawa, Matthew P. Herbst, and Nelson D. Horseman. 2003. “Receptor Activator of NF-kappaB Ligand Induction via Jak2 and Stat5a in Mammary Epithelial Cells.” *The Journal of Biological Chemistry* 278 (46): 46171–78. doi:10.1074/jbc.M308545200.

Stingl, John, Connie J. Eaves, Iman Zandieh, and Joanne T. Emerman. 2001. “Characterization of Bipotent Mammary Epithelial Progenitor Cells in Normal Adult Human Breast Tissue.” *Breast Cancer Research and Treatment* 67 (2): 93–109. doi:10.1023/A:1010615124301.

Stingl, John, Peter Eirew, Ian Ricketson, Mark Shackleton, François Vaillant, David Choi, Haiyan I. Li, and Connie J. Eaves. 2006. “Purification and Unique Properties of Mammary Epithelial Stem Cells.” *Nature* 439 (7079): 993–97. doi:10.1038/nature04496.

Sun, Shao-Cong, and Steven C. Ley. 2008. “New Insights into NF-kappaB Regulation and Function.” *Trends in Immunology* 29 (10): 469–78. doi:10.1016/j.it.2008.07.003.

Sun, Peng, Yuanyang Yuan, Aihua Li, Boan Li, and Xing Dai. 2010. “Cytokeratin Expression during Mouse Embryonic and Early Postnatal Mammary Gland Development.” *Histochemistry and Cell Biology* 133 (2): 213–21. doi:10.1007/s00418-009-0662-5.

Sutherland, Kate D., Geoffrey J. Lindeman, and Jane E. Visvader. 2007. “Knocking off SOCS Genes in the Mammary Gland.” *Cell Cycle (Georgetown, Tex.)* 6 (7): 799–803.

Sutherland, Kate D, François Vaillant, Warren S Alexander, Tim M Wintermantel, Natasha C Forrest, Sheridan L Holroyd, Edward J McManus, et al. 2006. “C-Myc as a Mediator of Accelerated Apoptosis and Involution in Mammary Glands Lacking Socs3.” *The EMBO Journal* 25 (24): 5805–15. doi:10.1038/sj.emboj.7601455.

Takayanagi, Hiroshi. 2007. “Osteoimmunology: Shared Mechanisms and Crosstalk between the Immune and Bone Systems.” *Nature Reviews. Immunology* 7 (4): 292–304. doi:10.1038/nri2062.

Taneja, Pankaj, Donna P. Frazier, Robert D. Kendig, Dejan Maglic, Takayuki Sugiyama, Fumitake Kai, Neetu K. Taneja, and Kazushi Inoue. 2009. “MMTV Mouse Models and the Diagnostic Values of MMTV-like Sequences in Human Breast Cancer.” *Expert Review of Molecular Diagnostics* 9 (5): 423–40. doi:10.1586/erm.09.31.

Tanos, Tamara, George Sflomos, Pablo C. Echeverria, Ayyakkannu Ayyanan, Maria Gutierrez, Jean-Francois Delaloye, Wassim Raffoul, et al. 2013. “Progesterone/RANKL Is a Major Regulatory Axis in the Human Breast.” *Science Translational Medicine* 5 (182): 182ra55. doi:10.1126/scitranslmed.3005654.

Tan, Wei, Weizhou Zhang, Amy Strasner, Sergei Grivennikov, Jin Q. Cheng, Robert M. Hoffman, and Michael Karin. 2011. “Tumour-Infiltrating Regulatory T Cells Stimulate Mammary Cancer Metastasis through RANKL-RANK Signalling.” *Nature* 470 (7335): 548–53. doi:10.1038/nature09707.

Teglund, S., C. McKay, E. Schuetz, J. M. van Deursen, D. Stravopodis, D. Wang, M. Brown, S. Bodner, G. Grosveld, and J. N. Ihle. 1998. “Stat5a and Stat5b Proteins Have Essential and Nonessential, or Redundant, Roles in Cytokine Responses.” *Cell* 93 (5): 841–50.

Theill, Lars E., William J. Boyle, and Josef M. Penninger. 2002. “RANK-L and RANK: T Cells, Bone Loss, and Mammalian Evolution.” *Annual Review of Immunology* 20: 795–823. doi:10.1146/annurev.immunol.20.100301.064753.

Thomas, R. S., A. N. Ng, J. Zhou, M. J. Tymms, W. Doppler, and I. Kola. 2000. “The Elf Group of Ets-Related Transcription Factors. ELF3 and ELF5.” *Advances in Experimental Medicine and Biology* 480: 123–28. doi:10.1007/0-306-46832-8_15.

Tiffen, Paul G., Nader Omidvar, Nuria Marquez-Almuina, Dawn Croston, Christine J. Watson, and Richard W. E. Clarkson. 2008. “A Dual Role for Oncostatin M Signaling in the Differentiation and Death of Mammary Epithelial Cells in Vivo.” *Molecular Endocrinology (Baltimore, Md.)* 22 (12): 2677–88. doi:10.1210/me.2008-0097.

Ukaji, Tamami, and Kazuo Umezawa. 2014. “Novel Approaches to Target NF-κB and Other Signaling Pathways in Cancer Stem Cells.” *Advances in Biological Regulation*, Targeting Signaling Pathways in Stem Cells, 56 (September): 108–15. doi:10.1016/j.jbior.2014.06.001.

Vaillant, François, Marie-Liesse Asselin-Labat, Mark Shackleton, Natasha C. Forrest, Geoffrey J. Lindeman, and Jane E. Visvader. 2008. “The Mammary Progenitor Marker CD61/beta3 Integrin Identifies Cancer Stem Cells in Mouse Models of Mammary Tumorigenesis.” *Cancer Research* 68 (19): 7711–17. doi:10.1158/0008-5472.CAN-08-1949.

Valentino, Lyne, and Josiane Pierre. 2006. “JAK/STAT Signal Transduction: Regulators and Implication in Hematological Malignancies.” *Biochemical Pharmacology* 71 (6): 713–21. doi:10.1016/j.bcp.2005.12.017.

Vallabhapurapu, Sivakumar, and Michael Karin. 2009. “Regulation and Function of NF-kappaB Transcription Factors in the Immune System.” *Annual Review of Immunology* 27: 693–733. doi:10.1146/annurev.immunol.021908.132641.

van Amerongen, Renée, Angela N. Bowman, and Roel Nusse. 2012. “Developmental Stage and Time Dictate the Fate of Wnt/β-Catenin-Responsive Stem Cells in the Mammary Gland.” *Cell Stem Cell* 11 (3): 387–400. doi:10.1016/j.stem.2012.05.023.

Van Keymeulen, Alexandra, Ana Sofia Rocha, Marielle Ousset, Benjamin Beck, Gaëlle Bouvencourt, Jason Rock, Neha Sharma, Sophie Dekoninck, and Cédric Blanpain. 2011. “Distinct Stem Cells Contribute to Mammary Gland Development and Maintenance.” *Nature* 479 (7372): 189–93. doi:10.1038/nature10573.

Vargo-Gogola, Tracy, and Jeffrey M. Rosen. 2007. “Modelling Breast Cancer: One Size Does Not Fit All.” *Nature Reviews Cancer* 7 (9): 659–72. doi:10.1038/nrc2193.

Vici, Patrizia, Laura Pizzuti, Clara Natoli, Teresa Gamucci, Luigi Di Lauro, Maddalena Barba, Domenico Sergi, et al. 2015. “Triple Positive Breast Cancer: A Distinct Subtype?” *Cancer Treatment Reviews* 41 (2): 69–76. doi:10.1016/j.ctrv.2014.12.005.

Visvader, Jane E. 2011. “Cells of Origin in Cancer.” *Nature* 469 (7330): 314–22. doi:10.1038/nature09781.

Wada, Teiji, Tomoki Nakashima, Nishina Hiroshi, and Josef M. Penninger. 2006. “RANKL-RANK Signaling in Osteoclastogenesis and Bone Disease.” *Trends in Molecular Medicine* 12 (1): 17–25. doi:10.1016/j.molmed.2005.11.007.

Wagner, Kay-Uwe, and Hallgeir Rui. 2008. “Jak2/Stat5 Signaling in Mammogenesis, Breast Cancer Initiation and Progression.” *Journal of Mammary Gland Biology and Neoplasia* 13 (1): 93–103. doi:10.1007/s10911-008-9062-z.

Wagner, K. U., K. McAllister, T. Ward, B. Davis, R. Wiseman, and L. Hennighausen. 2001. “Spatial and Temporal Expression of the Cre Gene under the Control of the MMTV-LTR in Different Lines of Transgenic Mice.” *Transgenic Research* 10 (6): 545–53.

Wagner, K U, R J Wall, L St-Onge, P Gruss, A Wynshaw-Boris, L Garrett, M Li, P A Furth, and L Hennighausen. 1997. “Cre-Mediated Gene Deletion in the Mammary Gland.” *Nucleic Acids Research* 25 (21): 4323–30.

Wajapeyee, Narendra, Ryan W. Serra, Xiaochun Zhu, Meera Mahalingam, and Michael R. Green. 2008. “Oncogenic BRAF Induces Senescence and Apoptosis through Pathways Mediated by the Secreted Protein IGFBP7.” *Cell* 132 (3): 363–74. doi:10.1016/j.cell.2007.12.032.

Watkin, Harriet, Monica M Richert, Andrew Lewis, Kristina Terrell, James P McManaman, and Steven M Anderson. 2008. “Lactation Failure in Src Knockout Mice Is due to Impaired Secretory Activation.” *BMC Developmental Biology* 8 (January): 6. doi:10.1186/1471-213X-8-6.

Watson, Christine J., and Walid T. Khaled. 2008. “Mammary Development in the Embryo and Adult: A Journey of Morphogenesis and Commitment.” *Development (Cambridge, England)* 135 (6): 995–1003. doi:10.1242/dev.005439.

Watson, Christine J., and Peter A. Kreuzaler. 2011. “Remodeling Mechanisms of the Mammary Gland during Involution.” *The International Journal of Developmental Biology* 55 (7-9): 757–62. doi:10.1387/ijdb.113414cw.

Watt, Fiona M., and Kim B. Jensen. 2009. “Epidermal Stem Cell Diversity and Quiescence.” *EMBO Molecular Medicine* 1 (5): 260–67. doi:10.1002/emmm.200900033.

Weigelt, Britta, Johannes L. Peterse, and Laura J. van’t Veer. 2005. “Breast Cancer Metastasis: Markers and Models.” *Nature Reviews Cancer* 5 (8): 591–602. doi:10.1038/nrc1670.

Weinstein, I. Bernard. 2002. “Cancer. Addiction to Oncogenes--the Achilles Heal of Cancer.” *Science (New York, N.Y.)* 297 (5578): 63–64. doi:10.1126/science.1073096.

Whyte, Jacqueline, Orla Bergin, Alessandro Bianchi, Sara McNally, and Finian Martin. 2009. “Key Signalling Nodes in Mammary Gland Development and Cancer. Mitogen-Activated Protein Kinase Signalling in Experimental Models of Breast Cancer Progression and in Mammary Gland Development.” *Breast Cancer Research: BCR* 11 (5): 209. doi:10.1186/bcr2361.

Wiseman, Bryony S., and Zena Werb. 2002. “Stromal Effects on Mammary Gland Development and Breast Cancer.” *Science* 296 (5570): 1046–49. doi:10.1126/science.1067431.

Wong, B. R., J. Rho, J. Arron, E. Robinson, J. Orlinick, M. Chao, S. Kalachikov, et al. 1997. “TRANCE Is a Novel Ligand of the Tumor Necrosis Factor Receptor Family That Activates c-Jun N-Terminal Kinase in T Cells.” *The Journal of Biological Chemistry* 272 (40): 25190–94.

Wu, Wen-Jun, Chin-Feng Lee, Chung-Han Hsin, Jyun-Yi Du, Tsai-Ching Hsu, Ting-Hui Lin, Tsung-You Yao, Cheng-Hsieh Huang, and Yi-Ju Lee. 2008. “TGF-Beta Inhibits Prolactin-Induced Expression of Beta-Casein by a Smad3-Dependent Mechanism.” *Journal of Cellular Biochemistry* 104 (5): 1647–59. doi:10.1002/jcb.21734.

Xing, Lianping, Edward M. Schwarz, and Brendan F. Boyce. 2005. “Osteoclast Precursors, RANKL/RANK, and Immunology.” *Immunological Reviews* 208 (December): 19–29. doi:10.1111/j.0105-2896.2005.00336.x.

Xu, Yingxi, Na Li, Rong Xiang, and Peiqing Sun. 2014. “Emerging Roles of the p38 MAPK and PI3K/AKT/mTOR Pathways in Oncogene-Induced Senescence.” *Trends in Biochemical Sciences* 39 (6): 268–76. doi:10.1016/j.tibs.2014.04.004.

Yagata, Hiroshi, Yuka Kajiura, and Hideko Yamauchi. 2011. “Current Strategy for Triple-Negative Breast Cancer: Appropriate Combination of Surgery, Radiation, and Chemotherapy.” *Breast Cancer (Tokyo, Japan)* 18 (3): 165–73. doi:10.1007/s12282-011-0254-9.

Yamaji, Daisuke, Keunsoo Kang, Gertraud W. Robinson, and Lothar Hennighausen. 2013. “Sequential Activation of Genetic Programs in Mouse Mammary Epithelium during Pregnancy Depends on STAT5A/B Concentration.” *Nucleic Acids Research* 41 (3): 1622–36. doi:10.1093/nar/gks1310.

Yamaji, Daisuke, Risu Na, Yonatan Feuermann, Susanne Pechhold, Weiping Chen, Gertraud W. Robinson, and Lothar Hennighausen. 2009. “Development of Mammary Luminal Progenitor Cells Is Controlled by the Transcription Factor STAT5A.” *Genes & Development* 23 (20): 2382–87. doi:10.1101/gad.1840109.

Yarden, Y., and M. X. Sliwkowski. 2001. “Untangling the ErbB Signalling Network.” *Nature Reviews. Molecular Cell Biology* 2 (2): 127–37. doi:10.1038/35052073.

Yasuda, H., N. Shima, N. Nakagawa, K. Yamaguchi, M. Kinosaki, S. Mochizuki, A. Tomoyasu, et al. 1998a. “Osteoclast Differentiation Factor Is a Ligand for Osteoprotegerin/osteoclastogenesis-Inhibitory Factor and Is Identical to TRANCE/RANKL.” *Proceedings of the National Academy of Sciences of the United States of America* 95 (7): 3597–3602.

Zeng, Yi Arial, and Roel Nusse. 2010. “Wnt Proteins Are Self-Renewal Factors for Mammary Stem Cells and Promote Their Long-Term Expansion in Culture.” *Cell Stem Cell* 6 (6): 568–77. doi:10.1016/j.stem.2010.03.020.

Zhang, Weizhou, Wei Tan, Xuefeng Wu, Maxim Poustovoitov, Amy Strasner, Wei Li, Nicholas Borcherding, Majid Ghassemian, and Michael Karin. 2013. “A NIK-IKKα Module Expands ErbB2-Induced Tumor-Initiating Cells by Stimulating Nuclear Export of p27/Kip1.” *Cancer Cell* 23 (5): 647–59. doi:10.1016/j.ccr.2013.03.012.

Zhang, Yang, Hua Zhang, Xueqing Wang, Jiancheng Wang, Xuan Zhang, and Qiang Zhang. 2012. “The Eradication of Breast Cancer and Cancer Stem Cells Using Octreotide Modified Paclitaxel Active Targeting Micelles and Salinomycin Passive Targeting Micelles.” *Biomaterials* 33 (2): 679–91. doi:10.1016/j.biomaterials.2011.09.072.

Zhou, Jiong, Renee Chehab, Josephine Tkalcevic, Matthew J. Naylor, Jessica Harris, Trevor J. Wilson, Sue Tsao, et al. 2005. “Elf5 Is Essential for Early Embryogenesis and Mammary Gland Development during Pregnancy and Lactation.” *The EMBO Journal* 24 (3): 635–44. doi:10.1038/sj.emboj.7600538.

Zhou, Y., B. C. Xu, H. G. Maheshwari, L. He, M. Reed, M. Lozykowski, S. Okada, et al. 1997. “A Mammalian Model for Laron Syndrome Produced by Targeted Disruption of the Mouse Growth Hormone Receptor/binding Protein Gene (the Laron Mouse).” *Proceedings of the National Academy of Sciences of the United States of America* 94 (24): 13215–20.

Zomer, Anoek, Saskia Inge Johanna Ellenbroek, Laila Ritsma, Evelyne Beerling, Nienke Vrisekoop, and Jacco Van Rheenen. 2013. “Brief Report: Intravital Imaging of Cancer Stem Cell Plasticity in Mammary Tumors.” *Stem Cells (Dayton, Ohio)* 31 (3): 602–6. doi:10.1002/stem.1296.